SCUOLA DI DOTTORATO
UNIVERSITÀ DEGLI STUDI DI MILANO-BICOCCA

Dipartimento di / Department of

Earth and Environmental Sciences

Dottorato di Ricerca in / PhD program Geological Sciences Ciclo / Cycle XXXII

Curriculum in (se presente / if it is) Chemical, Geologial and Enviromental Sciences

Petrology and multimineral fingerprinting of modern sand derived from the Himalayan orogen

Cognome / Surname Liang Nome / Name Wendong

Matricola / Registration number 823486

Tutore / Tutor: Eduardo Garzanti

Cotutore / Co-tutor: Mara Limonta, Alberto Resentini
(se presente / if there is one)

Supervisor:
(se presente / if there is one)

Coordinatore / Coordinator: Maria Luce Frezzotti

ANNO ACCADEMICO / ACADEMIC YEAR 2019/2020

Abstract

Sediment and sedimentary rocks can be considered as geological archives that faithfully reflect their provenance information if the bias introduced by physical and chemical processes during transport and deposition can be properly recognized and corrected for. The sediment provenance analysis both in modern and ancient settings is crucial to trace the sediment sources, reconstruct paleoclimate and paleoenvironment, and interpret the evolution of the Earth's surface.

Modern sediment, unaffected by diagenesis, with transport and deposit under climatic conditions that are fully known, can provide valuable information on the interactions among the different controlling factors that govern source-to-sink systems. Rivers draining the Himalayan orogen provide the good opportunity to trace the source fingerprinting that is documented in modern fluvial and eolian sand and how these signatures reflect the erosion patterns of the modern and paleo-river systems. A multidisciplinary approach based on petrography, minerology, geochemistry and geochronology is emphasized in this research, in order to obtain a comprehensive provenance information.

Our research area focused on the modern sand in two river systems: Yarlung Tsangpo and Indus River. In the Yarlung Tsangpo system, the Nianchu River was chosen to investigate the petrographic, mineralogical and chronological signature of sediment from the Tethys Himalaya, Greater Himalaya, Kangmar gneiss dome and Transhimalayan ophiolitic suture. Different tectonic domains are characterized by distinct heavy mineral assemblages, e.g., the first-cycle sillimanite and garnet in Greater Himalaya, young titanite and monazite in Greater Himalaya or Kangmar dome, chloritoid in the low-grade metapelites surrounding the Kangmar dome, and clinopyroxene, olivine and enstatite in the forearc ophiolites. Sand carried by the Nianchu River and its major tributaries, mainly reflects Tethys Himalayan characteristics, consistent with the geochronological results. Erosion rates were also evaluated and circumscribed in the middle Yarlung Tsangpo catchment. The average erosion rate in the Nianchu catchment is estimated at ~ 0.10 mm a^{-1}, about twice as that in the middle Yarlung Tsangpo catchment (0.05 mm a^{-1}) and about five times as that of the Lhasa River catchment (0.02 mm a^{-1}). This marked difference is principally ascribed to the higher erodibility of the Tethys Himalayan sedimentary strata. Within the Nianchu basin, low precipitation in the rain shadow of the high Himalayan range may

explain a lower erosion rate in the headwaters (0.07 mm a^{-1}) than in the less steep lower reaches (0.14 mm a^{-1}).

In the Indus River system, minerochemical analysis of amphibole, garnet, epidote and pyroxene grains, and geochronological analysis of detrital zircons, associated with analysis on petrography, bulk-sediment geochemistry and isotopic geochemistry, in eolian sand from the Thal Desert and fluvial sand in selected tributaries draining one specific tectonic domain in the upper Indus catchment, were carried out to discriminate compositional signatures, decipher the provenance information, and trace the erosional evolution of the western Himalaya syntaxis. The compositional fingerprints of the Thal Desert sand are characterized by litho-feldspatho-quartzose to quartzo-feldspatho-lithic detrital modes and very rich amphibole-dominated heavy-mineral assemblages. The high heavy mineral concentration, less negative ε_{Nd}, abundant zircon ages at 40-100 Ma, and specific mineral varietal fingerprints, consistently reflect that the Kohistan arc has acted as the main sediment source. The Karakorum appears to contribute less while the Himalaya shows higher influence on the Thal Desert sand than modern river sand from the Indus River. The Nanga Parbat was also revealed as important sources of garnet, amphibole and zircon grains. As a Quaternary repository of wind-reworked Indus River sand at the entry point in the Himalayan foreland basin, the Thal Desert sand document higher erosion rates than today in the glaciated areas formed largely by batholites granitoids of the Asian active margin. The close compositional and chronological connection between the Thal Desert and the ancient Indus Delta and Fan deposits, shed new light on the reconstructing of paleodrainage and the understanding of relationship between climatic and tectonic forcing that controlled the erosional evolution of the western Himalayan-Karakorum orogen.

Index

1. Introduction

1.1 General remarks

Provenance analysis of sediment/sedimentary rocks had always been a thorny business, due to the physical and chemical modification both before ("environmental bias") and after deposition process ("diagenetic bias") (Zuffa, 1987; Garzanti, 2016).

However, tracing the detrital sand from generation, transport to deposition in modern setting, can help to understand the roles that tectonic or climate played in the source-to-sink system. Provenance analysis is considered as the efficient way to understand the sediment behaviour during the transport process in the modern river system where the diagenesis effect is negligible and the geological, geomorphological and climatic information are fully known. Studies on provenance can also help to correct for hydraulic-sorting effects, evaluate the importance of weathering and recycling, and realize the uncertainties and potential pitfalls in our thinking (Garzanti, 2016). As we always said that the present is the key to the past, the increasing understanding of the modern sediment can directly benefit the reconstructing of paleoclimate and paleoenvironment, unraveling of clastic rock provenance, and interpreting of the evolution of the Earth's surface.

Terrigenous detritus has a wide spectrum ranging from few microns to several meters, which is difficult to study with one single method. Coarse detritus like pebbles, cobbles and boulders carry lithology, provenance, ages and exhumation information (Dunkl et al., 2009; Spalla et al., 2009; Garzanti et al., 2018a). However, they are better tackled in field instead of laboratory. Fine detritus, as the major part of the fluvial sediment, is difficult dealt with by optical methods or single-grain techniques, and relying deeply on the improvement of the measuring techniques such as X-ray diffraction, Raman spectroscopy and QEMSCAN microscopy (Bunaciu et al., 2015; Andò et al., 2017; Caracciolo et al., 2019). Sand is the best study object because it is widespread in various tectonic domains and its grain-size is suitable for most of research techniques.

High-resolution petrographic and mineralogical studies now become the primary and essential step for the provenance analysis, which can provide the integral detrital composition and indicative information of source area. However, petrography and heavy mineral analysis may suffer great challenges in complicated orogenic setting because signatures of diverse tectonic domains maybe overlapped and difficult to differentiate. The petrography study alone cannot discriminate detritus young or old, allochthonous or autochthonous, and orogenic or anorogenic itself (Garzanti, 2016). Therefore, detailed and characteristic geochemical and geochronological analysis are needed to better trace the provenance.

1.2 Aims and outline of the thesis

The present thesis is devoted to the multimineral fingerprinting analysis in modern river and desert sand, to explore petrographic, mineralogical, geochemical and geochronological applications of the detrital mineral in provenance analysis, quantify the sediment budget, and trace the erosional evolution within the Himalayan orogen.

The thesis first reviews the previous research on the composition of modern sand derived from the Himalayan orogen, and the analytical methods including bulk-sediment, multimineral and single-mineral methods commonly used in provenance study. The main part of the thesis focuses on the specific modern sand studies in the Yarlung Tsangpo and the Indus River systems.

In the Yarlung Tsangpo catchment, we present the first detailed compositional fingerprinting of detritus released from the Tethys Himalaya in southern Tibet drained by the Nianchu River. Integrated with geochronological and geochemical signatures of zircon grains (Guo et al., in press), and previous petrographic and multimineral results on Lhasa River catchment (Garzanti et al., 2018a), the sediment budget and erosion rates and their controlling factors in middle Yarlung Tsangpo catchment were also estimated and evaluated.

In the Indus River system, multi-methods have been applied in the modern river and dune sand. Minerochemical analysis of amphibole, garnet, epidote and pyroxene grains, the four dominant heavy-mineral species in orogenic sediment worldwide, and petrographic, mineralogical, geochemical and geochronological analysis of sand collected in the Thal Desert and selected tributaries draining one specific tectonic domain each in the upper Indus catchment were determined to quantitatively identify compositional and chronological signatures of diverse Himalayan tectonic units, trace the distinct erosion patterns in the Indus catchment, and unravel the relationship between climatic and tectonic forces that controlled the erosional evolution of the western Himalayan-Karakorum orogen in space and time.

Chapter 1 gives a brief introduction and an outline of the thesis.

Chapter 2 briefly reviews the previous research on sediment compositions derived from the Himalayan orogen.

Chapter 3 describes the multi-methods including petrographic, mineralogical, geochemical and chronological methods used in provenance study.

Chapter 4 illustrates the petrographic and multimineral fingerprinting of modern sand in the Nianchu River draining the Tethys Himalaya, Kangmar dome and Indus-Yarlung suture zone. Sediment budget and erosion pattern among the Nianchu and the middle Yarlung Tsangpo catchments are also evaluated integrated with the suspended sediment load and forward mixing calculations.

Chapter 5 focuses on the provenance information carried in amphibole, garnet, epidote and pyroxene, the four main group minerals in the Thal Desert and selective tributaries of the upper Indus catchment with the combination of Raman spectroscopy and SEM-EDS spectroscopy.

Chapter 6 shows the petrographic, geochemical and geochronological analysis on the same dune and river sand samples in the Indus River system, and the different erosion pattern of Indus River in the western Himalayan syntaxis and adjacent orogenic segments throughout the Neogene.

2. Modern River Sand in the Himalayan Orogen

The two main river systems in the Himalayan orogen are the Indus system and Ganga-Brahmaputra system, which deliver abundant sediment to the Indus and Bengal fan, respectively. The Indus and Brahmaputra rivers both originate from the Tibet, draining symmetrically the western and eastern Himalaya syntaxes and extra-Himalayan tectonic units, whereas the Ganga River originate within the Himalaya, receiving major detritus from the Himalaya in the north and minor detritus from the Indian Shield in the south (Garzanti, 2019a). The Ganga River joins into the Brahmaputra River in Bangladesh before draining into the Bay of Bengal (Fig. 2.1).

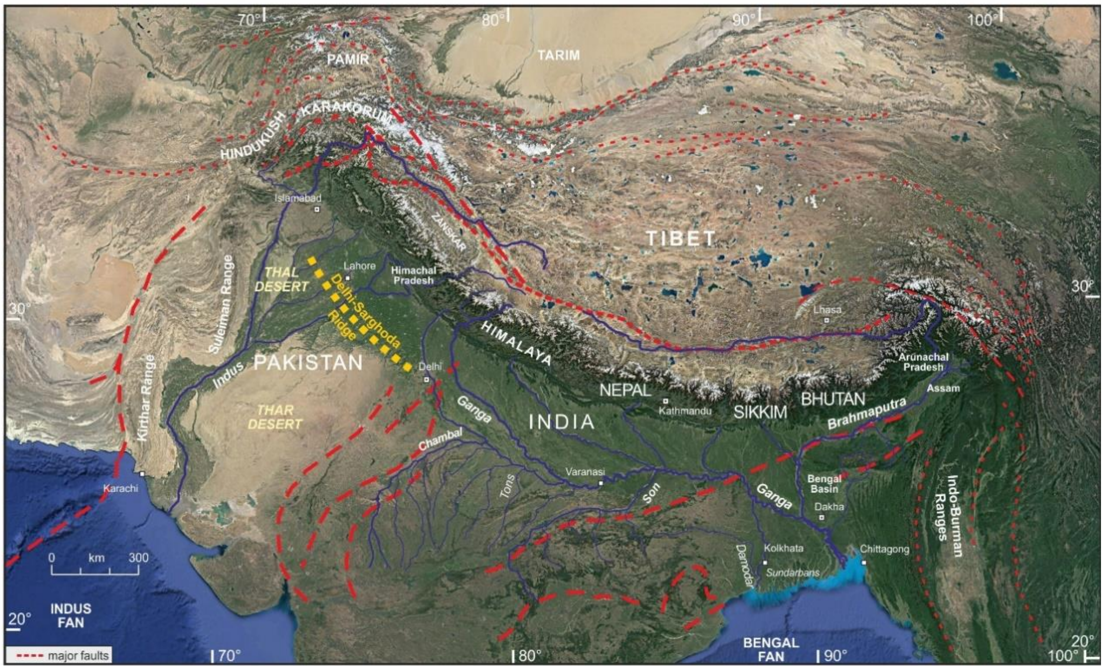

Figure 2.1 The sketch of Himalayan derived rivers and tectonic structures. Modified after Garzanti (2019a).

Different geological domains shed different petrographic characteristics and mineral assemblages, which can be directly seen from their thin sections under the microscope. Tributaries draining diverse geological domains (e.g., Gangdese arc, Ladakh-Kohistan Arc, Karakorum, Nanga Parbat, Namche Barwa syntaxis, Tethys, Greater, Lesser Himalaya, and Indian shield) of the Himalayan orogen, as the major sand carriers, deliver detritus with distinctive petrographic and mineralogic compositions, which provide the best materials for provenance study (Fig. 2.2).

Figure 2.2 End-member orogenic signatures in the Indus and Ganga-Brahmaputra catchments. (modified from fig. 7 and 8 in Garzanti, 2019a). (A) Feldspatho-quartzo-lithic metasedimenticlastic sand with moderately poor amphibole-dominated tHM-suite; (B) litho-

feldspatho-quartzose metamorphiclastic sand with rich amphibole–epidote–garnet tHM-suite; (C) quartzo-feldspathic plutoniclastic sand with rich hornblende dominated tHM-suite; (D) litho-feldspatho-quartzose plutoniclastic sand with very rich hornblende-dominated tHM-suite; (E) quartzo-lithic ophioliticlastic sand with very rich epidote–clinopyroxene–enstatite–amphibole–olivine tHM-suite; and (F) feldspatho-quartzose gneissiclastic sand with a very rich hornblende-dominated tHM-suite; (G) quartzo-feldspathic plutoniclastic sand with moderately rich hornblende-dominated tHM-suite; (H) feldspatho-quartzose gneissiclastic sand with very rich hornblende-diopside tHM-suite; (I) quartzo-lithic sedimenticlastic sand with poor tourmaline-dominated tHM-suite; (J) litho-feldspatho-quartzose metamorphiclastic sand with very rich diopside-dominated tHM-suite; (K) litho-quartzose metamorphiclastic sand with rich amphibole–garnet–epidote tHM-suite; (L) quartzo-lithic metasedimenticlastic sand with very poor tourmaline-dominated tHM-suite; (M) feldspatho-quartzose sand with rich hornblende-dominated tHM-suite. Q, quartz; P, plagioclase; K, K-feldspar; L, lithic fragment (Lc, carbonate; Lmf, higher-rank metasedimentary; Lms, lower-rank metasedimentary; Lu, ultramafic); a, amphibole; b, biotite; e, epidote; p, clinopyroxene; s, fibrolitic sillimanite. The blue bar for scale is 150 μm.

2.1 Indus River

The Indus River consistently carries feldspatho-litho-quartzose to litho-feldspatho-quartzose sand along its trunk drainage, with subequal amounts of quartz (invariably < 50% of the total framework), feldspars and lithic grains (Fig. 2.3). Detritus entering the foreland basin contains subequal amounts of plagioclase and K-feldspar, a variety of sedimentary (limestone, siltstone/shale, dolostone), very-low- to very-high-rank metamorphic lithic fragments (slate, phyllite, schist, gneiss, metabasite), and common mica (biotite > muscovite). Suture zone signals such as volcanic grains, serpentinite and chert are very weak. The rich heavy mineral assemblage is characterized by dominant blue-green hornblende to subordinate green-brown hornblende, associated with epidote and minor garnet, clinopyroxene, hypersthene, staurolite, kyanite and sillimanite (Garzanti et al., 2005; Garzanti, 2019a).

The Indus River sediment in the delta is somewhat rich in quartz and sedimentary grains (e.g. limestone), displaying a lower average rank of metamorphic grains, and depleted heavy minerals (especially amphibole and pyroxene), with a small relative increase in epidote and durable ZTR minerals (Clift et al. 2010). Indus Fan turbidites retain the litho-feldspatho-quartzose signature but with only minor garnet, suggesting hydrodynamic fractionation of denser minerals between the delta and the deep sea (Suczek and Ingersoll 1985; Andò et al. 2019).

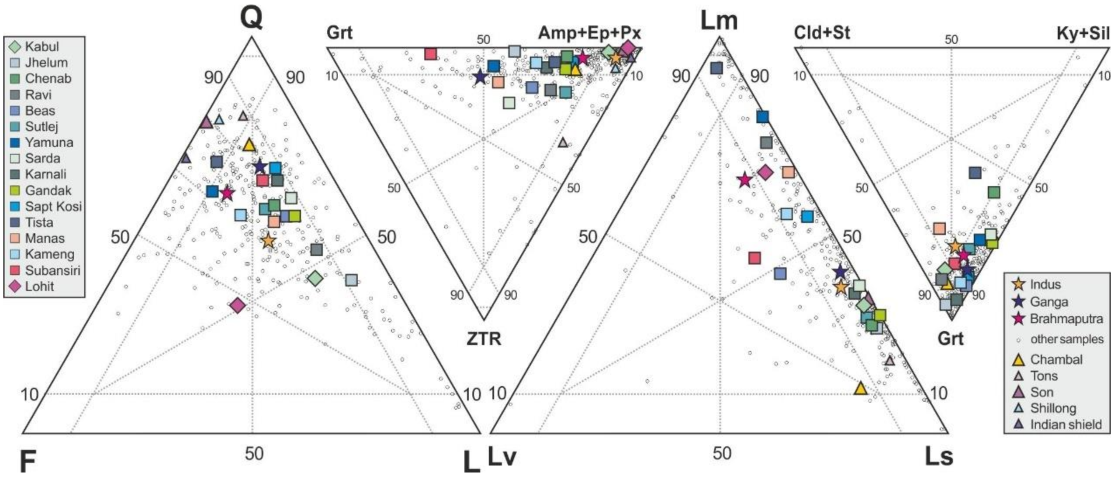

Figure 2.3 Detrital modes of modern sand derived from Hiamlaya (fig. 9 in Garzanti, 2019a). Major Himalayan rivers carry feldspatho-litho-quartzose to litho-feldspatho-quartzose sand rich in metamorphic and sedimentary lithics, with moderately rich to very rich amphibole–epidote–garnet tHM-suites almost invariably including staurolite, kyanite, sillimanite and clinopyroxene. Rivers draining the Indian Shield or Shillong Plateau carry instead mainly feldspatho-quartzose sand but locally include sedimentary and a few volcanic lithic fragments; moderately rich to very rich tHM-suites range from hornblende-dominated to amphibole–epidote–garnet–pyroxene with staurolite, kyanite and sillimanite. Feldspathoquartzo-lithic Kabul sand and litho-quartzo-feldspathic Lohit sand are supplied to the NW and NE ends of the Himalayan foreland basin. Q= quartz; F = feldspar; L = lithic grains (Lv = volcanic; Ls = sedimentary; Lm = metamorphic); ZTR = zircon + tourmaline + rutile; Amp = amphibole; Px = pyroxene; Ep = epidote; Grt = garnet; Cld = chloritoid; St = staurolite; Ky = kyanite; Sil = sillimanite.

Nd and Sr isotope of bulk-sediment (Clift et al., 2002; Alizai et al., 2011a; Jonell et al., 2018), ^{10}Be cosmogenic nuclides (Munack et al., 2014) and clay mineralogy (Alizai et al., 2012) in sand of the Indus River and Thar Desert have been investigated to trace the provenance. For detrital minerals, major and trace elements study in amphibole (Lee et al., 2003), geochemical study in garnet (Alizai et al., 2016), Pb isotopes in detrital K-feldspar (Clift et al., 2002; Alizai et al., 2011a), U-Pb or ^{39}Ar/^{40}Ar chronological studies on zircon or mica and fission-track or (U–Th)/He thermochronology study on apatite (Clift et al., 2004; Campbell et al., 2005; Alizai et al., 2011b) in sand of the middle Indus catchment and its Punjab tributaries have also been carried out to trace the erosional history and climatic or tectonic controls on the erosion pattern.

2.2 Ganga River

The Ganga River carries feldspatho-litho-quartzose sand characterized by K-feldspar ≈ plagioclase, mainly medium- to high-rank metamorphic rock fragments, limestone and dolostone grains lithics, common mica (biotite > muscovite), and a rich garnet-amphibole heavy mineral assemblage including epidote, clinopyroxene, kyanite, staurolite and sillimanite. Across the foreland basin, the Ganga River receives feldspatho-litho-quartzose sand from the Yamuna, Karnali and Gandak rivers and litho-feldspatho-quartzose sand from the Sapt Kosi river (Fig. 2.3) (Garzanti et al., 2007a; Garzanti, 2019a).

There is plenty of geochemical work focused on the sand of Ganga River and its tributaries, especially the geochemical analysis on major, trace elements and rare earth elements (REE) (Singh, 2009, 2010; Garzanti et al., 2010a, 2011; Rai et al., 2010; Lupker et al., 2011, 2012a), to identify the provenance and reconstruct the erosion process. Isotopic analysis, as an efficient complementary approach, is extensive applied in the modern sediment studies in Ganga catchment. These related studies including the He-Pb double dating of detrital zircons (Campbell et al., 2005), U-series disequilibria in suspended load (Granet et al., 2010), Sr and Nd isotopes (Singh et al., 2008; Rengarajan et al., 2009; Rai et al., 2010; Tripathy and Singh, 2010; Garçon et al., 2014), Hf, Pb isotopes and trace element contents of detrital minerals (K-feldspar, plagioclase, muscovite, biotite, magnetite, zircon, titanite, apatite, monazite/allanite, amphibole, epidote, garnet, carbonate and clay) (Garçon et al., 2014), ^{10}Be concentrations on quartz (Lupker et al., 2012b), and so on.

2.3 Brahmaputra River

The Yarlung Tsangpo, as the upper reaches of the Brahmaputra River located in the Chinese part, flows eastwards along the Indus-Yarlung suture zone and receives litho-feldspatho-quartzose sand from northern tributaries draining the Lhasa Block (Garzanti et al., 2018a), and feldspatho-quartzo-lithic sand from southern tributaries draining the Tethys and northern Himalaya. Even so, the erosion rate is low (< 0.1 mm a^{-1}; Garzanti et al., 2004a) and sediment load is negligible (1.5% of Brahmaputra River; Shi et al., 2018) in the Yarlung Tsangpo catchment.

The Brahmaputra River then drains southward at the eastern syntaxis and cuts across the Himalaya. This part of river is also named as Siang, which carries litho-feldspatho-quartzose sand, with high-rank metamorphic rock fragments (paragneiss, metabasite), dolomite grains and micas (biotite > muscovite). The very rich heavy mineral assemblages are dominated by hornblende associated with epidote, garnet and diopsidic clinopyroxene (Fig. 2.3).

After flowing into the foreland basin, the river sand is gradually mixed by plagioclase-rich sand from several major tributaries draining the Transhimalayan arcs from the east, quartz and metamorphic minerals rich sand derived from the Arunachal Pradesh, Bhutan and Sikkim Himalayas from the north, and feldspatho-quartzose sand from small tributaries draining the Indo-Burman Ranges and Shilong Plateau (Fig. 2.1; Fig. 2.3). The Brahmaputra River carries litho-feldspatho-quartzose sand, with higher plagioclase, dominant metamorphic lithic grains, and a very rich amphibole-epidote-garnet heavy mineral assemblage including minor pyroxenes, titanite, sillimanite and apatite (Fig. 2.3). As the twice higher sediment contribution from Brahmaputra than that of Ganga, the mixed sand in Bengal estuary is litho-feldspatho-quartzose, showing a similar composition with the Brahmaputra sand (Garzanti et al., 2004a; Garzanti, 2019a).

The channel processes and sedimentation of the Brahmaputra River (Coleman, 1969) and the mineralogy, morphology, magnetic property and composition of the sand of Brahmaputra River (Rahmanb et al., 2012) have already been detailed investigated. Many research also focused on the geochemical signatures, e.g., major, trace elements, REE (Sarin et al., 1989; Datta and Subramanian, 1997; Galy and France-Lanord, 2001; Li et al., 2009; Garzanti et al., 2010a, 2011a; Bhuiyan et al., 2011), Be, U, Th, Hf, Sr, Rb, Os and Nd isotopes (Sarin et al., 1990; Krishnaswami et al., 1992; Singh and France-Lanord, 2002; Singh et al., 2003; Zhang et al., 2012; Goodbred et al., 2014; Lupker et al., 2017), to track weathering processes and sediment supply. An increasing number of work on geochronological study has been carried out, mainly focused on the fission-track and U-Pb zircon grains (Stewart et al., 2008; Cina et al., 2009; Enkelmann et al., 2011; Zhang et al., 2012) in sediment of the Brahmaputra River and Yarlung Tsangpo recently.

2.3.1 Lhasa River

Mineralogical composition of sediment derived from orogenic setting can provide the key information to reconstruct the erosional evolution of the source area in time

(Dickinson, 1985; Garzanti et al., 2018a). The Lhasa River, as the largest northern Tibetan tributary of the Yarlung Tsangpo, drains entirely within the Lhasa block. Detritus carried by the Lhasa River, provides an exemplary case to define the petrographic, mineralogical, geochemical, and geochronological signatures of sediment shed today by a continental-arc terrane incorporated within a large collision orogen, and offers an important complement for the following studies on modern sand derived from the Himalayan orogen (Garzanti et al., 2018a).

Sand from the very low-grade Paleozoic metasedimentary cover strata, is quartzo-lithic sedimentaclastic, dominated by siltstone/metasiltstone and shale/slate with some metarhyolite/metadacite lithic grains. Its very poor heavy mineral suite mainly consists of amphibole, pyroxene, epidote and garnet. Sand from the Cretaceous to Cenozoic granitoid rocks is quartzo-feldspathic to feldspatho-quartzose plutoniclastic, with plagioclase ≥ K-feldspar, a few high to very high-rank metamorphic rock fragments. Its poor to moderately rich heavy-mineral assemblage dominated by hornblende associated with garnet, apatite, epidote, zircon, clinopyroxene and titanite. The Lhasa River sand is litho-feldspatho-quartzose with microlitic and felsitic volcanic, shale/slate/phyllite, siltstone/metasiltstone, metadacite, chloritoschist, and rarer higher-rank metamorphic rock fragments, resulting from the mixture of the two end members in proportion of 1:4. The moderately rich, amphibole-dominated heavy-mineral assemblage contains epidote, and minor garnet, zircon, apatite, and clinopyroxene (Garzanti et al., 2018a).

The studies on chemically resistant detrital minerals which are more easily survive from diagenesis, can help to define a modern-sand reference useful to constrain provenance diagnoses for ancient stratigraphic record. Combined with the zircon data of Zhang et al. (2012), zircon ages mainly distribute in Cenozoic, minor in Mesozoic and the remaining values ranging from 450 Ma to 1800 Ma. The Upper Cretaceous to Eocene magmatic rocks of the Gangdese batholith are characterized by young ages between 40 and 100 Ma and positive $\varepsilon_{Hf}(t)$ values, whereas the magmatic rocks of central Lhasa terrane are characterized by the Early Cretaceous to Jurassic ages and negative $\varepsilon_{Hf}(t)$ values. The zircon grains older than 400 Ma are ascribed to the recycling of the Paleozoic to Mesozoic sedimentary and volcaniclastic strata (Garzanti et al., 2018a). As for geochemical analysis, most apatite grains show comparable compositions to those grains in the Gangdese batholith (negative ε_{Nd} and $^{147}Sm/^{144}Nd$ ratios ~ 0.1). The dominant Nb-rich rutile indicates a felsic source, and minor Cr-rich rutile suggests a mafic source. Virtually all detrital garnets are derived from intermediate-felsic magmatic batholith or rocks (Suggate and Hall, 2014; Mange and Morton, 2007). Monazite grains are characterized by relative high Th content, marked light REE (LREE) enrichment, and negative Eu anomaly, showing their granitoid provenance (Garzanti et al., 2018a).

3. Petrographic and Mineralogical Methods in Modern Sand

A multidisciplinary approach is the most secure way to trace provenance by combining a diversified set of analytical methods and provenance tracers (Najman, 2006; Garzanti, 2016). Only by the careful integration of these disparate pieces of information obtained from diverse techniques can we hope to get a glimpse of the general picture of the source area.

3.1 Bulk-sediment methods

3.1.1 Petrography

To avoid losing the representative of the sample, bulk-sediment approach should always be considered primarily in the provenance analysis. In order to investigate the entire spectrum of grain-sized sediment, petrographic study with the microscope is considered as the most straightforward, cheap and efficient means to determine the mineralogical characteristics and textural parameters (Garzanti, 2016).

In the preparation of thin section, a quartered fraction of each bulk sand sample was impregnated with araldite before cutting into a standard thin section. To better distinguish calcite and dolomite, alizarine red was used for mineral staining. 400-500 grains were analysed for each sample under the microscope, with the Gazzi-Dickinson point counting method independently developed by Gazzi (1966) and Dickinson (1970), which help to minimize variation of composition with grain size (Ingersoll et al., 1984). Results are reported in terms of percentage of quartz (Q), feldspars (F) and lithic fragments (L). They are further used for sand classification according to these three main components which exceeding 10%QFL (e.g., in a litho-feldspatho-quartzose sand, Q > F > L > 10% QFL, in a feldspatho-lithic sand L > F > 10%QFL > Q; Garzanti, 2016, 2019a).

Rock fragments contain rich indicative information of parent rocks. Diverse aphanitic lithic fragments (L pole), including volcanic, ultramafic, metamorphic, sedimentary types, as well as chert, limestone, and dolostone grains larger than 62.5 μm (conventional boundary between silt and sand, Dickinson, 1970), need to be considered and classified. Four main groups of metamorphic rock fragments (metapelite, metapsammite/metafelsite, metacarbonate, metabasite) were recognized according to protolith composition. In each group, five classes of increasing metamorphic grade

(Rank 1 to Rank 5) were defined based on the degree of recrystalization and the progressive formation of cleavage and schistosity (Garzanti and Vezzoli, 2003). The metamorphic index (MI):

MI = (Rank 1 × 1 + Rank 2 × 2 + Rank 3 × 3 + Rank 4 × 4 + Rank 5 × 5) / (Rank 1 + Rank 2 + Rank 3 + Rank 4 + Rank 5) × 100;

ranging respectively from 0 (detritus from sedimentary and volcanic rocks) or 100 (detritus from very low-grade metamorphic rocks) to 500 (detritus from high-grade metamorphic rocks) can thus be calculated, and the crustal level reached by erosion in source area can thus be estimated (Garzanti et al., 2006, 2010b). Considering the various rock-fragment types, a suitable prefix is needed to directly recognize the common rock-fragment group (e.g., volcaniclastic, carbonaticlastic, metamorphiclastic, ultramaficlastic; Ingersoll, 1983).

3.1.2 Bulk-sediment geochemistry

Bulk-sediment geochemistry including the wide spectrum of chemical elements and different behaviour in sediment process, represents an important complementary way in sediment- generation studies. The dissolution and leaching which may considerably alter the original geochemical signatures of buried sediment in diagenesis, have only negligible influence on modern sand. Usually, the analysed sediment geochemical compositions are normalized to the estimated average concentration of upper continental crust elements (UCC; McLennan, 2001; Rudnick and Gao, 2003; Hu and Gao, 2008), whereas the rare earth elements (REE) data are normalized to CI carbonaceous chondrites (McDonough and Sun, 1995). REE are grouped here as light REE (LREE; La, Ce, Pr, Nd and Sm), middle REE (MREE; Eu, Gd, Tb and Dy) and heavy REE (HREE; Ho, Er, Tm, Yb and Lu). Medium REE/MREE* is the ratio between the average of Eu, Gd, Tb, and Dy normalized to Post-Archean Average Austrilian Sedimentary rock (PAAS) and the average of light REE and heavy REE values (Haley et al. 2004).

Geochemistry could be used to assess the fertility of detrital minerals derived from diverse sediment sources (Dickinson, 2008). For example, Zr and Hf elements mainly hosted in the ultradense zircon mineral and REE extremely enriched in monazite, xenotime and allanite (Garzanti et al., 2010a, 2011a). Similar cases such as the richer Na, Sr, Cr, Co and Ni in plagioclase, amphibole and Cr-spinel, and Ca in carbonate, both obtained from the comparation between chemical modes and mineral modes in sediment provenance research (Garzanti et al, 2010a, 2011a).

The primary chemical signatures of sediment generated from the source area can be considerably affected and transformed by the hydrodynamic effects. The sediment homogenization during the downstream transport in higher order rivers to the sea (Ingersoll, 1990; Garzanti et al., 2014a) also make the geochemistry rather blunt for provenance analysis, except some element (i.e. Cr, Ni and to a lesser extent Mg; von Eynatten et al., 2003) preferentially hosted in mafic and ultramafic rocks (Amorosi, 2012; Garzanti et al., 2012). However, hydraulic-sorting effects which lead to the anomalous concentration of minerals in terms of their different density or size classes, can be directly reflected by REE enrichment or depletion, for example, the strongly positive Eu anomaly due to selective entrainment of feldspar, or strongly negative Eu anomaly because of the progressive accumulation of ultradense monazite and allanite (Garzanti et al., 2010a).

Sediment geochemistry is also an efficient tool to assess the chemical weathering (Nesbitt and Young, 1982; Price and Velbel, 2003; Borges et al., 2008; Shao et al., 2012), such as geochemical parameters (e.g., Al/Ti, Ga/Al; Shiller and Frilot, 1996; Young and Nesbitt, 1998), REE parameters (McLennan, 1989; Brown et al., 2003; Haley et al., 2004). The chemical index of alteration (CIA; Nesbitt and Young, 1982) and the weathering index (WIP; Parker, 1970), are both calculated by molecular proportions of mobile alkali and alkaline earth metals and correcting for CaO in apatite and carbonates:

$CIA = 100 \times A1_2O_3/ (A1_2O_3 + CaO^* + Na_2O + K_2O)$,

$WIP = 100 \times (CaO^*/0.7 + 2\ Na_2O/0.35 + 2\ K_2O / 0.25 + MgO / 0.9)$;

where CaO* is CaO associated with the silicate fraction. Stronger weathering is indicated by a higher CIA value and lower WIP value. The CIA is chiefly used to measure the extent of conversion of feldspars to clays such as kaolinite, whereas the WIP is most appropriate for heterogeneous sources including metamorphic rocks (Price and Velbel, 2003; Borges and Huh, 2007; Shao et al., 2012). The WIP is markedly affected by quartz dilution and may cause overestimating of weathering in polycyclic quartzose sand (Garzanti et al. 2013a). That is why the quartz-rich sand samples commonly have lower WIP compared with that of mud samples. Chemical indices of weathering may not reflect weathering only, or even principally (Garzanti and Resentini, 2016). The comparison of CIA and WIP indices provides a key to discriminate compositional modifications caused by weathering and recycling (Garzanti et al., 2013b). A modified CIX index: CIX = 100 × $A1_2O_3$/ ($A1_2O_3$ + Na_2O + K_2O), in which Ca was ignored, has also been introduced because of the weathering underestimation of CIA and WIP in sediment containing carbonate rock fragments, reworked caliche or intrabasinal allochems (Garzanti et al., 2014b).

To circumvent this problem, weathering intensities can be calculated for each single mobile element during incongruent weathering of silicates (e.g., Mg, Ca, Na, Sr, K, Ba) by comparing its concentration to that of a non-mobile element with similar magmatic compatibility (Al, Ti, Sm, Nd, Th) in our samples and in UCC (α values; Gaillardet et al., 1999). This ratio minimizes the uncertainty existing on the composition of crustal source rocks as well as the effect of quartz dilution, partly of grain size and recycling (Garzanti et al., 2013b). As mentioned before, the non-mobile elements Th, Nd, Sm, and to a lesser extent Ti are preferentially hosted in monazite, allanite, titanite, ilmenite, and rutile etc., the dense and ultradense minerals that easily accumulate by hydrodynamic processes (Garzanti et al., 2009). Therefore, the non-mobile elements which are not concentrated in ultradense minerals (e.g. Al for any element E, $\alpha^{Al}_{E} = [Al/E]_{sample}/[Al/E]_{UCC}$) can be used to calculate weathering intensities (Garzanti et al., 2013b), even though the α^{Al} values tend to emphasize the more subtle effects associated with suspension sorting (Bouchez et al., 2011a; Garzanti et al., 2011a).

3.1.3 Bulk-sediment isotope geochemistry

Radioisotope systems, especially the isotope ratios (e.g., $^{87}Sr/^{86}Sr$, $^{143}Nd/^{144}Nd$), are commonly used together to characterize fine-grained siliciclastic sediments worldwide, providing important information on crustal evolution (Goldstein and Jacobsen, 1988), and of course, sediment provenance analysis (e.g., France-Lanord et al., 1993; Clift et al., 2002; Meyer et al., 2011; Singh et al., 2008).

Nd isotope is an efficient tool in provenance discrimination in the Himalayan orogen, whose compositions usually expressed with the ε_{Nd} notation:

$\varepsilon_{Nd} = [(^{143}Nd/^{144}Nd)_{\text{sample}} / (^{143}Nd/^{144}Nd)_{\text{CHUR}} - 1] * 10^4$, where $(^{143}Nd/^{144}Nd)_{CHUR}$ is referred to the Chondritic Uniform Reservoir in value of 0.512630 (Bouvier et al., 2008). Nd isotopic signatures in bulk sediment can reflect the compositional information of source area because isotopic fractionation is negligible in weathering, transport and even diagenesis processes (e.g., Goldstein and Jacobsen, 1988; Goldstein and Hemming, 2003). Combined with the Sr isotope, the radioisotope system may also be used to characterise the chemical weathering intensity in siliciclastic sediment within the source to sink system over geological timescales (Derry and France-Lanord, 1996; Quade et al., 2003; Jonell et al., 2018).

The grain size, especially the fine size (< 63 μm fraction), can affect the Nd isotope composition, which may blur the specific signatures of provenance change (Jonell et al., 2018) and chemical weathering (e.g., Garçon et al., 2014). The Nd-rich monazite and allanite, and feldspar, Sr-rich epidote, carbonate indeed control the bulk sediment isotopic compositions, especially when these minerals are enriched or depleted caused by hydraulic sorting, whereas other minerals (e.g. quartz) contained virtually no trace elements have negligible impact on most isotope ratios (Garçon et al., 2014; Garzanti et al., 2009; Bouchez et al., 2011a; Bouchez et al., 2011b). Even though, the grain size biases are not big enough to dim the bulk sediment Nd isotopic compositions of the provenance-driven trends over the last 15 ka (Jonell et al., 2018). Case study from the Indus delta shows that the ε_{Nd} excursions larger than 1.04, while $^{87}Sr/^{86}Sr$ larger than 0.0099 can be considered as the provenance induced (Jonell et al., 2018).

To assess the relative role played by diverse tectonic domains with overlapping isotopic signatures, supplementary methods independently from environmental and diagenetic biases should always be combined (Clift et al., 2002; Padoan et al., 2011).

3.2 Multimineral methods

Heavy minerals are sensitive indicators of provenance analysis (Morton, 1985a), and the distinct heavy mineral assemblages carry abundant provenance information (Garzanti and Andò, 2007a). The book “Heavy Minerals in Use” edited by Mange and Weight (2007) and the subsequent detailed update review by Morton (2012), provide a complete panorama of the great potential of heavy-mineral studies.

3.2.1 Heavy-mineral suites

Sampling and preparation

Samples are usually taken at regular intervals as well as after changes of lithologic units, stratigraphy, facies, flow regime, bed configurations, etc. To get a complete heavy-mineral assemblage, the fine to medium sized sand samples are recommended. Meanwhile, samples whether enriched or depleted in high density minerals caused by hydraulic sorting should be avoid for better representing the entire sand samples.

Grain size window is the first choice we need to make deliberately, otherwise, irresponsible conclusions would be made with non-representative samples. There are some misunderstandings, for example, increasing the consistency by narrowing the size-window to less than 1ϕ or even only 0.5ϕ wide (125-250 μm, Carver, 1971; 63-125 μm, Morton, 1985a; 90-125 μm, Bateman and Catt, 2007) (Fig. 3.1). The different grain-size classes of a sorted sediment contain notably different heavy mineral compositions, because the high-density minerals settle and deposit together with coarse but low-density or platy minerals (Rubey, 1933; Garzanti et al., 2008). Therefore, bulk-sample for the well-sorted sand, or widest possible size-window centered about the mean for poor-sorted sediment can be the best choice to accurately estimate the percentages of detrital minerals (Garzanti et al., 2009).

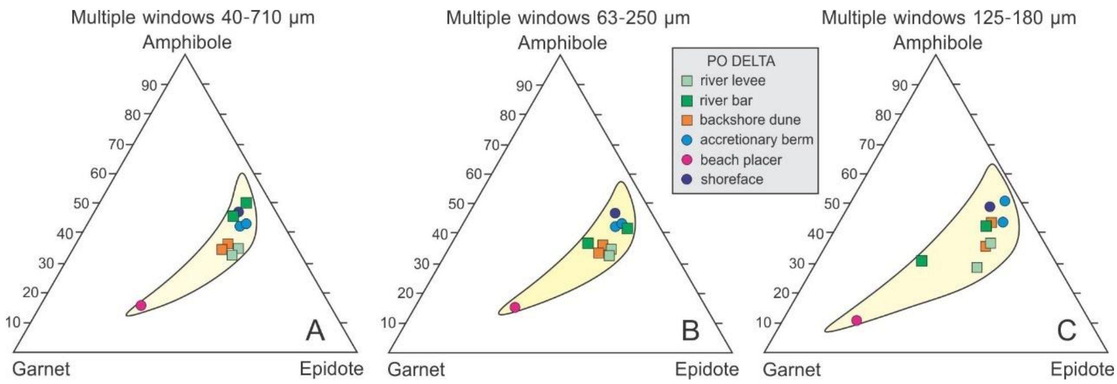

Figure 3.1 Analytical bias caused by size-window (after fig.3 in Garzanti and Andò, 2019). Multiple-window analyses at 0.25ϕ or 0.5ϕ sieve intervals faithfully assess natural intersample mineralogical variability in Po Delta sand (A). Instead, single-window analyses introduce bias which decreases with the width of the analysed size class (B, C). All pale-yellow fields are 90% predictive regions for data points. Data after Garzanti et al. (2009).

The required quantity of sediment varies depending on sample availability, sorting, grain size, and geological setting for modern sand and weathered ancient sandstones. Usually a small amount of 10 g for well-sorted and 15 g for poorly sorted modern sand, whereas 30-50 g for sandstone and 2-5 g for siltstone are taken for heavy mineral extraction in each sample. A disaggregation step with grinding machine or a steel or agate mortar is necessary for sandstone and siltstone.

Spliting is the primary step in sediment preparation to get the appropriate amount of sediment (Krumbein and Pettijohn, 1938; Hutton, 1950). Acid is used to eliminating carbonate, organic substances, and freeing grains from clays and iron oxides-coating (Leith, 1950), authigenic minerals (Milner, 1962). Sieving is the next operation to obtain sand in required size classes with dry method suit for fine-to-medium grained beach, dune and bar sand with mechanical shaker, or wet method used for poor-sorted bank sand or loess with a significant amount of silt or clay with tap water. Weighing of the dry sand is required in every step.

Separating

The watersoluble sodium polytungstate (SPT, $3Na_2WO_4 \cdot 9WO_3 \cdot H_2O$, δ_{used} = 2.90 g cm^{-3}) is usually used as the heavy liquid to separate the heavy (> 2.90 g cm^{-3}) and light minerals (< 2.90 g cm^{-3}) according to their density. The minerals denser than the heavy liquid will sink to the bottom while lighter ones will float on the top. Adding dry sediment and appropriate heavy liquid into the tube to reach a certain weight (usually 100.00 g) for every sample, and next putting them in the centrifuge in three minutes at the speed of 3000 rpm.

After the centrifugation, immerging the lower part of the tube which contains the heavy fraction into the liquid nitrogen to make the lower part freeze in a few minutes. Then recovering the non-frozen upper part (light fraction) firstly and heavy fraction part secondly. Cleaning the recovered fraction with distilled water, and then recycling the heavy liquid at last.

making slides

Splitting moderate amount of heavy minerals with the micro-splitter and mounting grains on the slide with Canada balsam (n = 1.538) on the hot plate (130 °C). Spreading the heavy minerals on the slide to avoid overlap and then coating with the cover glass. The ready-made slide can be moved to the microscope for the heavy mineral identification and counting, according to their diagnostic optical properties (Mange and Maurer, 2012).

Grain counting

The area (or ribbon) method and point counting method are commonly used in grain counting (Galehouse, 1969, 1971). For the slide with well-sorted sediment or quite few transparent grains, area method is applied by counting all grains in the randomly selected area (ribbon), to get the mineral number percentages. For the slide with bulk-samples or wide grain-size windows, point-counting method (Fig. 3.2) is highly recommended for heavy mineral analysis, by counting all the grains on the grid points in a fixed distance (Garzanti and Andò, 2019). This counting method converts the number frequencies to real volume percentages, avoiding the systematically overestimate for denser minerals that are smaller than settling-equivalent lower-density minerals (Galehouse, 1971).

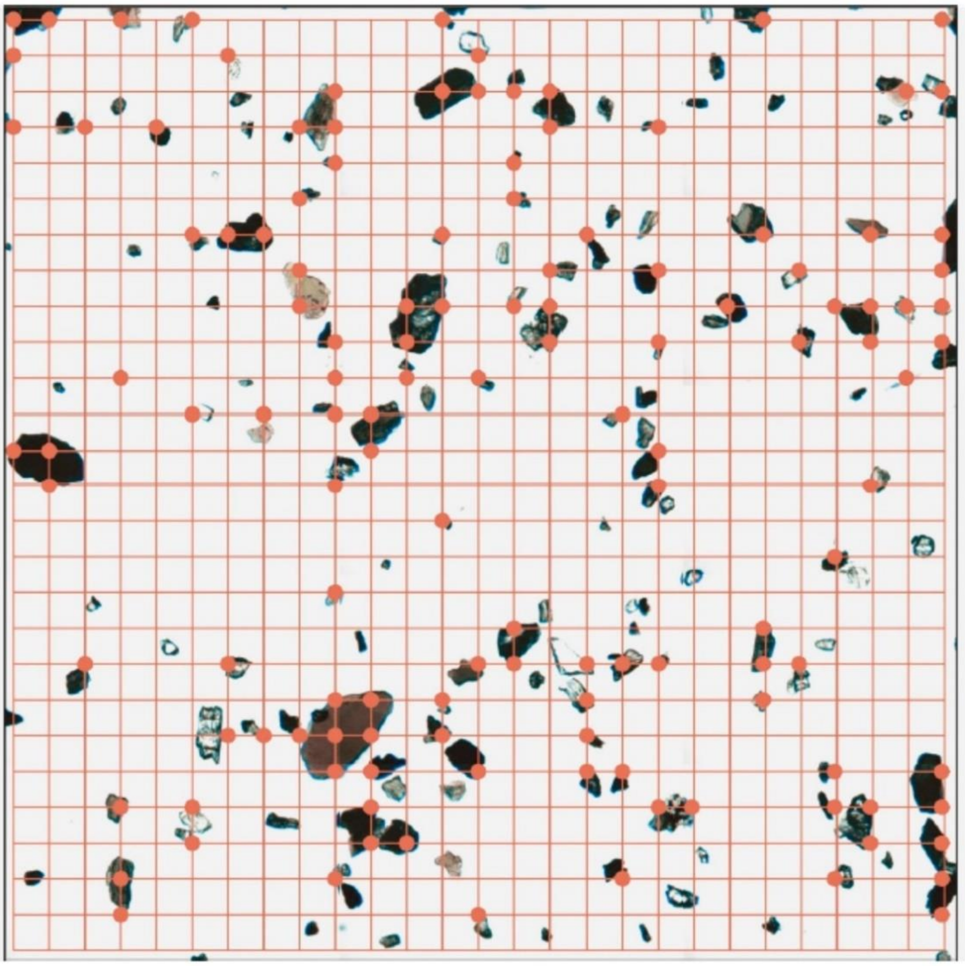

Figure 3.2 Point-counting methods (after fig. 4 in Garzanti and Andò, 2019). It allows obtaining real areal and therefore volumetric percentages of heavy minerals in grain mounts (Galehouse, 1971). Choosing an appropriate grid is critical. In the case represented here—heavy mineral mount from the size window 15–500 μm of a turbiditic silty sand from the Indus

Fan (IODP1456A), square grid 125 μm —several grains are counted more than once, but with a larger spacing more than a single slide would be needed to count a representative number of transparent heavy minerals (usually ⩾ 200).

Heavy mineral parameters

The relative abundance of heavy minerals is considered as an important parameter, as well as their absolute abundance. The Heavy Mineral Concentration index (HMC; Garzanti and Andò, 2007b) and transparent Heavy Mineral Concentration index (tHMC; Garzanti and Andò, 2007b) generally controlled by their parent rocks and their crustal level positions, which means that denser rocks, equilibrated at depth, contain and consequently shed much more heavy minerals than shallower located rocks (Garzanti et al., 2006). The similar HMC and tHMC values can be generated in detritus from high-grade metamorphic rocks, whereas great differences (tHMC much lower than HMC) are commonly seen in detritus generated from very low-grade and retrogressed metamorphic rocks. Similarly, HMC values are deeply influenced by lithology, which are high in mafic igneous and metamorphic rocks and lower in limestone, chert, shale, and granite. This distortive fertility effect indicating that different potential of heavy-mineral generation in different rock types, should be considered in the interpretation of provenance. HMC and tHMC values can be dramatically modified by the selective entrainment of low-density grains (Garzanti et al., 2010a) and selective leaching of unstable minerals during diagenetic process (Gazzi, 1965; Andò et al., 2012), which should also be taken into full account in provenance analysis.

Source Rock density (SRD) index is another parameter that can be used to estimate the crustal level of source rock and hydraulic sorting effect (Garzanti et al., 2006; Garzanti and Andò, 2007b). SRD is defined as:

$$SRD = [\Delta_{tHM}\ (1\text{– }\%\ opaque) + 5.00 \times \%\ opaque)\ HMC + 2.65 \times (100 - HMC)]/100,$$

where delta Δ_{tHM} is the weighted average density of transparent dense mineral. The average density of opaque grains is taken as 5.00 g/cm^3, and the average density of “light” grains is taken as 2.65 g/cm^3.

The average metamorphic grade of metasedimentary source rocks can be estimated by Metasedimentary Minerals Index (MMI, Garzanti and Andò, 2007a) with these high-rank metamorphic minerals expressed as:

MMI = [(1/3 staurolite + 2/3 kyanite + sillimanite) / (chloritoid + staurolite + kyanite + sillimanite)] × 100.

As for the medium-to-high grade metaigneous rocks, Hornblende Colour Index (HCI, Garzanti et al., 2004b, 2006) is calculated based on the relative abundance of blue-green, green, green-brown and brown hornblende grains, represents a useful indicator of average source rock grade and an efficient tool in tracing metamorphic provenance (Garzanti et al., 2004b; Andò et al., 2014). The HCI index is defined as:

HCI = (1/3 green hornblende + 2/3 green-brown hornblende + brown hornblende) / hornblende × 100,

which may provide unambiguous results because it considers only one single mineral that selective dissolution would be neglectable. The index has been proved work well in both metamorphic rocks and metamorphiclastic sediment, irrespective of the colour identification of different operators. MMI and HCI indices both range from 0 in sediment generated from greenschist facies to lowermost amphibolite facies rocks shedding chloritoid and blue/green amphibole to 100 in sediment generated from granulite facies rocks yielding sillimanite and brown hornblende (Garzanti et al. 2004, 2006).

Some ratio parameters are also commonly used in provenance analysis. Parameters (e.g., % opaque, % ultradense) based on density contrast (Garzanti and Andò, 2007b), can reveal the effect of hydraulic sorting and diagenetic dissolution. There are some parameters based on stability contrast, for example the ZTR index (Hubert, 1962), is defined as the percentage of chemically ultrastable species (zircon, tourmaline, and rutile) over total transparent detrital heavy minerals. Sand derived from collision orogens, magmatic arcs, volcanic rifted margins, dissected rift shoulders and cratonic shields, usually observed to have lower ZTR index (mostly < 10, Garzanti and Andò, 2007a), whereas sand derived from undissected rift shoulders and cratonic shields have higher ZTR values, corresponding with their abundant ultradense heavy minerals.

Raman spectroscopy

As a user-friendly, accurate, efficient and versatile technique, Raman spectroscopy is the ideal complementary tool for heavy mineral analysis and detrital geochronology in provenance study (Andò and Garzanti, 2014). This method is considered as nondestructive to minerals without specific preparation on both heavy mineral slides and thin sections (Griffith, 1969; McMillan, 1989; Hope et al., 2001; Nasdala et al., 2004). Another advantage is that it can help to distinguish similar grains, colourless crystals with uncertain orientation and rounded morphology, opaque and altered heavy minerals under the optical microscope.

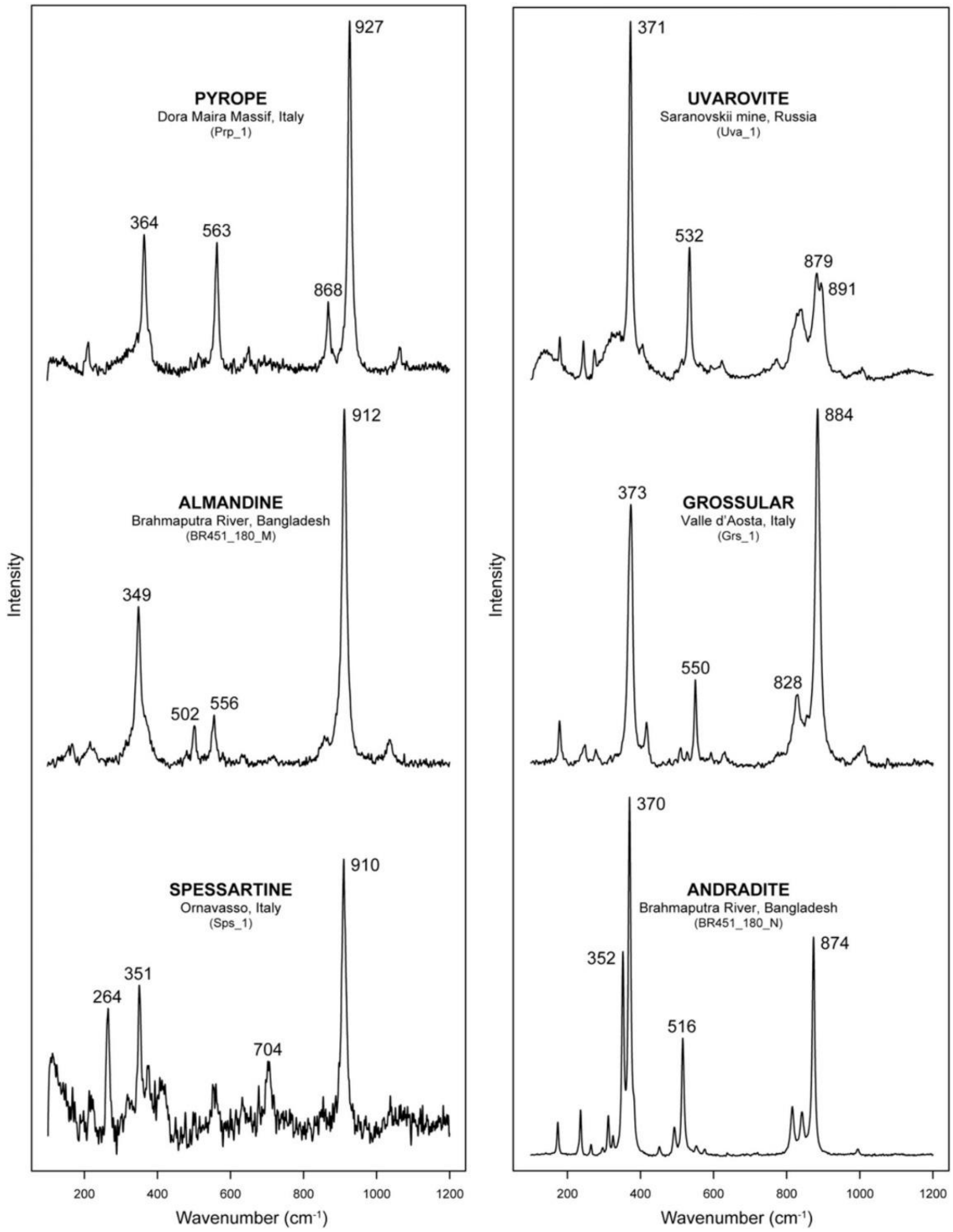

Figure 3.3 Discriminating within the isomorphous series of garnets (fig. 2 in Andò and Garzanti, 2014). Pyralspite and ugrandite garnets can be distinguished by the position of peaks found at high frequencies and caused by Si–O stretching modes (873–880 cm^{-1} in ugrandites, 907–926 cm^{-1} in pyralspites; Bersani et al., 2009).

With the Raman spectroscopy, additional information on polymorphs, solid, liquid and gaseous inclusions within single grains can also be obtained (Mernagh and Liu, 1991; Beyssac et al., 2002; Stefaniak et al., 2006; Bersani et al., 2009; Frezzotti et al., 2011). Besides, Raman spectroscopy allows to determine minerals in a few microns (Garzanti et al., 2011a), even finer grains (Villanueva et al., 2008), which is not feasible with the optical techniques. The accurate and efficient analysis of finer minerals on atmospheric particles (Godoi et al. 2006; Potgieter-Vermaak et al. 2011), suspended load in rivers, distal turbidites and wind-laid loess deposits (Blatt 1985; Godoi et al. 2006; Totten and Hanan 2007; Potgieter-Vermaak et al. 2011), bring a promising prospect for provenance research.

The Raman identification relies on the recognition and comparison of diagnostic peaks of distinct minerals and different species within one mineral group with reference spectra. The constant position of a Raman peak, independent of the orientation, reflects the crystallographic structure and mineral chemistry only. Peak intensity strongly depends on crystal orientation. The ratio between the intensities of different peaks help to identify the isomorphous series of isotropic minerals (e.g. garnets, Fig. 3.3). The Raman spectroscopy identification on group minerals (e.g., garnet, amphibole, pyroxene and epidote) according to these distinct peaks and intensities, has been applied in provenance analysis (Andò and Garzanti, 2014; Garzanti et al., 2018a). Semi-automated heavy-mineral analysis has also been applied by combining Raman spectroscopy with high-resolution geochemical techniques applied to single grains (Lünsdorf et al., 2019), which can greatly improve the efficiency of heavy mineral identification in the future.

3.3 Single-mineral methods

The detailed studies on heavy mineral (e.g., zircon) chemistry began from the 1980s (Morton, 1985b; Dodson et al., 1988). The subsequent studies proved that single detrital mineral serves well in tracing provenance and reconstructing the generation process of sediment (Lawrence et al., 2011; von Eynatten and Dunkl, 2012), especially from the coarse silt to lower medium sand, even though it may bring on risk of ignoring the information of remaining huge part of bulk sediment. One of the principle advantages of single mineral studies is that the detailed geochemical and isotopic composition within single mineral phase can be considered negligibly affected by physical processes during erosion, transport and deposition, and by chemical processes during weathering and diagenesis.

The studies investigated on chemical signatures of single mineral phase, have been developing in an increasing speed recent years, with the evolutive techniques on geochemistry and isotope geochemistry, such as the Raman Spectroscopy (e.g., Andò and Garzanti, 2014), X-ray diffraction (XRD; e.g., Norrish and Chappell, 1977), Cathodoluminescence spectroscopy (CL; e.g., Kempe and Götze, 2002), Scanning Electron Microscope-Energy Dispersive X-Ray Spectroscopy (SEM-EDS; e.g. Liang et al. 2019), Electron-probe Microanalysis (EMP; e.g., Morton, 1984) and Laser-Ablation Inductively-Coupled-Plasma Mass-Spectrometry (LA-ICP-MS; e.g., Jarvis and Williams, 1993).

3.3.1 Single-mineral chemistry

More and more sophisticated geochemical methods are being applied to trace the source information on an increasing number of target minerals (von Eynatten and Dunkl, 2012). Multiple chemical signatures for example, the major elements in amphibole (Winkler and Bernoulli, 1986; Morton, 1991), garnet (Morton, 1985b), pyroxene (Krawinkel et al., 1999), spinel (Pober and Faupl, 1988; Hu et al., 2014), tourmaline (von Eynatten and Gaupp, 1999), Fe-Ti-oxides (Grigsby, 1990); the trace elements in amphibole (Lee et al., 2003), apatite (Morton and Yaxley, 2007), titanite (Aleinikoff et al., 2002), zircon (Belousova et al., 2002a); REE in amphibole (Decou et al., 2011), apatite (Belousova et al., 2002b), epidote (Liang et al., 2019), Monazite (Williams et al., 2007), titanite (Tiepolo et al., 2002), zircon (Belousova et al., 2002a); isotopes in apatite (Bizzarro et al., 2003; Foster and Carter, 2007), epidote (Spiegel et al., 2002), K-feldspar (Tyrrell et al., 2010), rutile (Meinhold, 2010) tourmaline (Shabaga et al., 2010) and zircon (e.g., Knudsen et al., 2001), have been applied to discriminate the source lithology and trace the provenance.

The varietal studies focused on the characteristics and variability of single minerals have been proved to be an efficient provenance indicator, especially on detrital garnet, amphibole, pyroxene and epidote (Morton, 1985b; Liang et al., 2019). Different heavy minerals are expected to carry different provenance signals, thus the multimineral fingerprinting obtained by the integration of several different mineral groups can help to get a comprehensive understanding of source area. The more mineral species investigated, the more abundant provenance information we can get.

3.3.2 Single-mineral geochronology

Compared with minerochemical methods which can be applied to any detrital minerals with significant compositional variability, the geochronological and thermochronological methods can be only applied to suitable minerals displaying unstable isotopes. The diverse time structures of source terranes (Vermeesch et al., 2009) supported by single-grain geochronology and thermochronology can provide additional essential provenance information beyond the ability of traditional petrographic and geochemical approaches.

Single-grain geochronological method consists of high-temperature chronology (e.g., zircon U-Pb age) and low-temperature chronology (e.g., apatite (U–Th)/He age) methods according to the closure temperatures. The high-temperature chronology refers to igneous activities, re-crystallization and metamorphic event at mid crustal levels, reflecting major geodynamic events in source area. The low-temperature chronology relates to exhumation and sediment generation processes, reflecting cooling histories in shallow crustal levels (von Eynatten and Dunkl, 2012). Multiple methods generally include Ar/Ar chronology on amphibole (Cohen et al., 1995), U-Pb chronology(Chew et al., 2011), AHe (Stock et al., 2006) and fission track (AFT, e.g., Laslett et al., 1987) on apatite, Ar/Ar chronology on K-feldspar (Chetel et al., 2005), Th-U-Pb chronology (Hietpas et al., 2010) and MHe (Boyce et al., 2006) on monazite, U-Pb (Zack et al., 2011) and RtHe (Stockli et al., 2007) on rutile, U-Pb (McAteer et al., 2010) and fission track (Gleadow, 1978) on titanite, Ar/Ar (Brewer et al., 2006) or Rb/Sr (Chen et al., 2009) on white mica, U-Pb (Gehrels et al., 1995) and fission track (ZFT, Huford et al., 1984) or ZHe (Reiners et al., 2005) on zircon.

The highly diagnostic signatures of age spectrum provide the direct provenance information, especially combining with heavy mineral study (e.g., von Eynatten et al., 1996). Zircon is the most common mineral used for geochronology study, because it is stable in weathering and diagenesis. Even though its average content in sediment is only 2 grains out of 10,000 (Fig. 3.4; Garzanti et al., 2018a), roughly corresponding to 200 ppm of Zr in the upper continental crust (Taylor and McLennan, 1995). However, the geochronological results can be significantly influenced by the number of grains dated as well as the method of grain selection (e.g. Vermeesch, 2004; Andersen, 2005). Another problem is that the zircon age spectra tend to display homogeneous characteristics in time and space in some cases because of the successive recycling (Garzanti et al., 2013c). Besides, enrichment or depletion of zircon grains may occur in hydrodynamic processes (Lawrence et al., 2011). The research focused on zircon exclusively, may result in misunderstanding or even wrong interpretation in provenance analysis (Garzanti et al., 2018a).

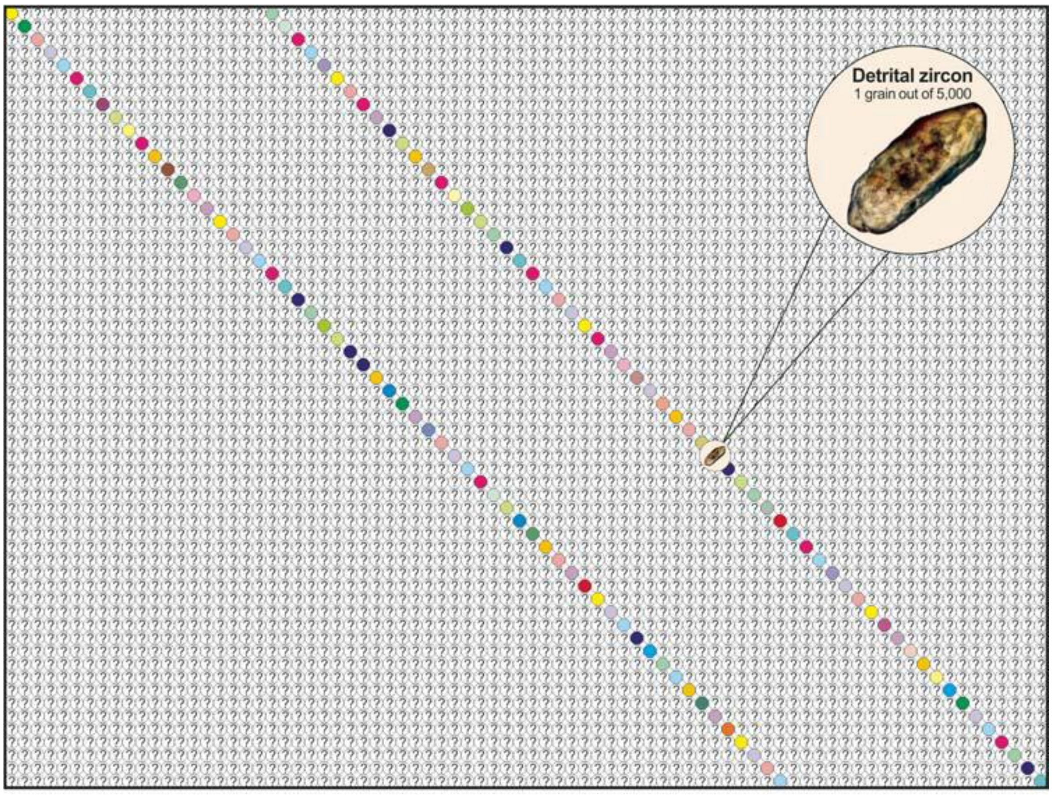

Figure 3.4 Zircon is not enough (fig.2 in Garzanti et al., 2018a). This emblematic sand contains 2.5% heavy minerals (depicted as 120 coloured circles out of 4800), with the one zircon grain representing ~ 0.8% of heavy minerals and ~ 0.02% of the bulk sample. Provenance studies relying exclusively on zircon dating neglect all of the information potentially retrieved from the other 99.98% of detrital grains, generally including not only quartz and feldspar, but also a variety of diagnostic rock fragments and accessory minerals.

4. Multimineral fingerprinting of modern sand generated from the Tethys Himalaya (Nianchu River, Tibet)

Submitted for publication in Sedimentary Geology as “Multimineral fingerprinting of modern sand generated from the Tethys Himalaya (Nianchu River, Tibet)” by Wendong Liang, Alberto Resentini, Ronghua Guo and Eduardo Garzanti.

4.1 Introduction

Orogenic belts are composed of a series of distinct tectonic domains, generally arranged roughly subparallel to tectonic strike. Each of these domains consists of an assemblage of diverse lithological units, which may shed a wide range of sediment compositions (Garzanti et al., 2007b). In order to unravel the erosional evolution of a huge orogenic belt such as the Himalayas, we need to quantitatively identify the signature of detritus derived from each one of these tectonic domains (“first order sampling scale” of Ingersoll, 1990; Garzanti et al., 2007a).

The Himalayan orogen is a thick-skinned thrust belt produced by collision between the Indian passive and Asian active continental margins along the Indus-Yarlung ophiolitic suture zone (Gansser, 1980; Hodges, 2000). The Yarlung Tsangpo (the headwater branch of the Brahmaputra River in south Tibet; *tsangpo* means big river in Tibetan language) flows eastward along the ophiolitic suture zone over a total length of 2057 km (Guan et al., 1984), and receives detritus from both the Lhasa Block in the north, representing the original Trashimalayan active margin of Neotethys (Zhu et al., 2011) and from the Tethys Himalaya in the south, representing the former passive continental margin of India facing Neotethys (Sciunnach and Garzanti, 2012).

Assessing the fingerprint of each detrital source-rock domain in an orogenic belt is a fundamental step to understand its erosional evolution (Garzanti et al., 2004a). Our paper is the first one that describes in detail the compositional fingerprints of detritus released from the Tethys Himalaya in southern Tibet, thus providing a reference for comparison for any provenance studies of ancient Himalayan sandstones. The Nianchu (*chu* = water, river in Tibetan language), a relatively large river that drains northward across the entire Tethys Himalayan zone, cutting across the North Himalayan Kangmar gneiss dome (Fig.1; Chen et al., 1990; Hauck et al., 1998; Lee et al., 2000), provides an excellent case in which to define the petrographic, mineralogical, and geochronological signatures of sediment shed today by Tethys Himalayan strata (Guo et al., in press).

Unraveling the complex mutual interactions among climatic, geomorphological and tectonic processes remains as a major challenge in the field of orogenic research (e.g. Lavé and Avouac, 2001; Burbank et al., 2003; Godard et al., 2014). In symmetry with the previous provenance study of the Lhasa River (Garzanti et al., 2018a), and combined with recent detrital geochronology work (Guo et al., in press), we can tentatively estimate the relative sediment contribution from diverse tectonic domains, useful to trace regional erosion patterns, and to better understand and disentangle the lithological (e.g. Carrapa et al., 2017; Garzanti et al., 2018a) and climatic (e.g. Bookhagen and Burbank, 2006; Shi et al., 2018) influence on erosional processes.

4.1.1 Geological framework

The continental collision between India and Asia took place around 60 Ma (DeCelles et al., 2014; Hu et al., 2015, 2016). The Tethys Himalayan stratigraphic sequence (Fig. 4.1), representing the sedimentary succession of northernmost India (Sciunnach and Garzanti, 2012), is bounded to the north by the south-dipping Great Counter Thrust and traditionally subdivided into southern and northern zones by the Lhagoi Kangri anticline (Burg et al., 1987; Ratschbacher et al., 1994). The southern Tethys Himalaya includes platform carbonates and siliciclastic rocks of Paleozoic to Eocene age that have undergone thrust-sheet deformation and mainly very-low grade metamorphism after continental collision (Willems et al., 1996; Jadoul et al., 1998; Hu et al., 2012). Differently, the northern Tethys Himalaya includes outer shelf, continental slope, and rise deposits of Mesozoic to Paleogene age, and a series of gneiss domes exposed along the axis of the Lhagoi Kangri (Hu et al., 2008; Cai et al., 2011). These domes are in fault contact with the overlying Tethys Himalaya sequence, and were mainly exhumed during the middle Miocene (e.g., Maluski et al., 1988; Chen et al., 1990). The Kangmar Dome, perhaps the best studied example, has a core of Cambrian orthogneiss mantled by Carboniferous and Permian metapelites overlain by low-grade Triassic metasedimentary rocks intruded by mafic and aplite dikes (Lee et al., 2000; Wagner et al., 2010). South of the Tethys Himalaya and comprised between the South Tibetan Detachment in the north and the Main Central Thrust in the south, the Greater Himalaya forms the axial core of the orogen, consisting of medium to locally high-grade metasedimentary rocks and Cambro-Ordovician orthogneiss (Aikman et al., 2008; Carosi et al., 2018). North of the Tethys Himalaya, the Indus-Yarlung suture zone includes mélange units (An et al., 2017) and the Cretaceous Xigaze forearc basin stratigraphically overlying the Yarlung-Tsangpo forearc ophiolite (An et al., 2014; Hu et al., 2016; Wang et al., 2017).

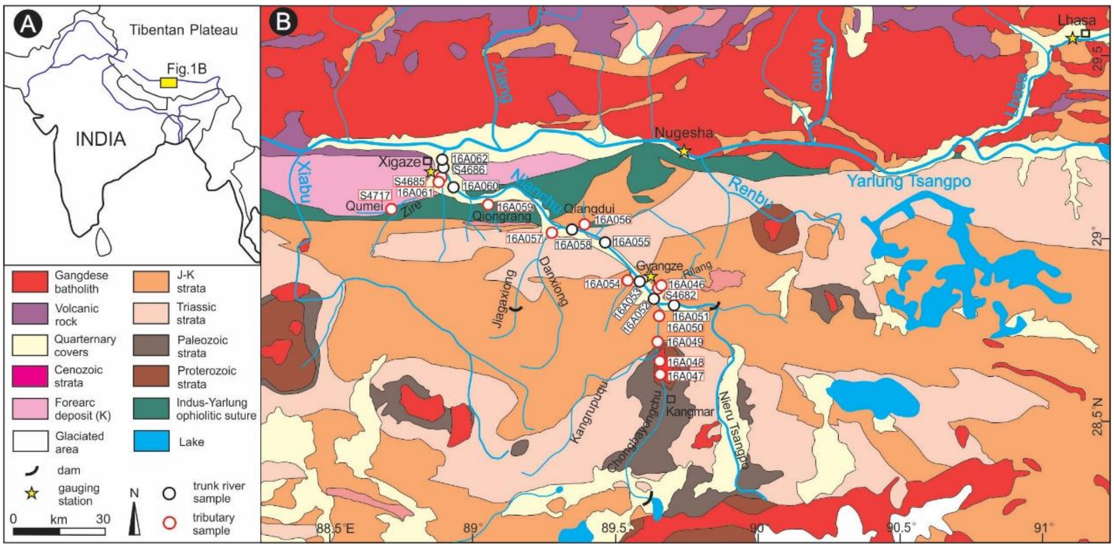

Figure 4.1. Location of the study area (A) and geological setting (B) after Pan et al. (2004). Detailed information on sample locations is provided in Appendix Table A1.

4.2 The Nianchu River

The Nianchu is sourced from the northern slope of the Greater Himalaya and cuts northward across the Tethys Himalayan zone to eventually join the Yarlung Tsangpo near the Xigaze city. As the largest southern tributary of the middle reaches of the Yarlung Tsangpo, the Nianchu originates from the Noijinkangsang Glacier (90.20° E, 29.04° N, 5,950 m above sea level) and flows for 217 km north-westward covering a drainage area of 11,130 km^2 (Fig. 4.2A). The upper reaches of the Nianchu catchment are narrow and steep (average gradient 9.6‰), whereas the lower reaches northwest of Gyangze are broad and open (average gradient 2.2‰). The largest tributary is the Chongbayongchu (length 105 km, drainage area 2864 km^2), also originating from the northern slope of the Greater Himalaya and flowing northward to join the Nianchu at Gyangze. Two major dams are built on the river for hydropower and flood regulation, the Manla reservoir (2001) at the confluence with the Nieru Tsangpo tributary, and the Chongbahu reservoir (1989) in the upstream reaches of the Chongbayongchu. The smaller Chusong reservoir (2000) was built on the Jiagaxiong tributary.

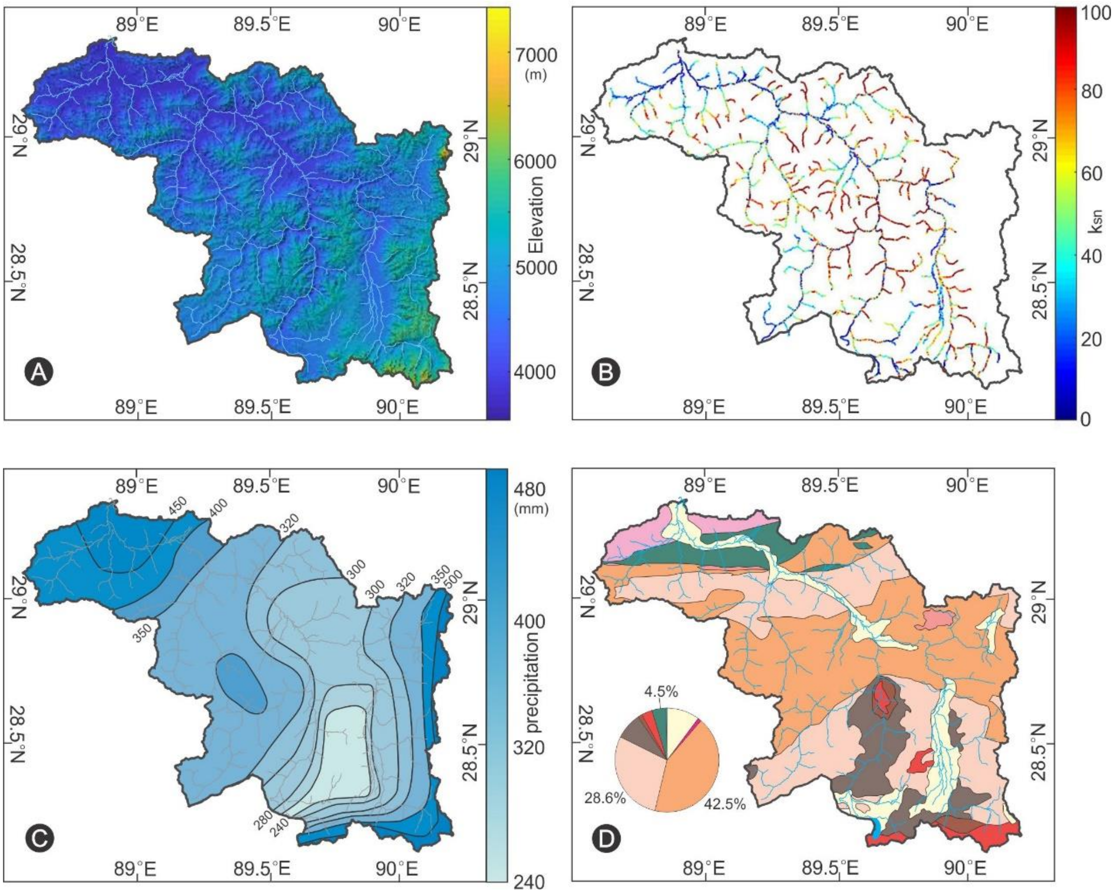

Figure 4.2 Topography (A), channel steepness (B), precipitation (C) and relative distribution of geological units (D) in the Nianchu catchment. Relief and fluvial network are delineated in TopoToolbox from a 30-m-resolution digital elevation model provided by Advanced Spaceborne Thermal Emission and Reflection Radiometer (ASTER) global digital elevation model. Precipitation data after Liu and Chen (1995). The area of the Nianchu catchment was calculated with QGIS based on the 1:1500 000 geological map of Pan et al. (2004). Geological units as in Fig. 4.1.

Climatic conditions in the Nianchu catchment are plateau semi-arid with humid summer and dry winter seasons. The period from June to September accounts for 90% of the annual precipitation (Yang et al., 2011), which is on average 430 mm at Xigaze (3836 m a.s.l.), 288 mm at Gyangze (4090 m a.s.l.), and much lower in the Chongbayongchu and Nieru Tsangpo catchments in the rain shadow of the high Himalayan range (Liu and Chen, 1995; Fig. 4.2C). The average annual temperature is 4.7 °C at Gyangze and 6.3 °C at Xigaze (Zhou et al., 2009), usually below zero in winter and relatively warm in summer (average temperature 13 °C). Because of cold semiarid climate, the effect of chemical weathering on sand mineralogy can be considered as very minor. Wind storms are frequent in late winter to spring. The annual water discharge recorded at the Gyangze and Xigaze stations are 33 $m^3 s^{-1}$ and 51 $m^3 s^{-1}$, respectively; 65% of total discharge occurs in the wet season (Yang et al., 2011). The mean sediment concentration is 1.25 kg m^{-3}. The annual suspended load of the Nianchu measured at Gyangze gauging station was estimated as 0.90×10^6 t a^{-1} (Guan et al., 1984) and 1.10×10^6 t a^{-1} (Liu, 1999) and at Xigaze gauging station as 2.44×10^6 t a^{-1} in the 1980s and as 3.13×10^6 t a^{-1} in the 1990s (Li, 2001). The glaciated area (Fig. 4.1; 224 km^2) represents ~ 2% of the Nianchu catchment. Ice and snow melting in summer contributes largely to peak discharge, which occurs in August accounting for 24% of the annual flux. Summer floods may occur, whereas the river has lowest levels in winter when it commonly freezes.

4.2.1 Geology of the catchment

Tethys Himalayan sedimentary rocks represent 72% of the Nianchu catchment. The rest is accounted for by Quaternary cover (10%), Kangmar Dome and surrounding Paleozoic strata (9%), ophiolites, mélange, and forearc turbidites (5%), other igneous rocks (3%), and Proterozoic metamorphic rocks (1%; Fig. 4.2D). The Greater Himalaya represents the largely snow-covered southernmost part of the catchment, with igneous and metamorphic rocks characterized by U-Pb zircon ages clustering around 500 Ma, 850 Ma, 1.1 Ga, 1.5–1.8 Ga, and 2.5–2.6 Ga (DeCelles et al., 2000, 2004; Gehrels et al., 2011). Paleozoic strata are exposed along the north-dipping Gyirong–Kangmar thrust (Ratschbacher et al., 1994), with the Chongbayongchu branch cutting across the orthogneiss core of the Kangmar Dome. Zircon ages in the Kangmar Dome cluster around 500 Ma (Lee et al, 2000; Wu et al., 2015), with much younger zircon rims dated between 30 Ma and 21 Ma (Hacker et al., 2011). The mainly Mesozoic sedimentary rocks of the Northern Tethys Himalaya yielded zircon age spectra with three modes at 480–570 Ma, 750–1200 Ma, and 2430–2560 Ma (Gehrels et al., 2003, 2011). An additional minor cluster at 220–280 Ma may reflect foreign sediment provenance from either the Lhasa block (Li et al., 2010; Webb et al., 2013) or far-away sources in the Gondwanide orogen (Wang J. et al., 2016). The ophiolite sequence, formed at 125–130 Ma (Li et al., 2009; Hébert et al., 2012; Dai et al., 2013), is exposed along the Indus-Yarlung suture and is drained by the Qiangdui, Qiongrang and Zire tributaries. Strata in the Xigaze forearc basin yielded mostly Cretaceous, some Jurassic, and a few older zircon ages (Wu et al., 2010; Aitchison et al., 2011; An et al., 2014).

4.3 Analytical methods

Twenty-one samples of fine-grained to coarse-grained sand were collected during the summers of 2013 and 2016 from active river bars, eight from the Nianchu trunk river and thirteen from tributaries draining different geological domains. Another set of five samples draining forearc ophiolites exposed in adjacent drainage basins were also analysed for heavy minerals. Information on sampling sites and the petrographic and heavy-mineral datasets are provided in Appendices Tables A1, A2 and A3.

4.3.1 Framework petrography

Fourteen samples were prepared for the petrographic framework. For each bulk sand sample, a quartered fraction was impregnated with araldite and cut into a standard thin section stained with alizarine red to distinguish calcite from dolomite. On each thin section, 350 sand grains were counted for each sample under the microscope (Gazzi-Dickinson method; Ingersoll et al., 1984). Sand were classified by their three main components quartz (Q), feldspars (F), and lithic fragments (L), considered if >10% QFL (e.g., a sand sample is called litho-feldspatho-quartzose if Q > F > L > 10% QFL; Garzanti, 2016, 2019b). The metamorphic indices MI or MI*, ranging respectively from 0 (detritus from sedimentary and volcanic rocks) or 100 (detritus from very low-grade metamorphic rocks) to 500 (detritus from high-grade metamorphic rocks; Garzanti and Vezzoli, 2003), were used to express the average rank of metamorphic rock fragments. Median grain size was also determined in thin section by ranking and visual comparison with sieved standards of $\phi/4$ classes.

4.3.2 Heavy minerals

Twenty-one samples were prepared for the heavy mineral analyses. Heavy minerals were separated with sodium polytungstate (~ 2.90 g/cm^3) from a quartered aliquot of the 32–500 μm class obtained by sieving, recovered by partial freezing with liquid nitrogen, and mounted on a glass slide with Canada balsam. For each sample, between 200 and 250 transparent heavy mineral grains were either grain-counted under the petrographic microscope with the area method, or point-counted at a suitable regular spacing to obtain real volume percentages (Galehouse, 1971). Raman spectroscopy was applied to check dubious grains (Andò and Garzanti, 2014; Lünsdorf et al., 2019). The sum of zircon, tourmaline, and rutile over total transparent heavy minerals (ZTR index of Hubert, 1962) provides information on the extent of recycling (Garzanti, 2017). The transparent heavy mineral concentration (tHMC), calculated as the volume percentage of transparent heavy minerals (Garzanti and Andò, 2007b, 2019), ranges from very poor ($0.1 \leq$ tHMC < 0.5), poor ($0.5 \leq$ tHMC < 1) and moderately poor ($1 \leq$ tHMC < 2), to moderately rich ($2 \leq$ tHMC < 5) and rich ($5 \leq$ tHMC < 10).

The Source Rock Density (SRD; g cm^{-3}) index, defined as the weighted average density of terrigenous grains, is used to estimate the average density of source rocks and to check for significant hydraulic-sorting modifications of sand composition (Garzanti et al., 2009).

4.3.3 Areal exposures and river morphometry

The areal exposure of each lithological unit exposed in the Nianchu catchment was calculated with QGIS using STRM DEM data and based on the 1:1500 000 geological map of Pan et al. (2004). The relief and fluvial network of Nianchu catchment were delineated in TopoToolbox (software shell implemented in MATLAB; Schwanghart and Scherler, 2014) from a 30-m-resolution digital elevation model provided by Advanced Spaceborne Thermal Emission and Reflection Radiometer Global Digital Elevation Model (ASTER GDEM; http://www.gdem.aster.ersdac.or.jp). The channel-steepness index k_s, used to measure the bedrock-channel response to differential rock uplift (Whipple and Tucker, 1999; Kirby et al., 2003), is defined according to the power-law relationship: $S = k_s A^{-\theta}$ (S: local channel slope; A: contributing drainage area; θ: concavity index; Flint, 1974). This equation assumes that other controls such as lithology, climate, flood hydrology, or sediment flux are negligible or sufficiently well constrained (Kirby et al., 2003; Whipple, 2004). The concavity index θ is the rate of change of local slope as a function of increasing drainage area, generally found to lie within a narrow range between 0.3 and 0.6 under a steady-state bedrock channel profile (Tucker and Whipple, 2002; Whipple, 2004). A normalized channel steepness index, k_{sn}, is calculated using a fixed reference concavity $\theta_{ref} = 0.45$ to compare channel slopes with markedly different drainage areas and concavities (Korup and Schlunegger, 2009).

4.3.4 Statistical tools

Relative sediment budgets (i.e., the relative amount of detritus contributed by different tributaries to the trunk river) were assessed by forward mixing models based on integrated bulk petrography and heavy mineral data on bedload sand (method illustrated in Garzanti et al., 2012). The Aitchison distance was used to measure the goodness of fit between theoretical detrital modes of sediment supplied by different combinations of diverse end-member sources and the observed detrital mode of the trunk river sediment (Resentini et al., 2017). In order to improve on the accuracy of calculations, we analysed two replicate samples each for the Zire tributary and the Nianchu upstream of the Yarlung Tsangpo confluence.

Statistical/graphical techniques used to illustrate our petrographic and heavy-mineral datasets include the compositional biplot (Gabriel, 1971), which allows discrimination among multivariate observations (points) while shedding light on the mutual relationships among variables (rays). The length of each ray is proportional to the variance of the corresponding variable in the dataset. If the angle between two rays is close to 0°, 90° or 180°, then the corresponding variables are directly correlated, uncorrelated or inversely correlated, respectively.

4.3.5 Erosion rate calculations

The sediment yield (t a^{-1} km^{-2}) of a given source was calculated as the ratio of sediment flux (10^6 t a^{-1}) and the area of the source obtained from the digital geological map. The erosion rate (mm a^{-1}) is estimated next by calculating the ratio between the sediment yield and the estimated average density of exposed source rocks.

4.4 Results

Table 4.1 Petrographic and heavy-mineral signatures of Nianchu sand. Q = quartz; KF = K-feldspar; P = plagioclase; L = lithic grains (Lvm = volcanic and low-rank metavolcanic; Lsm = sedimentary and low-rank metasedimentary; Lmfb = high-rank metamorphic; Lu = ultramafic); HM = heavy minerals; MI and MI = metamorphic indices (Garzanti and Vezzoli, 2003). tHMC = transparent heavy-mineral concentration; ZTR = zircon + tourmaline + rutile; Ttn = titanite; Ap = apatite; Ep = epidote-group minerals; Grt = garnet; Cld = chloritoid; HgM = staurolite + andalusite + kyanite + sillimanite; Amp = amphibole; Px = pyroxene; OS = olivine + spinel; &HM = other transparent heavy minerals (monazite, barite, vesuvianite, prehnite).*

River	Sample	Q	KF	P	Lvm	Lsm	Lmfb	Lu	mica	HM	total	MI*	MI
Greater Himalaya and dome													

Chongbayongchu	16A047	53	3	11	0.3	22	9	0	0.3	1	100	130	85
Chongbayongchu	16A048	43	3	5	0.1	30	12	0	3	3	100	196	148
Chongbayongchu	16A050	23	1	6	1	49	18	0	2	1	100	162	95
Mesozoic strata													
Rilang	S4682	39	2	5	1	38	14	0	1	0.3	100	110	63
Danxiong	16A057	46	3	6	0.1	34	6	1	0	3	100	136	47
Including													
Qiangdui	16A056	25	1	7	0.3	13	9	40	1	6	100	134	101
Qiongrang	16A059	20	1	9	2	20	18	22	1	7	100	155	133
Other tributaries													
Zire	16A061	49	0	4	1	26	6	9	0.3	5	100	142	71
Zire	S4685	43	1	6	2	29	11	7	0.3	1	100	127	76
Trunk river													
Nianchu @upper	16A051	20	2	5	0.3	59	11	0	1	0.3	100	142	45
Nianchu @lower	16A055	36	1	4	0.1	46	10	0	1	2	100	140	55
Nianchu @lower	16A060	47	2	7	1	24	8	5	1	4	100	128	74
Nianchu @final 1	S4686	35	1	6	1	33	13	9	0.3	2	100	135	81
Nianchu @final 2	16A062	30	2	9	3	30	20	3	0.3	2	100	141	105

River	Sample	tHM	ZT	Ttn	Ap	Ep	Grt	Cld	Hg	Amp	Px	OS	& H M	Tot
Greater Himalaya and dome														
Chongbayongchu	16A047	0.8	7	1	10	8	33	0.5	19	15	7	0	0	100
Chongbayongchu	16A048	0.9	12	0.5	7	9	15	4	7	41	5	0	0.5	100
Chongbayongchu	16A049	1.7	14	3	5	17	14	15	4	22	6	0	0.4	100
Chongbayongchu	16A050	0.7	16	2	4	8	11	38	2	17	3	0	0	100
Mesozoic strata														
Rilang	16A046	0.5	23	4	8	15	16	10	3	14	7	0	0.4	100
Rilang	S4682	1.1	13	3	5	11	32	8	9	13	5	0	1	100
Sala	16A054	1.3	16	6	7	22	12	13	2	18	3	0.	0	100
Danxiong	16A057	1.0	21	4	8	16	12	4	5	16	10	1	3	100
Including														
Qiangdui	16A056	2.8	4	0	4	20	9	5	5	14	26	8	4	100
Qiongrang	16A059	3.2	6	0.4	3	28	4	8	1	34	8	3	4	100
Other tributaries														
Qumei	S4717	0.5	11	4	6	20	11	9	3	17	12	2	3	100
Zire	16A061	2.6	29	3	4	10	7	10	2	17	10	6	2	100

Zire	S4685	2.1	12	3	7	13	6	8	0.5	16	24	9	1	100
Trunk river														
Nianchu @upper	16A051	0.3	13	2	9	22	8	18	1	12	14	2	0	100
Nianchu @upper	16A052	0.7	12	1	9	18	9	21	3	14	12	1	0	100
Nianchu @upper	16A053	0.4	13	2	9	18	12	11	3	10	18	1	1	100
Nianchu @lower	16A055	0.8	23	3	6	16	11	15	3	17	6	0	0.4	100
Nianchu @lower	16A058	0.9	9	4	4	19	21	7	2	15	15	3	1	100
Nianchu @lower	16A060	1.4	15	1	7	21	4	14	1	24	8	1	2	100
Nianchu @final 1	S4686	1.3	14	3	5	14	4	11	1	23	21	1	2	100
Nianchu @final 2	16A062	1.6	10	1	1	13	17	11	0.5	13	21	10	2	100

4.4.1 Modern sand of Nianchu tributaries

The Chongbayongchu carries feldspatho-litho-quartzose sedimentaclastic sand with plagioclase > K-feldspar, pelitic, sparitic, and metasedimentary lithic grains, and some plutonic rock fragments and mica (Fig. 4.3A, Fig. 4.4A, B). The poor to moderately poor heavy-mineral assemblage includes amphibole and garnet, associated with epidote, tourmaline, sillimanite, apatite, and clinopyroxene (Fig. 4.4C, Table 4.1). Common sillimanite and garnet in sample 16A047, where chloritoid is rare (Table 4.1), reflect Greater Himalaya contribution. Metamorphic detritus from the Greater Himalaya is however subordinate, because of both limited exposure area (~ 3% of the catchment) and presence of the Manla and Chongbahu reservoirs that may have trapped part of the sediment flux generated in the headwaters. Sedimentary lithics thus prevail over metamorphic lithics, and metamorphic indices are very low (Table 4.1). Additional metamorphic detritus from the Kangmar gneiss dome is reflected by an only slight downstream increase in metamorphic lithics, metamorphic indices, mica (biotite ≈ muscovite), heavy-mineral concentration, epidote and chloritoid, but otherwise overwhelmed by a further increase of sedimentary to low grade metasedimentary grains including sparite (Table 4.1).

The Rilang and Danxiong tributaries, draining Mesozoic Tethys Himalayan strata, carry quartzo-lithic to litho-quartzose sand with dominant shale/slate, siltstone/metasiltstone, phyllite, and schist fragments (Fig. 4.3B, Fig. 4.4A, B). Their poor to moderately poor heavy-mineral suites mainly include garnet, amphibole, epidote and tourmaline, with minor clinopyroxene, chloritoid, apatite, zircon, and titanite (Fig. 4.4C, Table 4.1). The

Sala tributary, mostly draining Jurassic strata, carries a moderately poor assemblage mainly including epidote, amphibole, tourmaline and garnet (Table 4.1).

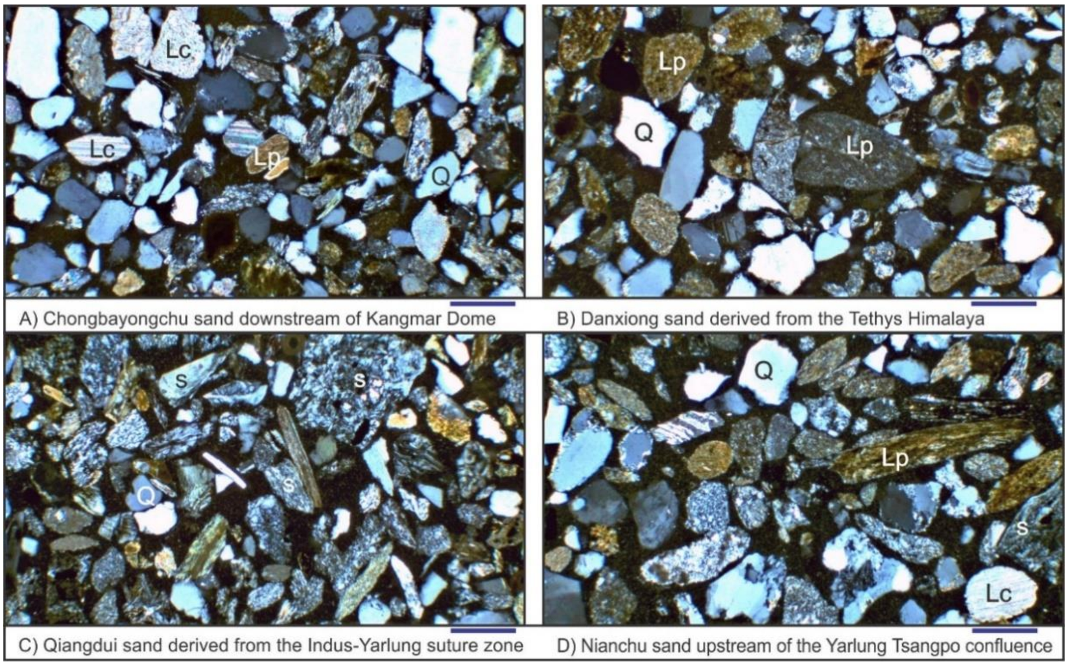

Figure 4.3 Photomicrographs illustrating the variability of sand composition in the Nianchu catchment. (A) Litho-quartzose sand derived from orthogneisses and surrounding Paleozoic strata of the Kangmar dome; (B) litho-quartzose sedimenticlastic/low-rank metasedimenticlastic sand derived from weakly metamorphosed Mesozoic strata of the Tethys Himalaya; (C) quartzo-lithic sand with dominant serpentinite grains derived from ophioltes of the Yarlung suture zone; (D) feldspatho-quartzo-lithic Nianchu sand. Q = quartz; Lc = carbonate, Lp = pelitic/low-rank metapelitic, and s = serpentinite rock fragments. All photos were taken with crossed polars; blue bar for scale is 250 μm.

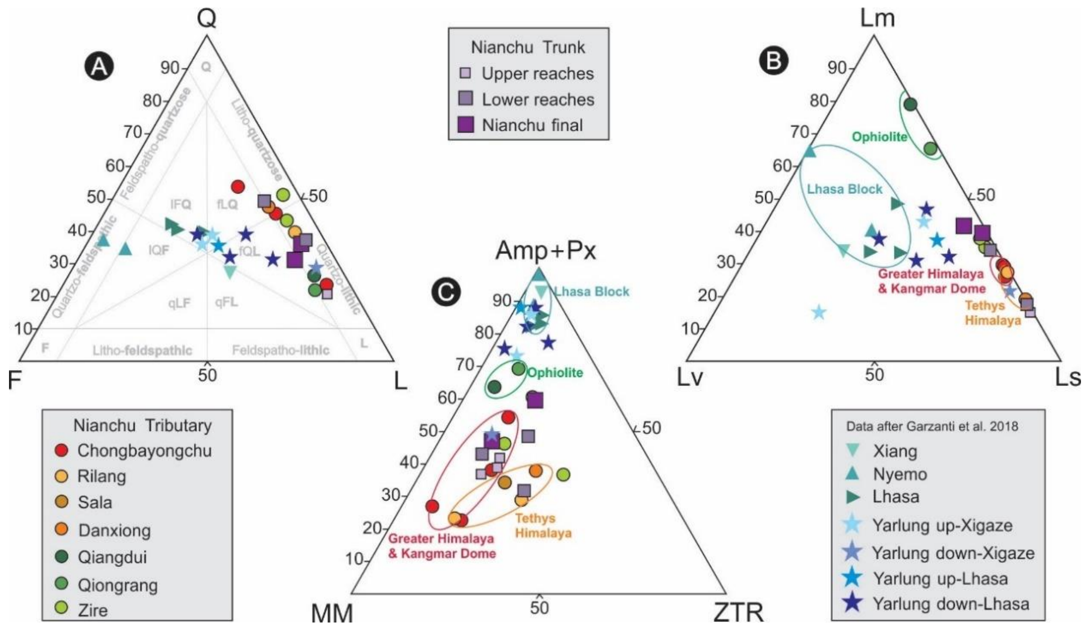

Figure 4.4 Sand petrography (A, B) and heavy mineral assemblages (C). Data from Xiang, Nyemo, Lhasa and Yarlung Tsangpo sand after Garzanti et al. (2018a). QFL (A) and LmLvLs (B) diagrams after Garzanti (2016, 2019b). Q = quartz; F = feldspars; L = lithic grains (Lm = metamorphic; Lv = volcanic; Ls = sedimentary). ZTR = zircon + tourmaline + rutile; MM = chloritoid + garnet + staurolite + andalusite + kyanite + sillimanite; Amp = amphibole; Px = pyroxene.

Different to the Chongbayongchu, Rilang and Danxiong, the Qiangdui and Qiongrang tributaries, carry quartzo-lithic to feldspatho-quartzo-lithic ultramaficlastic sand dominated by serpentinite grains associated with metapelite, metasandstone, shale/slate, and metabasite rock fragments (Fig. 4.3C, Fig. 4.4A, B). Moderately rich heavy-mineral assemblages mostly include amphibole, clinopyroxene and epidote, with subordinate garnet, olivine, prehnite, apatite, chloritoid, tourmaline, and rare spinel and orthopyroxene (Fig. 4.4C, Table 4.1).

The Zire tributary carries quartzo-lithic to litho-quartzose sand with sedimentary, metasedimentary lithics and serpentinite rock fragments (Fig. 4.4A, B), reflecting provenance from both low-rank sedimentary rocks and ophiolite. The moderately rich transparent-heavy-mineral assemblage includes mainly amphibole, clinopyroxene and epidote, associated with chloritoid, garnet, tourmaline, zircon, apatite, olivine, spinel, titanite and orthopyroxene (Fig. 4.4C, Table 4.1). The Qumei tributary carries a poor assemblage mainly consisting of epidote, amphibole, clinopyroxene, garnet, tourmaline and chloritoid (Table 4.1).

The SRD values (Appendices Tables A3) obtained for sand samples derived from Tethys Himalayan strata (SRD 2.56–2.67 g cm^{-3}) and partly supplied by forearc ophiolites (SRD 2.74–2.77 g cm^{-3}) are well within the range expected for the corresponding source rocks (Garzanti et al., 2009), indicating minor hydraulic-sorting bias, if any.

4.4.2 Modern Nianchu river sand

Nianchu sand at Xigaze, just upstream of the Yarlung Tsangpo confluence, is feldspatho-quartzo-lithic and dominated by shale/slate and metasandstone grains associated with serpentinite, sparite, metafelsite and metabasite rock fragments (Fig. 4.3D, Fig. 4.4A, B). The moderately poor transparent heavy-mineral suite includes amphibole, clinopyroxene (mostly green augite), epidote, chloritoid, garnet and tourmaline, with minor olivine, zircon, enstatite, apatite, titanite, prehnite and Cr-spinel (Fig. 4.4C, Table 4.1).

In the upper reaches (Nieru Tsangpo), sand is quartzo-lithic sedimentaclastic with dominant shale/slate and metasandstone grains (Fig. 4.4A, B). The very poor transparent heavy-mineral assemblage includes epidote, chloritoid, clinopyroxene (mostly green augite), amphibole, tourmaline, apatite and garnet (Fig. 4.4C, Table 4.1). Sand collected from the lower reaches upstream of the Indus-Yarlung suture zone displays a relative increase in quartz indicating considerable supply from tributaries draining Mesozoic sedimentary and very-low-grade metasedimentary rocks of the Tethys Himalaya. Additional quartz is contributed by the Danxiong tributary. High-rank metamorphic rock fragments constantly decrease from upper reaches to Nianchu final because of progressive dilution by sedimentary/metasedimentary and eventually ultramafic detritus (Fig. 4.4B). Downstream of the suture zone, the increase in ultramafic lithic grains at the expense of sedimentary lithic clasts, and of clinopyroxene, enstatite and olivine indicate significant local supply from the forearc ophiolites.

4.4.3 River morphometry

The Nianchu catchment shows a relatively homogeneous morphology. Although slope gradients are higher in the upper reaches than in the lower reaches, channel steepness remains in a narrow range for most stream segments ($60 < k_{sn} < 90$; Fig. 4.2B). The Nieru Tsangpo ($k_{sn} = 87$) and Chongbayongchu ($k_{sn} = 79$) have relatively high steepness, whereas other tributaries display lower values ($k_{sn} \sim 60$) (Fig. 4.2B).

4.5 Detrital sources and Nianchu sand budget

4.5.1 Heavy mineral sources

In the Nianchu catchment, in particular sillimanite, garnet, chloritoid, enstatite, and olivine identify specific source-rock domains. Sillimanite, associated with garnet (sample 16A047), is shed from upper-amphibolite-facies metasedimentary rocks exposed in the upper tectonic levels of the Greater Himalaya. Metamorphic rocks surrounding the Kangmar Dome display a zonation from kyanite to chloritoid (Lee et al., 2000), which is particularly abundant (Sample 16A050 and 16A051) in low-grade

Mesozoic metapelites in the outer part of the dome. Enstatite and olivine are derived from ultramafic forearc ophiolites of the Indus-Yarlung suture zone.

Among other minerals, mostly augitic to diopsidic clinopyroxenes are supplied in limited amount not only from mafic rocks of the suture zone but also from mafic volcanic and volcaniclastic rocks interbedded or intruded in Triassic (Wang J. et al., 2016; Meng et al., 2019) and Cretaceous strata (Jadoul et al., 1998; Hu et al., 2008; Wang Y. et al., 2016).

4.5.2 Endmembers and provenance budget

The accurate definition of end-member sources, which are represented by either tributaries or specific geological domains, is an essential prerequisite to calculate a reliable provenance budget (Garzanti et al., 2012). The Chongbayongchu tributary, sourced in the Greater Himalaya and draining the Kangmar dome, provides information on the mineralogy of detritus shed from metamorphic rocks (Fig. 4.1B). Ultramafic lithic grains, olivine, enstatite, and Cr-spinel characterizing sand of the Qiangdui and Qiongrang tributaries offer indications on the ophiolite end-member. Unfortunately all five samples exclusively or mostly draining different lithospheric levels (mantle to diabase dykes and pillow lavas) of forearc ophiolites exposed in adjacent drainage basins yielded mixed heavy-mineral assemblages including large amounts of garnet or other minerals recycled from sedimentary strata, suggesting contamination by fine sand windblown during the dry season. A pure ophiolite end-member could thus not be obtained. Sand in the Rilang, Sala, and Danxiong tributaries, draining Mesozoic strata exclusively, best represent detritus derived from Tethys Himalayan strata.

The Nianchu sand in its final reach is dominantly supplied by Tethys Himalayan strata and subordinately by forearc-basin ophiolites and overlying strata. Contribution from the Greater Himalaya and Kangmar dome, significant in the upper reaches, is progressively diluted downstream (Fig. 4.5).

Forward mixing calculations suggest that the Zire tributary provides 30 ± 11% of total Nianchu sand flux, whereas the Qiongrang, Danxiong, Rilang + Sala tributaries may account for 15–20% of the total sand budget each. Supply from the Chongbayongchu and Nieru Tsangpo headwater branches is limited to 11 ± 9% and 8 ± 8% only, whereas other tributaries contribute very little (e.g., ~ 1% from the Qiangdui).

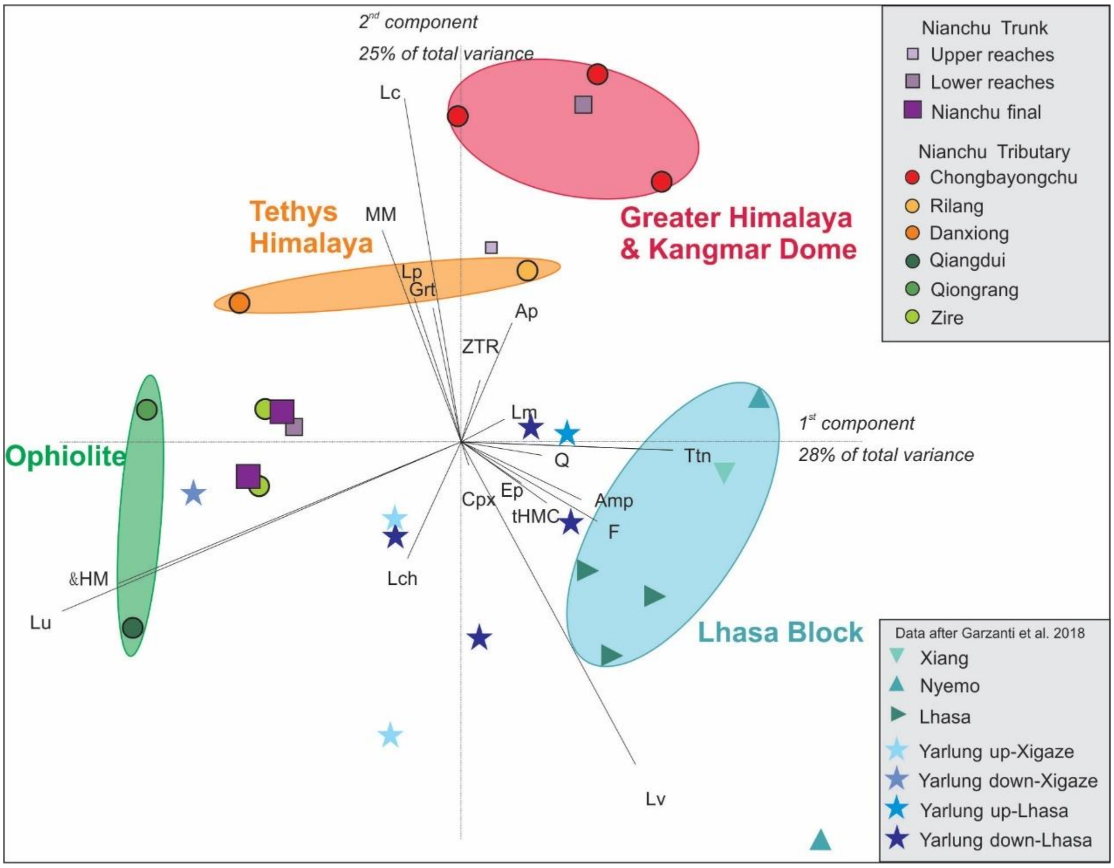

Figure 4.5 Compositional biplot (Gabriel, 1971) based on all petrographic and mineralogical parameters. Data for Yarlung Tsangpo, Xiang, Nyemo, and Lhasa Rivers draining the Lhasa block after Garzanti et al. (2018a). Lch = chert; other petrographic and heavy mineral parameters as in Table 4.1 and Figure 4.3.

Sand collected in Qiangdui and Qiongrang tributaries consist of ophiolite and Mesozoic sedimentary detritus in similar proportions. The petrographic and heavy-mineral datasets (Table 4.1) combined indicate that most of Nianchu sand (79 ± 10%) is generated from erosion of very low-grade Mesozoic strata of the Tethys Himalaya, with a subordinate but significant contribution from forearc ophiolites and overlying siliciclastic rocks (11 ± 8%) and limited supply from igneous and metamorphic rocks of the Greater Himalaya and Kangmar dome (9 ± 7%; Table 4.2).

The Nianchu sand provenance budget can be refined using the information available on age spectra of detrital zircon grains. The U-Pb age distribution of zircon grains obtained from our same final Nianchu sample 16A062 displays three main peaks at ca. 500 Ma, 900 Ma and 1150 Ma, and minor clusters in the 53–200 Ma, and 2400–2800 Ma range (Guo et al., in press). This geochronological data from Nianchu sand is consistent with the age distributions observed in other rivers chiefly draining Tethys Himalaya strata (i.e., Xiabu: Carrapa et al., 2017, and Renbu Rivers: Zhang et al., 2012) (Fig. 4.1B). Unlike the Xiabu River draining the Mabja Dome (Kouwu granite: 14.4 Ma; Kuday granite: 27.5 Ma; Zhang et al., 2004) and the Kampa Dome (Kampa leucogranite: 26.8–24.9 Ma; Liu et al., 2016), the Kangmar granite contains only a few newly grown zircons (Wu et al., 2015). This explains the lack of zircon grains younger than 50 Ma in Nianchu sand. All zircon grains younger than 200 Ma (8%) found in sample 16A062 were thus derived from forearc ophiolites (dated as 130–125 Ma; Li et al., 2009; Dai et al., 2013) or stratigraphically overlying forearc-basin turbidites (main age cluster at 130–80 Ma; Wu et al., 2010; Aitchison et al., 2011; An et al., 2014) exposed along the Indus-Yarlung suture zone. Because age spectra of detrital zircons are not markedly different in Greater Himalayan metamorphic rocks, Tethys Himalayan sedimentary rocks, and Kangmar gneiss dome (Lee et al, 2000; Gehrels et al., 2003, 2011), the much larger age population older than 200 Ma, accounting for about 92% of detrital zircons in sample 16A062 cannot be partitioned accurately among these three sources. Textural evidence, however, provides a clue useful to distinguish between first-cycle euhedral grains and recycled abraded grains. Most zircon grains in Nianchu sand are rounded, and they thus appear to be largely recycled from siliciclastic Tethys Himalayan strata. Besides, at least 5% zircon grains aged between 670–1200 Ma are characterized by Th/U < 0.1 (Guo et al., in press), suggesting origin from metamorphic rocks (Hartmann and Santos, 2004) and thus provenance from the Kangmar Dome or Greater Himalaya.

Provenance budgets based on the age spectra of zircon grains are inevitably far less accurate than bulk-sediment provenance budgets, because zircon is only a rare accessory component, generally representing only ~ 0.02% of the sediment (Vezzoli et al., 2016; Garzanti et al., 2018a), and because the zircon fertility of different end-member sources needs to be known and corrected for (Malusà et al., 2016; Malusà and Garzanti, 2019). Nevertheless, detrital zircon is a powerful carrier of provenance information.

Dominant zircon contribution from the Tethys Himalaya relative to other sources is explained also in the light of heavy-mineral analyses, which point out the notable differences in zircon concentration among different source rocks. Under the assumption of negligible hydraulic-sorting bias, a zircon concentration of ~ 0.04% is indicated for Tethys Himalayan strata (average between samples S4682 and 16A057), which is notably higher than in samples derived partly from forearc rocks, Greater Himalaya, or Kangmar dome (Table 4.2).

These considerations support the conclusions based on the integrated petrographic and heavy-mineral dataset, allowing us to refine our best estimate for sand generation in the Nianchu catchment, inferred to be ~ 81% recycled from the Tethys Himalayan zone, with subordinate supply from forearc rocks of the Indus-Yarlung suture zone (~ 10%) and from the Kangmar Dome + Greater Himalaya (~ 9%) (Table 4.2).

Table 4.2 Tentative sand provenance budget and erosion rates in Nianchu, Lhasa and middle Yarlung Tsangpo catchments. Provenance calculations are based on integrated forward mixing modelling considering bulk-petrography, heavy mineral, and zircon age data. Erosion rates are based on suspended sediment load measured at gauging stations.

	Nianchu						**Yarlung Tsangpo**	**Lhasa**
	Dome + Greater Himalaya	Tethys Himalaya	Suture zone	Total (Xigaze)	Upper Reaches (Gyangze)	Lower Reaches	Nugesha	Total (Lhasa)
Contribution PTHM	**9%**	**79%**	**11%**					
	7%	*10%*	*8%*					
Contrib. Age	> 5%	< 87%	8%					
Avg. Contrib.	**9%**	**81%**	**10%**					
Area (%)	12%	83%	5%					
Area (km^2)	1336	9238	557	11130	~ 6020	~ 5110	106060	32470
Suspended load (10^6 t a^{-1})	0.25	2.26	0.28	2.00-2.79	1.02	1.77	12.23	1.80
Sdm. load (10^6 t a^{-1})	0.28	2.49	0.31	2.20-3.07	1.12	1.95	13.45	1.98
Sdm. yield (t a^{-1} km^{-2})	207	269	552	198-276	186	381	127	61
SRD (g cm^{-3})	2.66	2.61	2.76	2.66	2.62	2.66	2.66	2.67
Erosion rate (mm a^{-1})	0.08	0.10	0.20	0.07-0.10	0.07	0.14	0.05	0.02

Note: Gauging stations are shown in Figure 1; PTHM—petrography + heavy minerals; Sdm.—sediment; SRD—average grain density of analysed sand samples (Garzanti and Andò, 2007b); Mean values are in **bold**, and standard deviations in *italics*. Gyangze gauging station information after Guan et al. (1994) and Liu (1999); Xigaze, Lhasa gauging station information after Li (2001); Yarlung gauging information after Shi et al. (2018). Bedload is considered as 10% of the suspended load.

It is noteworthy that these values are similar to the percentage of the exposure areas of the corresponding geological domains (Table 4.2), which suggests – within the major uncertainties involved in our assessments – similar sand-generation potential for all lithologies. The Tethys Himalaya thus provides, as expected, the bulk of the sand because of its wide exposure area. Our dataset apparently suggests a greater potential for sand generation only in the case of suture-zone ophiolites. However, this may be artefact created by an underestimation of the extreme heavy-mineral concentration in dense mafic and ultramafic rocks. Conversely, the contribution from granitoid and metamorphic rocks exposed in the Greater Himalaya and Kangmar dome is apparently lower than expected, which may be partly ascribed to the presence of reservoirs in the Nianchu headwaters.

The petrographic and heavy-mineral signatures of Yarlung Tsangpo sand downstream of Xigaze is similar to those of Nianchu sand (Fig. 4.4, Fig. 4.5), which indicates significant contribution from Tethys Himalayan rocks upstream. Suspended-load measurements in the Nugesha gauging station (Fig. 4.1) on the Yarlung Tsangpo, located 80 km downstream of the Nianchu confluence, suggests that supply from the Nianchu may account for as much as ~ 23% of Yarlung Tsangpo suspended load (Table 4.2).

4.6 Erosion rates and controlling factors

The total sediment flux from a river catchment includes suspended load, which may be estimated from measurements in gauging stations, and bedload, which so far has proved to be too hard to measure directly and is thus generally roughly calculated as a proportion of suspended load (e.g. 6%, Fergusson, 1984; ~ 10%, Summerfield and Hulton, 1994). Considering bedload equal to 10% of suspended load and an average suspended load of ~ 2×10^6 t a^{-1} or 2.79×10^6 t a^{-1} as estimated by Shi et al. (2018) or measured at Xigaze gauging station (Li, 2001), the total Nianchu sediment flux can be constrained as 2.20–3.07×10^6 t a^{-1}, corresponding to a sediment yield of 198–276 t a^{-1} km^{-2}. Taking an average source-rock density of 2.66 g cm^{-3}, based on the SRD index of Nianchu sand, the average erosion rate for the entire catchment is estimated as 0.07–0.10 mm a^{-1} (Table 4.2), which is fully consistent with the erosion rate assessed as < 0.1 mm a^{-1} for southern Tibet by Garzanti et al. (2004a).

Within the Nianchu basin, we can calculate, from suspended-load measurements carried out in the Gyangze gauging station (~ 10^6 t a^{-1}; Guan et al., 1984; Liu, 1999), an erosion rate of ~ 0.07 mm a^{-1} for the catchment upstream and of ~ 0.14 mm a^{-1} for the catchment downstream (Table 4.2).

Based on the Yarlung Tsangpo suspended load measured at Nugesha gauging station (Table 4.2), the average erosion rate for the entire middle Yarlung Tsangpo catchment is estimated at 0.05 mm a^{-1}, which is only half of the average erosion rate in the Nianchu catchment. An even lower average erosion rate (0.02 mm a^{-1}) is calculated for the Lhasa River catchment based on the flux of suspended sediment measured at Lhasa gauging station (Li, 2001; Table 4.2).

Such low erosion rates, compared to superfast erosion across both the eastern and western Himalayan syntaxes, explains why sediment contribution from dry southern Tibet to the Himalayan foreland basin is very minor (3% ± 2%: Garzanti et al., 2004a, 2005; 1.5%: Shi et al., 2018).

4.6.1 Lithological versus climatic control on sand generation

If indeed a similar sand generation potential characterizes all diverse geological domains within the Nianchu basin, as suggested by the broad correspondence between exposure area and sediment supply from each, then we can readily draw general inferences on the relative effect of lithological and climatic control on erosion efficiency. The Tethys Himalaya sedimentary and very-low-grade metasedimentary rocks contain a greater proportion of shale and slate grains, which are prone to be comminuted to silt and clay particles preferentially entrained in suspension (McBride and Picard, 1987; Garzanti et al., 2013d). Such mechanical comminution explains the much higher annual concentration of suspended sediment in the Nianchu (2.19 kg m^{-3} in 1980s, 2.55 kg m^{-3} in 1990s, Li, 2001) than in the Lhasa River catchment (0.15 kg m^{-3}, Guan et al., 1984; 0.13 kg m^{-3}, Li, 2001), where nearly a half of exposed bedrock is represented by tougher granitoids and volcanic rocks (Garzanti et al., 2018a). The higher erodibility of sedimentary rocks (Morel et al., 2003) represents a most plausible explanation why average erosion rate is so notably higher in the Nianchu than in the Lhasa River catchment, even though the annual precipitation is less in the Nianchu basin (300–450 mm) than in the Lhasa River basin (450–500 mm) (Garzanti et al., 2018a). Land use (Shi et al., 2018) and river channel morphology (Wang et al., 2015), being similar in the two regions, are consequently held not represent relevant factors.

Moreover, if indeed the diverse geological domains have similar capacity to generate sand in the Nianchu basin, then the higher erosion rate by a factor of 2 in the lower reaches than in the upper reaches, where slope gradient is much higher (Fig. 4.2B), would be best explained by the notably higher precipitation in the lower reaches (Liu and Chen, 1995; Fig. 4.2C). The possibly less extensive land use (Zhang et al., 2010) and dominance of dam in the upper part of the river system may represent additional explanations.

4.7 Conclusions

The Yarlung Tsangpo (upper Brahmaputra River) flows along the Indus-Yarlung suture zone separating the former continental margins of India and Asia and receives detritus from both the Lhasa block in the north and the Himalaya in the south. The Nianchu River, as the major southern tributary of the Yarlung Tsangpo in the region, drains mainly Tethys Himalaya sedimentary and very-low-grade metasedimentary rocks, and carries quartzo-lithic to litho-quartzose sedimentaclastic/metasedimentaclastic sand with a few metamorphic, volcanic, and ultramafic lithic grains. The moderately poor heavy-mineral assemblage is mainly composed of amphibole, clinopyroxene and epidote, with minor garnet, sillimanite, chloritoid, olivine and enstatite, which are derived from different geological domains in the Nianchu catchment.

From the combination of high-resolution petrographic, heavy-mineral and detrital-geochronology datasets we could estimate that four/fifths of total sediment in the Nianchu catchment are recycled from Tethys Himalayan strata, the rest being supplied in subequal proportions by forearc ophiolites and overlying siliciclastic rocks and by metamorphic rocks of the Greater Himalaya and Kangmar dome.

Mineralogical fingerprints of end-member sources, combined with gauged sediment fluxes, helped us to disentangle the interplay of lithological and climatic control on erosion patterns. Under the assumption that bedload is equal to 10% of suspended load, we could thus estimate for the Nianchu catchment an average erosion rate of about 0.10 mm a^{-1}. Lithological control explains the much higher erosion rate in the Nianchu catchment than in the Lhasa River catchment draining the Lhasa block to the north. Climatic control represents the most plausible reason why erosion rates surprisingly appear to be double in the lower Nianchu reaches than in the upper reaches despite the notably higher slope gradients. Sediment sequestration in artificial reservoirs and less extensive land use in the upper reaches represent additional explanations.

The petrographic, heavy-mineral, and geochronological signatures of Nianchu sand accurately defined in this study, especially as Tethys Himalayan source rocks are concerned, provide a useful reference for provenance studies based of ancient sandstones derived from the Himalayan orogen.

5. Multimineral Fingerprinting of Transhimalayan and Himalayan Sources of Indus-derived Thal Desert Sand (Central Pakistan)

Published in Minerals volume on Heavy mineral as “Multimineral fingerprinting of Transhimalayan and Himalayan sources of Indus-derived Thal Desert sand (central Pakistan)” by Wendong Liang, Eduardo Garzanti, Sergio Andò, Paolo Gentile and Alberto Resentini.

5.1 Introduction

Heavy minerals provide detailed information on the geology of source areas, which is particularly useful in the study of modern sand unmodified by diagenesis (Mange and Wright, 2007). Subtler distinctions, however, may be required in provenance analysis wherever several different potential sources of sediment consist of similar lithological assemblages shedding similar heavy-mineral assemblages. This is often the case in orogenic sediment containing transparent-heavy-mineral suites typically dominated by amphibole, garnet, epidote, and pyroxene in various proportions (Garzanti et al., 2004b, 2010b, 2016). In this case, distinctive geochemical signatures of single groups of detrital minerals can be used as a genetic tool to trace their provenance (“varietal studies”; Mange and Morton, 2007).

After the pioneering study dedicated to tourmaline by Krynine (1946), and since modern geochemical techniques were applied on garnet (Morton, 1985b), single-mineral analyses have been frequently used and proved to be an efficient means to trace sediment provenance (e.g. Morton, 1991; von Eynatten and Gaupp, 1999; Meinhold, 2010; Andò et al., 2014; Malusà et al., 2017). More and more sophisticated geochemical and geochronological methods are being applied with the aim to fingerprint the source of an increasing number of target minerals (e.g., von Eynatten and Dunkl, 2012). Single-mineral studies have the advantage that fractionation by physical processes during erosion, transport and deposition, and by chemical processes during weathering and diagenesis, can in general be held as minimal. On the other hand, the information obtained from single-mineral datasets needs to be deciphered by correcting for the generally strong differences in mineral fertility of different potential source rocks (Moecher and Samson, 2006; Malusà et al., 2016). This thorny fertility problem is best tackled when several mineral groups are investigated (“multimineral fingerprinting”; Garzanti et al., 2018a; Guo et al., in press), because provenance signals carried by different minerals are expected to differ, reflecting their different abundance in different source-rock domains. Emphasizing this crucial point is one of the goals of this article, which focuses on Transhimalayan and Himalayan sources of detritus transported by the Indus River across northern Pakistan to pinpoint the provenance of heavy minerals contained in eolian sand of the Thal Desert. This small dune field is located in central-northern Pakistan, confined between the Indus River in the west and the course of its major Punjab tributaries in the east (Fig. 5.1). The overall petrographic, mineralogical, and geochemical signatures of Thal dunes indicate that the contribution of Himalayan-derived Punjab tributaries is negligible (Garzanti et al., 2005). The Thal Desert, therefore, can be safely considered as representing a relict Quaternary repository of wind-reworked alluvial-fan sediment originally deposited by the upper Indus at the entry point in the Himalayan foreland basin. The detailed compositional fingerprint of Thal Desert sand, if contrasted with that of Punjab tributaries exclusively draining the Himalayan belt, thus provides an additional actualistic key to trace changes in erosion patterns within the huge catchment that has fed detritus to the Indus delta and deep-sea fan throughout the late Neogene (Clift et al., 2001, 2010). To this goal, our dataset complements a previous work on major and trace elements in amphibole (Lee et al., 2003) and integrates the geochemical study of detrital garnet in sand of the middle Indus course and its Punjab tributaries (Alizai, et al., 2016). We chose to focus on the chemical composition of detrital amphibole, garnet, epidote, and pyroxene because these four minerals, all solid-solution series, represent the four dominant species in orogenic sediments worldwide (Garzanti and Andò, 2007a). Other studies investigating provenance of Indus sediments focused on Pb isotopes in detrital K-feldspar and bulk-sediment Nd and Sr isotope fingerprints (Clift et al., 2002; Alizai et al., 2011a; Jonell et al., 2018), zircon U-Pb or mica $^{39}Ar/^{40}Ar$ geochronology and apatite fission-track or (U–Th)/He thermochronology (Clift et al., 2004; Campbell et al., 2005; Alizai et al., 2011b), sand petrography, heavy minerals, ^{10}Be cosmogenic nuclides (Garzanti et al., 2005; Munack et al., 2014), and clay mineralogy (Alizai et al., 2012). Such multi-technique approaches have shed new light on the relative role played by the interacting climatic and tectonic forces that controlled the erosional evolution of the western Himalayan-Karakorum orogen.

5.2 The Indus River and the Thal Desert

The Indus River, sourced from the central southern Tibetan Plateau, flows in its upper course along the suture zone and the Transhimalayan forearc basin, while receiving detritus from both the Ladakh arc in the north and the northern side of the Himalayan belt in the south (Munack et al., 2014). Next, it cuts a deep gorge through the western Himalayan syntaxis, where very rapid erosion rates generate large amounts of detritus from the Karakorum belt, the Nanga Parbat crystalline massif, and the Kohistan arc (Treloar et al., 1996; DiPietro and Pogue, 2004; Pêcher et al., 2008; Burg, 2011). Farther downstream, the Indus flows across the Himalayan belt and the Potwar Plateau (Khan et al., 1997) where it is joined by the Kabul River draining the Hindukush belt (Hildebrand et al., 2001), crosses the Salt Range, and eventually reaches the foreland basin where it flows southward, confined between the front of the Sulaiman Range in the west and the Thal Desert in the east (Fig. 5.1).

The upper Indus River is mainly fed by melting of ice and snow, and sediment flux consequently increases by two to three orders of magnitudes during the summer (Ferguson, 1984). The annual suspended load of the Indus River, estimated as ~ 14 × 10^6 t upstream of the Shyok confluence (Fig. 5.1), increases rapidly downstream owing to major contributions from the Shyok River (~ 23 × 10^6 t a^{-1}), Karakorum tributaries (≤ 100 × 10^6 t, ~ 18 × 10^6 t of which from the Hunza River), the Astor River draining Nanga Parbat (~ 2 × 10^6 t), and diverse tributaries draining the Kohistan arc, summing up to ~ 176 × 10^6 t at the Besham gauging station (Faran Ali and De Boer, 2008). The annual sediment load reaching the Tarbela Dam, which was closed in 1974 in northern Pakistan, has been estimated at 200 × 10^6 t (Einsele and Hinderer, 1997; Tate and Farquharson, 2000) or even at 287 × 10^6 t (Rehman et al., 1997).

The hydrology of the Indus River has been so intensely regulated since the 1930s that most of its sediment has been trapped in artificial reservoirs and canals, and the annual flux in the lower course has been reduced to ~ 50 × 10^6 t (Rehman et al., 1997). The Indus Waters Treaty signed in 1960 gave rights to the entire flow of the Indus, Jhelum, and Chenab Rivers to Pakistan, and of the Ravi, Beas, and Sutlej Rivers to India. Subsequently, all Punjab tributaries have been dammed and linked by canals to irrigate the arid lowlands and compensate for lost waters in eastern Pakistan. Water discharge dropped sharply, and flow in the Ravi and Sutlej rivers ceased altogether except during monsoon floods. The Mangla Dam, completed in 1967, reduced sediment load of the Jhelum River from 45 × 10^6 t a^{-1} to < 0.5 × 10^6 t a^{-1} (Milliman et al., 1984; Meadows and Meadows, 1999). Among Indus tributaries draining the Sulaiman Range in western Pakistan, the Gomal River (basin area 36,000 km^2) is characterized by extreme concentration of suspended solids (42 g l^{-1}) and high sediment load (30×10^6 t a^{-1}), followed by the Kurram River (3×10^6 t a^{-1}; Rehman et al., 1997). Other rivers are minor and mostly flow during flash floods.

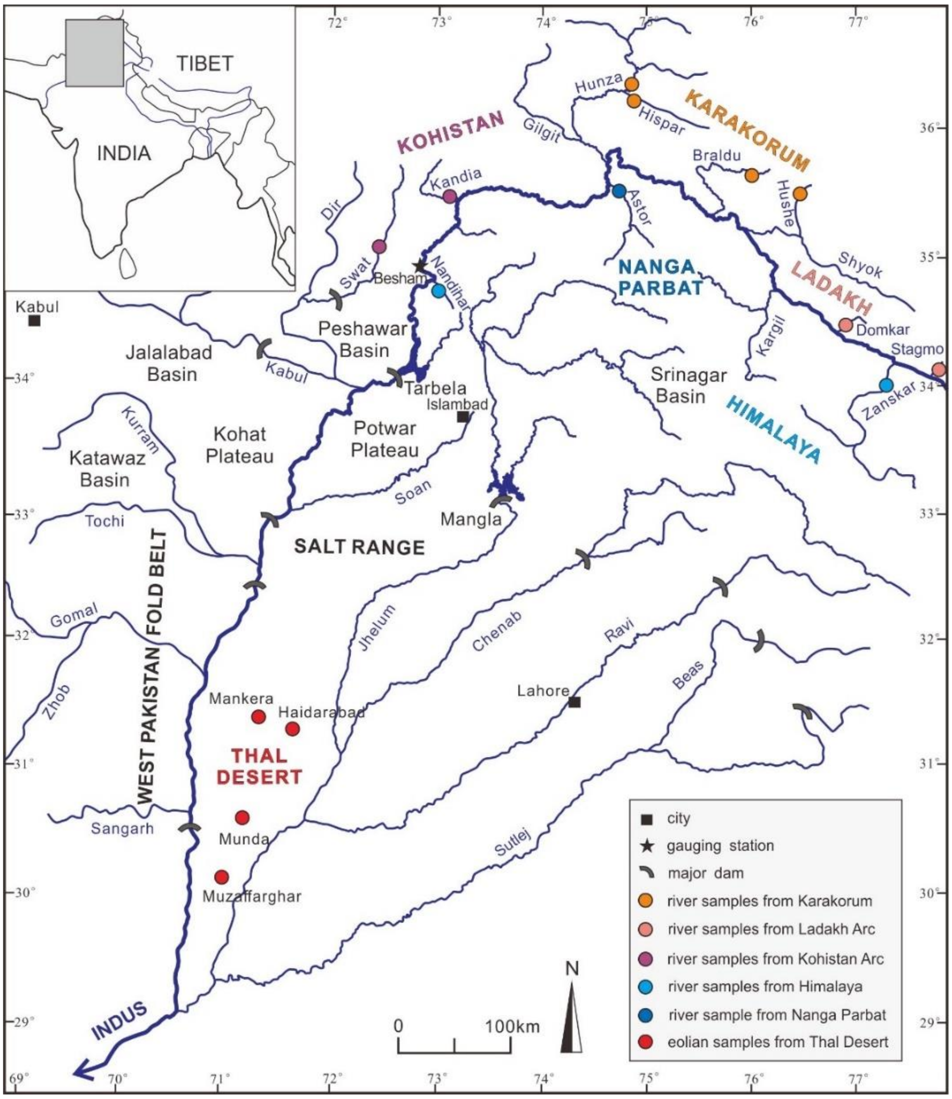

Figure 5.1 The Indus drainage system and sample locations in northern Pakistan.

5.2.1 Karakorum Belt

The composite Karakorum belt includes the Northern Karakorum sedimentary domain, the Central Karakorum batholith, and the Southern Karakorum metamorphic belt (Fig. 5.2; Searle et al., 1999; Hildebrand et al., 2000). In the Northern Karakorum, an Ordovician to Upper Cretaceous sedimentary succession lying non-conformably onto crystalline basement is exposed (Gaetani et al., 1990). Black slates in the north, intruded by calc-alkaline gabbro-diorite, granodiorite, granite, and tonalite, contain andalusite, chloritoid, and epidote (Zanchi and Gaetani, 2011). The Central Karakorum batholith comprises mid-Cretaceous granitoids intruded before the India-Asia collision, and containing amphibole with residual clinopyroxene and accessory titanite, epidote, allanite, apatite, zircon, and opaque minerals (Crawford and Searle, 1992). Post-collisional leucogranites were intruded between 13 Ma and 25 Ma (e.g., Baltoro batholith; Searle et al., 2010). The Southern Karakorum belt includes migmatitic domes undergoing rapid erosional exhumation and displays a northeastward increase in metamorphic grade from structurally lower phyllites to staurolite-, kyanite-, and eventually sillimanite-bearing metasedimentary rocks at the top. Impure dolomitic marbles containing diopside and corundum, and amphibolites with hornblende and garnet also occur (Searle and Tirrul 1991; Rolland et al. 2001; Palin et al., 2012).

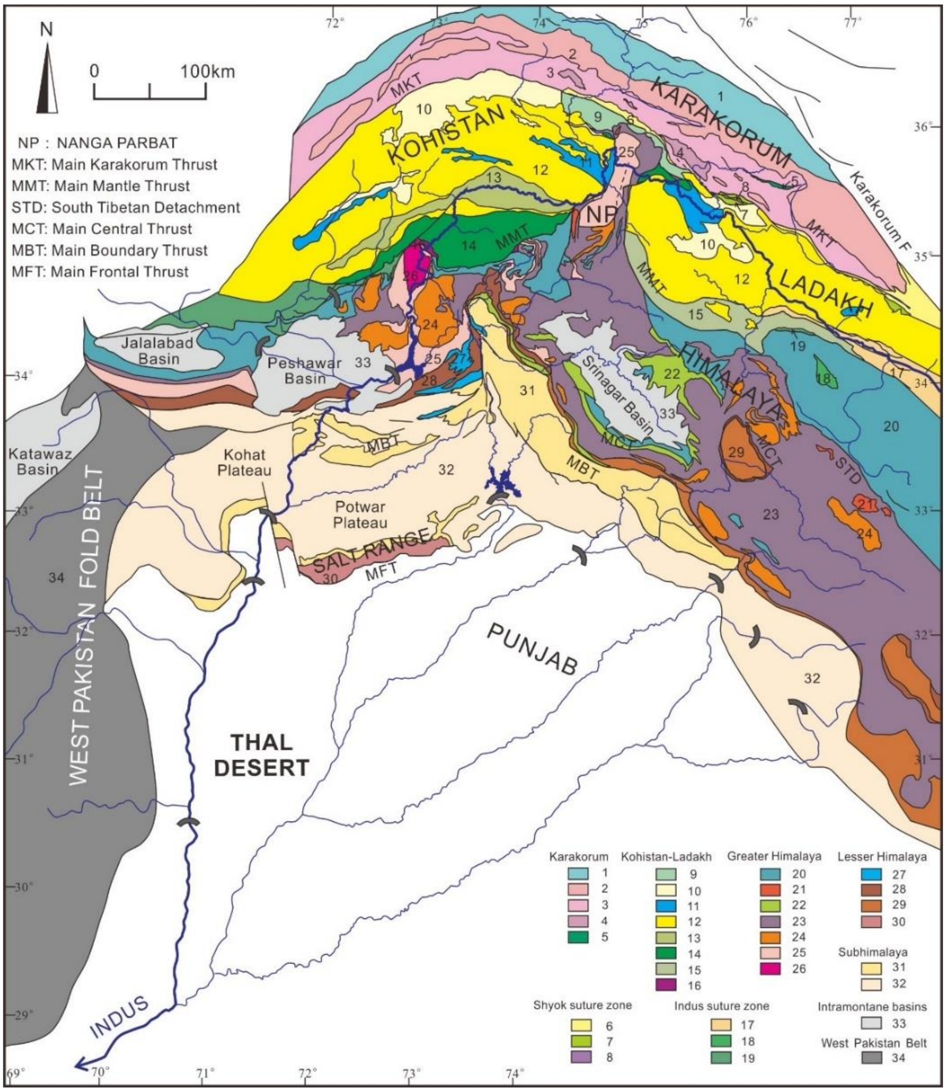

Figure 5.2 Geological map of the Indus catchment in northern Pakistan (modified from Pêcher

et al., 2008). Geological units, from north to south: Karakorum belt: 1: northern sedimentary belt; 2: axial batholith and other granitoid rocks; 3: southern metamorphic belt; 4: felsic gneiss; 5: Masherbrum Greenstone Complex. Shyok suture zone: 6: mostly terrigeneous strata; 7: mélange zone (mainly volcanic rocks); 8: ultramafic rocks (Shyok and Dobani-Dassu lineament). Kohistan and Ladakh arcs: 9: Paleogene Chalt (Kohistan) and Khardung (Ladakh) volcanic rocks, Turmik volcaniclastic rocks; 10: undifferentiated volcano-sedimentary group; 11: metasedimentary rocks; 12: plutonic rocks; 13: gabbronorite (Chilas complex); 14: southern amphibolite; 15: Dras volcano-sedimentary group; 16: ultramafic rocks (Jijal complex). Indus suture zone: 17: Indus Group; 18: Spontang ophiolite; 19: imbricate thrust units with blueschist. Tethys and Greater Himalaya: 20: Paleozoic-Eocene sedimentary rocks; 21: Miocene leucogranite; 22: Permian Panjal Traps; 23: Greater Himalayan neometamorphic rocks; 24: Paleozoic intrusives; 25: mainly Paleoproterozoic orthogneiss; 26: Besham metaigneous rocks. Lesser Himalaya: 27: Paleozoic-Eocene strata; 28: upper nappe (mostly Mesoproterozoic metasedimentary rocks); 29: lower nappe (mostly Neoproterozoic and Paleozoic metasedimentary rocks); 30: Salt Range (Neoproterozoic to Eocene Indian margin strata). Sub-Himalaya: 31: Muree and Subathu Formations (Cenozoic); 32: Siwalik Group (Neogene); 33: Peshawar and Srinagar Quaternary intramontane basins. West Pakistan Belt: 34: Sulaiman Range.

5.2.2 Ladakh and Kohistan Arcs

The Ladakh and Kohistan batholiths expose a complete section of mantle to upper crustal igneous rocks representing the dissected remnants of magmatic arcs fed by northern subduction of Neotethyan lithosphere during the Cretaceous to earliest Paleogene. The arcs are delimited by the Shyok ophiolitic suture in the north, generally ascribed to Upper Cretaceous (pre-Campanian) collision with the Karakorum block (Treloar et al., 1989; Gaetani et al., 1993; Robertson and Collins, 2002; Rehman et al., 2011; Borneman et al., 2015), and the Indus ophiolitic suture in the south, closed when India collided with Asia during the Paleocene (Garzanti et al., 1987; Najman et al., 2017).

The Kohistan arc is composed of six main units from bottom to top (south to north): 1) Jijal ultramafic-mafic complex yielding garnet, amphibole, clinopyroxene, and minor olivine, orthopyroxene, spinel and zoisite; 2) Kamila amphibolite; 3) Chilas ultramafic-mafic complex, containing orthopyroxene and clinopyroxene with minor olivine, magnetite, ilmenite, hornblende, and spinel; 4) Kohistan batholith, yielding mainly hornblende and locally clinopyroxene; 5) Jurassic-Cretaceous metavolcanic and metasedimentary rocks of the Jaglot and Chalt Groups, and the Aptian-Albian volcano-sedimentary Yasin Group (Jan and Howie, 1981; Jagoutz et al., 2007; Dhuime et al., 2009).

The Ladakh batholith consists of a suite of Cretaceous to Paleogene mafic to felsic rocks (olivine norite to granite) yielding hornblende, augite, titanite, apatite, epidote, and zircon (Honegger et al. 1982; Weinberg and Dunlap, 2000). The batholith is non conformably overlain by Upper Cretaceous to Paleogene strata of the Indus Group (Garzanti and van Haver, 1988; Henderson et al., 2010). Rocks exposed along the Indus suture also include Lower Cretaceous carbonates, ophiolitic mélange, and blueschists (Anczkiewicz et al., 1998; Mahéo et al., 2006).

5.2.3 Himalayan Belt and Nanga Parbat Massif

The Himalayan Range formed as a consequence of continental collision between the Indian passive margin and the Asian active margin at ~ 60 Ma (DeCelles et al., 2014; Hu et al., 2016). The orogenic belt consists of a series of southward propagating thrust sheets, which resulted in crustal thickening starting from the Eocene (Ratschbacher et al., 1994; Searle et al., 1997). The Neoproterozoic to Eocene Tethys Himalayan succession consists of siliciclastic and carbonate rocks originally deposited onto the northern continental margin of India (Gaetani and Garzanti, 1991; Sciunnach and Garzanti, 2012). The Greater Himalaya, including slate intruded by Ordovician granitoids and sillimanite-bearing metasedimentary rocks at the top, represents the axial crystalline backbone of the range (Pognante and Lombardo, 1989; DiPietro and Pogue, 2004). It is delimited to the north by the South Tibetan Detachment system lined with Miocene tourmaline-bearing leucogranite intrusions (Herren, 1987) and by the Main Central Thrust to the south (Steck, 2003). Lesser Himalayan and Sub-Himalayan rocks exposed farther south include, respectively, Paleoproterozoic basement and Mesoproterozoic to Cenozoic cover strata displaying southward decreasing metamorphic grade (Greco and Spencer, 1993; Vannay et al., 2004) and orogen-derived Cenozoic molasse (Bossart and Ottiger, 1989; Najman and Garzanti, 2000; White et al., 2002). These rocks are drained by Punjab tributaries and shed detritus that contributes to Indus River load only downstream of the Thal Desert.

Only the Indus River cuts across the western Himalayan syntaxis, where the N/S-elongated crustal-scale Nanga Parbat antiform exposing Precambrian Indian gneissic basement overprinted by Himalayan metamorphism is bounded to the north by the Karakorum belt and flanked to the west and east by the Kohistan and Ladakh arcs. In the Nanga Parbat massif, sillimanite-bearing gneisses are structurally overlain by kyanite-bearing schists (Zeitler et al., 1993; Chamberlain et al., 1995). Leucogranite intrusions yielding tourmaline, apatite, zircon, monazite, and garnet (Zeitler et al., 1991) are as young as 1.4 Ma. Cooling ages of 5 Ma or even 1 Ma in the core of the dome (Schneider et al., 2001) testify to ultra-rapid exhumation and very fast fluvial incision (Burbank et al., 1996a; Shroder and Bishop, 2000), with high denudation rates of 3-5 mm a^{-1} (Whittington, 1996; Moore and England, 2001; Zeitler et al., 2001). Upstream of the entry point in the foreland basin, the Indus River traverses the Potwar Plateau, where Himalayan-derived molassic Cenozoic rocks are widely exposed (Johnson et al., 1985; Najman et al., 2003), and finally cuts across the Salt Range, including Paleozoic to Paleogene strata detached over uppermost Neoproterozoic/Cambrian salt and uplifted during the latest Miocene (Burbank et al., 1996b).

5.2.4 Thal Desert

The Thal Desert, a triangular region located in central northern Pakistan between ~ 30° and 32°30' N and between ~ 71° and 72° E (Fig. 5.2), is characterised by arid to semi-arid subtropical climate. This desert occupies the Sind-Sagar or Thal Doab (*doab* = land between two rivers, from *do* = two and *ab* = water in Urdu and Farsi), the region extending between the course of the Indus River in the west and the Punjab in the east, the fertile region crossed by the Himalayan rivers Jhelum, Chenab, Ravi, Beas, and Sutlej (*punjab* = five waters, from *panj* = five and *ab* = water).

The Thal Desert is delimited by the Salt Range foothills to the north, whereas the Indus floodplain is bounded by the Sulaiman Range to the west (Fig. 5.1). The desert area is covered by low sand dunes (1 - 2 m in height) or rolling sand plains alternating with narrow valleys of cultivable land, and is underlain by Quaternary fluvial and eolian deposits more than 350 m-thick in the south and even thicker in the central part of the desert (Nickson et al., 2005). The underlying alluvium mostly consists of laterally continuous fine to coarse sand, with minor gravel and isolated mud lenses. The coarsest deposits occur in the north close to the Salt Range, but otherwise the distribution of grain size is irregular, reflecting deposition by the constantly shifting paleo-Indus River.

5.3 Methods

5.3.1 Sampling

The sample set considered in this study includes four eolian-dune sand samples collected in February 2001 from the Thal Desert, along with 11 sand samples collected during 2001 and 2011 from active river bars in 11 tributaries draining each a different geological domain in the upper Indus River catchment ("first-order sampling scale" of Ingersoll, 1990). These samples were accurately selected from a much larger sample set, described elsewhere (Garzanti et al., 2005; Munack et al., 2014; Garzanti, 2019a), as the best suited to represent end-member sources of detritus from the Karakorum belt (upper Hushe, upper Braldu, upper Hunza, and Hispar samples), the Ladakh (Stagmo and Domkar samples) and Kohistan arcs (Kandia and Swat samples), the Nanga Parbat massif (Astor sample), and the Himalayan belt (Zanskar and Nandihar samples). The Thal dune samples are upper very fine to lower fine and well to moderately sorted sand (3.05 - 2.67 ϕ, 0.43 - 0.84 σ_ϕ); fluvial samples are upper very fine to lower medium and moderately-well to moderately sorted sand (3.20 - 1.51 ϕ, 0.63 - 0.97 σ_ϕ) (Appendix Table B1).

5.3.2 Heavy mineral analyses

For each of the 15 selected samples, heavy minerals were separated with sodium polytungstate (density ~ 2.90 g cm^{-3}) from a split aliquot of the 63-250 μm or 32-500 μm fraction obtained by sieving, recovered by partial freezing with liquid nitrogen, and mounted on a glass slide. A polished thin section was also prepared, and mineralogical composition was determined by both counting under the microscope of ≥ 200 transparent heavy minerals on the glass slide and by semi-automated analysis of the polished thin section with a Raman spectrometer (Andò and Garzanti, 2014).

Heavy-mineral concentration, calculated as the volume percentage of total (HMC) and transparent (tHMC) heavy minerals in the bulk sample, ranges from poor (tHMC < 1), moderately poor (1 ≤ tHMC < 2) and moderately rich (2 ≤ tHMC < 5), to rich (5 ≤ tHMC < 10), very rich (10 ≤ tHMC < 20) and extremely rich (20 ≤ tHMC < 50) (Garzanti and Andò, 2007b, 2019).

5.3.3 Sources of bias

As a consequence of choosing a 2ϕ to 4ϕ-wide size window for analysis in order to reduce technical problems during separation, mounting on the glass slide, and identification under the microscope caused by detrital grains with great size differences, heavy minerals occurring in the finest tail of the size distribution (3 ± 2% of each bulk sample) and in the coarse tail (32 ± 22% of each bulk sample) were discarded. The sediment fraction considered for analysis ranged between 58 ± 21% for fluvial samples to 85 ± 9% for the better sorted Thal eolian-dune samples. The analytical bias thus introduced can be considered as minor, because the fine tail was almost entirely included whereas the coarse tail is strongly depleted in heavy minerals as the concentration of denser grains drops rapidly in the coarser classes of sediments deposited by tractive currents (Rubey, 1933; Garzanti et al., 2008).

Another potential source of bias is represented by hydraulic-sorting processes, which may concentrate different minerals in distinct depositional sub-environments based on their size, density, and shape (Briggs et al., 1962; Komar, 2007). An efficient way to test for heavy-mineral enrichment or depletion in sediment samples is provided by chemical analyses, which readily reveal anomalous concentrations of chemical elements such as rare earth elements (REE) or zirconium preferentially hosted in ultradense minerals (Garzanti and Andò, 2019). Among the four Thal dune samples, heavy-mineral enrichment is apparent for the Muzaffarghar sample S1470 containing much more Zr than the Munda sample S1474 (524 *vs.* 106 ppm), whereas the other two samples S1462 and S1463 have Zr concentrations very close to the Upper Continental Crust standard (UCC; 195 - 213 *versus* 190 - 193 ppm in the UCC; Taylor and McLennan, 1995; Rudnick and Gao, 2003) (Appendix Table B1). Among river sand, only the Hispar sample shows high concentration of Zr, Th, and REE relative to all other samples (Zr 395 *vs.* 110 - 186 ppm; Th 52 *vs.* 3 - 14 ppm; La 117 *vs.* 12 - 55 ppm and Y 41 *vs.* 12 - 27 ppm), suggesting hydraulic enrichment in heavy minerals. The heavy-mineral spectrum of samples systematically showing anomalous concentrations in these elements is expected to be enriched in denser heavy minerals such as garnet relative to low-density heavy minerals such as amphibole.

5.3.4 Microchemical analyses

The polished thin sections, in a photographic image of which all grains were properly identified and numbered, were carbon-coated and analysed by Energy Dispersive X-Ray Spectroscopy (EDS) under the scanning electron microscope (SEM) to obtain quantitative chemical information on the four most common detrital minerals in orogenic sediments (i.e., amphibole, garnet, epidote, and pyroxene). Microchemical analyses were carried out at the Department of Earth and Environmental Sciences, University of Milano-Bicocca (Milano, Italy), using a TESCAN TS5136XM with an electronic microprobe EDAX GENESIS 4000 XMS Imaging 60 SEM, voltage 20 KeV, detection time 20 s, spot size 250 nm and absorption current 190 ± 1 pA measured in Faraday cup, medium heating, take off angle 45°, working distance 23 mm.

In each thin section, we counted ~ 100 grains for each mineral group (or all of those present in case we did not find enough). In the four Thal Desert samples, 400 amphibole, 395 epidote, 317 pyroxene, and 280 garnet grains were analyzed, thus allowing identification even of small detrital populations (Vermeesch, 2004). Overall, we analyzed 1504 amphibole, 1129 epidote, 861 pyroxene, and 755 garnet grains in the 15 selected samples.

Information on sample locations, the result of heavy-mineral analyses, and the complete geochemical dataset including the percentages of each mineral variety in each sample are provided in Appendices Tables B1 to B10. Statistical techniques used to illustrate our dataset include multidimensional scaling, which produces a map of points in which samples with similar mineralogical signature cluster closely together and dissimilar samples plot far apart (Vermeesch and Garzanti, 2015) and the biplot (Gabriel, 1971), which allows us not only to discriminate among multivariate observations (data points) but also to visualize the mutual relationships among an even large number of variables (rays). The length of each ray is proportional to the variance of the corresponding parameter in the dataset, whereas if the angle between two rays is close to 0°, 90°, or 180°, then the corresponding elements are directly correlated, uncorrelated or inversely correlated, respectively.

5.3.5 Amphibole chemistry

The general chemical formula of the amphibole supergroup is $AB_2C_5T_8O_{22}W_2$, where

A, B, and C are cations and W anions (A = □, Na, K, Ca, Pb, Li; B = Na, Ca, Mn^{2+}, Fe^{2+}, Mg, Li; C = Mg, Fe^{2+}, Mn^{2+}, Al, Fe^{3+}, Mn^{3+}, Ti^{4+}, Li; T = Si, Al, Ti^{4+}, Be; W = (OH), F, Cl, O^{2-} ; Hawthorne et al., 2012; Oberti et al., 2012). Following the recommendation of the International Mineralogical Association, amphibole minerals are divided into two groups based on the dominant anions at site W, i.e. $(OH,F,Cl)^{-}$ *versus* oxo-amphiboles. The $(OH,F,Cl)^{-}$ group is further subdivided into eight subgroups based on B cations. An Excel spreadsheet developed by Locock (2014) was used to calculate the chemical formula and classify detrital amphiboles. The $Fe^{3+}/\Sigma Fe$ and $Mn^{3+}/\Sigma Mn$ ratios were calculated based on charge balance by normalizing the formula to one or more sets of cation sums because the valence state of Fe and Mn was not measured. All amphibole grains were considered to be monoclinic because only a few (< 2%) orthorhombic amphibole grains were detected with Raman spectroscopy. For amphibole with W = 2 (OH, F, Cl), sufficient OH content was calculated to reach 2 (OH, F, Cl) per formula unit because H_2O+ was not measured and OH could not be estimated (Locock, 2014).

5.3.6 Garnet chemistry

The general formula of garnet contains 8 cations and 12 anions: $X_3Y_2Z_3\Phi_{12}$, where X = Na, Mg, Ca, Mn^{2+}, Fe^{2+}, Y; Y = Mg, Al, Si, Sc, Ti, V, Cr, Mn^{3+}, Fe^{2+}, Fe^{3+}, Zr, Sn; Z = Al, Si, Fe^{3+}. The Excel spreadsheet developed by Locock (2008), which considers 15 different garnet varieties and 14 endmembers, was used to calculate the molar proportion of garnet endmembers from chemical data. The iron was entered as FeO_{tot} in the spreadsheet and the amount of Fe^{2+} and Fe^{3+} were calculated by stoichiometric constraints because the proportion of FeO *versus* Fe_2O_3 was not determined. Mn^{3+} was calculated only for compositions that cannot charge balance with Fe^{3+} alone.

Garnet, common in orogenic sediments derived from metasedimentary rocks, is a particularly valuable provenance tracer because it displays a wide range of major-element compositions and resists diagenetic dissolution better than epidote, amphibole, and pyroxene (Morton and Hallsworth 2007; Andò et al., 2012; Garzanti et al., 2018b). Different types of detrital garnets can be empirically distinguished according to their provenance by the use of the Fe+Mn–Mg–Ca ternary plot (Morton et al., 2004; Mange and Morton, 2007). Type A garnet (high Mg, low Ca) is mainly shed by granulite-facies metasedimentary rocks, charnockites, and intermediate-felsic igneous rocks. Type B garnet (low Mg, variable Ca) is derived from either intermediate-felsic igneous rock (sub-type Bi; X_{Mg} < 20%, X_{Ca} < 10%) or amphibolite-facies metasedimentary rocks (sub-type Bii). Type C garnet (high Mg, high Ca) is preferentially contained in high-grade metabasite (sub-type Ci) or ultramafic rocks such as pyroxenite and peridotite (sub-type Cii; X_{Mg} > 40%, X_{Ca} > 10%), and type D garnet (low Mg, very high Ca) in metasomatic rocks (skarn), very low-grade metabasite, and high-grade calc-silicate rocks.

The different origins of detrital garnet are also highlighted by the use of the Mn–Mg–Ca diagram, based on the observation that Mg^{2+} progressively substitutes for Mn^{2+} and Fe^{2+} in pyralspite garnet with increasing metamorphic temperature, whereas Ca^{2+} increases at increasing pressures (Win et al., 2007)

5.3.7 Epidote chemistry

For the classification of epidote-group minerals we used the *Windows*™ program *WinEpclas* developed by Yavuz and Yildirim (2018) and based on the nomenclature recommended by the Comission on New Minerals and Mineral Names of the International Mineralogical Association. The structural formula of monoclinic epidote-group minerals can be expressed as A1A2M1M2M3 $[T_2O_7][TO_4](O4)(O10)$, where A1 = Ca, Mn^{2+}; A2 = Ca, Sr, Pb, Ce^{3+}, $(REE)^{3+}$; M1 = Mg, Fe^{2+}, Mn^{2+}, Al, Fe^{3+}, V^{3+}, Mn^{3+}, Cr^{3+}; M2 = Al, Fe^{3+}; M3 = Mg, Fe^{2+}, Mn^{2+}, Al, Fe^{3+}, V^{3+}, Mn^{3+}, Cr^{3+}; T = Si; O4 = O^{2-}, F^-; and O10 = OH^-, O^{2-} (Armbruster et al., 2006). The normalization scheme based on the $\Sigma(A+M+T) = 8.0$ determines the mineral species on the basis of the dominant cations at sites A1, A2, M1, M2 and M3, and of anions at sites O4 and O10. Zoisite, the orthorhombic polymorph of clinozoisite, cannot be distinguished chemically from its monoclinic polymorph clinozoisite, and consequently is not considered as a distinct species by *WinEpclas* software.

5.3.8 Pyroxene chemistry

The general formula of orthorhombic or monoclinic pyroxene can be expressed as: ABZ_2O_6, where A = Ca, Fe^{2+}, Li, Mg, Mn^{2+}, Na, Zn; B = Al, Cr^{3+}, Fe^{2+}, Fe^{3+}, Mg, Mn^{2+}, Sc, Ti, V^{3+}; Z = Al, Si. Composition of detrital pyroxene was calculated on the basis of 6 oxygen atoms in the chemical formula, using the software developed by Sturm (2002). The nomenclature follows the rules set in Morimoto et al. (1988). The prefixes "aluminian" or "sodian" are added for clinopyroxene with $Al^{3+} > 0.1$ atoms per formula unit (a.p.f.u.) or $Na^{+} > 0.1$ a.p.f.u., respectively. The prefix "subsilicic" is added if Si^{4+} is < 1.75 a.p.f.u. Most pyroxene grains belong to the Quad chemical group (i.e., plot in the classical pyroxene quadrilateral, part of the Ca-Mg-Fe classification triangle; Morimoto et al., 1988). The J parameter is twice Na a.p.f.u.; the Q parameter is Ca + Mg + Fe^{2+} a.p.f.u..

5.4 Heavy mineral sources

Transparent heavy-mineral suites in all analyzed samples mostly consist (84% on average) of amphibole (47 ± 17%), epidote (17 ± 9%), pyroxene (12 ± 9%), and garnet grains (9 ± 8%).

Heavy-mineral concentration results to be much higher in river sand derived from the Kohistan arc (19-44%) than from the Ladakh arc (5-20%), and higher in river sand derived from the Nanga Parbat massif (6-17%) than from both the Karakorum belt and the Greater Himalaya (3-9%). Heavy mineral concentration is remarkably high in dune sand of the Thal Desert (12-26%; Table 5.1).

Table 5.1 Heavy-mineral assemblages in river sand of the upper Indus catchment (end-member sources) and eolian dunes of the Thal Desert (sediment sink) performed by semi-automated Raman spectroscopy. On average, over 700 transparent heavy minerals were counted per sample (ranging from 275 for S4426 to 1300 for S1748; Appendix Table B2). HMC = heavy mineral concentration; tHMC = transparent heavy mineral concentration; Zrn = zircon; Tur = tourmaline; Rt = rutile; Ttn = titanite; Ap = apatite; Amp = amphibole; Cpx = clinopyroxene; Opx = orthopyroxene; Ol = olivine; Zo = zoisite; Czo = clinozoisite; &Ep = allanite and other epidote-group minerals; Grt = garnet; Cld = chloritoid; St = staurolite; And = andalusite; Ky = kyanite; Sil = sillimanite; &HM = other transparent heavy minerals (monazite, anatase, brookite, prehnite, axinite, gahnite, barite, vesuvianite). Percentages of amphibole, garnet, epidote, and pyroxene on each bulk sample are given in the four last columns to the right.

Sample	River/Dune	Domain	HM	tHM	Zr	Tur	Rt	Tt	A	Am	Cp	Op
S1749	Hushe	Karakorum	4.8	2.5	2	0.2	1	9	6	60	5	0
S1748	Braldu	Karakorum	6.5	4.5	0.9	1	3	8	6	42	11	0
S1437	Hunza	Karakorum	2.9	1.5	0.5	2	9	10	5	45	8	0.2
S1438	Hispar	Karakorum	8.7	6.7	2	1	1	10	3	26	6	0
S4426	Stagmo	Ladakh arc	12.6	12.0	0.4	0.4	0.4	6	0.9	82	6	0
S4430	Domkar	Ladakh arc	9.7	8.1	2	0.3	1	7	1	73	6	0.3
S1439	Kandia	Kohistan arc	44.2	33.4	0	0	0.5	7	0.5	51	4	0
S1440	Swat	Kohistan arc	31.4	27.5	0.2	0	2	1	0.6	49	37	4

S4419	Zanskar	G. Himalaya	4.8	4.6	1	5	2	8	8	21	11	0
S1426	Nandihar	G. Himalaya	4.8	4.0	0.6	8	1	5	3	32	13	2
S1432	Astor	Nanga Parbat	17.9	16.9	0.2	1	2	1	0.3	64	6	0
S1462	Mankera	Thal Desert	21.2	15.3	0	1	1	4	0.3	40	10	1
S1463	Haidarabad	Thal Desert	24.2	18.6	0	0.4	2	6	1	36	11	3
S1470	Muzaffargha	Thal Desert	26.4	17.7	0.3	0.8	2	4	1	35	13	2
S1474	Munda	Thal Desert	12.3	10.0	0.3	1	1	4	1	40	13	2

Sample	Ol	Zo	Czo	&Ep	Grt	Cld	St	And	Ky	Sil	&HM	Tot
S1749	0.5	0	1	11	4	0	0	0	0	0.2	0.6	100.0
S1748	0.5	0.1	5	11	7	1	0.4	0.8	0	0.4	1	100.0
S1437	0	0.2	6	13	1	0	0.2	0.3	0	0	0.5	100.0
S1438	0.2	0	9	15	26	0.2	0.5	0	0	0	0.2	100.0
S4426	0	0	0	3	0	0	0	0	0	0	0	100.0
S4430	0	0	0.5	7	1	0	0	0	0	0	0.8	100.0
S1439	0.2	2	22	10	2	0	0	0	0	0	0	100.0
S1440	0	0	2	4	0.6	0	0	0	0	0	0	100.0
S4419	0.2	0	0.3	11	21	0	0.3	0	0.5	9	1	100.0
S1426	0	0.6	1	2	22	0	2	0	8	0.6	0.4	100.0
S1432	0.2	0.6	5	9	9	0	0.2	0.2	0.8	0.2	0.2	100.0
S1462	0.5	0.5	15	9	14	0.3	0.8	0	1	0.2	0.7	100.0
S1463	0.4	0.9	11	13	14	0	0.6	0.2	0.4	1	0	100.0
S1470	1	0.7	14	11	11	0	0.5	0	0.8	0.5	0.5	100.0
S1474	0.3	0.3	11	12	10	0	0.6	0	1	0.3	0.1	100.0

5.4.1 Karakorum

The studied river sand derived from the Karakorum contain moderately poor to rich transparent-heavy-mineral suites dominated by amphibole, with subordinate epidote, clinopyroxene, titanite, and rare clinozoisite, apatite and garnet. The Hispar River, draining mid-crustal rocks rapidly exhumed in metamorphic domes of the Southern Karakorum Belt, carries the richest transparent-heavy-mineral suite containing subequal amounts of garnet and amphibole (Table 5.1).

Amphibole grains in sand of the upper Hushe River, which largely drains granitoid rocks, are mainly pargasite (52%), hastingsite (26%), and hornblende (Fig. 5.3A). Garnet grains mainly plot in the Bi field of the Fe+Mn–Mg–Ca plot and in the low P/T field of the Ca–Mg–Mn plot (Fig. 5.4A), reflecting provenance from intermediate-felsic igneous rocks. Epidote-group minerals include REE-rich allanite (11% on average) and detrital pyroxene is mainly diopside with subordinate augite with low wollastonite (Wo) value and negligible orthopyroxene (Fig. 5.5A and 5.6A).

Sand of the upper Braldu River draining the axial part of the Karakorum belt contains mainly hornblende prevailing over pargasite and actinolite, and mainly Bi with subordinate Bii garnet plotting in the low and intermediate P/T fields (Fig. 5.4A). Epidote dominates over allanite and clinozoisite. Pyroxene is mostly diopside, largely derived from upper-amphibolite facies metasedimentary rocks (99%; Fig. 5.6A). Similar mineralogical signatures characterize upper Hunza and Hispar sands, mainly derived from the Northern Karakorum sedimentary domain and from the Southern Karakorum belt, respectively. Hispar sand, however, lacks allanite (Fig. 5.5A), whereas upper Hunza sand contains only a few garnet grains, dominantly of type D (Fig. 5.4A), and some ferroaugite grains (Fig. 5.6A).

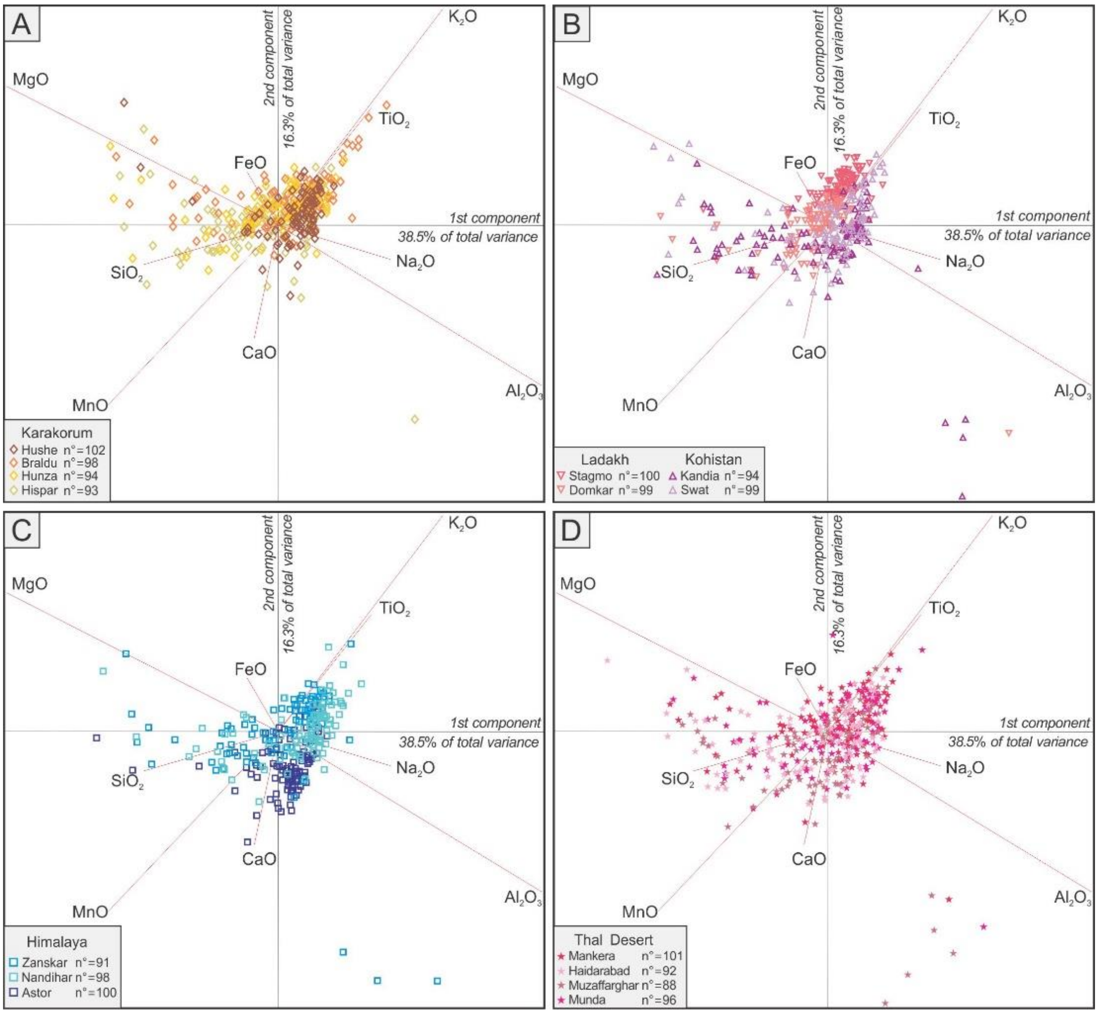

Figure 5.3 Chemical composition of detrital amphibole in river and eolian sand of northern Pakistan. All data were plotted in one single biplot, and next separated into four panels to allow comparison between the end-member sources (A = Karakprum, B = Ladakh and Kohistan arcs, C = Himalaya) and the sediment sink (D = Thal Desert).

5.4.2 Ladakh and Kohistan Arcs

Stream sand derived from the Ladakh arc contain rich to very rich, amphibole-dominated transparent heavy-mineral suites including minor titanite, clinopyroxene, epidote, and only rare garnet (Fig. 5.4B). Amphibole grains are mostly hornblende (~ 81% on average; Fig. 5.3B). Epidote is dominant (allanite is rare in Stagmo sand and absent in Domkar sand; Fig. 5.5B). Detrital pyroxene is mainly diopside and augite (Fig. 5.6B); Domkar sand includes a few orthopyroxene grains.

The very rich to extremely rich transparent heavy-mineral suites shed from the Kohistan arc are more varied (Table 5.1). Kandia sand yields mainly pargasite, hornblende and actinolite among the amphibole group, abundant epidote-group minerals (mostly clinozoisite; Fig. 5.5B), mostly high-Ca garnet of type D (Fig. 5.4B), and only a few diopside and orthopyroxene grains (Fig. 5.6B). In Swat sand, common detrital amphibole is mainly hornblende (42%), with minor pargasite and hastingsite, and rare actinolite and tschermakite. Clinopyroxene (diopside, minor augite) is abundant and orthopyroxene minor (Fig. 5.6B). Epidote-group minerals are represented by epidote and clinozoisite (Fig. 5.5B). The rare garnet grains are high in Ca and Mg (Fig. 5.4B).

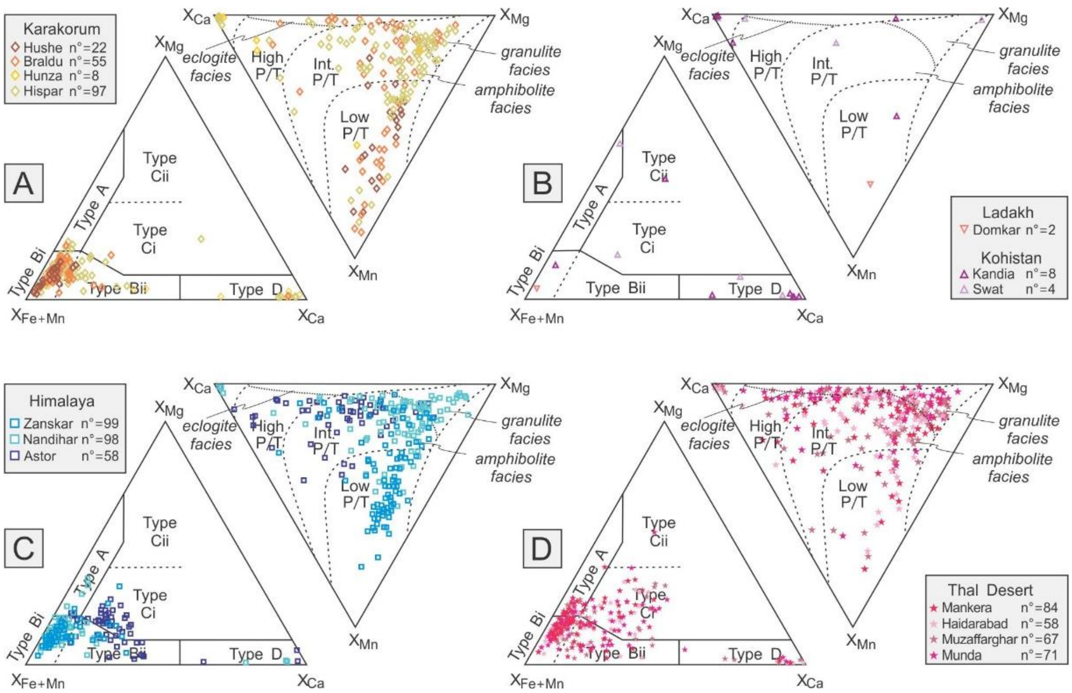

Figure 5.4 Chemical composition of detrital garnet in river sand of northern Pakistan (A = Karakorum, B = Ladakh and Kohistan arcs, C = Himalaya) and in the (D) Thal Desert (Fe+Mn–Mg–Ca plot after Mange & Morton, 2007; Ca–Mg–Mn plot after Win et al., 2007). X_{Fe}, X_{Mg}, X_{Ca}, X_{Mn} = molecular proportions of Fe^{2+}, Mg, Ca, and Mn.

5.4.3 Greater Himalaya

Rivers draining amphibolite-facies metamorphic rocks of the Greater Himalaya carry moderately rich transparent heavy-mineral suites including amphibole, garnet, clinopyroxene and epidote, with minor titanite, tourmaline, apatite, sillimanite and kyanite (Table 5.1).

The Zanskar River, sourced from the topmost part of the Greater Himalaya and cutting across the Tethys Himalaya, carries pargasite and hornblende with minor hastingsite, mainly Bi garnet with a few Bii and Ci grains (Fig. 5.4C), and dominant epidote with minor allanite (Fig. 5.5C). Diopside accounts for the vast majority of pyroxene grains (Fig. 5.6C).

Similar amphibole varieties characterize Nandihar river sand, which contains mainly Bi garnet with minor A, Bii, and D grains (Fig. 5.4C), epidote-clinozoisite but no allanite (Fig. 5.5C), and a higher proportion of augite (30%) and orthopyroxene (25%) (Fig. 5.6C).

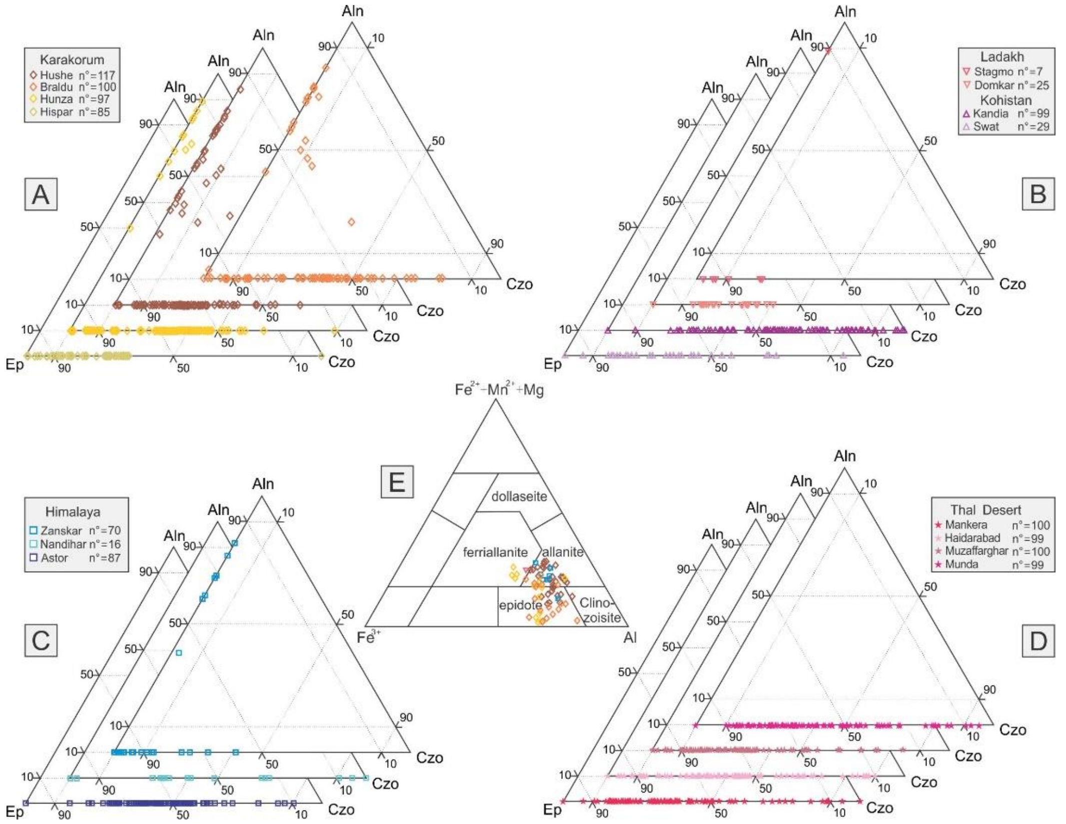

Figure 5.5 Chemical composition of detrital epidote-group minerals in river sand of northern Pakistan (A = Karakorum, B = Ladakh and Kohistan arcs, C = Himalaya) and in the (D) Thal Desert. A to D) The proportion of clinozoisite, allanite, and epidote were calculated as Al

(a.p.f.u.) – 2, if Al (a.p.f.u.) > 2 (otherwise the proportion was taken as zero), as REE (a.p.f.u.), and as 1 - allanite - clinozoisite, respectively (Graser and Markl, 2007). Aln: allanite; Ep: epidote; Czo: clinozoisite. E) Classification of REE-bearing epidote grains after Kartashov (2014).

5.4.4 Nanga Parbat

The very rich transparent-heavy-mineral suite of Astor River sand draining the Nanga Parbat massif is dominated by amphibole with subordinate epidote-group minerals, garnet, and clinopyroxene (Table 5.1). Detrital amphibole is mainly hornblende with common tschermakite (14%) and minor pargasite (Fig. 5.3C). Garnet grains are mainly Ci (57%) and minor Bii types (Fig. 5.4C). Epidote and clinozoisite occur whereas allanite is lacking (Fig. 5.5C), and detrital pyroxene is dominantly diopside with rare augite and orthopyroxene (Fig. 5.6C).

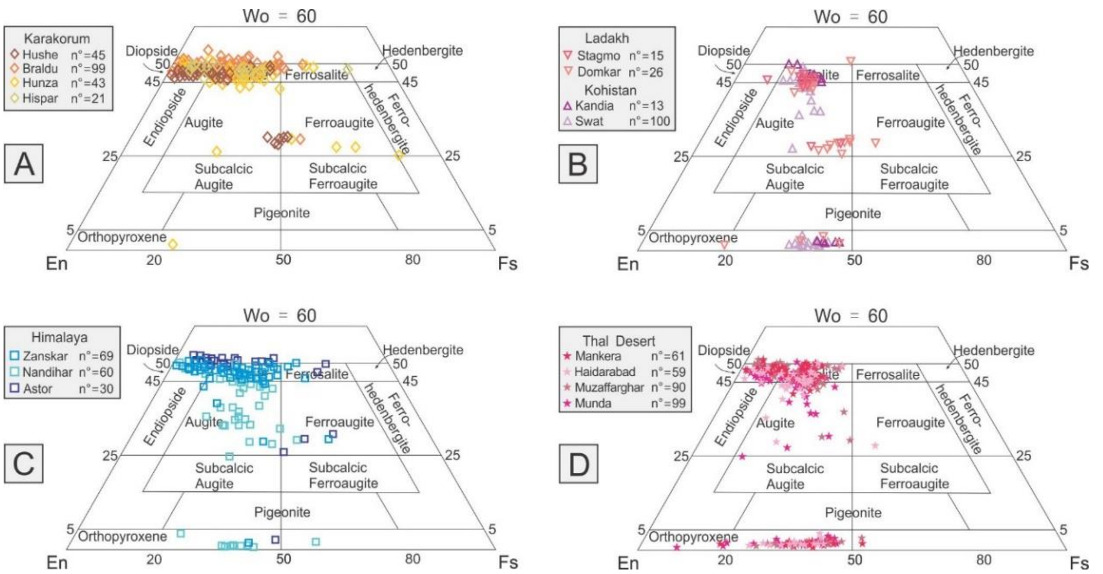

Figure 5.6 Chemical composition of detrital pyroxene in river sand of northern Pakistan (A = Karakorum, B = Ladakh and Kohistan arcs, C = Himalaya) and in the (D) Thal Desert. Pyroxene quadrilateral from Poldervaart and Hess (1951) and Morimoto et al. (1988). Wo: Wollastonite ($Ca_2Si_2O_6$); En: enstatite ($Mg_2Si_2O_6$); Fs: ferrosilite ($Fe_2Si_2O_6$).

5.5 Heavy-mineral provenance tracers in Thal Desert sand

Transparent-heavy-mineral suites of Thal Desert sand reflect the mineralogy of their diverse magmatic and metamorphic sources. As each source-rock domain contributes detrital species to the sediment load of the upper Indus River in different proportions, depending not only on exposure area and erosion rate but also on the different mineral concentrations (fertilities), every detrital mineral is expected to carry a distinct provenance signal (Fig. 5.7). A source-rock domain may contribute one mineral (e.g., amphibole) in large proportion, but another mineral (e.g., garnet) in negligible proportion; as a consequence, that domain will be over-represented in the detrital-amphibole spectrum but hardly seen in the detrital-garnet spectrum.

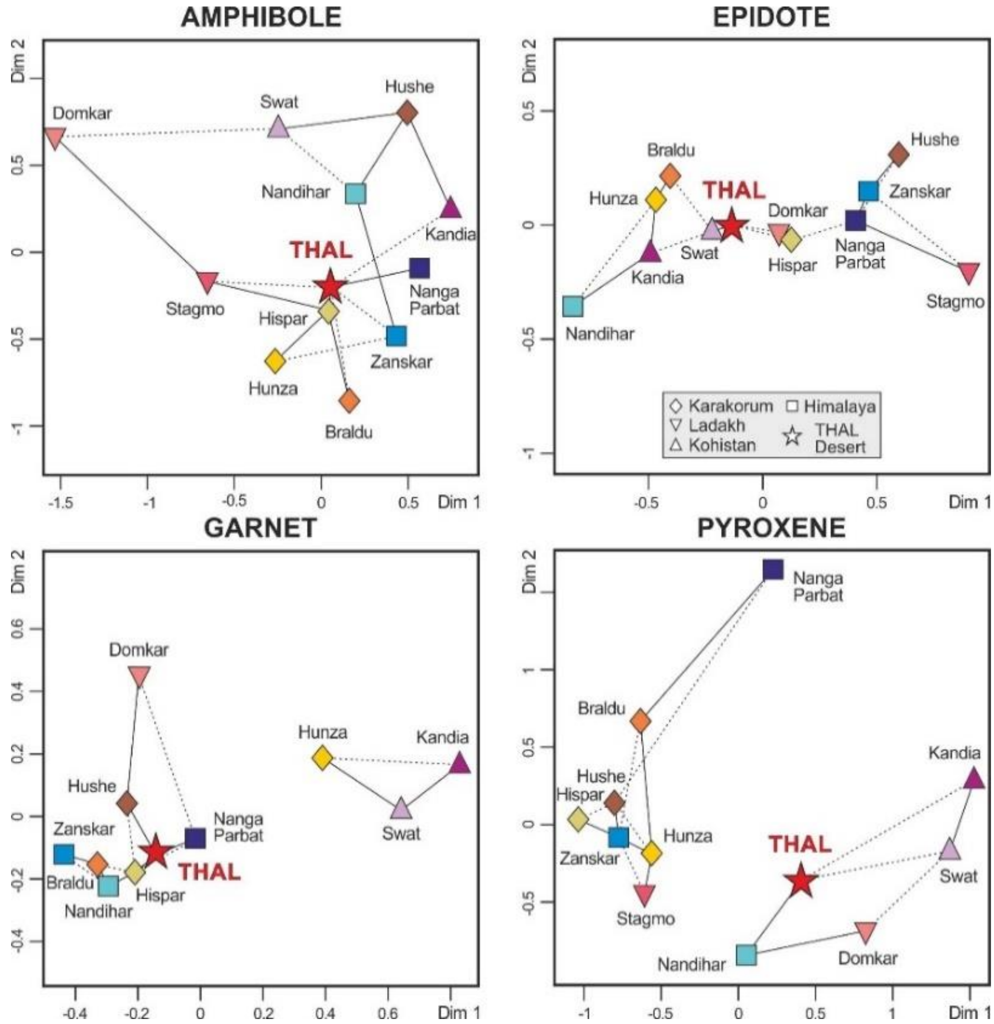

Figure 5.7 Multidimensional scaling maps based on the chemical signatures of the four studied mineral groups in river sand of northern Pakistan and in the Thal Desert (Appendices Tables B7 to B10). The four Thal dune samples are considered as subsamples of the same unitary population. Solid and dashed lines link closest and second-closest neighbors, respectively. The higher "stress" values (poorer fit) obtained for the amphibole (11.2%) and pyroxene maps (8.9%) than for the garnet (2.4%) and epidote maps (0.8%) largely reflect the higher number of varieties identified for amphibole (32) and pyroxene (39) than for epidote and garnet (6 each). The four maps – plotted using the provenance package of Vermeesch et al. (2016) – differ because different minerals are contained in markedly different proportions (fertilities) in different source-rock domains. Similarities among mineralogical spectra indicate the

Kohistan arc as the main supplier of epidote and pyroxene, whereas amphibole and garnet were largely derived also from the Karakorum (Southern Karakorum gneiss domes drained by the Hispar River) and Himalaya (Nanga Parbat massif). The shape and colour of sample symbols are same with those of Figure 5.3-5.6.

5.5.1 The Thal Desert as a Quaternary sediment sink

The very rich transparent-heavy-mineral suite of Thal Desert sand (tHMC 15.4 ± 3.9) mainly consists of amphibole, with common epidote, clinozoisite, clinopyroxene, and garnet. Detrital amphibole includes mainly hornblende, subordinate pargasite, actinolite (11% on average), hastingsite, and minor tschermakite (up to 5%; Fig. 5.3D). Detrital garnet mainly consists of Bi grains with minor Ci (23%), Bii (18%), A (13%), and a few D grains (Fig. 5.4D). Epidote-group minerals are mainly clinozoisite (54% on average) and epidote (Fig. 5.5D). Detrital pyroxene is mainly diopside with common orthopyroxene (32% on average) and minor augite (Fig. 5.6D).

The four studied dune samples are compositionally homogeneous (Table 5.1) and can thus be considered as subsamples of the same unitary population. Minor differences, however, are observed for instance between the adjacent Mankera and Haidarabad samples (Fig. 5.1). Sample S1462 yielded more hornblende and more Bii than Ci garnets (20% *vs.* 18%), whereas sample S1463 yielded more hastingsite (27%), less Bii than Ci garnets (12% *vs.* 26%), and a lower diopside/augite ratio (Fig. 5.8 and 5.9).

5.5.2 Heavy mineral concentration and provenance estimates

A fundamental parameter in provenance analysis is represented by heavy-mineral concentration (HMC; Garzanti and Andò, 2007b, 2019), which depends originally on the mineralogy and on the average density of parent rocks. The denser a rock is, the greater amount of dense minerals it contains and therefore can shed. Heavy-mineral concentration in sediments, however, can be modified even by an order of magnitude or more by hydraulic sorting during erosion, transport and sedimentation (Garzanti et al., 2009), or by chemical processes including weathering in soils and intrastratal dissolution during burial diagenesis (Garzanti et al., 2013b, 2018). Only in the absence of such environmental and diagenetic bias can terrigenous detritus be considered as produced purely by physical comminution and the mineralogy of daughter sand held to faithfully reflect the mineralogy of parent rocks. Under this strict assumption, the concentration (fertility) of each mineral can be determined for any specific source by the mineralogical analysis of daughter sand (Malusà et al., 2016).

Our mineralogical dataset, integrated by data from Garzanti et al. (2005) and Munack et al. (2014), indicates that erosion in the diverse tectonic domains of the upper Indus catchment generate different amounts of heavy minerals. This depends principally on arc *versus* continental protoliths and crustal level exposed to erosion in each domain, because continental crust is more felsic and therefore less dense than arc crust, and because the Earth's crust is markedly stratified by density (Garzanti et al., 2006).

The very high transparent-heavy-mineral concentration in all of our four Thal dune-sand samples, which are not systematically enriched in densest minerals by selective-entrainment effects (Appendix Table B1), points by itself to major heavy-mineral supply especially from dense mafic rocks exposed in deep tectonostratigraphic levels of the Kohistan arc and minor heavy-mineral supply from either the Karakorum or the Greater Himalaya. Similarity analysis (Garzanti et al., 2011b) indicates that heavy-mineral suites resembling more closely those of Thal Desert dunes are those of Braldu and Hispar sand derived from the Central-Southern Karakorum, whereas the least similar are those of stream sand derived from the Ladakh arc. Forward-mixing calculations based on heavy-mineral data shown in Table 5.1 (mathematical method illustrated in Weltje, 1997 and Garzanti et al., 2012) confirm the Kohistan arc and the Central-Southern Karakorum as major sources of sediment for the Thal dunes.

5.5.3 The amphibole signal

The composite amphibole population of Thal Desert sand includes hornblende as well as other species identified in sand carried by diverse mountain tributaries of the Indus River, pointing to mixing from several sources (Fig. 5.8). The relatively high amount of actinolite suggests contribution from Karakorum and/or Kohistan, and the presence of tschermakite indicates significant supply from Nanga Parbat.

The massive appearance of blue-green hornblende in Upper Miocene foreland-basin strata of northern Pakistan was used as an indicator of rapid exhumation of the Kohistan arc (Cerveny et al., 1989). Geochemical data from Lee et al. (2003) confirm the Kohistan arc as a major source of amphibole, whereas the Nanga Parbat massif together with the Himalayan belt and the Ladakh arc in the uppermost catchment were held to be minor contributors. Major supply from the Kohistan arc was principally ascribed to high fertility, whereas the Southern Karakorum Belt was identified as the dominant source of bulk sediment also based on Nd isotope fingerprints (Clift et al., 2002).

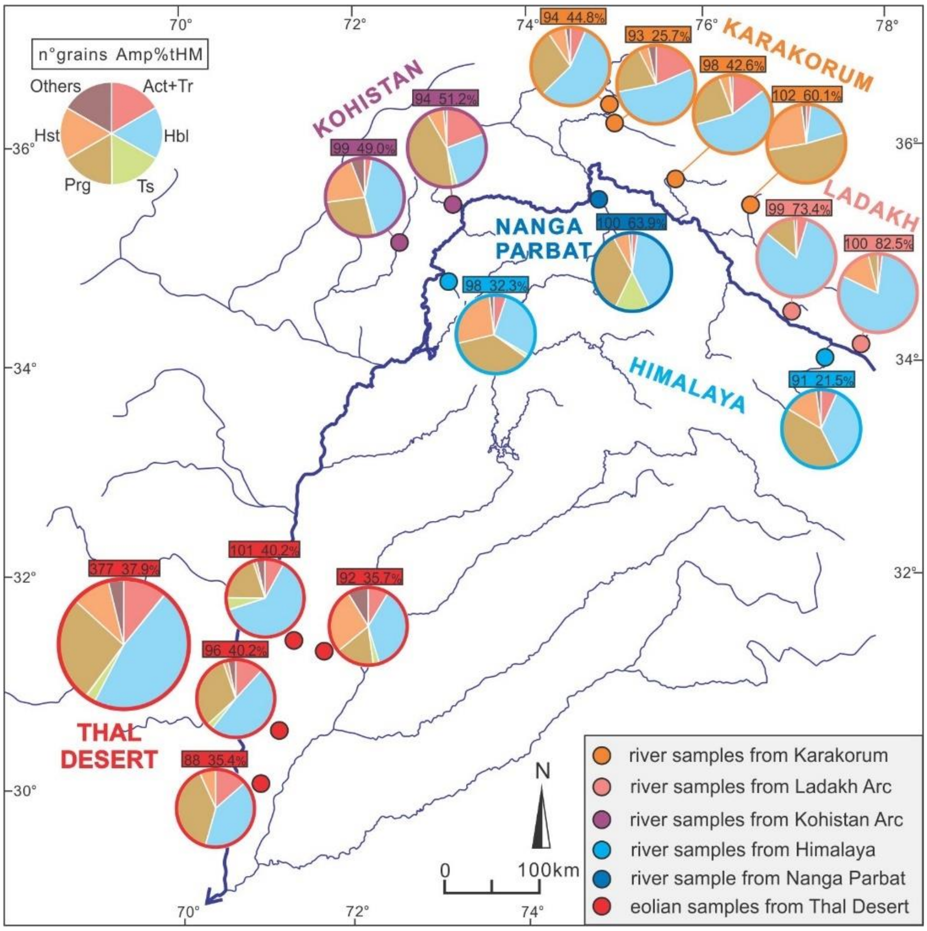

Figure 5.8 Calculated proportions of different varieties of detrital amphibole found in river and eolian sand of northern Pakistan. Act: actinolite; Hbl: hornblende; Hst: hastingsite; Prg: pargasite; Tr: tremolite; Ts: tschermakite.

5.5.4 The garnet signal

As the studied rivers draining the Ladakh and Kohistan arcs carry little garnet, most of which are Ca-rich type-D grains, the arcs cannot be considered as significant sources for garnet (Fig. 5.9). However, Thal Desert dunes contain common high-Mg Ci and A garnet grains, which may have been derived not only from Nanga Parbat and the Greater Himalaya, respectively, but also from granulite-facies metagabbros and metasedimentary rocks exposed in the southern part of the Kohistan arc drained by the Indus River. These high-grade rocks of the lower arc crust may in fact contain up to 20 - 30% garnet (Yamamoto, 1993; Jagoutz and Schmidt, 2012). High-Mn garnets plotting in the low P/T field are sporadic in Thal Desert dunes, but common in all river sand derived from the Karakorum belt and the Greater Himalaya (Fig. 5.4), which argues against dominant garnet contribution from these sources.

Geochemical data from Alizai et al. (2016) indicate that garnet in Kabul sand has intermediate signatures between those of the Karakorum belt and the Kohistan arc, and that Punjab rivers draining the Himalayan belt carry mainly Bi and Bii garnets with minor Ci grains (Fig. 5.9). Type D garnet occurs in all geological domains drained by the Indus River upstream of the Thal Desert but not in Punjab tributaries (Fig. 5.9), which do not contribute significant amounts of sediment to the Thal Desert. Mg-rich garnet derived from the Kohistan arc and subordinately from the Karakorum belt, characteristic of Indus sand, are still the mark of the Thar Desert dune field in southern Pakistan, chiefly representing wind-reworked alluvial fan of the Indus River (Alizai et al., 2016).

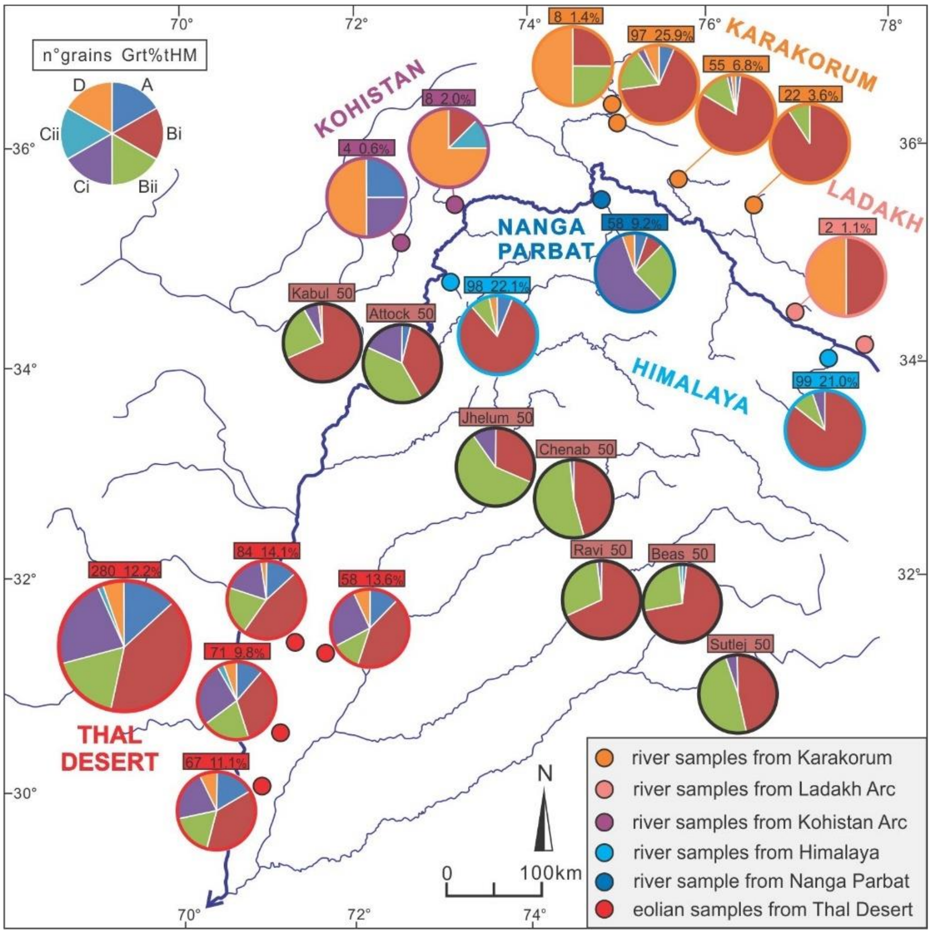

Figure 5.9 Calculated proportions of different varieties of detrital garnet (as defined in Mange & Morton, 2007) found in river and eolian sand of northern Pakistan. Data for Kabul, Indus, Jhelum, Chenab, Ravi, Beas, and Sutlej sand, circled in black, are from Alizai et al. (2016). Garnet types are explained in the text (section 5.3.6).

5.5.5 The epidote signal

Although epidote has been generally used as a provenance tracer based on isotopic fingerprints (Keane and Morrison, 1997; Spiegel et al., 2002), major element geochemistry also provides critical information. Most important, allanite grains were not detected in all four Thal sand samples, which precludes significant contribution from the Northern and Central Karakorum drained by the upper Hunza, upper Braldu, and upper Hushe rivers, and by the upper part of the Greater Himalaya drained by the Zanskar River (Fig. 5.10). The abundance of clinozoisite favours instead major contribution from the Kohistan arc and possibly from the Southern Karakorum, drained by the Hispar which is the only Karakorum river that does not carry allanite. Subordinate supply from the Nanga Parbat massif, mainly shedding epidote, and from the Greater Himalaya in Pakistan, dominantly shedding clinozoisite, cannot be ruled out. Although zoisite cannot be identified from geochemical data by *WinEpclas* software (Yavuz and Yildirim, 2018), Raman spectroscopy revealed its abundance in both Thal Desert and Kandia River sand (Table 5.1), confirming the Kohistan arc as a major source of detrital epidote for Thal dunes.

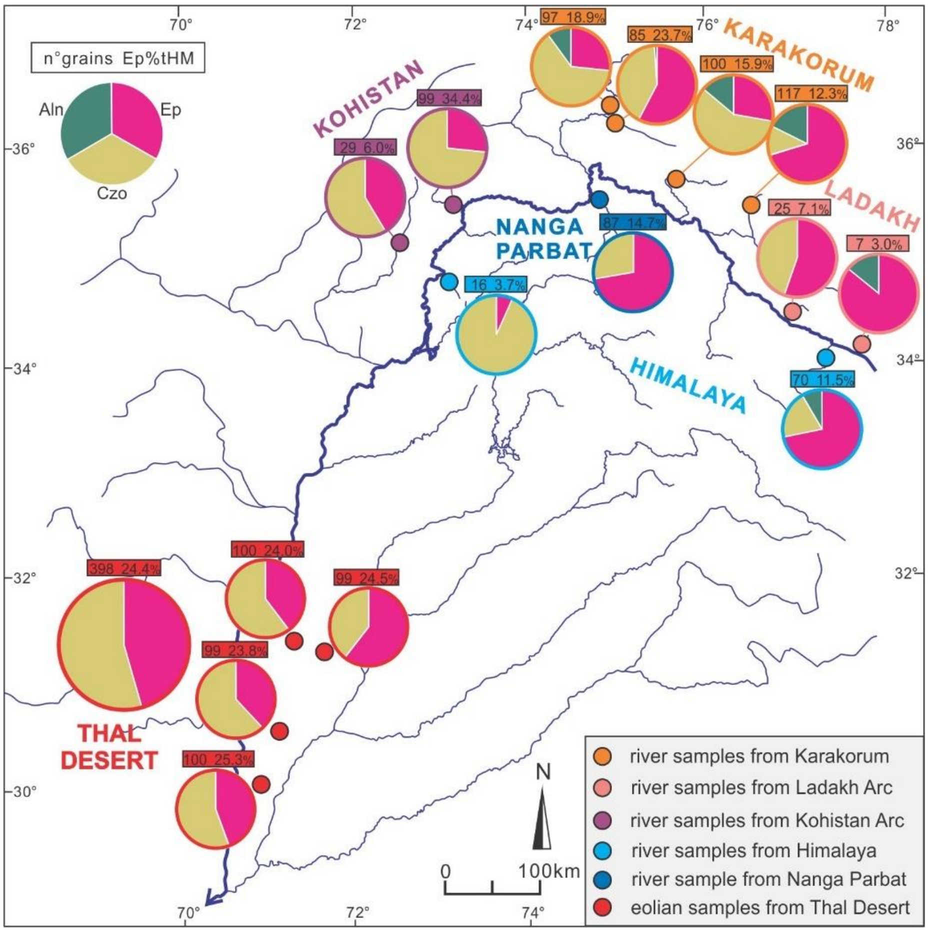

Figure 5.10 Calculated proportions of different varieties of detrital epidote-group minerals found in river and eolian sand of northern Pakistan. Note that Thal dunes, as well as sand from Kohistan and Nanga Parbat, lack allanite. Among Karakorum rivers, only the Hispar does not carry allanite, which singles out the Southern Karakorum as the only domain potentially representing a major source of epidote within the belt. Aln: allanite; Czo: clinozoisite; Ep: epidote.

5.5.6 The pyroxene signal

The abundance of orthopyroxene in Thal Desert dunes points to dominant contribution from the Kohistan arc, with minor to negligible additional contributions from other sources (Fig. 5.11). In fact, the Ladakh arc (Wo < 30), the Karakorum belt (upper Hushe sand; Wo ~ 30), and the Greater Himalaya (Nandihar sand; Wo < 40) shed mostly Ca-poor augite (Fig. 5.6), whereas augite grains in Thal Desert dunes are mostly Ca-rich (Wo > 40). Detrital ferroaugite is negligible in Thal dunes, whereas it occurs in sand derived from the Nanga Parbat, Greater Himalaya, and Karakorum belt (upper Hunza sand) (Fig. 5.6).

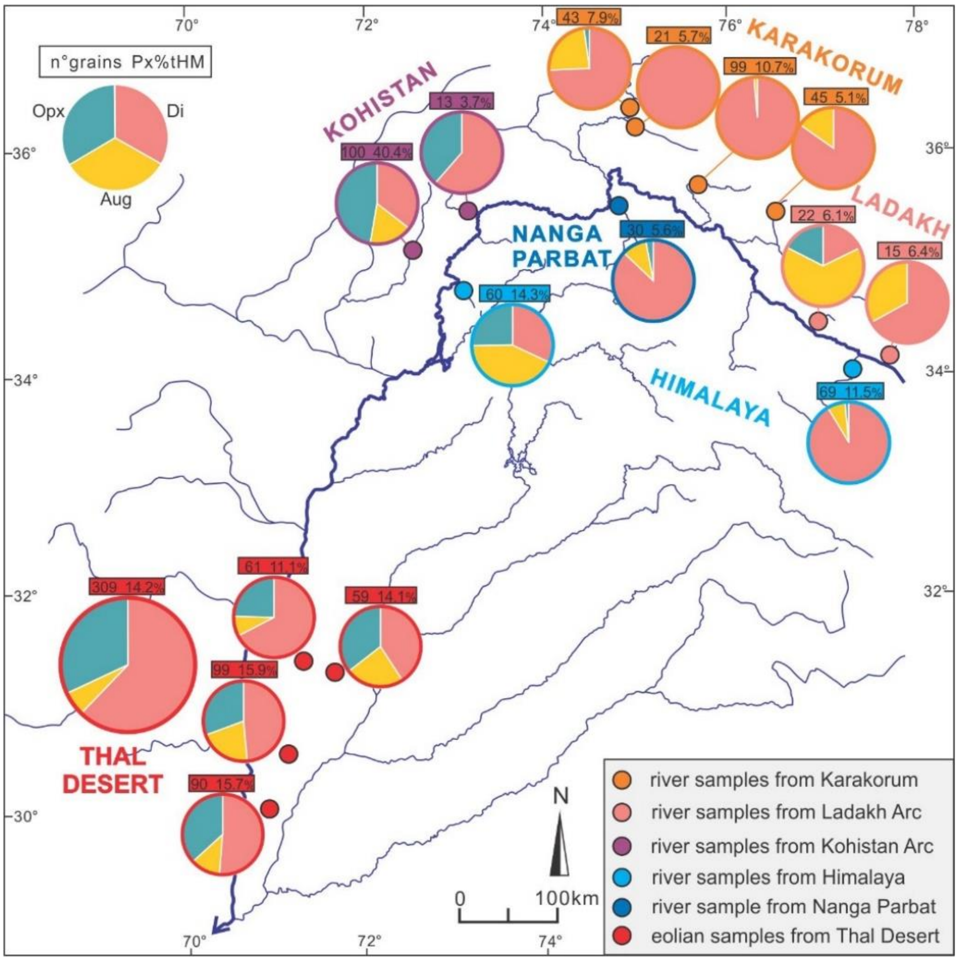

Figure 5.11 Calculated proportions of different varieties of detrital pyroxene found in river and eolian sand of northern Pakistan. Aug: augite (25 < Wo < 45); Di: diopside (Wo > 45); Opx: orthopyroxene (Wo < 5).

5.6 Conclusions

Varietal studies of heavy minerals have long been proven to provide crucial information on sediment provenance. The present study focuses on the chemical composition of detrital amphibole, garnet, epidote, and pyroxene because these solid-solution series are the four dominant minerals in orogenic sediments worldwide. The rich minerochemical dataset produced is intended as a basis useful to discriminate among the diverse sources of detritus within the upper part of the Indus River catchment in northern Pakistan, upstream of its entry point in the Punjab foreland basin. Therefore, the thorough quantitative description of mineralogical signatures of Thal Desert dune sand, representing a relict sink of sediment entirely derived from the upper Indus River in the Quaternary, offers a complementary way to trace erosion patterns across the western Himalayan syntaxis and adjacent orogenic segments.

High-resolution analysis of Thal Desert dune sand indicates that the Kohistan arc has played the principal role as a source of heavy minerals, especially as pyroxene and epidote are concerned. The similarity among mineralogical spectra suggests that the Southern Karakorum gneiss domes undergoing fast exhumation and the Nanga Parbat massif were important suppliers of amphibole and garnet, reflecting high erosion rates in the western Himalaya syntaxis. Among other Himalayan domains, a minor amount of heavy minerals was supplied by the Greater Himalaya, whereas detritus from the Lesser Himalaya and Subhimalaya becomes significant in Indus sand only in southern Pakistan, downstream of the confluence with Punjab tributaries. The contrast between mineralogical fingerprints of Thal Desert sand, entirely derived from geological domains exposed around the western Himalayan syntaxis, and those of detritus carried by Punjab tributaries, which drain the Himalayan belt exclusively, can be exploited to assess how the relative contributions from these different parts of the Himalayan-Karakorum orogen to the Indus delta to huge deep-sea fan have changed through time. Such a clear differentiation between Transhimalayan and Himalayan sources of detritus provides a semi-actualistic key that can be used, together with complementary compositional datasets and geological information, to make a step forward in the understanding of the erosional evolution of the Himalayan orogen and of landscape changes in the Punjab foreland basin as controlled by the complex interplay between climatic and tectonic forces in the recent and less recent past.

6 Provenance of Thal Desert sand: a Pleistocene inland archive of Indus River sediment (central Pakistan)

Liang et al., in preparation

6.1 Introduction

The western Himalaya area has great height differences, resulting from the rapid uplift among Neogene and erosion unroofing of crystalline basement rocks (Shroder and Bishop, 2000). The complete transect across the collision area also exposed here, from the Asian margin to the Indian passive margin (Searle et al., 1999; Hodges, 2000). The Indus River, draining the various tectonic domains of western Himalaya, carries sand with distinct compositional signatures which can faithfully reflect the geology terranes (Garzanti et al., 2005), providing a superb opportunity for investigating the relationships of among orogenic processes, climate and erosional evolution among the western Himalayan Syntaxis.

Plenty of research has been focused on understanding how the Indus River system has evolved over time (e.g., Qayyum et al., 1997; Sinclair and Jaffey 2001; Clift et al 2001, 2002, 2014; Najman et al., 2003; Henderson et al., 2010; Zhuang et al., 2018). Desert, as a substantial sediment repository of rivers has drawn great attention recent years (Clift and Giosan, 2014; East et al., 2015), especially the Thar Desert (e.g. Singh et al., 1990; Enzel et al., 1999; Singhvi and Kar, 2004; Singhvi et al., 2010) with large amount of sediments recycled from the lower Indus River and delta (Clift and Giosan, 2014; East et al., 2015). However, the neighbouring Thal Desert, located at the entry point in the Himalayan foreland basin, and held the key information to interpret the stratigraphic record and understand the erosive dynamics of the recent Indus system, causes only little concern.

The arid desert characterized by negligible chemical weathering and minor effect of fluvial transport and human activities, can generally preserve provenance information perfectly. Most sand components of the dunes may survive for a million years (Vermeesch et al., 2010) with only considerable mechanical modification. Therefore, the desert area provides an excellent opportunity to investigate the interrelationships between tectonics and climate and their influence on sedimentation during Quaternary. Zircon geochronology represents one of the few available methods to trace the ultimate provenance of desert sand (Dickinson and Gehrels, 2009), because zircon is one of the few accessory minerals consisting the sand seas in the world (Muhs, 2004), although focusing on zircon only thus inevitably entails missing information on the remaining 99.98% of the sand composition (Garzanti, 2016).

We emphasize the importance of an integrated, multi-method and multi-mineral approach in provenance analysis (e.g., von Eynatten and Dunkl, 2012; Smyth et al., 2014; Garzanti et al., 2018a). The detailed provenance study on Thal Desert sand, using the high-resolution sand petrography and heavy mineral analysis, bulk sediment geochemistry, Nd isotopes and zircon chronology, integrated with previous analysis of Raman spectroscopy and varietal studies on amphibole, garnet, epidote and pyroxene grains (Liang et al., 2019), can help to document detritus signals in river and dune sand, distinguish the sand provenance, and identify distinct erosion patterns in the western Himalayan Syntaxis through the Quaternary.

6.2 The Thal Desert

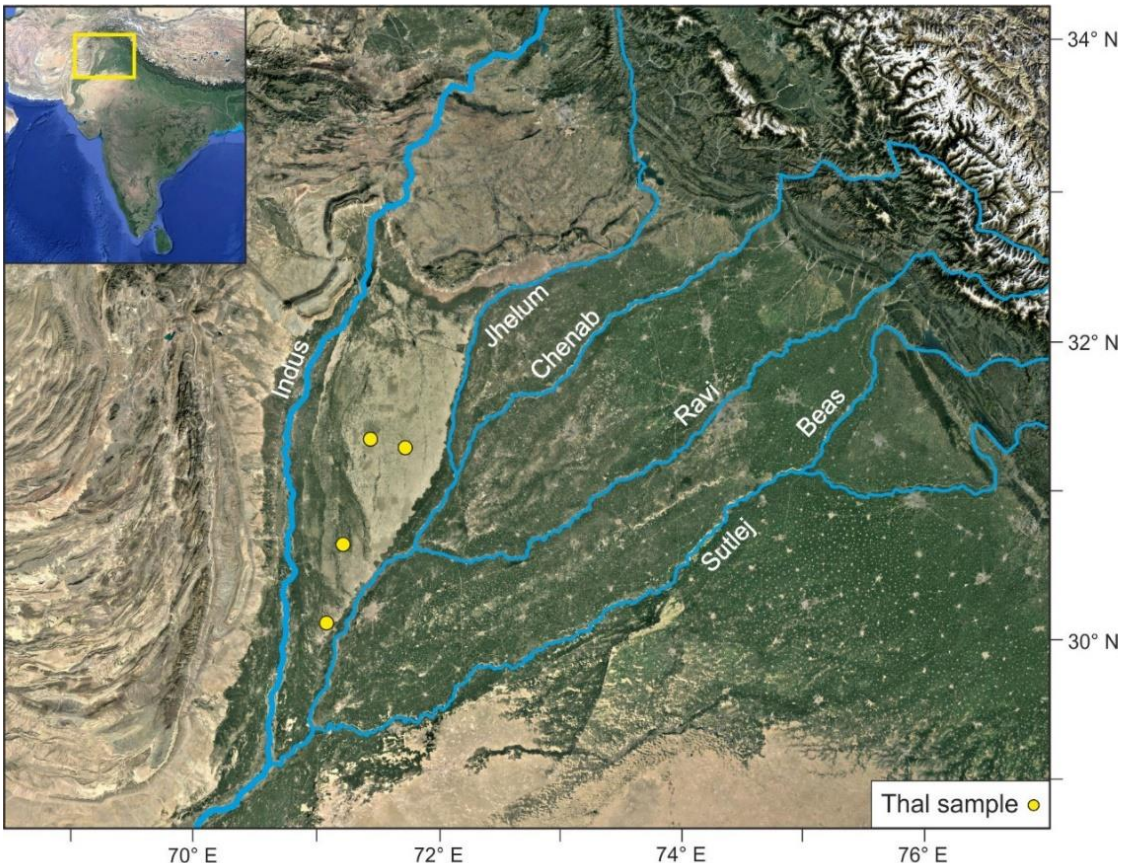

Figure 6.1 Google Map of Thal Desert and Thal Desert dune samples.

Central Pakistan is an arid to semi-arid subtropical region hosting in the south the large Thar Desert (~ 175,000 km^2), straddling the political border with India (Singhvi and Kar, 2004; East et al., 2015), and in the north the much smaller, 300 km-long and 100 km-wide Thal Desert, located between about 30° and 32°30' N and between about 71° and 72° E (Fig. 6.1). This triangular-shaped desert extending between the course of the Indus River in the west and the Punjab tributaries in the east.

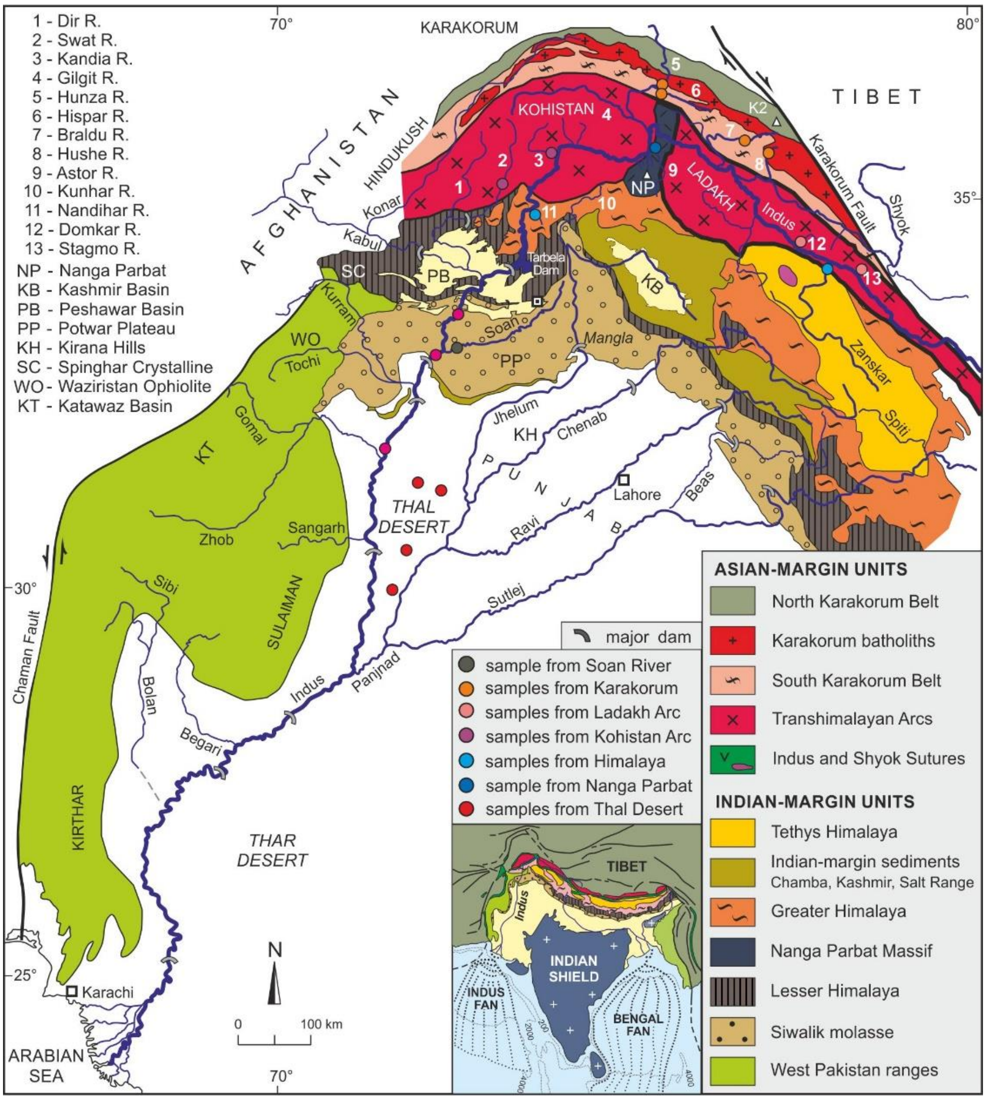

Figure 6.2 Geological sketch map of the Indus River catchment (redrawn after Garzanti et al. 2005), indicating the studied tributaries and sampling sites.

The Thal Desert, comprised between the Indus and Jhelum rivers, is delimited by the Salt Range foothills in the north, whereas the Indus floodplain is bounded by the Sulaiman Ranges in the west (Fig. 6.2). Exposed in the Salt Range are Neoproterozoic/Cambrian evaporites overlain by a fossiliferous Cambrian to Cenozoic succession (Shah, 1977). The Sulaiman fold-thrust belt includes largely shelfal upper

Paleozoic to Eocene strata, Neogene molasse, and deep-water turbidites underlain by ophiolitic complexes (Jadoon et al., 1994). The Punjab plains are underlain by up to 450 m-thick Quaternary alluvium and eolian deposits overlying semiconsolidated Cenozoic rocks or directly Precambrian crystalline basement, which crops out in the Kirana Hills straddling the Chenab River course and representing the topographic culmination of the Sargodha Ridge (Greenman et al., 1967; Kadri, 1995).

6.2.1 Climate

Summers are very hot in the Thal Desert, with average temperatures around 35°C in June to July, dropping to about 10°C in December to January. Average annual temperatures increase from ~ 24°C in the north and west to ~ 28°C in the south. Most of the region receives less than 350 mm of rain per year. Annual rainfall progressively decreases from the northern (annual average of 617 mm recorded from 1991 to 2013 in the Mianwali meteorological station; Shah and Ahmad, 2015) to the southern edges of the desert (150 mm; Greenman et al., 1967). Cold dry winds blow from the north in winter, whereas hot rain-bearing winds blow from the south in summer, with average speed of several km per hour. Between March and April, hailstorms generated by air turbulence owing to the high temperature difference between the warm surface and the cold upper atmosphere may cause major damage to crop and buildings (Gosal, 2004). In the summer, dust storms may be fostered by unsteady thermal conditions and north/south temperature gradients (Hussain et al., 2005).

6.2.2 Geomorphology, hydrology and hydrogeology

Different physiographic units can be distinguished in the Thal Desert, which lies at altitudes above sea-level decreasing from ~ 200 m in the north to ~ 120 m in the south. The piedmont area transitional to the Salt Range foothills hosts alluvial fans consisting of detritus reworked and deposited during sheet floods, and fining downstream within a distance of ~ 10 km. The Quaternary fluvial and eolian deposits in the south desert is ~ 350 m-thick and much thicker in the central desert (Nickson et al., 2005).

The underlying alluvium basically consists of laterally continuous fine to coarse sand bodies, with minor gravel, and isolated mud lenses. Fluvial environments can be distinguished into three categories, the active flood plain, the abandoned flood plain, and bar uplands. The present active floodplain of the Indus River reaches a width of more than 20 km in the south. The abandoned flood plain is even wider and includes areas of higher ground termed as bar upland. In the upper part of the desert, bar uplands are actively eroded by the Jhelum River with scarps locally up to 10 meters above the floodplain (Greenman et al., 1967).

The Thal Doab aquifer, consisting of Quaternary alluvial and eolian deposits with local mud lenses, is recharged rapidly from river water and rainfall. The Indus River and its tributaries to a lesser extent give rise to one of the largest irrigation systems in the world, including the Chashma-Jhelum link canal supplied with Indus waters and built between 1967 and 1971. A network of dams, barrages and canals aim to convert into cultivable land the Thal Desert, where the water table lies between 9 and 0.5 m from ground surface (Shah and Ahmad, 2016; Hussain et al., 2017).

Other detailed information on geomorphology, hydrology and hydrogeology are provided in Chapter 5.2.

6.3 Methods

6.3.1 Sand petrography and heavy minerals

Dune sand samples from the Thal Desert were collected in February 2001. Detailed information on sample location, petrography, heavy mineral, geochemistry and Nd isotopic data in Appendices Tables C1 to C5. A quartered aliquot of each bulk sand sample was impregnated with araldite, cut into a standard thin section stained with alizarine red to distinguish dolomite and calcite, and analyzed by counting 400 points by the Gazzi-Dickinson method (Ingersoll et al., 1984). Metamorphic grains were classified by protolith composition and metamorphic rank. Average rank of rock fragments in each sample was expressed by the metamorphic indices MI and MI*, ranging from 0 to 500 with the increasing metamorphic grade (Garzanti and Vezzoli, 2003). Sand classification is based on the main component quartz, feldspars and lithic fragments considered if exceeding 10% QFL (Garzanti, 2016, 2019b). Median grain size was determined in thin section by ranking and visual comparison with standards of $\phi/4$ classes prepared by sieving in our laboratory.

Heavy minerals were separated in sodium polytungstate (density ~ 2.90 g cm^{-3}), using the 63-250 μm fraction treated with oxalic and acetic acids. 200 to 225 transparent heavy minerals were counted on grain mounts by the area method (Mange and Maurer, 2012). Heavy-mineral concentrations, calculated as the volume percentage of total (HMC) and transparent (tHMC) heavy minerals (Garzanti and Andó, 2007b), range from "very poor" (tHMC < 0.5) and "poor" ($0.5 \leq$ tHMC < 1) to "rich" ($5 \leq$ tHMC < 10), "very-rich" ($10 \leq$ tHMC < 20) and "extremely rich" ($20 \leq$ tHMC < 50). The ZTR index (Hubert, 1962) estimates the durability of the assemblage (i.e., extent of recycling; Garzanti, 2017). The Hornblende Colour Index (HCI) varies from 0 to 100 and estimates formation temperatures of metamorphic and igneous rocks (Andò et al., 2014). Detrital components are listed in order of abundance throughout the text.

6.3.2 Bulk chemistry and Nd isotopes

Chemical analyses were carried out at ACME Laboratories (Vancouver) on a split aliquot of the 63-2000 µm fraction obtained by wet sieving. Major oxides and some minor elements were determined by ICP-ES and trace elements by ICP-MS, following a lithium metaborate/tetraborate fusion and nitric acid digestion. A separate split was digested in aqua regia and analysed for Mo, Ni, Cu, Ag, Au, Zn, Cd, Hg, Tl, Pb, As, Sb, Bi, Se, but the concentration of these elements may be underestimated because of only partial leaching of refractory minerals. For further information on adopted procedures, geostandards used and precision for various elements see http://acmelab.com (code LF200).

Several grams of the bulk sediment were powdered from each sample to ensure a good average composition. Each sample was then dissolved in a solvent and the Nd separated using standard column extraction techniques. Nd isotopic compositions were determined on VG354 mass spectrometer at Woods Hole Oceanographic Institution. $^{143}Nd/^{144}Nd$ values are normalized to $^{146}Nd/^{144}Nd = 0.7219$ and are relative to 0.511847 for the La Jolla standard. We calculated the parameter ε_{Nd} (DePaolo and Wasserburg, 1976) using a $^{143}Nd/^{144}Nd$ value of 0.512630 for the Chondritic Uniform Reservoir (Bouvier et al., 2008).

6.3.3 U-Pb zircon geochronology

On the heavy-mineral separates of 14 samples (3 from the Thal Desert, 2 from the Indus River and 9 from various end-member sources). Detrital zircons were identified by Automated Phase Mapping (Vermeesch et al., 2017) with a Renishaw inVia™ Raman microscope. U-Pb zircon ages were determined at the London Geochronology Centre using an Agilent 7700x LAICPMS (laser ablation-inductively coupled plasma-mass spectrometry) system, employing a NewWave NWR193 Excimer Laser operated at 10 Hz with a 35 μm spot size and ~ 2.5 J cm^{-2} fluence. No cathodoluminesce imaging was done, and the laser spot was always placed "blindly" in the interior of zircon grains. Data reduction was performed using GLITTER 4.4.2 software (Griffin et al., 2008). We used $^{206}Pb/^{238}U$ and $^{207}Pb/^{206}Pb$ ages for zircons younger and older than 1100 Ma, respectively. No common Pb correction was applied. Grains with > +5 / -15% age discordance were discarded, and 1392 concordant ages were obtained overall. The full geochronological dataset is provided in Appendix Table C7.

6.4 Compositional fingerprints of Thal Desert sand

6.4.1 Petrography and heavy minerals

All four Thal Desert samples are fine-grained, litho-feldspatho-quartzose to quartzo-feldspatho-lithic sand. Q/F and Q/L ratios are 1.1 ± 0.1 and 1.3 ± 0.5, respectively (Fig. 6.3). Quartz is mostly monocrystalline (Qp/Q 0.09 ± 0.03). K-feldspar and plagioclase occur in subequal amounts (P/F 0.51 ± 0.07). The varied rock-fragment population includes metasedimentary (paragneiss, schist, slate, calcschist, phyllite, metasandstone), metabasite (prasinite, chloritoschist, amphibolite), carbonate (limestone, dolostone), other sedimentary (shale, siltstone, minor chert), granitoid, felsic to mafic volcanic and metavolcanic, and minor ultramafic (serpentineschist, cellular serpentinite) grains (MI 253 ± 33, MI* 293 ± 20). A few muscovite and biotite occur. Very rich heavy-mineral assemblages (HMC 16 ± 4; tHMC 12 ± 2) are dominated by amphibole (mainly blue-green hornblende; HCI 9 ± 3) associated with epidote, garnet, green to colourless clinopyroxene, and hypersthene. Titanite, staurolite, kyanite, zircon, tourmaline, rutile, sillimanite, olivine, and chloritoid also occur (ZTR ≤ 4) (Table 6.1).

Table 6.1 Petrographic and heavy-mineral signatures of Thal Desert sand compared with that of sand carried by the Indus River and by its tributaries draining different source-rock domains. Q = quartz; F = feldspars; Lv = volcanic; Lc = carbonate and metacarbonate; Lp = shale, siltstone; Lh = chert; Lm = metamorphic; Lu = ultramafic; MI = metamorphic index. HM = heavy minerals; tHMC = transparent heavy-mineral concentration. ZTR = zircon + tourmaline + rutile; Ttn = titanite; Ep = epidote-group minerals; Gt = garnet; HgM = high-grade metasedimentary mineral (staurolite + kyanite + andalusite + sillimanite); Amp = amphibole;*

Cpx = clinopyroxene; Opx = orthopyroxene; &tHM = other transparent heavy minerals (apatite, olivine, spinel, prehnite, pumpellyite, brookite, barite).

	Sample	Q	F	Lv	Lc	Lp	Lh	Lm	Lu	total	MI*
End members											
Hushe	S1749	55	41	0	2	0	0	3	0	100.0	405
Braldu	S1748	50	26	0	18	0.3	0	6	0	100.0	350
Hunza	S1437	23	23	0	18	13	0	24	0	100.0	247
Hispar	S1438	58	31	0	5	1	0	5	0	100.0	381
Stagmo	S4426	41	57	0	0.4	0	0	1	0	100.0	456
Domkar	S4430	47	50	0	0.2	1	0	2	0	100.0	403
Kandia	S1439	32	18	0	2	0	0	48	0	100.0	320
Swat	S1440	26	47	2	0	0.5	0	21	3	100.0	339
Zanskar	S4419	49	15	0.3	29	1	0	6	0.3	100.0	356
Nandihar	S1426	59	25	0	0	0	0	16	0	100.0	411
Astor	S1432	67	30	0	0	0	0	3	0	100.0	390
Soan	S1454	48	18	1	11	10	4	9	0	100.0	192
Indus River											
Indus	S1447	42	22	0	9	6	1	21	0.4	100.0	292
Indus	S1455	43	16	1	15	11	1	11	1	100.0	253
Indus	S1461	45	24	2	12	4	3	11	0.4	100.0	296
Desert dunes											
Thal	S1462	39	34	1	5	1	1	18	1	100.0	317
Thal	S1463	35	33	1	7	2	0.4	22	0.4	100.0	283
Thal	S1470	30	34	3	8	2	0	23	0	100.0	294
Thal	S1474	43	36	0.4	7	5	0	9	0.4	100.0	273

	Sample	HMC	tHMC	ZTR	Ttn	Ep	Gt	HgM	Amp	CPX	OPX	&tHM	total
End members													
Hushe	S1749	4.8	2.5	7	10	11	2	1	67	1	0	0	100.0
Braldu	S1748	6.5	4.5	6	3	34	6	1	46	2	1	0	100.0
Hunza	S1437	2.9	1.5	5	4	20	2	0	66	2	0	0	100.0
Hispar	S1438	8.7	6.7	3	9	21	21	1	41	3	0	0	100.0
Stagmo	S4426	12.6	12.0	0	3	2	0	0	90	3	0	1	100.0
Domkar	S4430	9.7	8.1	2	2	7	0	0	86	0	1	0	100.0
Kandia	S1439	44.2	33.4	0	0	38	0	0	60	1	0	0	100.0
Swat	S1440	31.4	27.5	1	0	8	0	0	67	8	15	0	100.0
Zanskar	S4419	4.8	4.6	6	1	12	14	23	31	10	0	4	100.0
Nandihar Khwar	S1426	4.8	4.0	2	0	10	26	8	47	0	6	1	100.0
Astor	S1432	17.9	16.9	1	0	19	7	0	71	1	0	0	100.0
Soan	S1454	5.0	3.8	3	0	76	5	0	16	0	0	0	100.0
Indus River													
Indus	S1447	12.2	9.8	0	1	17	9	3	60	7	4	0	100.0
Indus	S1455	8.7	6.7	3	2	30	8	4	44	4	3	1	100.0
Indus	S1461	27.7	22.9	1	4	22	29	2	40	0	2	0	100.0
Desert dunes													
Thal	S1462	21.2	15.3	1	1	15	11	1	64	2	4	0	100.0
Thal	S1463	24.2	18.6	1	1	16	14	2	55	7	3	0	100.0
Thal	S1470	26.4	17.7	4	1	20	13	4	45	5	6	0	100.0
Thal	S1474	12.3	10.0	0	1	18	9	1	60	8	3	0	100.0

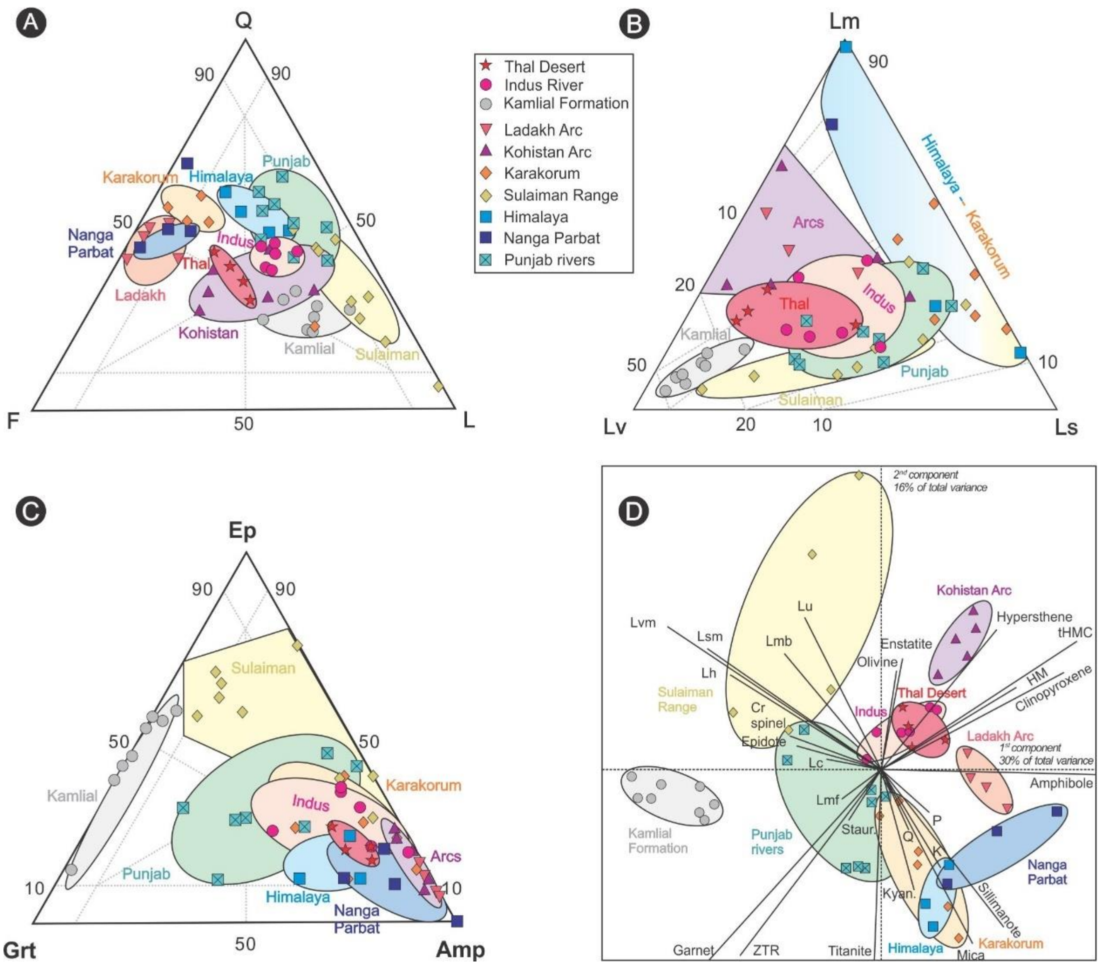

Figure 6.3 Detrital modes QFL (A), LmLvLs (B) (diagrams after Ingersoll et al., 1984 and Garzanti, 2019b), Ep-Grt-Amp (C) and biplot (D). Indus river sand downstream of the Kabul River confluence is a mixture of detritus derived from the Kohistan and Ladakh arcs, and the Himalaya, Karakorum, Hindukush and Sulaiman ranges. Thal Desert sand shows virtually the same composition, similar with that of the Indus River sand. The Thal dune sand is more feldspar-rich than that of modern Indus River sand, indicating a higher Kohistan Arc influence in dune sand than the river sand. The most abundant volcanic lithics occurs in the Kamlial Formation, reflecting only incipient dissection of the Kohistan Arc in mid-Miocene times (Najman et al., 2003). K = K-feldspar; P = plagioclase; L = lithic grains (Ls = sedimentary; Lvm = volcanic and metavolcanic; Lsm = shale, siltstone, slate and metasiltstone; Lmf = felsic metamorphic; Lmb = metabasite). Other parameters as Table 1. Data in the LmLvLs diagram were re-centered to allow better visualization. In the compositional biplot (Gabriel, 1971), all petrographic and mineralogical parameters are considered. The length of each ray is proportional to the variability of the corresponding compositional parameter in the data set. If the angle between two rays is close to 0°, 90°, or 180°, then the corresponding parameters are directly correlated, uncorrelated, or inversely correlated, respectively.

6.4.2 Geochemical signatures

The bulk geochemical composition of Thal Desert sand samples show similar pattern which is enriched in Be, Mg, Ca, Si and depleted in Na, K, Rb, Cs, Sr, Ba, Mo, Cu, Zn, Cd, Tl, Sn, Pb and Sb compared with the Upper Continental Crust standard (UCC). The samples S1462 and S1463 are slightly enriched in Y, REE, Th, Ti, V and Cr and depleted in U, Hf, Nb and Ta. The amounts of Y, REE, Th, U, Ti, Zr, Hf, V, Nb and Ta in sample S1470 are about three times higher than these elements in sample S1474 (Fig. 6.4A), reflecting a selective concentration of heavy minerals in sample S1470 (Garzanti et al., 2010a).

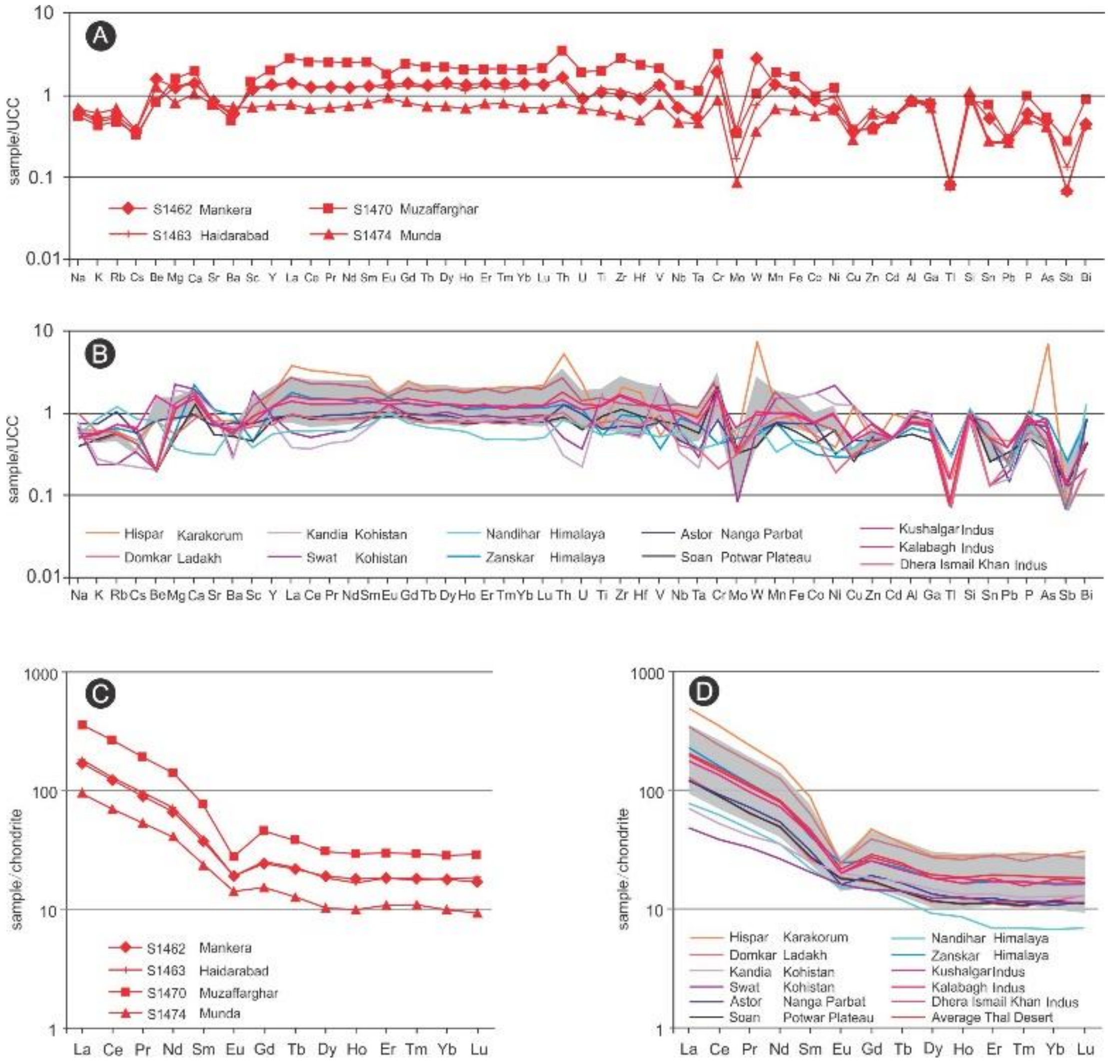

Figure 6.4 Geochemistry of eolian and river sand. UCC-normalized chemical composition of sand in Thal Desert samples (A) and in tributaries from the upper Indus catchment (B); Chondrite-normalized REE patterns in Thal Desert samples (C) and in tributaries from the upper Indus catchment (D). Elements in UCC-normalized diagrams are arranged following the

periodic table group by group. The REE enrichment in S1470 and depletion in S1474, reflect different heavy mineral concentration. Plutonic and volcaniclastic sediments from Kohistan and Ladakh arcs are enriched in Na, Mg, Ca, Sr, whereas metasedimentclastic and sedimentclastic sediments from the Himalaya and Nanga Parbat Massif are enriched in K, Rb, Ba. Sand of the Hispar River draining the Karakorum is rich in REE and Zr, Hf, suggesting hydraulic enrichment in heavy minerals (Garzanti et al., 2010a).

Chondrite-normalized REE patterns show classical LREE enrichment, flat HREE distribution, and negative Eu anomaly (Mcdogough and Sun, 1995), and vary slightly (La_N/Sm_N 4.5 ± 0.3, Gd_N/Ho_N 1.5 ± 0.1, Ho_N/Yb_N 1.0 ± 0.1) in Thal Desert samples (Fig. 6.4C). The Eu anomaly changes systematically from less negative value 0.74 in REE-poor S1474 to strongly negative value 0.46 in REE-rich S1470, reflecting a higher concentration of ultradense minerals (e.g., allanite and monazite with strongly negative Eu anomaly) in sample S1470, and a higher concentration of feldspar in sample S1474 (feldspar has strongly positive Eu anomaly).

6.4.3 Nd isotopic signatures

Neodymium isotope ratios range widely in the studied Thal Desert sand. Because their bulk-sediment mineralogy is rather homogeneous, indicating notably constant provenance, this marked variability is most likely controlled by local factors such as grain size and/or hydraulic sorting. All four samples are fine sand, but coarser-grained samples (2.0-2.2 ϕ) have less negative ε_{Nd} (-3.5 and -8.7) than finer-grained samples (2.3-2.7 ϕ; ε_{Nd} -10.9 and -13.2). Studies of Himalayan-derived sand have shown that their isotopic signatures are buffered by few minerals, and that the Nd budget is chiefly controlled by monazite and allanite despite their very low concentration (Garzanti et al., 2010a, 2011a; Garçon et al., 2014). We note that the two samples with less negative ε_{Nd} display the highest heavy-mineral concentration and are enriched in ultradense minerals including opaque Fe-Ti-Cr oxides, garnet, zircon.

6.4.4 Detrital geochronological signatures

91 concordant U-Pb ages were obtained from the zircon grains in Thal Desert sand, with half of them younger than 200 Ma. The two youngest ages are same at 21.6 ± 0.3 Ma, with discordances of 1.9% and 2.8%, respectively. The three main age clusters are

at 40-50 Ma, 70-100 Ma and 1800-1900 Ma with minor age populations at 100-110 Ma, 640-850 Ma and 2300-2500 Ma (Fig. 6.5).

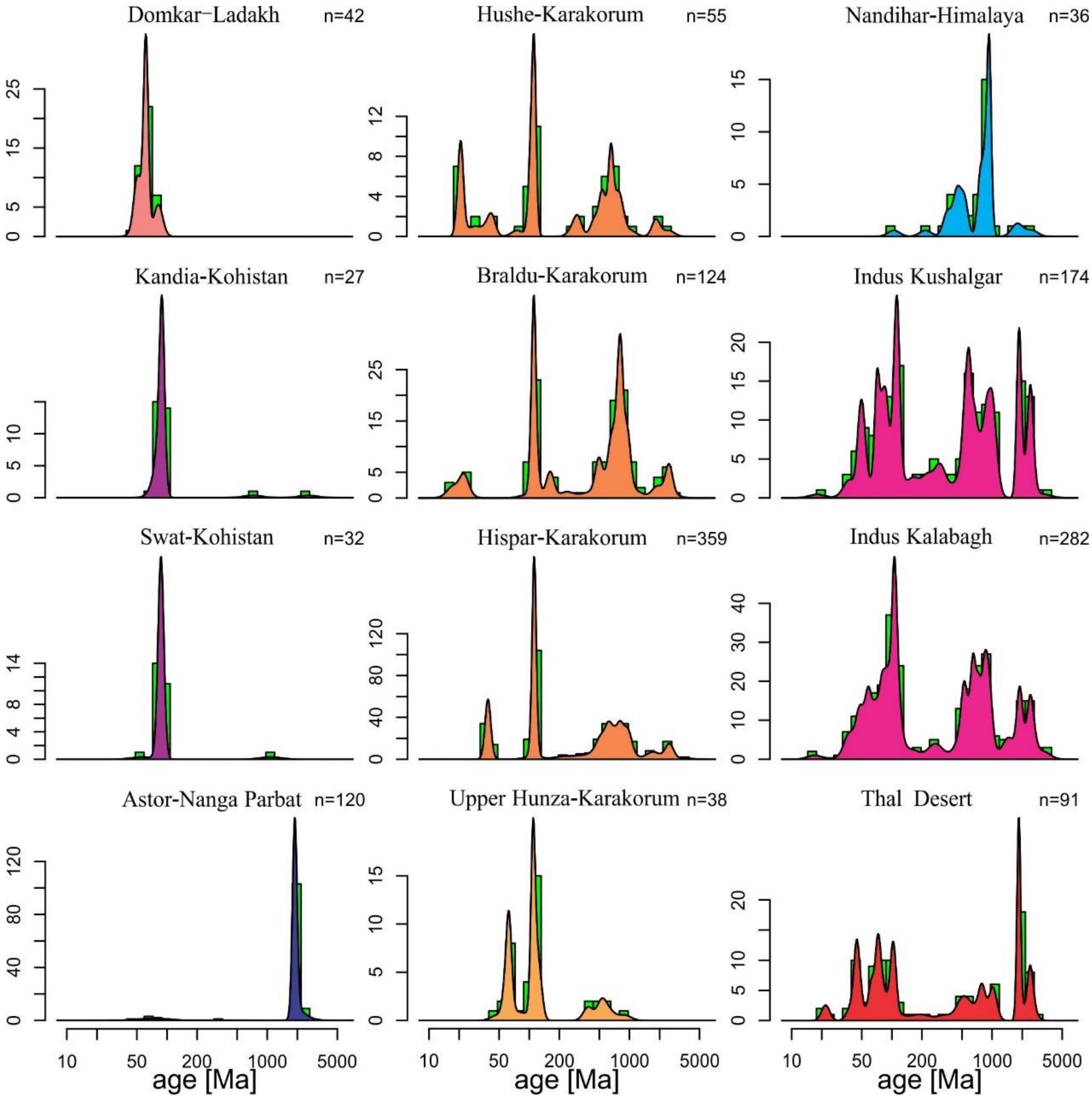

Figure 6.5 U-Pb age spectra of zircon grains in Indus drainage and Thal Desert. The KDEs (kernel density estimates) are shown with logarithmic abscissa (Vermeesch, 2018).

Zircon grains are more abundant in sample S1470 compared to S1474, due to its higher heavy mineral concentration. Zircon age distribution of S1470 concentrates in younger age clusters with 49% of zircons younger than 100 Ma, compared with 32% of grains in S1474. At the same time, sample S1474 contains a higher (24% of total grains) age population at ca. 850-1200 Ma which is about three times than that in S1470 (only ~ 9% of total grains).

6.5 Provenance of the Thal Desert

6.5.1 Signatures of potential sand sources

Potential sediment sources for Thal Desert sand include the major left-bank and right-bank tributaries of the Indus River, which drain the Ladakh and Kohistan arcs, the Himalayan belt including the Nanga Parbat massif, the Karakorum, and the Hindukush.

Petrographic and mineralogical signatures

The petrographic and mineralogical signatures (Appendix Table C6) of the diverse geological domains drained by these rivers are defined in Garzanti et al. (2005) and briefly summarized below. Complementary petrography and heavy mineral data from Ladakh and Zanskar tributaries are also included.

Tributaries of the Indus River

Indus tributaries draining the Ladakh arc carry quartzo-feldspathic and subordinately feldspatho-quartzose plutoniclastic sand with rich to very rich heavy-mineral assemblages dominated by blue-green hornblende (HCI 5 ± 5) with minor epidote, titanite, apatite, clinopyroxene and hypersthene. The Kohistan arc sheds sand ranging in composition from feldspatho-quartzo-lithic to litho-quartzo-feldspathic metamorphiclastic with common prasinite and epidote-amphibolite grains and very rich to extremely rich heavy-mineral assemblages dominated by blue-green hornblende (HCI 8 ± 3) and including epidote and minor hypersthene and clinopyroxene.

Indus tributaries draining the Karakorum carry sand ranging in composition from quartzo-feldspatho-lithic sedimentaclastic (North Karakorum) to quartzo-feldspathic plutoniclastic (Central Karakorum), and litho-feldspatho-quartzose metamorphiclastic with marble grains (South Karakorum). Heavy-mineral assemblages are mostly moderately rich and include dominant blue-green hornblende (HCI 8 ± 1; North and Central Karakorum) or amphibole associated with epidote, garnet, titanite, diopside, and minor kyanite, staurolite, and sillimanite (HCI 20 ± 5; South Karakorum). A similar mineralogy characterizes feldspatho-quartzo-lithic sedimentaclastic sand of the Kabul River upstream of the Swat confluence.

Detritus from the Greater Himalaya, contributed by the Zanskar River in Ladakh and by minor rivers in northern Pakistan, is litho-feldspatho-quartzose metamorphiclastic with moderately rich heavy-mineral assemblages including hornblende, garnet and kyanite or sillimanite (HCI 16 ± 6). Sand supplied by tributaries draining the Nanga Parbat massif is mainly feldspar-rich feldspatho-quartzose with up to very rich, amphibole-dominated heavy-mineral assemblage (HCI up to 52) including garnet, clinopyroxene, epidote, and sillimanite. The Soan River, recycling Cenozoic foreland-basin units of the Potwar Plateau, carries feldspatho-litho-quartzose sedimentaclastic sand with a moderately rich, epidote-dominated heavy-mineral assemblage with garnet, hornblende, and tourmaline. The Jhelum and Chenab Rivers as well as other major Himalayan tributaries of Punjab carry feldspatho-litho-quartzose sand with varied sedimentary and metamorphic rock fragments and mainly moderately rich amphibole-epidote-garnet heavy-mineral assemblages.

Right-bank tributaries in west central Pakistan mainly draining the sedimentary succession of the Sulaiman Range (Kurram, Gomal, Sanghar Rivers) carry quartzo-lithic to feldspatho-quartzo-lithic sedimentaclastic sand with poor to moderately rich heavy-mineral assemblages including epidote, amphibole, garnet, clinopyroxene, enstatite, and commonly rounded tourmaline zircon, and rutile. The Kurram River contributes granitoid and metamorphic detritus derived from the Indian basement rocks of the Spinghar Crystalline (Badhsah et al., 2000), whereas the Tochi tributary of the Kurram and the Zhob tributary of the Gomal carry ultramaficlastic detritus derived from the Waziristan, Zhob, and Muslim Bagh ophiolite complexes (Gnos et al., 1997).

Trunk-river sand through time

The modern Indus River carries to the Pakistan foreland basin feldspatho-litho-quartzose sand including a variety of sedimentary and metamorphic rock fragments, and rich hornblende-dominated heavy-mineral assemblages (HCI 13 ± 6) with epidote, garnet, and minor clinopyroxene, hypersthene, staurolite, titanite, kyanite, and sillimanite. Back in the mid-Miocene, the Burdigalian-Langhian (18-14 Ma) Kamlial Formation, exposed in the Chinji area of the Potwar Plateau and inferred to have been largely deposited by a paleo-Indus river, contains feldspatho-quartzo-lithic sandstones including sedimentary as well as rich volcanic, metavolcanic, and metabasite detritus (Najman et al., 2003). This may represent the time when a drainage system similar to the present one was first established, whereas the existence and compositional fingerprints of a paleo-Indus at older times remain loosely constrained (Garzanti et al., 1996; Clift et al., 2000a; Roddaz et al., 2011; Zhuang et al., 2015).

Geochemical signatures

Sand from the Hispar River draining the Karakorum displays an enrichment in REE and Zr, Hf, indicating a hydraulic enrichment in heavy minerals (Garzanti et al., 2010a). The Kohistan derived sediment tends to be richer in Na, Sr, Cr, Co, and Ni, while the Ladakh derived sand is low in Cr, Co and Ni, reflecting the influence of heterogeneous distribution of plagioclase, amphibole and Cr-spinel (Garzanti et al., 2010a). Plutonic and volcaniclastic sediments from the Kohistan and Ladakh arcs are rich in Na, Mg, Ca, Sr, whereas metasedimentclastic and sedimentclastic sediments from the Himalaya and Nanga Parbat enrich in K, Rb, Ba. Among sediments derived from the Himalayan orogen, sand from the Zanskar River is richer in REE, Th and U elements than the Nandihar River, indicating a hydraulic concentration of ultradense minerals. The Nandihar sand is rich in Na, K, Rb, Cs, Be, whereas the Zanskar sand is rich in Ca and Mg, reflecting the occurrence of carbonate rocks in the Tethys Himalaya. The Soan tributary draining the Potwar Plateau shows similar chemical variability as Thal Desert sand, as well as the Indus trunk sample collected upstream and downstream of the Soan confluence. Indus trunk sample (Dhera Ismail Khan) close to the Thal Desert, displays a hydraulic concentration characteristic similar as eolian sample S1470 (Fig. 6.4B).

The REE patterns show similar trend with a LREE enrichment and flat HREE distribution and mostly negative Eu anomaly (Fig. 6.4D). The strong negative Eu anomaly in Hispar sample (Eu/Eu* 0.37), results from the enrichment of the ultradense minerals. The slightly negative Eu anomaly in the Kohistan Arc (Eu/Eu* 0.94 in Kandia and 0.95 in Swat) and the Ladakh Arc (Eu/Eu* 0.87), reflecting the influence of abundant feldspar.

Nd isotope signatures

Nd isotopic compositions can be used to distinguish tectonic domains among the collision zone, including the Karakorum, Transhimalaya, Nanga Parbat, Greater Himalaya and Lesser Himalaya (Clift et al., 2002, 2010). The mean documented ε_{Nd} in the Transhimalaya arcs is about 3 (Petterson et al., 1993; Khan et al., 1997; Clift et al., 2000b, 2002), where the Kohistan arc is estimated at 2-7 (Petterson et al., 1993; Khan et al., 1997) and the Ladakh batholith is measured at -1 (Clift et al., 2002). Mean ε_{Nd} in the Karakorum can be estimated at-11(Schärer et al., 1990; Clift et al., 2002), where the batholith is about -10 and the metamorphic belt is -11 (Braldu tributary in Clift et al., 2002). ε_{Nd} measured in bedrock (-18 – -30, Whittington et al., 1999) and modern sand (-23 – -27, Clift et al., 2002) of the Nanga Parbat are strongly negative. The Greater Himalaya shows relatively radiogenic-intermediate feature with mean ε_{Nd} value estimated at -16 (Deniel et al., 1987; France-Lanord et al., 1993; Parrish and Hodges, 1996; Harrison et al., 1999; Whittington et al., 1999; Ahmad et al., 2000), whereas the Lesser Himalaya is considered to posses a much more negative value at about -25 (Parrish and Hodges, 1996; Ahmad et al., 2000).

Detrital zircon chronological signatures

The Domkar tributary entirely draining the Ladakh Arc carries young detrital zircon grains (< 100 Ma) with ages peaking at 60 Ma associated with minor populations at 50 Ma and 80 Ma (Fig. 6.5). The young age population is consistent with the previous research on bedrock (Schärer et al., 1984; Weinberg and Dunlap, 2000; Singh et al., 2007). Kohistan Arc-derived tributaries mostly yield ages 70-95 Ma (94% in Kandia; 96% in Swat) corresponding to the Kohistan batholith and Chilas complex ages (e.g. Schaltegger et al., 2002; Jagoutz et al., 2009), with few zircon grains older than 700 Ma. The Dir, tributary of the Swat River, draining Kohistan batholith and Dir-Utror groups (Treloar et al., 1989; Jagoutz et al., 2009) displays a younger age cluster at 40-50 Ma (Zhuang et al., 2018).

The Hushe and Braldu Rivers mainly draining the southern Karakorum metamorphic belt and batholith of the central Karakorum carry zircons that mainly cluster at 100-120 Ma and 600-1000 Ma with a minor young age cluster at ~ 20 Ma (e.g. Baltoro granite in Baltoro region; Schärer et al., 1990; Weinberg et al., 2000) and an old age cluster at 2300-2800 Ma. The Hispar River draining the southern Karakorum metamorphic belt shows similar age distribution, albeit with a more abundant Eocene age population. Zircon grains from the Upper Hunza River displays main age clusters at 100-120 Ma and 55-65 Ma, associated with a minor age cluster between 500 and 900 Ma (Fig. 6.5), corresponding well with the bedrock in the south Pamir (Blayney et al., 2016), northern Karakorum and axial granitoids (Fraser et al., 2001; Jain and Singh, 2008).

The Astor River draining mainly the Nanga Parbat Massif shows an age distribution with the main age peak at ~ 1850 Ma, which is consistent with the Gneiss basement (Zeitler et al., 1993), and a minor subordinate age population at 60-90 Ma. Detritus from the Greater Himalaya, contributed by the Zanskar River (Jonell et al., 2017) and

Nandihar River, mainly carry zircon grains with Neo-Proterozoic (700-1000 Ma) and Paleozoic ages (350-500 Ma) (Fig. 6.5), whereas Punjab tributaries draining the Greater and Lesser Himalaya show major age clusters at 750-1250 Ma and 1500-2300 Ma (Alizai et al., 2011b).

Samples collected in the trunk Indus River upstream of the Thal Desert show ages cluster at 40-50 Ma (17%), 70-100 Ma (15%), 100-130 Ma (17%), 450-800 Ma (22%) and 850-1100 Ma (12%). The age spectra of sand in Kushalgar (upstream of the Soan confluence) and Kalabagh (downstream of the Soan confluence) display extremely high similarity (Fig. 6.5).

6.5.2 Sediment provenance of the Thal Desert

Kohistan Arc and Ladakh Arc

The low Q/F ratio (~ 1) and abundant metabasite rock fragments (Fig. 6.3A and 6.3B), as well as the relatively higher clinopyroxene and hypersthene content (Fig. 6.3D), indicate the abundant contribution of the Kohistan Arc. The average heavy mineral concentration (HMC 21.0; tHMC 15.4) of Thal dune samples which are not affected by selective-entrainment (enriched S1470 and depleted S1474), is very rich, and points by itself to major heavy mineral supply from the dense mafic rocks exposed in Kohistan Arc with extremely rich heavy mineral concentration (average HMC 37.8; tHMC 30.5) (Table 6.1). The average ε_{Nd} value in Thal sand is -9.1, which is less negative than the Karakorum, Greater Himalaya and much less than the Nanga Parbat and Lesser Himalaya sand, indicating a significant contribution from the Transhimalaya arcs.

The young age clusters at 40-50 Ma and 70-100 Ma correspond well with the age distribution in sand of Kohistan derived from the Swat and Kandia Rivers (Fig. 6.5 and 6.6). Even though the Ladakh Arc is also characterized by young ages, the lack of age cluster at 60 Ma in Thal Desert sand speaks against the Ladakh Arc as a major source.

According to the detailed minerochemical fingerprints analysis, the relatively high amount of actinolite in amphibole group, clinozoisite and zoisite in epidote group, orthopyroxene in pyroxene group (Liang et al., 2019), certificate that the Kohistan Arc has played a major role as a source of Thal Desert sand. The abundant Ca-poor augite (Wo < 30) in Ladakh Arc is negligible in Thal Desert (Liang et al., 2019), which further indicates the minor contribution from Ladakh Arc.

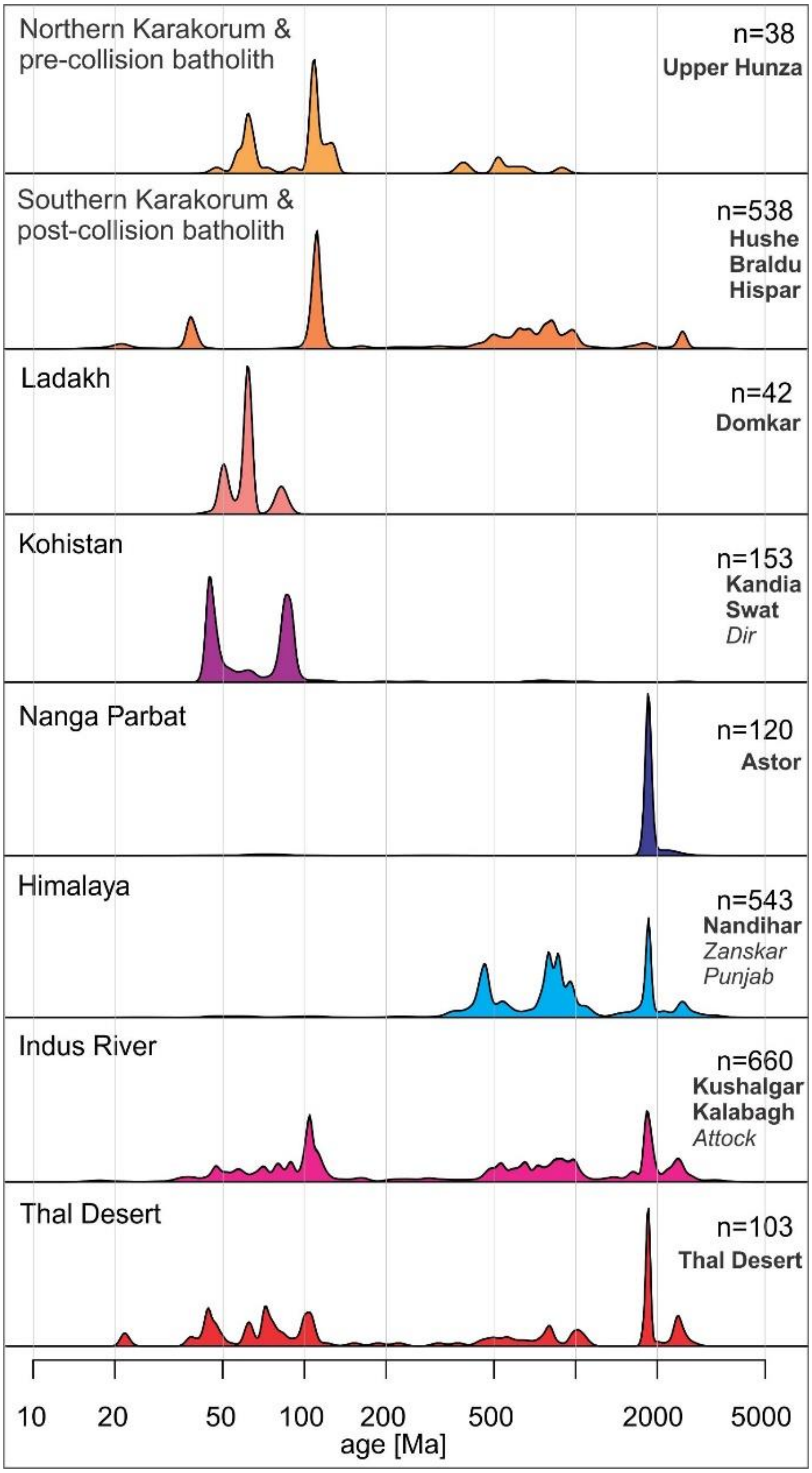

Figure 6.6 U-Pb age spectra of detrital zircons from river and eolian sand of northern Pakistan (age vs. frequencies plotted as KDEs using IsoplotR from Vermeesch, 2018). Tributaries in bold are from this study; Data of Dir tributary after Zhuang et al. (2018); Zanskar River after Jonell et al. (2017); Punjab (Jhelum, Chenab, Ravi, Beas and Sutlej) tributaries and Indus trunk @Attock after Alizai et al. (2011).

Karakorum

Tributaries draining the Karakorum carry abundant quartz and feldspar, and less volcanic lithic grains compared with the Thal Desert sand (Fig. 6.3A and 6.3B). However, the less negative ε_{Nd} value (Clift et al., 2002), comparable with the dune sand, indicate a significant influence on the Thal Desert.

Sand from the Northern and Central Karakorum (HCI 8 ± 1) and Southern Karakorum (HCI 20 ± 5) have apparent differences on their petrographic, mineralogical and chronological signatures (Fig. 6.3 and 6.6). The main age peak at ~ 60 Ma in Northern and Central Karakorum is negligible in the age spectrum of Thal Desert sand. Combined with the abundant high-Mn garnet, allanite and Ca-poor (Wo ~ 30) augite (Liang et al., 2019), a major contribution from the Northern and Central Karakorum can be ruled out. The Southern Karakorum belt drained by the Hispar tributary, was revealed as important provenance area, according to the corresponding garnet and amphibole species, and the zircon age distribution (100-120 Ma and ~ 20 Ma, Fig. 6.6). Besides, the chemical fingerprint of the Hispar sand correspond well with the Thal Desert sand, especially the sample S1470 (Fig. 6.4).

Nanga Parbat

The Nanga Parbat Massif sheds high rank quartzo-feldspathic detritus, which is different from Thal dune sand (Fig. 6.3A). The very negative ε_{Nd} value does not indicate a major sand contribution for the Thal Desert (Table 6.1). However, the characteristic age peak at ~ 1850 Ma occurs also in dune sand (Fig. 6.6). Mineral varietal studies show the presence of tschermakite and abundant type Ci garnets in Thal Desert sand, which may be explained by significant supply from the Nanga Parbat Massif (Liang et al., 2019).

Himalaya

Sediment delivered by Himalayan tributaries is characterized by high Q/F values of 2 ~ 3 and high amount of high-rank metamorphic minerals (e.g. garnet, kyanite, sillimanite), differing from the Thal Desert petrographic signatures (Table 6.1). The more negative ε_{Nd} value and distinct geochemical variability preclude the Himalaya as a major sand provenance to the Thal Desert. The U-Pb age spectrum indicate the zircon age clusters at 700-1000 Ma and 1500-2300 Ma may be supplied by the Himalaya, even though the Paleozoic age cluster at 350-500 Ma is lacking in eolian sand (Fig. 6.6). The varietal study shows that the common high-Mn garnets, Ca-poor augite (Wo < 40) in Greater Himalaya are sporadic in Thal dunes (Liang et al., 2019).

Sediment budget

Based on the signatures of all different potential sources illustrated above, the relative contributions from various rivers and geological domains can be tentatively calculated by forward mixing models (Garzanti et al., 2012). The calculation depending on a variety of assumptions (e.g., lack of mechanical breakdown, chemical dissolution, and/or hydraulic sorting), which are never strictly verified. Four samples from the Karakorum, and two from the Kohistan Arc, Ladakh Arc and Himalaya, respectively, were considered. Calculations according to the single groups of minerals (i.e., amphibole, epidote and pyroxene) were also carried out. This range of separate trials, together with isotopic and geochronological information, proved to be essential in testing the overall consistency of the results obtained.

The overall bulk-sediment budget calculated from the integrated petrographic-mineralogical data set indicates that the sediment was provided mainly by the Kohistan Arc (34%), the Karakorum (31%) and the Himalaya (24%), with the remaining 7% from the Ladakh Arc and 4% from the Nanga Parbat Massif. Calculation based on amphibole group mineral indicates that the major amphibole source in Thal Desert is represented by the Kohistan Arc (64%), with minor contribution from the Karakorum (17%), Ladakh Arc (10%) and Nanga Parbat Massif (9%). A majority of the pyroxene and epidote minerals (70%) were supplied by the Kohistan Arc.

Considering all potential source areas, the Kohistan Arc (40%) and the Himalaya (24%) have provided the major sediment in the Thal Desert, with subordinate contributions from the Karakorum (10%), Kabul River (9%), Nanga Parbat (7%), Soan River (7%) and Ladakh Arc (3%).

Zircon grains dated between 40 Ma and100 Ma, accounting for 42% of the total age spectrum, also reflect a major supply from the Kohistan Arc, which is consistent with the calculation from the bulk petrographic and mineralogical data.

6.6 Paleoclimates and paleodrainages

6.6.1 Distinct erosion pattern for the Thal Desert

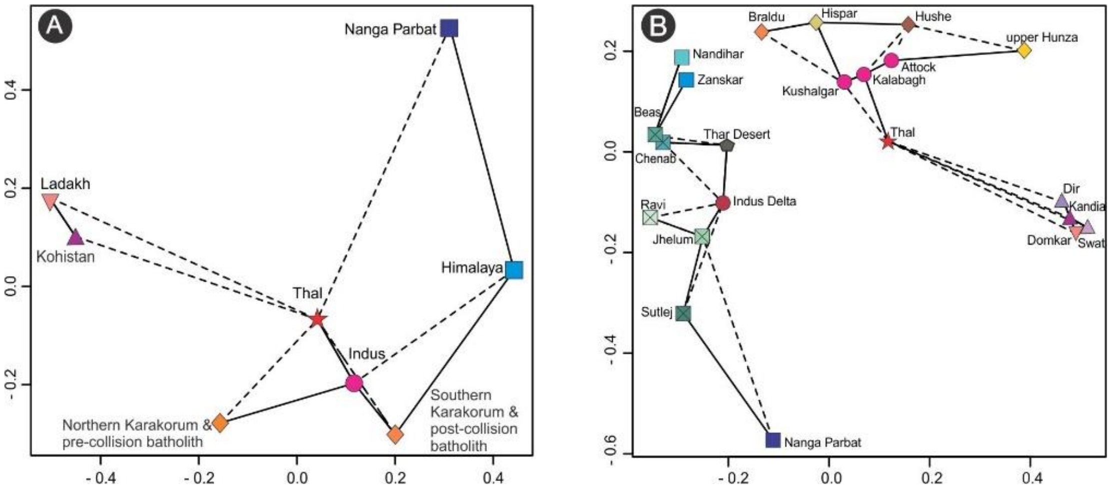

Figure 6.7 Multidimensional scaling (MDS) plot. (A) Thal Desert sample and its potential provenance end-members (Stress value, 10.9%). Thal Desert sand has closest connection with Indus sand upstream of the Thal Desert, and then the Karakorum, Kohistan and Ladakh arcs, and Nanga Parbat Massif. (B) Thal Desert sand and samples from Indus drainage (Stress value, 2.3%). Sediment in the lower reaches of the Indus River has close relationship with the Himalaya-derived detritus. The group configurations show the salient similarities and differences between samples as a 'map' in which similar samples plot close together and dissimilar samples plot far apart. Solid lines mark the closest neighbours and dashed lines the second closest neighbours. Data sources same as Fig. 6.6.

The closest connection between the Thal Desert sand and the modern Indus sand upstream of the Thal Desert (Fig. 6.7) reflects that the dune sand was mainly delivered by the Indus River. The eolian Thal sand have a peculiar composition, characterized by higher feldspars, more concentrated heavy mineral assemblages and less negative ε_{Nd} value with respect to the trunk river sand at the Salt Range front. The Indus trunk sediment at the Salt Range front was mainly from the Kabul River (33%) and Karakorum (32%), with subordinate contributions from Soan River (11%), Kohistan Arc (8%), Nanga Parbat (7%), and equally less contributions from Himalaya and Ladakh Arc (Garzanti et al., 2005). The Thal sand, by contrast, receives higher sediment supply from the Kohistan Arc (40% *vs.* 8%) and Himalaya (24% *vs.* 3%), and less from Karakorum (10% *vs.* 32%) and Kabul (9% *vs.* 33%).

Because the Karakorum (60%) rather than the Kohistan (14%) and Himalaya (6%) provides the majority of the pre-dam sediment (Garzanti et al., 2005), which is inconsistent with Thal Desert sand, the anthropic activities and the huge amount of sediment presently trapped in the Tarbela Reservoir cannot explain the great sediment budget differences.

In consideration of the all these compositional signatures in Thal Desert and its relationship with Indus River system, we tentatively interpret here the desert sand as fed from the trunk river carried much more feldspar sediment in a recent past period when more intense erosion happened in Asian margin batholiths and in general of granitoid bodies exposed at high altitudes.

6.6.2 When and how did the desert form?

The significant Kohistan Arc signatures in the Thal Desert sand, can be compared with those of the Indus Fan turbidites (Suczek and Ingersoll, 1985) and Indus Delta (Clift et al., 2010) deposited at Late Pleistocene – early Holocene when more intense erosion of granitoid bodies in high altitudes happened. The Indus Fan turbidites display more richer feldspars than sand of the modern Indus delta, resulting from the large contribution from Kohistan Arc. The river delta sand deposited at Last Glacial Maximum (LGM) shows less negative ε_{Nd} and higher Transhimalaya arcs age (30% - 45%) in sediment of Indus Delta deposited at 20 Ka to 7 Ka (Clift et al., 2010). Considering the ca. 7 - 14 Ka transport time of zircon grains in bedload (Clift and Giosan, 2014), these chronological signatures represent the zircon age spectra of deposit at least at LGM period, fitting well with the that of sand in Thal Desert.

The mountain glaciers and continental ice sheets during the last glacial cycle generally have diachronous maximum extents (Hughes et al., 2013), and the maximum extent of glaciation in Himalaya area may have occurred earlier than the LGM (Gillespie and Molnar, 1995; Benn and Owen, 1998). During the last glacial cycle, glaciation in the Kohistan (e.g., Swat Himalaya) area was extensive, and may be restricted in the LGM (Owen et al., 2002). The deglaciation during the late last glacial cycle caused the post-glacial rebound (Árnadóttir et al., 2009) and climate change, increasing the erosion rates in the Himalayan orogen, especially in the Kohistan Arc, and generating more detritus to the Indus River system. The intense erosion also fit well with the higher sediment discharge of Himalayan rivers until the early Holocene (Goodbred and Kuhel, 2000).

Another potential process is a high monsoon precipitation focused on the Kohistan Arc. The precipitation pattern in the Himalayan orogen is strongly controlled by topography and shows a marked gradient across the mountains from the dry area of Ladakh, Karakorum and Tibet in the north to the wet southern Himalaya and part Kohistan region (Anders et al., 2006). The higher rainfall during the intense monsoon in the early Holocene (Clift et al., 2008) may have driven the Kohistan Arc and Himalaya to provide more detritus into the Indus system, contributing the sand accumulation in Thal Desert, which is consistent with a slightly increase in hypersthene from 9 Ka in the Indus Delta (Clift et al., 2010).

The fluvial–eolian interactions (East et al., 2015) has been recognized as an important process buffering sedimentary signals in a sediment-routing system. In the Punjab plain, mixing with eolian sand (locally > 20% of bulk detritus) is consistently documented by both detrital modes (decreasing Q/F ratios, increasing rank of metamorphic grains) and dense minerals (increase in hornblende and pyroxenes, including hypersthene) all along the eastern side of the Thal Desert, from the lowest reaches of the Jhelum and Chenab to final Ravi and Punjab-Indus confluence (Garzanti et al., 2005).

Sediment in the lower Indus course can be considered as the mixing of the Punjab river sediment and Indus sediment upstream of the Thal Desert in relatively equal amount, whereas sediment in the Indus Delta cores can be considered as the mixing from the Punjab sediment and Thal Desert sediment in similar proportion (Fig. 6.8).

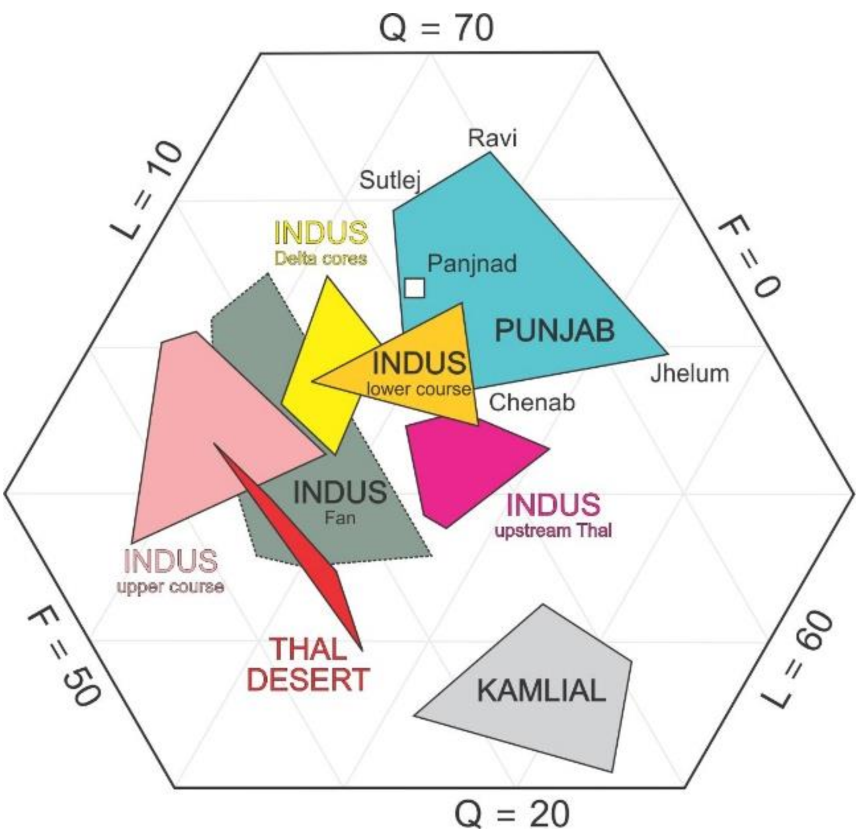

Figure 6.8 Petrographic signatures of sand from the Thal Desert and Indus system. Feldspar content showing a decreasing trend from the Thal Desert to Punjab, and the lower Indus sand could be regarded as the mixing of these two end-members. Petrographic data from the Kamlial Formation and the Indus Fan after Najman et al. 2003 and Suczek and Ingersoll, 1985, respectively.

The Indus Fan sediment is characterized by rich feldspar (Fig. 6.8) and less negative ε_{Nd} signatures (Clift et al., 2002), compared with the sediment of the current Indus lower course and delta. These significant differences can be hardly ascribed to sedimentary differentiation alone (e.g., Zuffa 1987). The Thal Desert sand may suggest a different idea, that the Indus Fan sediment can be better explained by mixing of major ancient feldspathic Indus sediment before the Punjab tributaries with minor Himalayan derived detritus (Fig. 6.8).

6.7 Conclusions

The Thal Desert, located at the entry point in the Himalayan foreland basin, provides the crucial information to understand the stratigraphic record of Indus River and helps to reconstruct the erosion history of the western Himalayan syntaxis in northern Pakistan. The Thal Desert sand is characterized by litho-feldspatho-quartzose to quartzo-feldspatho-lithic detrital modes and very rich heavy-mineral assemblages dominated by amphibole. The much less negative ε_{Nd} value, more young zircons aged at Paleocene to Late Cretaceous compared with those in the upstream of the Thal Desert, combined with the detailed mineral varietal studies, both reflects a great contribution from granitoid rocks.

The overall petrographic, mineralogical, isotopic and geochronological signatures of Thal dunes show the sediment was largely fed by the Kohistan Arc and Karakorum, with only minor supply from the Himalaya range. The distinct erosion pattern significantly different from the modern Indus system, indicates that the Thal dunes fed from the paleo-Indus River in the Late Pleistocene to early Holocene when erosion was focused in high glaciated areas formed largely around granitoids batholites of the Asian active margin. The distinct composition comparable with the LGM deposit in Indus Delta and Indus Fan turbidites sheds new light on the understanding of the paleo-Indus system and erosional evolution in the western Himalayan Syntaxis.

References

Ahmad, T., Harris, N., Bickle, M., Chapman, H., Bunbury, J., Prince, C., 2000. Isotopic constraints on the structural relationships between the lesser Himalayan series and the high Himalayan crystalline series, Garhwal Himalaya. Geological Society of America Bulletin, 112(3), 467-477.

Aitchison, J.C., Xia, X., Baxter, A.T., Ali, J.R., 2011. Detrital zircon U–Pb ages along the Yarlung-Tsangpo suture zone, Tibet: implications for oblique convergence and collision between India and Asia. Gondwana Research, 20 (4), 691-709.

Aikman, A.B., Harrison, T.M., Lin, D., 2008. Evidence for early (> 44 Ma) Himalayan crustal thickening, Tethyan Himalaya, southeastern Tibet. Earth and Planetary Science Letters, 274(1-2), 14-23.

Aleinikoff, J.N., Wintsch, R.P., Fanning, C.M., Dorais, M.J., 2002. U–Pb geochronology of zircon and polygenetic titanite from the Glastonbury Complex, Connecticut, USA: an integrated SEM, EMPA, TIMS, and SHRIMP study. Chemical Geology, 188, 125-147.

Alizai, A., Clift, P.D., Giosan, L., Van Laningham, S., Hinton, R., Tabrez, A.R., Danish, M., The Edinburgh Ion Microprobe Facility (EIMF), 2011a. Pb isotopic variability in the modern-Pleistocene Indus River system measured by ion microprobe in detrital K-feldspar grains. Geochemistry and Cosmochemistry Acta, 75, 4771-4795.

Alizai, A., Carter, A., Clift, P.D., Van Laningham, S., Williams, J.C., Kumar, R., 2011b. Sediment provenance, reworking and transport processes in the Indus River by U–Pb dating of detrital zircon grains. Global and Planetary Change, 76(1-2), 33-55.

Alizai, A., Hillier, S., Clift, P. D., Giosan, L., Hurst, A., VanLaningham, S., Macklin, M., 2012. Clay mineral variations in Holocene terrestrial sediments from the Indus Basin. Quaternary Research, 77(3), 368-381.

Alizai, A., Clift, P. D., Still, J., 2016. Indus Basin sediment provenance constrained using garnet geochemistry. Journal of Asian Earth Sciences, 126, 29-57.

Amorosi, A., 2012. Chromium and nickel as indicators of source-to-sink sediment transfer in a Holocene alluvial and coastal system (Po Plain, Italy). Sedimentary Geology, 280, 260-269.

An, W., Hu, X., Garzanti, E., BouDagher-Fadel, M. K., Wang, J., Sun, G., 2014. Xigaze forearc basin revisited (South Tibet): Provenance changes and origin of the Xigaze Ophiolite. Bulletin, 126(11-12), 1595-1613.

An, W., Hu, X., Garzanti, E., 2017. Sandstone provenance and tectonic evolution of the Xiukang Mélange from Neotethyan subduction to India–Asia collision (Yarlung-Zangbo suture, south Tibet). Gondwana Research, 41, 222-234.

Anczkiewicz, R., Burg, J.P., Hussain, S.S., Dawood, H., Ghazanfar, M., Chaudhry, M.N., 1998. Stratigraphy and structure of the Indus Suture in the lower Swat, Pakistan, NW Himalaya. Journal of Asian Earth Sciences, 16(2-3), 225-238.

Anders, A.M., Roe, G.H., Hallet, B., Montgomery, D.R., Finnegan, N.J., Putkonen, J., 2006. Spatial patterns of precipitation and topography in the Himalaya. In: Willet S.D., Hovius N., Brandon M.T., Fisher D.M. (Eds.) Tectonics, Climate, and Landscape Evolution. Geological Society of America Special Papers, 398, 39-53.

Andersen, T., 2005. Detrital zircons as tracers of sedimentary provenance: limiting conditions from statistics and numerical simulation. Chemical Geology, 216, 249-270.

Andò, S., 2017. Raman counting of heavy minerals in turbidites: Indus Fan, IODP Expedition 355. In EGU General Assembly Conference Abstracts (Vol. 19, p. 13814).

Andò S., Garzanti, E., 2014. Raman spectroscopy in heavy-mineral studies. In: Scott, R.A., Smyth. H.R., Morton, A.C., Richardson, N. (Eds.), Sediment Provenance Studies in Hydrocarbon Exploration and Production. Geological Society London, Special Publication 386(1), 395-412.

Andò, S., Garzanti, E., Padoan, M., Limonta, M., 2012. Corrosion of heavy minerals during weathering and diagenesis: a catalogue for optical analysis. In: von Eynatten, H., Critelli, S., Ingersoll, R.V., Weltje, G.J., Actualistic Models of Sediment Generation. Sedimentary Geology, 280, pp. 165-178.

Andò, S., Morton, A., Garzanti, E., 2014. Metamorphic grade of source rocks revealed by chemical fingerprints of detrital amphibole and garnet. In: Scott, R.A., Smyth, H.R., Morton, A.C., Richardson, N., (Eds.), Sediment Provenance Studies in Hydrocarbon Exploration and Production. Geological Society: London, UK; Special Publication 386; pp.351-371.

Andò, S., Aharonovich, S., Hahn, A., George, S.C., Clift, P.D., Garzanti, E., 2019. Integrating heavy-mineral, geochemical and biomarker analyses of Plio-Pleistocene sandy and silty turbidites: a novel approach for provenance studies (Indus Fan, IODP Expedition 355). Geological Magazine, 1-10.

Armbruster, T., Bonazzi, P., Akasaka, M., Bermanec, V., Chopin, C., Gieré, R., Heuss-Assbichler, S., Liebscher, A., Menchetti, S., Pan, Y., Pasero, M., 2006. Recommended nomenclature of epidote-group minerals. European Journal of Mineralogy, 18(5), 551-567.

Árnadóttir, T., Lund, B., Jiang, W., Geirsson, H., Björnsson, H., Einarsson, P., Sigurdsson, T., 2009. Glacial rebound and plate spreading: results from the first countrywide GPS observations in Iceland. Geophysical Journal International, 177(2), 691-716.

Badshah, M.S., Gnos, E., Jan, M.Q., Afridi, M.I., 2000. Stratigraphic and tectonic evolution of the northwestern Indian plate and Kabul Block. In: Khan, M.A. (Ed.), Tectonics of the Nanga Parbat Syntaxis and the Western Himalaya. Geological Society, London, Special Publications, 170, 467-476.

Bateman, R.M., Catt, J.A., 2007. Provenance and palaeoenvironmental interpretation of superficial deposits, with particular reference to post-depositional modification of heavy-mineral assemblages. In: Mange, M.A., Wright, D.T. (Eds.), Heavy Minerals in Use, Developments in Sedimentology Series 58. Elsevier, Amsterdam, pp. 151-188.

Belousova, E.A., Griffin, W.L., O'Reilly, S.Y., Fisher, N.I., 2002a. Igneous zircon: trace element composition as an indicator of source rock type. Contributions to Mineralogy and Petrology, 143, 602-622.

Belousova, E.A., Griffin, W.L., O'Reilly, S.Y., Fisher, N.I., 2002b. Apatite as an indicator mineral for mineral exploration: trace-element compositions and their relationship to host rock type. Journal of Geochemical Exploration, 76, 45-69.

Benn, D. I., Owen, L.A., 1998. The role of the Indian summer monsoon and the mid-latitude westerlies in Himalayan glaciation: review and speculative discussion. Journal of the Geological Society, 155(2), 353-363.

Bersani, D., Andò, S., Vignola, P., Moltifiori, G., Marino, I.G, Lottici, P.P, and Diella, V., 2009. Micro-Raman spectroscopy as a routine tool for garnet analysis. Spectrochimica Acta Part A: Molecular and Biomolecular Spectroscopy, 73(3), 484-491.

Beyssac, O., Rouzaud, J.N., Goffe, B., Brunet, F., Chopin, C., 2002. Graphitization in a high-pressure, low-temperature metamorphic gradient: a Raman microspectroscopy and HRTEM study. Contributions to Mineralogy and Petrology, 143(1), 19-31.

Bhuiyan, M.A.H., Rahman, M.J.J., Dampare, S.B., Suzuki, S., 2011. Provenance, tectonics and source weathering of modern fluvial sediments of the Brahmaputra–Jamuna River, Bangladesh: inference from geochemistry. Journal of Geochemical Exploration, 111(3), 113-137.

Bizzarro, M., Simonetti, A., Stevenson, R.K., Kurslaukis, S., 2003. In situ $^{87}Sr/^{86}Sr$ investigation of igneous apatites and carbonates using laser-ablation MC-ICP-MS. Geochimica et Cosmochimica Acta, 67, 289-302.

Blatt, H., 1985. Provenance studies and mudrocks. Journal of Sedimentary Research, 55(1), 69-75.

Blayney, T., Najman, Y., Dupont-Nivet, G., Carter, A., Millar, I., Garzanti, E., Sobel, E.R., Rittner, M., Andò, S., Guo, Z., Vezzoli, G., 2016. Indentation of the Pamirs with respect to the northern margin of Tibet: Constraints from the Tarim basin sedimentary record. Tectonics, 35(10), 2345-2369.

Bookhagen, B., Burbank, D.W., 2006. Topography, relief, and TRMM-derived rainfall variations along the Himalaya. Geophysical Research Letters, 33, L08405. https://doi.org/10.1029/2006GL026037

Borges, J.B., Huh, Y., Moon, S., Noh, H., 2008. Provenance and weathering control on river-bed sediments of the eastern Tibetan Plateau and the Russian Far East. Chemical Geology, 254, 52-72.

Borges, J., Huh, Y., 2007. Petrography and chemistry of the bed sediments of the Red River in China and Vietnam: provenance and chemical weathering. Sedimentary Geology, 194, 155-168.

Borneman, N.L., Hodges, K.V., Van Soest, M.C., Bohon, W., Wartho, J.A., Cronk, S.S., Ahmad, T., 2015. Age and structure of the Shyok sutures in the Ladakh region of northwestern India: implications for slip on the Karakoram fault system. Tectonics, 34(10), 2011-2033.

Bossart, P., Ottiger, R., 1989. Rocks of the Murree Formation in northern Pakistan: indicators of descending for the basin of late Paleocene to middle Eocene age. Eclogae Geologicae Helvetiae, 82 (1), 133-165.

Bouchez, J., Lupker, M., Gaillardet, J., France-Lanord, C., Maurice, L., 2011a. How important is it to integrate riverine suspended sediment chemical composition with depth? Clues from Amazon River depth-profiles. Geochimica et Cosmochimica Acta, 75(22), 6955-6970.

Bouchez, J., Gaillardet, J., France-Lanord, C., Maurice, L., Dutra-Maia, P., 2011b. Grain size control of river suspended sediment geochemistry: Clues from Amazon River depth profiles. Geochemistry, Geophysics, Geosystems, 12(3), Q03008.

Bouvier, A., Vervoort, J.D., Patchett, P.J., 2008. The Lu–Hf and Sm–Nd isotopic composition of CHUR: constraints from unequilibrated chondrites and implications for the bulk composition of terrestrial planets. Earth and Planetary Science Letters, 273(1-2), 48-57.

Boyce, J., Hodges, K.V., Olszewski, W.J., Jercinovic, M.J., Carpenter, B.D., Reiners, P.W., 2006. Laser microprobe (U–Th)/He geochronology. Geochimica et Cosmochimica Acta, 70, 3031-3039.

Brewer, I.D., Burbank, D.W., Hodges, K.V., 2006. Downstream development of a detrital cooling-age signal: insights from $^{40}Ar/^{39}Ar$ muscovite thermochronology in the Nepalese Himalaya. In: Willett, S.D., Hovius, N., Brandon, M.T., Fisher, D. (Eds.), Tectonics, Climate, and Landscape Evolution: Geological Society of America Special Paper: Penrose Conference Series, 398, pp. 321-338.

Briggs, L.I., McCulloch, D.S., Moser, F., 1962. The hydraulic shape of sand particles. Journal of Sedimentary Research, 32(4), 645-656.

Brown, D.J., Helmke, P.A., Clayton, M.K., 2003. Robust geochemical indices for redox and weathering on a granitic laterite landscape in central Uganda. Geochimica et Cosmochimica Acta, 67(15), 2711-2723.

Bunaciu, A.A., UdriŞTioiu, E.G., Aboul-Enein, H.Y., 2015. X-ray diffraction: instrumentation and applications. Critical Reviews in Analytical Chemistry, 45(4), 289-299.

Burbank, D.W., Leland, J., Fielding, E., Anderson, R.S., Brozovic, N., Reid, M.R., Duncan, C., 1996a. Bedrock incision, rock uplift and threshold hillslopes in the northwestern Himalayas. Nature, 379(6565), 505-510.

Burbank, D.W., Beck, R.A., Mulder, T., 1996b. The Himalayan foreland basin. In: Yin, A., Harrison, T.M., (eds.), The Tectonic Evolution of Asia (World and regional geology). Cambridge University Press: Cambridge, UK; pp.149-188.

Burbank, D.W., Blythe, A.E., Putkonen, J., Pratt-Sitaula, B., Gabet, E., Oskin, M., Barros, A., Ojha, T.P., 2003. Decoupling of erosion and precipitation in the Himalayas. Nature, 426 (6967), 652-655.

Burg, J.P., 2011. The Asia–Kohistan–India collision: review and discussion. In: Brown, D., Ryan, P.D., (Eds.), Arc-Continent Collision. Springer-Verlag Berlin Heidelberg, Berlin, Germany; pp. 279-309.

Burg, J.P., Leyreloup, A., Girardeau, J., Chen, G.M., 1987. Structure and metamorphism of a tectonically thickened continental crust: the Yalu Tsangpo suture zone (Tibet). Philosophical transactions of the Royal Society of London. Series A, Mathematical and Physical Sciences, 321(1557), 67-86.

Cai, F., Ding, L., Yue, Y., 2011. Provenance analysis of upper Cretaceous strata in the Tethys Himalaya, southern Tibet: implications for timing of India–Asia collision. Earth and Planetary Science Letters, 305(1-2), 195-206.

Campbell, I.H., Reiners, P.W., Allen, C.M., Nicolescu, S., Upadhyay, R., 2005. He–Pb double dating of detrital zircons from the Ganges and Indus Rivers: implication for quantifying sediment recycling and provenance studies. Earth and Planetary Science Letters, 237(3-4), 402-432.

Caracciolo, L., Andò, S., Vermeesch, P., Garzanti, E., McCabe, R., Barbarano, M., Pareari, C., Rittner, M., Pearce, T., 2019. A multidisciplinary approach for the quantitative provenance analysis of siltstone: Mesozoic Mandawa Basin, southeastern Tanzania. In: DOWEY, P., OSBORNE, M., VOLK, H. (Eds.), Application of Analytical Techniques to Petroleum Systems. Geological Society, London, Special Publications, 484, https://doi.org/10.1144/SP484-2018-136.

Carosi, R., Montomoli, C., Iaccarino, S., 2018. 20 years of geological mapping of the metamorphic core across Central and Eastern Himalayas. Earth-Science Reviews, 177, 124-138.

Carrapa, B., Faiz bin Hassim, M., Kapp, P. A., DeCelles, P. G., Gehrels, G., 2017. Tectonic and erosional history of southern Tibet recorded by detrital chronological signatures along the Yarlung River drainage. Bulletin, 129(5-6), 570-581.

Carver, R.E., 1971. Heavy-mineral separation. In: Carver, R.E. (Ed.), Procedures in Sedimentary Petrology. Wiley, New York, pp. 427-452.

Cerveny, P.F., Johnson, N.M., Tahirkheli, R.A.K., Bonis, N.R., 1989. Tectonic and geomorphic implications of Siwalik group heavy minerals, Potwar plateau, Pakistan. In: Malinconico, L.L., Lillie, R.J., (Eds.), Tectonics of the Western Himalayas. Geological Society of America, Special Papers, 232, 129-136.

Chamberlain, C.P., Zeitler, P.K., Barnett, D.E., Winslow, D., Poulson, S.R., Leahy, T., Hammer, J.E., 1995. Active hydrothermal systems during the recent uplift of Nanga Parbat, Pakistan Himalaya. Journal of Geophysical Research: Solid Earth, 100(B1), 439-453.

Chen, F., Zhu, X., Wang, W., Wang, F., Hieu, P.T., Siebel,W., 2009. Single-grain detrital muscovite Rb–Sr isotopic composition as an indicator of provenance for the Carboniferous sedimentary rocks in northern Dabie, China. Geochemical Journal, 43, 257-273.

Chetel, L.M., Simo, J.A., Singer, B.S., 2005. $^{40}Ar/^{39}Ar$ geochronology and provenance of detrital K-feldspars, Ordovician, Upper Mississippi Valley. Sedimentary Geology, 182, 163-181.

Chen, Z., Liu, Y., Hodges, K.V., Burchfiel, B.C., Royden, L.H., Deng, C., 1990. The Kangmar Dome: A metamorphic core complex in southern Xizang (Tibet). Science, 250 (4987), 1552-1556.

Chew, D.M., Sylvester, P.J., Tubrett, M.N., 2011. U–Pb and Th–Pb dating of apatite by LA-ICPMS. Chemical Geology, 280, 200-216.

Cina, S.E., Yin, A., Grove, M., Dubey, C.S., Shukla, D.P., Lovera, O.M., Kelty, T.K., Gehrels, G.E., Foster, D.A., 2009. Gangdese arc detritus within the eastern Himalayan Neogene foreland basin: implications for the Neogene evolution of the Yalu–Brahmaputra River system. Earth and Planetary Science Letters, 285(1-2), 150-162.

Clift, P. D., Giosan, L., 2014. Sediment fluxes and buffering in the post-glacial Indus Basin. Basin Research, 26(3), 369-386.

Clift, P., Shimizu, N., Layne, G., Gaedicke, C., Schlter, H.U., Clark, M., Amjad, S., 2000a. Fifty-five million years of Tibetan evolution recorded in the Indus Fan. Eos, Transactions American Geophysical Union, 81(25), 277-281.

Clift, P.D., Degnan, P.J., Hannigan, R., Blusztajn, J., 2000b. Sedimentary and geochemical evolution of the Dras forearc basin, Indus suture, Ladakh Himalaya, India. Geological Society of America Bulletin, 112(3), 450-466.

Clift, P.D., Shimizu, N., Layne, G.D., Blusztajn, J.S., Gaedicke, C., Schluter, H.U., Clark, M.K, Amjad, S., 2001. Development of the Indus Fan and its significance for the erosional history of the Western Himalaya and Karakoram. Geological Society of America Bulletin, 113(8), 1039-1051.

Clift, P.D., Lee, J.I., Hildebrand, P., Shimizu, N., Layne, G.D., Blusztajn, J., Blum, J.D., Garzanti, E., Khan, A.A., 2002. Nd and Pb isotope variability in the Indus River system: implications for sediment provenance and crustal heterogeneity in the Western Himalaya. Earth and Planetary Science Letters, 200, 91-106.

Clift, P.D., Campbell, I.H., Pringle, M.S., Carter, A., Zhang, X., Hodges, K.V., Khan, A.A., Allen, C.M., 2004. Thermochronology of the modern Indus River bedload: New insight into the controls on the marine stratigraphic record. Tectonics, 23, TC5013.

Clift, P.D., Giosan, L., Blusztajn, J., Campbell, I.H., Allen, C., Pringle, M., Tabrez, A.R., Danish, M., Rabbani, M.M., Alizai, A., Carter, A., Lückge, A., 2008. Holocene erosion of the Lesser Himalaya triggered by intensified summer monsoon. Geology, 36(1), 79-82.

Clift, P.D., Giosan, L., Carter, A., Garzanti, E., Galy, V., Tabrez, A.R., Pringle, M., Campbell, I.H., France-Lanord, C., Blusztajn,J., Allen, C., Alizai, A., Lückge, A., Danish, M., Rabbani, M.M., 2010. Monsoon control over erosion patterns in the western Himalaya: possible feed-back into the tectonic evolution. In: Clift, P.D., Tada, R., Zheng, H., (Eds.), Monsoon Evolution and Tectonic-Climate Linkage in Asia. Geological Society, London, Special Publications, 342(1), 185-218.

Clift, P.D., Giosan, L., Henstock, T.J., and Tabrez, A.R., 2014. Sediment storage and reworking on the shelf and in the Canyon of the Indus River-Fan System since the last glacial maximum. Basin Research, 26(1), 183-202.

Cohen, H.A., Hall, C.M., Lundberg, N., 1995. Dating of detrital grains constrains the provenance and stratigraphy of the Gravina belt, Southeastern Alaska. Journal of Geology, 103, 327-337.

Coleman, J.M., 1969. Brahmaputra River: channel processes and sedimentation. Sedimentary geology, 3(2-3), 129-239.

Crawford, MB, Searle, MP, 1992. Field relationships and geochemistry of pre-collisional (India-Asia) granitoid magmatism in the central Karakoram, northern Pakistan. Tectonophysics, 206 (1-2), 171-192.

Dai, J., Wang, C., Polat, A., Santosh, M., Li, Y., Ge, Y., 2013. Rapid forearc spreading between 130 and 120 Ma: evidence from geochronology and geochemistry of the Xigaze ophiolite, southern Tibet. Lithos, 172, 1-16.

Datta, D. K., Subramanian, V., 1997. Texture and mineralogy of sediments from the Ganges-Brahmaputra-Meghna river system in the Bengal Basin, Bangladesh and their environmental implications. Environmental Geology, 30(3-4), 181-188.

DeCelles, P.G., Gehrels, G.E., Quade, J., Lareau, B., Spurlin, M., 2000. Tectonic Implications of U-Pb Zircon Ages of the Himalayan Orogenic Belt in Nepal. Science, 288(5465): 497-499.

DeCelles, P.G., Gehrels, G.E., Najman, Y., Martin, A.J., Carter, A., Garzanti, E., 2004. Detrital geochronology and geochemistry of Cretaceous Early Miocene strata of Nepal: implications for timing and diachroneity of initial Himalayan orogenesis. Earth Planetary Science Letters, 227(3): 313-330.

DeCelles, P.G., Kapp, P., Gehrels, G.E., Ding, L., 2014. Paleocene-Eocene foreland basin evolution in the Himalaya of southern Tibet and Nepal: Implications for the age of initial India-Asia collision. Tectonics, 33(5), 824-849.

Decou, A., von Eynatten, H., Mamani, M., Sempere, T., Wörner, G., 2011. Cenozoic forearc basin sediments in Southern Peru (15–18°S): stratigraphic and heavy mineral constraints for Eocene to Miocene evolution of the Central Andes. Sedimentary Geology, 237, 55-72.

Deniel, C., Vidal, P., Fernandez, A., Le Fort, P., Peucat, J.J., 1987. Isotopic study of the Manaslu granite (Himalaya, Nepal): inferences on the age and source of Himalayan leucogranites. Contributions to Mineralogy and Petrology, 96(1), 78-92.

DePaolo, D.J., Wasserburg, G.J., 1976. Nd isotopic variations and petrogenetic models. Geophysical Research Letters, 3, 249-252.

Derry, L.A., France-Lanord, C., 1996. Neogene Himalayan weathering history and river $^{87}Sr/^{86}Sr$; impact on the marine Sr record. Earth and Planetary Science Letters, 142(1-2), 59-74.

Dhuime, B., Bosch, D., Garrido, C.J., Bodinier, J.L., Bruguier, O., Hussain, S.S., Dawood, H., 2009. Geochemical architecture of the lower-middle section of a paleo-island arc (Kohistan Complex, Jijal – Kamila area, northern Pakistan): implications for the evolution of an oceanic subduction zone. Journal of Petrology, 50 (3), 531-569.

Dickinson, W.R., 1970. Interpreting detrital modes of graywacke and arkose. Journal of Sedimentary Research, 40 (2), 695-707.

Dickinson, W.R., 1985, Interpreting provenance relations from detrital modes of sandstones, In: Zuffa, G.G., (Ed.), Provenance of Arenites. Reidel, Dordrecht, Netherlands, NATO ASI Series, 148, 333-361.

Dickinson, W.R., 2008. Impact of differential zircon fertility of granitoid basement rocks in North America on age populations of detrital zircons and implications for granite petrogenesis. Earth and Planetary Science Letters, 275, 80-92.

Dickinson, W.R., Gehrels, G.E., 2009. U-Pb ages of detrital zircons in Jurassic eolian and associated sandstones of the Colorado Plateau: Evidence for transcontinental dispersal and intraregional recycling of sediment. Geological Society of America Bulletin, 121(3-4), 408-433.

DiPietro, J.A., Pogue, K.R., 2004. Tectonostratigraphic subdivisions of the Himalaya: A view from the west. Tectonics, 23(5). TC5001.

Dodson, M.H., Compston, W., Williams, I.S., Wilson, J.F., 1988. A search for ancient detrital zircons in Zimbabwean sediments. Journal of the Geological Society, 145, 977-983.

Dunkl, I., Frisch, W., Kuhlemann, J., Brügel, A., 2009. Pebble population dating as an additional tool for provenance studies-examples from the Eastern Alps. Geological Society, London, Special Publications, 324(1), 125-140.

East, A.E., Clift, P.D., Carter, A., Alizai, A., VanLaningham, S., 2015. Fluvial-eolian interactions in sediment routing and sedimentary signal buffering: an example from the Indus Basin and Thar Desert. Journal of Sedimentary Research, 85 (6), 715-728.

Einsele, G., Hinderer, M., 1997. Terrestrial sediment yield and the lifetimes of reservoirs, lakes, and larger basins. Geologische Rundschau, 86 (2), 288-310.

Enkelmann, E., Ehlers, T.A., Zeitler, P.K., Hallet, B., 2011. Denudation of the Namche Barwa antiform, eastern Himalaya. Earth and Planetary Science Letters, 307(3-4), 323-333.

Enzel, Y., Ely, L.L., Mishra, S., Ramesh, R., Amit, R., Lazar, B., Rajaguru, S.N., Baker, V.R., Sandler, A., 1999. High-resolution Holocene environmental changes in the Thar Desert, northwestern India. Science, 284(5411), 125-128.

Faran Ali, K., de Boer, D.H., 2008. Factors controlling specific sediment yield in the upper Indus River basin, northern Pakistan. Hydrological Processes, 22(16), 3102-3114.

Ferguson, R.I., 1984. Sediment load of the Hunza River. In: Miller, K.J., (Ed.), The International Karakoram Project. Cambridge University Press: Cambridge, UK; Volume 2, pp. 581-598.

Flint, J.J., 1974. Stream gradient as a function of order, magnitude, and discharge. Water Resources Research, 10(5), 969-973.

Foster, G.L., Carter, A., 2007. Insights into the patterns and locations of erosion in the Himalaya — a combined fission-track and in situ Sm–Nd isotopic study of detrital apatite. Earth and Planetary Science Letters, 257, 407-418.

France-Lanord, C., Derry, L., Michard, A., 1993. Evolution of the Himalaya since Miocene time: isotopic and sedimentological evidence from the Bengal Fan. In: Treloar, P.J., Searle, M.P., (Eds.), Himalayan Tectonics. Geological Society, London, Special Publications, 74(1), 603-621.

Fraser, J.E., Searle, M.P., Parrish, R.R., Noble, S.R., 2001. Chronology of deformation, metamorphism, and magmatism in the southern Karakoram Mountains. Geological Society of America Bulletin, 113(11), 1443-1455.

Frezzotti, M.L., Selverstone, J., Sharp, Z.D., Compagnoni, R., 2011. Carbonate dissolution during subduction revealed by diamond-bearing rocks from the Alps. Nature Geoscience, 4(10), 703.

Gabriel, K.R., 1971. The biplot graphic display of matrices with application to principal component analysis. Biometrika, 58, 453-467.

Gaetani, M., Garzanti, E., 1991. Multicyclic history of the Northern India continental margin (Northwestern Himalaya) (1). AAPG Bulletin, 75 (9), 1427-1446.

Gaetani, M., Garzanti, E., Jadoul, F., Nicora, A., Tintori, A., Pasini, M., Khan, K.S.A., 1990. The north Karakorum side of the Central Asia geopuzzle. Geological Society of America Bulletin, 102 (1), 54-62.

Gaetani, M., Jadoul, F., Erba, E., Garzanti, E., 1993. Jurassic and Cretaceous orogenic events in the North Karakoram: age constraints from sedimentary rocks. In: Treloar, P.J., Searle, M.P., (Eds.), Himalayan Tectonics. Geological Society, London, Special Publications, 74 (1), 39-52.

Gaillardet, J., Dupré, B., Allègre, C.J., 1999. Geochemistry of large river suspended sediments: silicate weathering or recycling tracer? Geochemistry and Cosmochemistry Acta, 63 (23-24), 4037-4051.

Galehouse, J.S., 1969. Counting grain mounts: number percentage vs. number frequency. Journal of Sedimentary Petrology, 39, 812-815.

Galehouse, J.S., 1971. Point counting, in Carver, R.E., (Ed.), Procedures in Sedimentary Petrology. New York, Wiley, pp:385-407.

Galy, A., France-Lanord, C., 2001. Higher erosion rates in the Himalaya: Geochemical constraints on riverine fluxes. Geology, 29(1), 23-26.

Gansser, A., 1980. The significance of the Himalayan suture zone. Tectonophysics, 62(1-2), 37-52.

Garçon, M., Chauvel, C., France-Lanord, C., Limonta, M., Garzanti, E., 2014. Which minerals control the Nd–Hf–Sr–Pb isotopic compositions of river sediments? Chemical Geology, 364, 42-55.

Garzanti, E., 2016. From static to dynamic provenance analysis—Sedimentary petrology upgraded. Sedimentary Geology, 336, 3-13.

Garzanti, E., 2017. The Maturity Myth in Sedimentology and Provenance. Journal of Sedimentary Research, 87(4), 353-365.

Garzanti, E., 2019a. The Himalayan Foreland Basin from collision onset to the present: a sedimentary–petrology perspective. In: Treloar P.J., Searle M.P., (Eds), Himalayan Tectonics: A Modern Synthesis. Geological Society, London, Special Publications, 483, https://doi.org/10.1144/SP483.17.

Garzanti, E., 2019b. Petrographic classification of sand and sandstone. Earth-Science Reviews, 192, 545-563.

Garzanti, E., Andò, S., 2007a. Plate tectonics and heavy mineral suites of modern sands. In: Mange, M.A., Wright D.T., (Eds.), Heavy Minerals in Use, Developments in Sedimentology Series. Elsevier, Amsterdam,58, 741-763.

Garzanti, E., Andò, S., 2007b. Heavy-mineral concentration in modern sands: Implications for provenance interpretation. In: Mange, M.A., Wright D.T., (Eds.), Heavy Minerals in Use, Developments in Sedimentology Series. Elsevier, Amsterdam, 58, pp: 517-545.

Garzanti, E., Andò, S., 2019. Heavy Minerals for Junior Woodchucks. Minerals, 9(3), 148.

Garzanti, E., Resentini, A., 2016. Provenance control on chemical indices of weathering (Taiwan river sands). Sedimentary geology, 336, 81-95.

Garzanti, E., Van Haver, T., 1988. The Indus clastics: forearc basin sedimentation in the Ladakh Himalaya (India). Sedimentary Geology, 59 (3-4), 237-249.

Garzanti, E., Vezzoli, G., 2003. A classification of metamorphic grains in sands based on their composition and grade. Journal of Sedimentary Research, 73, 830-837.

Garzanti, E., Casnedi, R., Jadoul F., 1986. Sedimentary evidence of a Cambro-Ordovician orogenic event in the northwestern Himalaya. Sedimentary Geology, 48, 237-265.

Garzanti, E., Baud, A., Mascle, G., 1987. Sedimentary record of the northward flight of India and its collision with Eurasia (Ladakh Himalaya, India). Acta geodynamics, 1 (4-5), 297-312.

Garzanti, E., Critelli, S., Ingersoll, R.V., 1996. Paleogeographic and paleotectonic evolution of the Himalayan Range as reflected by detrital modes of Tertiary sandstones and modern sands (Indus transect, India and Pakistan). Geological Society of America Bulletin, 108, 631-642.

Garzanti, E., Vezzoli, G., Andò, S., France-Lanord, C., Singh, S. K., Foster, G., 2004a. Sand petrology and focused erosion in collision orogens: the Brahmaputra case. Earth and Planetary Science Letters, 220(1-2), 157-174.

Garzanti, E., Vezzoli, G., Lombardo, B., Ando, S., Mauri, E., Monguzzi, S., Russo, M., 2004b. Collision-orogen provenance (western Alps): Detrital signatures and unroofing trends. The Journal of Geology, 112 (2), 145-164.

Garzanti, E., Vezzoli, G., Ando, S., Paparella, P., Clift, P.D., 2005. Petrology of Indus River sands: a key to interpret erosion history of the Western Himalayan Syntaxis. Earth and Planetary Science Letters, 229(3-4), 287-302.

Garzanti, E., Ando, S., Vezzoli, G., 2006. The continental crust as a source of sand (Southern Alps cross section, northern Italy). The Journal of Geology, 114(5), 533-554.

Garzanti, E., Vezzoli, G., Andò, S., Lavé, J., Attal, M., France-Lanord, C., DeCelles, P., 2007a. Quantifying sand provenance and erosion (Marsyandi River, Nepal Himalaya). Earth and Planetary Science Letters, 258 (3-4), 500-515.

Garzanti, E., Doglioni, C., Vezzoli, G., Ando, S., 2007b. Orogenic belts and orogenic sediment provenance. The Journal of Geology, 115(3), 315-334.

Garzanti, E., Andò, S., Vezzoli, G., 2008. Settling equivalence of detrital minerals and grainsize dependence of sediment composition. Earth and Planetary Science Letters, 273, 138-151.

Garzanti, E., Andò, S., Vezzoli, G., 2009. Grain-size dependence of sediment composition and environmental bias in provenance studies. Earth and Planetary Science Letters, 277(3-4), 422-432.

Garzanti, E., Andò, S., France-Lanord, C., Vezzoli, G., Censi, P., Galy, V., Najman, Y., 2010a. Mineralogical and chemical variability of fluvial sediments: 1. Bedload sand (Ganga–Brahmaputra, Bangladesh). Earth and Planetary Science Letters, 299(3-4), 368-381.

Garzanti, E., Resentini, A., Vezzoli, G., Andò, S., Malusà, M.G., Padoan, M., Paparella, P., 2010b. Detrital fingerprints of fossil continental-subduction Zones (axial belt provenance, European Alps). The Journal of Geology, 118, 341-362.

Garzanti, E., Andó, S., France-Lanord, C., Censi, P., Vignola, P., Galy, V., Lupker, M., 2011a. Mineralogical and chemical variability of fluvial sediments 2. Suspended-load silt (Ganga–Brahmaputra, Bangladesh). Earth and Planetary Science Letters, 302(1-2), 107-120.

Garzanti, E., Vezzoli, G., Andò, S., 2011b. Paleogeographic and paleodrainage changes during Pleistocene glaciations (Po Plain, northern Italy). Earth-Science Reviews, 105 (1-2), 25-48.

Garzanti, E., Resentini, A., Vezzoli, G., Andò, S., Malusà, M., Padoan, M., 2012. Forward compositional modelling of Alpine orogenic sediments. Sedimentary Geology, 280, 149-164.

Garzanti, E., Padoan, M., Andò, S., Resentini, A., Vezzoli, G., Lustrino, M., 2013a. Weathering and relative durability of detrital minerals in equatorial climate: sand petrology and geochemistry in the East African Rift. The Journal of Geology, 121, 547-580.

Garzanti, E., Padoan, M., Setti, M., Najman, Y., Peruta, L., Villa, I.M., 2013b. Weathering geochemistry and Sr-Nd fingerprints of equatorial upper Nile and Congo muds. Geochemistry, Geophysics, Geosystems, 14 (2), 292-316.

Garzanti, E., Vermeesch, P., Andò, S., Vezzoli, G., Valagussa, M., Allen, K., Khadi, K.A., Al-Juboury, I.A., 2013c. Provenance and recycling of Arabian desert sand. Earth-Science Reviews, 120, 1-19.

Garzanti, E., Limonta, M., Resentini, A., Bandopadhyay, P.C., Najman, Y., Andò, S., Vezzoli, G., 2013d. Sediment recycling at convergent plate margins (Indo-Burman Ranges and Andaman-Nicobar Ridge). Earth-Science Reviews, 123, 113-132.

Garzanti, E., Vermeesch, P., Padoan, M., Resentini, A., Vezzoli, G., Andò, S., 2014a. Provenance of passive-margin sand (southern Africa). The Journal of Geology, 122, 17-42.

Garzanti, E., Padoan, M., Setti, M., López-Galindo, A., Villa, I.M., 2014b. Provenance versus weathering control on the composition of tropical river mud (southern Africa). Chemical Geology, 366, 61-74.

Garzanti, E., Al-Juboury, A.I., Zoleikhaei, Y., Vermeesch, P., Jotheri, J., Akkoca, D.B., Obaid, A.K., Allen, M.B., Ando, S., Limonta, M., Padoan, M., 2016. The Euphrates-Tigris-Karun river system: Provenance, recycling and dispersal of quartz-poor foreland-basin sediments in arid climate. Earth-Science Reviews, 162, 107-128.

Garzanti, E., Limonta, M., Vezzoli, G., An, W., Wang, J., Hu, X., 2018a. Petrology and multimineral fingerprinting of modern sand generated from a dissected magmatic arc (Lhasa River, Tibet). In: Ingersoll, R.V., Lawton, T.F., Graham S.A., (Eds.), Tectonics, Sedimentary Basins, and Provenance: A Celebration of William R. Dickinson's Career. Geological Society of America, Special Paper 540, 197-221.

Garzanti, E., Andò, S., Limonta, M., Fielding, L., Najman, Y., 2018b. Diagenetic control on mineralogical suites in sand, silt, and mud (Cenozoic Nile Delta): Implications for provenance reconstructions. Earth-Science Reviews, 185, 122-139.

Gazzi, P., 1965. On the heavy mineral zones in the geosyncline series, recent studies in the Northern Apennines, Italy. Journal of Sedimentary Petrology, 35, 109-115.

Gazzi, P., Zuffa, G.G., Gandolfi, G., Paganelli, L., 1973. Provenance and coastal dispersion of the sands of the Adriatic beaches between the mouths of the Isonzo and of the Foglia: regional framework. Memories of the Italian Geological Society, 12 (1), 1-37.

Gehrels, G.E., Dickinson, W.R., Ross, G.M., Stewert, J.H., Howell, D.G., 1995. Detrital zircon reference for Cambrian to Triassic miogeoclinal strata of western North America. Geology, 23, 831-834.

Gehrels, G.E., DeCelles, P.G., Martin, A., Ojha, T.P., Pinhassi, G., Upreti, B.N., 2003. Initiation of the Himalayan orogen as an early Paleozoic thin-skinned thrust belt. GSA today, 13(9), 4-9.

Gehrels, G., Kapp, P., DeCelles, P., Pullen, A., Blakey, R., Weislogel, A., Ding, L., Guynn, J., Martin, A., McQuarrie, N., Yin, A., 2011. Detrital zircon geochronology of pre-Tertiary strata in the Tibetan-Himalayan orogen. Tectonics, 30(5), TC5016, https://doi.org/10.1029/2011TC002868

Gillespie, A., Molnar, P., 1995. Asynchronous maximum advances of mountain and continental glaciers. Reviews of Geophysics, 33(3), 311-364.

Gleadow, A.J.W., 1978. Anisotropic and variable track etching characteristics in natural sphenes. Nuclear Track Detection, 2, 105-117.

Gnos, E., Immenhauser, A., Peters, T.J., 1997. Late Cretaceous/early Tertiary convergence between the Indian and Arabian plates recorded in ophiolites and related sediments. Tectonophysics, 271, 1-19.

Godard, V., Bourlès, D.L., Spinabella, F., Burbank, D.W., Bookhagen, B., Fisher, G.B., Moulin, A., Léanni, L., 2014. Dominance of tectonics over climate in Himalayan denudation. Geology, 42(3), 243-246.

Godoi, R.H.M., Potgieter-Vermaak, S., De Hoog, J., Kaegi, R., Van Grieken, R., 2006. Substrate selection for optimum qualitative and quantitative single atmospheric particles analysis using nano-manipulation, sequential thin-window electron probe X-ray microanalysis and micro-Raman spectrometry. Spectrochimica Acta Part B: Atomic Spectroscopy, 61 (4), 375-388.

Goldstein, S.L., Hemming, S.R., 2003. Long-lived isotopic tracers in oceanography, paleoceanography, and ice-sheet dynamics. Treatise on Geochemistry, 6 (6), 453-489.

Goldstein, S.J., Jacobsen, S.B., 1988. The Nd and Sr isotopic systematics of river water suspended material: implications for crustal evolution. Earth and Planetary Science Letters, 87, 249-265.

Goodbred Jr, S.L., Kuehl, S.A., 2000. Enormous Ganges-Brahmaputra sediment discharge during strengthened early Holocene monsoon. Geology, 28(12), 1083-1086.

Goodbred Jr, S.L., Paolo, P.M., Ullah, M.S., Pate, R.D., Khan, S.R., Kuehl, S.A., Singh, S.K., Rahaman, W., 2014. Piecing together the Ganges-Brahmaputra-Meghna River delta: Use of sediment provenance to reconstruct the history and interaction of multiple fluvial systems during Holocene delta evolution. Bulletin, 126(11-12), 1495-1510.

Gosal, G., 2004. Physical geography of the Punjab. Journal of Punjab Studies, 11, 19-37.

Granet, M., Chabaux, F., Stille, P., Dosseto, A., France-Lanord, C., Blaes, E., 2010. U-series disequilibria in suspended river sediments and implication for sediment transfer time in alluvial plains: the case of the Himalayan rivers. Geochimica et Cosmochimica Acta, 74(10), 2851-2865.

Graser, G., Markl, G., 2007. Ca-rich ilvaite–epidote–hydrogarnet endoskarns: a record of late-magmatic fluid influx into the Persodic Ilímaussaq Complex, South Greenland. Journal of Petrology, 49(2), 239-265.

Greco, A., Spencer, D.A., 1993. A section through the Indian plate, Kaghan valley, NW Himalaya, Pakistan. In: Treloar, P.J., Searle, M.P., (Eds.), Himalayan Tectonics. Geological Society, London, Special Publications, 74(1), 221-236.

Greenman, D.W., Swarzenski, W.V., Bennett, G.D., 1967. Ground-water hydrology of the Punjab, West Pakistan, with emphasis on problems caused by canal irrigation. United States Government Printing Office, Washington, United Stated Geological Survey, Water-supply paper 1608H, 1-66.

Griffith, W.P., 1969. Raman spectroscopy of minerals. Nature, 224, 264-266.

Griffin, W.L., Powell, W.J., Pearson, N.J., O'Reilly, S.Y., 2008, GLITTER: data reduction software for laser ablation ICP–MS. In: Sylvester, P. (Ed.), Laser ablation–ICP–MS in the earth sciences: current practices and outstanding issues. Mineralogical Association of Canada, Short Course 40, pp: 204-207.

Grigsby, J.D., 1990. Detrital magnetite as a provenance indicator. Journal of Sedimentary Petrology, 60, 940-951.

Guan, Z., Chen, C., Qu, Y., 1984. Rivers and lakes in Tibet. Beijing: Science and Technology Press. (in Chinese).

Guo, R., Hu, X.M., Garzanti, E., Lai, W., Yan, B., 2020. Magmatic and metamorphic events in Himalaya and Tibet traced by geochronological and geochemical fingerprinting of detrital zircon, monazite, rutile, and titanite. Earth-Science Review. (in press).

Haley, B.A., Klinkhammer, G.P., McManus, J., 2004. Rare earth elements in pore waters of marine sediments. Geochemistry and Cosmochemistry Acta, 68, 1265-1279.

Hacker, B.R., Kylander-Clark, A., Lee, J., Cottle, J., Stearns, M., 2011. Laser-Ablation Split-Stream Petrochronology of Kangmar and Mabja North Himalayan Gneiss Domes. Journal of Himalayan Earth Sciences, 44(1), 25.

Harrison, M.T., Grove, M., Mckeegan, K.D., Coath, C.D., Lovera, O.M., Fort, P.L., 1999. Origin and episodic emplacement of the Manaslu intrusive complex, central Himalaya. Journal of Petrology, 40(1), 3-19.

Hartmann, LA, Santos, J.O.S., 2004. Predominance of high Th / U, magmatic zircon in Brazilian Shield sandstones. Geology, 32(1), 73-76.

Hauck, M.L., Nelson, K.D., Brown, L.D., Zhao, W., Ross, A.R., 1998. Crustal structure of the Himalayan orogen at ~ 90 east longitude from Project INDEPTH deep reflection profiles. Tectonics, 17(4), 481-500.

Hawthorne, F.C., Oberti, R., Harlow, G.E., Maresch, W.V., Martin, R.F., Schumacher, J.C., Welch, M.D., 2012. Nomenclature of the amphibole supergroup. American Mineralogist, 97, 2031-2048.

Hébert, R., Bezard, R., Guilmette, C., Dostal, J., Wang, C., Liu, Z., 2012. The Indus–Yarlung Zangbo ophiolites from Nanga Parbat to Namche Barwa syntaxes, southern Tibet: First synthesis of petrology, geochemistry, and geochronology with incidences on geodynamic reconstructions of Neo-Tethys. Gondwana Research, 22, 377-397.

Henderson, A.L., Najman, Y., Parrish, R., BouDagher - Fadel, M., Barford, D., Garzanti, E., Andò, S., 2010. Geology of the Cenozoic Indus Basin sedimentary rocks: Paleo-environmental interpretation of sedimentation from the western Himalayas during the early phases of India-Eurasia collision. Tectonics, 29 (6). TC6015.

Herren, E., 1987. Zanskar shear zone: Northeast-southwest extension within the Higher Himalayas (Ladakh, India). Geology, 15(5), 409-413.

Hietpas, J., Samson, S., Moecher, D., Schmitt, A.K., 2010. Recovering tectonic events from the sedimentary record: detrital monazite plays in high fidelity. Geology, 38, 167-170.

Hildebrand, P.R., Searle, M.P., Khan, Z., Van Heijst, H.J., 2000. Geological evolution of the Hindu Kush, NW Frontier Pakistan: active margin to continent-continent collision zone. In: Khan M.A., Treloar P.J., Searle M.P., Jan M.Q., (Eds.), Tectonics of the Nanga Parbat Syntaxis and the Western Himalaya. Geological Society: London, UK; Special Publication 170; pp: 277-293.

Hildebrand, P.R., Noble, S.R., Searle, M.P., Waters, D.J., Parrish, R.R., 2001. Old origin for an active mountain range: Geology and geochronology of the eastern Hindu Kush, Pakistan. Geological Society of America Bulletin, 113(5), 625-639.

Hodges, K.V., 2000. Tectonics of the Himalaya and southern Tibet from two perspectives. Geological Society of America Bulletin, 112(3), 324-350.

Honegger, K., Dietrich, V., Frank, W., Gansser, A., Thöni, M., Trommsdorff, V., 1982. Magmatism and metamorphism in the Ladakh Himalayas (the Indus-Tsangpo suture zone). Earth and Planetary Science Letters, 60(2), 253-292.

Hope, G.A., Woods, R., Munce, C.G., 2001. Raman microprobe mineral identification. Minerals Engineering, 14 (12), 1565-1577.

Hu, X., Jansa, L., Wang, C., 2008. Upper Jurassic–Lower Cretaceous stratigraphy in south-eastern Tibet: a comparison with the western Himalayas. Cretaceous Research, 29(2), 301-315.

Hu, X., Sinclair, HD, Wang, J., Jiang, H., Wu, F., 2012. Late Cretaceous-Palaeogene stratigraphic evolution in the Zhepure Mountain of southern Tibet: implications for the timing of India-Asia initial collision. Basin Research, 24 (5), 520-543.

Hu, X., An, W., Wang, J., Garzanti, E., Guo, R., 2014. Himalayan detrital chromatic spinels and timing of Indus-Yarlung ophiolite erosion. Tectonophysics, 621, 60-68.

Hu, X., Garzanti, E., Moore, T., Raffi, I., 2015. Direct stratigraphic dating of India-Asia collision onset at the Selandian (middle Paleocene, 59 ± 1 Ma). Geology, 43, 859-862.

Hu, X., Garzanti, E., Wang, J., Huang, W., An, W., Webb, A., 2016. The timing of India-Asia collision onset–Facts, theories, controversies. Earth-Science Reviews, 160, 264-299.

Hu, Z., Gao, S., 2008. Upper crustal abundances of trace elements: a revision and update. Chemical Geology, 253, 205-221.

Hubert, J.F., 1962. A zircon–tourmaline–rutile maturity index and the interdependence of the composition of heavy minerals assemblages with the gross composition and texture of sandstones. Journal of Sedimentary Petrology, 32, 440-450.

Hughes, P.D., Gibbard, P.L., Ehlers, J., 2013. Timing of glaciation during the last glacial cycle: evaluating the concept of a global 'Last Glacial Maximum'(LGM). Earth-Science Reviews, 125, 171-198.

Hurford, A.J., Fitch, F.J., Clarke, A., 1984. Resolution of the age structure of the detrital zircon populations of two Lower Cretaceous sandstones from the Weald of England by fission track dating. Geological Magazine, 121, 269-277.

Hussain, A., Mir, H., Afzal, M., 2005. Analysis of dust storms frequency over Pakistan during 1961-2000. Pakistan Jounal of Meteorology, 2, 49-68.

Hussain, Y., Ullah, S.F., Hussain, M.B., Aslam, A.Q., Akhter, G., Martinez-Carvajal, H., Cárdenas-Soto, M., 2017. Modelling the vulnerability of groundwater to contamination in an unconfined alluvial aquifer in Pakistan. Environmental Earth Sciences, 76(2), 84, https://doi.org/10.1007/s12665-017-6391-5.

Hutton, C.O., 1950. Studies of heavy detrital minerals. Geological Society of America Bulletin, 61, 635-710.

Ingersoll, R.V., 1983. Petrofacies and provenance of late Mesozoic forearc basin, northern and central California. AAPG Bulletin, 67(7), 1125-1142.

Ingersoll, R.V., 1990. Actualistic sandstone petrofacies: discriminatingmodern and ancient source rocks. Geology, 18, 733-736.

Ingersoll, R.V., Bullard, T.F., Ford, R.L., Grimm, J.P., Pickle, J.D., Sares, S.W., 1984. The effect of grain size on detrital modes: a test of the Gazzi-Dickinson point-counting method. Journal of Sedimentary Research, 54(1), 103-116.

Jadoon, I.A., Lawrence, R.D., Lillie, R.J., 1994. Seismic data, geometry, evolution, and shortening in the active Sulaiman fold-and-thrust belt of Pakistan, southwest of the Himalayas. American Association of Petroleum Geologists Bulletin, 78, 758-774.

Jadoul, F., Berra, F., Garzanti, E., 1998. The Tethys Himalayan passive margin from Late Triassic to Early Cretaceous (South Tibet). Journal of Asian Earth Sciences, 16(2-3), 173-194.

Jagoutz, O., Schmidt, M.W., 2012. The formation and bulk composition of modern juvenile continental crust: The Kohistan arc. Chemical Geology, 298, 79-96.

Jagoutz, O., Müntener, O., Ulmer, P., Pettke, T., Burg, J.P., Dawood, H., Hussain, S., 2007. Petrology and mineral chemistry of lower crustal intrusions: the Chilas Complex, Kohistan (NW Pakistan). Journal of Petrology, 48 (10), 1895-1953.

Jagoutz, O. E., Burg, J. P., Hussain, S., Dawood, H., Pettke, T., Iizuka, T., Maruyama, S., 2009. Construction of the granitoid crust of an island arc part I: geochronological and geochemical constraints from the plutonic Kohistan (NW Pakistan). Contributions to Mineralogy and Petrology, 158(6), 739-755.

Jain, A. K., Singh, S., 2008. Tectonics of the southern Asian Plate margin along the Karakoram Shear Zone: Constraints from field observations and U–Pb SHRIMP ages. Tectonophysics, 451(1-4), 186-205.

Jan, M.Q., Howie, R.A.,1981. The mineralogy and geochemistry of the metamorphosed basic and ultrabasic rocks of the Jijal complex, Kohistan, NW Pakistan. Journal of Petrology, 22 (1), 85-126.

Jarvis, K.E., Williams, J.G., 1993. Laser ablation inductively coupled plasma mass spectrometry (LA-ICP-MS): a rapid technique for the direct, quantitative determination of major, trace and rare-earth elements in geological samples. Chemical Geology, 106(3-4), 251-262.

Johnson, N.M., Stix, J., Tauxe, L., Cerveny, P.F., Tahirkheli, R.A., 1985. Paleomagnetic chronology, fluvial processes, and tectonic implications of the Siwalik deposits near Chinji village, Pakistan. The Journal of Geology, 93(1), 27-40.

Jonell, T.N., Carter, A., Böning, P., Pahnke, K., Clift, P.D., 2017. Climatic and glacial impact on erosion patterns and sediment provenance in the Himalayan rain shadow, Zanskar River, NW India. Bulletin, 129(7-8), 820-836.

Jonell, T.N., Li, Y., Blusztajn, J., Giosan, L., Clift, P.D., 2018. Signal or noise? Isolating grain size effects on Nd and Sr isotope variability in Indus delta sediment provenance. Chemical Geology, 485, 56-73.

Kadri, I.B., 1995. Petroleum Geology of Pakistan. Pakistan Petroleum Limited, Karachi. p.273.

Kartashov, P.M., 2014. Classification diagram for REE-bearing members of the epidote group based on crystallochemical data. In Proceedings of Workshop on acessory minerals; University of Warsaw, Poland; pp: 19-21.

Keane, S.D., Morrison, J., 1997. Distinguishing magmatic from subsolidus epidote: laser probe oxygen isotope compositions. Contributions to Mineralogy and Petrology, 126(3), 265-274.

Kempe, U., Götze, J., 2002. Cathodoluminescence (CL) behaviour and crystal chemistry of apatite from rare-metal deposits. Mineralogical Magazine, 66(1), 151-172.

Khan, I.A., Bridge, J.S., Kappelman, J., Wilson, R., 1997. Evolution of Miocene fluvial environments, eastern Potwar plateau, northern Pakistan. Sedimentology, 44(2), 221-251.

Khan, M.A., Stern, R.J., Gribble, R.F., Windley, B.F., 1997. Geochemical and isotopic constraints on subduction polarity, magma sources, and palaeogeography of the Kohistan intra-oceanic arc, northern Pakistan Himalaya. Journal of the Geological Society, 154(6), 935-946.

Kirby, E., Whipple, K.X., Tang, W., Chen, Z., 2003. Distribution of active rock uplift along the eastern margin of the Tibetan Plateau: Inferences from bedrock channel longitudinal profiles: Journal of Geophysical Research, 108, B4, ETG16, https://doi.org/10.1029/2001JB000861

Knudsen, T.L., Griffin, W., Hartz, E., Andresen, A., Jackson, S., 2001. In-situ hafnium and lead isotope analyses of detrital zircons from the Devonian sedimentary basin of NE Greenland: a record of repeated crustal reworking. Contributions to Mineralogy and Petrology, 141, 83-94.

Komar, P.D., 2007. The entrainment, transport and sorting of heavy minerals by waves and currents. In: Mange,M.A.,Wright, D.T., (Eds.), Heavy Minerals in Use, Developments in Sedimentology Series. Elsevier: Amsterdam, Volume 58, pp: 3-48.

Korup, O., Schlunegger, F., 2009. Rock-type control on erosion-induced uplift, eastern Swiss Alps. Earth and Planetary Science Letters, 278(3-4), 278-285.

Krawinkel, H., Wozazek, S., Krawinkel, J., Hellmann, W., 1999. Heavy-mineral analysis and clinopyroxene geochemistry applied to provenance analysis of lithic sandstones from the Azuero–Soná Complex (NW Panama). Sedimentary Geology, 124,149-168.

Krishnaswami, S., Trivedi, J.R., Sarin, M.M., Ramesh, R., Sharma, K.K., 1992. Strontium isotopes and rubidium in the Ganga-Brahmaputra river system: weathering in the Himalaya, fluxes to the Bay of Bengal and contributions to the evolution of oceanic$^{87}Sr/^{86}Sr$. Earth and Planetary Science Letters, 109(1-2), 243-253.

Krumbein, W.C., Pettijohn, F.J., 1938. Manual of sedimentary petrography. Appleton-Centuary, New York, pp: 549.

Krynine, P.D., 1946. The tourmaline group in sediments. The Journal of Geology, 54(2), 65-87.

Laslett, G.M., Green, P.F., Duddy, I.R., Gleadow, A.J.W., 1987. Thermal annealing of fission tracks in apatite. II: a quantitative analysis. Chemical Geology, 65, 1-13.

Lavé, L., Avouac, J.P., 2001, Fluvial incision and tectonic uplift across the Himalayas of central Nepal. Journal of Geophysical Research: Solid Earth, 106, 26561-26591.

Lawrence, R.L., Cox, R., Mapes, R.W., Coleman, D.S., 2011. Hydrodynamic fractionation of zircon age populations. Geological Society of America Bulletin, 123, 295-305.

Lee, J., Hacker, B.R., Dinklage, W.S., Wang, Y., Gans, P., Calvert, A., Wan, J., Chen, W., Blythe, A.E., McClelland, W., 2000. Evolution of the Kangmar Dome, southern Tibet: Structural, petrologic, and thermochronologic constraints. Tectonics, 19(5), 872-895.

Lee, J.I., Clift, P.D., Layne, G., Blum, J., Khan, A.A., 2003. Sediment flux in the modern Indus River inferred from the trace element composition of detrital amphibole grains. Sedimentary Geology, 160, 243-257.

Lee, J., Hacker, B., Wang, Y., 2004. Evolution of North Himalayan gneiss domes: structural and metamorphic studies in Mabja Dome, southern Tibet. Journal of Structural Geology, 26(12), 2297-2316.

Leith, C.J., 1950. Removal of iron oxide coating from mineral grains. Journal of Sedimentary Petrology, 20, 174-176.

Li, C., Kang, S., Zhang, Q., Wang, F., 2009. Rare earth elements in the surface sediments of the Yarlung Tsangbo (Upper Brahmaputra River) sediments, southern Tibetan Plateau. Quaternary International, 208(1-2), 151-157.

Li, D., 2001. Initial analysis for water and soil moving distribution and its damage and difficulty of management in Tibet. Tibet Science and Technology. (1).21-24. (in Chinese).

Li, G., Liu, X., Alex, P., Wei, L., Liu, X., Huang, F., Zhou, X., 2010. In-situ detrital zircon geochronology and Hf isotopic analyses from Upper Triassic Tethys sequence strata. Earth and Planetary Science Letters, 297(3-4), 461-470.

Li, J., Xia, B., Liu, L., Xu, L., He, G., Wang, H., Zhang, Y., Yang, Z., 2009. SHRIMP U-Pb dating for the Gabbro in Qunrang Ophiolite, Tibet: the geochronology constraint for the development of eastern Tetys basin. Geotectonica et Metallogenia, 33(2), 294-298. (in chinese).

Liang, W., Garzanti, E., Andò, S., Gentile, P., Resentini, A., 2019. Multimineral fingerprinting of Transhimalayan and Himalayan sources of Indus-derived Thal Desert sand (central Pakistan). Minerals, 9(8), 457.

Liu, T., 1999. Hydrological characteristics of Yarlung Zangbo river. Acta Geographica Sinica, 54(Suppl 1), 157-164. (in Chinese).

Liu, T., Chen A., 1995. The characteristics of the precipitation of Nian-chu River basin. Journal of Chengdu University of Science and Technology, 85, 12-18. (in Chinese).

Liu, X., Wu, F., Yu, L., Liu, Z., Ji, W., Wang, J., 2016. Emplacement age of leucogranite in the Kampa Dome, southern Tibet. Tectonophysics, 667, 163-175.

Locock, A.J., 2008. An Excel spreadsheet to recast analyses of garnet into end-member components, and a synopsis of the crystal chemistry of natural silicate garnets. Computers & Geosciences, 34(12), 1769-1780.

Locock, A.J., 2014. An Excel spreadsheet to classify chemical analyses of amphiboles following the IMA 2012 recommendations. Computers & Geosciences, 62, 1-11.

Lünsdorf, N.K., Kalies, J., Ahlers, P., Dunkl, I., von Eynatten, H., 2019. Semi-Automated Heavy-Mineral Analysis by Raman Spectroscopy. Minerals, 9 (7), 385.

Lupker, M., France-Lanord, C., Lavé, J., Bouchez, J., Galy, V., Métivier, F., Gaillardet, J., Lartiges, B., Mugnier, J.L., 2011. A Rouse-based method to integrate the chemical composition of river sediments: Application to the Ganga basin. Journal of Geophysical Research: Earth Surface, 116(F4), https://doi.org/10.1029/2010JF001947

Lupker, M., France-Lanord, C., Galy, V., Lavé, J., Gaillardet, J., Gajurel, A.P., Guilmette, C., Rahman, M., Singh, S.K., Sinha, R., 2012a. Predominant floodplain over mountain weathering of Himalayan sediments (Ganga basin). Geochimica et Cosmochimica Acta, 84, 410-432.

Lupker, M., Blard, P.H., Lavé, J., France-Lanord, C., Leanni, L., Puchol, N., Charreau, J., Bourlès, D., 2012b. ^{10}Be-derived Himalayan denudation rates and sediment budgets in the Ganga basin. Earth and Planetary Science Letters, 333, 146-156.

Lupker, M., Lavé, J., France-Lanord, C., Christl, M., Bourlès, D., Carcaillet, J., Maden, C., Woeler, R., Rahman, M., Bezbaruah, D., Xiaohan, L., 2017. ^{10}Be systematics in the

Tsangpo-Brahmaputra catchment: the cosmogenic nuclide legacy of the eastern Himalayan syntaxis. Earth Surface Dynamics, 5(3), 429-449.

Mahéo, G., Fayoux, X., Guillot, S., Garzanti, E., Capiez, P., Mascle, G., 2006. Relicts of an intra-oceanic arc in the Sapi-Shergol mélange zone (Ladakh, NW Himalayas, India): implications for the closure of the Neo-Tethys Ocean. Journal of Asian Earth Sciences, 26 (6), 695-707.

Malusà, M.G., Garzanti, E., 2019. The sedimentology of detrital thermochronology. In: Malusà, M.G., Fitzgerald, P.G., (Eds.), Fission-track Thermochronology and its Application to Geology. Springer, Cham, Switzerland, pp:123-143.

Malusà, M.G., Resentini, A., Garzanti, E., 2016. Hydraulic sorting and mineral fertility bias in detrital geochronology. Gondwana Research, 31, 1-19.

Malusà, M.G., Wang, J., Garzanti, E., Liu, Z.C., Villa, I.M., Wittmann, H., 2017. Trace-element and Nd-isotope systematics in detrital apatite of the Po river catchment: Implications for provenance discrimination and the lag-time approach to detrital thermochronology. Lithos, 290, 48-59.

Maluski, H., Matte, P., Brunel, M., Xiao, X., 1988. Argon 39-argon 40 dating of metamorphic and plutonic events in the north and high Himalaya belts (southern Tibet-China). Tectonics, 7(2), 299-326.

Mange, M.A., Maurer, H., 2012. Heavy minerals in colour. Springer Science & Business Media.

Mange, M.A., Morton, A.C., 2007. Geochemistry of heavy minerals. In: Mange, M.A., Wright, D.T., (Eds.), Heavy Minerals in Use, Developments in Sedimentology Series. Elsevier: Amsterdam, The Netherlands; Volume 58, pp: 345-391.

McAteer, C.A., Daly, J.S., Flowerdew, M.J., Connelly, J.N., Housh, T.B., Whitehouse, M.J., 2010. Detrital zircon, detrital titanite and igneous clast U–Pb geochronology and basement-cover relationships of the Colonsay Group, SW Scotland: Laurentian provenance and correlation with the Neoproterozoic Dalradian Supergroup. Precambrian Research, 181, 21-42.

McBride, E., Picard, D.M., 1987. Downstream changes in sand composition, roundness and gravel size in a short-headed, high-gradient stream, Northwestern Italy. Journal of Sedimentary Petrology, 57, 1018-1026.

McDonough, W.F., Sun, S.S., 1995. The composition of the Earth. Chemical Geology, 120(3-4), 223-253.

McLennan, S.M., 1989. Rare earth elements in sedimentary rocks: influence of provenance and sedimentary processes. Reviews in Mineralogy and Geochemistry, 21, 169-200.

McLennan, S.M., 2001. Relationships between the trace element composition of sedimentary rocks and upper continental crust. Geochemistry, Geophysics, Geosystem, 2(4), https://doi.org/10.1029/2000GC000109 .

McMillan, P.F., 1989. Raman spectroscopy in mineralogy and geochemistry. Annual Review of Earth and Planetary Sciences, 17, 255-283.

Meadows, A., Meadows, P.S., 1999. The Indus River: biodiversity, resources, humankind. Oxford University Press, Oxford, UK, pp.441.

Meinhold, G., 2010. Rutile and its applications in earth sciences. Earth-Science Reviews, 102, 1-28.

Meng, Z., Wang, J., Ji, W., Zhang, H., Wu, F., Garzanti, E., 2019. The Langjiexue Group is an in situ sedimentary sequence rather than an exotic block: Constraints from coeval Upper Triassic strata of the Tethys Himalaya (Qulonggongba Formation). Science China Earth Sciences, 62, 783-797.

Mernagh, T.P., Liu, L.G., 1991. Raman spectra from the Al2SiO5 polymorphs at high pressures and room temperatures. Physics and Chemistry of Minerals, 18 (2), 126-130.

Meyer, K.M., Yu, M., Jost, A.B., Kelley, B.M., Payne, J.L., 2011. $\delta^{13}C$ evidence that high primary productivity delayed recovery from end-Permian mass extinction. Earth and Planetary Science Letters, 302(3-4), 378-384.

Milliman, J.D., Quraishee, G.S., Beg, M.A.A., 1984. Sediment discharge from the Indus River to the ocean: past, present and future. In: Haq, B.U., Milliman J.D., (Eds.), Marine Geology and Oceanography of the Arabian Sea and Coastal Pakistan. Van Nostrand Reynolds: New York, USA; pp: 65-70.

Milner, H. B., 1962. Sedimentary petrography: Methods in sedimentary petrography. London: George Allen & Unwin.

Moecher, D.P., Samson, S.D., 2006. Differential zircon fertility of source terranes and natural bias in the detrital zircon record: Implications for sedimentary provenance analysis. Earth and Planetary Science Letters, 247 (3-4), 252-266.

Moore, M.A., England, P.C., 2001. On the inference of denudation rates from cooling ages of minerals. Earth and Planetary Science Letters, 185(3-4), 265-284.

Morel, P., Von Blanckenburg, F., Schaller, M., Kubik, P.W., Hinderer, M., 2003. Lithology, landscape dissection and glaciation controls on catchment erosion as determined by cosmogenic nuclides in river sediment (the Wutach Gorge, Black Forest). Terra Nova, 15(6), 398-404.

Morimoto, N., Fabries, J., Ferguson, A.K., Ginzburg, I.V., Ross, M., Seifert, F.A., Zussman, J., Aoki, K., Gottardi, G., 1988. Nomenclature of pyroxenes. Mineralogy and Petrology, 39, 55-76.

Morton, A.C., 1984. Stability of detrital heavy minerals in Tertiary sandstones of the North Sea Basin. Clay Mineralogy, 19, 287-308.

Morton, A.C., 1985a. Heavy minerals in provenance studies. In: Zuffa, G.G. (Ed.), Provenance of Arenites. Springer, Dordrecht, pp: 249-277.

Morton, A.C., 1985b. A new approach to provenance studies: electron microprobe analysis of detrital garnets from Middle Jurassic sandstones of the northern North Sea. Sedimentology, 32(4), 553-566.

Morton, A.C., 1991. Geochemical studies of detrital heavy minerals and their application to provenance research. In: Morton, A.C., Todd, S.P., Haughton, P.D.W. (Eds.), Developments in Sedimentary Provenance Studies. Geological Society, London, Special Publications, 57(1), 31-45.

Morton, A.C., 2012. Value of heavy minerals in sediments and sedimentary rocks for provenance, transport history and stratigraphic correlation. In: Sylvester, P. (Ed.), Quantitative Mineralogy and Microanalysis of Sediments and Sedimentary Rocks. Mineralogical Association of Canada Short Course Series 42, pp: 133-165.

Morton, A.C., Hallsworth, C., 2007. Stability of detrital heavy minerals during burial diagenesis. In: M. Mange, D.T., Wright, (Eds.), Heavy Minerals in Use, Developments in Sedimentology. 58, 215-245.

Morton, A.C., Yaxley, G., 2007. Detrital apatite geochemistry and its application in provenance studies. In: Arribas, J., Critelli, S., Johnsson, M.J. (Eds.), Sedimentary Provenance and Petrogenesis: Perspectives from Petrography and Geochemistry. Geological Society of America Special Paper, 420, 319-344.

Morton, A., Hallsworth, C., Chalton, B., 2004. Garnet compositions in Scottish and Norwegian basement terrains: a framework for interpretation of North Sea sandstone provenance. Marine and Petroleum Geology, 21(3), 393-410.

Munack, H., Korup, O., Resentini, A., Limonta, M., Garzanti, E., Blöthe, J.H., Scherler, D., Wittmann, H., Kubik, P.W., 2014. Postglacial denudation of western Tibetan Plateau margin outpaced by long-term exhumation. Bulletin, 126(11-12), 1580-1594.

Muhs, D.R., 2004. Mineralogical maturity in dunefields of North America, Africa and Australia. Geomorphology, 59(1-4), 247-269.

Najman, Y., 2006. The detrital record of orogenesis: a review of approaches and techniques used in the Himalayan sedimentary basins. Earth-Science Reviews, 74, 1-72.

Najman, Y., Garzanti, E., 2000. Reconstructing early Himalayan tectonic evolution and paleogeography from Tertiary foreland basin sedimentary rocks, northern India. Geological Society of America Bulletin, 112(3), 435-449.

Najman, Y., Garzanti, E., Pringle, M., Bickle, M., Stix, J., Khan, I., 2003. Early-Middle Miocene paleodrainage and tectonics in the Pakistan Himalaya. Geological Society of America Bulletin, 115(10), 1265-1277.

Najman, Y., Jenks, D., Godin, L., Boudagher-Fadel, M., Millar, I., Garzanti, E., Horstwood, M, Bracciali, L., 2017. The Tethyan Himalayan detrital record shows that India–Asia terminal collision occurred by 54 Ma in the Western Himalaya. Earth and Planetary Science Letters, 459, 301-310.

Nasdala, L., Smith, D.C., Kaindl, R., Ziemann, M.A., 2004. Raman spectroscopy: analytical perspectives in mineralogical research. In: Beran, A.B., Libowitzki, E., (Eds.), Spectroscopic Methods in Mineralogy. European Mineralogical Union Notes in Mineralogy, 6, 281-343.

Nesbitt, H.W., Young, G.M., 1982. Early Proterozoic climates and plate motions inferred from major element chemistry of lutites. Nature, 299, 715-717.

Nickson, R.T., McArthur, J.M., Shrestha, B., Kyaw-Myint, T.O., Lowry, D., 2005. Arsenic and other drinking water quality issues, Muzaffargarh District, Pakistan. Applied Geochemistry, 20(1), 55-68.

Norrish, K., Chappell, B.W., 1977. X-ray fluorescence spectrometry. In: Zussman (Ed.), Physical Methods in Determinative Mineralogy. Academic Press, London, 201-272.

Oberti, R., Cannillo, E., Toscani, G., 2012. How to name amphiboles after the IMA2012 report: rules of thumb and a new PC program for monoclinic amphiboles. Periodico di Mineralogia, 81(2), 257-267.

Owen, L.A., Finkel, R.C., Caffee, M.W., 2002. A note on the extent of glaciation throughout the Himalaya during the global Last Glacial Maximum. Quaternary Science Reviews, 21(1-3), 147-157.

Padoan, M., Garzanti, E., Haravan, Y., Villa, I.M., 2011. Tracing Nile sediment sources by Sr and Nd isotope signatures (Uganda, Ethiopia, Sudan). Geochimica et Cosmochimica Acta, 75, 3627-3644.

Pan, G., Ding, J., Yao, D., Wang, L., 2004. Geological map of the Qinghai-Xizang (Tibet) plateau and adjacent areas (1:1,500,000). Chengdu Institute of Geology and Mineral Resources, China Geological Survey, Chengdu Cartographic Publishing House, Chengdu, China.

Palin, R.M., Searle, M.P., Waters, D.J., Horstwood, M.S.A., Parrish, R.R., 2012. Combined thermobarometry and geochronology of peraluminous metapelites from the Karakoram metamorphic complex, North Pakistan; New insight into the tectonothermal evolution of the Baltoro and Hunza Valley regions. Journal of Metamorphic Geology, 30 (8), 793-820.

Parker, A., 1970. An index of weathering for silicate rocks. Geological Magazine, 107, 501-504.

Parrish, R.R., Hodges, V., 1996. Isotopic constraints on the age and provenance of the Lesser and Greater Himalayan sequences, Nepalese Himalaya. Geological Society of America Bulletin, 108(7), 904-911.

Pecher, A., Seeber, L., Guillot, S., Jouanne, F., Kausar, A., Latif, M., Majid, A., Mahéo, G., Mugnier, J.L., Rolland, Y., Van Der Beek, P., Van Melle, J., 2008. Stress field evolution in the northwest Himalayan syntaxis, northern Pakistan. Tectonics, 27(6). TC6005, https://doi.org/10.1029/2007TC002252.

Petterson, M.G., Crawford, M.B., Windley, B.F., 1993. Petrogenetic implications of neodymium isotope data from the Kohol bathistan, North Pakistan. Journal of the Geological Society, 150(1), 125-129.

Pober, E., Faupl, P., 1988. The chemistry of detrital chromian spinels and its implications for the geodynamic evolution of the Eastern Alps. Geologische Rundschau, 77, 641-670.

Pognante, U.T., Lombardo, B., 1989. Metamorphic evolution of the High Himalayan crystallines in SE Zanskar, India. Journal of Metamorphic Geology, 7(1), 9-17.

Poldervaart, A., Hess, H.H., 1951. Pyroxenes in the crystallization of basaltic magma. The Journal of Geology, 59(5), 472-489.

Potgieter-Vermaak, S., Worobiec, A., Darchuk, L., Van Grieken, R., 2011. Micro-Raman spectroscopy for the analysis of environmental particles. Fundamentals and Applications in Aerosol Spectroscopy, 193-208.

Price, J.R., Velbel, M.A., 2003. Chemical weathering indices applied to weathering profiles developed on heterogeneous felsic metamorphic parent rocks. Chemical Geology, 202, 397-416.

Qayyum, M., Lawrence, R.D., Niem, A.R., 1997. Discovery of the palaeo-Indus delta-fan complex. Journal of the Geological Society, 154(5), 753-756.

Quade, J., English, N., DeCelles, P.G., 2003. Silicate versus carbonate weathering in the Himalaya; a comparison of the Arun and Seti River watersheds. Chemical Geology, 202 (3-4), 275-296.

Rahmanb, M.A., Biswasb, P.K., Zamanb, M.N., Miah, M.Y., Hossain, T., Huq, S.I., 2012. Characterization of the sand of Brahmaputra river of Bangladesh. Bangladesh Journal of Scientific and Industrial Research, 47(2), 167-172.

Rai, S.K., Singh, S.K., Krishnaswami, S., 2010. Chemical weathering in the plain and peninsular sub-basins of the Ganga: impact on major ion chemistry and elemental fluxes. Geochimica et Cosmochimica Acta, 74(8), 2340-2355.

Ratschbacher, L., Frisch, W., Liu, G., Chen, C., 1994. Distributed deformation in southern and western Tibet during and after the India-Asia collision. Journal of Geophysical Research: Solid Earth, 99(B10), 19917-19945.

Rehman, H.U., Seno, T., Yamamoto, H., Khan, T., 2011. Timing of collision of the Kohistan–Ladakh Arc with India and Asia: debate. Island Arc, 20(3), 308-328.

Rehman, S.S., Sabir, M.A., Khan, J., 1997. Discharge characteristics and suspended load from rivers of Northern Indus Basin, Pakistan. Geological Bulletin (University of Peshawar), 30, 325-336.

Reiners, P.W., Campbell, I.H., Nicolescu, S., Allen, C.M., Hourigan, J.K., Garver, J.I., Mattinson, J.M., Cowan, D.S., 2005. (U–Th)/(He–Pb) double dating of detrital zircons. American Journal of Science, 305, 259-311.

Rengarajan, R., Singh, S.K., Sarin, M.M., Krishnaswami, S., 2009. Strontium isotopes and major ion chemistry in the Chambal River system, India: implications to silicate erosion rates of the Ganga. Chemical Geology, 260(1-2), 87-101.

Resentini, A., Goren, L., Castelltort, S., Garzanti, E., 2017. Partitioning the sediment flux by provenance and tracing erosion patterns in Taiwan. Journal of Geophysical Research: Earth Surface, 122(7), 1430-1454.

Robertson, A.H., Collins, A.S., 2002. Shyok Suture Zone, N Pakistan: late Mesozoic–Tertiary evolution of a critical suture separating the oceanic Ladakh Arc from the Asian continental margin. Journal of Asian Earth Sciences, 20 (3), 309-351.

Roddaz, M., Said, A., Guillot, S., Antoine, P.O., Montel, J.M., Martin, F., Darrozes, J., 2011. Provenance of Cenozoic sedimentary rocks from the Sulaiman fold and thrust belt, Pakistan: implications for the palaeogeography of the Indus drainage system. Journal of the Geological Society, 168, 499-516.

Rolland, Y., Mahéo, G., Guillot, S., Pêcher, A., 2001. Tectono-metamorphic evolution of the Karakorum Metamorphic complex (Dassu–Askole area, NE Pakistan): exhumation of mid-crustal HT–MP gneisses in a convergent context. Journal of Metamorphic Geology, 19(6), 717-737.

Rubey, W.W., 1933. The size distribution of heavy minerals within a water-laid sandstone. Journal of Sedimentary Research, 3(1), 3-29.

Rudnick, R.L., Gao, S., 2003. Composition of the continental crust. In: Rudnick, R.L., Holland, H.D., Turekian, K.K., (Eds.), Treatise on Geochemistry, The Crust. Elsevier Pergamon: Oxford, UK; Volume 3, pp: 1-64.

Sarin, M.M., Krishnaswami, S., Dilli, K., Somayajulu, B.L.K., Moore, W.S., 1989. Major ion chemistry of the Ganga-Brahmaputra river system: Weathering processes and fluxes to the Bay of Bengal. Geochimica et cosmochimica acta, 53(5), 997-1009.

Sarin, M.M., Krishnaswami, S., Moore, W.S., 1990. Chemistry of uranium, thorium, and radium isotopes in the Ganga-Brahmaputra river system: Weathering processes and fluxes to the Bay of Bengal. Geochimica et Cosmochimica Acta, 54(5), 1387-1396.

Schaltegger, U., Zeilinger, G., Frank, M., Burg, J.P., 2002. Multiple mantle sources during island arc magmatism: U–Pb and Hf isotopic evidence from the Kohistan arc complex, Pakistan. Terra Nova, 14(6), 461-468.

Schärer, U., Hamet, J., Allègre, C.J., 1984. The Transhimalaya (Gangdese) plutonism in the Ladakh region: a U-Pb and Rb-Sr study. Earth and Planetary Science Letters, 67(3), 327-339.

Schärer, U., Copeland, P., Harrison, T.M., Searle, M.P., 1990. Age, cooling history, and origin of post-collisional leucogranites in the Karakoram Batholith; a multi-system isotope study. The Journal of Geology, 98(2), 233-251.

Schneider, D.A., Zeitler, P.K., Kidd, W.S.F., Edwards, M.A., 2001. Geochronologic constraints on the tectonic evolution and exhumation of Nanga Parbat, western Himalaya syntaxis, revisited. The Journal of Geology, 109 (5), 563-583.

Schwanghart, W., Scherler, D., 2014. TopoToolbox 2 – MATLAB-based software for topographic analysis and modeling in Earth surface sciences. Earth Surface Dynamics, 2, 1-7.

Sciunnach, D., Garzanti, E., 2012. Subsidence history of the Tethys Himalaya. Earth-Science Reviews, 111(1-2), 179-198.

Searle, MP, Tirrul, R., 1991. Structural and thermal evolution of the Karakoram crust. Journal of the Geological Society, 148(1), 65-82.

Searle, M., Corfield, R.I., Stephenson, B.E.N., McCarron, J.O.E., 1997. Structure of the North Indian continental margin in the Ladakh – Zanskar Himalayas: implications for the timing of the obduction of the Spontang ophiolite, India–Asia collision and deformation events in the Himalayas. Geological Magazine, 134(3), 297-316.

Searle, M.P., Khan, M.A., Fraser, J.E., Gough, S.J., Jan, M.Q., 1999. The tectonic evolution of the Kohistan-Karakoram collision belt along the Karakoram Highway transect, north Pakistan. Tectonics, 18(6), 929-949.

Searle, M.P., Parrish, R.R., Thow, A.V., Noble, S.R., Phillips, R.J., Waters, D.J., 2010. Anatomy, age and evolution of a collisional mountain belt: the Baltoro granite batholith and Karakoram Metamorphic Complex, Pakistani Karakoram. Journal of the Geological Society, 167 (1), 183-202.

Shabaga, B.M., Fayek, M., Hawthorne, F.C., 2010. Boron and lithium isotopic compositions as provenance indicators of Cu-bearing tourmalines. Mineralogical Magazine, 74, 241-255.

Shah, I., 1977. Stratigraphy of Pakistan: Memoirs of the Geological Survey of Pakistan, 12,138.

Shah, Z.U.H., Ahmad, Z., 2015. Hydrochemical mapping of the Upper Thal Doab (Pakistan) using the geographic information system. Environmental Earth Sciences, 74, 2757-2773.

Shah, Z.U.H., Ahmad, Z., 2016. Hydrogeology and hydrochemistry of the Upper Thal Doab (Pakistan). Environmental Earth Sciences, 75(6), 527.

Shao, J., Yang, S., Li, C., 2012. Chemical indices (CIA and WIP) as proxies for integrated chemical weathering in China: inferences from analysis of fluvial sediments. Sedimentary Geology, 265, 110-120.

Shi, X., Zhang, F., Lu, X., Wang, Z., Gong, T., Wang, G., Zhang, H., 2018. Spatiotemporal variations of suspended sediment transport in the upstream and midstream of the Yarlung Tsangpo River (the upper Brahmaputra), China. Earth Surface Processes and Landforms, 43(2), 432-443.

Shiller, A.M., Frilot, D.M., 1996. The geochemistry of gallium relative to aluminum in Californian streams. Geochimica et Cosmochimica Acta, 60(8), 1323-1328.

Shroder, J.F., Bishop, M.P., 2000. Unroofing of Nanga Parbat Himalaya, In: Khan M.A., Treloar P.J., Searle M.P., Jan M.Q., (Eds.), Tectonics of the Nanga Parbat Syntaxis and the Western Himalaya. Geological Society: London, UK; Special Publication 170; pp: 163-179.

Sinclair, H.D., Jaffey, N., 2001. Sedimentology of the Indus Group, Ladakh, northern India: implications for the timing of initiation of the palaeo-Indus River. Journal of the Geological Society, 158(1), 151-162.

Singh, G., Wasson, R.J., Agrawal, D.P., 1990. Vegetational and seasonal climatic changes since the last full glacial in the Thar Desert, northwestern India. Review of Palaeobotany and Palynology, 64(1-4), 351-358.

Singh, P., 2009. Major, trace and REE geochemistry of the Ganga River sediments: influence of provenance and sedimentary processes. Chemical Geology, 266(3-4), 242-255.

Singh, P., 2010. Geochemistry and provenance of stream sediments of the Ganga River and its major tributaries in the Himalayan region, India. Chemical Geology, 269(3-4), 220-236.

Singh, S. K., France-Lanord, C., 2002. Tracing the distribution of erosion in the Brahmaputra watershed from isotopic compositions of stream sediments. Earth and Planetary Science Letters, 202(3-4), 645-662.

Singh, S. K., Reisberg, L., France-Lanord, C., 2003. Re-Os isotope systematics of sediments of the Brahmaputra River system. Geochimica et cosmochimica acta, 67(21), 4101-4111.

Singh, S., Kumar, R., Barley, M.E., Jain, A.K., 2007. SHRIMP U–Pb ages and depth of emplacement of Ladakh Batholith, Eastern Ladakh, India. Journal of Asian Earth Sciences, 30(3-4), 490-503.

Singh, S.K., Rai, S.K., Krishnaswami, S., 2008. Sr and Nd isotopes in river sediments from the Ganga Basin: sediment provenance and spatial variability in physical erosion. Journal of Geophysical Research: Earth Surface, 113(F3), https://doi.org/10.1029/2007JF000909.

Singhvi, A.K., Kar, A., 2004. The aeolian sedimentation record of the Thar Desert. Journal of Earth System Science, 113(3), 371-401.

Singhvi, A.K., Williams, M.A.J., Rajaguru, S.N., Misra, V.N., Chawla, S., Stokes, S., Chauhan, N., Francis, T., Ganjoo, R.K., Humphreys, G.S., 2010. A ~ 200 ka record of climatic change and dune activity in the Thar Desert, India. Quaternary Science Reviews, 29(23-24), 3095-3105.

Smyth, H.R., Morton, A., Richardson, N., Scott, R.A., 2014, Sediment provenance studies in hydrocarbon exploration and production: An introduction. In: Scott, R.A., Smyth, H.R., Morton, A.C., Richardson, N., (Eds.), Sediment Provenance Studies in Hydrocarbon Exploration and Production. Geological Society, London, Special Publication 386, p:1-6.

Spalla, M.I., Zanoni, D., Gosso, G., Zucali, M., 2009. Deciphering the geologic memory of a Permian conglomerate of the Southern Alps by pebble P–T estimates. International Journal of Earth Sciences, 98(1), 203-226.

Spiegel, C., Siebel, W., Frisch, W., Berner, Z., 2002. Nd and Sr isotopic ratios and trace element geochemistry of epidote from the Swiss Molasse Basin as provenance indicators: implications for the reconstruction of the exhumation history of the Central Alps. Chemical Geology, 189, 231-250.

Steck, A., 2003. Geology of the NW Indian Himalaya. Eclogae Geologicae Helvetiae, 96, 147-196.

Stefaniak, E.A., Worobiec, A., Potgieter-Vermaak, S., Alsecz, A., Török, S., Van Grieken, R., 2006. Molecular and elemental characterisation of mineral particles by means of parallel micro-Raman spectrometry and Scanning Electron Microscopy/Energy Dispersive X-ray Analysis. Spectrochimica Acta Part B: Atomic Spectroscopy, 61(7), 824-830.

Stewart, R.J., Hallet, B., Zeitler, P.K., Malloy, M.A., Allen, C.M., Trippett, D., 2008. Brahmaputra sediment flux dominated by highly localized rapid erosion from the easternmost Himalaya. Geology, 36(9), 711-714.

Stock, G.M., Ehlers, T.A., Farley, K.A., 2006. Where does sediment come from? Quantifying catchment erosion with detrital apatite (U–Th)/He thermochronometry. Geology, 34, 725-728.

Stockli, D.F., Wolfe, M.R., Blackburn, T.J., Zack, T., Walker, J.D., Luvizotto, G.L., 2007. He diffusion and (U–Th)/He thermochronometry of rutile. Eos, Transactions of the American Geophysical Union, Fall Meeting Supplement, Abstract, V23C-1548.

Sturm, R., 2002. PX-NOM—an interactive spreadsheet program for the computation of pyroxene analysis derived from the electron microprobe. Computers &Geosciences, 28 (4), 473-483.

Suczek, C.A., Ingersoll, R.V., 1985. Petrology and provenance of Cenozoic sand from the Indus Cone and the Arabian Basin, DSDP sites 221, 222, and 224. Journal of Sedimentary Research, 55(3), 340-346.

Suggate, S.M., Hall, R., 2014. Using detrital garnet compositions to determine provenance: A new compositional database and procedure. In: Scott, R.A., Smyth, H.R., Morton, A.C., Richardson, N., (Eds.), Sediment Provenance Studies in Hydrocarbon Exploration and Production. Geological Society, London, Special Publication 386, p. 373-393.

Summerfield, M.A., Hulton, N.J., 1994. Natural controls of fluvial denudation rates in major world drainage basins. Journal of Geophysical Research: Solid Earth, 99 (B7), 13871-13883.

Tate, E.L., Farquharson, F.A., 2000. Simulating reservoir management under the threat of sedimentation: the case of Tarbela dam on the river Indus. Water Resources Management, 14(3), 191-208.

Taylor, S.R., McLennan, S.M., 1995. The geochemical evolution of the continental crust. Reviews of Geophysics, 33, 241-265.

Tiepolo, M., Oberti, R., Vannucci, R., 2002. Trace-element incorporation in titanite: constraints from experimentally determined solid/liquid partition coefficients. Chemical Geology, 191, 105-119.

Totten, M.W., Hanan, M.A., 2007. Heavy minerals in shales. Developments in Sedimentology, 58, 323-341.

Treloar, P.J., Rex, D.C., Guise, P.G., Coward, M.P., Searle, M.P., Windley, B.F., Petterson, M.G., Jan, M.Q., Luff, I.W., 1989. K-Ar and Ar-Ar geochronology of the Himalayan collision in NW Pakistan: Constraints on the timing of suturing, deformation, metamorphism and uplift. Tectonics, 8(4), 881-909.

Treloar, P.J., Petterson, M.G., Jan, M.Q., Sullivan, M.A., 1996. A re-evaluation of the stratigraphy and evolution of the Kohistan arc sequence, Pakistan Himalaya: implications for magmatic and tectonic arc-building processes. Journal of the Geological Society, 153(5), 681-693.

Tripathy, G.R., Singh, S.K., 2010. Chemical erosion rates of river basins of the Ganga system in the Himalaya: Reanalysis based on inversion of dissolved major ions, Sr, and 87Sr/86Sr. Geochemistry, Geophysics, Geosystems, 11(3), https://doi.org/10.1029/2009GC002862.

Tucker, G.E., Whipple, K.X., 2002. Topographic outcomes predicted by stream erosion models: Sensitivity analysis and intermodel comparison. Journal of Geophysical Research: Solid Earth, 107(B9), ETG-1, https://doi.org/10.1029/2001JB000162.

Tyrrell, S., Souders, A.K., Haughton, P.D.W., Daly, J.S., Shannon, P.H., 2010. Sedimentology, sandstone provenance and palaeodrainage on the eastern Rockall Basin margin: evidence from the Pb isotopic composition of detrital K-feldspar. Petroleum Geology Conference series, 7, 937-952.

Vannay, J.C., Grasemann, B., Rahn, M., Frank, W., Carter, A., Baudraz, V., Cosca, M., 2004. Miocene to Holocene exhumation of metamorphic crustal wedges in the NW Himalaya: Evidence for tectonic extrusion coupled to fluvial erosion. Tectonics, 23(1). TC1014, https://doi.org/10.1029/2002TC001429.

Vermeesch, P., 2004. How many grains are needed for a provenance study? Earth and Planetary Science Letters, 224, 351-441.

Vermeesch, P., 2018. IsoplotR: a free and open toolbox for geochronology. Geoscience Frontiers, 9(5), 1479-1493.

Vermeesch, P., Garzanti, E., 2015. Making geological sense of ‘Big Data’ in sedimentary provenance analysis. Chemical Geology, 409, 20-27.

Vermeesch, P., Avigad, D., McWilliams, M.O., 2009. 500 my of thermal history elucidated by multi-method detrital thermochronology of North Gondwana Cambrian sandstone (Eilat area, Israel). Geological Society of America Bulletin, 121, 1204-1216.

Vermeesch, P., Fenton, C.R., Kober, F., Wiggs, G.F.S., Bristow, C.S., Xu, S., 2010. Sand residence times of one million years in the Namib Sand Sea from cosmogenic nuclides. Nature Geoscience, 3(12), 862.

Vermeesch, P., Resentini, A., Garzanti, E., 2016. An R package for statistical provenance analysis. Sedimentary Geology, 336, 14-25.

Vermeesch, P., Rittner, M., Petrou, E., Omma, J., Mattinson, C., Garzanti, E., 2017. High throughput petrochronology and sedimentary provenance analysis by automated phase mapping and LAICPMS. Geochemistry, Geophysics, Geosystems, 18(11), 4096-4109.

Vezzoli, G., Garzanti, E., Limonta, M., Andó, S., Yang, S., 2016. Erosion patterns in the Changjiang (Yangtze River) catchment revealed by bulk-sample versus single-mineral provenance budgets: Geomorphology, 261,177-192.

Villanueva, U., Raposo, J.C., Castro, K., de Diego, A., Arana, G., Madariaga, J.M., 2008. Raman spectroscopy speciation of natural and anthropogenic solid phases in river and estuarine sediments with appreciable amount of clay and organic matter. Journal of Raman Spectroscopy: An International Journal for Original Work in All Aspects of Raman Spectroscopy, Including Higher Order Processes, and also Brillouin and Rayleigh Scattering, 39 (9), 1195-1203.

von Eynatten, H., Dunkl, I., 2012. Assessing the sediment factory: the role of single grain analysis. Earth-Science Reviews, 115(1-2), 97-120.

von Eynatten, H., Gaupp, R., 1999. Provenance of Cretaceous synorogenic sandstones in the Eastern Alps: constraints from framework petrography, heavy mineral analysis and mineral chemistry. Sedimentary Geology, 124(1-4), 81-111.

von Eynatten, H., Gaupp, R., Wijbrans, J.R., 1996. $^{40}Ar/^{39}Ar$ laser-probe dating of detrital white micas from Cretaceous sedimentary rocks of the Eastern Alps: evidence for Variscan high-pressuremetamorphismand implications for Alpine orogeny. Geology, 24, 691-694.

von Eynatten, H., Schlunegger, F., Gaupp, R., Wijbrans, J.R., 1999. Exhumation of the Central Alps: evidence from $^{40}Ar/^{39}Ar$ laserprobe dating of detrital white micas from the Swiss Molasse Basin. Terra Nova, 11, 284-289.

von Eynatten, H., Barcelò-Vidal, C., Pawlowsky-Glahn, V., 2003. Composition and discrimination of sandstones: a statistical evaluation of different analytical methods. Journal of Sedimentary Research, 73, 47-57.

Wang, J., Wu, F., Garzanti, E., Hu, X., Ji, W., Liu, Z., Liu, X., 2016. Upper Triassic turbidites of the northern Tethyan Himalaya (Langjiexue Group): The terminal of a sediment-routing system sourced in the Gondwanide Orogen. Gondwana Research, 34, 84-98.

Wang, J., Hu, X., Garzanti, E., An, W., Liu, X., 2017. The birth of the Xigaze forearc basin in southern Tibet. Earth and Planetary Science Letters, 465, 38-47.

Wang, Y., Gao, L., Zeng, L., Chen, F., Hou, K., Wang, Q., Zhao, L., Gao, J., 2016. Multiple phases of cretaceous mafic magmatism in the Gyangze-Kangma area, Tethyan Himalaya, southern Tibet. Acta Petrologica Sinica, 32(12), 3572-3596. (in chinese).

Wang, Z., Yu, G., Wang, X., Melching, C.S., Liu, L., 2015. Sediment storage and morphology of the Yalu Tsangpo valley due to uneven uplift of the Himalaya. Science China Earth Sciences, 58(8), 1440-1445.

Webb, A.A.G., Yin, A., Dubey, C.S., 2013. U-Pb zircon geochronology of major lithologic units in the eastern Himalaya: Implications for the origin and assembly of Himalayan rocks. Bulletin, 125(3-4), 499-522.

Weltje, G.J., 1997. End-member modeling of compositional data: Numerical-statistical algorithms for solving the explicit mixing problem. Mathematical Geology, 29(4), 503-549.

Weinberg, R.F., Dunlap, W.J., 2000. Growth and deformation of the Ladakh Batholith, Northwest Himalayas: implications for timing of continental collision and origin of calc-alkaline batholiths. The Journal of Geology, 108(3), 303-320.

Weinberg, R.F., Dunlap, W.J., Whitehouse, M., 2000. New field, structural and geochronological data from the Shyok and Nubra valleys, northern Ladakh: linking Kohistan to Tibet. In: Khan, M.A., Treloar, P.J., Searle, M.P., Jan, M.Q., (Eds.), Tectonics of the Nanga Parbat Syntaxis and the Western Himalaya. Geological Society, London, Special Publications, 170(1), 253-275.

Whipple, K.X., 2004. Bedrock rivers and the geomorphology of active orogens. Annual Review of Earth and Planetary Sciences, 32, 151-185.

Whipple, K.X., Tucker, G.E., 1999. Dynamics of the stream-power river incision model: Implications for height limits of mountain ranges, landscape response timescales, and research needs: Journal of Geophysical Research, 104,17661-17674.

White, N. M., Pringle, M., Garzanti, E., Bickle, M., Najman, Y., Chapman, H., Friend, P., 2002. Constraints on the exhumation and erosion of the High Himalayan Slab, NW

India, from foreland basin deposits. Earth and Planetary Science Letters, 195(1-2), 29-44.

Whittington, A.G., 1996. Exhumation overrated at Nanga Parbat, northern Pakistan. Tectonophysics, 260(1-3), 215-226.

Whittington, A., Foster, G., Harris, N., Vance, D., Ayres, M., 1999. Lithostratigraphic correlations in the western Himalaya—an isotopic approach. Geology, 27(7), 585-588.

Willems, H., Zhou, Z., Zhang, B., Gräfe, K.U., 1996. Stratigraphy of the Upper Cretaceous and lower Tertiary strata in the Tethyan Himalayas of Tibet (Tingri area, China). Geologische Rundschau, 85(4), 723.

Williams, M.L., Jercinovic, M.J., Hetherington, C.J., 2007. Microprobe monazite geochronology: understanding geologic processes by integrating composition and chronology. Annual Review of Earth and Planetary Sciences, 35, 137-175.

Win, K.S., Takeuchi, M., Tokiwa, T., 2007. Changes in detrital garnet assemblages related to transpressive uplifting associated with strike–slip faulting: an example from the Cretaceous System in Kii Peninsula, Southwest Japan. Sedimentary Geology, 201(3-4), 412-431.

Winkler, W., Bernoulli, D., 1986. Detrital high-pressure/low-temperature minerals in a late Turonian flysch sequence of the Eastern Alps (western Austria): Implications for early Alpine tectonics. Geology, 14, 598-601.

Wu, F., Ji, W., Liu, C., Chung, S., 2010. Detrital zircon U–Pb and Hf isotopic data from the Xigaze fore-arc basin: constraints on Transhimalayan magmatic evolution in southern Tibet. Chemical Geology, 271(1-2), 13-25.

Wu, F., Liu, Z., Liu, X., Ji, W., 2015. Himalaya Leucogranite: petrogenesis and implication to orogenesis and plateu uplift. Acta Petrologica Sinica, 31(1), 1-36. (in chinese).

Yamamoto, H., 1993. Contrasting metamorphic P–T–time paths of the Kohistan granulites and tectonics of the western Himalayas. Journal of the Geological Society, 150(5), 843-856.

Yang, D., Oyang, H., Zhou, C., Chen, C., 2011. Runoff Characteristics of the Nyangqu River Basin on the Qinghai-Tibet Plateau. Resources Science, 33(7),1272-1277. (in chinese).

Yavuz, F., Yildirim, D.K., 2018. A Windows program for calculation and classification of epidote-supergroup minerals. Periodical of Mineralogy, 87(3), 269-285.

Young, G.M., Nesbitt, H.W., 1998. Processes controlling the distribution of Ti and Al in weathering profiles, siliciclastic sediments and sedimentary rocks. Journal of Sedimentary research, 68(3), 448-455.

Zack, T., Stockli, D.F., Luvizotto, G.L., Barth, M.G., Belousova, E., Wolfe, M.R., Hinton, R.W., 2011. In situ U–Pb rutile dating by LA-ICP-MS: ^{208}Pb correction and prospects for geological applications. Contributions to Mineralogy and Petrology, 162, 515-530.

Zanchi, A., Gaetani, M., 2011. The geology of the Karakoram range, Pakistan: the new 1: 100,000 geological map of Central-Western Karakoram. Italian journal of Geosciences, 130(2), 161-262.

Zeitler, P.K., Chamberlain, C.P., 1991. Petrogenetic and tectonic significance of young leucogranites from the northwestern Himalaya, Pakistan. Tectonics, 10(4), 729-741.

Zeitler, P.K., Chamberlain, C.P., Smith, H.A., 1993. Synchronous anatexis, metamorphism, and rapid denudation at Nanga Parbat (Pakistan Himalaya). Geology, 21(4), 347-350.

Zeitler, P.K., Meltzer, A.S., Koons, P.O., Craw, D., Hallet, B., Chamberlain, C.P., Kidd, W.S., Park, S.K., Seeber, L., Bishop, M., Shroder, J., 2001. Erosion, Himalayan geodynamics, and the geomorphology of metamorphism. GSA Today, 11(1), 4-9.

Zhang, H., Harris, N., Parrish, R., Kelley, S., Zhang, L., Rogers, N., Argles, T., King, J., 2004. Causes and consequences of protracted melting of the mid-crust exposed in the North Himalayan antiform. Earth and Planetary Science Letters, 228(1-2), 195-212.

Zhang, J., Yin, A., Liu, W., Wu, F., Lin, D., Grove, M., 2012. Coupled U-Pb dating and Hf isotopic analysis of detrital zircon of modern river sand from the Yalu River (Yarlung Tsangpo) drainage system in southern Tibet: Constraints on the transport processes and evolution of Himalayan rivers. Bulletin, 124(9-10), 1449-1473.

Zhang, X., Wang, X., Chen C., 2010. Dynamic analysis of land use change in Nianchu river basin supported by RS&GIS. In The 2nd International Conference on Information Science and Engineering (pp. 3665-3668). IEEE.

Zhou, C., Yang, W., Wu, L., Liu, S., 2009. Glacier changes from a new inventory, Nianchu river basin, Tibetan Plateau. Annals of Glaciology, 50(53), 87-92.

Zhu, D., Zhao, Z., Niu, Y., Mo, X., Chung, S., Hou, Z., Wang, L., Wu, F., 2011. The Lhasa Terrane: Record of a microcontinent and its histories of drift and growth. Earth and Planetary Science Letters, 301(1-2), 241-255.

Zhuang, G., Najman, Y., Guillot, S., Roddaz, M., Antoine, P.O., Métais, G., Carter, A., Marivaux, L., Solangi, S.H., 2015. Constraints on the collision and the pre-collision tectonic configuration between India and Asia from detrital geochronology, thermochronology, and geochemistry studies in the lower Indus basin, Pakistan. Earth and Planetary Science Letters, 432, 363-373.

Zhuang, G., Najman, Y., Tian, Y., Carter, A., Gemignani, L., Wijbrans, J., Qasim Jan, M., Khan, M.A., 2018. Insights into the evolution of The Hindu Kush-Kohistan-Karakoram from modern river sand detrital geo-and thermochronological studies. Journal of the Geological Society, 175(6), 934-948.

Zuffa, G.G., 1987. Unravelling hinterland and offshore palaeogeography from deep-water arenites. In: Leggett, J.K., Zuffa, G.G., (Eds.), Marine Clastic Sedimentology, Graham and Trotman, London, pp: 39-61.

Appendices

Appendix Table A1 Detailed information of samples in Nianchu catchment.

River	Site	Sample	Year	Received from	Latitude	Longitude	Drainage
Nianchu Basin							
Chongbayongchu	Canguo, Kangmar	16A047	2016	An Wei / Fu Hanpu	28°40′16″N	89°39′47″E	Nianchu
Chongbayongchu	Shaogang, Kangmar	16A048	2016	An Wei / Fu Hanpu	28°41′08″N	89°38′09″E	Nianchu
Chongbayongchu	Yawen	16A049	2016	An Wei / Fu Hanpu	28°44′15″N	89°39′12″E	Nianchu
Chongbayongchu	Baisu, Kangmar	16A050	2016	An Wei / Fu Hanpu	28°50′17″N	89°39′11″E	Nianchu
Nieru	Baizha, Gyangze	16A051	2016	An Wei / Fu Hanpu	28°51′03″N	89°41′28″E	Nianchu headwaters
Nianchu	Zaxixiong	16A052	2016	An Wei / Fu Hanpu	28°52′35″N	89°37′27″E	Yarlung Tsangpo
Rilang	Gyangze	16A046	2016	An Wei / Fu Hanpu	28°54′29″N	89°37′04″E	Nianchu
Rilang	Gyangze	S4682	2013	E.Garzanti	28°54′24″N	89°37′00″E	Nianchu
Nianchu	Gyangze	16A053	2016	An Wei / Fu Hanpu	28°54′19″N	89°36′02″E	Yarlung Tsangpo
Sala	Sala	16A054	2016	An Wei / Fu Hanpu	28°56′56″N	89°32′47″E	Nianchu
Nianchu	Dazi, Bailang	16A055	2016	An Wei / Fu Hanpu	29°02′41″N	89°27′38″E	Yarlung Tsangpo
Qiangdui	Jiebai, Bailang	16A056	2016	An Wei / Fu Hanpu	29°06′47″N	89°22′53″E	Nianchu
Nianchu	Bailang	16A058	2016	An Wei / Fu Hanpu	29°05′16″N	89°17′00″E	Yarlung Tsangpo
Danxiong	Qiaga, Bailang	16A057	2016	An Wei / Fu Hanpu	29°04′07″N	89°16′03″E	Nianchu
Qiangrang	Qiongrang, Xigaze	16A059	2016	An Wei / Fu Hanpu	29°10′07″N	89°03′23″E	Nianchu
Nianchu	Jiacuoxiong, Xigaze	16A060	2016	An Wei / Fu Hanpu	29°12′07″N	88°57′03″E	Yarlung Tsangpo
Qumei	Qumei	S4717	2013	E.Garzanti	29°09′09″N	88°43′54″E	Zire
Zire	Sixia, Xigaze	16A061	2016	An Wei / Fu Hanpu	29°13′36″N	88°54′09″E	Nianchu
Zire	Xigaze	S4685	2013	E.Garzanti	29°13′47″N	88°54′51″E	Nianchu
Nianchu	Xigaze	S4686	2013	E.Garzanti	29°16′28″N	88°53′51″E	Yarlung Tsangpo
Nianchu	Ama, Xigaze	16A062	2016	An Wei / Fu Hanpu	29°17′05″N	88°53′41″E	Yarlung Tsangpo
Other river catchments							
Naixia	Naixia	S4715	2013	E.Garzanti	29°09′05″N	88°26′27″E	Shapu
Pading	Pading	S4716	2013	E.Garzanti	29°07′57″N	88°23′54″E	Shapu
Bangale	upstream	S4708	2013	E.Garzanti	29°20′43″N	86°40′28″E	Doxu Tsangpo
Lai Wu Lu Su	Liuxiang	S4714	2013	E.Garzanti	29°10′47″N	88°10′45″E	Liuchu
Jianen	Jianen	S4701	2013	E.Garzanti	29°20′04″N	85°24'18″E	Yarlung Tsangpo

Appendix Table A2 Petrography in samples of Nianchu catchment.

River	Sample	Operator	Q	K	P	Lvf	Lvm	Lcc	Lcd	Lp	Lch	Lms	Lmv	Lmf	Lmb	Lu	mica	HM	total
Chongbayongqu	16A047	A.Resentini	53	3	11	0	0	3	1	10	0	16	1	1	0	0	0.3	1	100.0
Chongbayongqu	16A048	A.Resentini	43	3	5	0	0	16	1	6	0	13	0.3	5	0.3	0	3	3	100.0
Chongbayongqu	16A050	A.Resentini	23	1	6	1	0.3	11	0	23	0	29	1	3	0.1	0	2	1	100.0
Nianchu	16A051	A.Resentini	20	2	5	0.1	0.1	5	1	45	0	17	0	3	0	0	1	0.3	100.0
Gyangze	S4682	A.Resentini	39	2	5	0.2	0.4	3	0.3	20	0	29	0.3	0	0	0	1	0.3	100.0
Nianchu	16A055	A.Resentini	36	1	4	0	0	5	0.3	32	0.3	17	0.3	1	0.3	0	1	2	100.0
Qiangdui	16A056	A.Resentini	25	1	7	0	0.3	0	0	5	0	16	0	0	1	40	1	6	100.0
Danxiongqu	16A057	A.Resentini	46	3	6	0	0	2	0	25	1	11	0.3	1	0	1	0	3	100.0
Qiongrang	16A059	A.Resentini	20	1	9	0	0	1	0	6	0.3	26	3	1	3	22	1	7	100.0
Nianchu	16A060	A.Resentini	47	2	7	0.3	1	2	0.3	14	0	15	0	0.4	0.1	5	1	4	100.0
Zire	16A061	A.Resentini	49	0.3	4	1	1	7	5	10	0	10	0.3	1	1	9	0.3	5	100.0
Zire	S4685	A.Resentini	43	1	6	1	1	5	0	13	0.3	22	0.3	0	0.3	7	0.3	1	100.0
Nianchu	S4686	A.Resentini	35	1	6	1	0	4	0.3	17	0	22	1	1	0.3	9	0.3	2	100.0
Nianchu	16A062	A.Resentini	30	2	9	1	0.3	4	0.4	11	1	29	4	4	0	3	0.3	2	100.0

River	Sample	MI*	MI	Q	F	L		Lm	Lv	Ls		Q	P	K		Qp/Q	P/F
Chongbayongqu	16A047	130	85	54	15	31	100.0	30	1	70	100.0	78	17	5	100.0	31	78
Chongbayongqu	16A048	196	148	46	9	46	100.0	29	0	71	100.0	84	10	6	100.0	14	61
Chongbayongqu	16A050	162	95	23	6	70	100.0	26	2	72	100.0	79	19	2	100.0	11	91
Nianchu	16A051	142	45	21	7	72	100.0	16	0	84	100.0	73	18	8	100.0	18	69
Gyangze	S4682	110	63	40	7	54	100.0	27	1	71	100.0	85	10	4	100.0	29	71
Nianchu	16A055	140	55	37	5	58	100.0	18	0	82	100.0	88	10	2	100.0	23	84
Qiangdui	16A056	134	101	26	8	65	100.0	79	0	21	100.0	76	21	3	100.0	17	89
Danxiongqu	16A057	136	47	48	10	43	100.0	19	0	81	100.0	83	11	6	100.0	9	67
Qiongrang	16A059	155	133	22	10	68	100.0	65	3	32	100.0	68	30	2	100.0	17	94
Nianchu	16A060	128	74	49	10	41	100.0	34	2	64	100.0	83	13	4	100.0	7	78
Zire	16A061	142	71	51	4	45	100.0	35	3	62	100.0	93	7	1	100.0	10	93
Zire	S4685	127	76	43	7	50	100.0	37	3	59	100.0	86	13	1	100.0	13	92
Nianchu	S4686	135	81	36	7	57	100.0	39	2	59	100.0	83	13	3	100.0	17	79
Nianchu	16A062	141	105	31	11	58	100.0	41	5	53	100.0	74	22	4	100.0	25	83

Appendix Table A3 Heavy minerals in samples of Nianchu catchment.

River	Site	Sample	Class	Method	Operator	zircon	tourmaline	rutile	Ti Oxides	titanite	apatite	monazite	barite	vesuvianite	epidote	prehnite	garnet	chloritoid	staurolite	andalusite	kyanite	sillimanite	amphibole	clinopyroxene	hypersthene	enstatite	olivine	spinel	Total
Nianchu Basin			(µm)																										
Chongbayongchu	Canguo, Kangmar	16A047	32-500	Point	W.Liang	1	6	0	0	1	10	0	0	0	8	0	33	0.5	0	1	0	17	15	7	0	0	0	0	100.0
Chongbayongchu	Shaogang, Kangmar	16A048	32-500	Point	W.Liang	0.5	11	1	0.5	0.5	7	0	0	0	9	0	15	4	0	1	0.5	6	41	5	0	0	0	0	100.0
Chongbayongchu	Yawen	16A049	32-500	Area	W.Liang	4	9	1	0	3	5	0.4	0	0	17	0	14	15	0	1	0.4	2	22	6	0	0	0	0	100.0
Chongbayongchu	Baisu, Kangmar	16A050	32-500	Area	W.Liang	2	13	1	0	2	4	0	0	0	8	0	11	38	0	1	1	1	17	3	0	0	0	0	100.0
Nieru	Baizha, Gyangze	16A051	32-500	Area	W.Liang	2	10	1	0	2	9	0	0	0	22	0	8	18	0	1	0	1	12	14	0	0	0	2	100.0
Nianchu	Zhaxixiong	16A052	32-500	Area	W.Liang	2.2	7	3	0	1	9	0	0	0	18	0	9	21	0	1	0	2	14	11	0	0.4	0	1	100.0
Rilang	Gyangze	16A046	32-500	Area	W.Liang	6.7	15	1	0	4	8	0	0	0	15	0.4	16	10	0	1	0	2	14	7	0	0	0	0	100.0
Rilang	Gyangze	S4682	32-500	Point	W.Liang	4	8	1	0	3	5	0	0	0.9	11	0	32	8	0	3	0.5	5	13	5	0	0	0	0	100.0
Nianchu	Gyangze	16A053	32-500	Area	W.Liang	3	7	3	0	2	9	1	0	0	18	1	12	11	0	1	0	2	10	18	0	0	1	0	100.0
Sala	Sala	16A054	32-500	Area	W.Liang	2	13	1	0	6	7	0	0	0	22	0	12	13	0	0	0	2	18	3	0	0	0	0	100.0
Nianchu	Dazi, Bailang	16A055	32-500	Area	W.Liang	3	19	1	0	3	6	0	0	0	16	0	11	15	0	1	0	2	17	6	0	0.4	0	0	100.0
Qiangdui	Jiebai, Bailang	16A056	32-500	Point	W.Liang	1	3	0	0	0	4	0	0	0	20	4	9	5	0.5	0.5	0	4	14	25	0	2	5	2	100.0
Nianchu	Bailang	16A058	32-500	Area	W.Liang	4	4	1	0	4	4	0	0	0.6	19	1	21	7	0	1	0	1	15	15	0	0	2	1	100.0
Danxiong	Qiaga, Bailang	16A057	32-500	Point	W.Liang	5	15	1	0	4	8	0	0	0	16	3	12	4	2	3	0	0.5	16	10	0	0	0	1	100.0
Qiongrang	Qiongrang, Xigaze	16A059	32-500	Point	W.Liang	0.4	4	1	0	0.4	3	0	0.4	0	28	4	4	8	0	0.4	0	0.4	34	8	0	0	0.4	3	100.0
Nianchu	Jiacuoxiong, Xigaze	16A060	32-500	Point	W.Liang	3	11	0.5	0	1	7	0	0.5	0	21	2	4	14	0	0.5	0	0.5	24	8	0	0	1	0.5	100.0
Qumei	Qumei	S4717	32-500	Area	W.Liang	2	9	0	0.5	4	6	0	0	0	20	2	11	9	2	0.5	0	0.5	17	12	0	0.5	1	1	100.0
Zire	Sixia, Xigaze	16A061	32-500	Area	W.Liang	18	9	2	0	3	4	1	1	0	10	0	7	10	0	0	2	0	17	9	0	2	2	4	100.0
Zire	Xigaze	S4685	32-500	Area	W.Liang	2	10	0	1	3	7	0	0	0	13	0.5	6	8	0	0	0.5	0	16	21	0	3	7	1	100.0
Nianchu	Xigaze	S4686	32-500	Area	W.Liang	6	8	0.5	0	3	5	0.5	0	0.5	14	1	4	11	0	0.5	0	1	23	18	0.5	3	0.5	1	100.0
Nianchu	Ama, Xigaze	16A062	32-500	Area	W.Liang	3	7	0.5	0	1	1	0	0	0	13	2	17	11	0	0.5	0	0	13	18	0	4	9	1	100.0

River	Site	Sample	SRD	HM %weight	tHM %weight	%finer	%class	%coarser	ZTR	HCI	MMI	% transparent	% opaque	% Fe Oxide	% Ti Oxide	% turbid HM	% rock fragments	% soils, turbids	% chlorite	% biotite	% carbonates	% light minerals	Total
Nianchu Basin																							
Chongbayongchu	Canguo, Kangmar	16A047	2.64	0.9	0.8	2%	85%	14%	7	22	97	50%	3%	1%	1%	0%	7%	29%	6%	3%	0%	0%	100.0%
Chongbayongchu	Shaogang, Kangmar	16A048	2.67	1.1	0.9	8%	92%	0%	12	7	58	30%	2%	0%	3%	0%	4%	20%	12%	28%	0%	0%	100.0%
Chongbayongchu	Yawen	16A049	2.68	2.6	1.7	3%	86%	12%	14	11	16	40%	6%	6%	4%	5%	8%	20%	4%	4%	0%	1%	100.0%
Chongbayongchu	Baisu, Kangmar	16A050	2.63	1.2	0.7	3%	37%	61%	16	12	4	11%	3%	2%	2%	0%	6%	60%	11%	4%	0%	1%	100.0%
Nieru	Baizha, Gyangze	16A051	2.56	0.5	0.3	18%	82%	0%	13	18	3	14%	2%	2%	1%	0%	4%	51%	16%	1%	8%	1%	100.0%
Nianchu	Zhaxixiong	16A052	2.67	1.9	0.7	24%	76%	0%	12	7	10	14%	2%	12%	2%	9%	10%	26%	5%	3%	15%	2%	100.0%
Rilang	Gyangze	16A046	2.66	0.7	0.5	4%	73%	23%	23	16	14	20%	4%	1%	3%	1%	8%	42%	7%	2%	12%	1%	100.0%
Rilang	Gyangze	S4682	2.62	2.0	1.1	4%	94%	2%	13	15	42	36%	4%	14%	6%	3%	3%	28%	3%	2%	0%	0%	100.0%
Nianchu	Gyangze	16A053	2.66	0.8	0.4	5%	94%	1%	13	13	15	16%	2%	5%	7%	7%	5%	36%	11%	3%	10%	1%	100.0%
Sala	Sala	16A054	2.67	1.7	1.3	15%	83%	2%	16	17	16	21%	1%	2%	2%	0%	6%	62%	2%	0%	1%	1%	100.0%
Nianchu	Dazi, Bailang	16A055	2.59	1.0	0.8	8%	53%	39%	23	6	11	26%	3%	1%	2%	0%	3%	54%	6%	1%	3%	1%	100.0%
Qiangdui	Jiebai, Bailang	16A056	2.77	3.5	2.8	16%	84%	0%	4	19	47	40%	5%	2%	4%	0%	2%	41%	4%	1%	0%	2%	100.0%
Nianchu	Bailang	16A058	2.67	1.7	0.9	2%	80%	18%	9	0	14	27%	7%	8%	5%	6%	5%	29%	9%	0%	1%	1%	100.0%
Danxiong	Qiaga, Bailang	16A057	2.60	1.4	1.0	4%	85%	11%	21	30	17	21%	2%	4%	3%	0%	5%	61%	4%	1%	0%	0%	100.0%
Qiongrang	Qiongrang, Xigaze	16A059	2.74	3.7	3.2	12%	86%	2%	6	25	6	33%	2%	1%	2%	0%	2%	52%	6%	1%	1%	1%	100.0%
Nianchu	Jiacuoxiong, Xigaze	16A060	2.65	1.6	1.4	11%	89%	0%	15	19	3	30%	1%	1%	2%	0%	4%	50%	10%	1%	1%	0%	100.0%
Qumei	Qumei	S4717	2.67	0.7	0.5	4%	71%	25%	11	8	11	31%	6%	0%	5%	0%	4%	52%	1%	1%	1%	0%	100.0%
Zire	Sixia, Xigaze	16A061	2.70	5.4	2.6	3%	86%	11%	29	8	10	25%	12%	6%	9%	0%	4%	44%	0%	1%	0%	0%	100.0%
Zire	Xigaze	S4685	2.67	2.5	2.1	6%	82%	12%	12	6	4	33%	1%	1%	5%	0%	5%	46%	7%	0%	0%	1%	100.0%
Nianchu	Xigaze	S4686	2.66	1.8	1.3	5%	95%	0%	14	19	8	29%	4%	1%	7%	0%	3%	49%	4%	1%	1%	1%	100.0%
Nianchu	Ama, Xigaze	16A062	2.66	2.3	1.6	3%	91%	5%	10	8	0	32%	5%	6%	3%	0%	3%	46%	3%	0%	0%	1%	100.0%

Appendix Table B1 Detailed sample information from Thal Desert and Upper Indus tributaries

Sample	River bars	Location	Country	Collected by	Year	Latitude	Longitude	Tectonic domain	Grain size		Sorting	Zr	REE
									μm	ϕ units	σφ	ppm	ppm
	End members												
S1749	Hushe	downstream Charakusa	Pakistan	Mike Searle	2001	35°30'55" N	76°24'23" E	Karakorum	140	2.83	0.97	n.d.	n.d.
S1748	Braldu	downstream Baltoro	Pakistan	Mike Searle	2001	35°40'14" N	76°06'58" E	Karakorum	109	3.20	0.69	n.d.	n.d.
S1437	Hunza	Altit	Pakistan	Giacomo Ghielmi, Filippo Lazzati	2001	36°18'52" N	74°41'07" E	Northern Karakorum	213	2.23	0.63	n.d.	n.d.
S1438	Hispar	Nagar	Pakistan	Giacomo Ghielmi, Filippo Lazzati	2001	36°17'57" N	74°40'33" E	Southern Karakorum	259	1.95	0.67	395	479
S4426	Stagmo	Stagmo	India	Jan Blöthe, Henry Munack	2011	34°07'00" N	77°42'00" E	Ladakh arc	164	2.61	n.d.	n.d.	n.d.
S4430	Domkar	Domkar	India	Jan Blöthe, Henry Munack	2011	34°23'27" N	76°46'21" E	Ladakh arc	351	1.51	n.d.	157	130
S1439	Kandia	Halil	Pakistan	Giacomo Ghielmi, Filippo Lazzati	2001	35°26'46" N	73°12'31" E	Kohistan arc	215	2.22	0.83	113	88
S1440	Swat	Fatepur	Pakistan	Giacomo Ghielmi, Filippo Lazzati	2001	35°03'16" N	72°28'30" E	Kohistan arc	330	1.60	0.63	110	66
S4419	Zanskar	Rumbak	India	Jan Blöthe, Henry Munack	2011	34°08'34" N	77°17'04" E	Greater+Tethys Himalaya	223	2.17	n.d.	186	227
S1426	Nandihar	Daut	Pakistan	Giacomo Ghielmi, Filippo Lazzati	2001	34°46'16" N	72°55'50" E	Greater Himalaya	244	2.03	0.84	113	90
S1432	Astor	Bunji	Pakistan	Giacomo Ghielmi, Filippo Lazzati	2001	35°34'27" N	74°39'12" E	Nanga Parbat	233	2.10	0.75	134	135
	Desert dunes												
S1462	Thal	Mankera	Pakistan	Giacomo Ghielmi, Filippo Lazzati	2001	31°23'47" N	71°25'27" E	Thal Desert	125	3.00	0.50	195	179
S1463	Thal	Haidarabad	Pakistan	Giacomo Ghielmi, Filippo Lazzati	2001	31°20'42" N	71°42'12" E	Thal Desert	157	2.67	0.84	213	188
S1470	Thal	Muzaffarghar	Pakistan	Giacomo Ghielmi, Filippo Lazzati	2001	30°04'18" N	71°08'40" E	Thal Desert	152	2.72	0.52	524	371
S1474	Thal	Munda	Pakistan	Giacomo Ghielmi, Filippo Lazzati	2001	30°34'56" N	71°15'16" E	Thal Desert	121	3.05	0.43	106	104

Appendix Table B2 Heavy minerals from the Raman spectroscopy in Thal Desert and Upper Indus tributaries

								Zrn	tourmaline			Ti oxides			Ttn	apatite			epidote					garnet						Cld	St	An
River	Sample	counted class	% fine tail cut	% class	% coarse tail cut	HMC	tHMC	zircon	dravite	schorlite	others	rutile	anatase	brookite	titanite	F-apatite	others	Fe-rich	zoisite	clinozoisite	allanite	piemontite	others	spessartine	grossular	pyrope	andradite	uvarovite	others	chloritoid	staurolite	andalusite
SOURCE		µm																														
Hushe	S1749	63-250	5%	75%	20%	4.8	2.5	1	0.2	0	0	1	0.3	0.1	8	0.6	4	3	0	1	3	1	3	1	0.3	0	0	0	1	0	0	0
Braldu	S1748	63-250	5%	84%	11%	6.5	4.5	0.7	0.8	0.2	0	3	0	0.2	7	0.3	5	2	0.1	4	2	1	3	1	0.1	0.2	0	0	4	1	0.3	0.
Hunza	S1437	63-250	2%	62%	36%	2.9	1.5	0.4	0.9	0.6	0.1	8	0.1	0	8	0.3	4	5	0.1	5	2	1	3	0.3	0.3	0	0	0.3	0.3	0	0.1	0.
Hispar	S1438	63-250	2%	48%	50%	8.7	6.7	2	0.8	0.2	0	1	0.2	0	8	0.2	2	3	0	7	2	2	5	4	1	0.2	0	0	16	0.2	0.4	0
Stagmo	S4426	32-500	1%	58%	41%	12.6	12.0	0.4	0.4	0	0	0.4	0	0	5	0	0.7	0.7	0	0	0.4	0.7	0.7	0	0	0	0	0	0	0	0	0
Domkar	S4430	32-500	1%	47%	51%	9.7	8.1	2	0	0.2	0	1	0	0.2	4	0.5	0.3	2	0	0.3	0.2	1	1	0.3	0.2	0	0.2	0	0	0	0	0
Kandia	S1439	63-250	5%	51%	44%	44.2	33.4	0	0	0	0	0.4	0	0	6	0.2	0.2	2	2	19	0	2	4	0	0	1	0	0	0.4	0	0	0
Swat	S1440	63-250	0%	23%	77%	31.4	27.5	0.2	0	0	0	2	0	0	1	0	0.6	0.4	0	2	0.2	1	1	0.2	0.2	0	0	0	0.2	0	0	0
Zanskar	S4419	32-500	1%	99%	0%	4.8	4.6	0.7	2	2	0.7	1	0.1	0.1	7	0.1	6	3	0	0.2	1	1	3	3	0	0	0.1	0	14	0	0.2	0
Nandihar	S1426	63-250	3%	47%	50%	4.8	4.0	0.5	4	3	0.5	0.9	0.2	0	4	0.3	2	0.7	0.5	0.9	0.5	0.3	0.3	3	0.5	0	0	0	16	0	2	0
Astor	S1432	63-250	5%	45%	50%	17.9	16.9	0.1	0.6	0.3	0.1	2	0	0	1	0.1	0.1	4	0.6	4	0.4	1	3	4	0.3	0.1	0	0.1	4	0	0.1	0.
SINK																																
Thal Desert	S1462	63-250	4%	89%	7%	21.2	15.3	0	0.7	0.1	0.3	1	0.1	0.1	4	0.1	0.1	4	0.4	13	0.1	1	2	3	0.3	0.1	0	0.1	8	0.3	0.7	0
Thal Desert	S1463	63-250	5%	72%	24%	24.2	18.6	0	0	0.4	0	2	0	0	5	0	1	6	0.8	9	0.6	0.8	4	4	0.4	0.6	0	0	7	0	0.6	0.
Thal Desert	S1470	63-250	0%	87%	13%	26.4	17.7	0.3	0.3	0.3	0.1	2	0.1	0	4	0.1	1	4	0.5	12	0.1	1	3	3	0.1	0.3	0	0	6	0	0.4	0
Thal Desert	S1474	63-250	3%	92%	5%	12.3	10.0	0.2	0.2	0.4	0.5	1	0	0	4	0	1	5	0.2	10	0	0.8	5	3	0	0.4	0	0	5	0	0.5	0

amphibole						clinopyroxene					En	Hy	olivine		other transparent minerals						opaque minerals								phyllosilicates				carbonate		light minerals				Gyp		
hornblende	kaersutite	actinolite	tremolite	anthophyllite	pargasite	augite	diopside	pigeonite	aegirine	others	enstatite	hypersthene	Fe-rich	others	monazite	ghanite	barite	vesuvianite	prehnite	axinite	magnetite	ilmenite	hematite	goethite	Fe-hydroxide	chromite	sphalerite	pyrite	muscovite	biotite	chlorite	others	calcite	dolomite	quartz	K-feldspar	sanidine	plagioclase	gypsum		n° total grains
47	0	0.1	0.6	0.1	0	1	2	0	0	0.6	0	0	0.1	0.3	0.1	0	0	0	0	0	0.5	0	0	6	0.1	2	0.1	0.6	0	10	0.1	0	0	0	0.4	0.1	0	0.3	0	100.0	1263
33	0.2	0.5	0.7	0.1	0.2	1	5	0.1	0.1	2	0	0	0	0.4	0.5	0.1	0.2	0	0	0	1	0.2	0	5	0.1	0.5	0.2	0.4	0.5	6	0.2	0	0.5	1	2	0.2	0	1	0.1	100.0	1300
36	0	0	0	0.3	0	0.7	3	0	0	2	0	0.1	0	0	0.3	0	0	0	0	0	1	0	0	3	0	0.9	0	2	0.3	7	0.7	0	0.9	0	2	0.1	0	0.4	0	100.0	698
20	0	0	0.4	0.6	0	0	2	0	0	2	0	0	0	0.2	0	0	0	0	0	0	4	2	0	6	0.4	0.4	0.2	1	0	2	0	0	0.2	0.2	1	0	0	0.6	0	100.0	494
70	0	0	0	0	0	0.7	1	0	0	4	0	0	0	0	0	0	0	0	0	0	0.4	0	0	11	0	1	0	0	0	0.4	0	0	0	0	1	0	0	0.4	0	100.0	275
48	0.2	0.2	0.2	0	0	1	0.3	0.5	0	2	0	0.2	0	0	0	0	0	0	0.3	0	0.2	0.2	0	30	0	0.5	0.2	0	0	0.3	0.2	0	0	0	1	0.2	0.2	1	0	100.0	579
43	0	0.4	0.4	0	0	0.4	0.9	1	0	0.9	0	0	0	0.2	0	0	0	0	0	0	1	0	0	1	0	0	0.2	0	0	0	0	0.2	0	0.2	1	0	0	10	0	100.0	468
45	0	0	0	0.4	0.2	6	2	15	0	10	0	4	0	0	0	0	0	0	0	0	0.2	0.2	0	4	0	0	0.2	0	0	1	0	0	0	0	2	0	0	0	0	100.0	538
15	1	0	0.5	0.2	0	0.6	4	0.1	0	4	0	0	0	0.1	0.5	0.1	0	0	0	0	0.2	0.5	0	2	0	0.7	0.1	0.4	0.7	7	0.2	0	0.1	1	5	0	0	0.6	0	100.0	821
27	0.5	0.3	0.2	0	0.2	4	2	2	0	3	0	2	0	0	0	0	0	0	0	0.2	2	1	0	1	0	0.7	0.3	0	0.2	2	0	0	0	0	4	0	0	0.5	0	100.0	587
56	0.3	0.8	0.7	0.1	1	0.4	3	0.6	0	1	0	0	0	0.1	0	0	0	0	0	0.1	5	0.1	0	0.7	0	1	0	0.4	0	0.4	0	0	0	0	1	0	0	0.1	0	100.0	721
32	0	0.9	1	0.4	0	0.4	5	2	0	2	0.3	0.9	0	0.4	0.3	0	0	0	0	0	5	1	0.1	0	0.1	0.1	0	0	0.3	0.4	0.1	0	0	0	3	0.3	0	2	0.1	100.0	700
29	0	0.4	1	0.2	0.2	0.6	4	3	0	3	0	2	0	0.4	0	0	0	0	0	0	3	2	0	1	0.2	0.2	0	0	1	0.2	0	0	0	0	3	0.2	0	2	0	100.0	526
28	0.1	0.1	0.5	0.1	0.3	1	4	3	0	2	0	2	0	1	0	0	0	0.1	0.1	0	1	1	0	3	0	0.5	0	0	0.3	0.8	0.3	0	0	0	3	0.3	0.1	6	0	100.0	730
34	0.2	0.4	0.4	0.2	0.1	1	4	3	0	4	0.1	2	0	0.2	0.1	0	0	0	0	0	3	1	0.2	0.5	0	0.4	0	0	0.1	2	0	0	0	0	3	0.2	0.1	3	0	100.0	831

Appendix Table B3 SEM-EDS data and chemical calculations in amphibole of Thal Desert and Upper Indus tributaries.

Point	Sample	River/Dune	Domain	Na_2O	MgO	Al_2O_3	SiO_2	K_2O	CaO	TiO_2	MnO	FeO	Total	Group	Subgroup	Species
				wt%	wt%	wt%	wt%	wt%	wt%	wt%	wt%	wt%			of (OH,F,Cl)	
7-1	1749	Hushe	Karakorum	1.28	11.78	10.01	46.71	0.88	12.06	0.86	0.29	14.98	98.84	OH,F,Cl	Ca	magnesio-hornblende
10-1	1749	Hushe	Karakorum	1.51	9.20	10.77	42.87	1.78	11.63	1.12	0.56	19.51	98.95	OH,F,Cl	Ca	ferro-pargasite
14-1	1749	Hushe	Karakorum	1.55	12.28	8.73	46.83	0.54	10.88	0.85	0.33	16.69	98.69	OH,F,Cl	Ca	magnesio-hornblende
15-1	1749	Hushe	Karakorum	1.59	9.96	11.81	41.62	1.60	12.08	0.95	0.54	18.03	98.18	OH,F,Cl	Ca	magnesio-hastingsite
16-1	1749	Hushe	Karakorum	1.61	11.25	10.66	43.60	1.00	11.34	0.82	0.50	16.67	97.46	OH,F,Cl	Ca	magnesio-hastingsite
21-1	1749	Hushe	Karakorum	1.59	10.40	10.74	43.14	1.61	11.48	0.97	0.60	17.24	97.77	OH,F,Cl	Ca	pargasite
206-1	1749	Hushe	Karakorum	1.32	10.54	10.87	43.88	1.50	11.55	1.09	0.43	16.72	97.92	OH,F,Cl	Ca	pargasite
207-1	1749	Hushe	Karakorum	1.51	11.36	8.49	45.77	0.95	11.54	1.12	0.39	16.73	97.87	OH,F,Cl	Ca	pargasite
209-1	1749	Hushe	Karakorum	1.34	8.91	13.13	41.83	1.44	11.64	0.76	0.55	18.45	98.05	OH,F,Cl	Ca	pargasite
214-1	1749	Hushe	Karakorum	1.55	9.51	12.32	42.35	1.66	11.71	0.50	0.35	18.09	98.03	OH,F,Cl	Ca	pargasite
216-1	1749	Hushe	Karakorum	1.41	10.67	10.21	45.05	1.28	12.01	0.69	0.46	18.46	100.22	OH,F,Cl	Ca	magnesio-hastingsite
221-1	1749	Hushe	Karakorum	1.08	10.59	8.90	46.51	1.09	11.95	0.88	0.54	16.79	98.33	OH,F,Cl	Ca	magnesio-hornblende
225-1	1749	Hushe	Karakorum	1.88	10.41	14.35	43.05	0.39	11.09	1.18	0.38	14.53	97.26	OH,F,Cl	Ca	magnesio-hornblende
228-1	1749	Hushe	Karakorum	0.64	16.36	7.90	49.88	0.34	11.46	0.63	0.22	11.01	98.44	OH,F,Cl	Ca	magnesio-ferri-hornblende
230-1	1749	Hushe	Karakorum	0.47	19.96	2.76	53.87	0.50	12.91	0.55	0.35	6.96	98.31	OH,F,Cl	Ca	actinolite
237-1	1749	Hushe	Karakorum	1.82	11.14	10.17	43.73	1.04	11.28	1.20	0.55	16.14	97.09	OH,F,Cl	Ca	pargasite
239-1	1749	Hushe	Karakorum	1.35	10.66	11.54	43.65	1.01	11.41	1.23	0.52	16.81	98.19	OH,F,Cl	Ca	magnesio-hornblende
242-1	1749	Hushe	Karakorum	2.18	11.19	12.15	43.37	0.78	11.55	0.82	0.23	16.14	98.40	OH,F,Cl	Ca	pargasite
246-1	1749	Hushe	Karakorum	1.61	11.80	10.33	43.89	0.82	11.90	0.60	0.39	15.48	96.82	OH,F,Cl	Ca	magnesio-hastingsite
250-1	1749	Hushe	Karakorum	1.33	16.20	7.43	48.80	0.87	12.50	1.05	0.39	10.61	99.18	OH,F,Cl	Ca	magnesio-ferri-hornblende
253-1	1749	Hushe	Karakorum	1.24	16.13	6.55	48.92	0.60	11.94	0.46	0.33	11.43	97.59	OH,F,Cl	Ca	magnesio-ferri-hornblende
254-1	1749	Hushe	Karakorum	1.73	10.78	11.19	44.01	1.12	12.03	0.88	0.35	17.60	99.69	OH,F,Cl	Ca	pargasite
258-1	1749	Hushe	Karakorum	2.16	12.34	11.86	44.90	1.06	11.47	1.08	0.28	15.49	100.64	OH,F,Cl	Ca	pargasite
259-1	1749	Hushe	Karakorum	1.39	10.68	11.63	42.75	1.58	11.09	1.04	0.48	16.96	97.61	OH,F,Cl	Ca	potassic-magnesio-hastingsite
263-1	1749	Hushe	Karakorum	1.97	12.29	10.70	44.23	0.93	11.59	1.21	0.30	15.59	98.80	OH,F,Cl	Ca	magnesio-hastingsite
267-1	1749	Hushe	Karakorum	1.41	9.31	10.80	42.92	1.64	11.57	1.07	0.43	18.90	98.04	OH,F,Cl	Ca	ferro-pargasite
268-1	1749	Hushe	Karakorum	2.60	11.12	13.97	42.98	0.54	11.37	0.94	0.23	14.26	98.02	OH,F,Cl	Ca	pargasite
270-1	1749	Hushe	Karakorum	1.79	11.39	11.78	45.35	0.83	11.27	0.83	0.35	15.09	98.67	OH,F,Cl	Ca	pargasite
271-1	1749	Hushe	Karakorum	1.92	13.10	9.70	45.16	1.21	11.68	0.81	0.26	14.26	98.09	OH,F,Cl	Ca	pargasite
273-1	1749	Hushe	Karakorum	2.09	13.86	6.86	46.98	1.44	11.59	0.94	0.56	14.13	98.44	OH,F,Cl	Ca	edenite
274-1	1749	Hushe	Karakorum	1.66	10.72	11.12	42.82	1.48	11.97	1.10	0.72	17.60	99.19	OH,F,Cl	Ca	magnesio-hastingsite
537-1	1749	Hushe	Karakorum	1.70	9.18	11.73	42.23	1.32	11.32	1.41	0.54	18.13	97.58	OH,F,Cl	Ca	ferro-pargasite
539-1	1749	Hushe	Karakorum	1.87	9.62	11.08	43.15	1.73	11.95	0.80	0.49	17.63	98.33	OH,F,Cl	Ca	ferro-pargasite
540-1	1749	Hushe	Karakorum	1.62	11.80	9.54	44.49	1.46	11.96	1.06	0.43	15.53	97.89	OH,F,Cl	Ca	pargasite
549-1	1749	Hushe	Karakorum	1.97	11.58	10.02	43.08	1.52	11.46	1.67	0.34	16.08	97.72	OH,F,Cl	Ca	pargasite
551-1	1749	Hushe	Karakorum	1.67	11.77	10.57	45.16	0.95	11.28	1.22	0.47	16.34	99.44	OH,F,Cl	Ca	pargasite
552-1	1749	Hushe	Karakorum	1.78	11.22	12.28	43.13	0.93	11.64	1.12	0.35	15.53	97.98	OH,F,Cl	Ca	pargasite
554-1	1749	Hushe	Karakorum	1.43	9.78	11.77	43.20	1.64	11.82	0.82	0.36	17.40	98.22	OH,F,Cl	Ca	pargasite
559-1	1749	Hushe	Karakorum	1.67	11.16	12.68	42.82	0.78	11.90	0.83	0.36	15.99	98.21	OH,F,Cl	Ca	magnesio-hastingsite
567-1	1749	Hushe	Karakorum	1.40	10.13	12.17	42.66	1.63	11.54	0.62	0.55	17.84	98.55	OH,F,Cl	Ca	magnesio-hastingsite
569-1	1749	Hushe	Karakorum	1.73	12.15	11.61	44.15	0.55	11.37	0.66	0.44	16.14	98.79	OH,F,Cl	Ca	magnesio-ferri-hornblende
570-1	1749	Hushe	Karakorum	1.08	18.47	7.11	49.86	0.50	12.54	0.62	0.21	7.05	97.45	OH,F,Cl	Ca	magnesio-ferri-hornblende
576-1	1749	Hushe	Karakorum	1.34	9.36	11.11	42.15	1.75	11.68	0.75	0.50	18.75	97.39	OH,F,Cl	Ca	magnesio-hastingsite
579-1	1749	Hushe	Karakorum	2.23	10.65	14.11	41.25	0.99	11.56	1.32	0.49	14.62	97.21	OH,F,Cl	Ca	pargasite
580-1	1749	Hushe	Karakorum	1.20	11.89	10.49	42.97	1.63	11.95	1.30	0.42	15.74	97.60	OH,F,Cl	Ca	potassic-magnesio-hastingsite
583-1	1749	Hushe	Karakorum	1.48	9.72	10.47	42.89	1.40	11.32	1.26	0.41	18.80	97.77	OH,F,Cl	Ca	magnesio-hastingsite
593-1	1749	Hushe	Karakorum	1.58	12.46	10.55	44.47	1.16	12.24	0.53	0.69	15.22	98.90	OH,F,Cl	Ca	magnesio-hastingsite
598-1	1749	Hushe	Karakorum	1.85	10.62	10.55	43.34	1.69	11.38	0.90	0.30	17.09	97.73	OH,F,Cl	Ca	pargasite
2-2	1749	Hushe	Karakorum	1.56	8.82	12.35	41.29	1.91	11.67	0.98	0.28	18.11	96.98	OH,F,Cl	Ca	ferro-pargasite
4-2	1749	Hushe	Karakorum	1.70	11.28	10.36	43.02	1.40	11.60	1.06	0.34	16.60	97.38	OH,F,Cl	Ca	magnesio-hastingsite
6-2	1749	Hushe	Karakorum	1.41	11.16	11.14	44.52	0.99	11.45	0.85	0.16	15.49	97.17	OH,F,Cl	Ca	pargasite
10-2	1749	Hushe	Karakorum	1.35	11.76	10.73	46.14	0.63	11.71	0.89	0.46	16.27	99.94	OH,F,Cl	Ca	magnesio-hornblende
11-2	1749	Hushe	Karakorum	2.23	10.56	9.56	43.27	1.53	11.12	0.89	0.59	17.74	97.51	OH,F,Cl	Ca	pargasite
13-2	1749	Hushe	Karakorum	1.17	8.38	12.42	41.18	1.64	11.70	1.04	0.60	18.48	96.59	OH,F,Cl	Ca	potassic-ferro-pargasite
18-2	1749	Hushe	Karakorum	1.47	10.57	10.76	42.54	1.40	11.64	1.18	0.53	18.62	98.70	OH,F,Cl	Ca	magnesio-hastingsite
30-2	1749	Hushe	Karakorum	1.51	12.14	9.42	44.46	1.42	11.74	0.93	0.55	15.67	97.84	OH,F,Cl	Ca	magnesio-hastingsite
31-2	1749	Hushe	Karakorum	1.24	14.57	8.02	47.27	0.70	12.29	0.86	0.55	12.77	98.27	OH,F,Cl	Ca	magnesio-ferri-hornblende
32-2	1749	Hushe	Karakorum	2.00	10.75	13.36	42.22	1.04	11.31	0.96	0.45	15.91	98.01	OH,F,Cl	Ca	pargasite
33-2	1749	Hushe	Karakorum	0.92	15.78	7.67	48.63	0.59	11.64	0.86	0.49	11.06	97.64	OH,F,Cl	Ca	magnesio-ferri-hornblende
252-2	1749	Hushe	Karakorum	1.40	16.61	6.79	50.71	0.63	12.09	0.58	0.25	10.38	99.44	OH,F,Cl	Ca	magnesio-hornblende
253-2	1749	Hushe	Karakorum	1.51	9.23	12.65	41.94	1.64	11.52	0.77	0.58	18.08	97.92	OH,F,Cl	Ca	pargasite
254-2	1749	Hushe	Karakorum	1.99	9.82	11.28	45.08	0.76	11.45	1.08	0.40	16.55	98.41	OH,F,Cl	Ca	pargasite
255-2	1749	Hushe	Karakorum	1.65	14.69	8.81	48.61	1.01	11.83	0.89	0.16	11.94	99.61	OH,F,Cl	Ca	pargasite
256-2	1749	Hushe	Karakorum	1.73	8.77	12.34	42.28	0.80	11.53	1.31	0.42	19.10	98.29	OH,F,Cl	Ca	ferro-pargasite
257-2	1749	Hushe	Karakorum	1.63	12.73	9.73	44.52	1.25	12.07	0.57	0.37	16.72	99.59	OH,F,Cl	Ca	magnesio-hastingsite
258-2	1749	Hushe	Karakorum	1.47	10.57	11.54	43.63	1.00	12.50	0.77	0.37	15.89	97.75	OH,F,Cl	Ca	pargasite
262-2	1749	Hushe	Karakorum	1.34	15.19	8.91	46.90	0.64	11.70	0.77	0.32	12.18	97.96	OH,F,Cl	Ca	magnesio-ferri-hornblende
263-2	1749	Hushe	Karakorum	1.50	13.54	10.41	45.74	0.82	11.64	1.45	0.23	13.51	98.84	OH,F,Cl	Ca	magnesio-hornblende
264-2	1749	Hushe	Karakorum	1.91	11.38	11.46	44.21	0.83	11.66	1.08	0.33	16.90	99.76	OH,F,Cl	Ca	magnesio-hastingsite
284-2	1749	Hushe	Karakorum	0.36	22.22	0.87	57.37	0.37	12.92	0.44	0.25	5.93	100.72	OH,F,Cl	Ca	actinolite
286-2	1749	Hushe	Karakorum	1.19	11.26	11.38	43.29	0.83	11.19	0.86	0.36	16.03	96.39	OH,F,Cl	Ca	magnesio-ferri-hornblende
291-2	1749	Hushe	Karakorum	1.52	14.69	9.20	46.23	1.54	12.27	0.89	0.37	12.39	99.10	OH,F,Cl	Ca	magnesio-hastingsite
294-2	1749	Hushe	Karakorum	2.56	11.84	12.84	43.53	0.73	10.96	1.01	0.48	14.13	98.09	OH,F,Cl	Ca	pargasite
296-2	1749	Hushe	Karakorum	1.40	10.19	11.07	44.71	0.74	12.14	0.67	0.40	15.82	97.12	OH,F,Cl	Ca	pargasite
297-2	1749	Hushe	Karakorum	1.40	9.36	12.37	43.57	0.82	11.77	0.99	0.27	16.41	96.97	OH,F,Cl	Ca	magnesio-hornblende
298-2	1749	Hushe	Karakorum	1.54	14.13	8.96	46.03	1.29	11.75	0.98	0.20	12.96	97.85	OH,F,Cl	Ca	pargasite
299-2	1749	Hushe	Karakorum	1.93	10.19	9.84	42.29	1.64	11.33	1.39	0.35	18.45	97.40	OH,F,Cl	Ca	magnesio-hastingsite
300-2	1749	Hushe	Karakorum	1.22	10.90	9.95	45.85	0.57	11.62	0.61	0.68	15.55	96.94	OH,F,Cl	Ca	magnesio-hornblende
303-2	1749	Hushe	Karakorum	1.65	11.01	11.68	43.93	1.33	11.91	1.02	0.24	16.32	99.08	OH,F,Cl	Ca	pargasite
304-2	1749	Hushe	Karakorum	1.37	9.76	11.52	42.99	1.51	12.08	1.10	0.70	18.46	99.49	OH,F,Cl	Ca	magnesio-hastingsite
306-2	1749	Hushe	Karakorum	1.52	10.14	11.21	44.04	1.08	12.28	1.08	0.53	18.33	100.22	OH,F,Cl	Ca	pargasite
307-2	1749	Hushe	Karakorum	1.78	12.94	8.06	46.27	0.68	11.59	0.61	0.42	14.86	97.21	OH,F,Cl	Ca	magnesio-hastingsite
309-2	1749	Hushe	Karakorum	2.06	12.95	10.57	45.78	0.77	10.92	0.75	0.42	13.92	98.15	OH,F,Cl	Ca	pargasite
310-2	1749	Hushe	Karakorum	1.36	10.02	10.84	42.80	1.35	11.59	1.10	0.53	17.63	97.20	OH,F,Cl	Ca	pargasite
319-2	1749	Hushe	Karakorum	1.46	9.91	11.30	42.97	1.58	11.82	0.94	0.28	17.33	97.57	OH,F,Cl	Ca	pargasite
322-2	1749	Hushe	Karakorum	1.64	8.76	12.36	41.98	1.47	11.69	0.61	0.44	19.46	98.41	OH,F,Cl	Ca	ferro-pargasite
323-2	1749	Hushe	Karakorum	1.90	10.00	11.01	41.87	1.62	11.79	1.08	0.35	17.79	97.42	OH,F,Cl	Ca	pargasite
324-2	1749	Hushe	Karakorum	1.78	11.58	11.01	43.98	1.38	12.04	1.18	0.35	16.37	99.67	OH,F,Cl	Ca	pargasite
326-2	1749	Hushe	Karakorum	1.85	9.30	12.67	43.67	1.30	11.64	0.86	0.34	17.86	99.49	OH,F,Cl	Ca	ferro-pargasite
327-2	1749	Hushe	Karakorum	1.77	12.76	10.77	44.32	1.01	11.64	0.96	0.42	14.64	98.28	OH,F,Cl	Ca	magnesio-hastingsite
329-2	1749	Hushe	Karakorum	1.26	10.19	11.03	43.72	1.33	11.91	0.76	0.50	16.77	97.47	OH,F,Cl	Ca	pargasite
334-2	1749	Hushe	Karakorum	2.22	14.12	12.55	44.45	0.51	11.65	0.70	0.27	12.24	98.71	OH,F,Cl	Ca	pargasite
338-2	1749	Hushe	Karakorum	0.51	28.77	0.69	58.31	0.21	0.58	0.50	0.27	9.75	99.60	OH,F,Cl	Mg-Fe-Mn	cummingtonite
339-2	1749	Hushe	Karakorum	1.64	11.12	10.37	44.13	1.52	11.46	0.96	0.33	15.96	97.50	OH,F,Cl	Ca	pargasite
340-2	1749	Hushe	Karakorum	1.54	9.74	11.10	42.70	1.48	11.84	0.81	0.44	19.13	98.79	OH,F,Cl	Ca	magnesio-hastingsite
341-2	1749	Hushe	Karakorum	1.36	12.20	9.95	45.20	1.30	11.82	0.54	0.32	16.28	98.97	OH,F,Cl	Ca	magnesio-hastingsite
342-2	1749	Hushe	Karakorum	1.74	11.21	10.10	45.40	1.12	11.45	0.80	0.41	16.11	98.32	OH,F,Cl	Ca	pargasite
344-2	1749	Hushe	Karakorum	1.69	11.38	9.96	44.96	1.24	11.64	0.78	0.47	16.69	98.80	OH,F,Cl	Ca	pargasite
718-2	1749	Hushe	Karakorum	1.50	10.64	10.46	43.79	1.45	12.26	0.89	0.45	17.35	98.79	OH,F,Cl	Ca	pargasite
719-2	1749	Hushe	Karakorum	1.68	10.86	11.27	44.44	0.90	11.56	1.13	0.38	16.66	98.89	OH,F,Cl	Ca	pargasite
725-2	1749	Hushe	Karakorum	2.06	12.28	11.52	43.28	0.70	11.22	0.74	0.47	14.98	97.26	OH,F,Cl	Ca	magnesio-hastingsite
730-2	1749	Hushe	Karakorum	1.40	9.42	11.61	42.15	1.58	11.80	1.17	0.49	18.48	98.10	OH,F,Cl	Ca	pargasite

Point	Sample	River/Dune	Domain	Na_2O	MgO	Al_2O_3	SiO_2	K_2O	CaO	TiO_2	MnO	FeO	Total	Group	Subgroup	Species
				wt%	wt%	wt%	wt%	wt%	wt%	wt%	wt%	wt%			of (OH,F,Cl)	
7-1	1748	Braldu	Karakorum	1.51	8.27	11.76	44.77	0.91	10.52	1.08	0.18	19.52	98.52	OH,F,Cl	Ca	ferro-hornblende
9-1	1748	Braldu	Karakorum	0.99	8.32	13.72	44.08	1.50	11.84	0.78	0.30	16.98	98.51	OH,F,Cl	Ca	ferro-hornblende
20-1	1748	Braldu	Karakorum	1.03	7.62	11.41	42.79	1.93	11.78	1.31	0.12	19.29	97.28	OH,F,Cl	Ca	potassic-ferro-pargasite
24-1	1748	Braldu	Karakorum	1.08	10.79	10.32	46.73	0.67	11.46	0.99	0.17	15.79	97.99	OH,F,Cl	Ca	magnesio-hornblende
26-1	1748	Braldu	Karakorum	2.17	11.25	8.35	45.81	1.55	10.88	1.05	0.31	17.11	98.50	OH,F,Cl	Ca	pargasite
27-1	1748	Braldu	Karakorum	1.73	11.18	10.67	45.47	1.06	11.63	0.87	0.22	15.07	97.88	OH,F,Cl	Ca	pargasite
28-1	1748	Braldu	Karakorum	1.48	10.16	10.09	44.19	1.39	11.14	1.00	0.36	18.89	98.69	OH,F,Cl	Ca	magnesio-hastingsite
30-1	1748	Braldu	Karakorum	0.60	16.10	3.33	53.48	0.21	12.28	0.29	0.19	11.12	97.60	OH,F,Cl	Ca	actinolite
31-1	1748	Braldu	Karakorum	0.82	9.91	9.00	47.52	0.85	11.63	0.56	0.17	18.17	98.63	OH,F,Cl	Ca	magnesio-hornblende
33-1	1748	Braldu	Karakorum	0.38	16.10	2.25	54.55	0.26	11.84	0.30	0.26	11.42	97.36	OH,F,Cl	Ca	actinolite
35-1	1748	Braldu	Karakorum	0.81	15.75	4.86	53.07	0.63	11.26	0.50	0.22	12.93	100.02	OH,F,Cl	Ca	magnesio-hornblende
36-1	1748	Braldu	Karakorum	1.28	11.90	7.83	46.99	0.73	11.31	0.70	0.21	17.17	98.12	OH,F,Cl	Ca	magnesio-ferri-hornblende
37-1	1748	Braldu	Karakorum	1.82	10.36	12.35	44.46	0.90	10.96	0.98	0.21	16.91	98.95	OH,F,Cl	Ca	pargasite
48-1	1748	Braldu	Karakorum	1.08	8.69	10.95	45.29	1.32	11.12	0.70	0.27	18.47	97.89	OH,F,Cl	Ca	ferro-hornblende
53-1	1748	Braldu	Karakorum	0.98	11.25	7.12	49.29	0.68	11.49	0.65	0.24	16.84	98.53	OH,F,Cl	Ca	magnesio-hornblende
54-1	1748	Braldu	Karakorum	0.97	13.74	9.73	47.50	0.46	11.23	0.89	0.21	12.84	97.57	OH,F,Cl	Ca	magnesio-hornblende
60-1	1748	Braldu	Karakorum	0.52	15.78	4.16	51.39	0.31	12.19	0.55	0.19	12.35	97.43	OH,F,Cl	Ca	magnesio-ferri-hornblende
62-1	1748	Braldu	Karakorum	1.21	9.69	9.62	45.66	1.34	11.87	0.74	0.25	16.98	97.36	OH,F,Cl	Ca	pargasite
63-1	1748	Braldu	Karakorum	1.72	8.44	10.74	43.99	0.58	10.91	0.81	0.25	20.78	98.23	OH,F,Cl	Ca	ferro-pargasite
66-1	1748	Braldu	Karakorum	1.61	12.77	7.43	48.24	0.96	10.91	1.21	0.21	15.67	99.02	OH,F,Cl	Ca	magnesio-hornblende
69-1	1748	Braldu	Karakorum	0.78	14.68	5.56	50.94	0.78	11.96	0.47	0.13	12.50	97.80	OH,F,Cl	Ca	magnesio-hornblende
70-1	1748	Braldu	Karakorum	0.95	10.09	8.65	47.01	1.43	11.72	0.99	0.25	17.93	99.01	OH,F,Cl	Ca	magnesio-hornblende
78-1	1748	Braldu	Karakorum	1.04	9.06	11.76	44.40	1.38	11.46	0.59	0.18	18.55	98.42	OH,F,Cl	Ca	ferro-hornblende
80-1	1748	Braldu	Karakorum	0.66	12.73	7.74	48.63	0.98	11.84	0.66	0.24	15.17	98.63	OH,F,Cl	Ca	magnesio-hornblende
82-1	1748	Braldu	Karakorum	0.95	12.59	6.56	48.90	0.75	10.97	0.45	0.26	16.30	97.74	OH,F,Cl	Ca	magnesio-ferri-hornblende
84-1	1748	Braldu	Karakorum	1.35	11.30	10.04	46.89	0.31	11.05	0.63	0.23	16.43	98.25	OH,F,Cl	Ca	magnesio-hornblende
86-1	1748	Braldu	Karakorum	0.59	15.87	2.27	53.70	0.43	11.84	0.50	0.31	12.69	98.19	OH,F,Cl	Ca	actinolite
87-1	1748	Braldu	Karakorum	0.92	15.69	7.60	49.79	0.74	11.92	0.74	0.20	10.91	98.51	OH,F,Cl	Ca	magnesio-hornblende
88-1	1748	Braldu	Karakorum	0.94	10.28	7.99	46.97	1.14	11.71	1.06	0.31	18.10	98.51	OH,F,Cl	Ca	magnesio-hornblende
89-1	1748	Braldu	Karakorum	0.77	9.88	9.68	46.24	1.27	11.39	0.90	0.26	18.21	98.60	OH,F,Cl	Ca	magnesio-hornblende
95-1	1748	Braldu	Karakorum	0.55	9.98	8.33	46.94	1.12	11.87	0.66	0.31	17.49	97.25	OH,F,Cl	Ca	magnesio-hornblende
96-1	1748	Braldu	Karakorum	1.14	20.20	2.33	53.68	0.50	11.29	0.56	0.28	6.98	96.96	OH,F,Cl	Ca	actinolite
101-1	1748	Braldu	Karakorum	2.75	10.83	12.71	41.85	0.44	11.31	1.57	0.22	17.45	99.12	OH,F,Cl	Ca	magnesio-hastingsite
109-1	1748	Braldu	Karakorum	1.21	9.62	10.26	45.59	1.31	11.50	0.94	0.20	17.72	98.36	OH,F,Cl	Ca	magnesio-hornblende
116-1	1748	Braldu	Karakorum	1.47	10.43	11.13	44.06	1.51	11.58	1.57	0.26	17.74	99.74	OH,F,Cl	Ca	pargasite
117-1	1748	Braldu	Karakorum	0.84	13.99	7.15	50.06	0.59	12.18	0.67	0.22	13.33	99.03	OH,F,Cl	Ca	magnesio-hornblende
123-1	1748	Braldu	Karakorum	2.60	12.87	12.53	42.34	1.20	10.91	2.23	0.05	12.85	97.59	OH,F,Cl	Ca	pargasite
124-1	1748	Braldu	Karakorum	0.52	16.99	4.74	53.99	0.28	11.81	0.42	0.21	8.97	97.93	OH,F,Cl	Ca	actinolite
127-1	1748	Braldu	Karakorum	0.95	10.43	8.74	46.88	0.93	11.92	0.66	0.30	18.08	98.89	OH,F,Cl	Ca	magnesio-hornblende
128-1	1748	Braldu	Karakorum	1.37	8.68	10.11	43.48	0.70	10.64	0.87	0.21	21.87	97.94	OH,F,Cl	Ca	magnesio-ferri-hornblende
130-1	1748	Braldu	Karakorum	1.52	8.05	12.39	42.86	1.86	11.17	1.25	0.27	18.34	97.70	OH,F,Cl	Ca	potassic-ferro-pargasite
131-1	1748	Braldu	Karakorum	1.18	9.53	9.93	43.06	1.54	11.27	0.67	0.25	20.27	97.71	OH,F,Cl	Ca	potassic-magnesio-hastingsite
136-1	1748	Braldu	Karakorum	1.07	14.64	5.97	50.66	0.47	11.15	0.72	0.27	12.29	97.23	OH,F,Cl	Ca	magnesio-hornblende
137-1	1748	Braldu	Karakorum	0.90	13.13	8.23	48.11	0.70	11.88	0.74	0.23	14.29	98.21	OH,F,Cl	Ca	magnesio-hornblende
139-1	1748	Braldu	Karakorum	0.22	16.08	0.33	54.76	0.32	23.98	0.35	0.16	3.51	99.71	OH,F,Cl	Ca	edenite
145-1	1748	Braldu	Karakorum	1.37	10.45	9.78	45.14	1.50	11.32	0.83	0.25	17.38	98.02	OH,F,Cl	Ca	pargasite
153-1	1748	Braldu	Karakorum	1.41	14.98	8.64	48.56	0.74	11.10	0.73	0.17	11.93	98.26	OH,F,Cl	Ca	magnesio-hornblende
157-1	1748	Braldu	Karakorum	1.23	7.51	11.83	42.53	1.81	11.54	0.86	0.32	21.27	98.89	OH,F,Cl	Ca	potassic-ferro-pargasite
166-1	1748	Braldu	Karakorum	0.51	13.95	2.31	53.00	0.46	11.64	0.51	0.32	15.37	98.07	OH,F,Cl	Ca	actinolite
167-1	1748	Braldu	Karakorum	0.38	18.56	1.62	56.23	0.25	11.76	0.49	0.16	9.06	98.51	OH,F,Cl	Ca	actinolite
169-1	1748	Braldu	Karakorum	1.40	10.80	11.15	44.57	1.18	11.07	1.05	0.23	15.14	96.58	OH,F,Cl	Ca	magnesio-hornblende
206-1	1748	Braldu	Karakorum	0.82	12.19	6.74	50.34	0.69	11.92	0.78	0.19	15.29	98.96	OH,F,Cl	Ca	magnesio-hornblende
208-1	1748	Braldu	Karakorum	1.52	9.04	11.12	43.29	1.02	11.08	0.99	0.23	19.33	97.61	OH,F,Cl	Ca	ferro-pargasite
211-1	1748	Braldu	Karakorum	1.46	8.35	13.05	43.03	1.10	11.03	1.17	0.21	20.16	99.56	OH,F,Cl	Ca	ferro-pargasite
213-1	1748	Braldu	Karakorum	1.54	10.31	11.21	45.64	0.80	11.41	0.88	0.22	17.21	99.23	OH,F,Cl	Ca	magnesio-hornblende
215-1	1748	Braldu	Karakorum	1.18	15.06	7.53	49.46	0.73	11.85	0.96	0.15	11.87	98.80	OH,F,Cl	Ca	magnesio-hornblende
223-1	1748	Braldu	Karakorum	1.10	13.04	8.37	49.03	0.45	11.57	0.67	0.22	13.71	98.15	OH,F,Cl	Ca	magnesio-hornblende
224-1	1748	Braldu	Karakorum	1.48	10.75	12.60	45.23	0.40	11.00	0.71	0.20	15.12	97.50	OH,F,Cl	Ca	magnesio-hornblende
228-1	1748	Braldu	Karakorum	1.44	9.27	12.61	43.43	1.12	11.97	0.80	0.24	18.87	99.75	OH,F,Cl	Ca	pargasite
230-1	1748	Braldu	Karakorum	0.85	8.98	10.90	44.95	1.56	11.58	0.66	0.25	17.98	97.71	OH,F,Cl	Ca	ferro-hornblende
235-1	1748	Braldu	Karakorum	0.93	12.27	6.87	49.18	0.53	11.16	0.71	0.26	15.79	97.70	OH,F,Cl	Ca	magnesio-ferri-hornblende
237-1	1748	Braldu	Karakorum	1.20	8.78	11.13	44.76	1.60	11.80	0.95	0.20	18.55	98.98	OH,F,Cl	Ca	potassic-ferro-pargasite
239-1	1748	Braldu	Karakorum	1.09	12.67	6.31	50.78	0.50	11.59	0.70	0.24	15.70	99.57	OH,F,Cl	Ca	magnesio-hornblende
240-1	1748	Braldu	Karakorum	0.82	9.82	10.95	46.10	0.79	11.80	0.94	0.26	17.42	98.92	OH,F,Cl	Ca	magnesio-hornblende
241-1	1748	Braldu	Karakorum	1.19	16.57	5.74	50.97	0.69	11.32	0.68	0.16	10.65	97.96	OH,F,Cl	Ca	magnesio-ferri-hornblende
242-1	1748	Braldu	Karakorum	1.23	9.88	10.08	45.62	1.17	11.04	0.47	0.23	18.56	98.28	OH,F,Cl	Ca	magnesio-hornblende
245-1	1748	Braldu	Karakorum	0.63	15.74	3.40	53.80	0.37	11.46	0.42	0.18	13.05	99.06	OH,F,Cl	Ca	actinolite
248-1	1748	Braldu	Karakorum	0.65	10.32	4.91	50.35	0.87	11.90	0.41	0.21	19.74	99.36	OH,F,Cl	Ca	ferro-actinolite
251-1	1748	Braldu	Karakorum	1.55	9.94	11.59	44.81	0.79	11.19	1.06	0.21	18.78	99.91	OH,F,Cl	Ca	magnesio-hornblende
254-1	1748	Braldu	Karakorum	1.15	5.83	16.81	42.05	0.72	10.58	0.54	0.09	20.78	98.55	OH,F,Cl	Ca	ferro-tschermakite
260-1	1748	Braldu	Karakorum	1.21	11.13	9.14	46.14	0.83	11.89	0.90	0.25	16.51	98.01	OH,F,Cl	Ca	magnesio-hornblende
262-1	1748	Braldu	Karakorum	2.37	13.81	12.72	41.91	1.62	11.42	2.10	0.18	11.80	97.93	OH,F,Cl	Ca	pargasite
263-1	1748	Braldu	Karakorum	0.62	16.58	2.96	54.66	0.37	12.30	0.32	0.24	10.97	99.01	OH,F,Cl	Ca	actinolite
266-1	1748	Braldu	Karakorum	0.38	23.24	1.68	57.87	0.21	13.45	0.31	0.12	0.78	98.04	OH,F,Cl	Ca	tremolite
267-1	1748	Braldu	Karakorum	1.16	8.75	11.61	43.45	1.09	11.40	1.13	0.09	18.72	97.40	OH,F,Cl	Ca	ferro-hornblende
271-1	1748	Braldu	Karakorum	1.20	9.71	11.33	44.91	1.10	11.69	1.03	0.20	17.10	98.27	OH,F,Cl	Ca	magnesio-hornblende
285-1	1748	Braldu	Karakorum	0.69	16.29	5.56	52.82	0.40	10.63	0.34	0.29	11.14	98.17	OH,F,Cl	Ca	magnesio-hornblende
289-1	1748	Braldu	Karakorum	0.70	13.40	4.85	51.18	0.29	11.27	0.78	0.24	15.54	98.24	OH,F,Cl	Ca	magnesio-hornblende
294-1	1748	Braldu	Karakorum	0.78	13.11	5.00	51.57	0.58	11.79	0.34	0.29	15.06	98.50	OH,F,Cl	Ca	actinolite
302-1	1748	Braldu	Karakorum	1.15	12.05	5.32	49.78	0.82	11.96	0.41	0.33	16.88	98.71	OH,F,Cl	Ca	actinolite
303-1	1748	Braldu	Karakorum	2.40	12.52	13.41	40.37	1.97	11.60	2.46	0.16	12.80	97.68	OH,F,Cl	Ca	pargasite
311-1	1748	Braldu	Karakorum	2.49	11.51	13.15	39.58	1.90	11.82	2.23	0.16	14.27	97.10	OH,F,Cl	Ca	pargasite
319-1	1748	Braldu	Karakorum	1.41	9.84	11.31	43.90	1.33	10.98	1.04	0.23	17.65	97.69	OH,F,Cl	Ca	pargasite
320-1	1748	Braldu	Karakorum	0.52	21.71	1.27	55.42	0.25	1.44	0.34	0.23	18.04	99.20	OH,F,Cl	Mg-Fe-Mn	cummingtonite
358-1	1748	Braldu	Karakorum	0.95	13.60	8.74	50.48	0.43	10.90	0.70	0.22	13.25	99.28	OH,F,Cl	Ca	magnesio-hornblende
360-1	1748	Braldu	Karakorum	1.55	13.00	9.64	47.93	0.68	11.14	0.83	0.21	13.09	98.08	OH,F,Cl	Ca	magnesio-hornblende
365-1	1748	Braldu	Karakorum	1.30	10.24	10.95	43.93	1.06	11.25	1.01	0.26	17.69	97.68	OH,F,Cl	Ca	magnesio-hornblende
368-1	1748	Braldu	Karakorum	1.62	12.11	10.60	46.51	0.54	11.00	0.60	0.20	15.07	98.23	OH,F,Cl	Ca	magnesio-hornblende
371-1	1748	Braldu	Karakorum	1.29	8.97	11.77	43.96	1.84	11.11	0.76	0.21	18.40	98.31	OH,F,Cl	Ca	potassic-ferro-pargasite
374-1	1748	Braldu	Karakorum	0.95	7.89	12.74	42.65	2.22	11.37	0.54	0.21	20.90	99.48	OH,F,Cl	Ca	potassic-ferro-pargasite
375-1	1748	Braldu	Karakorum	0.96	10.78	8.09	48.37	0.66	11.22	0.82	0.13	17.20	98.21	OH,F,Cl	Ca	magnesio-hornblende
380-1	1748	Braldu	Karakorum	1.31	11.93	10.87	47.38	0.58	10.66	0.61	0.28	15.13	98.75	OH,F,Cl	Ca	magnesio-hornblende
386-1	1748	Braldu	Karakorum	2.54	10.82	13.48	39.64	1.94	11.44	2.63	0.06	15.92	98.48	OH,F,Cl	Ca	magnesio-hastingsite
398-1	1748	Braldu	Karakorum	1.28	10.54	12.41	46.13	0.42	10.82	0.69	0.21	16.44	98.95	OH,F,Cl	Ca	magnesio-hornblende
399-1	1748	Braldu	Karakorum	2.45	14.05	12.34	41.86	1.32	12.00	1.80	0.10	12.56	98.49	OH,F,Cl	Ca	magnesio-hastingsite
401-1	1748	Braldu	Karakorum	1.33	14.17	8.52	49.02	0.82	12.11	0.92	0.24	11.70	98.83	OH,F,Cl	Ca	magnesio-hornblende
405-1	1748	Braldu	Karakorum	1.27	9.35	11.25	42.98	1.69	11.35	0.79	0.26	18.62	97.54	OH,F,Cl	Ca	potassic-pargasite
415-1	1748	Braldu	Karakorum	0.47	24.01	0.62	59.06	0.21	12.90	0.13	0.11	0.69	98.18	OH,F,Cl	Ca	tremolite
426-1	1748	Braldu	Karakorum	1.55	8.59	13.34	42.69	1.26	11.26	1.03	0.24	18.93	98.89	OH,F,Cl	Ca	ferro-pargasite
446-1	1748	Braldu	Karakorum	1.20	10.57	10.79	45.60	1.14	11.49	1.06	0.25	15.51	97.61	OH,F,Cl	Ca	magnesio-hornblende

Point	Sample	River/Dune	Domain	Na_2O	MgO	Al_2O_3	SiO_2	K_2O	CaO	TiO_2	MnO	FeO	Total	Group	Subgroup	Species
				wt%	wt%	wt%	wt%	wt%	wt%	wt%	wt%	wt%			of (OH,F,Cl)	
5-1	1437	Upper Hunza	Karakorum	0.22	14.59	0.66	53.76	0.31	1.26	0.66	1.06	28.77	101.30	OH,F,Cl	Mg-Fe-Mn	grunerite
7-1	1437	Upper Hunza	Karakorum	0.74	12.14	6.35	50.12	0.78	12.24	0.89	0.60	15.46	99.32	OH,F,Cl	Ca	magnesio-hornblende
11-1	1437	Upper Hunza	Karakorum	1.61	10.80	6.92	45.18	1.22	11.70	2.47	0.55	18.39	98.85	OH,F,Cl	Ca	magnesio-hastingsite
12-1	1437	Upper Hunza	Karakorum	0.57	11.96	3.67	51.40	0.45	11.06	0.67	0.70	19.46	99.94	OH,F,Cl	Ca	actinolite
13-1	1437	Upper Hunza	Karakorum	1.17	13.86	5.12	49.72	0.76	11.86	1.14	0.40	15.09	99.12	OH,F,Cl	Ca	magnesio-ferri-hornblende
14-1	1437	Upper Hunza	Karakorum	1.11	8.40	10.23	45.13	1.47	11.65	1.31	0.58	18.57	98.46	OH,F,Cl	Ca	ferro-hornblende
15-1	1437	Upper Hunza	Karakorum	1.30	9.60	8.49	44.58	1.26	11.12	1.67	0.66	19.59	98.26	OH,F,Cl	Ca	ferro-pargasite
19-1	1437	Upper Hunza	Karakorum	0.92	9.16	10.16	44.39	1.40	11.67	1.41	0.48	19.03	98.62	OH,F,Cl	Ca	ferro-hornblende
21-1	1437	Upper Hunza	Karakorum	1.18	13.06	8.25	49.01	0.65	12.33	1.15	0.27	13.55	99.46	OH,F,Cl	Ca	magnesio-hornblende
27-1	1437	Upper Hunza	Karakorum	0.75	11.14	5.87	49.81	0.64	11.53	0.94	0.55	20.42	101.65	OH,F,Cl	Ca	magnesio-ferri-hornblende
29-1	1437	Upper Hunza	Karakorum	0.99	8.71	10.82	45.10	1.47	11.95	1.46	0.29	19.53	100.32	OH,F,Cl	Ca	ferro-hornblende
30-1	1437	Upper Hunza	Karakorum	1.42	8.14	13.14	42.23	1.11	12.15	1.54	0.34	19.44	99.51	OH,F,Cl	Ca	ferro-pargasite
37-1	1437	Upper Hunza	Karakorum	1.03	7.85	11.55	42.26	1.59	11.98	0.96	0.39	20.67	98.28	OH,F,Cl	Ca	potassic-ferro-pargasite
38-1	1437	Upper Hunza	Karakorum	0.74	10.79	9.07	47.47	0.85	11.99	0.99	0.41	16.30	98.62	OH,F,Cl	Ca	magnesio-hornblende
40-1	1437	Upper Hunza	Karakorum	0.78	9.58	5.43	48.00	0.73	11.37	1.62	0.45	20.18	98.14	OH,F,Cl	Ca	ferro-ferri-hornblende
43-1	1437	Upper Hunza	Karakorum	0.65	18.14	2.52	55.19	0.37	12.65	0.65	0.46	9.20	99.83	OH,F,Cl	Ca	actinolite
44-1	1437	Upper Hunza	Karakorum	0.85	14.59	6.96	50.47	0.73	12.54	0.87	0.59	10.73	98.33	OH,F,Cl	Ca	magnesio-hornblende
46-1	1437	Upper Hunza	Karakorum	0.57	10.07	7.34	48.49	0.97	12.13	1.17	0.52	18.85	100.11	OH,F,Cl	Ca	magnesio-hornblende
59-1	1437	Upper Hunza	Karakorum	0.64	10.52	6.32	50.15	0.72	12.45	0.99	0.55	19.24	101.58	OH,F,Cl	Ca	magnesio-hornblende
60-1	1437	Upper Hunza	Karakorum	1.65	11.96	7.11	46.66	1.20	12.04	1.35	0.33	15.79	98.09	OH,F,Cl	Ca	pargasite
61-1	1437	Upper Hunza	Karakorum	1.18	8.30	12.15	43.85	1.71	12.06	0.90	0.34	19.24	99.75	OH,F,Cl	Ca	potassic-ferro-pargasite
64-1	1437	Upper Hunza	Karakorum	0.56	13.54	3.22	53.25	0.30	12.99	0.50	0.63	15.02	100.00	OH,F,Cl	Ca	actinolite
65-1	1437	Upper Hunza	Karakorum	0.93	8.63	10.96	44.22	1.59	11.47	0.90	0.38	20.17	99.26	OH,F,Cl	Ca	ferro-hornblende
69-1	1437	Upper Hunza	Karakorum	0.83	10.90	5.81	48.64	0.86	11.51	0.98	0.55	18.70	98.78	OH,F,Cl	Ca	magnesio-ferri-hornblende
76-1	1437	Upper Hunza	Karakorum	0.45	14.13	1.01	54.03	0.13	24.10	0.35	0.32	6.74	101.25	OH,F,Cl	Ca	edenite
77-1	1437	Upper Hunza	Karakorum	1.04	12.09	6.40	48.50	0.71	11.45	0.75	0.48	17.66	99.09	OH,F,Cl	Ca	magnesio-ferri-hornblende
84-1	1437	Upper Hunza	Karakorum	0.69	14.56	5.65	53.19	0.37	11.52	0.25	0.49	14.99	101.70	OH,F,Cl	Ca	magnesio-hornblende
85-1	1437	Upper Hunza	Karakorum	1.19	9.87	11.18	45.47	1.68	12.02	1.39	0.34	16.40	99.54	OH,F,Cl	Ca	potassic-pargasite
90-1	1437	Upper Hunza	Karakorum	0.97	9.39	9.86	45.94	1.00	11.38	1.01	0.44	20.13	100.13	OH,F,Cl	Ca	magnesio-hornblende
92-1	1437	Upper Hunza	Karakorum	1.42	12.24	8.34	45.84	1.09	12.28	2.19	0.40	15.48	99.27	OH,F,Cl	Ca	pargasite
98-1	1437	Upper Hunza	Karakorum	1.15	9.00	12.55	44.61	1.13	12.47	1.13	0.13	17.57	99.75	OH,F,Cl	Ca	ferro-pargasite
99-1	1437	Upper Hunza	Karakorum	1.20	11.42	6.45	48.16	1.02	11.68	2.01	0.76	17.09	99.79	OH,F,Cl	Ca	magnesio-hornblende
101-1	1437	Upper Hunza	Karakorum	0.71	10.17	9.56	46.43	1.39	11.84	1.13	0.35	16.82	98.40	OH,F,Cl	Ca	magnesio-hornblende
105-1	1437	Upper Hunza	Karakorum	1.23	10.30	7.37	46.19	1.11	11.04	2.13	0.51	19.80	99.67	OH,F,Cl	Ca	magnesio-ferri-hornblende
112-1	1437	Upper Hunza	Karakorum	0.96	10.94	5.93	49.21	0.44	11.42	0.86	0.75	20.33	100.84	OH,F,Cl	Ca	magnesio-ferri-hornblende
121-1	1437	Upper Hunza	Karakorum	1.08	8.69	12.02	43.36	1.51	12.03	1.25	0.64	20.10	100.68	OH,F,Cl	Ca	potassic-ferro-pargasite
123-1	1437	Upper Hunza	Karakorum	0.94	12.08	5.60	48.79	0.94	12.12	1.36	0.40	17.77	100.00	OH,F,Cl	Ca	magnesio-ferri-hornblende
124-1	1437	Upper Hunza	Karakorum	1.28	11.39	6.72	46.40	1.18	11.91	1.99	0.31	17.53	98.70	OH,F,Cl	Ca	magnesio-hastingsite
129-1	1437	Upper Hunza	Karakorum	1.44	12.18	7.66	46.02	1.16	11.32	1.47	0.61	16.22	98.09	OH,F,Cl	Ca	magnesio-hastingsite
132-1	1437	Upper Hunza	Karakorum	0.90	9.99	9.93	46.93	0.77	11.77	0.90	0.31	19.65	101.16	OH,F,Cl	Ca	magnesio-hornblende
134-1	1437	Upper Hunza	Karakorum	2.13	13.55	11.47	43.64	0.68	10.99	1.66	0.64	14.79	99.56	OH,F,Cl	Ca	magnesio-hastingsite
136-1	1437	Upper Hunza	Karakorum	0.52	11.27	8.13	48.44	0.89	11.87	0.73	0.67	17.99	100.51	OH,F,Cl	Ca	magnesio-ferri-hornblende
138-1	1437	Upper Hunza	Karakorum	0.91	10.27	8.36	45.49	1.25	11.89	1.66	0.44	20.34	100.62	OH,F,Cl	Ca	magnesio-ferri-hornblende
145-1	1437	Upper Hunza	Karakorum	1.16	10.79	7.83	45.13	1.21	11.88	1.45	0.35	18.80	98.60	OH,F,Cl	Ca	magnesio-hastingsite
148-1	1437	Upper Hunza	Karakorum	1.13	7.82	10.33	44.78	1.35	12.18	1.05	0.46	19.90	99.00	OH,F,Cl	Ca	ferro-pargasite
150-1	1437	Upper Hunza	Karakorum	0.92	8.43	9.32	44.59	1.23	12.34	1.03	0.57	20.73	99.16	OH,F,Cl	Ca	ferro-hornblende
151-1	1437	Upper Hunza	Karakorum	0.92	11.75	6.47	48.49	0.75	12.10	1.26	0.51	17.31	99.57	OH,F,Cl	Ca	magnesio-ferri-hornblende
152-1	1437	Upper Hunza	Karakorum	1.16	9.86	9.23	44.63	1.12	11.36	1.54	0.49	19.21	98.60	OH,F,Cl	Ca	magnesio-ferri-hornblende
154-1	1437	Upper Hunza	Karakorum	1.09	10.26	11.41	44.72	1.79	11.47	1.20	0.65	15.92	98.51	OH,F,Cl	Ca	potassic-pargasite
159-1	1437	Upper Hunza	Karakorum	1.27	8.26	12.05	43.77	1.74	11.44	1.38	0.69	19.61	100.21	OH,F,Cl	Ca	potassic-ferro-pargasite
163-1	1437	Upper Hunza	Karakorum	1.11	9.78	9.50	45.48	1.09	11.89	0.91	0.63	17.95	98.35	OH,F,Cl	Ca	magnesio-hornblende
164-1	1437	Upper Hunza	Karakorum	0.99	8.40	11.07	43.37	1.50	11.62	1.14	0.40	19.76	98.26	OH,F,Cl	Ca	potassic-ferro-pargasite
165-1	1437	Upper Hunza	Karakorum	1.22	9.74	10.62	43.97	1.55	11.98	1.46	0.39	17.69	98.61	OH,F,Cl	Ca	pargasite
166-1	1437	Upper Hunza	Karakorum	1.05	10.60	9.41	46.10	1.15	11.92	1.11	0.64	16.74	98.72	OH,F,Cl	Ca	magnesio-hornblende
167-1	1437	Upper Hunza	Karakorum	0.98	10.98	8.72	47.04	1.15	11.96	0.90	0.59	16.98	99.31	OH,F,Cl	Ca	magnesio-hornblende
172-1	1437	Upper Hunza	Karakorum	1.04	8.82	9.47	44.10	1.42	11.83	1.30	0.73	19.94	98.65	OH,F,Cl	Ca	potassic-ferro-pargasite
175-1	1437	Upper Hunza	Karakorum	1.27	10.09	11.19	43.15	1.78	12.29	1.55	0.63	17.22	99.17	OH,F,Cl	Ca	pargasite
177-1	1437	Upper Hunza	Karakorum	1.21	5.03	12.20	40.65	1.34	10.97	0.28	0.42	27.89	99.99	OH,F,Cl	Ca	ferro-ferri-hornblende
179-1	1437	Upper Hunza	Karakorum	0.76	16.03	4.98	51.28	0.45	11.96	1.43	0.51	10.79	98.20	OH,F,Cl	Ca	magnesio-ferri-hornblende
180-1	1437	Upper Hunza	Karakorum	0.88	10.61	8.92	46.25	0.63	11.48	0.68	0.57	18.77	98.79	OH,F,Cl	Ca	magnesio-ferri-hornblende
181-1	1437	Upper Hunza	Karakorum	0.82	10.55	6.53	48.51	0.75	11.41	1.14	0.64	20.27	100.62	OH,F,Cl	Ca	magnesio-ferri-hornblende
183-1	1437	Upper Hunza	Karakorum	1.17	13.73	5.26	49.37	0.84	11.34	1.02	0.62	14.76	98.12	OH,F,Cl	Ca	magnesio-ferri-hornblende
187-1	1437	Upper Hunza	Karakorum	0.88	7.76	11.71	43.33	1.82	11.90	1.39	0.56	18.82	98.17	OH,F,Cl	Ca	potassic-ferro-pargasite
210-1	1437	Upper Hunza	Karakorum	0.56	18.14	1.24	55.61	0.22	1.99	0.40	0.48	21.90	100.56	OH,F,Cl	Mg-Fe-Mn	cummingtonite
214-1	1437	Upper Hunza	Karakorum	1.31	8.30	12.05	41.83	1.94	12.56	0.93	0.34	19.70	98.96	OH,F,Cl	Ca	ferro-pargasite
220-1	1437	Upper Hunza	Karakorum	0.12	16.11	0.87	54.72	0.24	13.28	0.38	0.38	12.98	99.08	OH,F,Cl	Ca	actinolite
234-1	1437	Upper Hunza	Karakorum	0.76	13.80	5.37	51.07	0.39	11.95	0.59	0.53	15.13	99.59	OH,F,Cl	Ca	magnesio-ferri-hornblende
237-1	1437	Upper Hunza	Karakorum	0.86	9.46	9.48	45.17	1.26	11.84	1.07	0.42	18.68	98.24	OH,F,Cl	Ca	ferro-hornblende
245-1	1437	Upper Hunza	Karakorum	1.12	8.49	12.29	43.89	1.88	12.08	1.37	0.17	18.22	99.51	OH,F,Cl	Ca	potassic-ferro-pargasite
246-1	1437	Upper Hunza	Karakorum	1.04	13.81	6.30	50.87	0.90	11.75	0.95	0.49	13.49	99.60	OH,F,Cl	Ca	magnesio-hornblende
265-1	1437	Upper Hunza	Karakorum	0.82	12.04	6.08	49.48	0.81	12.04	0.58	0.53	15.85	98.24	OH,F,Cl	Ca	magnesio-hornblende
267-1	1437	Upper Hunza	Karakorum	1.03	10.65	7.45	47.24	1.04	11.49	1.36	0.58	19.67	100.52	OH,F,Cl	Ca	magnesio-ferri-hornblende
268-1	1437	Upper Hunza	Karakorum	1.35	8.76	10.20	44.19	1.53	11.35	1.02	0.43	19.36	98.19	OH,F,Cl	Ca	ferro-pargasite
272-1	1437	Upper Hunza	Karakorum	1.14	6.53	12.59	42.27	1.88	11.34	1.15	0.56	22.84	100.30	OH,F,Cl	Ca	potassic-ferro-pargasite
273-1	1437	Upper Hunza	Karakorum	0.93	8.80	8.58	45.90	1.32	11.72	1.30	0.64	20.10	99.28	OH,F,Cl	Ca	ferro-hornblende
274-1	1437	Upper Hunza	Karakorum	1.10	9.94	9.78	46.91	1.10	11.63	0.86	0.32	17.79	99.44	OH,F,Cl	Ca	magnesio-hornblende
276-1	1437	Upper Hunza	Karakorum	1.10	9.43	9.58	45.10	1.18	11.85	1.40	0.62	19.43	99.69	OH,F,Cl	Ca	ferro-hornblende
277-1	1437	Upper Hunza	Karakorum	1.51	8.17	11.61	43.63	0.97	10.79	0.67	0.33	22.32	100.00	OH,F,Cl	Ca	ferro-ferri-hornblende
279-1	1437	Upper Hunza	Karakorum	0.53	13.82	4.11	53.02	0.53	11.78	0.53	0.57	16.02	100.90	OH,F,Cl	Ca	actinolite
282-1	1437	Upper Hunza	Karakorum	0.89	8.95	9.93	44.91	1.32	11.71	1.11	0.31	20.23	99.37	OH,F,Cl	Ca	ferro-hornblende
283-1	1437	Upper Hunza	Karakorum	1.70	11.95	11.73	44.35	1.41	12.25	1.25	0.31	13.54	98.50	OH,F,Cl	Ca	pargasite
285-1	1437	Upper Hunza	Karakorum	1.33	11.44	10.44	47.56	1.25	11.75	0.93	0.48	15.61	100.77	OH,F,Cl	Ca	magnesio-hornblende
286-1	1437	Upper Hunza	Karakorum	1.36	12.08	7.01	46.08	1.09	11.72	1.66	0.36	17.99	99.34	OH,F,Cl	Ca	magnesio-hastingsite
291-1	1437	Upper Hunza	Karakorum	1.35	7.01	12.06	42.32	1.78	11.14	1.16	0.49	22.56	99.85	OH,F,Cl	Ca	potassic-ferro-pargasite
293-1	1437	Upper Hunza	Karakorum	0.77	13.15	4.14	53.19	0.69	11.86	0.49	0.43	16.68	101.39	OH,F,Cl	Ca	magnesio-ferri-hornblende
298-1	1437	Upper Hunza	Karakorum	1.30	9.08	11.14	44.94	1.62	11.92	1.11	0.27	18.45	99.84	OH,F,Cl	Ca	potassic-ferro-pargasite
301-1	1437	Upper Hunza	Karakorum	0.61	13.18	5.55	51.73	0.57	12.48	0.48	0.33	15.30	100.22	OH,F,Cl	Ca	actinolite
302-1	1437	Upper Hunza	Karakorum	0.77	13.61	5.61	51.64	0.31	11.75	0.69	0.40	13.79	98.57	OH,F,Cl	Ca	magnesio-hornblende
303-1	1437	Upper Hunza	Karakorum	0.92	12.71	7.51	47.80	0.90	11.47	0.74	0.48	16.45	98.99	OH,F,Cl	Ca	magnesio-ferri-hornblende
306-1	1437	Upper Hunza	Karakorum	0.64	10.38	6.12	48.43	0.63	10.93	1.39	0.79	20.97	100.26	OH,F,Cl	Ca	magnesio-ferri-hornblende
307-1	1437	Upper Hunza	Karakorum	1.11	9.35	9.42	44.24	1.42	11.78	1.62	0.40	20.72	100.07	OH,F,Cl	Ca	potassic-hastingsite
308-1	1437	Upper Hunza	Karakorum	1.31	10.81	9.32	46.01	1.29	11.95	0.90	0.50	17.56	99.65	OH,F,Cl	Ca	pargasite
345-1	1437	Upper Hunza	Karakorum	1.10	8.92	10.63	46.04	1.22	11.96	1.08	0.38	20.07	101.42	OH,F,Cl	Ca	ferro-hornblende
349-1	1437	Upper Hunza	Karakorum	0.90	8.25	10.36	44.25	1.68	12.08	1.22	0.61	19.13	98.48	OH,F,Cl	Ca	potassic-ferro-pargasite
352-1	1437	Upper Hunza	Karakorum	0.79	12.52	6.41	49.93	0.76	11.99	0.43	0.35	16.18	99.35	OH,F,Cl	Ca	magnesio-hornblende
366-1	1437	Upper Hunza	Karakorum	0.73	10.94	2.95	52.32	0.57	8.79	0.88	0.40	24.16	101.74	OH,F,Cl	Ca	actinolite
395-1	1437	Upper Hunza	Karakorum	1.29	12.77	6.68	47.81	0.96	12.17	1.09	0.43	15.79	99.00	OH,F,Cl	Ca	pargasite

Point	Sample	River/Dune	Domain	Na_2O	MgO	Al_2O_3	SiO_2	K_2O	CaO	TiO_2	MnO	FeO	Total	Group	Subgroup	Species
				wt%	wt%	wt%	wt%	wt%	wt%	wt%	wt%	wt%			of (OH,F,Cl)	
10-1	1438	Hispar	Karakorum	0.45	19.96	1.01	54.72	0.20	1.23	0.35	0.62	19.61	98.16	OH,F,Cl	Mg-Fe-Mn	cummingtonite
11-1	1438	Hispar	Karakorum	0.28	12.72	3.80	50.10	0.29	12.48	0.58	0.59	16.78	97.63	OH,F,Cl	Ca	magnesio-ferri-hornblende
21-1	1438	Hispar	Karakorum	0.67	13.86	4.59	51.14	0.51	12.48	0.27	0.49	13.88	97.89	OH,F,Cl	Ca	actinolite
23-1	1438	Hispar	Karakorum	1.04	11.61	8.64	46.16	0.81	12.49	0.94	0.45	16.38	98.53	OH,F,Cl	Ca	magnesio-ferri-hornblende
24-1	1438	Hispar	Karakorum	1.05	14.66	7.93	48.12	0.43	11.55	1.34	0.20	11.78	97.06	OH,F,Cl	Ca	magnesio-hornblende
44-1	1438	Hispar	Karakorum	2.15	7.66	15.81	41.36	0.51	10.94	0.58	0.60	17.16	96.76	OH,F,Cl	Ca	ferro-pargasite
46-1	1438	Hispar	Karakorum	1.41	7.97	13.76	42.87	0.49	12.21	0.40	0.34	17.73	97.18	OH,F,Cl	Ca	ferro-hornblende
51-1	1438	Hispar	Karakorum	0.81	13.47	4.96	51.39	0.52	12.05	0.39	0.56	16.54	100.69	OH,F,Cl	Ca	magnesio-ferri-hornblende
57-1	1438	Hispar	Karakorum	0.72	13.50	7.33	48.53	0.64	11.54	0.93	0.68	15.02	98.91	OH,F,Cl	Ca	magnesio-ferri-hornblende
59-1	1438	Hispar	Karakorum	0.98	12.19	4.97	47.24	0.73	11.72	0.81	0.44	16.01	95.10	OH,F,Cl	Ca	actinolite
75-1	1438	Hispar	Karakorum	1.53	8.74	13.71	42.10	0.64	12.23	0.75	0.36	18.29	98.36	OH,F,Cl	Ca	pargasite
76-1	1438	Hispar	Karakorum	0.61	11.93	7.09	48.55	0.69	12.44	0.73	0.57	17.29	99.90	OH,F,Cl	Ca	magnesio-ferri-hornblende
77-1	1438	Hispar	Karakorum	0.90	10.89	9.61	45.06	0.97	12.70	1.18	0.47	16.45	98.25	OH,F,Cl	Ca	magnesio-hornblende
78-1	1438	Hispar	Karakorum	0.81	13.71	9.99	48.97	0.47	12.27	0.94	0.50	12.94	100.60	OH,F,Cl	Ca	magnesio-hornblende
82-1	1438	Hispar	Karakorum	1.36	12.71	10.76	46.53	0.63	12.51	1.00	0.31	13.01	98.81	OH,F,Cl	Ca	magnesio-hornblende
85-1	1438	Hispar	Karakorum	1.19	10.13	10.48	45.10	1.30	12.17	0.65	0.42	17.39	98.84	OH,F,Cl	Ca	pargasite
101-1	1438	Hispar	Karakorum	0.13	16.43	3.21	53.28	0.62	12.60	0.55	0.28	10.95	98.05	OH,F,Cl	Ca	actinolite
104-1	1438	Hispar	Karakorum	0.90	16.12	4.52	51.07	0.41	11.90	0.85	0.29	11.36	97.43	OH,F,Cl	Ca	magnesio-ferri-hornblende
118-1	1438	Hispar	Karakorum	0.70	20.53	1.73	55.40	0.16	13.12	0.43	0.34	6.83	99.26	OH,F,Cl	Ca	actinolite
119-1	1438	Hispar	Karakorum	0.64	18.58	1.77	55.09	0.00	12.16	0.43	0.57	10.29	99.54	OH,F,Cl	Ca	actinolite
120-1	1438	Hispar	Karakorum	1.04	10.02	8.83	46.36	0.86	13.18	1.17	0.41	17.36	99.23	OH,F,Cl	Ca	pargasite
125-1	1438	Hispar	Karakorum	0.56	11.47	7.28	46.88	0.95	12.47	1.05	0.56	15.93	97.15	OH,F,Cl	Ca	magnesio-hornblende
126-1	1438	Hispar	Karakorum	0.64	10.49	7.31	46.66	0.70	12.14	0.38	0.48	18.63	97.42	OH,F,Cl	Ca	magnesio-ferri-hornblende
133-1	1438	Hispar	Karakorum	1.19	11.14	7.37	46.58	0.99	12.31	1.00	0.54	16.86	97.98	OH,F,Cl	Ca	pargasite
138-1	1438	Hispar	Karakorum	1.50	11.11	9.46	45.42	0.82	11.93	1.98	0.62	16.52	99.37	OH,F,Cl	Ca	pargasite
140-1	1438	Hispar	Karakorum	0.99	12.61	8.98	46.95	0.41	12.48	0.73	0.32	14.24	97.72	OH,F,Cl	Ca	magnesio-hornblende
142-1	1438	Hispar	Karakorum	0.87	14.82	7.13	49.59	0.42	12.04	0.70	0.45	12.04	98.06	OH,F,Cl	Ca	magnesio-hornblende
145-1	1438	Hispar	Karakorum	0.62	17.53	3.80	52.59	0.39	13.15	0.51	0.24	8.45	97.27	OH,F,Cl	Ca	actinolite
146-1	1438	Hispar	Karakorum	1.62	8.65	12.32	42.20	0.83	12.61	1.36	0.47	18.34	98.40	OH,F,Cl	Ca	ferro-pargasite
155-1	1438	Hispar	Karakorum	1.62	11.17	7.90	46.32	0.92	12.15	1.25	0.69	18.07	100.08	OH,F,Cl	Ca	magnesio-hastingsite
162-1	1438	Hispar	Karakorum	1.72	10.41	10.69	41.68	1.41	11.92	1.43	0.19	16.38	95.84	OH,F,Cl	Ca	pargasite
165-1	1438	Hispar	Karakorum	1.63	12.15	10.83	45.34	0.65	10.50	1.84	0.35	15.82	99.12	OH,F,Cl	Ca	magnesio-hornblende
172-1	1438	Hispar	Karakorum	1.13	12.45	5.44	48.87	0.77	12.52	0.78	0.40	17.58	99.94	OH,F,Cl	Ca	actinolite
175-1	1438	Hispar	Karakorum	1.04	12.33	9.49	45.96	0.98	10.92	1.76	0.46	15.04	98.00	OH,F,Cl	Ca	magnesio-ferri-hornblende
206-1	1438	Hispar	Karakorum	1.35	11.05	11.22	44.80	0.80	11.81	0.79	0.31	15.39	97.52	OH,F,Cl	Ca	magnesio-hornblende
210-1	1438	Hispar	Karakorum	1.53	9.77	11.79	42.96	0.90	11.48	1.38	0.42	17.39	97.64	OH,F,Cl	Ca	pargasite
212-1	1438	Hispar	Karakorum	1.05	8.62	11.19	41.99	1.79	12.23	2.09	0.48	18.73	98.17	OH,F,Cl	Ca	potassic-ferro-pargasite
213-1	1438	Hispar	Karakorum	0.47	15.65	5.19	49.66	0.33	11.71	1.06	0.43	13.40	97.90	OH,F,Cl	Ca	magnesio-ferri-hornblende
6-2	1438	Hispar	Karakorum	0.48	23.10	1.11	54.58	0.30	0.81	0.41	0.39	14.92	96.11	OH,F,Cl	Mg-Fe-Mn	cummingtonite
7-2	1438	Hispar	Karakorum	0.36	0.26	23.94	36.68	0.23	22.52	0.75	0.30	12.19	97.23	OH,F,Cl	Ca	ferro-sadanagaite
8-2	1438	Hispar	Karakorum	0.96	13.95	4.24	51.38	0.38	12.36	0.30	0.38	14.04	97.98	OH,F,Cl	Ca	actinolite
15-2	1438	Hispar	Karakorum	0.65	13.09	4.05	49.74	0.44	12.32	0.36	0.53	15.16	96.35	OH,F,Cl	Ca	actinolite
22-2	1438	Hispar	Karakorum	1.24	9.78	8.02	46.24	0.96	12.25	0.71	0.62	17.79	97.59	OH,F,Cl	Ca	ferro-pargasite
23-2	1438	Hispar	Karakorum	0.58	15.51	4.50	51.81	0.61	12.66	0.51	0.45	11.59	98.21	OH,F,Cl	Ca	actinolite
24-2	1438	Hispar	Karakorum	0.48	16.77	3.43	52.62	0.18	13.01	0.44	0.33	10.71	97.98	OH,F,Cl	Ca	actinolite
25-2	1438	Hispar	Karakorum	1.30	12.19	9.85	43.82	1.27	12.16	1.48	0.20	14.79	97.06	OH,F,Cl	Ca	magnesio-hastingsite
34-2	1438	Hispar	Karakorum	0.84	12.46	9.28	46.57	0.86	12.05	1.22	0.31	14.82	98.41	OH,F,Cl	Ca	magnesio-hornblende
35-2	1438	Hispar	Karakorum	1.27	9.83	7.81	46.16	1.02	11.76	1.29	0.69	19.16	98.99	OH,F,Cl	Ca	ferro-pargasite
39-2	1438	Hispar	Karakorum	0.00	3.60	21.07	36.58	0.30	1.92	0.34	0.92	34.92	99.65	OH,F,Cl	Mg-Fe-Mn	grunerite
44-2	1438	Hispar	Karakorum	0.87	11.49	6.35	47.92	0.80	12.23	0.95	0.41	16.97	98.00	OH,F,Cl	Ca	magnesio-hornblende
46-2	1438	Hispar	Karakorum	0.37	13.58	3.98	50.16	0.56	12.40	0.42	0.53	14.92	96.91	OH,F,Cl	Ca	actinolite
67-2	1438	Hispar	Karakorum	0.72	8.06	13.26	41.05	1.73	11.89	1.53	0.37	18.50	97.10	OH,F,Cl	Ca	potassic-ferro-pargasite
68-2	1438	Hispar	Karakorum	1.03	11.10	10.59	43.83	0.94	12.19	0.67	0.45	16.35	97.15	OH,F,Cl	Ca	magnesio-ferri-hornblende
77-2	1438	Hispar	Karakorum	0.50	14.88	2.84	51.68	0.24	13.03	0.39	0.45	14.74	98.74	OH,F,Cl	Ca	actinolite
83-2	1438	Hispar	Karakorum	1.28	10.08	9.26	44.51	1.29	11.74	1.41	0.36	19.10	99.03	OH,F,Cl	Ca	magnesio-hastingsite
94-2	1438	Hispar	Karakorum	1.40	11.36	9.76	45.21	0.56	11.54	2.04	0.37	15.34	97.60	OH,F,Cl	Ca	magnesio-hornblende
113-2	1438	Hispar	Karakorum	0.94	12.01	6.43	48.14	0.73	12.11	0.78	0.57	16.91	98.61	OH,F,Cl	Ca	magnesio-ferri-hornblende
119-2	1438	Hispar	Karakorum	0.82	18.15	3.26	53.46	0.32	11.92	0.23	0.52	8.83	97.53	OH,F,Cl	Ca	actinolite
130-2	1438	Hispar	Karakorum	1.06	15.63	5.60	51.23	0.46	11.72	1.38	0.43	12.67	100.18	OH,F,Cl	Ca	magnesio-ferri-hornblende
132-2	1438	Hispar	Karakorum	0.85	12.70	6.90	47.70	0.46	8.77	1.01	0.39	18.48	97.26	OH,F,Cl	Ca	magnesio-ferri-hornblende
133-2	1438	Hispar	Karakorum	1.02	12.05	8.22	47.25	0.99	12.15	0.43	0.35	15.44	97.90	OH,F,Cl	Ca	magnesio-hornblende
147-2	1438	Hispar	Karakorum	0.82	12.20	5.23	48.80	0.58	11.94	0.70	0.63	17.43	98.34	OH,F,Cl	Ca	magnesio-ferri-hornblende
152-2	1438	Hispar	Karakorum	1.57	7.94	12.21	42.58	0.61	11.50	1.01	0.36	19.46	97.24	OH,F,Cl	Ca	ferro-pargasite
153-2	1438	Hispar	Karakorum	0.47	17.68	0.94	54.73	0.27	12.89	0.24	0.52	10.56	98.30	OH,F,Cl	Ca	actinolite
166-2	1438	Hispar	Karakorum	0.37	14.98	2.36	52.06	0.42	12.19	0.80	0.49	15.65	99.31	OH,F,Cl	Ca	actinolite
176-2	1438	Hispar	Karakorum	1.34	14.38	8.35	48.62	1.01	11.80	1.20	0.32	11.15	98.18	OH,F,Cl	Ca	magnesio-hornblende
181-2	1438	Hispar	Karakorum	0.16	12.15	4.87	51.62	0.48	12.02	0.73	0.37	15.98	98.39	OH,F,Cl	Ca	magnesio-hornblende
186-2	1438	Hispar	Karakorum	1.33	11.85	10.18	48.36	0.78	10.68	1.47	0.38	14.86	99.88	OH,F,Cl	Ca	magnesio-hornblende
190-2	1438	Hispar	Karakorum	1.11	15.62	8.32	49.12	0.74	11.46	1.13	0.29	10.02	97.82	OH,F,Cl	Ca	magnesio-hornblende
196-2	1438	Hispar	Karakorum	1.33	10.66	10.30	45.22	1.33	11.98	1.50	0.54	15.61	98.48	OH,F,Cl	Ca	pargasite
210-2	1438	Hispar	Karakorum	1.33	11.39	12.23	44.17	0.43	11.67	0.63	0.26	15.45	97.55	OH,F,Cl	Ca	magnesio-hornblende
211-2	1438	Hispar	Karakorum	0.62	19.01	2.38	55.36	0.11	11.91	0.31	0.43	9.25	99.37	OH,F,Cl	Ca	actinolite
217-2	1438	Hispar	Karakorum	0.34	16.89	1.57	52.23	0.26	1.78	0.64	0.63	23.40	97.75	OH,F,Cl	Mg-Fe-Mn	cummingtonite
229-2	1438	Hispar	Karakorum	1.04	10.96	8.71	47.67	0.89	12.20	0.79	0.53	16.60	99.40	OH,F,Cl	Ca	magnesio-hornblende
238-2	1438	Hispar	Karakorum	0.68	12.95	6.66	48.61	0.43	12.16	1.26	0.32	14.80	97.88	OH,F,Cl	Ca	magnesio-hornblende
242-2	1438	Hispar	Karakorum	1.17	13.30	8.98	46.06	0.51	12.07	1.38	0.49	13.45	97.42	OH,F,Cl	Ca	magnesio-ferri-hornblende
244-2	1438	Hispar	Karakorum	1.34	9.50	11.29	41.75	1.69	12.37	1.81	0.35	18.01	98.11	OH,F,Cl	Ca	pargasite
247-2	1438	Hispar	Karakorum	0.46	10.97	5.48	51.15	0.61	11.59	0.80	0.56	16.37	97.99	OH,F,Cl	Ca	magnesio-hornblende
251-2	1438	Hispar	Karakorum	1.13	9.66	10.83	44.74	1.19	12.19	1.39	0.38	16.26	97.77	OH,F,Cl	Ca	pargasite
257-2	1438	Hispar	Karakorum	1.01	17.28	6.42	52.55	0.44	11.74	0.58	0.40	8.92	99.33	OH,F,Cl	Ca	magnesio-hornblende
260-2	1438	Hispar	Karakorum	1.50	11.62	11.60	46.80	0.28	11.40	0.44	0.31	14.17	98.10	OH,F,Cl	Ca	magnesio-hornblende
265-2	1438	Hispar	Karakorum	0.98	9.01	9.78	44.54	1.23	11.93	2.06	0.56	17.23	97.32	OH,F,Cl	Ca	ferro-hornblende
1-3	1438	Hispar	Karakorum	0.91	13.58	8.31	46.12	0.80	12.07	1.23	0.34	13.32	96.67	OH,F,Cl	Ca	magnesio-ferri-hornblende
2-3	1438	Hispar	Karakorum	1.25	14.12	9.62	47.66	0.57	11.89	0.90	0.29	11.54	97.85	OH,F,Cl	Ca	magnesio-hornblende
4-3	1438	Hispar	Karakorum	0.94	11.58	7.19	46.74	0.74	12.04	0.95	0.44	17.08	97.71	OH,F,Cl	Ca	magnesio-ferri-hornblende
7-3	1438	Hispar	Karakorum	0.30	11.57	5.73	49.08	0.52	11.79	0.53	0.40	16.36	96.27	OH,F,Cl	Ca	magnesio-hornblende
9-3	1438	Hispar	Karakorum	1.87	10.13	11.95	43.82	0.59	11.04	1.13	0.20	16.21	96.94	OH,F,Cl	Ca	pargasite
13-3	1438	Hispar	Karakorum	1.54	12.69	10.65	44.44	0.79	11.80	1.86	0.28	13.60	97.65	OH,F,Cl	Ca	pargasite
35-3	1438	Hispar	Karakorum	0.57	13.70	3.02	52.69	0.48	12.35	0.62	0.39	15.76	99.58	OH,F,Cl	Ca	actinolite
40-3	1438	Hispar	Karakorum	1.56	8.17	12.31	42.56	0.94	11.14	1.12	0.44	19.26	97.50	OH,F,Cl	Ca	ferro-pargasite
41-3	1438	Hispar	Karakorum	1.67	9.56	11.63	42.85	0.79	11.64	1.41	0.36	19.93	99.83	OH,F,Cl	Ca	magnesio-hastingsite
42-3	1438	Hispar	Karakorum	0.92	11.79	5.71	49.24	0.87	12.23	0.97	0.39	16.98	99.11	OH,F,Cl	Ca	actinolite
50-3	1438	Hispar	Karakorum	0.80	12.37	5.93	51.35	0.62	11.93	0.51	0.48	15.87	99.86	OH,F,Cl	Ca	magnesio-hornblende
57-3	1438	Hispar	Karakorum	1.17	9.27	10.67	45.31	1.41	12.02	1.15	0.27	16.38	97.65	OH,F,Cl	Ca	potassic-pargasite
58-3	1438	Hispar	Karakorum	1.57	10.65	10.35	47.67	0.87	11.71	0.88	0.20	16.08	99.98	OH,F,Cl	Ca	magnesio-hornblende
59-3	1438	Hispar	Karakorum	1.38	9.63	13.85	45.54	0.65	11.65	0.65	0.26	14.32	97.93	OH,F,Cl	Ca	magnesio-hornblende
70-3	1438	Hispar	Karakorum	0.61	10.63	7.29	47.43	0.87	11.85	1.07	0.63	18.49	98.87	OH,F,Cl	Ca	magnesio-ferri-hornblende
71-3	1438	Hispar	Karakorum	1.30	11.73	7.03	47.06	0.82	12.18	1.13	0.59	17.45	99.29	OH,F,Cl	Ca	magnesio-ferri-hornblende
83-3	1438	Hispar	Karakorum	1.00	10.62	8.93	46.02	0.94	11.78	0.84	0.41	17.39	97.93	OH,F,Cl	Ca	magnesio-hornblende
96-3	1438	Hispar	Karakorum	0.75	10.59	6.82	47.74	0.68	11.61	1.12	0.71	18.45	98.47	OH,F,Cl	Ca	magnesio-ferri-hornblende
109-3	1438	Hispar	Karakorum	1.46	11.13	10.36	46.83	1.37	12.11	1.55	0.48	15.14	100.44	OH,F,Cl	Ca	pargasite

Point	Sample	River/Dune	Domain	Na_2O	MgO	Al_2O_3	SiO_2	K_2O	CaO	TiO_2	MnO	FeO	Total	Group	Subgroup	Species
				wt%	wt%	wt%	wt%	wt%	wt%	wt%	wt%	wt%			of (OH,F,Cl)	
2-1	4426	Stagmo	Ladakh	1.31	12.12	8.05	46.96	0.75	11.78	1.23	0.27	17.23	99.70	OH,F,Cl	Ca	magnesio-ferri-hornblende
9-1	4426	Stagmo	Ladakh	0.88	13.60	6.17	48.71	0.81	11.91	1.27	0.24	15.48	99.08	OH,F,Cl	Ca	magnesio-ferri-hornblende
12-1	4426	Stagmo	Ladakh	1.04	11.60	6.93	47.92	0.82	11.21	1.01	0.27	16.65	97.46	OH,F,Cl	Ca	magnesio-hornblende
13-1	4426	Stagmo	Ladakh	1.24	11.73	7.13	46.18	1.04	11.82	1.62	0.30	16.59	97.66	OH,F,Cl	Ca	pargasite
15-1	4426	Stagmo	Ladakh	1.06	12.48	7.39	46.71	0.82	11.95	1.34	0.30	15.72	97.76	OH,F,Cl	Ca	magnesio-ferri-hornblende
17-1	4426	Stagmo	Ladakh	1.04	10.52	8.60	45.38	0.90	11.10	0.87	0.26	19.22	97.91	OH,F,Cl	Ca	magnesio-ferri-hornblende
20-1	4426	Stagmo	Ladakh	1.19	10.54	8.60	44.83	1.13	11.72	1.91	0.31	18.64	98.86	OH,F,Cl	Ca	magnesio-ferri-hornblende
21-1	4426	Stagmo	Ladakh	1.31	12.55	7.05	47.65	0.78	12.19	1.24	0.27	14.69	97.73	OH,F,Cl	Ca	magnesio-hornblende
22-1	4426	Stagmo	Ladakh	1.12	11.75	7.56	46.25	1.12	12.15	1.58	0.30	17.09	98.92	OH,F,Cl	Ca	magnesio-ferri-hornblende
24-1	4426	Stagmo	Ladakh	1.08	11.68	7.27	46.80	1.06	11.33	1.38	0.25	16.79	97.65	OH,F,Cl	Ca	magnesio-ferri-hornblende
47-1	4426	Stagmo	Ladakh	1.23	13.58	6.83	47.18	0.83	11.01	1.42	0.27	15.74	98.09	OH,F,Cl	Ca	magnesio-ferri-hornblende
53-1	4426	Stagmo	Ladakh	1.22	11.34	8.10	45.98	1.10	11.35	1.36	0.19	17.81	98.46	OH,F,Cl	Ca	magnesio-hornblende
59-1	4426	Stagmo	Ladakh	1.03	11.46	7.84	47.25	1.09	11.38	1.49	0.23	16.97	98.74	OH,F,Cl	Ca	magnesio-hornblende
60-1	4426	Stagmo	Ladakh	0.72	11.14	7.50	46.47	0.97	11.68	1.23	0.22	18.50	98.43	OH,F,Cl	Ca	magnesio-ferri-hornblende
63-1	4426	Stagmo	Ladakh	1.14	10.76	8.72	46.24	0.95	11.62	0.80	0.17	17.57	97.97	OH,F,Cl	Ca	magnesio-hornblende
64-1	4426	Stagmo	Ladakh	1.13	11.13	8.34	46.03	1.07	11.40	1.19	0.21	16.99	97.49	OH,F,Cl	Ca	magnesio-hornblende
65-1	4426	Stagmo	Ladakh	1.23	8.07	11.09	41.53	1.10	12.17	1.61	0.31	20.28	97.38	OH,F,Cl	Ca	hastingsite
66-1	4426	Stagmo	Ladakh	0.76	12.68	7.12	49.03	0.79	12.80	0.73	0.29	15.74	99.94	OH,F,Cl	Ca	magnesio-hornblende
87-1	4426	Stagmo	Ladakh	1.27	12.11	7.90	46.42	0.84	12.17	1.33	0.33	15.11	97.49	OH,F,Cl	Ca	magnesio-hornblende
88-1	4426	Stagmo	Ladakh	0.87	9.96	8.71	46.64	0.78	11.31	0.80	0.26	19.31	98.63	OH,F,Cl	Ca	magnesio-hornblende
89-1	4426	Stagmo	Ladakh	1.24	11.39	6.88	46.71	0.81	11.73	1.08	0.31	17.70	97.84	OH,F,Cl	Ca	magnesio-ferri-hornblende
91-1	4426	Stagmo	Ladakh	1.39	11.76	7.76	46.66	1.04	11.60	1.35	0.36	16.25	98.18	OH,F,Cl	Ca	pargasite
94-1	4426	Stagmo	Ladakh	0.97	10.18	9.38	44.58	1.03	11.60	1.50	0.31	17.88	97.43	OH,F,Cl	Ca	magnesio-hornblende
96-1	4426	Stagmo	Ladakh	1.00	11.18	7.89	46.37	0.97	11.95	0.96	0.20	17.37	97.89	OH,F,Cl	Ca	magnesio-hornblende
101-1	4426	Stagmo	Ladakh	0.73	10.75	8.61	45.71	1.21	11.92	1.50	0.27	16.44	97.13	OH,F,Cl	Ca	magnesio-hornblende
113-1	4426	Stagmo	Ladakh	1.05	10.92	8.68	45.05	1.17	12.20	1.51	0.29	18.11	98.98	OH,F,Cl	Ca	magnesio-ferri-hornblende
114-1	4426	Stagmo	Ladakh	1.17	11.02	7.64	46.17	0.90	12.00	1.39	0.37	18.33	98.98	OH,F,Cl	Ca	magnesio-ferri-hornblende
115-1	4426	Stagmo	Ladakh	1.07	10.73	7.49	46.24	0.96	11.68	0.94	0.25	17.93	97.30	OH,F,Cl	Ca	magnesio-hornblende
119-1	4426	Stagmo	Ladakh	1.31	12.36	7.83	46.50	1.10	11.12	1.78	0.19	15.53	97.72	OH,F,Cl	Ca	magnesio-hornblende
120-1	4426	Stagmo	Ladakh	1.04	13.37	5.86	50.86	0.69	11.20	1.00	0.27	14.12	98.39	OH,F,Cl	Ca	magnesio-hornblende
122-1	4426	Stagmo	Ladakh	1.39	10.98	8.51	45.08	1.21	11.67	1.03	0.28	18.54	98.68	OH,F,Cl	Ca	magnesio-hastingsite
128-1	4426	Stagmo	Ladakh	0.58	11.05	7.68	47.22	0.78	11.86	1.02	0.34	17.65	98.18	OH,F,Cl	Ca	magnesio-ferri-hornblende
129-1	4426	Stagmo	Ladakh	1.25	9.91	8.99	44.96	1.09	12.42	1.30	0.19	18.45	98.56	OH,F,Cl	Ca	pargasite
135-1	4426	Stagmo	Ladakh	1.39	11.18	8.37	46.83	1.03	11.13	1.32	0.18	17.28	98.71	OH,F,Cl	Ca	magnesio-hornblende
136-1	4426	Stagmo	Ladakh	1.74	10.60	8.66	45.01	1.01	11.02	1.26	0.25	17.64	97.18	OH,F,Cl	Ca	pargasite
142-1	4426	Stagmo	Ladakh	1.28	11.22	8.34	45.41	0.79	11.47	1.31	0.17	17.06	97.05	OH,F,Cl	Ca	magnesio-ferri-hornblende
144-1	4426	Stagmo	Ladakh	1.82	8.81	11.15	41.61	0.95	10.90	2.26	0.23	19.46	97.18	OH,F,Cl	Ca	ferro-pargasite
152-1	4426	Stagmo	Ladakh	1.34	12.24	8.16	45.95	1.01	11.76	1.16	0.25	16.84	98.71	OH,F,Cl	Ca	magnesio-ferri-hornblende
154-1	4426	Stagmo	Ladakh	1.02	11.97	8.01	47.40	0.92	11.57	1.17	0.32	17.56	99.94	OH,F,Cl	Ca	magnesio-ferri-hornblende
161-1	4426	Stagmo	Ladakh	1.17	13.54	6.38	48.47	0.62	12.20	1.20	0.26	14.10	97.93	OH,F,Cl	Ca	magnesio-hornblende
165-1	4426	Stagmo	Ladakh	1.13	13.08	6.46	48.40	0.77	11.97	0.98	0.32	16.21	99.30	OH,F,Cl	Ca	magnesio-ferri-hornblende
166-1	4426	Stagmo	Ladakh	0.74	13.14	4.75	50.15	0.67	12.44	0.60	0.36	16.37	99.21	OH,F,Cl	Ca	actinolite
167-1	4426	Stagmo	Ladakh	1.21	10.36	9.08	44.42	1.17	11.37	1.08	0.14	18.38	97.23	OH,F,Cl	Ca	magnesio-ferri-hornblende
171-1	4426	Stagmo	Ladakh	1.04	11.43	8.09	45.82	1.10	12.23	1.51	0.31	16.52	98.06	OH,F,Cl	Ca	magnesio-hornblende
174-1	4426	Stagmo	Ladakh	0.38	16.93	1.38	58.37	0.28	11.41	0.31	0.28	10.15	99.51	OH,F,Cl	Ca	actinolite
177-1	4426	Stagmo	Ladakh	1.07	12.70	9.69	46.22	0.51	11.79	1.01	0.26	14.69	97.94	OH,F,Cl	Ca	magnesio-ferri-hornblende
183-1	4426	Stagmo	Ladakh	1.18	11.21	8.05	47.09	0.59	11.70	0.71	0.12	16.54	97.19	OH,F,Cl	Ca	magnesio-hornblende
192-1	4426	Stagmo	Ladakh	1.29	10.91	8.47	45.92	1.13	11.61	1.58	0.32	17.96	99.20	OH,F,Cl	Ca	pargasite
195-1	4426	Stagmo	Ladakh	1.35	10.16	9.11	45.18	1.27	11.76	0.87	0.29	19.85	99.84	OH,F,Cl	Ca	magnesio-hastingsite
206-1	4426	Stagmo	Ladakh	0.86	10.70	8.28	44.91	1.05	11.60	1.43	0.23	17.91	96.96	OH,F,Cl	Ca	magnesio-ferri-hornblende
208-1	4426	Stagmo	Ladakh	1.18	11.11	8.60	45.15	1.20	11.44	1.13	0.29	17.53	97.61	OH,F,Cl	Ca	magnesio-ferri-hornblende
210-1	4426	Stagmo	Ladakh	0.59	11.94	7.28	47.25	0.68	11.74	1.16	0.18	16.66	97.47	OH,F,Cl	Ca	magnesio-ferri-hornblende
212-1	4426	Stagmo	Ladakh	1.27	10.99	8.54	44.95	1.17	11.51	1.67	0.34	18.50	98.93	OH,F,Cl	Ca	magnesio-ferri-hornblende
218-1	4426	Stagmo	Ladakh	1.01	11.96	7.59	47.20	0.96	11.81	1.45	0.31	15.73	98.00	OH,F,Cl	Ca	magnesio-hornblende
227-1	4426	Stagmo	Ladakh	0.99	11.30	8.20	45.44	0.94	11.43	1.03	0.27	18.00	97.59	OH,F,Cl	Ca	magnesio-ferri-hornblende
230-1	4426	Stagmo	Ladakh	1.45	12.72	7.73	46.86	0.88	11.70	0.81	0.22	15.31	97.69	OH,F,Cl	Ca	pargasite
233-1	4426	Stagmo	Ladakh	0.95	12.39	7.15	47.42	0.87	11.49	1.30	0.32	16.28	98.17	OH,F,Cl	Ca	magnesio-ferri-hornblende
234-1	4426	Stagmo	Ladakh	0.96	10.90	8.97	46.11	0.92	11.76	1.10	0.21	16.19	97.13	OH,F,Cl	Ca	magnesio-hornblende
238-1	4426	Stagmo	Ladakh	0.87	10.80	8.29	45.94	0.85	11.71	0.94	0.25	16.71	96.36	OH,F,Cl	Ca	magnesio-hornblende
243-1	4426	Stagmo	Ladakh	1.56	11.38	8.03	45.69	0.94	11.37	1.27	0.25	16.60	97.10	OH,F,Cl	Ca	pargasite
251-1	4426	Stagmo	Ladakh	0.96	10.83	8.66	46.03	0.83	11.55	1.25	0.32	17.68	98.10	OH,F,Cl	Ca	magnesio-ferri-hornblende
255-1	4426	Stagmo	Ladakh	1.30	10.62	9.28	44.43	1.06	11.30	1.06	0.28	18.28	97.61	OH,F,Cl	Ca	magnesio-ferri-hornblende
259-1	4426	Stagmo	Ladakh	1.50	11.22	8.17	46.25	1.11	12.17	1.46	0.20	16.51	98.59	OH,F,Cl	Ca	pargasite
261-1	4426	Stagmo	Ladakh	0.86	14.05	5.85	49.74	0.63	12.01	0.72	0.20	14.01	98.06	OH,F,Cl	Ca	magnesio-hornblende
267-1	4426	Stagmo	Ladakh	1.33	13.06	6.64	49.50	0.85	11.35	1.11	0.12	15.31	99.25	OH,F,Cl	Ca	magnesio-hornblende
269-1	4426	Stagmo	Ladakh	1.48	11.27	8.81	46.07	1.20	11.08	1.53	0.29	17.89	99.61	OH,F,Cl	Ca	pargasite
277-1	4426	Stagmo	Ladakh	1.35	10.58	7.78	45.90	0.97	11.00	1.04	0.23	17.96	96.82	OH,F,Cl	Ca	magnesio-hornblende
287-1	4426	Stagmo	Ladakh	0.77	12.68	7.07	48.66	0.81	11.38	0.63	0.21	15.10	97.30	OH,F,Cl	Ca	magnesio-ferri-hornblende
295-1	4426	Stagmo	Ladakh	1.24	10.27	8.80	45.46	1.17	12.26	1.27	0.30	18.13	98.90	OH,F,Cl	Ca	pargasite
297-1	4426	Stagmo	Ladakh	1.30	14.33	6.40	49.31	0.62	11.51	1.33	0.42	14.37	99.57	OH,F,Cl	Ca	magnesio-ferri-hornblende
298-1	4426	Stagmo	Ladakh	0.99	10.47	8.17	44.94	1.18	11.90	1.02	0.22	18.95	97.84	OH,F,Cl	Ca	magnesio-ferri-hornblende
299-1	4426	Stagmo	Ladakh	0.88	11.30	7.62	47.02	0.70	11.64	1.00	0.12	19.34	99.62	OH,F,Cl	Ca	magnesio-ferri-hornblende
300-1	4426	Stagmo	Ladakh	0.60	13.24	5.79	51.03	0.70	11.84	1.10	0.38	15.64	100.34	OH,F,Cl	Ca	magnesio-hornblende
310-1	4426	Stagmo	Ladakh	0.85	11.59	7.31	45.78	0.83	11.94	1.38	0.21	16.28	96.18	OH,F,Cl	Ca	magnesio-ferri-hornblende
313-1	4426	Stagmo	Ladakh	0.89	10.83	8.10	45.31	0.77	11.79	1.27	0.24	17.46	96.66	OH,F,Cl	Ca	magnesio-ferri-hornblende
315-1	4426	Stagmo	Ladakh	1.03	11.50	8.94	46.85	1.02	11.75	1.20	0.30	16.91	99.50	OH,F,Cl	Ca	magnesio-hornblende
316-1	4426	Stagmo	Ladakh	1.27	12.22	7.26	47.48	1.06	11.70	1.38	0.29	17.45	100.11	OH,F,Cl	Ca	magnesio-ferri-hornblende
318-1	4426	Stagmo	Ladakh	1.16	11.16	7.59	45.98	0.80	11.56	1.19	0.20	17.72	97.37	OH,F,Cl	Ca	magnesio-ferri-hornblende
327-1	4426	Stagmo	Ladakh	0.97	10.62	8.18	47.24	0.91	11.96	0.88	0.21	17.65	98.62	OH,F,Cl	Ca	magnesio-hornblende
332-1	4426	Stagmo	Ladakh	1.30	11.02	9.01	45.33	0.99	11.34	0.97	0.36	18.10	98.42	OH,F,Cl	Ca	magnesio-ferri-hornblende
334-1	4426	Stagmo	Ladakh	1.17	12.28	7.62	47.35	0.81	11.59	1.35	0.39	15.93	98.48	OH,F,Cl	Ca	magnesio-ferri-hornblende
335-1	4426	Stagmo	Ladakh	1.34	11.51	7.75	46.27	0.88	11.20	1.41	0.25	17.43	98.04	OH,F,Cl	Ca	magnesio-hornblende
340-1	4426	Stagmo	Ladakh	1.11	11.06	7.15	46.88	0.84	11.87	0.82	0.25	17.50	97.48	OH,F,Cl	Ca	magnesio-hornblende
341-1	4426	Stagmo	Ladakh	1.13	12.54	7.14	46.28	1.05	11.82	1.40	0.25	15.87	97.48	OH,F,Cl	Ca	magnesio-ferri-hornblende
344-1	4426	Stagmo	Ladakh	1.29	10.46	8.27	45.85	1.09	11.73	1.49	0.18	17.72	98.09	OH,F,Cl	Ca	pargasite
348-1	4426	Stagmo	Ladakh	1.39	11.65	8.25	46.20	0.88	11.20	1.08	0.21	17.04	97.89	OH,F,Cl	Ca	magnesio-hornblende
354-1	4426	Stagmo	Ladakh	0.86	16.69	5.15	51.50	0.34	11.54	0.44	0.14	10.47	97.14	OH,F,Cl	Ca	magnesio-ferri-hornblende
355-1	4426	Stagmo	Ladakh	1.07	11.27	7.96	45.38	1.13	11.55	1.41	0.31	17.89	97.96	OH,F,Cl	Ca	magnesio-ferri-hornblende
359-1	4426	Stagmo	Ladakh	1.26	12.06	7.67	45.28	1.24	10.93	1.40	0.20	17.21	97.26	OH,F,Cl	Ca	magnesio-ferri-hornblende
48-2	4426	Stagmo	Ladakh	1.08	10.92	8.70	46.22	0.91	11.79	1.07	0.24	17.28	98.21	OH,F,Cl	Ca	magnesio-hornblende
59-2	4426	Stagmo	Ladakh	1.25	11.11	8.02	45.64	0.68	11.56	1.25	0.15	17.32	96.98	OH,F,Cl	Ca	magnesio-ferri-hornblende
61-2	4426	Stagmo	Ladakh	1.22	10.84	7.15	46.49	0.95	11.63	1.09	0.36	17.33	97.06	OH,F,Cl	Ca	magnesio-hornblende
62-2	4426	Stagmo	Ladakh	0.92	10.18	8.68	45.26	0.92	11.62	0.93	0.25	18.62	97.37	OH,F,Cl	Ca	magnesio-ferri-hornblende
63-2	4426	Stagmo	Ladakh	1.35	10.64	7.81	45.35	1.26	11.71	1.68	0.25	18.11	98.16	OH,F,Cl	Ca	pargasite
64-2	4426	Stagmo	Ladakh	1.12	11.66	7.51	46.69	0.95	11.47	1.51	0.32	16.55	97.77	OH,F,Cl	Ca	magnesio-ferri-hornblende
69-2	4426	Stagmo	Ladakh	1.37	11.69	8.48	45.59	0.94	11.61	1.43	0.22	17.31	98.65	OH,F,Cl	Ca	magnesio-ferri-hornblende
84-2	4426	Stagmo	Ladakh	1.43	11.34	8.07	45.71	1.12	11.71	1.36	0.27	17.50	98.50	OH,F,Cl	Ca	pargasite
85-2	4426	Stagmo	Ladakh	1.09	11.83	7.80	46.81	0.82	11.61	1.12	0.20	17.23	98.52	OH,F,Cl	Ca	magnesio-ferri-hornblende
94-2	4426	Stagmo	Ladakh	0.92	11.83	7.60	46.26	0.73	11.57	1.20	0.25	16.79	97.17	OH,F,Cl	Ca	magnesio-ferri-hornblende
241-2	4426	Stagmo	Ladakh	1.42	12.47	6.94	45.27	1.03	11.76	1.64	0.25	16.95	97.74	OH,F,Cl	Ca	magnesio-hastingsite

Point	Sample	River/Dune	Domain	Na_2O	MgO	Al_2O_3	SiO_2	K_2O	CaO	TiO_2	MnO	FeO	Total	Group	Subgroup	Species
				wt%	wt%	wt%	wt%	wt%	wt%	wt%	wt%	wt%			of (OH,F,Cl)	
34-1	4430	Domkar	Ladakh	1.19	10.12	9.15	43.74	0.96	12.05	1.44	0.40	19.98	99.02	OH,F,Cl	Ca	magnesio-ferri-hornblende
39-1	4430	Domkar	Ladakh	1.31	11.22	9.46	44.41	0.90	12.05	1.68	0.40	17.72	99.15	OH,F,Cl	Ca	magnesio-ferri-hornblende
40-1	4430	Domkar	Ladakh	0.99	14.29	4.25	50.74	0.36	11.67	1.06	0.90	15.38	99.64	OH,F,Cl	Ca	magnesio-ferri-hornblende
44-1	4430	Domkar	Ladakh	0.28	15.18	3.28	52.56	0.32	11.69	0.31	0.67	13.94	98.23	OH,F,Cl	Ca	actinolite
50-1	4430	Domkar	Ladakh	1.75	16.52	12.07	46.39	0.36	11.32	0.56	0.39	9.01	98.37	OH,F,Cl	Ca	magnesio-ferri-hornblende
52-1	4430	Domkar	Ladakh	1.18	11.51	9.17	46.94	0.57	12.13	0.82	0.56	17.98	100.85	OH,F,Cl	Ca	magnesio-ferri-hornblende
55-1	4430	Domkar	Ladakh	1.10	11.04	8.49	46.37	0.86	12.05	0.96	0.58	19.30	100.75	OH,F,Cl	Ca	magnesio-ferri-hornblende
56-1	4430	Domkar	Ladakh	0.93	10.80	6.93	47.06	0.73	11.63	1.27	0.31	18.26	97.92	OH,F,Cl	Ca	magnesio-ferri-hornblende
62-1	4430	Domkar	Ladakh	0.73	13.32	5.15	50.48	0.49	12.44	1.23	0.43	14.77	99.05	OH,F,Cl	Ca	magnesio-hornblende
65-1	4430	Domkar	Ladakh	1.08	10.88	8.33	45.35	0.48	11.75	2.30	0.60	19.56	100.33	OH,F,Cl	Ca	magnesio-ferri-hornblende
69-1	4430	Domkar	Ladakh	1.05	12.89	7.22	47.79	0.36	11.53	1.42	0.57	16.91	99.74	OH,F,Cl	Ca	magnesio-ferri-hornblende
73-1	4430	Domkar	Ladakh	1.65	10.10	11.44	41.93	0.73	11.99	2.62	0.54	18.56	99.56	OH,F,Cl	Ca	magnesio-hastingsite
75-1	4430	Domkar	Ladakh	1.47	11.73	10.32	44.06	0.30	11.00	2.77	0.74	16.27	98.67	OH,F,Cl	Ca	Ti-rich magnesio-ferri-hornblend
77-1	4430	Domkar	Ladakh	1.56	9.99	9.49	44.04	0.86	11.49	1.08	0.42	20.93	99.86	OH,F,Cl	Ca	magnesio-hastingsite
79-1	4430	Domkar	Ladakh	1.57	10.76	7.29	45.68	0.74	10.86	1.34	0.60	19.74	98.57	OH,F,Cl	Ca	magnesio-ferri-hornblende
84-1	4430	Domkar	Ladakh	1.27	11.29	6.56	46.84	0.84	11.75	1.63	0.42	18.68	99.29	OH,F,Cl	Ca	magnesio-ferri-hornblende
87-1	4430	Domkar	Ladakh	1.15	10.87	6.94	46.20	0.89	11.91	1.91	0.74	17.98	98.59	OH,F,Cl	Ca	magnesio-ferri-hornblende
193-1	4430	Domkar	Ladakh	1.24	11.82	7.91	46.13	0.70	11.57	1.58	0.30	16.95	98.20	OH,F,Cl	Ca	magnesio-ferri-hornblende
194-1	4430	Domkar	Ladakh	1.54	12.03	9.54	43.45	0.90	11.80	2.19	0.35	16.72	98.52	OH,F,Cl	Ca	magnesio-hastingsite
196-1	4430	Domkar	Ladakh	1.51	10.77	7.73	45.63	0.88	11.35	1.44	0.70	18.97	98.98	OH,F,Cl	Ca	magnesio-ferri-hornblende
198-1	4430	Domkar	Ladakh	1.09	9.97	8.58	43.47	1.01	11.44	1.64	0.54	20.44	98.18	OH,F,Cl	Ca	magnesio-ferri-hornblende
200-1	4430	Domkar	Ladakh	1.05	13.50	6.02	48.55	0.56	11.26	1.60	0.60	15.93	99.07	OH,F,Cl	Ca	magnesio-ferri-hornblende
206-1	4430	Domkar	Ladakh	0.97	11.20	6.87	46.89	0.78	11.92	1.26	0.59	18.05	98.54	OH,F,Cl	Ca	magnesio-ferri-hornblende
208-1	4430	Domkar	Ladakh	1.38	11.73	8.64	45.80	0.71	11.65	2.07	0.37	17.88	100.24	OH,F,Cl	Ca	magnesio-ferri-hornblende
210-1	4430	Domkar	Ladakh	0.67	11.46	7.64	47.34	0.73	11.68	0.92	0.45	18.34	99.23	OH,F,Cl	Ca	magnesio-ferri-hornblende
211-1	4430	Domkar	Ladakh	1.30	10.52	8.77	46.46	0.57	11.75	1.69	0.34	20.17	101.59	OH,F,Cl	Ca	magnesio-ferri-hornblende
214-1	4430	Domkar	Ladakh	0.73	10.60	7.38	46.31	0.61	11.52	1.69	0.60	19.07	98.50	OH,F,Cl	Ca	magnesio-ferri-hornblende
218-1	4430	Domkar	Ladakh	2.77	14.06	12.15	43.33	0.54	11.22	2.51	0.51	13.19	100.28	OH,F,Cl	Ca	magnesio-hastingsite
220-1	4430	Domkar	Ladakh	0.67	13.80	5.41	50.43	0.15	11.07	0.46	0.31	16.24	98.53	OH,F,Cl	Ca	magnesio-ferri-hornblende
224-1	4430	Domkar	Ladakh	1.45	9.36	9.54	43.85	1.12	11.16	1.55	0.51	20.11	98.65	OH,F,Cl	Ca	magnesio-hastingsite
225-1	4430	Domkar	Ladakh	1.39	11.67	7.95	45.93	0.76	11.66	1.88	0.55	17.47	99.25	OH,F,Cl	Ca	magnesio-ferri-hornblende
226-1	4430	Domkar	Ladakh	1.65	11.94	8.49	45.44	0.83	11.60	1.63	0.37	18.69	100.63	OH,F,Cl	Ca	magnesio-hastingsite
227-1	4430	Domkar	Ladakh	2.06	12.73	11.46	43.56	0.55	11.75	1.98	0.38	14.77	99.23	OH,F,Cl	Ca	magnesio-hastingsite
228-1	4430	Domkar	Ladakh	1.31	10.95	8.73	44.17	0.64	11.55	1.81	0.53	18.36	98.06	OH,F,Cl	Ca	magnesio-ferri-hornblende
230-1	4430	Domkar	Ladakh	1.00	11.77	7.28	47.87	0.55	12.17	0.47	0.51	19.15	100.77	OH,F,Cl	Ca	magnesio-ferri-hornblende
231-1	4430	Domkar	Ladakh	1.13	12.89	6.68	48.41	0.27	12.44	0.83	0.49	16.44	99.58	OH,F,Cl	Ca	magnesio-ferri-hornblende
233-1	4430	Domkar	Ladakh	1.35	10.87	8.13	45.38	0.83	11.82	1.61	0.42	18.82	99.23	OH,F,Cl	Ca	magnesio-ferri-hornblende
234-1	4430	Domkar	Ladakh	0.84	10.88	7.55	45.15	0.73	12.46	1.50	0.40	19.18	98.68	OH,F,Cl	Ca	magnesio-ferri-hornblende
235-1	4430	Domkar	Ladakh	0.91	11.02	7.63	47.36	0.64	11.60	1.07	0.56	19.11	99.90	OH,F,Cl	Ca	magnesio-ferri-hornblende
236-1	4430	Domkar	Ladakh	1.45	11.54	7.94	46.07	0.93	11.74	1.67	0.62	17.98	99.93	OH,F,Cl	Ca	magnesio-ferri-hornblende
238-1	4430	Domkar	Ladakh	1.35	9.00	9.65	44.00	0.76	11.72	1.19	0.82	22.05	100.55	OH,F,Cl	Ca	magnesio-ferri-hornblende
239-1	4430	Domkar	Ladakh	0.49	19.42	3.23	54.69	0.22	12.25	0.49	0.38	6.38	97.56	OH,F,Cl	Ca	actinolite
242-1	4430	Domkar	Ladakh	2.12	13.89	10.41	44.61	0.58	11.31	1.81	0.31	13.54	98.58	OH,F,Cl	Ca	magnesio-hastingsite
327-1	4430	Domkar	Ladakh	1.12	12.33	6.77	47.81	0.63	12.19	0.85	0.94	17.05	99.68	OH,F,Cl	Ca	magnesio-ferri-hornblende
328-1	4430	Domkar	Ladakh	1.39	9.40	9.72	41.70	1.18	11.63	1.88	0.63	20.74	98.26	OH,F,Cl	Ca	magnesio-hastingsite
329-1	4430	Domkar	Ladakh	0.71	11.55	6.67	47.96	0.49	11.98	0.74	0.37	17.72	98.20	OH,F,Cl	Ca	magnesio-ferri-hornblende
332-1	4430	Domkar	Ladakh	1.11	12.37	4.84	49.42	0.43	11.63	0.85	0.37	18.55	99.57	OH,F,Cl	Ca	magnesio-ferri-hornblende
333-1	4430	Domkar	Ladakh	1.07	9.03	8.97	44.82	0.61	11.29	0.71	0.76	21.79	99.06	OH,F,Cl	Ca	magnesio-ferri-hornblende
338-1	4430	Domkar	Ladakh	1.46	10.65	9.19	44.28	0.95	11.58	2.06	0.50	18.50	99.19	OH,F,Cl	Ca	magnesio-hastingsite
342-1	4430	Domkar	Ladakh	0.92	12.39	6.07	48.64	0.62	12.15	1.06	0.33	16.84	99.03	OH,F,Cl	Ca	magnesio-ferri-hornblende
343-1	4430	Domkar	Ladakh	0.99	9.99	9.21	43.34	1.08	11.78	1.33	0.49	20.68	98.90	OH,F,Cl	Ca	magnesio-ferri-hornblende
43-2	4430	Domkar	Ladakh	0.84	17.42	5.46	51.22	0.30	8.73	0.23	0.46	13.19	97.85	OH,F,Cl	Ca	magnesio-ferri-hornblende
50-2	4430	Domkar	Ladakh	5.13	0.40	27.49	53.21	0.24	10.69	0.24	0.11	0.92	98.43	OH,F,Cl	Ca	ferro-sadanagaite
52-2	4430	Domkar	Ladakh	1.38	11.28	7.60	46.11	0.83	11.39	1.86	0.51	18.95	99.92	OH,F,Cl	Ca	magnesio-ferri-hornblende
54-2	4430	Domkar	Ladakh	1.23	8.71	9.95	43.34	0.44	10.96	1.91	0.33	21.28	98.14	OH,F,Cl	Ca	ferro-ferri-hornblende
56-2	4430	Domkar	Ladakh	1.12	9.74	8.85	43.81	0.81	11.21	1.38	0.57	21.31	98.80	OH,F,Cl	Ca	magnesio-ferri-hornblende
57-2	4430	Domkar	Ladakh	1.48	10.85	7.64	46.34	0.77	11.71	1.36	0.68	20.69	101.52	OH,F,Cl	Ca	magnesio-ferri-hornblende
60-2	4430	Domkar	Ladakh	1.22	8.77	10.09	43.27	0.57	10.99	1.75	0.64	22.46	99.76	OH,F,Cl	Ca	magnesio-ferri-hornblende
61-2	4430	Domkar	Ladakh	0.34	15.30	1.15	52.25	0.24	1.55	0.52	2.19	26.08	99.60	OH,F,Cl	Mg-Fe-Mn	cummingtonite
63-2	4430	Domkar	Ladakh	0.48	19.61	2.05	55.86	0.21	12.34	0.42	0.25	6.96	98.17	OH,F,Cl	Ca	actinolite
64-2	4430	Domkar	Ladakh	1.51	12.83	5.35	49.11	0.56	11.47	1.03	0.70	16.99	99.56	OH,F,Cl	Ca	magnesio-ferri-hornblende
65-2	4430	Domkar	Ladakh	1.07	12.22	7.69	44.53	0.82	11.95	1.59	0.61	17.75	98.23	OH,F,Cl	Ca	magnesio-ferri-hornblende
67-2	4430	Domkar	Ladakh	1.28	12.04	8.01	46.86	0.71	11.20	1.88	0.55	16.15	98.70	OH,F,Cl	Ca	magnesio-ferri-hornblende
70-2	4430	Domkar	Ladakh	1.24	11.25	9.28	45.94	0.67	12.06	1.42	0.46	18.68	101.00	OH,F,Cl	Ca	magnesio-ferri-hornblende
72-2	4430	Domkar	Ladakh	1.37	11.18	7.50	45.84	0.66	11.60	1.64	0.72	18.43	98.94	OH,F,Cl	Ca	magnesio-ferri-hornblende
73-2	4430	Domkar	Ladakh	0.94	11.93	8.00	48.38	0.44	12.08	1.24	0.33	16.90	100.25	OH,F,Cl	Ca	magnesio-hornblende
74-2	4430	Domkar	Ladakh	0.93	12.06	6.61	48.71	0.62	11.65	1.22	0.41	18.21	100.41	OH,F,Cl	Ca	magnesio-ferri-hornblende
75-2	4430	Domkar	Ladakh	1.25	11.02	7.75	45.54	0.79	11.48	1.27	0.54	18.83	98.48	OH,F,Cl	Ca	magnesio-ferri-hornblende
79-2	4430	Domkar	Ladakh	1.51	11.99	5.75	48.43	0.53	10.81	1.52	1.15	18.64	100.32	OH,F,Cl	Ca	magnesio-ferri-hornblende
80-2	4430	Domkar	Ladakh	0.33	15.47	1.20	54.18	0.26	10.72	0.60	1.20	14.69	98.65	OH,F,Cl	Ca	actinolite
216-2	4430	Domkar	Ladakh	2.08	10.43	13.98	40.55	1.05	12.36	2.48	0.58	17.53	101.04	OH,F,Cl	Ca	magnesio-hastingsite
220-2	4430	Domkar	Ladakh	1.08	9.77	8.59	45.05	0.78	11.60	0.96	0.81	20.74	99.40	OH,F,Cl	Ca	magnesio-ferri-hornblende
222-2	4430	Domkar	Ladakh	1.61	13.75	9.71	48.08	0.42	11.85	1.15	0.42	14.52	101.51	OH,F,Cl	Ca	magnesio-ferri-hornblende
225-2	4430	Domkar	Ladakh	1.10	10.42	8.05	46.09	0.88	11.16	1.59	0.30	18.73	98.32	OH,F,Cl	Ca	magnesio-ferri-hornblende
226-2	4430	Domkar	Ladakh	1.64	11.52	7.44	46.62	0.72	11.19	1.67	0.84	19.04	100.69	OH,F,Cl	Ca	magnesio-ferri-hornblende
227-2	4430	Domkar	Ladakh	0.87	12.53	6.96	47.08	0.32	11.82	1.44	0.48	16.76	98.26	OH,F,Cl	Ca	magnesio-ferri-hornblende
229-2	4430	Domkar	Ladakh	1.21	10.11	8.37	45.47	0.93	11.86	1.50	0.47	18.83	98.75	OH,F,Cl	Ca	magnesio-ferri-hornblende
232-2	4430	Domkar	Ladakh	1.04	9.48	8.55	46.13	0.71	11.45	0.97	1.14	21.64	101.11	OH,F,Cl	Ca	magnesio-ferri-hornblende
235-2	4430	Domkar	Ladakh	1.02	10.02	9.37	44.53	0.75	12.01	0.88	0.42	20.56	99.55	OH,F,Cl	Ca	magnesio-ferri-hornblende
236-2	4430	Domkar	Ladakh	0.51	11.99	7.34	46.25	0.65	12.08	1.23	0.42	18.51	98.98	OH,F,Cl	Ca	magnesio-ferri-hornblende
239-2	4430	Domkar	Ladakh	1.12	12.70	7.71	46.98	0.48	11.71	1.32	0.41	16.21	98.64	OH,F,Cl	Ca	magnesio-ferri-hornblende
240-2	4430	Domkar	Ladakh	1.10	10.58	8.09	45.00	0.83	11.43	1.60	0.48	19.35	98.46	OH,F,Cl	Ca	magnesio-ferri-hornblende
241-2	4430	Domkar	Ladakh	1.01	11.10	6.32	46.65	0.69	11.63	0.56	0.75	19.92	98.63	OH,F,Cl	Ca	magnesio-ferri-hornblende
245-2	4430	Domkar	Ladakh	1.24	11.04	8.13	45.42	0.85	11.57	1.32	0.58	20.28	100.43	OH,F,Cl	Ca	magnesio-ferri-hornblende
248-2	4430	Domkar	Ladakh	0.79	13.12	7.27	48.27	0.49	11.90	1.71	0.45	15.27	99.27	OH,F,Cl	Ca	magnesio-ferri-hornblende
250-2	4430	Domkar	Ladakh	1.34	9.67	8.75	44.03	0.97	11.33	1.53	0.59	20.86	99.07	OH,F,Cl	Ca	magnesio-ferri-hornblende
253-2	4430	Domkar	Ladakh	1.18	11.00	8.26	43.88	0.74	12.05	1.83	0.36	19.38	98.68	OH,F,Cl	Ca	magnesio-ferri-hornblende
257-2	4430	Domkar	Ladakh	0.95	12.15	6.25	47.25	0.43	11.61	1.51	0.74	18.72	99.62	OH,F,Cl	Ca	magnesio-ferri-hornblende
262-2	4430	Domkar	Ladakh	0.91	12.24	7.38	47.04	0.66	11.62	1.30	0.50	17.43	99.09	OH,F,Cl	Ca	magnesio-ferri-hornblende
264-2	4430	Domkar	Ladakh	1.10	12.70	6.24	48.10	0.36	11.67	0.77	0.52	17.85	99.30	OH,F,Cl	Ca	magnesio-ferri-hornblende
267-2	4430	Domkar	Ladakh	1.14	12.37	8.57	47.10	0.31	11.17	0.86	0.44	16.67	98.63	OH,F,Cl	Ca	magnesio-ferri-hornblende
269-2	4430	Domkar	Ladakh	1.00	11.58	7.82	46.97	0.83	11.48	1.24	0.62	18.70	100.24	OH,F,Cl	Ca	magnesio-ferri-hornblende
273-2	4430	Domkar	Ladakh	1.12	12.35	7.50	46.23	0.77	11.37	1.51	0.47	17.08	98.39	OH,F,Cl	Ca	magnesio-ferri-hornblende
274-2	4430	Domkar	Ladakh	2.57	14.84	12.57	43.89	0.46	12.01	1.24	0.40	11.05	99.03	OH,F,Cl	Ca	magnesio-hastingsite
277-2	4430	Domkar	Ladakh	0.81	11.55	7.31	47.03	0.80	11.87	0.98	0.46	18.18	99.00	OH,F,Cl	Ca	magnesio-ferri-hornblende
278-2	4430	Domkar	Ladakh	1.11	9.85	8.92	46.05	0.68	11.61	1.43	0.49	21.50	101.66	OH,F,Cl	Ca	magnesio-ferri-hornblende
280-2	4430	Domkar	Ladakh	1.17	11.94	8.48	46.44	0.34	11.66	1.27	0.42	17.49	99.20	OH,F,Cl	Ca	magnesio-ferri-hornblende
329-2	4430	Domkar	Ladakh	0.90	10.99	6.59	46.92	0.60	12.19	1.22	0.29	18.37	98.08	OH,F,Cl	Ca	magnesio-ferri-hornblende
332-2	4430	Domkar	Ladakh	0.61	11.07	7.49	46.81	0.68	11.73	1.31	0.91	18.56	99.19	OH,F,Cl	Ca	magnesio-ferri-hornblende
333-2	4430	Domkar	Ladakh	2.12	11.47	11.25	41.22	0.63	11.56	2.64	0.48	14.97	96.34	OH,F,Cl	Ca	magnesio-hastingsite

Point	Sample	River/Dune	Domain	Na_2O	MgO	Al_2O_3	SiO_2	K_2O	CaO	TiO_2	MnO	FeO	Total	Group	Subgroup	Species
				wt%	wt%	wt%	wt%	wt%	wt%	wt%	wt%	wt%			of (OH,F,Cl)	
30-1	1439	Kandia	Kohistan	0.43	15.79	2.58	51.86	0.13	12.36	0.68	0.4	13.35	97.569	OH,F,Cl	Ca	actinolite
32-1	1439	Kandia	Kohistan	2.38	10.79	13.57	41.93	0.58	11.84	2.41	0.44	15.5	99.44	OH,F,Cl	Ca	pargasite
34-1	1439	Kandia	Kohistan	1.86	14.52	9.77	46.43	0.43	11.26	0.71	0.46	10.93	96.374	OH,F,Cl	Ca	magnesio-hornblende
35-1	1439	Kandia	Kohistan	2.62	12.02	11.33	42.98	0.52	10.9	1.26	0.22	13.4	95.257	OH,F,Cl	Ca	pargasite
36-1	1439	Kandia	Kohistan	2.39	10.61	13.01	41.83	0.89	11.8	1.54	0.37	15.75	98.175	OH,F,Cl	Ca	pargasite
46-1	1439	Kandia	Kohistan	1.98	10.8	12.43	43.1	0.8	11.3	1.52	0.45	16.48	98.86	OH,F,Cl	Ca	pargasite
50-1	1439	Kandia	Kohistan	0.82	19.49	0.89	56.64	0.05	12.74	0.43	0.35	8.71	100.11	OH,F,Cl	Ca	actinolite
52-1	1439	Kandia	Kohistan	0.26	0.27	28.55	38.06	0.24	23.52	0.74	0.37	4.98	96.983	OH,F,Cl	Ca	ferro-sadanagaite
55-1	1439	Kandia	Kohistan	0.66	19.42	2.68	53.72	0.24	12.02	0.36	0.47	8.35	97.93	OH,F,Cl	Ca	actinolite
204-1	1439	Kandia	Kohistan	1.15	13.09	9.53	45.62	0.85	11.6	1.52	0.28	14.93	98.57	OH,F,Cl	Ca	magnesio-ferri-hornblende
207-1	1439	Kandia	Kohistan	1.5	11.58	11.06	44.68	0.4	12.42	1.32	0.36	13.71	97.031	OH,F,Cl	Ca	magnesio-hornblende
208-1	1439	Kandia	Kohistan	0.7	13.27	2.86	49.73	0.2	21.82	0.65	0.45	9.58	99.26	OH,F,Cl	Ca	edenite
210-1	1439	Kandia	Kohistan	1.81	11.51	11.39	42.92	1.24	11.51	1.34	0.41	15.56	97.692	OH,F,Cl	Ca	pargasite
212-1	1439	Kandia	Kohistan	1.49	9.91	11.47	42.16	1.25	11.88	1.41	0.46	16.84	96.86	OH,F,Cl	Ca	pargasite
213-1	1439	Kandia	Kohistan	1.9	10.79	11.64	43.96	0.75	11.43	1.77	0.37	17.42	100.03	OH,F,Cl	Ca	pargasite
216-1	1439	Kandia	Kohistan	1.23	15.09	6.16	50.61	0.35	11.23	0.63	0.52	14.39	100.21	OH,F,Cl	Ca	magnesio-ferri-hornblende
219-1	1439	Kandia	Kohistan	1.78	11.34	10.65	43.05	0.62	10.99	1.12	0.13	16.66	96.334	OH,F,Cl	Ca	magnesio-hastingsite
220-1	1439	Kandia	Kohistan	0.52	19.4	1.06	53.62	0.26	13.11	0	0.35	8.41	96.74	OH,F,Cl	Ca	actinolite
224-1	1439	Kandia	Kohistan	1.27	15.03	6.41	49.62	0.36	11.65	0.61	0.34	13.11	98.413	OH,F,Cl	Ca	magnesio-ferri-hornblende
231-1	1439	Kandia	Kohistan	1.62	9.74	12.88	44.71	0.54	11.71	1.01	0.47	16.38	99.061	OH,F,Cl	Ca	magnesio-hornblende
233-1	1439	Kandia	Kohistan	0.78	17.49	2.27	53.34	0.31	12.9	0.26	0.43	9.72	97.51	OH,F,Cl	Ca	actinolite
235-1	1439	Kandia	Kohistan	0.61	15.92	2.56	54.12	0.24	12.3	0.64	0.18	12.95	99.513	OH,F,Cl	Ca	actinolite
239-1	1439	Kandia	Kohistan	0.8	15.72	5.46	51.51	0.28	12.08	0.58	0.18	11.88	98.502	OH,F,Cl	Ca	magnesio-hornblende
240-1	1439	Kandia	Kohistan	2.71	12.84	13.57	43.16	0.18	11.18	2.05	0.36	13.66	99.69	OH,F,Cl	Ca	pargasite
241-1	1439	Kandia	Kohistan	2.41	12.39	11.26	44.52	0.82	11.52	1.33	0.52	14.17	98.949	OH,F,Cl	Ca	pargasite
245-1	1439	Kandia	Kohistan	0.27	0.26	26.55	37.16	0.32	24.25	0.8	0.4	8.69	98.702	OH,F,Cl	Ca	ferro-sadanagaite
251-1	1439	Kandia	Kohistan	1.62	9.31	12.01	44.52	0.63	12.23	0.9	0.51	17.75	99.482	OH,F,Cl	Ca	ferro-pargasite
254-1	1439	Kandia	Kohistan	0.38	0.41	25.18	37.52	0.19	23.67	0.27	0.17	10.67	98.457	OH,F,Cl	Ca	ferro-sadanagaite
256-1	1439	Kandia	Kohistan	1.1	10.19	13.16	42.82	0.76	10.81	1.36	0.42	16.6	97.231	OH,F,Cl	Ca	tschermakite
259-1	1439	Kandia	Kohistan	1.88	11.1	11.66	44.99	0.77	11.95	1.48	0.55	14.7	99.075	OH,F,Cl	Ca	pargasite
262-1	1439	Kandia	Kohistan	1.53	14.19	7.95	49.56	0.23	11.72	0.71	0.35	13.32	99.555	OH,F,Cl	Ca	magnesio-hornblende
264-1	1439	Kandia	Kohistan	1.42	13.7	10.27	47.18	0.47	11.39	1.09	0.36	12.04	97.917	OH,F,Cl	Ca	magnesio-hornblende
265-1	1439	Kandia	Kohistan	0.44	17.87	1.61	54.31	0.23	12.68	0.21	0.38	12.21	99.935	OH,F,Cl	Ca	actinolite
266-1	1439	Kandia	Kohistan	0.75	14.99	4.98	51.5	0.39	13.35	0.21	0.53	12.14	98.842	OH,F,Cl	Ca	actinolite
267-1	1439	Kandia	Kohistan	1.85	12.81	9.11	46.95	0.51	11.18	1.09	0.17	13.91	97.582	OH,F,Cl	Ca	magnesio-hornblende
268-1	1439	Kandia	Kohistan	1.01	15.3	4.25	51.63	0.39	10.9	0.47	0.42	14.89	99.264	OH,F,Cl	Ca	magnesio-ferri-hornblende
270-1	1439	Kandia	Kohistan	0.39	15.6	1.55	53.22	0.36	12.54	0.48	0.46	14.36	98.971	OH,F,Cl	Ca	actinolite
275-1	1439	Kandia	Kohistan	1.5	14.26	7.82	49.25	0.44	11.9	0.31	0.22	12.68	98.379	OH,F,Cl	Ca	magnesio-hornblende
277-1	1439	Kandia	Kohistan	2.48	10.43	12.56	43.81	0.8	11.39	1.75	0.46	15.01	98.687	OH,F,Cl	Ca	pargasite
288-1	1439	Kandia	Kohistan	0.9	14.16	7.48	47.88	0.59	12.14	0.21	0.21	14.92	98.493	OH,F,Cl	Ca	magnesio-ferri-hornblende
290-1	1439	Kandia	Kohistan	2.26	10.49	12.68	43.79	0.31	11.17	1.19	0.25	16.52	98.668	OH,F,Cl	Ca	pargasite
292-1	1439	Kandia	Kohistan	2.12	10.71	14.06	43.11	0.73	11.83	1.08	0.37	16.22	100.24	OH,F,Cl	Ca	pargasite
22-2	1439	Kandia	Kohistan	2.27	9.64	12.46	42.75	0.5	11.36	1.43	0.45	15.91	96.757	OH,F,Cl	Ca	pargasite
23-2	1439	Kandia	Kohistan	1.83	11.74	8.83	42.27	1.44	12.08	2.17	0.53	16.51	97.395	OH,F,Cl	Ca	magnesio-hastingsite
24-2	1439	Kandia	Kohistan	1.86	10.39	11	45.23	0.56	11.82	1.01	0.41	16.54	98.815	OH,F,Cl	Ca	pargasite
26-2	1439	Kandia	Kohistan	1.88	12.52	11.67	44.5	0.7	11.85	0.66	0.47	13.62	97.874	OH,F,Cl	Ca	pargasite
28-2	1439	Kandia	Kohistan	0.61	17.09	1.94	53.78	0.28	13.05	0.56	0.45	11.58	99.356	OH,F,Cl	Ca	actinolite
29-2	1439	Kandia	Kohistan	1.66	10.2	12.2	41.56	0.73	11.04	1.89	0.5	19.08	98.859	OH,F,Cl	Ca	ferri-tschermakite
30-2	1439	Kandia	Kohistan	2.7	12.89	13.93	42.76	0.18	11.77	1.82	0.49	12.09	98.62	OH,F,Cl	Ca	pargasite
31-2	1439	Kandia	Kohistan	0.49	19.15	1.83	55.68	0.2	12.5	0.5	0.56	6.49	97.416	OH,F,Cl	Ca	actinolite
32-2	1439	Kandia	Kohistan	1.9	13.37	9.3	47.73	0.46	11.58	1.26	0.54	14.21	100.36	OH,F,Cl	Ca	magnesio-hornblende
38-2	1439	Kandia	Kohistan	2.15	11.82	11.65	45.34	0.55	11.67	0.96	0.29	15.72	100.15	OH,F,Cl	Ca	pargasite
40-2	1439	Kandia	Kohistan	0.76	16.09	1.37	54.03	0.29	11.83	0.48	0.43	14.69	99.973	OH,F,Cl	Ca	actinolite
41-2	1439	Kandia	Kohistan	1.9	10.84	12.53	43.15	0.59	12.1	0.79	0.21	15	97.102	OH,F,Cl	Ca	pargasite
42-2	1439	Kandia	Kohistan	2.07	11.62	12.36	41.7	0.83	12.29	3.14	0.55	14.45	99.02	OH,F,Cl	Ca	Ti-rich pargasite
43-2	1439	Kandia	Kohistan	1.86	11.92	11	42.29	0.61	11.26	1.83	0.48	15.9	97.156	OH,F,Cl	Ca	magnesio-hastingsite
44-2	1439	Kandia	Kohistan	1.83	10.46	11.8	42.23	0.79	11.82	1.76	0.47	16.34	97.5	OH,F,Cl	Ca	pargasite
46-2	1439	Kandia	Kohistan	2.21	10	12.94	42.75	0.56	11.39	1.5	0.53	16.51	98.388	OH,F,Cl	Ca	pargasite
50-2	1439	Kandia	Kohistan	1.87	13.83	9.88	46.55	0.41	11.76	1.07	0.36	14.67	100.4	OH,F,Cl	Ca	magnesio-ferri-hornblende
51-2	1439	Kandia	Kohistan	1.55	12.14	11.99	44.12	0.79	11.82	2.44	0.41	14.41	99.657	OH,F,Cl	Ca	pargasite
53-2	1439	Kandia	Kohistan	1.12	15.25	4.42	50.45	0.27	11.94	0.68	0.77	14.62	99.523	OH,F,Cl	Ca	magnesio-ferri-hornblende
58-2	1439	Kandia	Kohistan	1.15	15.51	3.51	52.65	0.25	13.71	0.62	0.44	11.75	99.585	OH,F,Cl	Ca	edenite
65-2	1439	Kandia	Kohistan	2.06	11.1	10.7	43.91	0.6	11.45	1.43	0.56	15.39	97.195	OH,F,Cl	Ca	pargasite
73-2	1439	Kandia	Kohistan	0.82	16.38	3.95	52.52	0.32	12.94	0.61	0.35	11.8	99.695	OH,F,Cl	Ca	actinolite
75-2	1439	Kandia	Kohistan	1.13	16.87	4.59	51.35	0.31	11.65	0.78	0.49	11.54	98.708	OH,F,Cl	Ca	magnesio-ferri-hornblende
77-2	1439	Kandia	Kohistan	1.35	16.47	5.31	51.1	0.48	12.98	0.6	0.44	11.34	100.07	OH,F,Cl	Ca	actinolite
78-2	1439	Kandia	Kohistan	2.02	11.31	12.13	43.68	0.7	11.28	1.55	0.38	14.93	97.976	OH,F,Cl	Ca	pargasite
81-2	1439	Kandia	Kohistan	1.92	13.42	11.26	45.74	0.48	11.03	0.8	0.33	13.34	98.311	OH,F,Cl	Ca	pargasite
83-2	1439	Kandia	Kohistan	1.97	14.65	8.69	48.17	0.41	11.04	1.2	0.42	13.11	99.65	OH,F,Cl	Ca	magnesio-hornblende
84-2	1439	Kandia	Kohistan	1	13.54	4.37	51.73	0.26	12.72	0.63	0.12	15.08	99.45	OH,F,Cl	Ca	actinolite
86-2	1439	Kandia	Kohistan	1.53	13.93	7.45	48.86	0.39	12.74	0.78	0.36	13.47	99.504	OH,F,Cl	Ca	magnesio-hornblende
87-2	1439	Kandia	Kohistan	2.33	12.16	13.72	42.8	0.59	11.83	1.95	0.38	13.77	99.547	OH,F,Cl	Ca	pargasite
88-2	1439	Kandia	Kohistan	2.35	11.5	12.07	42.95	0.7	11.27	1.47	0.42	14.83	97.559	OH,F,Cl	Ca	pargasite
96-2	1439	Kandia	Kohistan	0.73	16.65	3.01	54.6	0.32	12.23	0.34	0.4	12.47	100.76	OH,F,Cl	Ca	actinolite
99-2	1439	Kandia	Kohistan	2.86	11.64	13.44	43.18	0.69	10.55	1.16	0.43	15.36	99.315	OH,F,Cl	Ca	pargasite
100-2	1439	Kandia	Kohistan	0.44	16.21	1.26	52.55	0.27	12.72	0.62	0.41	12.94	97.43	OH,F,Cl	Ca	actinolite
101-2	1439	Kandia	Kohistan	0.83	18.05	2.2	53.26	0.22	12.43	0.52	0.54	9.45	97.523	OH,F,Cl	Ca	actinolite
106-2	1439	Kandia	Kohistan	0.96	15.07	4.24	49.77	0.35	12.89	1.1	0.45	13.31	98.157	OH,F,Cl	Ca	actinolite
108-2	1439	Kandia	Kohistan	1.27	10.67	10.97	44.14	1.14	12.09	1.07	0.59	17.66	99.592	OH,F,Cl	Ca	magnesio-hastingsite
109-2	1439	Kandia	Kohistan	0.18	0.14	29.44	38.03	0.11	23.59	0.6	0.38	4.46	96.911	OH,F,Cl	Ca	ferro-sadanagaite
110-2	1439	Kandia	Kohistan	2.78	13.26	12.27	44.58	0.95	10.97	2.69	0.41	12.7	100.61	OH,F,Cl	Ca	pargasite
114-2	1439	Kandia	Kohistan	2.07	10.39	10.9	44.37	0.66	10.87	1.11	0.41	17.96	98.741	OH,F,Cl	Ca	pargasite
178-2	1439	Kandia	Kohistan	3.78	11.23	14.74	41.46	0.59	10.26	1.15	0.33	16.27	99.798	OH,F,Cl	Ca	magnesio-hastingsite
179-2	1439	Kandia	Kohistan	0.55	21.01	1.59	50.83	0.26	0.95	0.36	0.54	24.65	100.74	OH,F,Cl	Mg-Fe-Mn	cummingtonite
182-2	1439	Kandia	Kohistan	0.93	12.73	4.34	49.14	0.49	12.32	0.73	0.62	15.7	96.996	OH,F,Cl	Ca	actinolite
184-2	1439	Kandia	Kohistan	1.85	10.8	12.83	43.28	0.32	10.89	1.36	0.33	17.04	98.705	OH,F,Cl	Ca	magnesio-ferri-hornblende
186-2	1439	Kandia	Kohistan	2.14	11.62	13.38	42.05	0.62	11.57	1.7	0.34	14.47	97.883	OH,F,Cl	Ca	pargasite
190-2	1439	Kandia	Kohistan	1.37	13.57	7.13	48.94	0.53	12.09	1.35	0.56	14.22	99.746	OH,F,Cl	Ca	magnesio-hornblende
191-2	1439	Kandia	Kohistan	1.63	11.83	11.04	41.96	1.37	12.09	2.19	0.39	15.94	98.447	OH,F,Cl	Ca	magnesio-hastingsite
195-2	1439	Kandia	Kohistan	2.2	10.14	14.13	42.89	0.37	10.42	1.12	0.55	16.16	97.975	OH,F,Cl	Ca	pargasite
203-2	1439	Kandia	Kohistan	2.11	11.67	12.36	43.35	0.62	11.31	1.86	0.46	13.91	97.657	OH,F,Cl	Ca	pargasite
204-2	1439	Kandia	Kohistan	2.27	14.07	11.45	46.82	0.32	11.48	0.82	0.32	12.02	99.572	OH,F,Cl	Ca	pargasite
205-2	1439	Kandia	Kohistan	0.27	0.2	1.21	30.92	0.24	28.62	38.26	0.42	1.42	101.55	OH,F,Cl	Ca	ferro-rootname4
207-2	1439	Kandia	Kohistan	1.45	10.73	11.55	43.68	0.64	11.9	0.99	0.64	18.99	100.56	OH,F,Cl	Ca	magnesio-ferri-hornblende
213-2	1439	Kandia	Kohistan	2.03	11.9	11.96	43.38	0.63	11.08	1.39	0.43	15.31	98.109	OH,F,Cl	Ca	magnesio-hastingsite
215-2	1439	Kandia	Kohistan	2.19	12.29	12.16	45.31	0.51	11.2	0.77	0.3	12.92	97.649	OH,F,Cl	Ca	pargasite
216-2	1439	Kandia	Kohistan	1.89	10.72	12.9	43.16	0.81	11.28	1.79	0.52	15.89	98.965	OH,F,Cl	Ca	pargasite
218-2	1439	Kandia	Kohistan	0.84	13.01	2.85	50.61	0.27	22.33	0.84	0.36	9.92	101.02	OH,F,Cl	Ca	edenite
222-2	1439	Kandia	Kohistan	2.22	11.83	12.4	43.6	0.99	11.5	1.66	0.36	13.15	97.701	OH,F,Cl	Ca	pargasite
223-2	1439	Kandia	Kohistan	1.35	11.46	11.38	44.74	0.94	11.81	0.9	0.41	16.82	99.822	OH,F,Cl	Ca	magnesio-ferri-hornblende
228-2	1439	Kandia	Kohistan	1.97	13.65	9.94	49.5	0.61	11.03	0.61	0.38	12.63	100.32	OH,F,Cl	Ca	magnesio-hornblende
231-2	1439	Kandia	Kohistan	1.84	12.29	13.01	44.53	0.55	11.86	2.29	0.41	12.38	99.148	OH,F,Cl	Ca	magnesio-hornblende
234-2	1439	Kandia	Kohistan	2.61	10.85	13.48	41.66	0.63	11.83	1.7	0.39	15.63	98.78	OH,F,Cl	Ca	pargasite
238-2	1439	Kandia	Kohistan	0.73	18.48	3.15	53.3	0.3	12.94	0.54	0.4	8.14	97.977	OH,F,Cl	Ca	actinolite
239-2	1439	Kandia	Kohistan	2.62	12.25	13.01	44.66	0.59	10.83	0.83	0.45	13.61	98.856	OH,F,Cl	Ca	pargasite

Point	Sample	River/Dune	Domain	Na_2O	MgO	Al_2O_3	SiO_2	K_2O	CaO	TiO_2	MnO	FeO	Total	Group	Subgroup	Species
				wt%	wt%	wt%	wt%	wt%	wt%	wt%	wt%	wt%			of (OH,F,Cl)	
1-1	1440	Swat	Kohistan	1.79	11.44	14.08	41.68	0.45	10.41	0.99	0.34	14.93	96.116	OH,F,Cl	Ca	ferri-tschermakite
3-1	1440	Swat	Kohistan	1.39	15.41	5.68	49.65	0.34	11.56	0.59	0.56	12.62	97.797	OH,F,Cl	Ca	magnesio-ferri-hornblende
4-1	1440	Swat	Kohistan	1.89	12.29	11.7	44.57	0.74	10.62	1.1	0.44	15.31	98.662	OH,F,Cl	Ca	pargasite
7-1	1440	Swat	Kohistan	2.33	11.92	15.16	42.7	0.5	9.96	0.7	0.39	13.89	97.555	OH,F,Cl	Ca	pargasite
8-1	1440	Swat	Kohistan	1.28	11.09	11.4	43.48	0.8	11.74	0.94	0.57	17.32	98.629	OH,F,Cl	Ca	magnesio-ferri-hornblende
9-1	1440	Swat	Kohistan	0.21	15.92	1.32	53.26	0.12	12.65	0.16	0.28	12.8	96.713	OH,F,Cl	Ca	actinolite
10-1	1440	Swat	Kohistan	1.05	14.67	7.08	49.17	0.25	10.9	0.58	0.34	12.95	96.989	OH,F,Cl	Ca	magnesio-ferri-hornblende
11-1	1440	Swat	Kohistan	1.38	11.74	9.97	43.77	1.22	11.72	1.58	0.44	15.61	97.432	OH,F,Cl	Ca	magnesio-hastingsite
16-1	1440	Swat	Kohistan	1.87	11.35	13.13	41.66	0.8	11.36	1.38	0.35	15.39	97.282	OH,F,Cl	Ca	magnesio-hastingsite
65-1	1440	Swat	Kohistan	1.17	11.58	7.61	45.35	0.76	11.17	1.57	0.47	16.95	96.628	OH,F,Cl	Ca	magnesio-ferri-hornblende
72-1	1440	Swat	Kohistan	1.28	11.39	10.04	44.17	0.64	10.66	1.17	0.41	18.34	98.099	OH,F,Cl	Ca	magnesio-ferri-hornblende
73-1	1440	Swat	Kohistan	1.93	10.7	13.8	41.73	0.88	10.98	0.95	0.39	15.75	97.11	OH,F,Cl	Ca	pargasite
74-1	1440	Swat	Kohistan	1.66	9.99	11.81	42.08	1.17	11.31	1.78	0.19	17.78	97.782	OH,F,Cl	Ca	pargasite
75-1	1440	Swat	Kohistan	1.68	10.93	14.41	42.02	0.78	11.48	0.83	0.32	14.06	96.527	OH,F,Cl	Ca	pargasite
82-1	1440	Swat	Kohistan	1.98	11.43	14.13	41.62	0.73	10.91	1.29	0.65	15.54	98.276	OH,F,Cl	Ca	ferri-sadanagaite
86-1	1440	Swat	Kohistan	1.42	11.63	10.62	43.68	1.16	11.56	1.62	0.45	16.08	98.227	OH,F,Cl	Ca	magnesio-hastingsite
89-1	1440	Swat	Kohistan	1.64	10.98	11.14	42.23	1.57	12	1.56	0.52	17.32	98.956	OH,F,Cl	Ca	magnesio-hastingsite
92-1	1440	Swat	Kohistan	1.16	12.05	9.85	43.41	1.12	11.82	0.63	0.66	16.15	96.852	OH,F,Cl	Ca	magnesio-ferri-hornblende
94-1	1440	Swat	Kohistan	1.51	11.56	9.93	43.07	1.3	12.27	1.49	0.33	16.24	97.69	OH,F,Cl	Ca	magnesio-hastingsite
98-1	1440	Swat	Kohistan	1.43	11.5	10.63	44.42	0.58	11.53	1.19	0.62	16.2	98.093	OH,F,Cl	Ca	magnesio-ferri-hornblende
99-1	1440	Swat	Kohistan	1.82	12.35	9.42	43.78	1.26	11.11	1.92	0.48	16.12	98.255	OH,F,Cl	Ca	magnesio-hastingsite
100-1	1440	Swat	Kohistan	1.69	12.52	12.91	44.9	0.57	11.64	0.81	0.31	13.73	99.074	OH,F,Cl	Ca	magnesio-hornblende
102-1	1440	Swat	Kohistan	1.33	12.93	9.94	45.51	0.68	10.94	1.29	0.34	13.86	96.818	OH,F,Cl	Ca	magnesio-hornblende
103-1	1440	Swat	Kohistan	1.81	11.68	13.61	42.81	0.78	11.45	0.92	0.4	14.55	98.006	OH,F,Cl	Ca	pargasite
104-1	1440	Swat	Kohistan	1.27	12.92	10.4	45.03	0.47	8.33	1.39	0.45	18.14	98.403	OH,F,Cl	Ca	magnesio-ferri-hornblende
106-1	1440	Swat	Kohistan	1.94	11.26	13.74	42.58	0.5	11.51	0.5	0.38	15.26	97.683	OH,F,Cl	Ca	pargasite
107-1	1440	Swat	Kohistan	1.23	11.18	10.71	42.73	1.53	11.74	1.99	0.38	15.34	96.82	OH,F,Cl	Ca	pargasite
108-1	1440	Swat	Kohistan	2.02	14.02	9.61	46.78	0.59	12.19	0.68	0.37	13.77	100.03	OH,F,Cl	Ca	magnesio-hastingsite
112-1	1440	Swat	Kohistan	1.47	11.16	12.31	42.4	0.64	11.24	1.08	0.32	16.26	96.886	OH,F,Cl	Ca	magnesio-ferri-hornblende
213-1	1440	Swat	Kohistan	0.39	18.02	2.16	52.7	0.22	12.05	0.57	0.39	11.4	97.901	OH,F,Cl	Ca	actinolite
214-1	1440	Swat	Kohistan	1.78	11.48	11.01	44.47	0.22	11.61	0.87	0.44	15.26	97.142	OH,F,Cl	Ca	magnesio-hornblende
217-1	1440	Swat	Kohistan	1.52	9.58	14.41	41.68	0.87	11.67	1.22	0.4	16.3	97.632	OH,F,Cl	Ca	pargasite
220-1	1440	Swat	Kohistan	2.39	16.49	10.95	44.47	0.63	11.16	0.86	0.29	9.41	96.642	OH,F,Cl	Ca	magnesio-hastingsite
221-1	1440	Swat	Kohistan	1.28	8.33	8.79	42.98	1.16	10.65	1.98	0.36	21.7	97.244	OH,F,Cl	Ca	ferro-ferri-hornblende
226-1	1440	Swat	Kohistan	1.35	11.38	11.33	43.81	0.65	11.9	0.92	0.29	15.79	97.413	OH,F,Cl	Ca	magnesio-ferri-hornblende
227-1	1440	Swat	Kohistan	2.21	10.14	11.17	41.81	0.44	11.59	1.13	0.29	18.28	97.063	OH,F,Cl	Ca	magnesio-hastingsite
230-1	1440	Swat	Kohistan	1.52	10.9	13.65	41.49	0.95	12.17	1.35	0.36	15.19	97.587	OH,F,Cl	Ca	pargasite
231-1	1440	Swat	Kohistan	1.95	10.73	13.24	42.97	0.51	11.33	0.9	0.39	15.56	97.588	OH,F,Cl	Ca	pargasite
234-1	1440	Swat	Kohistan	1.44	11.55	9.55	44.02	1.1	11.86	1.83	0.55	17.22	99.116	OH,F,Cl	Ca	magnesio-hastingsite
235-1	1440	Swat	Kohistan	0	18.49	1.69	49.69	0.2	1.01	0.63	0.55	26.85	99.121	OH,F,Cl	Mg-Fe-Mn	cummingtonite
239-1	1440	Swat	Kohistan	1.94	17.26	7.3	48.67	0.32	9.08	0.53	0.5	10.58	96.182	OH,F,Cl	Ca	magnesio-ferri-hornblende
240-1	1440	Swat	Kohistan	1.48	12.09	11.51	43.11	1.38	11.97	1.66	0.23	13.54	96.969	OH,F,Cl	Ca	pargasite
242-1	1440	Swat	Kohistan	1.97	11.74	11.67	42.94	0.78	11.07	1.48	0.42	16.47	98.537	OH,F,Cl	Ca	magnesio-hastingsite
245-1	1440	Swat	Kohistan	0.74	16.88	3.96	50.86	0.33	11.64	0.62	0.41	11.37	96.829	OH,F,Cl	Ca	magnesio-ferri-hornblende
248-1	1440	Swat	Kohistan	1.45	11.55	10.82	43.06	0.57	11.82	1.18	0.44	17.36	98.258	OH,F,Cl	Ca	magnesio-ferri-hornblende
249-1	1440	Swat	Kohistan	1.38	10.61	8.1	45.56	0.81	11.83	1.75	0.56	19.28	99.879	OH,F,Cl	Ca	magnesio-ferri-hornblende
251-1	1440	Swat	Kohistan	0.97	11.61	8.56	44.77	0.89	11.68	1.8	0.53	17.22	98.027	OH,F,Cl	Ca	magnesio-ferri-hornblende
253-1	1440	Swat	Kohistan	1.66	11.67	10.73	42.16	0.99	11.99	1.6	0.26	16.42	97.472	OH,F,Cl	Ca	magnesio-hastingsite
255-1	1440	Swat	Kohistan	0.11	19.39	1.83	49.61	0.21	0.81	0.52	0.41	25.79	98.676	OH,F,Cl	Mg-Fe-Mn	cummingtonite
4-2	1440	Swat	Kohistan	1.32	13.39	8.2	46.32	0.41	11.73	1.29	0.37	13.17	96.175	OH,F,Cl	Ca	magnesio-hornblende
5-2	1440	Swat	Kohistan	1.43	13.17	11.34	45.81	0.44	11.78	1.18	0.41	13.08	98.647	OH,F,Cl	Ca	magnesio-hornblende
9-2	1440	Swat	Kohistan	1.02	15.45	6.48	48.45	0.31	12.51	0.83	0.28	11.95	97.279	OH,F,Cl	Ca	magnesio-ferri-hornblende
12-2	1440	Swat	Kohistan	0.86	16.9	3.88	51.81	0.36	10.88	0.74	0.3	11.89	97.629	OH,F,Cl	Ca	magnesio-ferri-hornblende
15-2	1440	Swat	Kohistan	1.77	11.77	12.7	43.42	0.48	11.3	1.06	0.42	13.86	96.797	OH,F,Cl	Ca	pargasite
18-2	1440	Swat	Kohistan	1.54	10.67	11.3	43.05	1.45	11.53	1.98	0.24	17.1	98.875	OH,F,Cl	Ca	pargasite
98-2	1440	Swat	Kohistan	1.86	10.53	13.3	42.8	0.53	11.18	0.46	0.54	16.11	97.311	OH,F,Cl	Ca	pargasite
99-2	1440	Swat	Kohistan	1.4	13.09	10.11	45.22	0.48	10.36	1.18	0.41	13.91	96.161	OH,F,Cl	Ca	magnesio-ferri-hornblende
101-2	1440	Swat	Kohistan	1.51	11.13	12.41	43.31	0.62	11.73	0.85	0.37	15.09	97.023	OH,F,Cl	Ca	magnesio-hornblende
102-2	1440	Swat	Kohistan	1.8	11.56	12.26	42.72	0.8	11.59	1.6	0.48	15.28	98.09	OH,F,Cl	Ca	magnesio-hastingsite
103-2	1440	Swat	Kohistan	1.45	11.66	11.23	43.05	0.45	10.9	1.78	0.42	16.48	97.426	OH,F,Cl	Ca	magnesio-ferri-hornblende
105-2	1440	Swat	Kohistan	1.24	12.74	7.55	46.86	0.5	12.03	1.51	0.37	16.23	99.033	OH,F,Cl	Ca	magnesio-ferri-hornblende
107-2	1440	Swat	Kohistan	1.49	12.62	10.45	43.31	1.39	11.89	1.54	0.16	15.29	98.127	OH,F,Cl	Ca	magnesio-hastingsite
108-2	1440	Swat	Kohistan	0.98	11.26	7.22	46.99	0.81	10.85	1.93	0.59	18.38	99.009	OH,F,Cl	Ca	magnesio-ferri-hornblende
111-2	1440	Swat	Kohistan	1.75	10.86	13.02	41.78	0.77	11.56	1.42	0.3	15.61	97.067	OH,F,Cl	Ca	pargasite
112-2	1440	Swat	Kohistan	1.97	12.12	12.11	44.47	0.53	11.6	0.58	0.49	14.61	98.488	OH,F,Cl	Ca	pargasite
116-2	1440	Swat	Kohistan	2.15	11.84	12.66	42.44	0.62	11.13	1.67	0.28	15.29	98.073	OH,F,Cl	Ca	magnesio-hastingsite
117-2	1440	Swat	Kohistan	1.72	16.11	10.37	43.68	0.53	12.66	2.34	0.44	11.16	98.996	OH,F,Cl	Ca	magnesio-hastingsite
121-2	1440	Swat	Kohistan	2.02	13	10.48	45.38	0.52	11.8	1.18	0.35	13.14	97.858	OH,F,Cl	Ca	pargasite
123-2	1440	Swat	Kohistan	1.71	10.78	12.18	44.25	0.68	11.78	1.03	0.32	15.92	98.667	OH,F,Cl	Ca	pargasite
124-2	1440	Swat	Kohistan	0.16	22.38	0.91	51.69	0.25	1.34	0.52	0.7	21.95	99.899	OH,F,Cl	Mg-Fe-Mn	cummingtonite
127-2	1440	Swat	Kohistan	1.63	10.88	9.98	43.52	1.11	11.65	1.35	0.37	17.94	98.43	OH,F,Cl	Ca	magnesio-hastingsite
130-2	1440	Swat	Kohistan	1.11	11.08	10.31	44.33	0.79	11.65	1.19	0.62	16.96	98.029	OH,F,Cl	Ca	magnesio-ferri-hornblende
131-2	1440	Swat	Kohistan	1.65	11.79	9.7	46.16	0.56	12.11	0.8	0.16	15.81	98.735	OH,F,Cl	Ca	pargasite
133-2	1440	Swat	Kohistan	1.58	10.38	10.55	42.88	1.78	11.43	1.81	0.35	16.76	97.521	OH,F,Cl	Ca	pargasite
139-2	1440	Swat	Kohistan	0.81	14.54	4.61	49.66	0.51	11.97	0.99	0.39	15.68	99.151	OH,F,Cl	Ca	magnesio-ferri-hornblende
141-2	1440	Swat	Kohistan	2.47	13.27	15.31	40.7	0.66	12.8	0.98	0.28	9.86	96.33	OH,F,Cl	Ca	pargasite
142-2	1440	Swat	Kohistan	2.3	11.04	14.15	41.22	0.98	11.82	1.29	0.31	14.93	98.054	OH,F,Cl	Ca	pargasite
143-2	1440	Swat	Kohistan	1.41	11.25	10.7	44.25	0.71	11.46	1.08	0.54	16.7	98.087	OH,F,Cl	Ca	magnesio-ferri-hornblende
150-2	1440	Swat	Kohistan	1.8	12.74	12.33	42.46	0.66	11.52	2.08	0.26	15.17	99.02	OH,F,Cl	Ca	magnesio-hastingsite
152-2	1440	Swat	Kohistan	1.24	12.82	8.96	46.37	0.56	11.54	0.64	0.41	14.53	97.073	OH,F,Cl	Ca	magnesio-ferri-hornblende
153-2	1440	Swat	Kohistan	1.34	10.77	10.12	44.23	1.1	11.58	2.14	0.46	16.42	98.159	OH,F,Cl	Ca	pargasite
154-2	1440	Swat	Kohistan	1.92	11.62	10.85	43.47	0.87	10.68	1.31	0.1	16.39	97.214	OH,F,Cl	Ca	pargasite
241-2	1440	Swat	Kohistan	1.45	11.25	12.2	43.42	0.5	10.95	1.17	0.41	16.15	97.499	OH,F,Cl	Ca	magnesio-ferri-hornblende
242-2	1440	Swat	Kohistan	1.32	11.72	9.63	44.32	1.09	11.53	1.09	0.42	17.65	98.75	OH,F,Cl	Ca	magnesio-ferri-hornblende
246-2	1440	Swat	Kohistan	0.96	10.98	10.48	43.72	0.7	11.18	1.11	0.44	16.97	96.534	OH,F,Cl	Ca	magnesio-ferri-hornblende
262-2	1440	Swat	Kohistan	0.99	12.7	5.45	48.28	0.39	11.65	0.55	0.35	15.37	95.736	OH,F,Cl	Ca	magnesio-ferri-hornblende
264-2	1440	Swat	Kohistan	1.96	10.07	14.38	41.33	0.68	11.49	1.25	0.31	15.9	97.366	OH,F,Cl	Ca	pargasite
267-2	1440	Swat	Kohistan	0.53	19.34	1.31	53.66	0.16	2	0.41	0.63	19.56	97.591	OH,F,Cl	Mg-Fe-Mn	cummingtonite
268-2	1440	Swat	Kohistan	1.44	11.6	12.62	42.66	0.53	12.09	1.26	0.19	13.09	95.49	OH,F,Cl	Ca	magnesio-hornblende
271-2	1440	Swat	Kohistan	1.27	14	9.69	46.99	0.37	11.21	0.37	0.43	13.4	97.723	OH,F,Cl	Ca	magnesio-ferri-hornblende
273-2	1440	Swat	Kohistan	1.67	11.68	12.33	42.44	0.74	11.35	1.75	0.29	16.25	98.486	OH,F,Cl	Ca	magnesio-ferri-hornblende
274-2	1440	Swat	Kohistan	1.67	11.68	12.33	42.44	0.74	11.35	1.75	0.29	16.25	98.486	OH,F,Cl	Ca	magnesio-ferri-hornblende
276-2	1440	Swat	Kohistan	0.26	19.33	0.98	53.66	0.29	1.81	0.37	0.58	21.72	98.989	OH,F,Cl	Mg-Fe-Mn	cummingtonite
277-2	1440	Swat	Kohistan	1.77	10.69	12.63	41.55	0.72	11.86	0.9	0.16	16.6	96.868	OH,F,Cl	Ca	magnesio-hastingsite
278-2	1440	Swat	Kohistan	1.83	11.48	11.13	41.46	1.54	11.56	2.34	0.41	15.48	97.229	OH,F,Cl	Ca	magnesio-hastingsite
279-2	1440	Swat	Kohistan	0.19	16.34	1.04	53.32	0.25	12.74	0.43	0.34	12.12	96.766	OH,F,Cl	Ca	actinolite
281-2	1440	Swat	Kohistan	1.28	10.9	10.71	44.49	0.41	10.83	0.89	0.47	16.77	96.747	OH,F,Cl	Ca	magnesio-ferri-hornblende
335-2	1440	Swat	Kohistan	1.66	10.55	14.7	41.93	0.88	11.76	0.83	0.31	14.12	96.746	OH,F,Cl	Ca	pargasite
344-2	1440	Swat	Kohistan	1.63	12.91	9.03	46.59	0.19	10.47	0.68	0.56	14.67	96.744	OH,F,Cl	Ca	magnesio-ferri-hornblende
345-2	1440	Swat	Kohistan	1.58	11.68	8.24	43.51	1.08	11.69	0.9	0.45	18.16	97.299	OH,F,Cl	Ca	magnesio-hastingsite
348-2	1440	Swat	Kohistan	0.76	12.79	2.92	49.49	0.17	21.17	0.47	0.29	9.65	97.705	OH,F,Cl	Ca	edenite

Point	Sample	River/Dune	Domain	Na_2O	MgO	Al_2O_3	SiO_2	K_2O	CaO	TiO_2	MnO	FeO	Total	Group	Subgroup	Species
				wt%	wt%	wt%	wt%	wt%	wt%	wt%	wt%	wt%			of (OH,F,Cl)	
2-2	4419	Zanskar	Himalaya	1.22	9.68	9.05	44.47	1.62	11.62	1.26	0.50	19.05	98.46	OH,F,Cl	Ca	potassic-ferro-pargasite
12-2	4419	Zanskar	Himalaya	1.32	12.40	7.13	47.08	1.25	11.82	1.20	0.63	14.99	97.82	OH,F,Cl	Ca	pargasite
31-2	4419	Zanskar	Himalaya	1.56	9.60	8.75	43.81	1.52	11.45	1.39	0.50	18.35	96.93	OH,F,Cl	Ca	ferro-pargasite
41-2	4419	Zanskar	Himalaya	0.70	11.30	9.97	46.92	0.68	11.46	0.95	0.47	14.97	97.43	OH,F,Cl	Ca	magnesio-hornblende
44-2	4419	Zanskar	Himalaya	0.66	17.42	1.14	56.99	0.24	12.73	0.21	0.27	9.05	98.72	OH,F,Cl	Ca	actinolite
56-2	4419	Zanskar	Himalaya	1.60	9.28	10.25	41.71	1.59	11.10	1.25	0.44	20.04	97.25	OH,F,Cl	Ca	magnesio-hastingsite
64-2	4419	Zanskar	Himalaya	1.87	6.16	6.49	44.96	0.77	10.63	1.04	0.65	25.21	97.77	OH,F,Cl	Ca	ferro-pargasite
74-2	4419	Zanskar	Himalaya	1.31	13.04	7.72	48.08	0.96	11.07	0.86	0.68	14.04	97.74	OH,F,Cl	Ca	magnesio-hornblende
75-2	4419	Zanskar	Himalaya	1.80	17.12	6.52	49.42	0.64	11.89	0.86	0.69	8.93	97.88	OH,F,Cl	Ca	pargasite
83-2	4419	Zanskar	Himalaya	1.82	8.79	10.66	41.49	1.88	11.12	1.89	0.43	19.26	97.34	OH,F,Cl	Ca	ferro-pargasite
97-2	4419	Zanskar	Himalaya	1.60	11.80	7.64	46.84	1.03	11.60	0.58	0.50	15.63	97.22	OH,F,Cl	Ca	pargasite
111-2	4419	Zanskar	Himalaya	1.79	7.37	11.53	40.66	1.79	11.56	1.57	0.79	20.02	97.08	OH,F,Cl	Ca	ferro-pargasite
113-2	4419	Zanskar	Himalaya	1.71	8.73	11.03	41.88	1.92	11.28	1.48	0.55	17.97	96.55	OH,F,Cl	Ca	ferro-pargasite
116-2	4419	Zanskar	Himalaya	0.93	20.53	0.72	57.96	0.26	12.28	0.25	0.34	7.06	100.32	OH,F,Cl	Ca	actinolite
119-2	4419	Zanskar	Himalaya	1.65	11.37	9.56	45.47	0.73	11.15	1.00	0.70	14.93	96.56	OH,F,Cl	Ca	magnesio-hornblende
139-2	4419	Zanskar	Himalaya	1.97	8.62	8.97	43.04	1.42	10.93	1.97	0.68	21.25	98.85	OH,F,Cl	Ca	hastingsite
142-2	4419	Zanskar	Himalaya	1.49	11.82	13.04	44.67	1.04	10.82	0.98	0.51	13.25	97.62	OH,F,Cl	Ca	magnesio-hornblende
158-2	4419	Zanskar	Himalaya	1.65	11.21	10.50	44.94	0.59	10.54	1.23	0.66	16.94	98.26	OH,F,Cl	Ca	magnesio-hornblende
159-2	4419	Zanskar	Himalaya	0.95	12.16	10.57	47.06	0.87	11.36	1.47	0.78	13.85	99.07	OH,F,Cl	Ca	magnesio-hornblende
174-2	4419	Zanskar	Himalaya	1.70	11.87	8.43	45.73	1.09	11.81	1.13	0.42	16.36	98.54	OH,F,Cl	Ca	pargasite
176-2	4419	Zanskar	Himalaya	2.06	8.60	11.62	43.05	1.83	11.03	1.89	0.55	19.17	99.80	OH,F,Cl	Ca	ferro-pargasite
177-2	4419	Zanskar	Himalaya	1.04	12.42	8.67	46.06	1.33	11.76	0.90	0.48	14.61	97.27	OH,F,Cl	Ca	pargasite
180-2	4419	Zanskar	Himalaya	1.35	11.94	8.49	46.34	1.14	11.46	1.05	0.33	14.94	97.03	OH,F,Cl	Ca	magnesio-hornblende
188-2	4419	Zanskar	Himalaya	1.75	10.31	10.82	45.72	0.81	10.89	1.27	0.34	17.02	98.92	OH,F,Cl	Ca	magnesio-hornblende
192-2	4419	Zanskar	Himalaya	0.74	11.81	5.72	50.83	0.63	11.92	0.57	0.72	17.51	100.45	OH,F,Cl	Ca	magnesio-hornblende
202-2	4419	Zanskar	Himalaya	1.94	10.00	10.79	43.34	1.85	11.03	1.10	0.63	18.36	99.05	OH,F,Cl	Ca	pargasite
214-2	4419	Zanskar	Himalaya	0.78	10.77	4.21	48.79	0.66	12.23	0.45	1.05	18.18	97.12	OH,F,Cl	Ca	actinolite
230-2	4419	Zanskar	Himalaya	0.36	21.14	0.95	56.46	0.32	1.03	0.36	0.64	16.91	98.17	OH,F,Cl	Mg-Fe-Mn	cummingtonite
245-2	4419	Zanskar	Himalaya	1.79	9.53	10.64	42.48	1.68	11.20	1.53	0.40	17.62	96.87	OH,F,Cl	Ca	pargasite
257-2	4419	Zanskar	Himalaya	0.00	2.32	19.03	37.53	0.22	2.75	0.28	16.08	17.27	95.48	OH,F,Cl	Mg-Fe-Mn	clino-ferro-suenoite
305-2	4419	Zanskar	Himalaya	1.43	9.13	12.22	43.08	1.06	11.76	1.72	0.50	17.87	98.77	OH,F,Cl	Ca	ferro-pargasite
311-2	4419	Zanskar	Himalaya	0.89	13.89	5.35	52.52	0.30	11.25	0.63	0.56	13.52	98.90	OH,F,Cl	Ca	magnesio-hornblende
322-2	4419	Zanskar	Himalaya	1.19	11.77	9.97	47.72	0.47	11.10	0.98	0.41	14.62	98.23	OH,F,Cl	Ca	magnesio-hornblende
372-2	4419	Zanskar	Himalaya	1.48	9.46	11.96	41.21	1.72	11.70	1.71	0.76	19.29	99.29	OH,F,Cl	Ca	magnesio-hastingsite
374-2	4419	Zanskar	Himalaya	1.53	6.83	13.94	42.05	0.73	10.46	0.48	0.80	20.79	97.61	OH,F,Cl	Ca	ferro-hornblende
396-2	4419	Zanskar	Himalaya	0.83	15.95	4.85	51.44	0.71	11.99	0.74	0.59	11.02	98.11	OH,F,Cl	Ca	magnesio-hornblende
401-2	4419	Zanskar	Himalaya	2.64	9.65	14.30	40.93	0.39	12.10	0.89	0.36	16.04	97.30	OH,F,Cl	Ca	pargasite
405-2	4419	Zanskar	Himalaya	1.65	8.36	10.70	41.31	2.04	10.95	1.42	0.96	20.51	97.91	OH,F,Cl	Ca	potassic-hastingsite
440-2	4419	Zanskar	Himalaya	1.03	0.32	32.90	45.22	0.23	17.80	0.29	0.24	0.51	98.53	OH,F,Cl	Ca	sadanagaite
444-2	4419	Zanskar	Himalaya	1.98	3.32	10.87	39.72	1.79	10.62	1.88	0.90	27.56	98.64	OH,F,Cl	Ca	ferro-pargasite
454-2	4419	Zanskar	Himalaya	1.02	15.70	4.88	52.54	0.70	12.47	0.86	0.62	10.50	99.29	OH,F,Cl	Ca	actinolite
458-2	4419	Zanskar	Himalaya	1.30	10.05	7.26	47.24	0.96	11.05	0.94	0.82	19.02	98.64	OH,F,Cl	Ca	magnesio-hornblende
485-2	4419	Zanskar	Himalaya	1.30	10.05	7.26	47.24	0.96	11.05	0.94	0.82	19.02	98.64	OH,F,Cl	Ca	magnesio-hornblende
488-2	4419	Zanskar	Himalaya	1.65	8.70	9.95	43.57	1.74	11.07	1.83	0.13	19.14	97.76	OH,F,Cl	Ca	potassic-ferro-pargasite
499-2	4419	Zanskar	Himalaya	1.80	9.26	10.19	42.95	1.58	10.58	1.33	0.69	19.68	98.06	OH,F,Cl	Ca	ferro-pargasite
509-2	4419	Zanskar	Himalaya	1.77	10.24	8.08	46.03	1.31	10.74	1.04	0.70	19.72	99.63	OH,F,Cl	Ca	magnesio-hastingsite
514-2	4419	Zanskar	Himalaya	0.81	8.93	10.01	45.91	0.73	10.53	1.37	0.46	18.97	97.72	OH,F,Cl	Ca	ferro-hornblende
519-2	4419	Zanskar	Himalaya	1.49	9.75	9.62	43.84	1.40	11.00	1.84	0.67	18.07	97.68	OH,F,Cl	Ca	pargasite
524-2	4419	Zanskar	Himalaya	1.76	10.13	11.35	43.85	1.16	11.53	1.87	0.31	17.24	99.20	OH,F,Cl	Ca	pargasite
533-2	4419	Zanskar	Himalaya	1.10	7.35	11.57	41.94	1.73	11.24	1.64	0.41	20.04	97.01	OH,F,Cl	Ca	potassic-ferro-pargasite
536-2	4419	Zanskar	Himalaya	1.42	10.08	10.71	43.40	1.78	11.36	1.44	0.61	17.37	98.16	OH,F,Cl	Ca	potassic-pargasite
542-2	4419	Zanskar	Himalaya	1.70	8.99	10.38	42.46	1.82	10.68	1.46	0.46	19.59	97.54	OH,F,Cl	Ca	ferro-pargasite
546-2	4419	Zanskar	Himalaya	1.62	10.63	8.40	44.49	1.51	11.46	1.45	0.63	18.59	98.78	OH,F,Cl	Ca	magnesio-hastingsite
547-2	4419	Zanskar	Himalaya	1.83	12.41	11.68	44.71	0.64	10.78	1.09	0.58	13.70	97.43	OH,F,Cl	Ca	magnesio-hornblende
552-2	4419	Zanskar	Himalaya	1.14	15.90	5.67	50.75	0.65	11.48	0.49	0.32	9.82	96.22	OH,F,Cl	Ca	magnesio-hornblende
589-2	4419	Zanskar	Himalaya	0.78	14.50	8.14	49.21	0.48	10.45	0.95	0.39	14.56	99.46	OH,F,Cl	Ca	magnesio-ferri-hornblende
595-2	4419	Zanskar	Himalaya	1.64	11.39	9.63	44.04	1.35	11.74	1.31	0.27	17.47	98.85	OH,F,Cl	Ca	magnesio-hastingsite
596-2	4419	Zanskar	Himalaya	1.65	8.80	10.59	41.87	1.87	11.08	1.31	0.42	20.63	98.22	OH,F,Cl	Ca	hastingsite
598-2	4419	Zanskar	Himalaya	1.06	15.62	5.88	49.66	0.56	11.38	0.62	0.58	13.38	98.75	OH,F,Cl	Ca	magnesio-ferri-hornblende
600-2	4419	Zanskar	Himalaya	1.75	7.83	10.96	42.35	1.62	10.58	1.33	0.51	23.05	99.98	OH,F,Cl	Ca	hastingsite
604-2	4419	Zanskar	Himalaya	1.63	9.06	9.11	43.95	1.33	11.04	1.16	0.89	20.28	98.46	OH,F,Cl	Ca	ferro-pargasite
615-2	4419	Zanskar	Himalaya	1.49	11.88	9.52	44.05	1.43	11.35	1.31	0.41	15.04	96.46	OH,F,Cl	Ca	pargasite
620-2	4419	Zanskar	Himalaya	0.81	14.19	7.19	48.69	0.50	11.05	0.51	0.49	12.79	96.22	OH,F,Cl	Ca	magnesio-hornblende
621-2	4419	Zanskar	Himalaya	2.20	13.36	9.30	46.44	0.50	10.73	0.87	0.38	13.88	97.67	OH,F,Cl	Ca	pargasite
664-2	4419	Zanskar	Himalaya	0.91	8.14	10.08	46.12	0.84	11.58	0.77	0.36	18.04	96.85	OH,F,Cl	Ca	ferro-hornblende
668-2	4419	Zanskar	Himalaya	0.62	13.59	4.82	52.92	0.38	11.93	0.57	0.39	12.14	97.34	OH,F,Cl	Ca	magnesio-hornblende
686-2	4419	Zanskar	Himalaya	1.09	9.20	10.42	43.91	1.50	11.62	1.59	0.43	18.25	98.01	OH,F,Cl	Ca	potassic-ferro-pargasite
688-2	4419	Zanskar	Himalaya	0.57	14.88	4.83	52.93	0.27	11.14	0.49	0.19	12.87	98.18	OH,F,Cl	Ca	magnesio-hornblende
696-2	4419	Zanskar	Himalaya	1.45	10.37	11.49	42.30	1.98	12.08	1.95	0.52	16.47	98.62	OH,F,Cl	Ca	pargasite
714-2	4419	Zanskar	Himalaya	0.97	13.29	5.44	51.78	0.55	11.45	0.59	0.68	14.93	99.67	OH,F,Cl	Ca	magnesio-hornblende
715-2	4419	Zanskar	Himalaya	1.23	9.34	10.09	43.11	1.94	11.62	0.96	0.45	18.99	97.72	OH,F,Cl	Ca	potassic-ferro-pargasite
716-2	4419	Zanskar	Himalaya	1.28	10.61	9.07	45.76	1.66	11.68	1.09	0.31	16.77	98.24	OH,F,Cl	Ca	potassic-pargasite
730-2	4419	Zanskar	Himalaya	1.16	10.46	11.14	43.81	1.20	11.78	1.11	0.49	15.12	96.26	OH,F,Cl	Ca	pargasite
751-2	4419	Zanskar	Himalaya	1.61	14.63	8.05	47.76	0.39	11.21	0.92	0.47	13.42	98.46	OH,F,Cl	Ca	magnesio-ferri-hornblende
753-2	4419	Zanskar	Himalaya	1.45	8.66	10.98	42.31	1.78	11.25	1.25	0.55	18.70	96.95	OH,F,Cl	Ca	ferro-pargasite
758-2	4419	Zanskar	Himalaya	1.75	8.74	10.23	42.30	1.82	11.06	1.57	0.52	21.45	99.43	OH,F,Cl	Ca	hastingsite
764-2	4419	Zanskar	Himalaya	1.30	16.54	8.15	49.37	0.45	9.54	0.91	0.57	10.48	97.32	OH,F,Cl	Ca	magnesio-ferri-hornblende
767-2	4419	Zanskar	Himalaya	1.58	10.97	8.92	44.57	1.17	10.46	1.49	0.50	18.53	98.18	OH,F,Cl	Ca	magnesio-hastingsite
773-2	4419	Zanskar	Himalaya	0.20	0.51	20.85	38.54	0.13	21.51	0.39	0.49	15.14	97.76	OH,F,Cl	Ca	ferro-sadanagaite
776-2	4419	Zanskar	Himalaya	0.97	24.42	4.69	54.42	0.06	0.49	0.37	0.29	11.50	97.22	OH,F,Cl	Mg-Fe-Mn	cummingtonite
782-2	4419	Zanskar	Himalaya	0.97	14.73	8.87	47.44	0.58	11.58	0.63	0.63	12.21	97.65	OH,F,Cl	Ca	magnesio-ferri-hornblende
785-2	4419	Zanskar	Himalaya	0.88	12.14	5.66	48.54	0.60	11.47	0.31	0.72	17.44	97.75	OH,F,Cl	Ca	magnesio-ferri-hornblende
793-2	4419	Zanskar	Himalaya	1.43	13.04	11.25	46.44	0.37	10.83	1.09	0.43	12.05	96.94	OH,F,Cl	Ca	magnesio-hornblende
798-2	4419	Zanskar	Himalaya	1.48	10.34	9.99	44.09	1.31	11.51	1.36	0.66	17.98	98.72	OH,F,Cl	Ca	magnesio-hastingsite
801-2	4419	Zanskar	Himalaya	1.47	9.90	10.10	43.75	1.57	11.23	1.32	0.59	18.11	98.04	OH,F,Cl	Ca	pargasite
802-2	4419	Zanskar	Himalaya	0.64	17.56	1.18	56.59	0.24	12.04	0.37	0.58	9.01	98.20	OH,F,Cl	Ca	actinolite
807-2	4419	Zanskar	Himalaya	1.43	7.80	10.95	42.71	1.41	10.63	1.48	0.62	20.33	97.36	OH,F,Cl	Ca	ferro-pargasite
809-2	4419	Zanskar	Himalaya	0.17	0.20	21.80	37.63	0.14	22.30	0.32	0.46	13.06	96.09	OH,F,Cl	Ca	ferro-sadanagaite
810-2	4419	Zanskar	Himalaya	1.11	10.41	10.12	42.84	1.69	11.29	1.48	0.77	17.54	97.26	OH,F,Cl	Ca	potassic-magnesio-hastingsite
812-2	4419	Zanskar	Himalaya	1.36	15.84	6.10	49.80	0.78	11.62	0.73	0.43	11.30	97.96	OH,F,Cl	Ca	magnesio-ferri-hornblende
813-2	4419	Zanskar	Himalaya	1.30	15.64	9.65	48.48	0.41	10.20	0.60	0.39	10.01	96.69	OH,F,Cl	Ca	magnesio-hornblende
819-2	4419	Zanskar	Himalaya	1.76	11.23	11.67	44.65	0.90	11.63	1.61	0.82	15.08	99.36	OH,F,Cl	Ca	pargasite
826-2	4419	Zanskar	Himalaya	1.98	5.87	9.76	41.64	1.86	10.74	1.44	1.32	24.50	99.11	OH,F,Cl	Ca	ferro-pargasite
844-2	4419	Zanskar	Himalaya	0.58	13.83	7.98	49.94	0.43	11.53	1.22	0.31	11.62	97.44	OH,F,Cl	Ca	magnesio-hornblende
848-2	4419	Zanskar	Himalaya	0.42	20.12	2.08	57.78	0.10	12.65	0.76	0.34	4.67	98.93	OH,F,Cl	Ca	actinolite

Point	Sample	River/Dune	Domain	Na_2O	MgO	Al_2O_3	SiO_2	K_2O	CaO	TiO_2	MnO	FeO	Total	Group	Subgroup	Species
				wt%	wt%	wt%	wt%	wt%	wt%	wt%	wt%	wt%			of (OH,F,Cl)	
31-1	1426	Nandihar	Himalaya	1.28	9.46	12.90	42.36	1.02	11.80	1.55	0.36	17.79	98.54	OH,F,Cl	Ca	magnesio-hornblende
41-1	1426	Nandihar	Himalaya	1.71	12.74	9.67	47.08	0.38	11.49	0.76	0.43	15.15	99.41	OH,F,Cl	Ca	magnesio-hornblende
42-1	1426	Nandihar	Himalaya	2.04	9.58	13.32	42.44	0.92	10.92	1.03	0.48	18.92	99.67	OH,F,Cl	Ca	magnesio-hastingsite
43-1	1426	Nandihar	Himalaya	1.88	8.24	15.37	42.34	0.75	11.64	0.33	0.18	18.72	99.45	OH,F,Cl	Ca	ferro-pargasite
44-1	1426	Nandihar	Himalaya	2.03	9.33	12.80	42.46	0.81	11.18	1.21	0.41	17.97	98.22	OH,F,Cl	Ca	pargasite
46-1	1426	Nandihar	Himalaya	2.02	8.88	15.85	41.88	0.68	11.30	0.71	0.17	19.04	100.53	OH,F,Cl	Ca	pargasite
51-1	1426	Nandihar	Himalaya	1.48	9.76	12.12	44.77	0.42	11.59	0.73	0.23	16.99	98.09	OH,F,Cl	Ca	magnesio-hornblende
54-1	1426	Nandihar	Himalaya	1.78	8.89	12.56	43.90	0.90	11.05	1.16	0.33	19.42	99.99	OH,F,Cl	Ca	ferro-pargasite
57-1	1426	Nandihar	Himalaya	1.51	14.40	7.74	48.42	0.36	11.69	0.83	0.36	13.73	99.04	OH,F,Cl	Ca	magnesio-ferri-hornblende
60-1	1426	Nandihar	Himalaya	2.09	8.10	17.55	41.84	0.57	10.73	0.62	0.27	17.10	98.87	OH,F,Cl	Ca	sadanagaite
62-1	1426	Nandihar	Himalaya	1.98	8.45	13.60	41.87	0.68	11.29	1.04	0.39	20.39	99.69	OH,F,Cl	Ca	hastingsite
66-1	1426	Nandihar	Himalaya	1.87	8.60	14.75	41.85	1.08	11.20	1.13	0.38	19.85	100.70	OH,F,Cl	Ca	pargasite
69-1	1426	Nandihar	Himalaya	3.11	12.78	13.76	42.86	0.78	10.65	1.85	0.29	12.55	98.63	OH,F,Cl	Ca	pargasite
76-1	1426	Nandihar	Himalaya	1.80	9.48	12.75	42.49	0.77	11.59	1.16	0.37	19.18	99.59	OH,F,Cl	Ca	magnesio-hastingsite
88-1	1426	Nandihar	Himalaya	1.66	9.73	11.83	45.02	0.67	11.15	0.91	0.46	18.88	100.32	OH,F,Cl	Ca	magnesio-hornblende
90-1	1426	Nandihar	Himalaya	1.01	16.67	5.79	51.06	0.34	11.38	1.44	0.26	10.34	98.30	OH,F,Cl	Ca	magnesio-ferri-hornblende
96-1	1426	Nandihar	Himalaya	1.39	9.98	10.44	46.23	0.62	12.45	1.00	0.57	18.76	101.45	OH,F,Cl	Ca	magnesio-hornblende
104-1	1426	Nandihar	Himalaya	1.30	9.81	11.61	45.40	0.63	11.25	1.09	0.36	18.19	99.64	OH,F,Cl	Ca	magnesio-hornblende
105-1	1426	Nandihar	Himalaya	1.30	9.81	11.61	45.40	0.63	11.25	1.09	0.36	18.19	99.64	OH,F,Cl	Ca	magnesio-hornblende
106-1	1426	Nandihar	Himalaya	2.42	9.46	12.98	41.57	0.81	11.40	1.36	0.44	18.95	99.41	OH,F,Cl	Ca	magnesio-hastingsite
107-1	1426	Nandihar	Himalaya	1.95	10.42	11.05	44.72	0.79	11.50	1.51	0.52	18.62	101.09	OH,F,Cl	Ca	pargasite
108-1	1426	Nandihar	Himalaya	0.77	14.25	6.58	51.20	0.40	11.42	0.63	0.66	14.21	100.12	OH,F,Cl	Ca	magnesio-hornblende
109-1	1426	Nandihar	Himalaya	1.89	8.75	13.81	41.13	0.90	11.20	1.31	0.27	20.12	99.39	OH,F,Cl	Ca	magnesio-hastingsite
119-1	1426	Nandihar	Himalaya	2.21	7.32	13.39	43.16	0.81	11.21	1.12	0.23	22.10	101.55	OH,F,Cl	Ca	ferro-pargasite
123-1	1426	Nandihar	Himalaya	1.86	7.73	14.51	43.01	0.66	11.55	1.13	0.28	20.95	101.68	OH,F,Cl	Ca	ferro-pargasite
124-1	1426	Nandihar	Himalaya	2.02	9.19	12.81	41.50	0.74	11.46	0.87	0.39	20.50	99.48	OH,F,Cl	Ca	magnesio-hastingsite
125-1	1426	Nandihar	Himalaya	1.60	11.17	12.06	43.40	1.13	11.50	2.40	0.31	17.22	100.79	OH,F,Cl	Ca	magnesio-hastingsite
139-1	1426	Nandihar	Himalaya	0.87	15.88	3.33	54.28	0.00	10.31	0.50	0.46	15.19	100.83	OH,F,Cl	Ca	actinolite
149-1	1426	Nandihar	Himalaya	1.94	10.15	12.64	43.45	0.74	11.43	1.14	0.32	18.29	100.10	OH,F,Cl	Ca	pargasite
155-1	1426	Nandihar	Himalaya	2.05	9.20	12.19	44.29	0.75	11.02	0.83	0.32	19.59	100.25	OH,F,Cl	Ca	ferro-pargasite
166-1	1426	Nandihar	Himalaya	1.56	12.68	14.10	45.69	0.62	11.89	0.71	0.28	12.91	100.45	OH,F,Cl	Ca	magnesio-hornblende
169-1	1426	Nandihar	Himalaya	1.89	8.73	14.47	42.55	1.04	11.65	1.40	0.15	18.66	100.53	OH,F,Cl	Ca	ferro-pargasite
172-1	1426	Nandihar	Himalaya	1.42	8.71	12.82	45.09	0.62	11.59	1.04	0.44	17.03	98.76	OH,F,Cl	Ca	ferro-hornblende
175-1	1426	Nandihar	Himalaya	1.91	17.80	4.94	52.17	0.29	10.42	0.72	0.49	9.04	97.79	OH,F,Cl	Ca	magnesio-ferri-hornblende
178-1	1426	Nandihar	Himalaya	1.76	9.76	11.21	43.55	0.61	11.23	1.42	0.24	19.25	99.04	OH,F,Cl	Ca	magnesio-hastingsite
190-1	1426	Nandihar	Himalaya	1.82	8.45	14.01	43.44	1.06	11.17	1.42	0.36	18.55	100.30	OH,F,Cl	Ca	ferro-pargasite
200-1	1426	Nandihar	Himalaya	1.54	5.95	11.20	41.99	1.22	10.45	1.37	0.26	27.49	101.48	OH,F,Cl	Ca	hastingsite
201-1	1426	Nandihar	Himalaya	1.92	9.97	10.90	44.27	1.17	12.10	1.36	0.19	17.95	99.83	OH,F,Cl	Ca	pargasite
204-1	1426	Nandihar	Himalaya	0.53	15.46	5.57	51.82	0.31	11.82	0.91	0.31	12.32	99.05	OH,F,Cl	Ca	magnesio-hornblende
205-1	1426	Nandihar	Himalaya	1.54	9.45	7.91	44.07	1.07	10.86	3.74	0.18	22.28	101.10	OH,F,Cl	Ca	Ti-rich hastingsite
214-1	1426	Nandihar	Himalaya	2.19	11.01	13.93	43.68	0.88	11.45	1.04	0.35	16.25	100.79	OH,F,Cl	Ca	pargasite
215-1	1426	Nandihar	Himalaya	0.40	19.61	0.68	55.95	0.15	1.03	0.41	0.60	21.65	100.48	OH,F,Cl	Mg-Fe-Mn	cummingtonite
224-1	1426	Nandihar	Himalaya	1.71	10.31	13.25	45.36	0.61	11.30	0.76	0.57	16.32	100.19	OH,F,Cl	Ca	magnesio-hornblende
230-1	1426	Nandihar	Himalaya	1.59	15.11	9.39	49.11	0.48	11.81	1.29	0.42	10.66	99.86	OH,F,Cl	Ca	magnesio-hornblende
232-1	1426	Nandihar	Himalaya	1.74	9.83	11.57	42.94	1.05	11.29	1.54	0.40	17.81	98.18	OH,F,Cl	Ca	pargasite
239-1	1426	Nandihar	Himalaya	2.05	9.29	12.25	41.87	0.85	11.77	1.15	0.42	19.10	98.75	OH,F,Cl	Ca	magnesio-hastingsite
251-1	1426	Nandihar	Himalaya	2.06	8.50	14.28	41.81	1.00	10.82	1.03	0.46	20.58	100.53	OH,F,Cl	Ca	magnesio-hastingsite
252-1	1426	Nandihar	Himalaya	1.83	10.18	12.02	42.88	1.15	11.59	1.76	0.30	19.20	100.91	OH,F,Cl	Ca	magnesio-hastingsite
257-1	1426	Nandihar	Himalaya	1.53	9.57	13.07	41.93	0.91	11.81	1.55	0.30	18.11	98.79	OH,F,Cl	Ca	pargasite
258-1	1426	Nandihar	Himalaya	1.83	8.32	11.30	40.78	1.34	11.60	1.55	0.54	22.45	99.71	OH,F,Cl	Ca	hastingsite
263-1	1426	Nandihar	Himalaya	1.81	9.08	12.98	41.79	1.09	11.43	1.80	0.30	19.12	99.41	OH,F,Cl	Ca	pargasite
265-1	1426	Nandihar	Himalaya	2.21	8.49	14.98	42.63	0.56	10.80	0.85	0.50	18.56	99.58	OH,F,Cl	Ca	ferro-pargasite
295-1	1426	Nandihar	Himalaya	1.31	8.74	12.99	41.36	1.60	11.92	1.59	0.32	19.61	99.44	OH,F,Cl	Ca	hastingsite
299-1	1426	Nandihar	Himalaya	1.21	9.88	11.58	43.21	1.22	12.21	1.24	0.33	19.05	99.93	OH,F,Cl	Ca	magnesio-hastingsite
302-1	1426	Nandihar	Himalaya	2.00	10.56	9.95	45.39	0.78	11.67	1.01	0.60	19.44	101.39	OH,F,Cl	Ca	magnesio-hastingsite
306-1	1426	Nandihar	Himalaya	2.19	8.20	12.37	42.61	0.99	10.64	1.16	0.59	22.17	100.92	OH,F,Cl	Ca	hastingsite
307-1	1426	Nandihar	Himalaya	1.71	9.47	11.44	43.51	0.93	11.16	1.63	0.43	18.95	99.23	OH,F,Cl	Ca	pargasite
308-1	1426	Nandihar	Himalaya	0.82	15.32	6.91	50.83	0.54	12.14	0.55	0.80	10.62	98.52	OH,F,Cl	Ca	magnesio-hornblende
310-1	1426	Nandihar	Himalaya	1.59	8.46	15.51	42.49	0.56	11.51	1.01	0.30	16.85	98.27	OH,F,Cl	Ca	ferro-hornblende
311-1	1426	Nandihar	Himalaya	0.82	14.02	5.32	51.12	0.40	11.52	1.16	0.46	14.65	99.48	OH,F,Cl	Ca	magnesio-ferri-hornblende
316-1	1426	Nandihar	Himalaya	1.93	9.72	12.64	42.98	0.54	11.31	1.13	0.41	19.23	99.88	OH,F,Cl	Ca	magnesio-hastingsite
320-1	1426	Nandihar	Himalaya	1.57	10.75	13.32	42.07	0.75	11.53	1.09	0.40	18.52	100.01	OH,F,Cl	Ca	ferri-tschermakite
321-1	1426	Nandihar	Himalaya	1.58	10.83	8.37	48.08	0.42	11.71	0.78	0.48	19.01	101.26	OH,F,Cl	Ca	magnesio-hornblende
322-1	1426	Nandihar	Himalaya	0.95	14.15	5.07	51.17	0.50	11.52	0.79	0.29	14.05	98.50	OH,F,Cl	Ca	magnesio-ferri-hornblende
326-1	1426	Nandihar	Himalaya	1.85	9.40	12.39	42.77	0.74	10.90	1.04	0.56	19.23	98.87	OH,F,Cl	Ca	magnesio-hastingsite
338-1	1426	Nandihar	Himalaya	1.94	10.14	11.39	43.78	1.27	11.48	1.55	0.13	18.18	99.87	OH,F,Cl	Ca	pargasite
349-1	1426	Nandihar	Himalaya	0.52	13.53	3.35	52.91	0.44	11.78	0.66	0.51	16.94	100.65	OH,F,Cl	Ca	actinolite
350-1	1426	Nandihar	Himalaya	1.70	10.05	11.04	43.54	1.03	11.69	1.46	0.29	18.75	99.54	OH,F,Cl	Ca	magnesio-hastingsite
351-1	1426	Nandihar	Himalaya	0.40	11.79	2.37	51.82	0.00	22.59	0.55	0.50	10.55	100.57	OH,F,Cl	Ca	edenite
441-1	1426	Nandihar	Himalaya	1.87	9.82	12.72	43.05	0.74	11.10	1.14	0.20	19.02	99.66	OH,F,Cl	Ca	magnesio-hastingsite
443-1	1426	Nandihar	Himalaya	0.73	13.89	3.21	53.08	0.29	11.93	0.50	0.43	16.19	100.26	OH,F,Cl	Ca	actinolite
446-1	1426	Nandihar	Himalaya	1.87	9.06	11.98	42.17	0.96	11.55	1.62	0.64	20.05	99.90	OH,F,Cl	Ca	magnesio-hastingsite
455-1	1426	Nandihar	Himalaya	1.85	7.73	12.70	42.49	0.70	11.14	0.92	0.28	21.67	99.47	OH,F,Cl	Ca	ferro-pargasite
462-1	1426	Nandihar	Himalaya	1.94	9.37	12.20	43.34	0.88	11.13	1.54	0.38	19.89	100.67	OH,F,Cl	Ca	magnesio-hastingsite
463-1	1426	Nandihar	Himalaya	1.79	8.00	13.74	42.25	0.97	11.31	1.05	0.42	20.89	100.42	OH,F,Cl	Ca	ferro-pargasite
465-1	1426	Nandihar	Himalaya	1.38	6.03	12.96	41.63	1.65	11.30	0.85	0.32	23.19	99.31	OH,F,Cl	Ca	potassic-ferro-pargasite
468-1	1426	Nandihar	Himalaya	1.99	9.70	13.89	42.71	1.22	11.63	1.42	0.38	18.75	101.69	OH,F,Cl	Ca	pargasite
473-1	1426	Nandihar	Himalaya	1.49	12.65	9.61	47.11	0.50	11.86	1.39	0.35	14.00	98.96	OH,F,Cl	Ca	magnesio-hornblende
44-2	1426	Nandihar	Himalaya	1.79	8.60	14.68	42.68	0.88	11.56	0.81	0.12	18.97	100.09	OH,F,Cl	Ca	ferro-pargasite
47-2	1426	Nandihar	Himalaya	0.57	22.39	3.06	56.86	0.22	13.45	0.88	0.35	0.98	98.75	OH,F,Cl	Ca	tremolite
51-2	1426	Nandihar	Himalaya	1.84	9.84	11.66	43.92	0.93	11.33	1.39	0.32	19.53	100.76	OH,F,Cl	Ca	magnesio-hastingsite
52-2	1426	Nandihar	Himalaya	1.94	10.63	12.86	42.46	1.44	11.71	1.18	0.39	16.97	99.58	OH,F,Cl	Ca	pargasite
58-2	1426	Nandihar	Himalaya	1.38	8.51	11.66	43.51	1.00	11.75	1.78	0.52	21.44	101.56	OH,F,Cl	Ca	ferro-ferri-hornblende
60-2	1426	Nandihar	Himalaya	1.79	12.14	11.53	45.33	0.28	11.11	0.88	0.66	15.60	99.33	OH,F,Cl	Ca	magnesio-ferri-hornblende
66-2	1426	Nandihar	Himalaya	2.03	11.12	11.44	45.50	0.49	11.14	1.05	0.35	16.92	100.05	OH,F,Cl	Ca	pargasite
67-2	1426	Nandihar	Himalaya	1.29	15.01	7.09	51.53	0.20	11.84	0.75	0.37	12.40	100.48	OH,F,Cl	Ca	magnesio-hornblende
73-2	1426	Nandihar	Himalaya	1.98	9.70	11.04	44.90	0.74	11.08	1.37	0.20	18.10	99.10	OH,F,Cl	Ca	pargasite
78-2	1426	Nandihar	Himalaya	0.88	14.28	4.84	51.92	0.43	11.56	0.74	0.65	14.43	99.72	OH,F,Cl	Ca	magnesio-ferri-hornblende
80-2	1426	Nandihar	Himalaya	1.86	8.68	15.02	41.95	1.28	11.24	1.59	0.28	20.04	101.94	OH,F,Cl	Ca	pargasite
82-2	1426	Nandihar	Himalaya	1.64	9.26	13.13	43.45	0.63	11.72	1.24	0.11	17.87	99.05	OH,F,Cl	Ca	pargasite
87-2	1426	Nandihar	Himalaya	2.07	9.12	15.17	43.21	0.96	11.37	1.02	0.46	16.65	100.03	OH,F,Cl	Ca	pargasite
90-2	1426	Nandihar	Himalaya	1.74	10.34	12.80	43.25	0.62	11.57	1.16	0.29	17.72	99.50	OH,F,Cl	Ca	magnesio-hastingsite
93-2	1426	Nandihar	Himalaya	0.55	20.03	1.21	57.79	0.25	12.93	0.39	0.53	6.92	100.61	OH,F,Cl	Ca	actinolite
96-2	1426	Nandihar	Himalaya	1.81	6.79	13.81	40.61	1.36	11.05	1.23	0.14	22.42	99.23	OH,F,Cl	Ca	ferro-pargasite
105-2	1426	Nandihar	Himalaya	0.92	13.30	9.73	47.97	0.50	11.85	1.02	0.20	12.61	98.10	OH,F,Cl	Ca	magnesio-hornblende
108-2	1426	Nandihar	Himalaya	1.07	11.84	7.95	47.38	0.89	11.58	1.46	0.34	18.24	100.75	OH,F,Cl	Ca	magnesio-ferri-hornblende
114-2	1426	Nandihar	Himalaya	1.68	9.22	12.02	43.05	1.26	11.25	1.95	0.40	19.57	100.40	OH,F,Cl	Ca	ferro-pargasite
115-2	1426	Nandihar	Himalaya	1.46	9.60	14.36	43.52	1.28	11.52	1.04	0.32	17.50	100.61	OH,F,Cl	Ca	pargasite
266-2	1426	Nandihar	Himalaya	1.96	9.74	12.26	43.14	0.75	11.58	1.05	0.32	18.95	99.75	OH,F,Cl	Ca	pargasite
273-2	1426	Nandihar	Himalaya	1.32	9.82	11.04	43.07	1.05	11.95	1.47	0.60	20.25	100.56	OH,F,Cl	Ca	magnesio-hastingsite

Point	Sample	River/Dune	Domain	Na_2O	MgO	Al_2O_3	SiO_2	K_2O	CaO	TiO_2	MnO	FeO	Total	Group	Subgroup	Species
				wt%	wt%	wt%	wt%	wt%	wt%	wt%	wt%	wt%			of (OH,F,Cl)	
61-1	1432	Astor	Nanga Parbat	1.71	9.52	14.43	41.89	0.92	11.17	0.87	0.94	16.98	98.42	OH,F,Cl	Ca	pargasite
63-1	1432	Astor	Nanga Parbat	0.98	11.76	10.68	46.56	1.26	12.22	0.72	0.93	15.35	100.47	OH,F,Cl	Ca	magnesio-hornblende
65-1	1432	Astor	Nanga Parbat	1.53	8.53	15.89	41.78	1.08	11.25	0.68	0.29	17.18	98.20	OH,F,Cl	Ca	pargasite
66-1	1432	Astor	Nanga Parbat	1.75	10.92	15.60	43.69	0.60	11.04	0.79	1.11	14.21	99.70	OH,F,Cl	Ca	magnesio-hornblende
69-1	1432	Astor	Nanga Parbat	1.77	10.44	14.98	43.81	0.84	11.59	0.69	0.78	14.71	99.62	OH,F,Cl	Ca	pargasite
70-1	1432	Astor	Nanga Parbat	1.99	8.94	14.64	42.58	0.75	10.80	0.99	0.46	19.69	100.84	OH,F,Cl	Ca	pargasite
77-1	1432	Astor	Nanga Parbat	1.79	10.95	13.98	42.53	1.04	11.61	1.36	1.10	15.27	99.64	OH,F,Cl	Ca	pargasite
78-1	1432	Astor	Nanga Parbat	1.83	12.85	14.00	44.72	0.63	11.63	0.77	0.54	12.27	99.25	OH,F,Cl	Ca	pargasite
84-1	1432	Astor	Nanga Parbat	1.71	9.42	13.85	42.71	0.81	10.78	0.91	0.99	18.43	99.59	OH,F,Cl	Ca	magnesio-ferri-hornblende
85-1	1432	Astor	Nanga Parbat	0.90	12.01	5.91	49.66	0.86	12.45	0.38	0.74	17.82	100.73	OH,F,Cl	Ca	magnesio-ferri-hornblende
86-1	1432	Astor	Nanga Parbat	1.85	9.95	15.35	42.83	0.62	10.84	0.90	0.76	15.84	98.94	OH,F,Cl	Ca	pargasite
92-1	1432	Astor	Nanga Parbat	1.02	10.01	15.24	43.08	0.85	11.25	0.94	1.08	15.22	98.68	OH,F,Cl	Ca	tschermakite
94-1	1432	Astor	Nanga Parbat	1.73	9.55	14.61	43.39	0.90	11.08	1.16	0.75	17.01	100.19	OH,F,Cl	Ca	pargasite
95-1	1432	Astor	Nanga Parbat	1.76	17.35	8.21	48.17	0.35	11.69	0.70	0.43	9.64	98.29	OH,F,Cl	Ca	magnesio-ferri-hornblende
96-1	1432	Astor	Nanga Parbat	0.46	20.86	0.64	57.85	0.23	12.56	0.35	0.85	6.15	99.94	OH,F,Cl	Ca	actinolite
99-1	1432	Astor	Nanga Parbat	1.21	8.99	12.39	43.48	1.66	11.84	1.14	0.73	18.83	100.27	OH,F,Cl	Ca	potassic-ferro-pargasite
101-1	1432	Astor	Nanga Parbat	1.93	9.51	11.55	43.67	1.14	11.06	1.49	0.39	19.34	100.10	OH,F,Cl	Ca	pargasite
105-1	1432	Astor	Nanga Parbat	1.42	9.42	15.03	41.94	0.61	10.70	0.78	0.74	17.73	98.36	OH,F,Cl	Ca	ferri-tschermakite
107-1	1432	Astor	Nanga Parbat	1.33	8.78	10.61	42.21	1.94	11.97	0.81	0.43	21.46	99.54	OH,F,Cl	Ca	potassic-hastingsite
108-1	1432	Astor	Nanga Parbat	1.16	10.90	11.84	45.14	0.67	11.99	0.87	0.65	14.94	98.16	OH,F,Cl	Ca	magnesio-hornblende
110-1	1432	Astor	Nanga Parbat	1.61	14.15	14.23	45.96	0.22	12.13	0.24	0.48	8.85	97.86	OH,F,Cl	Ca	magnesio-hornblende
111-1	1432	Astor	Nanga Parbat	1.62	11.52	9.62	45.83	1.23	12.13	0.85	0.81	18.38	102.00	OH,F,Cl	Ca	magnesio-hastingsite
115-1	1432	Astor	Nanga Parbat	1.75	13.08	10.30	46.05	0.82	11.33	1.19	0.78	13.28	98.58	OH,F,Cl	Ca	pargasite
116-1	1432	Astor	Nanga Parbat	1.82	10.18	14.95	42.59	0.53	11.24	0.75	0.66	16.15	98.87	OH,F,Cl	Ca	magnesio-hornblende
119-1	1432	Astor	Nanga Parbat	1.72	9.33	13.53	43.59	1.08	11.83	1.01	0.69	18.58	101.38	OH,F,Cl	Ca	pargasite
122-1	1432	Astor	Nanga Parbat	1.58	13.09	14.03	44.55	0.37	11.32	0.56	0.83	12.17	98.49	OH,F,Cl	Ca	magnesio-hornblende
124-1	1432	Astor	Nanga Parbat	1.33	10.79	13.84	44.33	0.66	11.33	0.61	0.48	15.93	99.29	OH,F,Cl	Ca	magnesio-hornblende
125-1	1432	Astor	Nanga Parbat	1.83	9.12	16.08	40.41	1.03	11.99	1.02	0.58	18.96	101.04	OH,F,Cl	Ca	ferri-sadanagaite
130-1	1432	Astor	Nanga Parbat	1.21	9.76	16.08	44.36	0.54	11.80	0.43	0.18	15.76	100.12	OH,F,Cl	Ca	magnesio-hornblende
132-1	1432	Astor	Nanga Parbat	1.77	10.99	12.21	44.60	0.62	11.32	1.08	0.73	15.64	98.95	OH,F,Cl	Ca	pargasite
133-1	1432	Astor	Nanga Parbat	1.43	9.79	15.17	43.39	1.26	11.35	0.53	0.30	16.33	99.56	OH,F,Cl	Ca	pargasite
134-1	1432	Astor	Nanga Parbat	1.47	9.59	13.95	44.01	0.97	11.26	0.87	0.63	19.14	101.90	OH,F,Cl	Ca	magnesio-hornblende
136-1	1432	Astor	Nanga Parbat	1.26	14.19	8.56	47.68	1.03	12.74	1.03	0.73	12.93	100.14	OH,F,Cl	Ca	pargasite
140-1	1432	Astor	Nanga Parbat	1.55	9.37	9.75	45.91	0.87	11.33	0.87	0.76	21.07	101.50	OH,F,Cl	Ca	ferro-ferri-hornblende
142-1	1432	Astor	Nanga Parbat	1.67	10.27	14.76	43.53	0.97	11.24	0.97	0.90	15.37	99.66	OH,F,Cl	Ca	pargasite
143-1	1432	Astor	Nanga Parbat	2.19	9.05	16.55	41.29	0.75	11.07	0.77	0.68	16.90	99.24	OH,F,Cl	Ca	pargasite
144-1	1432	Astor	Nanga Parbat	1.14	12.93	10.29	45.92	1.09	11.99	1.17	0.66	15.47	100.65	OH,F,Cl	Ca	magnesio-ferri-hornblende
146-1	1432	Astor	Nanga Parbat	1.98	9.31	15.81	42.30	1.05	10.73	1.10	0.86	17.80	100.91	OH,F,Cl	Ca	pargasite
147-1	1432	Astor	Nanga Parbat	2.16	10.01	15.97	42.48	0.46	10.67	0.85	0.68	16.89	100.18	OH,F,Cl	Ca	pargasite
148-1	1432	Astor	Nanga Parbat	1.56	10.25	16.13	42.06	0.52	11.45	0.66	0.43	15.15	98.21	OH,F,Cl	Ca	tschermakite
149-1	1432	Astor	Nanga Parbat	1.30	12.89	9.97	47.81	0.95	12.18	0.81	0.78	13.84	100.52	OH,F,Cl	Ca	magnesio-hornblende
150-1	1432	Astor	Nanga Parbat	0.86	9.60	8.44	47.39	1.01	12.48	0.64	0.82	19.85	101.10	OH,F,Cl	Ca	ferro-hornblende
155-1	1432	Astor	Nanga Parbat	1.27	8.88	15.85	42.60	0.50	10.93	0.79	0.61	16.77	98.19	OH,F,Cl	Ca	tschermakite
160-1	1432	Astor	Nanga Parbat	1.33	10.22	15.35	43.31	0.79	11.01	1.06	0.91	15.76	99.74	OH,F,Cl	Ca	tschermakite
161-1	1432	Astor	Nanga Parbat	1.88	14.22	9.95	47.38	0.52	10.78	0.88	0.86	12.56	99.03	OH,F,Cl	Ca	magnesio-hornblende
167-1	1432	Astor	Nanga Parbat	1.55	8.94	14.50	42.86	0.79	11.09	1.18	0.55	17.23	98.70	OH,F,Cl	Ca	magnesio-hornblende
168-1	1432	Astor	Nanga Parbat	1.90	8.70	12.79	42.16	1.21	11.15	1.19	0.68	19.99	99.76	OH,F,Cl	Ca	ferro-pargasite
169-1	1432	Astor	Nanga Parbat	1.70	10.97	11.75	44.10	0.56	11.37	0.77	0.70	18.15	100.06	OH,F,Cl	Ca	magnesio-ferri-hornblende
170-1	1432	Astor	Nanga Parbat	1.42	11.29	11.06	44.22	1.38	11.80	1.35	0.60	17.27	100.38	OH,F,Cl	Ca	magnesio-hastingsite
172-1	1432	Astor	Nanga Parbat	1.57	10.14	13.43	44.03	0.86	11.07	0.51	0.55	16.75	98.92	OH,F,Cl	Ca	pargasite
173-1	1432	Astor	Nanga Parbat	1.79	9.22	15.13	42.25	0.76	11.02	0.79	0.77	17.89	99.63	OH,F,Cl	Ca	magnesio-hornblende
174-1	1432	Astor	Nanga Parbat	1.84	12.98	12.23	46.13	0.75	11.70	1.14	0.89	13.35	101.01	OH,F,Cl	Ca	pargasite
291-1	1432	Astor	Nanga Parbat	1.69	8.84	15.36	41.66	0.87	11.09	1.19	0.66	17.55	98.90	OH,F,Cl	Ca	pargasite
293-1	1432	Astor	Nanga Parbat	1.70	9.13	15.47	43.62	0.70	11.26	0.68	0.62	17.45	100.61	OH,F,Cl	Ca	magnesio-hornblende
296-1	1432	Astor	Nanga Parbat	1.48	12.35	9.09	46.86	0.68	10.44	0.72	0.87	18.34	100.83	OH,F,Cl	Ca	magnesio-ferri-hornblende
299-1	1432	Astor	Nanga Parbat	1.48	8.70	17.21	42.22	0.76	11.14	0.54	0.68	17.56	100.28	OH,F,Cl	Ca	tschermakite
300-1	1432	Astor	Nanga Parbat	1.69	10.43	14.64	42.51	0.72	11.33	0.76	0.74	17.01	99.84	OH,F,Cl	Ca	ferri-tschermakite
301-1	1432	Astor	Nanga Parbat	1.07	10.19	12.09	43.57	1.58	11.95	0.76	0.82	18.83	100.87	OH,F,Cl	Ca	potassic-magnesio-hastingsite
323-1	1432	Astor	Nanga Parbat	1.06	8.19	10.55	44.38	1.27	12.24	1.03	0.31	21.94	100.97	OH,F,Cl	Ca	hastingsite
324-1	1432	Astor	Nanga Parbat	1.58	8.67	16.59	42.28	0.70	10.98	0.61	0.62	17.32	99.34	OH,F,Cl	Ca	magnesio-hornblende
328-1	1432	Astor	Nanga Parbat	1.84	9.75	14.61	43.32	0.88	11.06	0.86	0.82	18.37	101.51	OH,F,Cl	Ca	pargasite
330-1	1432	Astor	Nanga Parbat	0.60	13.61	4.70	51.45	0.62	12.38	0.64	1.44	16.24	101.69	OH,F,Cl	Ca	magnesio-ferri-hornblende
331-1	1432	Astor	Nanga Parbat	1.57	18.13	8.66	50.53	0.42	12.92	0.72	0.85	6.14	99.94	OH,F,Cl	Ca	magnesio-hornblende
332-1	1432	Astor	Nanga Parbat	1.39	12.86	11.88	45.85	0.74	11.38	0.81	0.71	13.18	98.80	OH,F,Cl	Ca	magnesio-hornblende
334-1	1432	Astor	Nanga Parbat	2.28	11.39	16.66	43.73	0.39	10.93	0.65	0.70	15.01	101.74	OH,F,Cl	Ca	pargasite
335-1	1432	Astor	Nanga Parbat	1.74	13.41	10.37	45.77	1.47	11.93	1.06	0.85	14.56	101.17	OH,F,Cl	Ca	magnesio-hastingsite
336-1	1432	Astor	Nanga Parbat	1.21	12.94	10.01	47.25	0.94	11.42	1.24	0.68	15.03	100.73	OH,F,Cl	Ca	magnesio-hornblende
338-1	1432	Astor	Nanga Parbat	1.60	7.95	14.78	42.06	0.86	11.34	0.67	0.61	19.32	99.19	OH,F,Cl	Ca	ferro-pargasite
341-1	1432	Astor	Nanga Parbat	1.22	9.99	10.35	45.47	0.71	12.56	1.02	0.32	18.80	100.45	OH,F,Cl	Ca	magnesio-hornblende
346-1	1432	Astor	Nanga Parbat	1.71	10.30	12.54	45.13	0.37	11.67	0.90	0.73	18.07	101.41	OH,F,Cl	Ca	magnesio-hornblende
348-1	1432	Astor	Nanga Parbat	0.49	20.27	1.67	56.89	0.22	12.65	0.38	0.85	5.95	99.37	OH,F,Cl	Ca	actinolite
350-1	1432	Astor	Nanga Parbat	1.44	9.22	16.47	42.17	0.93	11.32	0.81	0.51	17.64	100.51	OH,F,Cl	Ca	tschermakite
355-1	1432	Astor	Nanga Parbat	1.43	9.38	16.14	41.93	0.76	11.39	0.75	0.70	16.89	99.38	OH,F,Cl	Ca	tschermakite
356-1	1432	Astor	Nanga Parbat	1.71	9.64	15.02	42.36	0.75	10.92	1.21	0.86	17.02	99.49	OH,F,Cl	Ca	tschermakite
358-1	1432	Astor	Nanga Parbat	1.50	13.80	9.60	48.12	0.54	10.60	0.86	0.91	14.88	100.82	OH,F,Cl	Ca	magnesio-ferri-hornblende
362-1	1432	Astor	Nanga Parbat	1.60	9.55	14.80	43.14	1.11	11.04	0.89	0.73	18.02	100.89	OH,F,Cl	Ca	magnesio-hornblende
364-1	1432	Astor	Nanga Parbat	2.00	13.14	12.06	45.91	0.57	10.98	0.96	0.60	12.91	99.15	OH,F,Cl	Ca	magnesio-hornblende
365-1	1432	Astor	Nanga Parbat	1.87	13.04	14.86	45.29	0.54	11.13	0.61	0.70	11.35	99.40	OH,F,Cl	Ca	magnesio-hornblende
366-1	1432	Astor	Nanga Parbat	1.95	9.49	14.63	42.78	0.81	11.50	0.45	0.74	16.51	98.87	OH,F,Cl	Ca	pargasite
367-1	1432	Astor	Nanga Parbat	1.71	10.28	16.09	42.88	0.82	10.75	0.68	0.62	16.20	100.03	OH,F,Cl	Ca	pargasite
373-1	1432	Astor	Nanga Parbat	1.32	9.79	16.04	42.48	0.69	11.34	0.82	0.71	15.23	98.42	OH,F,Cl	Ca	tschermakite
374-1	1432	Astor	Nanga Parbat	1.60	9.07	15.06	42.92	0.77	11.15	0.74	0.73	18.31	100.35	OH,F,Cl	Ca	magnesio-hornblende
376-1	1432	Astor	Nanga Parbat	1.52	10.22	15.66	42.67	0.80	11.25	0.78	0.79	15.97	99.66	OH,F,Cl	Ca	tschermakite
377-1	1432	Astor	Nanga Parbat	1.82	10.29	15.48	43.94	0.48	11.16	0.66	0.86	15.77	100.47	OH,F,Cl	Ca	magnesio-hornblende
378-1	1432	Astor	Nanga Parbat	1.47	10.20	15.66	42.98	0.68	11.36	0.59	0.59	15.75	99.28	OH,F,Cl	Ca	tschermakite
382-1	1432	Astor	Nanga Parbat	1.58	9.19	16.84	43.07	0.86	10.91	0.62	0.62	17.17	100.86	OH,F,Cl	Ca	magnesio-hornblende
383-1	1432	Astor	Nanga Parbat	2.19	10.12	14.61	42.09	0.71	11.13	0.83	0.62	16.83	99.13	OH,F,Cl	Ca	pargasite
388-1	1432	Astor	Nanga Parbat	2.28	8.84	16.18	41.82	0.49	10.90	0.68	0.82	18.08	100.08	OH,F,Cl	Ca	pargasite
389-1	1432	Astor	Nanga Parbat	1.32	13.08	10.02	47.64	0.97	12.20	0.59	0.98	13.70	100.50	OH,F,Cl	Ca	magnesio-hornblende
390-1	1432	Astor	Nanga Parbat	1.81	8.96	16.57	43.28	0.61	11.17	0.78	0.76	16.22	100.16	OH,F,Cl	Ca	magnesio-hornblende
392-1	1432	Astor	Nanga Parbat	1.65	9.04	14.32	42.24	0.64	11.22	1.30	0.82	19.67	100.90	OH,F,Cl	Ca	ferri-tschermakite
393-1	1432	Astor	Nanga Parbat	1.99	11.38	15.69	43.82	0.44	11.46	0.83	0.84	11.89	98.34	OH,F,Cl	Ca	magnesio-hornblende
394-1	1432	Astor	Nanga Parbat	1.73	9.65	14.27	43.29	1.01	11.39	0.69	0.86	17.58	100.47	OH,F,Cl	Ca	pargasite
398-1	1432	Astor	Nanga Parbat	2.12	9.82	15.60	42.54	0.62	10.29	0.84	0.79	16.99	99.59	OH,F,Cl	Ca	pargasite
399-1	1432	Astor	Nanga Parbat	1.62	9.98	14.34	42.69	1.11	11.72	0.98	0.36	16.10	98.89	OH,F,Cl	Ca	pargasite
400-1	1432	Astor	Nanga Parbat	1.73	9.99	11.36	42.74	0.84	11.20	1.13	1.02	18.97	98.99	OH,F,Cl	Ca	magnesio-hastingsite
410-1	1432	Astor	Nanga Parbat	1.91	9.49	16.73	42.62	0.54	11.41	0.68	0.78	15.86	100.02	OH,F,Cl	Ca	pargasite
411-1	1432	Astor	Nanga Parbat	1.38	11.92	15.08	44.79	0.60	11.25	0.56	0.44	13.26	99.27	OH,F,Cl	Ca	magnesio-hornblende
521-1	1432	Astor	Nanga Parbat	1.63	8.43	14.66	42.62	0.54	11.69	1.09	0.37	19.60	100.62	OH,F,Cl	Ca	ferro-hornblende
522-1	1432	Astor	Nanga Parbat	1.54	8.50	12.16	43.80	1.05	11.90	1.03	0.56	21.14	101.67	OH,F,Cl	Ca	ferro-pargasite

Point	Sample	River/Dune	Domain	Na_2O	MgO	Al_2O_3	SiO_2	K_2O	CaO	TiO_2	MnO	FeO	Total	Group	Subgroup	Species
				wt%	wt%	wt%	wt%	wt%	wt%	wt%	wt%	wt%			of (OH,F,Cl)	
83	1462	Mankera	Thal	0.62	15.72	1.68	53.17	0.28	11.99	0.44	0.23	11.11	95.25	OH,F,Cl	Ca	actinolite
87	1462	Mankera	Thal	1.28	8.36	8.00	42.09	1.46	10.57	1.51	0.26	19.15	92.66	OH,F,Cl	Ca	potassic-ferro-pargasite
88	1462	Mankera	Thal	1.24	10.72	11.68	43.69	0.60	10.81	1.39	0.29	16.04	96.46	OH,F,Cl	Ca	magnesio-hornblende
90	1462	Mankera	Thal	1.46	13.08	10.30	45.33	0.65	9.77	0.48	0.29	13.98	95.35	OH,F,Cl	Ca	magnesio-hornblende
92	1462	Mankera	Thal	2.45	11.32	14.14	41.89	0.34	9.26	0.67	0.22	13.23	93.51	OH,F,Cl	Ca	pargasite
99	1462	Mankera	Thal	0.47	18.69	3.32	52.57	0.07	3.65	0.19	0.22	17.85	97.05	OH,F,Cl	Mg-Fe-Mn	cummingtonite
101	1462	Mankera	Thal	1.82	10.53	12.42	41.26	0.86	10.49	1.02	0.26	13.87	92.56	OH,F,Cl	Ca	pargasite
104	1462	Mankera	Thal	1.68	10.20	11.39	41.92	0.97	10.05	1.53	0.21	15.99	93.92	OH,F,Cl	Ca	pargasite
107	1462	Mankera	Thal	1.98	9.34	15.85	41.42	0.82	10.89	0.80	0.20	16.66	97.95	OH,F,Cl	Ca	pargasite
110	1462	Mankera	Thal	1.44	10.94	9.98	43.90	0.39	10.26	1.64	0.30	16.62	95.49	OH,F,Cl	Ca	magnesio-ferri-hornblende
123	1462	Mankera	Thal	1.18	11.92	7.92	46.04	0.56	10.95	1.25	0.46	17.37	97.65	OH,F,Cl	Ca	magnesio-ferri-hornblende
125	1462	Mankera	Thal	1.29	10.32	12.94	42.04	1.66	11.01	2.15	0.25	17.41	99.06	OH,F,Cl	Ca	potassic-magnesio-hastingsite
130	1462	Mankera	Thal	1.61	12.12	12.59	43.42	0.51	10.70	1.26	0.30	12.72	95.23	OH,F,Cl	Ca	magnesio-hornblende
132	1462	Mankera	Thal	1.80	9.56	14.13	40.60	1.18	10.00	1.65	0.28	16.79	96.00	OH,F,Cl	Ca	pargasite
135	1462	Mankera	Thal	0.45	16.05	0.79	52.32	0.14	10.46	0.30	0.24	10.20	90.95	OH,F,Cl	Ca	actinolite
140	1462	Mankera	Thal	0.85	10.40	9.39	45.22	0.46	10.58	0.93	0.34	17.90	96.08	OH,F,Cl	Ca	magnesio-ferri-hornblende
145	1462	Mankera	Thal	1.39	10.39	14.31	42.74	0.70	9.49	1.11	0.33	16.56	97.02	OH,F,Cl	Ca	magnesio-hornblende
158	1462	Mankera	Thal	1.04	11.03	7.09	47.00	0.78	11.93	0.97	0.35	17.30	97.50	OH,F,Cl	Ca	magnesio-hornblende
170	1462	Mankera	Thal	0.59	22.45	0.51	55.83	0.22	12.61	0.30	0.23	1.51	94.24	OH,F,Cl	Ca	tremolite
179	1462	Mankera	Thal	1.42	11.08	11.80	43.82	0.73	10.10	1.18	0.34	16.67	97.13	OH,F,Cl	Ca	magnesio-hornblende
183	1462	Mankera	Thal	0.89	11.37	9.13	46.15	0.50	10.28	1.38	0.20	13.51	93.41	OH,F,Cl	Ca	magnesio-hornblende
188	1462	Mankera	Thal	2.44	15.17	12.24	45.34	0.11	11.13	0.62	0.27	9.11	96.45	OH,F,Cl	Ca	pargasite
194	1462	Mankera	Thal	0.78	14.21	8.17	48.35	0.51	10.90	0.78	0.23	11.39	95.33	OH,F,Cl	Ca	magnesio-hornblende
197	1462	Mankera	Thal	1.59	11.33	11.96	43.71	0.35	11.02	0.96	0.18	12.96	94.06	OH,F,Cl	Ca	magnesio-hornblende
204	1462	Mankera	Thal	0.75	16.59	5.40	50.93	0.47	11.87	0.66	0.30	8.82	95.79	OH,F,Cl	Ca	magnesio-hornblende
206	1462	Mankera	Thal	1.23	11.94	9.86	44.10	0.53	8.70	1.31	0.29	15.46	93.41	OH,F,Cl	Ca	magnesio-hornblende
208	1462	Mankera	Thal	1.78	9.60	13.60	41.90	0.48	10.44	0.68	0.23	16.84	95.54	OH,F,Cl	Ca	pargasite
211	1462	Mankera	Thal	1.33	10.18	11.04	44.52	0.42	11.03	0.68	0.19	15.49	94.88	OH,F,Cl	Ca	magnesio-hornblende
217	1462	Mankera	Thal	1.70	11.77	10.63	47.11	1.39	10.82	0.91	0.66	16.78	101.76	OH,F,Cl	Ca	pargasite
223	1462	Mankera	Thal	1.12	15.33	5.64	50.78	0.22	11.02	0.63	0.18	10.29	95.22	OH,F,Cl	Ca	magnesio-hornblende
224	1462	Mankera	Thal	0.55	16.24	2.11	53.23	0.10	11.73	0.57	0.24	10.82	95.58	OH,F,Cl	Ca	actinolite
227	1462	Mankera	Thal	1.54	7.51	14.48	40.60	0.78	10.68	0.72	0.35	19.11	95.77	OH,F,Cl	Ca	ferro-hornblende
242	1462	Mankera	Thal	0.16	0.00	21.88	36.42	0.18	20.78	0.49	0.26	12.99	93.17	OH,F,Cl	Ca	ferro-sadanagaite
250	1462	Mankera	Thal	1.50	9.48	14.40	42.22	0.37	10.58	0.88	0.33	15.75	95.51	OH,F,Cl	Ca	tschermakite
252	1462	Mankera	Thal	1.49	9.46	10.25	42.46	1.43	10.52	1.77	0.14	18.00	95.51	OH,F,Cl	Ca	pargasite
607	1462	Mankera	Thal	1.36	9.62	10.89	42.80	1.11	10.25	1.11	0.26	16.97	94.36	OH,F,Cl	Ca	magnesio-hornblende
609	1462	Mankera	Thal	1.20	9.92	9.24	42.35	1.10	10.78	1.79	0.26	16.80	93.46	OH,F,Cl	Ca	pargasite
611	1462	Mankera	Thal	0.64	14.14	5.51	50.01	0.34	10.52	0.83	0.31	14.17	96.49	OH,F,Cl	Ca	magnesio-hornblende
613	1462	Mankera	Thal	0.63	15.08	3.59	51.22	0.21	9.90	0.20	0.30	12.70	93.84	OH,F,Cl	Ca	actinolite
620	1462	Mankera	Thal	1.18	11.03	12.16	42.21	1.03	10.87	1.04	0.30	13.57	93.39	OH,F,Cl	Ca	magnesio-hornblende
624	1462	Mankera	Thal	1.27	10.14	11.27	41.67	0.93	10.54	1.52	0.27	15.04	92.65	OH,F,Cl	Ca	magnesio-hornblende
628	1462	Mankera	Thal	1.32	10.59	10.27	43.18	0.66	10.95	1.18	0.22	16.40	94.78	OH,F,Cl	Ca	magnesio-hornblende
629	1462	Mankera	Thal	2.00	9.07	16.13	40.53	0.46	10.11	1.04	0.14	13.83	93.29	OH,F,Cl	Ca	tschermakite
634	1462	Mankera	Thal	1.07	15.59	7.13	49.67	0.55	11.76	0.42	0.24	10.72	97.14	OH,F,Cl	Ca	magnesio-hornblende
645	1462	Mankera	Thal	0.65	11.20	6.56	47.09	0.46	10.77	1.16	0.28	18.53	96.70	OH,F,Cl	Ca	magnesio-ferri-hornblende
647	1462	Mankera	Thal	1.58	9.28	9.09	43.58	1.48	10.86	1.47	0.40	19.85	97.59	OH,F,Cl	Ca	ferro-pargasite
649	1462	Mankera	Thal	0.90	13.50	7.18	48.24	0.55	11.28	1.15	0.34	13.89	97.03	OH,F,Cl	Ca	magnesio-ferri-hornblende
652	1462	Mankera	Thal	1.04	12.52	7.12	46.33	0.75	10.82	1.68	0.30	14.55	95.12	OH,F,Cl	Ca	magnesio-ferri-hornblende
653	1462	Mankera	Thal	1.14	12.41	7.44	45.13	0.70	10.73	1.99	0.36	15.57	95.46	OH,F,Cl	Ca	magnesio-ferri-hornblende
656	1462	Mankera	Thal	2.61	8.55	16.27	41.12	0.36	9.35	0.85	0.32	15.75	95.16	OH,F,Cl	Ca	sadanagaite
666	1462	Mankera	Thal	0.44	13.71	5.56	50.85	0.43	11.71	0.38	0.27	13.48	96.82	OH,F,Cl	Ca	magnesio-hornblende
668	1462	Mankera	Thal	0.48	18.20	2.57	53.19	0.28	1.40	0.24	0.37	21.68	98.41	OH,F,Cl	Mg-Fe-Mn	cummingtonite
672	1462	Mankera	Thal	2.70	13.18	13.87	41.61	1.36	11.57	1.25	0.16	11.01	96.72	OH,F,Cl	Ca	pargasite
674	1462	Mankera	Thal	1.60	11.22	12.80	45.65	0.59	11.13	1.12	0.30	16.12	100.52	OH,F,Cl	Ca	magnesio-hornblende
687	1462	Mankera	Thal	1.45	8.50	12.92	41.57	1.20	10.71	0.86	0.16	17.76	95.14	OH,F,Cl	Ca	ferro-pargasite
688	1462	Mankera	Thal	0.76	8.59	7.39	45.46	0.76	10.74	0.86	0.37	17.75	92.68	OH,F,Cl	Ca	ferro-hornblende
700	1462	Mankera	Thal	0.53	14.67	2.36	52.97	1.32	9.91	0.60	0.23	14.50	97.09	OH,F,Cl	Ca	actinolite
707	1462	Mankera	Thal	1.54	11.46	10.44	45.45	1.30	11.29	1.89	0.27	14.97	98.62	OH,F,Cl	Ca	pargasite
712	1462	Mankera	Thal	1.41	12.89	8.94	46.79	0.55	8.83	1.10	0.22	16.66	97.39	OH,F,Cl	Ca	magnesio-ferri-hornblende
718	1462	Mankera	Thal	1.24	11.13	11.07	44.07	0.69	11.16	1.17	0.24	13.94	94.71	OH,F,Cl	Ca	magnesio-hornblende
722	1462	Mankera	Thal	1.37	10.49	12.00	42.23	0.50	10.18	1.25	0.31	15.62	93.95	OH,F,Cl	Ca	magnesio-hornblende
726	1462	Mankera	Thal	1.56	8.52	12.23	40.84	1.76	10.66	1.09	0.29	18.50	95.44	OH,F,Cl	Ca	ferro-pargasite
728	1462	Mankera	Thal	1.11	14.98	5.80	48.72	0.31	9.92	1.32	0.23	12.82	95.21	OH,F,Cl	Ca	magnesio-ferri-hornblende
734	1462	Mankera	Thal	1.24	10.88	7.99	44.06	0.73	10.38	1.91	0.27	16.34	93.79	OH,F,Cl	Ca	magnesio-ferri-hornblende
735	1462	Mankera	Thal	0.95	11.64	8.04	45.59	1.03	11.24	1.48	0.29	14.36	94.62	OH,F,Cl	Ca	magnesio-hornblende
736	1462	Mankera	Thal	1.47	15.99	7.75	47.34	0.40	11.37	1.30	0.27	9.12	95.02	OH,F,Cl	Ca	magnesio-hornblende
740	1462	Mankera	Thal	0.87	6.16	10.42	35.88	0.99	10.42	0.78	0.27	20.52	86.32	OH,F,Cl	Ca	ferro-ferri-hornblende
741	1462	Mankera	Thal	0.89	14.49	5.93	48.14	0.50	10.47	1.47	0.28	13.08	95.25	OH,F,Cl	Ca	magnesio-ferri-hornblende
750	1462	Mankera	Thal	1.06	10.99	8.74	44.30	0.70	11.00	0.89	0.16	15.95	93.81	OH,F,Cl	Ca	magnesio-hornblende
757	1462	Mankera	Thal	1.74	9.97	11.02	42.11	0.35	9.98	0.90	0.29	17.80	94.15	OH,F,Cl	Ca	magnesio-ferri-hornblende
758	1462	Mankera	Thal	2.24	11.18	11.89	42.50	0.64	10.41	1.24	0.31	16.38	96.78	OH,F,Cl	Ca	pargasite
1043	1462	Mankera	Thal	0.92	9.71	11.13	39.60	1.00	10.19	1.24	0.20	17.20	91.17	OH,F,Cl	Ca	ferri-tschermakite
1062	1462	Mankera	Thal	1.61	9.81	7.08	44.75	1.04	10.29	1.67	0.38	18.64	95.26	OH,F,Cl	Ca	magnesio-hornblende
1066	1462	Mankera	Thal	0.21	0.42	25.30	37.29	0.25	21.43	0.52	0.19	9.67	95.27	OH,F,Cl	Ca	ferro-sadanagaite
1070	1462	Mankera	Thal	1.27	9.71	7.81	45.95	0.35	10.31	1.29	0.34	19.29	96.33	OH,F,Cl	Ca	magnesio-ferri-hornblende
1072	1462	Mankera	Thal	1.47	8.39	9.38	44.19	0.64	9.91	2.01	0.38	23.44	99.81	OH,F,Cl	Ca	ferro-ferri-hornblende
1075	1462	Mankera	Thal	0.00	18.61	0.84	54.32	0.11	1.05	0.28	0.38	20.22	95.81	OH,F,Cl	Mg-Fe-Mn	cummingtonite
1083	1462	Mankera	Thal	1.23	16.66	5.34	52.57	0.41	11.29	0.54	0.23	9.14	97.41	OH,F,Cl	Ca	magnesio-hornblende
1085	1462	Mankera	Thal	1.26	13.33	7.66	48.77	0.49	10.43	0.72	0.26	14.72	97.64	OH,F,Cl	Ca	magnesio-ferri-hornblende
1099	1462	Mankera	Thal	1.44	9.94	12.17	43.85	0.99	10.59	1.29	0.23	18.11	98.62	OH,F,Cl	Ca	magnesio-hornblende
1100	1462	Mankera	Thal	1.65	11.61	10.32	45.43	0.59	11.37	1.28	0.31	15.49	98.06	OH,F,Cl	Ca	magnesio-hornblende
1102	1462	Mankera	Thal	0.94	13.58	4.23	52.52	0.41	11.54	0.42	0.23	16.94	100.80	OH,F,Cl	Ca	magnesio-ferri-hornblende
1113	1462	Mankera	Thal	1.65	10.79	14.04	43.61	0.67	10.59	0.76	0.15	13.04	95.29	OH,F,Cl	Ca	magnesio-hornblende
1122	1462	Mankera	Thal	1.27	13.73	5.58	49.12	0.63	10.51	1.28	0.22	13.35	95.68	OH,F,Cl	Ca	magnesio-ferri-hornblende
1125	1462	Mankera	Thal	1.42	10.77	9.34	45.39	0.75	11.06	1.17	0.41	16.06	96.38	OH,F,Cl	Ca	magnesio-hornblende
1132	1462	Mankera	Thal	1.66	10.86	11.80	43.67	1.24	10.93	1.46	0.25	16.15	98.04	OH,F,Cl	Ca	pargasite
1139	1462	Mankera	Thal	1.87	9.00	13.49	42.63	0.52	10.32	1.14	0.15	18.14	97.26	OH,F,Cl	Ca	magnesio-hornblende
1141	1462	Mankera	Thal	0.72	13.96	2.56	53.68	0.36	11.86	0.41	0.46	13.52	97.54	OH,F,Cl	Ca	actinolite
1148	1462	Mankera	Thal	1.27	13.01	7.66	46.70	0.38	11.02	0.65	0.18	14.66	95.55	OH,F,Cl	Ca	magnesio-ferri-hornblende
1151	1462	Mankera	Thal	1.80	10.62	10.44	44.50	0.47	10.85	0.87	0.32	16.00	95.88	OH,F,Cl	Ca	magnesio-hornblende
1152	1462	Mankera	Thal	1.48	10.61	14.63	42.30	0.86	10.27	0.83	0.14	13.14	94.26	OH,F,Cl	Ca	tschermakite
1157	1462	Mankera	Thal	1.88	11.80	13.20	40.55	0.61	11.02	2.23	0.25	12.73	94.27	OH,F,Cl	Ca	pargasite
1170	1462	Mankera	Thal	0.98	14.34	6.20	48.07	0.24	10.90	0.77	0.19	10.46	92.14	OH,F,Cl	Ca	magnesio-hornblende
1173	1462	Mankera	Thal	1.35	9.74	10.15	42.57	0.81	10.70	1.30	0.35	17.22	94.19	OH,F,Cl	Ca	magnesio-hornblende
1182	1462	Mankera	Thal	0.28	14.75	1.50	52.28	0.37	12.21	0.55	0.34	12.72	95.00	OH,F,Cl	Ca	actinolite
1183	1462	Mankera	Thal	1.90	10.54	16.95	44.23	0.57	10.74	0.76	0.24	13.84	99.77	OH,F,Cl	Ca	tschermakite
1186	1462	Mankera	Thal	1.73	10.62	12.72	44.50	1.09	11.05	0.96	0.18	14.74	97.60	OH,F,Cl	Ca	pargasite
1187	1462	Mankera	Thal	1.15	10.60	9.62	45.02	0.76	11.49	0.55	0.24	17.33	96.75	OH,F,Cl	Ca	magnesio-hornblende
1189	1462	Mankera	Thal	1.56	11.26	11.40	43.19	0.56	10.10	1.26	0.29	15.87	95.49	OH,F,Cl	Ca	magnesio-hornblende
1191	1462	Mankera	Thal	0.72	12.32	7.39	46.54	0.30	9.01	0.90	0.41	15.31	92.90	OH,F,Cl	Ca	magnesio-hornblende
1202	1462	Mankera	Thal	1.20	11.04	9.57	43.29	1.00	10.23	0.37	0.35	16.36	93.40	OH,F,Cl	Ca	magnesio-ferri-hornblende
1203	1462	Mankera	Thal	0.75	11.86	7.43	45.94	0.50	10.85	1.04	0.32	14.38	93.05	OH,F,Cl	Ca	magnesio-hornblende
1214	1462	Mankera	Thal	1.18	10.98	8.49	43.91	1.24	10.33	1.49	0.51	16.37	94.50	OH,F,Cl	Ca	magnesio-hornblende

Point	Sample	River/Dune	Domain	Na_2O	MgO	Al_2O_3	SiO_2	K_2O	CaO	TiO_2	MnO	FeO	Total	Group	Subgroup	Species
				wt%	wt%	wt%	wt%	wt%	wt%	wt%	wt%	wt%			of (OH,F,Cl)	
3	1463	Haidarabad	Thal	1.07	13.42	6.90	50.80	0.67	11.71	0.55	0.44	14.11	99.65	OH,F,Cl	Ca	magnesio-hornblende
18	1463	Haidarabad	Thal	0.57	15.26	1.97	51.38	0.27	11.11	0.58	0.67	15.02	96.83	OH,F,Cl	Ca	actinolite
113	1463	Haidarabad	Thal	1.95	12.38	12.39	42.69	0.62	10.49	1.58	1.01	14.44	97.55	OH,F,Cl	Ca	magnesio-ferri-hornblende
115	1463	Haidarabad	Thal	1.81	8.12	13.26	40.46	0.79	10.59	0.66	0.91	18.01	94.60	OH,F,Cl	Ca	ferro-pargasite
119	1463	Haidarabad	Thal	0.81	15.18	2.92	52.29	0.15	11.34	0.69	0.77	13.64	97.78	OH,F,Cl	Ca	actinolite
130	1463	Haidarabad	Thal	0.66	16.21	3.64	49.55	0.24	12.48	0.51	0.45	13.09	96.83	OH,F,Cl	Ca	magnesio-ferri-hornblende
181	1463	Haidarabad	Thal	1.99	9.92	15.01	38.95	1.35	10.78	1.47	0.48	15.12	95.07	OH,F,Cl	Ca	pargasite
187	1463	Haidarabad	Thal	1.82	13.34	13.26	41.08	0.52	10.53	2.03	0.50	12.51	95.59	OH,F,Cl	Ca	ferri-tschermakite
188	1463	Haidarabad	Thal	2.20	8.81	16.68	41.10	0.60	10.35	0.75	0.43	15.17	96.09	OH,F,Cl	Ca	sadanagaite
199	1463	Haidarabad	Thal	0.00	0.00	27.02	39.98	0.20	22.26	0.37	0.22	8.83	98.88	OH,F,Cl	Ca	ferro-sadanagaite
206	1463	Haidarabad	Thal	2.61	10.82	17.68	40.92	0.78	10.25	0.91	0.24	12.25	96.46	OH,F,Cl	Ca	sadanagaite
260	1463	Haidarabad	Thal	1.14	10.07	11.63	42.13	2.16	11.49	1.84	0.47	16.61	97.54	OH,F,Cl	Ca	potassic-pargasite
261	1463	Haidarabad	Thal	1.55	11.49	12.39	45.11	1.05	11.18	1.38	0.48	14.01	98.64	OH,F,Cl	Ca	magnesio-hornblende
262	1463	Haidarabad	Thal	0.29	16.34	1.64	55.12	0.18	12.41	0.42	0.23	13.40	100.03	OH,F,Cl	Ca	actinolite
282	1463	Haidarabad	Thal	1.74	11.30	13.62	41.54	0.31	10.87	0.91	0.57	16.48	97.35	OH,F,Cl	Ca	ferri-tschermakite
290	1463	Haidarabad	Thal	0.75	12.29	5.47	48.68	0.49	12.28	0.60	0.71	18.33	99.60	OH,F,Cl	Ca	magnesio-ferri-hornblende
305	1463	Haidarabad	Thal	1.13	15.31	7.41	47.86	0.29	12.63	0.99	0.56	11.55	97.74	OH,F,Cl	Ca	magnesio-ferri-hornblende
309	1463	Haidarabad	Thal	1.54	9.51	11.78	40.49	1.98	11.42	2.45	0.42	19.29	98.87	OH,F,Cl	Ca	potassic-magnesio-hastingsite
310	1463	Haidarabad	Thal	0.51	13.76	2.92	49.58	0.42	11.96	0.75	0.86	16.05	96.80	OH,F,Cl	Ca	actinolite
314	1463	Haidarabad	Thal	1.78	7.18	14.17	39.18	1.16	11.65	0.90	0.93	21.24	98.19	OH,F,Cl	Ca	hastingsite
323	1463	Haidarabad	Thal	1.33	13.59	9.19	45.05	0.37	9.59	1.20	0.76	15.72	96.82	OH,F,Cl	Ca	magnesio-ferri-hornblende
329	1463	Haidarabad	Thal	0.88	17.75	5.17	50.06	0.73	11.95	1.57	0.80	11.23	100.14	OH,F,Cl	Ca	magnesio-ferri-hornblende
357	1463	Haidarabad	Thal	1.49	11.50	12.02	40.27	1.73	11.68	2.84	0.55	13.99	96.07	OH,F,Cl	Ca	Ti-rich magnesio-hastingsite
463	1463	Haidarabad	Thal	0.32	19.51	0.31	53.98	0.24	0.86	0.48	1.98	19.81	97.49	OH,F,Cl	Mg-Fe-Mn	cummingtonite
470	1463	Haidarabad	Thal	1.58	11.79	11.36	41.64	1.06	11.40	1.26	0.81	14.55	95.46	OH,F,Cl	Ca	magnesio-hastingsite
471	1463	Haidarabad	Thal	0.39	17.93	1.91	51.83	0.20	11.86	0.80	0.78	11.26	96.96	OH,F,Cl	Ca	actinolite
479	1463	Haidarabad	Thal	1.39	11.90	7.83	43.38	1.15	11.79	1.21	0.93	17.53	97.10	OH,F,Cl	Ca	magnesio-hastingsite
514	1463	Haidarabad	Thal	1.03	11.68	8.36	42.75	1.01	12.07	1.93	0.96	18.07	97.85	OH,F,Cl	Ca	magnesio-ferri-hornblende
522	1463	Haidarabad	Thal	0.91	7.12	13.63	40.15	1.83	11.71	1.16	1.01	20.02	97.53	OH,F,Cl	Ca	potassic-ferro-pargasite
541	1463	Haidarabad	Thal	0.00	0.14	26.01	37.92	0.20	23.27	0.58	0.48	8.61	97.22	OH,F,Cl	Ca	ferro-sadanagaite
560	1463	Haidarabad	Thal	1.58	14.98	8.41	48.71	0.54	11.61	0.70	0.79	12.70	100.01	OH,F,Cl	Ca	magnesio-hornblende
571	1463	Haidarabad	Thal	2.16	12.44	12.67	42.87	1.45	11.54	1.08	0.35	15.58	100.13	OH,F,Cl	Ca	magnesio-hastingsite
575	1463	Haidarabad	Thal	1.18	12.47	8.55	48.44	0.81	12.30	1.41	0.33	13.70	99.19	OH,F,Cl	Ca	magnesio-hornblende
588	1463	Haidarabad	Thal	1.75	11.81	12.89	46.83	1.84	10.70	0.79	0.29	12.37	99.28	OH,F,Cl	Ca	magnesio-hornblende
589	1463	Haidarabad	Thal	1.87	13.79	13.37	43.25	0.35	10.86	0.71	0.38	12.31	96.89	OH,F,Cl	Ca	magnesio-ferri-hornblende
607	1463	Haidarabad	Thal	1.81	8.43	16.85	40.96	0.78	10.53	0.78	0.31	17.01	97.46	OH,F,Cl	Ca	sadanagaite
614	1463	Haidarabad	Thal	0.96	16.75	3.44	52.19	0.35	10.11	0.48	0.37	13.00	97.63	OH,F,Cl	Ca	magnesio-ferri-hornblende
618	1463	Haidarabad	Thal	1.52	12.04	9.78	45.08	1.15	11.37	1.15	0.43	15.94	98.47	OH,F,Cl	Ca	magnesio-hastingsite
632	1463	Haidarabad	Thal	0.64	17.91	2.75	54.23	0.35	11.98	0.44	0.24	9.22	97.76	OH,F,Cl	Ca	actinolite
639	1463	Haidarabad	Thal	1.04	18.05	5.02	52.42	0.30	11.65	0.36	0.27	9.53	98.66	OH,F,Cl	Ca	magnesio-ferri-hornblende
643	1463	Haidarabad	Thal	0.12	12.65	1.32	52.13	0.41	1.53	0.51	0.92	26.33	95.90	OH,F,Cl	Mg-Fe-Mn	grunerite
644	1463	Haidarabad	Thal	1.72	12.44	8.73	47.58	0.69	10.84	0.84	0.34	15.56	98.75	OH,F,Cl	Ca	magnesio-hornblende
648	1463	Haidarabad	Thal	1.53	12.18	10.29	44.24	1.04	11.37	1.47	0.41	14.65	97.18	OH,F,Cl	Ca	pargasite
666	1463	Haidarabad	Thal	1.64	9.66	12.16	39.72	1.78	11.73	1.29	0.69	18.40	97.08	OH,F,Cl	Ca	magnesio-hastingsite
683	1463	Haidarabad	Thal	0.77	13.63	5.60	49.04	0.50	11.33	0.79	0.88	16.11	98.65	OH,F,Cl	Ca	magnesio-ferri-hornblende
691	1463	Haidarabad	Thal	0.77	11.80	6.63	46.72	0.59	11.53	1.02	1.19	18.80	99.07	OH,F,Cl	Ca	magnesio-ferri-hornblende
700	1463	Haidarabad	Thal	0.85	13.30	8.21	44.58	0.93	12.40	1.23	0.48	16.63	98.62	OH,F,Cl	Ca	magnesio-ferri-hornblende
717	1463	Haidarabad	Thal	3.04	14.75	15.55	41.12	0.43	11.39	1.21	0.44	10.28	98.21	OH,F,Cl	Ca	magnesio-hastingsite
738	1463	Haidarabad	Thal	2.01	12.59	15.27	42.59	0.95	11.89	0.89	0.57	11.75	98.51	OH,F,Cl	Ca	pargasite
740	1463	Haidarabad	Thal	1.45	10.46	11.84	40.61	1.05	11.73	2.35	0.74	17.72	97.96	OH,F,Cl	Ca	magnesio-hastingsite
741	1463	Haidarabad	Thal	1.80	11.35	14.01	42.00	0.73	11.71	1.26	0.54	15.15	98.54	OH,F,Cl	Ca	magnesio-hastingsite
743	1463	Haidarabad	Thal	1.45	11.12	9.04	43.15	1.03	11.59	1.54	1.15	18.60	98.67	OH,F,Cl	Ca	magnesio-hastingsite
749	1463	Haidarabad	Thal	1.78	11.64	12.33	42.96	0.57	12.31	1.07	0.64	16.12	99.41	OH,F,Cl	Ca	magnesio-hastingsite
753	1463	Haidarabad	Thal	1.74	10.85	13.71	41.36	1.02	11.71	1.51	0.68	14.60	97.17	OH,F,Cl	Ca	pargasite
786	1463	Haidarabad	Thal	4.32	11.32	13.10	42.95	0.45	8.78	0.80	0.52	14.87	97.11	OH,F,Cl	Ca	pargasite
787	1463	Haidarabad	Thal	1.13	12.60	4.52	46.76	0.73	11.74	1.44	0.78	17.82	97.52	OH,F,Cl	Ca	magnesio-ferri-hornblende
793	1463	Haidarabad	Thal	1.33	7.53	14.88	38.97	1.58	11.52	1.17	0.70	19.39	97.06	OH,F,Cl	Ca	ferro-pargasite
901	1463	Haidarabad	Thal	0.96	21.78	3.52	53.10	0.27	12.26	0.73	0.92	6.45	99.99	OH,F,Cl	Ca	magnesio-ferri-hornblende
915	1463	Haidarabad	Thal	1.32	9.11	12.08	41.26	1.62	11.90	1.26	0.75	19.18	98.48	OH,F,Cl	Ca	magnesio-hastingsite
921	1463	Haidarabad	Thal	2.14	8.42	15.97	39.17	0.95	10.85	0.96	0.42	19.01	97.89	OH,F,Cl	Ca	sadanagaite
970	1463	Haidarabad	Thal	1.49	8.40	13.78	41.17	1.31	11.34	0.96	0.66	20.16	99.28	OH,F,Cl	Ca	magnesio-hastingsite
976	1463	Haidarabad	Thal	1.49	10.38	10.44	40.92	1.64	12.52	1.59	0.71	19.25	98.93	OH,F,Cl	Ca	magnesio-hastingsite
979	1463	Haidarabad	Thal	2.99	8.27	13.57	40.14	0.37	10.79	1.28	0.67	20.71	98.78	OH,F,Cl	Ca	hastingsite
992	1463	Haidarabad	Thal	1.87	9.26	15.64	42.18	0.67	10.19	0.61	0.37	16.28	97.07	OH,F,Cl	Ca	magnesio-hornblende
993	1463	Haidarabad	Thal	0.90	14.49	5.99	49.77	0.91	11.82	0.69	0.39	13.51	98.47	OH,F,Cl	Ca	magnesio-ferri-hornblende
996	1463	Haidarabad	Thal	1.96	12.94	13.39	43.09	0.68	11.06	2.86	0.41	12.37	98.76	OH,F,Cl	Ca	Ti-rich pargasite
1057	1463	Haidarabad	Thal	0.64	13.70	2.55	56.23	0.21	10.09	0.28	0.55	15.46	99.71	OH,F,Cl	Ca	actinolite
1075	1463	Haidarabad	Thal	1.40	9.85	12.69	43.50	1.42	11.17	0.95	0.51	17.18	98.67	OH,F,Cl	Ca	pargasite
1086	1463	Haidarabad	Thal	2.69	9.20	13.12	41.83	0.53	10.57	0.71	0.45	19.55	98.65	OH,F,Cl	Ca	pargasite
1088	1463	Haidarabad	Thal	1.89	11.69	12.38	44.04	1.67	11.20	1.29	0.32	14.70	99.20	OH,F,Cl	Ca	pargasite
1093	1463	Haidarabad	Thal	0.54	13.80	3.82	48.80	0.38	12.69	0.73	0.70	15.57	97.04	OH,F,Cl	Ca	actinolite
1098	1463	Haidarabad	Thal	0.94	17.28	5.30	50.32	0.33	12.40	0.65	0.39	11.97	99.58	OH,F,Cl	Ca	magnesio-ferri-hornblende
1101	1463	Haidarabad	Thal	2.79	14.80	14.25	42.86	0.39	12.00	0.78	0.65	9.90	98.42	OH,F,Cl	Ca	pargasite
1121	1463	Haidarabad	Thal	2.17	11.65	11.06	44.00	0.31	10.03	1.11	0.98	17.48	98.79	OH,F,Cl	Ca	magnesio-ferri-hornblende
1125	1463	Haidarabad	Thal	1.38	11.99	11.50	43.30	1.17	11.81	1.80	0.68	16.48	100.12	OH,F,Cl	Ca	magnesio-hastingsite
1131	1463	Haidarabad	Thal	2.40	9.95	12.28	39.41	1.36	11.51	1.26	0.93	19.35	98.45	OH,F,Cl	Ca	magnesio-hastingsite
1134	1463	Haidarabad	Thal	0.90	21.06	2.71	52.75	0.23	12.42	0.22	0.61	6.45	97.35	OH,F,Cl	Ca	magnesio-ferri-hornblende
1147	1463	Haidarabad	Thal	1.49	11.25	9.46	42.37	1.03	11.07	2.89	0.53	17.47	97.56	OH,F,Cl	Ca	Ti-rich magnesio-hastingsite
1152	1463	Haidarabad	Thal	0.00	0.27	23.03	37.43	0.08	22.71	0.00	0.90	13.99	98.41	OH,F,Cl	Ca	ferro-sadanagaite
1158	1463	Haidarabad	Thal	2.22	9.48	15.91	40.60	0.72	10.86	0.59	0.57	17.18	98.14	OH,F,Cl	Ca	sadanagaite
1170	1463	Haidarabad	Thal	0.49	12.14	0.54	50.57	0.29	23.53	0.41	0.75	11.57	100.30	OH,F,Cl	Ca	edenite
1179	1463	Haidarabad	Thal	0.41	26.33	0.63	57.78	0.31	13.32	0.23	0.32	0.90	100.24	OH,F,Cl	Ca	tremolite
1370	1463	Haidarabad	Thal	1.93	9.79	12.19	41.55	1.25	12.13	1.44	0.69	19.27	100.24	OH,F,Cl	Ca	magnesio-hastingsite
1375	1463	Haidarabad	Thal	0.88	13.58	8.44	44.93	0.54	11.42	2.18	0.68	15.87	98.53	OH,F,Cl	Ca	magnesio-ferri-hornblende
1376	1463	Haidarabad	Thal	0.69	16.59	3.72	50.95	0.26	12.65	0.29	0.69	12.13	97.97	OH,F,Cl	Ca	magnesio-ferri-hornblende
1379	1463	Haidarabad	Thal	0.93	20.04	2.18	53.69	0.45	13.06	0.57	0.37	6.45	97.74	OH,F,Cl	Ca	actinolite
1393	1463	Haidarabad	Thal	1.37	10.95	8.99	44.83	0.55	11.55	0.96	0.79	17.58	97.58	OH,F,Cl	Ca	magnesio-ferri-hornblende
1406	1463	Haidarabad	Thal	1.81	9.00	8.84	41.80	1.53	12.19	1.24	1.06	21.09	98.55	OH,F,Cl	Ca	hastingsite
1411	1463	Haidarabad	Thal	0.52	17.78	2.01	51.50	0.23	1.88	0.52	1.10	23.09	98.63	OH,F,Cl	Mg-Fe-Mn	cummingtonite
1419	1463	Haidarabad	Thal	0.68	14.16	4.11	49.44	0.39	12.84	1.02	0.76	16.33	99.74	OH,F,Cl	Ca	magnesio-ferri-hornblende
1431	1463	Haidarabad	Thal	0.97	16.96	5.84	51.93	0.60	11.83	0.58	0.34	9.97	99.02	OH,F,Cl	Ca	magnesio-ferri-hornblende
1457	1463	Haidarabad	Thal	1.74	12.05	9.53	44.72	0.83	10.81	1.31	0.66	15.48	97.13	OH,F,Cl	Ca	pargasite
1469	1463	Haidarabad	Thal	5.95	0.10	27.69	54.19	0.35	9.43	0.09	0.15	0.81	98.77	OH,F,Cl	Na-Ca	ferro-taramite
1473	1463	Haidarabad	Thal	1.23	10.46	9.55	43.51	1.20	11.58	0.91	0.42	18.16	97.02	OH,F,Cl	Ca	magnesio-hastingsite
1487	1463	Haidarabad	Thal	1.50	12.57	9.35	44.12	1.81	11.68	1.78	0.49	15.33	98.64	OH,F,Cl	Ca	magnesio-hastingsite
1501	1463	Haidarabad	Thal	2.28	12.70	13.25	41.89	0.48	11.50	1.32	0.40	14.21	98.02	OH,F,Cl	Ca	magnesio-hastingsite
1526	1463	Haidarabad	Thal	0.64	13.88	5.08	47.38	0.57	11.94	1.04	0.94	16.29	97.75	OH,F,Cl	Ca	magnesio-ferri-hornblende
1533	1463	Haidarabad	Thal	0.94	16.68	6.49	47.64	0.33	12.16	0.41	0.51	12.06	97.22	OH,F,Cl	Ca	magnesio-ferri-hornblende
1541	1463	Haidarabad	Thal	2.08	13.73	9.91	43.87	1.32	11.68	1.58	0.50	13.01	97.69	OH,F,Cl	Ca	magnesio-hastingsite
1558	1463	Haidarabad	Thal	1.44	11.48	8.13	44.49	0.59	11.00	1.02	1.01	19.66	98.83	OH,F,Cl	Ca	magnesio-ferri-hornblende

Point	Sample	River/Dune	Domain	Na_2O	MgO	Al_2O_3	SiO_2	K_2O	CaO	TiO_2	MnO	FeO	Total	Group	Subgroup	Species
				wt%	wt%	wt%	wt%	wt%	wt%	wt%	wt%	wt%			of (OH,F,Cl)	
34	1470	Muzaffarghar	Thal	1.81	11.12	13.09	44.57	1.43	11.19	1.25	0.51	15.12	100.10	OH,F,Cl	Ca	pargasite
35	1470	Muzaffarghar	Thal	0.79	15.25	7.78	52.01	0.50	11.35	0.77	0.44	11.59	100.48	OH,F,Cl	Ca	magnesio-hornblende
36	1470	Muzaffarghar	Thal	0.99	13.34	10.22	48.17	0.44	10.88	0.47	0.52	14.03	99.05	OH,F,Cl	Ca	magnesio-hornblende
140	1470	Muzaffarghar	Thal	1.35	8.55	7.19	47.63	1.10	10.59	1.44	0.67	21.79	100.30	OH,F,Cl	Ca	ferro-ferri-hornblende
142	1470	Muzaffarghar	Thal	0.49	19.99	1.21	58.01	0.36	12.16	0.56	0.65	8.41	101.83	OH,F,Cl	Ca	actinolite
144	1470	Muzaffarghar	Thal	2.62	11.19	13.72	44.16	0.70	10.12	1.16	0.80	15.80	100.27	OH,F,Cl	Ca	pargasite
149	1470	Muzaffarghar	Thal	0.64	14.98	4.37	52.50	0.33	12.49	0.44	0.75	11.89	98.39	OH,F,Cl	Ca	actinolite
210	1470	Muzaffarghar	Thal	1.90	15.78	13.75	46.47	0.31	10.97	1.16	0.31	8.66	99.30	OH,F,Cl	Ca	magnesio-hornblende
223	1470	Muzaffarghar	Thal	2.19	13.65	13.55	43.78	0.56	10.56	1.50	0.73	12.73	99.25	OH,F,Cl	Ca	pargasite
229	1470	Muzaffarghar	Thal	1.71	12.78	11.67	45.97	1.73	10.84	1.30	0.61	13.03	99.64	OH,F,Cl	Ca	potassic-pargasite
266	1470	Muzaffarghar	Thal	1.21	11.32	10.25	43.62	1.99	12.13	2.67	1.02	15.14	99.33	OH,F,Cl	Ca	potassic-pargasite
293	1470	Muzaffarghar	Thal	1.33	12.81	10.10	46.59	0.64	10.25	1.14	0.86	14.12	97.83	OH,F,Cl	Ca	magnesio-hornblende
296	1470	Muzaffarghar	Thal	1.19	12.04	9.82	45.46	1.47	10.63	2.48	0.49	14.54	98.13	OH,F,Cl	Ca	magnesio-hornblende
336	1470	Muzaffarghar	Thal	0.52	17.68	1.75	55.87	0.47	13.09	0.60	0.65	9.26	99.89	OH,F,Cl	Ca	actinolite
345	1470	Muzaffarghar	Thal	0.58	15.08	1.73	55.16	0.33	12.11	0.30	0.57	14.12	99.99	OH,F,Cl	Ca	actinolite
354	1470	Muzaffarghar	Thal	0.51	17.83	3.74	54.72	0.23	12.83	0.60	0.80	7.65	98.91	OH,F,Cl	Ca	actinolite
381	1470	Muzaffarghar	Thal	0.17	0.33	24.27	40.17	0.31	21.95	0.82	0.64	9.50	98.16	OH,F,Cl	Ca	ferro-sadanagaite
394	1470	Muzaffarghar	Thal	0.46	14.41	1.39	55.34	0.29	11.11	0.52	0.67	16.56	100.76	OH,F,Cl	Ca	actinolite
424	1470	Muzaffarghar	Thal	0.28	14.77	1.10	56.63	0.31	12.74	0.20	0.39	13.87	100.30	OH,F,Cl	Ca	actinolite
444	1470	Muzaffarghar	Thal	0.88	13.74	6.08	49.07	0.52	13.64	0.58	0.53	13.30	98.32	OH,F,Cl	Ca	edenite
451	1470	Muzaffarghar	Thal	1.73	15.61	8.12	48.46	0.36	13.39	0.91	0.38	9.51	98.47	OH,F,Cl	Ca	pargasite
523	1470	Muzaffarghar	Thal	1.78	8.77	11.37	41.62	1.80	11.83	1.74	0.65	20.41	99.97	OH,F,Cl	Ca	hastingsite
617	1470	Muzaffarghar	Thal	0.92	14.38	8.54	49.22	0.44	12.75	0.60	0.84	10.46	98.15	OH,F,Cl	Ca	magnesio-hornblende
635	1470	Muzaffarghar	Thal	2.05	13.22	11.81	44.04	0.30	12.11	1.91	0.50	12.27	98.20	OH,F,Cl	Ca	pargasite
742	1470	Muzaffarghar	Thal	2.32	14.47	13.78	43.18	0.41	11.18	1.73	0.17	10.95	98.19	OH,F,Cl	Ca	pargasite
754	1470	Muzaffarghar	Thal	1.86	11.44	11.39	45.04	1.04	10.91	1.50	0.67	16.10	99.96	OH,F,Cl	Ca	pargasite
762	1470	Muzaffarghar	Thal	2.00	10.45	15.51	43.76	0.57	10.82	1.01	0.58	15.27	99.98	OH,F,Cl	Ca	magnesio-hornblende
765	1470	Muzaffarghar	Thal	1.80	8.97	13.89	43.60	0.73	10.65	0.80	0.85	16.73	98.02	OH,F,Cl	Ca	magnesio-hornblende
785	1470	Muzaffarghar	Thal	1.22	19.14	6.84	52.87	0.74	11.78	0.89	0.57	6.57	100.61	OH,F,Cl	Ca	magnesio-hornblende
795	1470	Muzaffarghar	Thal	2.05	10.58	16.12	42.61	0.58	11.14	0.97	0.89	13.61	98.55	OH,F,Cl	Ca	pargasite
849	1470	Muzaffarghar	Thal	1.08	17.72	8.73	50.19	0.39	12.46	0.75	0.55	7.55	99.41	OH,F,Cl	Ca	magnesio-hornblende
907	1470	Muzaffarghar	Thal	1.46	9.79	11.94	43.16	2.01	12.34	1.05	0.58	16.15	98.49	OH,F,Cl	Ca	pargasite
935	1470	Muzaffarghar	Thal	1.44	9.45	10.27	45.98	1.75	11.11	0.95	0.64	18.01	99.60	OH,F,Cl	Ca	potassic-ferro-pargasite
937	1470	Muzaffarghar	Thal	1.20	15.27	7.98	49.43	0.48	10.22	1.41	0.73	12.74	99.45	OH,F,Cl	Ca	magnesio-ferri-hornblende
943	1470	Muzaffarghar	Thal	1.47	12.31	13.54	44.17	0.99	11.37	1.13	0.48	13.33	98.79	OH,F,Cl	Ca	pargasite
1026	1470	Muzaffarghar	Thal	1.41	17.80	9.31	47.81	0.41	11.44	0.68	0.77	7.93	97.58	OH,F,Cl	Ca	magnesio-ferri-hornblende
1060	1470	Muzaffarghar	Thal	0.55	22.18	2.56	57.12	0.31	12.62	0.61	0.66	2.64	99.25	OH,F,Cl	Ca	tremolite
1091	1470	Muzaffarghar	Thal	1.05	12.33	6.54	50.80	0.88	12.68	0.73	0.69	14.92	100.61	OH,F,Cl	Ca	magnesio-hornblende
1127	1470	Muzaffarghar	Thal	1.58	12.55	13.38	44.91	0.78	11.22	0.88	0.63	12.84	98.77	OH,F,Cl	Ca	magnesio-hornblende
1129	1470	Muzaffarghar	Thal	0.81	16.84	6.76	51.08	0.66	11.89	0.70	0.54	10.60	99.89	OH,F,Cl	Ca	magnesio-ferri-hornblende
1142	1470	Muzaffarghar	Thal	1.97	16.61	9.97	47.89	0.35	12.21	0.87	0.33	8.74	98.95	OH,F,Cl	Ca	pargasite
1154	1470	Muzaffarghar	Thal	0.99	10.40	11.48	42.63	2.51	12.07	3.00	0.52	15.48	99.09	OH,F,Cl	Ca	Ti-rich potassic-pargasite
1155	1470	Muzaffarghar	Thal	0.83	11.64	3.48	50.60	0.11	21.30	0.99	0.88	10.81	100.64	OH,F,Cl	Ca	edenite
1211	1470	Muzaffarghar	Thal	1.55	11.57	11.15	46.47	1.17	10.87	1.73	0.36	14.65	99.52	OH,F,Cl	Ca	magnesio-hornblende
1332	1470	Muzaffarghar	Thal	1.46	9.22	11.32	44.67	1.51	11.32	0.91	0.80	19.38	100.60	OH,F,Cl	Ca	ferro-pargasite
1345	1470	Muzaffarghar	Thal	1.90	15.54	5.28	51.65	0.36	11.79	0.33	0.71	12.12	99.68	OH,F,Cl	Ca	actinolite
1405	1470	Muzaffarghar	Thal	0.59	13.88	7.18	51.33	0.88	12.02	0.80	0.83	12.64	100.14	OH,F,Cl	Ca	magnesio-hornblende
1423	1470	Muzaffarghar	Thal	1.10	13.95	11.11	47.22	0.70	10.41	1.54	0.64	13.61	100.28	OH,F,Cl	Ca	magnesio-hornblende
1441	1470	Muzaffarghar	Thal	2.94	13.42	12.41	43.11	0.44	11.79	1.89	0.71	12.77	99.46	OH,F,Cl	Ca	pargasite
1488	1470	Muzaffarghar	Thal	0.83	17.89	6.98	52.91	0.21	11.91	0.51	0.65	6.89	98.78	OH,F,Cl	Ca	magnesio-hornblende
1530	1470	Muzaffarghar	Thal	3.26	14.41	13.31	42.58	0.57	12.47	0.66	0.32	10.74	98.34	OH,F,Cl	Ca	pargasite
1539	1470	Muzaffarghar	Thal	1.63	8.94	13.16	43.91	1.26	11.50	1.46	0.53	16.38	98.77	OH,F,Cl	Ca	ferro-pargasite
1618	1470	Muzaffarghar	Thal	1.06	10.79	8.29	47.06	1.21	12.37	0.94	0.59	17.34	99.67	OH,F,Cl	Ca	pargasite
1626	1470	Muzaffarghar	Thal	0.82	12.58	6.45	49.89	0.86	12.53	1.00	0.83	13.79	98.76	OH,F,Cl	Ca	magnesio-hornblende
1671	1470	Muzaffarghar	Thal	0.00	0.15	24.36	39.57	0.21	22.63	0.34	0.69	9.71	97.67	OH,F,Cl	Ca	ferro-sadanagaite
1678	1470	Muzaffarghar	Thal	2.03	16.25	12.74	47.14	0.39	11.86	0.58	0.52	8.45	99.98	OH,F,Cl	Ca	pargasite
1691	1470	Muzaffarghar	Thal	1.45	11.43	12.03	45.34	0.67	11.32	1.49	0.84	15.48	100.05	OH,F,Cl	Ca	magnesio-hornblende
1707	1470	Muzaffarghar	Thal	0.58	12.79	1.32	53.84	0.34	12.66	0.60	0.90	15.50	98.53	OH,F,Cl	Ca	actinolite
1710	1470	Muzaffarghar	Thal	0.57	16.63	1.67	55.17	0.38	12.34	0.41	0.83	11.54	99.56	OH,F,Cl	Ca	actinolite
1774	1470	Muzaffarghar	Thal	0.18	0.00	25.17	40.26	0.23	22.35	0.29	0.56	8.36	97.38	OH,F,Cl	Ca	ferro-sadanagaite
1776	1470	Muzaffarghar	Thal	1.43	13.37	10.27	47.67	1.19	11.41	1.14	0.79	12.34	99.62	OH,F,Cl	Ca	magnesio-hornblende
1787	1470	Muzaffarghar	Thal	0.25	0.56	23.38	38.56	0.36	22.65	0.62	0.38	10.42	97.17	OH,F,Cl	Ca	ferro-sadanagaite
1789	1470	Muzaffarghar	Thal	0.11	0.32	22.74	40.07	0.08	22.56	0.39	0.68	12.02	98.96	OH,F,Cl	Ca	ferro-sadanagaite
1820	1470	Muzaffarghar	Thal	1.39	6.24	12.95	39.81	1.51	12.10	0.97	0.50	22.74	98.21	OH,F,Cl	Ca	hastingsite
1881	1470	Muzaffarghar	Thal	2.94	13.32	14.57	45.53	0.39	10.84	1.33	0.37	11.31	100.61	OH,F,Cl	Ca	pargasite
1895	1470	Muzaffarghar	Thal	1.96	10.14	12.94	43.01	1.49	11.17	1.74	0.27	16.28	98.99	OH,F,Cl	Ca	pargasite
1904	1470	Muzaffarghar	Thal	1.41	11.84	8.31	45.62	0.76	11.46	2.20	0.69	16.77	99.06	OH,F,Cl	Ca	magnesio-ferri-hornblende
1950	1470	Muzaffarghar	Thal	1.94	13.18	11.00	46.95	0.53	10.79	0.76	0.42	12.53	98.08	OH,F,Cl	Ca	magnesio-hornblende
1952	1470	Muzaffarghar	Thal	1.85	7.69	13.80	40.84	1.85	10.67	1.32	0.90	19.26	98.18	OH,F,Cl	Ca	ferro-pargasite
1973	1470	Muzaffarghar	Thal	1.43	12.71	11.45	46.58	1.42	12.02	1.33	0.52	12.46	99.92	OH,F,Cl	Ca	pargasite
1985	1470	Muzaffarghar	Thal	1.08	11.27	8.93	47.32	1.43	12.02	1.13	0.60	15.10	98.89	OH,F,Cl	Ca	magnesio-hornblende
1999	1470	Muzaffarghar	Thal	1.83	11.36	12.38	44.71	1.31	12.34	1.18	0.28	12.52	97.92	OH,F,Cl	Ca	pargasite
2051	1470	Muzaffarghar	Thal	1.29	9.94	9.75	45.22	1.19	10.98	1.32	1.00	17.64	98.33	OH,F,Cl	Ca	magnesio-hornblende
2059	1470	Muzaffarghar	Thal	2.29	10.25	16.63	43.08	0.75	10.73	0.89	0.39	14.99	100.01	OH,F,Cl	Ca	pargasite
2083	1470	Muzaffarghar	Thal	1.16	9.47	12.28	44.17	1.17	11.67	0.96	0.43	17.05	98.36	OH,F,Cl	Ca	magnesio-hornblende
2138	1470	Muzaffarghar	Thal	2.60	12.37	13.81	45.00	0.31	10.95	0.56	0.75	11.80	98.14	OH,F,Cl	Ca	pargasite
2151	1470	Muzaffarghar	Thal	1.71	10.94	12.19	44.91	0.56	11.25	1.68	0.62	15.93	99.78	OH,F,Cl	Ca	magnesio-hornblende
2159	1470	Muzaffarghar	Thal	1.98	11.43	14.03	43.82	1.00	11.00	1.08	0.61	14.10	99.05	OH,F,Cl	Ca	pargasite
2174	1470	Muzaffarghar	Thal	2.19	14.07	12.88	40.97	1.43	12.93	3.37	0.39	9.43	97.66	OH,F,Cl	Ca	Ti-rich pargasite
2175	1470	Muzaffarghar	Thal	1.55	7.56	12.43	41.12	1.98	11.97	1.26	0.55	18.85	97.27	OH,F,Cl	Ca	ferro-pargasite
2230	1470	Muzaffarghar	Thal	0.29	0.55	27.19	40.78	0.14	23.14	0.21	0.36	6.24	98.90	OH,F,Cl	Ca	ferro-sadanagaite
2353	1470	Muzaffarghar	Thal	1.35	11.95	11.82	44.73	0.40	11.84	1.47	0.85	13.64	98.04	OH,F,Cl	Ca	magnesio-hornblende
2355	1470	Muzaffarghar	Thal	2.93	17.58	13.84	45.43	0.44	11.40	0.65	0.51	7.67	100.46	OH,F,Cl	Ca	magnesio-hastingsite
2355	1470	Muzaffarghar	Thal	1.35	12.60	10.11	45.58	1.19	11.99	1.39	0.86	15.49	100.56	OH,F,Cl	Ca	magnesio-hastingsite
2356	1470	Muzaffarghar	Thal	2.04	9.31	14.16	44.49	0.52	11.93	0.64	0.59	15.97	99.65	OH,F,Cl	Ca	pargasite
2436	1470	Muzaffarghar	Thal	2.03	9.14	11.93	44.79	0.46	11.28	1.19	0.69	17.05	98.56	OH,F,Cl	Ca	ferro-pargasite
2472	1470	Muzaffarghar	Thal	1.82	8.89	13.99	42.97	0.99	11.74	1.47	0.61	16.69	99.16	OH,F,Cl	Ca	ferro-pargasite
2635	1470	Muzaffarghar	Thal	1.57	13.52	10.84	47.84	0.44	12.71	0.85	0.68	10.65	99.09	OH,F,Cl	Ca	magnesio-hornblende
2830	1470	Muzaffarghar	Thal	1.85	13.20	11.88	46.82	0.48	11.79	0.86	0.64	10.87	98.38	OH,F,Cl	Ca	magnesio-hornblende
2831	1470	Muzaffarghar	Thal	1.54	12.00	10.22	45.05	0.69	11.68	1.45	0.92	14.97	98.51	OH,F,Cl	Ca	magnesio-hornblende
2846	1470	Muzaffarghar	Thal	2.49	13.21	11.22	46.03	0.26	10.52	1.06	0.67	13.11	98.57	OH,F,Cl	Ca	pargasite
2849	1470	Muzaffarghar	Thal	0.26	17.92	0.73	56.87	0.10	13.70	0.00	0.70	10.15	100.42	OH,F,Cl	Ca	actinolite
2925	1470	Muzaffarghar	Thal	1.10	10.37	9.52	46.74	0.65	11.73	1.00	0.77	17.81	99.70	OH,F,Cl	Ca	magnesio-hornblende
2927	1470	Muzaffarghar	Thal	0.74	10.46	8.11	47.24	0.52	12.05	1.04	1.20	16.37	97.73	OH,F,Cl	Ca	magnesio-hornblende
3012	1470	Muzaffarghar	Thal	0.44	11.49	3.66	52.04	0.52	12.34	0.57	0.86	17.20	99.13	OH,F,Cl	Ca	actinolite
3212	1470	Muzaffarghar	Thal	2.16	11.14	13.68	43.88	0.44	12.42	0.99	0.53	14.09	99.32	OH,F,Cl	Ca	pargasite
3285	1470	Muzaffarghar	Thal	0.26	0.20	22.92	39.26	0.33	23.60	0.31	0.45	11.09	98.42	OH,F,Cl	Ca	ferro-sadanagaite
3299	1470	Muzaffarghar	Thal	1.35	12.95	6.62	49.74	0.36	11.68	0.36	0.64	15.28	98.99	OH,F,Cl	Ca	magnesio-hornblende
3384	1470	Muzaffarghar	Thal	1.43	11.28	8.52	44.99	1.13	11.86	1.34	1.00	17.72	99.27	OH,F,Cl	Ca	magnesio-hastingsite
3494	1470	Muzaffarghar	Thal	1.76	11.88	8.72	45.26	1.52	11.94	1.55	0.67	17.04	100.34	OH,F,Cl	Ca	magnesio-hastingsite

Point	Sample	River/Dune	Domain	Na_2O	MgO	Al_2O_3	SiO_2	K_2O	CaO	TiO_2	MnO	FeO	Total	Group	Subgroup	Species
				wt%	wt%	wt%	wt%	wt%	wt%	wt%	wt%	wt%			of (OH,F,Cl)	
4	1474	Munda	Thal	1.02	14.04	6.28	50.41	0.00	11.56	0.38	0.36	14.01	98.07	OH,F,Cl	Ca	magnesio-ferri-hornblende
5	1474	Munda	Thal	0.65	19.10	5.21	53.83	0.40	11.50	0.21	0.42	8.50	99.82	OH,F,Cl	Ca	magnesio-hornblende
11	1474	Munda	Thal	1.21	14.72	5.85	51.27	0.16	10.34	0.51	0.63	13.87	98.53	OH,F,Cl	Ca	magnesio-ferri-hornblende
119	1474	Munda	Thal	1.48	10.67	10.62	44.85	0.64	10.85	0.95	0.53	16.91	97.49	OH,F,Cl	Ca	magnesio-hornblende
124	1474	Munda	Thal	1.60	13.12	12.59	46.19	0.32	10.99	1.21	0.40	12.52	98.96	OH,F,Cl	Ca	magnesio-hornblende
126	1474	Munda	Thal	1.39	12.04	9.06	47.46	0.96	11.45	1.39	0.28	15.63	99.67	OH,F,Cl	Ca	magnesio-hornblende
129	1474	Munda	Thal	1.29	12.40	10.57	46.18	0.79	11.31	0.67	0.37	15.57	99.17	OH,F,Cl	Ca	magnesio-ferri-hornblende
130	1474	Munda	Thal	2.11	6.90	11.54	44.29	0.39	10.12	0.38	0.29	22.98	99.00	OH,F,Cl	Ca	ferro-hornblende
132	1474	Munda	Thal	1.95	10.54	10.97	42.66	1.20	11.37	1.60	0.40	16.35	97.03	OH,F,Cl	Ca	pargasite
134	1474	Munda	Thal	2.84	13.58	13.65	45.22	0.59	10.98	1.18	0.34	11.23	99.61	OH,F,Cl	Ca	pargasite
135	1474	Munda	Thal	1.37	10.83	11.30	43.52	1.57	11.64	1.21	0.36	16.08	97.87	OH,F,Cl	Ca	pargasite
141	1474	Munda	Thal	1.07	13.52	8.66	47.73	0.94	11.99	0.75	0.34	12.95	97.95	OH,F,Cl	Ca	magnesio-hornblende
142	1474	Munda	Thal	2.32	12.45	13.06	45.93	0.39	11.16	0.53	0.43	15.34	101.61	OH,F,Cl	Ca	pargasite
143	1474	Munda	Thal	1.65	14.84	11.53	45.86	0.88	11.12	1.28	0.33	12.23	99.72	OH,F,Cl	Ca	magnesio-ferri-hornblende
146	1474	Munda	Thal	0.53	19.23	1.50	54.11	0.23	0.82	0.46	0.68	20.91	98.45	OH,F,Cl	Mg-Fe-Mn	cummingtonite
148	1474	Munda	Thal	1.57	9.28	11.71	43.26	1.75	11.24	1.61	0.43	17.89	98.75	OH,F,Cl	Ca	potassic-ferro-pargasite
150	1474	Munda	Thal	0.92	11.05	9.95	45.76	1.34	11.84	1.57	0.41	16.84	99.69	OH,F,Cl	Ca	magnesio-hornblende
153	1474	Munda	Thal	0.79	16.47	4.96	50.94	0.68	12.98	1.53	0.07	8.72	97.15	OH,F,Cl	Ca	actinolite
155	1474	Munda	Thal	0.81	16.84	2.65	56.31	0.34	12.13	0.40	0.45	12.23	102.16	OH,F,Cl	Ca	actinolite
173	1474	Munda	Thal	1.39	16.12	9.33	47.31	0.55	11.49	1.94	0.38	11.06	99.57	OH,F,Cl	Ca	magnesio-ferri-hornblende
175	1474	Munda	Thal	1.67	13.47	8.53	48.45	0.24	11.03	0.73	0.28	13.78	98.18	OH,F,Cl	Ca	magnesio-hornblende
197	1474	Munda	Thal	1.21	17.38	8.55	51.24	0.80	12.33	0.31	0.16	7.81	99.80	OH,F,Cl	Ca	magnesio-hornblende
202	1474	Munda	Thal	2.36	14.23	12.46	47.97	0.46	10.84	0.56	0.18	10.56	99.62	OH,F,Cl	Ca	magnesio-hornblende
206	1474	Munda	Thal	2.02	9.79	17.59	43.20	0.66	10.52	0.59	0.31	13.86	98.54	OH,F,Cl	Ca	tschermakite
208	1474	Munda	Thal	0.49	16.95	3.68	55.55	0.23	12.17	0.36	0.51	12.12	102.06	OH,F,Cl	Ca	actinolite
210	1474	Munda	Thal	1.93	9.43	11.91	45.02	0.57	11.03	0.57	0.09	18.62	99.18	OH,F,Cl	Ca	pargasite
214	1474	Munda	Thal	1.86	12.99	12.90	44.54	1.23	11.86	1.19	0.35	12.13	99.05	OH,F,Cl	Ca	pargasite
220	1474	Munda	Thal	0.94	12.07	5.99	50.45	0.88	11.97	0.71	0.46	14.64	98.09	OH,F,Cl	Ca	magnesio-hornblende
221	1474	Munda	Thal	0.62	18.93	4.05	55.21	0.31	12.66	0.47	0.29	8.52	101.04	OH,F,Cl	Ca	magnesio-ferri-hornblende
234	1474	Munda	Thal	2.10	9.51	15.12	43.56	1.08	11.24	0.69	0.25	16.98	100.54	OH,F,Cl	Ca	pargasite
248	1474	Munda	Thal	0.83	24.05	3.24	56.38	0.18	13.75	0.35	0.12	1.11	100.00	OH,F,Cl	Ca	tremolite
249	1474	Munda	Thal	1.10	18.74	5.63	52.42	0.16	11.67	0.50	0.22	8.24	98.69	OH,F,Cl	Ca	magnesio-ferri-hornblende
251	1474	Munda	Thal	1.52	12.25	8.34	46.79	1.47	11.26	1.13	0.32	16.04	99.12	OH,F,Cl	Ca	pargasite
254	1474	Munda	Thal	0.41	12.56	3.16	54.21	0.50	11.84	0.65	0.28	13.73	97.35	OH,F,Cl	Ca	magnesio-hornblende
258	1474	Munda	Thal	1.62	9.78	14.15	43.84	0.69	11.09	0.84	0.26	14.94	97.22	OH,F,Cl	Ca	magnesio-hornblende
260	1474	Munda	Thal	2.29	15.13	13.37	47.38	0.46	10.87	0.73	0.07	10.30	100.62	OH,F,Cl	Ca	magnesio-hornblende
263	1474	Munda	Thal	1.60	14.54	11.38	46.95	0.55	11.27	0.79	0.25	11.39	98.71	OH,F,Cl	Ca	magnesio-hornblende
264	1474	Munda	Thal	1.59	9.46	12.65	41.88	1.98	11.73	1.44	0.42	18.36	99.52	OH,F,Cl	Ca	pargasite
493	1474	Munda	Thal	2.15	11.12	12.58	44.30	1.08	11.63	0.92	0.41	16.29	100.48	OH,F,Cl	Ca	pargasite
496	1474	Munda	Thal	1.23	11.98	8.99	46.33	1.15	12.00	1.35	0.39	16.24	99.66	OH,F,Cl	Ca	magnesio-hornblende
525	1474	Munda	Thal	1.46	13.05	10.48	46.94	1.26	12.03	0.97	0.22	12.94	99.35	OH,F,Cl	Ca	pargasite
529	1474	Munda	Thal	1.58	13.99	8.46	48.25	0.35	10.62	0.48	0.42	13.39	97.54	OH,F,Cl	Ca	magnesio-ferri-hornblende
540	1474	Munda	Thal	1.74	11.38	13.67	42.15	1.63	10.83	1.58	0.44	14.96	98.39	OH,F,Cl	Ca	pargasite
546	1474	Munda	Thal	1.67	8.48	18.17	41.95	0.70	11.13	0.96	0.37	15.66	99.08	OH,F,Cl	Ca	tschermakite
547	1474	Munda	Thal	1.86	14.75	11.53	47.49	0.75	11.05	1.00	0.51	11.03	99.96	OH,F,Cl	Ca	magnesio-hornblende
552	1474	Munda	Thal	1.64	15.13	10.97	47.29	0.43	12.26	0.60	0.46	9.92	98.72	OH,F,Cl	Ca	magnesio-hornblende
553	1474	Munda	Thal	1.27	19.17	7.35	53.02	0.34	12.05	0.51	0.37	6.83	100.89	OH,F,Cl	Ca	magnesio-hornblende
560	1474	Munda	Thal	0.00	3.04	21.07	38.39	0.28	3.22	0.39	0.52	33.08	99.99	OH,F,Cl	Mg-Fe-Mn	grunerite
565	1474	Munda	Thal	1.95	16.27	15.07	44.96	0.49	11.92	0.59	0.24	7.72	99.19	OH,F,Cl	Ca	magnesio-hornblende
566	1474	Munda	Thal	0.49	14.64	3.05	53.45	0.44	12.19	0.62	0.26	14.81	99.94	OH,F,Cl	Ca	actinolite
569	1474	Munda	Thal	2.28	9.76	17.33	41.62	0.67	10.85	0.96	0.26	14.33	98.06	OH,F,Cl	Ca	pargasite
570	1474	Munda	Thal	0.55	15.41	0.97	54.26	0.24	1.33	0.23	0.78	24.54	98.31	OH,F,Cl	Mg-Fe-Mn	cummingtonite
571	1474	Munda	Thal	1.89	9.81	12.53	41.82	2.00	11.19	1.04	0.43	17.07	97.78	OH,F,Cl	Ca	pargasite
574	1474	Munda	Thal	1.84	10.83	14.89	43.23	0.72	10.32	0.80	0.36	15.74	98.74	OH,F,Cl	Ca	magnesio-hornblende
575	1474	Munda	Thal	2.10	13.30	13.39	45.65	0.72	10.67	1.18	0.37	13.39	100.77	OH,F,Cl	Ca	pargasite
584	1474	Munda	Thal	1.26	8.97	15.90	42.26	1.28	11.84	0.80	0.21	16.72	99.25	OH,F,Cl	Ca	pargasite
586	1474	Munda	Thal	3.06	12.42	14.07	44.55	0.48	10.58	1.01	0.22	12.88	99.27	OH,F,Cl	Ca	pargasite
935	1474	Munda	Thal	0.71	15.67	4.35	52.08	0.25	10.13	0.41	0.33	13.82	97.75	OH,F,Cl	Ca	magnesio-ferri-hornblende
943	1474	Munda	Thal	1.87	11.47	11.94	44.63	0.56	11.78	1.44	0.15	14.70	98.55	OH,F,Cl	Ca	pargasite
944	1474	Munda	Thal	1.68	12.32	11.77	45.09	0.55	9.75	1.14	0.38	13.93	96.60	OH,F,Cl	Ca	magnesio-hornblende
949	1474	Munda	Thal	0.23	14.51	2.68	54.56	0.46	12.16	0.37	0.46	13.86	99.30	OH,F,Cl	Ca	actinolite
952	1474	Munda	Thal	0.32	16.19	4.19	54.64	0.20	12.01	0.28	0.40	12.58	100.81	OH,F,Cl	Ca	actinolite
954	1474	Munda	Thal	2.03	8.82	16.64	42.33	0.57	10.59	0.44	0.24	16.43	98.10	OH,F,Cl	Ca	magnesio-hornblende
957	1474	Munda	Thal	2.52	13.41	13.25	45.28	0.49	10.66	0.93	0.30	11.34	98.19	OH,F,Cl	Ca	pargasite
966	1474	Munda	Thal	1.23	13.91	7.39	50.30	0.58	11.54	0.40	0.35	13.15	98.84	OH,F,Cl	Ca	magnesio-hornblende
979	1474	Munda	Thal	1.26	14.93	10.12	48.74	0.46	11.33	0.45	0.22	11.94	99.47	OH,F,Cl	Ca	magnesio-hornblende
980	1474	Munda	Thal	1.56	9.27	12.14	43.48	1.68	11.85	0.74	0.27	18.74	99.72	OH,F,Cl	Ca	ferro-pargasite
983	1474	Munda	Thal	1.48	10.34	10.04	44.01	1.58	11.70	1.68	0.39	18.20	99.42	OH,F,Cl	Ca	pargasite
987	1474	Munda	Thal	1.60	10.97	14.15	42.55	1.13	11.58	0.89	0.48	15.77	99.12	OH,F,Cl	Ca	pargasite
989	1474	Munda	Thal	1.77	8.69	12.29	40.03	2.10	11.41	1.85	0.26	18.66	97.05	OH,F,Cl	Ca	ferro-pargasite
990	1474	Munda	Thal	1.73	12.25	13.17	40.80	1.77	11.54	1.70	0.50	13.80	97.26	OH,F,Cl	Ca	magnesio-hastingsite
991	1474	Munda	Thal	1.24	15.76	6.79	49.68	0.44	11.31	0.32	0.39	10.94	96.86	OH,F,Cl	Ca	magnesio-ferri-hornblende
993	1474	Munda	Thal	1.70	14.95	7.46	49.40	0.51	10.90	0.56	0.22	12.75	98.47	OH,F,Cl	Ca	magnesio-ferri-hornblende
997	1474	Munda	Thal	1.70	12.80	12.04	44.13	0.95	10.60	1.89	0.47	13.29	97.87	OH,F,Cl	Ca	magnesio-hornblende
1018	1474	Munda	Thal	2.31	9.01	14.11	41.81	1.05	11.01	1.11	0.37	17.34	98.12	OH,F,Cl	Ca	pargasite
1040	1474	Munda	Thal	1.21	18.48	4.27	54.26	0.39	11.77	0.31	0.24	8.21	99.14	OH,F,Cl	Ca	actinolite
1051	1474	Munda	Thal	0.62	18.04	3.12	54.03	0.00	12.52	0.19	0.28	9.38	98.19	OH,F,Cl	Ca	actinolite
1392	1474	Munda	Thal	0.47	18.70	2.33	54.34	0.28	3.62	0.35	0.58	18.09	98.75	OH,F,Cl	Mg-Fe-Mn	cummingtonite
1400	1474	Munda	Thal	1.97	11.82	14.01	43.97	0.65	9.96	0.41	0.28	14.06	97.14	OH,F,Cl	Ca	magnesio-hornblende
1402	1474	Munda	Thal	1.37	11.47	7.81	45.74	0.97	11.71	0.96	0.49	17.54	98.05	OH,F,Cl	Ca	magnesio-hastingsite
1403	1474	Munda	Thal	1.69	8.93	15.53	41.68	2.34	11.07	1.25	0.11	16.98	99.58	OH,F,Cl	Ca	potassic-pargasite
1407	1474	Munda	Thal	2.10	11.64	16.40	43.89	0.77	11.15	0.72	0.26	13.51	100.43	OH,F,Cl	Ca	pargasite
1412	1474	Munda	Thal	1.36	18.54	7.75	53.11	0.29	12.37	0.21	0.31	6.10	100.04	OH,F,Cl	Ca	magnesio-hornblende
1413	1474	Munda	Thal	1.28	12.81	10.32	46.22	0.79	11.05	0.84	0.37	13.78	97.45	OH,F,Cl	Ca	magnesio-hornblende
1416	1474	Munda	Thal	0.42	0.42	32.88	38.96	0.26	23.24	0.23	0.09	1.35	97.86	OH,F,Cl	Ca	ferro-sadanagaite
1417	1474	Munda	Thal	1.19	12.10	11.70	44.53	1.08	11.58	1.53	0.66	14.12	98.50	OH,F,Cl	Ca	magnesio-hornblende
1429	1474	Munda	Thal	0.59	16.90	3.01	53.24	0.15	11.88	0.59	0.40	11.64	98.40	OH,F,Cl	Ca	actinolite
1447	1474	Munda	Thal	2.06	9.70	16.41	42.64	0.78	10.81	0.98	0.31	14.96	98.65	OH,F,Cl	Ca	pargasite
1448	1474	Munda	Thal	1.69	11.39	11.53	45.40	1.18	11.42	1.91	0.30	13.88	98.70	OH,F,Cl	Ca	pargasite
1456	1474	Munda	Thal	0.91	13.20	7.34	49.17	0.97	11.77	0.88	0.34	13.89	98.45	OH,F,Cl	Ca	magnesio-hornblende
1457	1474	Munda	Thal	0.89	17.24	9.33	51.41	0.40	11.71	0.66	0.25	8.36	100.25	OH,F,Cl	Ca	magnesio-hornblende
1462	1474	Munda	Thal	1.36	14.56	10.70	47.94	0.71	12.16	0.57	0.42	9.72	98.14	OH,F,Cl	Ca	magnesio-hornblende
1474	1474	Munda	Thal	1.49	17.23	8.01	51.44	0.40	12.05	0.64	0.38	7.84	99.48	OH,F,Cl	Ca	magnesio-hornblende
1974	1474	Munda	Thal	1.91	9.02	13.22	43.30	1.29	11.45	1.52	0.28	17.92	99.92	OH,F,Cl	Ca	ferro-pargasite
1983	1474	Munda	Thal	1.30	14.38	9.83	48.06	0.39	11.32	0.91	0.50	11.48	98.16	OH,F,Cl	Ca	magnesio-hornblende
1986	1474	Munda	Thal	0.83	23.30	2.51	56.07	0.37	12.85	0.24	0.23	1.41	97.81	OH,F,Cl	Ca	tremolite
1999	1474	Munda	Thal	2.71	14.02	14.85	43.97	0.44	11.24	1.03	0.11	10.78	99.16	OH,F,Cl	Ca	pargasite
2013	1474	Munda	Thal	1.61	9.40	15.23	42.60	0.96	10.76	0.96	0.31	16.00	97.85	OH,F,Cl	Ca	magnesio-hornblende
2014	1474	Munda	Thal	0.75	8.28	6.67	47.08	0.62	12.19	0.32	0.31	20.62	96.83	OH,F,Cl	Ca	ferro-actinolite
2017	1474	Munda	Thal	0.97	12.31	8.85	48.40	0.65	11.69	0.74	0.42	14.03	98.06	OH,F,Cl	Ca	magnesio-hornblende

Appendix Table B4 SEM-EDS data and chemical calculations in garnet of Thal Desert and Upper Indus tributaries.

Sample	Points	River/Dune	Domain	SiO_2	Al_2O_3	FeO	MnO	MgO	CaO	Total	Majorite	Spessartine	Pyrope	Almandine	Grossular	Andradite	Total	Quality
				wt%	wt%	wt%	wt%	wt%	wt%		$\{Mg_3\}[SiMg](Si_3)O_{12}$	$\{Mn_3\}[Al_2](Si_3)O_{12}$	$\{Mg_3\}[Al_2](Si_3)O_{12}$	$\{Fe_3\}[Al_2](Si_3)O_{12}$	$\{Ca_3\}[Al_2](Si_3)O_{12}$	$\{Ca_3\}[Fe_2](Si_3)O_{12}$		index
1749	38-1	Hushe	Karakorum	37.82	16.90	7.29	0.32	0.52	34.85	97.70			0.020		0.739	0.227	1.000	Good
1749	110-1	Hushe	Karakorum	35.22	20.07	21.80	8.86	0.66	0.62	87.22		0.232	0.030	0.564	0.021		1.000	Poor
1749	178-1	Hushe	Karakorum	36.06	20.17	27.98	4.51	2.96	1.13	92.81		0.110	0.127	0.673	0.035		1.000	Poor
1749	205-1	Hushe	Karakorum	38.77	19.94	3.16	0.35	0.49	35.99	98.70			0.016		0.868	0.101	1.000	Excellent
1749	232-1	Hushe	Karakorum	35.74	20.49	32.26	4.05	1.83	0.65	95.02		0.098	0.078	0.768	0.020		1.000	Poor
1749	233-1	Hushe	Karakorum	36.91	20.76	30.00	2.26	3.44	3.64	97.02		0.052	0.140	0.687	0.107		1.000	Fair
1749	320-1	Hushe	Karakorum	35.78	19.73	15.08	14.60	0.41	0.51	86.12		0.387	0.019	0.395	0.017		1.000	Poor
1749	339-1	Hushe	Karakorum	36.40	20.59	27.16	5.17	2.75	1.03	93.09		0.126	0.118	0.652	0.032		1.000	Poor
1749	432-1	Hushe	Karakorum	35.91	20.00	25.08	7.74	0.64	0.60	89.97		0.197	0.029	0.631	0.019		1.000	Poor
1749	528-1	Hushe	Karakorum	36.47	20.43	30.39	2.67	2.71	1.57	94.24		0.064	0.115	0.721	0.048		1.000	Poor
1749	592-1	Hushe	Karakorum	35.95	19.92	27.17	8.01	0.54	0.76	92.36		0.200	0.024	0.669	0.024		1.000	Poor
1749	612-1	Hushe	Karakorum	37.17	20.22	27.84	4.91	2.95	1.39	94.48		0.118	0.124	0.658	0.042		1.000	Poor
1749	615-1	Hushe	Karakorum	36.37	20.09	28.89	7.02	0.64	0.42	93.44		0.173	0.028	0.704	0.013		1.000	Poor
1749	689-1	Hushe	Karakorum	38.04	18.68	3.34	0.30	0.00	34.19	94.55		0.007		0.014	0.862	0.066	1.000	Poor
1749	89-2	Hushe	Karakorum	36.90	20.52	28.57	5.84	1.80	1.39	95.02		0.140	0.076	0.677	0.042		1.000	Poor
1749	142-2	Hushe	Karakorum	34.35	19.25	20.96	6.37	1.38	1.03	83.34		0.173	0.066	0.562	0.035		1.000	Poor
1749	231-2	Hushe	Karakorum	35.60	19.67	20.98	10.65	1.11	0.86	88.87		0.274	0.050	0.532	0.028		1.000	Poor
1749	235-2	Hushe	Karakorum	35.36	19.68	23.08	9.70	0.34	0.64	88.81		0.251	0.016	0.590	0.021		1.000	Poor
1749	275-2	Hushe	Karakorum	36.69	20.43	21.19	9.25	1.31	2.48	91.36		0.230	0.057	0.520	0.078		1.000	Poor
1749	278-2	Hushe	Karakorum	35.35	19.79	24.52	7.19	1.81	1.71	90.37		0.181	0.080	0.609	0.054		1.000	Poor
1749	459-2	Hushe	Karakorum	36.12	20.05	26.91	7.26	1.37	0.81	92.52		0.180	0.060	0.657	0.025		1.000	Poor
1749	519-2	Hushe	Karakorum	35.38	19.84	25.13	4.71	2.53	1.75	89.34		0.119	0.113	0.627	0.056		1.000	Poor
1749	521-2	Hushe	Karakorum	35.12	19.13	22.36	8.20	0.67	0.95	86.43		0.217	0.031	0.584	0.032		1.000	Poor
1749	555-2	Hushe	Karakorum	36.91	20.13	27.78	4.51	2.78	1.56	93.67		0.109	0.118	0.663	0.048		1.000	Poor
1749	573-2	Hushe	Karakorum	36.08	20.65	27.85	6.53	1.23	0.72	93.06		0.161	0.053	0.676	0.022		1.000	Poor
1749	616-2	Hushe	Karakorum	36.00	20.67	26.92	3.73	3.01	3.16	93.50		0.090	0.127	0.639	0.096		1.000	Poor
1749	635-2	Hushe	Karakorum	36.39	20.17	22.45	8.09	1.87	1.96	90.93		0.202	0.082	0.552	0.062		1.000	Poor
1749	696-2	Hushe	Karakorum	38.50	18.65	5.00	0.27	0.25	35.61	98.27			0.010		0.830	0.154	1.000	Excellent
1749	706-2	Hushe	Karakorum	35.98	20.45	29.36	4.54	2.64	1.12	94.09		0.110	0.112	0.699	0.034		1.000	Poor
1749	731-2	Hushe	Karakorum	35.24	20.44	22.51	9.17	1.07	1.13	89.56		0.233	0.048	0.566	0.036		1.000	Poor
1749	803-2	Hushe	Karakorum	36.93	20.17	21.60	9.56	2.13	0.87	91.26		0.237	0.093	0.530	0.027		1.000	Poor
1749	823-2	Hushe	Karakorum	37.02	20.69	29.62	4.00	3.06	1.48	95.88		0.094	0.127	0.690	0.044		1.000	Poor
1749	901-2	Hushe	Karakorum	37.12	20.60	27.35	6.41	1.16	0.45	93.09		0.158	0.050	0.664	0.014		1.000	Poor
1749	1029-2	Hushe	Karakorum	37.12	20.59	27.85	4.39	3.57	1.41	94.93		0.104	0.149	0.652	0.042		1.000	Poor
1749	1039-2	Hushe	Karakorum	35.81	20.38	29.59	4.30	2.99	1.24	94.31		0.103	0.126	0.702	0.038		1.000	Poor
1748	25-1	Braldu	Karakorum	37.92	19.99	32.49	0.90	3.75	1.75	96.81		0.021	0.154	0.748	0.050		1.000	Poor
1748	58-1	Braldu	Karakorum	35.41	19.87	27.09	9.74	2.82	1.38	96.31		0.231	0.118	0.600	0.018	0.024	1.000	Good
1748	103-1	Braldu	Karakorum	36.42	20.21	34.70	0.77	2.56	1.77	96.43		0.018	0.106	0.809	0.053		1.000	Poor
1748	150-1	Braldu	Karakorum	36.06	19.37	33.72	5.91	2.05	0.98	98.11		0.139	0.085	0.725		0.029	1.000	Superior
1748	156-1	Braldu	Karakorum	35.61	18.88	26.55	1.57	1.16	7.69	91.46		0.039	0.051	0.648	0.237		1.000	Poor
1748	160-1	Braldu	Karakorum	34.82	19.83	26.00	16.86	0.88	0.42	98.81		0.397	0.036	0.492		0.013	1.000	Good
1748	184-1	Braldu	Karakorum	34.63	17.90	27.91	0.17	0.75	3.64	84.99		0.005	0.035	0.739	0.124		1.000	Poor
1748	185-1	Braldu	Karakorum	34.66	19.17	28.48	9.18	1.98	2.21	95.68		0.220	0.084	0.611	0.018	0.050	1.000	Good
1748	265-1	Braldu	Karakorum	36.17	19.90	33.22	9.72	1.82	1.78	102.62		0.219	0.072	0.588		0.051	1.000	Fair
1748	274-1	Braldu	Karakorum	36.82	19.94	35.75	0.89	3.51	1.56	98.47	0.010	0.021	0.130	0.795	0.016	0.030	1.000	Superior
1748	276-1	Braldu	Karakorum	36.72	19.53	36.72	0.25	1.83	1.97	97.02		0.006	0.076	0.858	0.025		1.000	Poor
1748	283-1	Braldu	Karakorum	36.67	19.39	34.49	0.05	1.95	3.69	96.24	0.002	0.001	0.079	0.807	0.072		1.000	Poor
1748	300-1	Braldu	Karakorum	36.76	19.70	29.21	5.39	1.49	7.32	99.87		0.123	0.060	0.596	0.144	0.067	1.000	Excellent
1748	310-1	Braldu	Karakorum	35.89	19.34	27.72	9.56	2.52	1.12	96.16	0.025	0.228	0.072	0.642	0.019	0.015	1.000	Excellent
1748	324-1	Braldu	Karakorum	39.89	20.55	31.88	1.00	3.90	1.92	99.15		0.023	0.156	0.715	0.055		1.000	Poor
1748	352-1	Braldu	Karakorum	39.52	21.59	30.54	2.02	2.50	3.10	99.26		0.046	0.100	0.686	0.089		1.000	Poor
1748	363-1	Braldu	Karakorum	36.30	19.85	26.06	13.00	2.87	0.87	98.94		0.301	0.117	0.527		0.025	1.000	Superior
1748	367-1	Braldu	Karakorum	35.73	19.61	36.74	0.95	1.95	1.94	96.92		0.023	0.081	0.837	0.027	0.031	1.000	Excellent
1748	384-1	Braldu	Karakorum	35.92	19.43	35.11	5.78	2.70	1.43	100.36		0.132	0.109	0.644		0.041	1.000	Good
1748	416-1	Braldu	Karakorum	36.78	19.13	36.59	0.84	3.20	1.42	97.95	0.036	0.020	0.084	0.819	0.008	0.034	1.000	Superior
1748	453-1	Braldu	Karakorum	37.51	20.55	34.35	1.08	2.94	3.42	99.86	0.018	0.025	0.093	0.766	0.091	0.007	1.000	Superior
1748	481-1	Braldu	Karakorum	36.69	20.15	36.91	0.10	2.11	3.85	99.82		0.002	0.085	0.793	0.070	0.041	1.000	Superior
1748	515-1	Braldu	Karakorum	34.94	19.00	30.72	11.12	1.23	0.82	97.81		0.264	0.051	0.595		0.025	1.000	Good
1748	581-1	Braldu	Karakorum	37.90	20.32	32.24	1.66	2.75	1.98	96.84		0.039	0.113	0.746	0.059		1.000	Poor
1748	653-1	Braldu	Karakorum	36.92	19.20	37.41	0.17	2.14	4.30	100.14		0.004	0.086	0.782	0.039	0.085	1.000	Superior
1748	659-1	Braldu	Karakorum	37.42	20.21	35.31	0.62	4.00	1.26	98.85	0.032	0.014	0.119	0.799	0.034		1.000	Excellent
1748	743-1	Braldu	Karakorum	35.88	19.20	36.14	2.14	3.16	1.24	97.75		0.050	0.130	0.743		0.037	1.000	Superior
1748	752-1	Braldu	Karakorum	35.50	19.55	33.03	3.96	3.00	1.37	96.41		0.094	0.125	0.732	0.002	0.039	1.000	Excellent
1748	776-1	Braldu	Karakorum	35.31	19.25	28.97	7.95	2.10	1.22	94.80	0.025	0.192	0.057	0.689	0.034	0.004	1.000	Good
1748	11-2	Braldu	Karakorum	35.59	19.23	26.95	14.92	1.23	0.93	98.85		0.350	0.051	0.520		0.028	1.000	Excellent
1748	28-2	Braldu	Karakorum	36.64	19.58	34.94	0.32	3.21	2.16	96.85	0.040	0.008	0.080	0.809	0.062		1.000	Good
1748	41-2	Braldu	Karakorum	37.39	19.91	34.37	0.44	5.60	1.10	98.81	0.006	0.010	0.215	0.718		0.032	1.000	Superior
1748	55-2	Braldu	Karakorum	36.49	19.23	37.06	0.18	0.75	3.49	97.20	0.022	0.004		0.869	0.080		1.000	Fair
1748	78-2	Braldu	Karakorum	36.85	20.03	34.92	1.09	2.94	1.21	97.04		0.026	0.121	0.809	0.025		1.000	Fair
1748	93-2	Braldu	Karakorum	38.67	19.46	31.80	4.30	4.63	2.09	100.95	0.064	0.096	0.098	0.684	0.031	0.028	1.000	Superior
1748	100-2	Braldu	Karakorum	35.88	18.85	28.83	15.69	0.69	0.81	100.74		0.364	0.028	0.494		0.024	1.000	Excellent
1748	146-2	Braldu	Karakorum	37.09	19.58	32.67	8.82	2.90	1.70	102.76		0.197	0.114	0.569		0.048	1.000	Fair
1748	182-2	Braldu	Karakorum	39.32	19.96	2.51	0.21	0.42	33.44	95.85		0.005	0.016	0.038	0.867		1.000	Poor
1748	201-2	Braldu	Karakorum	37.07	19.78	35.26	1.56	2.16	1.21	97.03		0.037	0.090	0.822	0.026		1.000	Poor
1748	213-2	Braldu	Karakorum	39.30	30.52	0.71	0.50	0.00	22.45	93.49		0.011		0.016	0.639		1.000	Poor
1748	215-2	Braldu	Karakorum	38.34	20.41	35.52	0.71	4.04	1.17	100.18	0.007	0.016	0.151	0.792	0.003		1.000	Fair
1748	226-2	Braldu	Karakorum	35.99	18.61	26.19	4.86	0.30	0.45	86.40		0.129	0.014	0.688	0.015		1.000	Poor
1748	245-2	Braldu	Karakorum	37.19	19.22	34.66	1.71	2.00	1.59	96.38		0.041	0.084	0.814	0.016		1.000	Poor
1748	261-2	Braldu	Karakorum	36.54	20.06	32.64	7.30	3.05	0.93	100.52		0.166	0.122	0.638		0.027	1.000	Excellent
1748	349-2	Braldu	Karakorum	36.67	18.93	30.16	3.57	1.55	0.86	91.74		0.089	0.068	0.744	0.027		1.000	Poor
1748	353-2	Braldu	Karakorum	37.14	19.33	38.23	0.66	2.55	1.60	99.50	0.033	0.015	0.060	0.846	0.010	0.037	1.000	Superior
1748	424-2	Braldu	Karakorum	37.40	19.86	35.75	0.34	2.47	2.11	97.93		0.008	0.101	0.823	0.034		1.000	Poor
1748	431-2	Braldu	Karakorum	36.05	19.64	33.44	1.86	1.66	1.22	93.88		0.045	0.071	0.806	0.038		1.000	Poor
1748	522-2	Braldu	Karakorum	36.64	19.15	26.16	4.97	0.00	0.80	87.73		0.130		0.677	0.027		1.000	Poor
1748	525-2	Braldu	Karakorum	37.53	20.30	38.30	0.14	1.96	1.89	100.11	0.011	0.003	0.064	0.867	0.037		1.000	Good
1748	611-2	Braldu	Karakorum	38.37	19.92	33.28	1.10	4.18	1.20	98.06		0.025	0.169	0.756	0.006		1.000	Poor
1748	621-2	Braldu	Karakorum	37.04	19.02	32.51	1.03	4.34	1.10	95.04	0.002	0.024	0.179	0.739			1.000	Poor
1748	628-2	Braldu	Karakorum	36.91	18.94	33.98	0.11	2.65	3.39	95.96	0.029	0.003	0.072	0.795	0.067		1.000	Poor
1748	657-2	Braldu	Karakorum	35.68	18.65	28.00	3.59	1.27	0.79	87.98		0.093	0.058	0.719	0.026		1.000	Poor
1748	659-2	Braldu	Karakorum	38.22	19.48	25.57	0.42	4.45	7.08	95.22		0.010	0.182	0.587	0.167		1.000	Poor
1748	749-2	Braldu	Karakorum	36.74	19.83	35.47	1.37	2.34	1.66	97.40	0.001	0.032	0.095	0.822	0.022		1.000	Fair
1748	752-2	Braldu	Karakorum	38.29	20.71	34.34	0.61	3.98	2.89	100.82	0.032	0.014	0.114	0.759	0.081		1.000	Excellent
1748	774-2	Braldu	Karakorum	36.95	20.00	37.99	0.20	2.57	1.99	99.71	0.003	0.005	0.099	0.835	0.019	0.039	1.000	Superior
1748	795-2	Braldu	Karakorum	37.02	19.65	33.78	1.48	2.85	1.39	96.17		0.035	0.119	0.790	0.028		1.000	Poor
1748	799-2	Braldu	Karakorum	37.73	19.70	33.86	1.71	1.68	1.93	96.61		0.041	0.070	0.793	0.058		1.000	Poor
1748	814-2	Braldu	Karakorum	36.37	19.44	31.69	1.13	3.20	1.99	93.82		0.027	0.136	0.755	0.061		1.000	Poor
1437	26-1	Upper Hunza	Karakorum	40.46	20.68	2.82	0.35	0.35	34.88	99.54		0.008	0.013	0.034	0.871	0.003	1.000	Fair
1437	212-1	Upper Hunza	Karakorum	39.69	23.38	12.46	0.36	0.22	22.94	99.05		0.008	0.009	0.270	0.637		1.000	Poor
1437	58-2	Upper Hunza	Karakorum	36.18	9.41	14.87	0.25	0.54	34.61	95.86					0.433	0.509	1.000	Poor
1437	62-2	Upper Hunza	Karakorum	39.06	20.96	38.23	1.35	3.63	1.48	104.71	0.008	0.029	0.128	0.794	0.000	0.041	1.000	Excellent
1437	81-2	Upper Hunza	Karakorum	39.23	20.17	22.12	3.37	1.16	14.69	100.74	0.029	0.075		0.485	0.375		1.000	Fair
1437	251-2	Upper Hunza	Karakorum	41.30	20.57	3.91	0.24	0.94	35.56	102.52	0.020	0.005		0.039	0.849	0.062	1.000	Fair
1437	257-2	Upper Hunza	Karakorum	38.16	19.73	34.10	5.36	1.42	1.78	100.55	0.012	0.123	0.042	0.772	0.008		1.000	Poor
1437	347-2	Upper Hunza	Karakorum	39.73	20.19	26.82	2.15	1.24	13.51	103.64	0.030	0.047		0.553	0.315	0.033	1.000	Fair

Sample	Points	River/Dune	Domain	SiO_2	Al_2O_3	FeO	MnO	MgO	CaO	Total	Majorite	Spessartine	Pyrope	Almandine	Grossular	Andradite	Total	Quality
				wt%	wt%	wt%	wt%	wt%	wt%		$\{Mg_3\}[SiMg](Si_3)O_{12}$	$\{Mn_3\}[Al_2](Si_3)O_{12}$	$\{Mg_3\}[Al_2](Si_3)O_{12}$	$\{Fe_3\}[Al_2](Si_3)O_{12}$	$\{Ca_3\}[Al_2](Si_3)O_{12}$	$\{Ca_3\}[Fe_2](Si_3)O_{12}$		index
1438	1-1	Hispar	Karakorum	37.81	21.22	32.76	1.51	3.55	2.00	98.85		0.035	0.143	0.739	0.058		1.000	Poor
1438	9-1	Hispar	Karakorum	37.56	21.30	19.07	10.11	1.56	5.35	94.95		0.240	0.065	0.447	0.161		1.000	Poor
1438	16-1	Hispar	Karakorum	38.11	21.68	31.08	0.78	5.88	1.04	98.57		0.018	0.233	0.692	0.030		1.000	Poor
1438	25-1	Hispar	Karakorum	36.95	21.01	31.30	0.53	2.75	5.35	97.89		0.012	0.111	0.711	0.156		1.000	Good
1438	47-1	Hispar	Karakorum	40.19	23.69	30.10	4.00	3.32	1.38	102.68		0.088	0.128	0.651	0.038		1.000	Poor
1438	49-1	Hispar	Karakorum	40.92	23.94	32.04	0.88	4.14	4.33	106.25		0.019	0.153	0.665	0.115		1.000	Poor
1438	54-1	Hispar	Karakorum	38.74	21.46	30.97	2.42	2.69	3.32	99.60		0.055	0.107	0.694	0.095		1.000	Poor
1438	65-1	Hispar	Karakorum	39.31	23.15	33.80	1.17	3.09	2.47	102.98		0.026	0.119	0.731	0.068		1.000	Poor
1438	66-1	Hispar	Karakorum	39.00	22.72	34.65	0.86	3.44	2.01	102.68		0.019	0.133	0.752	0.056		1.000	Poor
1438	67-1	Hispar	Karakorum	38.90	22.90	32.47	1.89	4.28	1.80	102.24		0.042	0.165	0.703	0.050		1.000	Poor
1438	87-1	Hispar	Karakorum	38.54	21.47	2.43	0.66	0.33	34.38	97.81		0.014	0.013	0.017	0.917	0.029	1.000	Superior
1438	88-1	Hispar	Karakorum	35.73	21.63	33.43	2.00	3.37	1.20	97.36		0.047	0.138	0.761	0.035		1.000	Excellent
1438	93-1	Hispar	Karakorum	37.15	21.01	33.68	1.12	4.30	1.35	98.61		0.026	0.173	0.760	0.039		1.000	Good
1438	107-1	Hispar	Karakorum	37.43	21.16	30.94	2.96	3.73	1.74	97.97		0.068	0.151	0.703	0.051		1.000	Poor
1438	108-1	Hispar	Karakorum	37.89	21.65	33.66	1.45	4.14	1.68	100.47		0.033	0.163	0.745	0.048		1.000	Fair
1438	110-1	Hispar	Karakorum	37.76	21.77	32.84	0.29	3.32	4.08	100.05		0.007	0.131	0.729	0.116		1.000	Fair
1438	111-1	Hispar	Karakorum	37.39	22.10	30.80	3.78	2.89	1.71	98.65		0.087	0.117	0.697	0.050		1.000	Poor
1438	114-1	Hispar	Karakorum	38.49	21.81	32.62	0.92	5.43	1.25	100.53		0.020	0.212	0.715	0.035		1.000	Fair
1438	127-1	Hispar	Karakorum	35.38	21.13	23.62	9.41	1.22	1.25	92.01		0.233	0.053	0.578	0.039		1.000	Poor
1438	132-1	Hispar	Karakorum	37.22	20.48	32.33	2.11	4.44	1.06	97.64		0.049	0.180	0.736	0.021		1.000	Fair
1438	147-1	Hispar	Karakorum	37.29	21.13	34.48	0.52	3.81	2.30	99.54		0.012	0.152	0.768	0.065	0.001	1.000	Superior
1438	148-1	Hispar	Karakorum	36.72	20.90	30.98	3.41	2.72	1.79	96.52		0.080	0.113	0.719	0.053		1.000	Poor
1438	149-1	Hispar	Karakorum	37.15	21.44	33.54	1.02	1.62	3.85	98.63		0.024	0.066	0.764	0.112		1.000	Poor
1438	151-1	Hispar	Karakorum	37.55	21.61	34.33	0.77	3.76	1.83	99.84		0.017	0.150	0.766	0.052		1.000	Fair
1438	157-1	Hispar	Karakorum	51.53	0.29	13.88	1.02	8.52	23.57	98.80	0.017	0.013					1.000	Poor
1438	182-1	Hispar	Karakorum	36.79	20.86	31.60	2.10	3.41	2.22	96.98		0.049	0.140	0.726	0.065		1.000	Poor
1438	190-1	Hispar	Karakorum	37.61	21.85	32.24	0.43	2.23	5.79	100.15		0.010	0.089	0.717	0.165		1.000	Fair
1438	204-1	Hispar	Karakorum	37.91	21.41	31.46	1.16	4.31	1.96	98.20		0.027	0.173	0.709	0.057		1.000	Poor
1438	205-1	Hispar	Karakorum	37.27	20.90	26.28	3.75	4.24	4.88	97.34		0.086	0.171	0.594	0.141		1.000	Good
1438	207-1	Hispar	Karakorum	36.28	21.44	34.78	0.99	3.17	0.88	97.54		0.023	0.130	0.799	0.026		1.000	Fair
1438	216-1	Hispar	Karakorum	37.32	21.44	34.21	1.03	3.82	1.45	99.27		0.023	0.153	0.768	0.042		1.000	Fair
1438	219-1	Hispar	Karakorum	37.14	20.98	30.46	4.10	2.71	1.38	96.78		0.096	0.112	0.705	0.041		1.000	Poor
1438	11-2	Hispar	Karakorum	36.65	20.41	20.45	12.89	0.81	0.69	91.89		0.321	0.036	0.503	0.022		1.000	Poor
1438	20-2	Hispar	Karakorum	36.65	21.76	32.87	0.96	2.17	3.75	98.15		0.022	0.088	0.749	0.110		1.000	Fair
1438	33-2	Hispar	Karakorum	37.07	21.00	36.09	0.42	2.27	3.00	99.86		0.010	0.091	0.812	0.087	0.000	1.000	Superior
1438	45-2	Hispar	Karakorum	37.73	21.81	31.83	1.57	2.44	5.11	100.50		0.035	0.097	0.706	0.145		1.000	Fair
1438	48-2	Hispar	Karakorum	37.98	20.83	34.00	1.53	3.74	1.50	99.58		0.035	0.150	0.763	0.041		1.000	Fair
1438	50-2	Hispar	Karakorum	37.52	22.01	35.21	0.92	3.34	1.45	100.44		0.021	0.133	0.784	0.041		1.000	Fair
1438	55-2	Hispar	Karakorum	37.19	22.14	24.41	9.47	2.35	0.54	96.10		0.223	0.098	0.568	0.016		1.000	Poor
1438	61-2	Hispar	Karakorum	38.43	22.48	34.90	1.00	4.55	1.49	102.85		0.022	0.175	0.753	0.041		1.000	Good
1438	63-2	Hispar	Karakorum	36.98	22.35	32.80	2.67	3.76	1.20	99.75		0.060	0.150	0.732	0.034		1.000	Fair
1438	66-2	Hispar	Karakorum	38.78	22.38	24.55	3.89	4.22	4.62	98.44		0.088	0.167	0.546	0.132		1.000	Poor
1438	84-2	Hispar	Karakorum	36.95	21.40	35.37	1.47	2.70	1.21	99.10		0.034	0.109	0.802	0.035		1.000	Fair
1438	85-2	Hispar	Karakorum	36.01	21.35	33.95	0.88	3.18	1.92	97.29		0.021	0.130	0.780	0.057		1.000	Good
1438	88-2	Hispar	Karakorum	37.10	21.08	31.08	1.04	0.86	6.10	97.27		0.024	0.035	0.717	0.180		1.000	Poor
1438	96-2	Hispar	Karakorum	37.27	21.73	31.05	3.34	3.32	1.21	97.93		0.077	0.135	0.707	0.035		1.000	Poor
1438	98-2	Hispar	Karakorum	36.88	21.39	32.93	0.89	2.37	3.37	97.82		0.021	0.097	0.753	0.099		1.000	Poor
1438	116-2	Hispar	Karakorum	36.30	21.56	33.81	1.64	2.88	1.74	97.93		0.038	0.117	0.773	0.051		1.000	Fair
1438	121-2	Hispar	Karakorum	37.32	21.56	31.60	1.38	5.39	1.20	98.46		0.031	0.215	0.707	0.034		1.000	Good
1438	123-2	Hispar	Karakorum	37.24	21.55	30.69	3.26	2.55	1.39	96.69		0.076	0.105	0.710	0.041		1.000	Poor
1438	129-2	Hispar	Karakorum	36.31	20.85	33.48	0.94	2.29	2.22	96.10		0.022	0.095	0.782	0.066		1.000	Poor
1438	135-2	Hispar	Karakorum	36.86	20.97	31.19	0.63	3.45	2.54	95.65		0.015	0.143	0.724	0.076		1.000	Poor
1438	136-2	Hispar	Karakorum	36.74	21.23	32.31	1.77	4.29	1.29	97.63		0.041	0.174	0.735	0.038		1.000	Good
1438	140-2	Hispar	Karakorum	37.90	21.52	30.13	4.04	3.19	1.57	98.35		0.093	0.129	0.683	0.046		1.000	Poor
1438	146-2	Hispar	Karakorum	37.89	22.27	23.11	4.25	3.75	6.94	98.22		0.096	0.149	0.515	0.198		1.000	Poor
1438	150-2	Hispar	Karakorum	37.66	22.50	30.81	1.01	5.63	1.81	99.42		0.023	0.221	0.679	0.051		1.000	Fair
1438	158-2	Hispar	Karakorum	36.67	21.82	32.49	1.81	3.74	1.45	98.00		0.042	0.151	0.738	0.042		1.000	Fair
1438	160-2	Hispar	Karakorum	37.78	22.04	32.08	2.65	3.24	1.76	99.54		0.060	0.129	0.719	0.051		1.000	Poor
1438	161-2	Hispar	Karakorum	36.60	21.63	34.86	1.45	2.61	2.17	99.34		0.033	0.105	0.788	0.063		1.000	Excellent
1438	165-2	Hispar	Karakorum	39.40	33.97	1.02	0.24	0.13	25.14	99.90		0.005	0.005	0.021	0.667		1.000	Poor
1438	173-2	Hispar	Karakorum	37.21	22.02	33.75	1.39	3.39	1.51	99.27		0.032	0.136	0.759	0.044		1.000	Fair
1438	177-2	Hispar	Karakorum	38.04	22.08	29.32	4.85	2.79	1.48	98.56		0.111	0.113	0.664	0.043		1.000	Poor
1438	179-2	Hispar	Karakorum	38.19	22.15	31.95	0.88	5.05	1.62	99.84		0.020	0.199	0.705	0.046		1.000	Poor
1438	199-2	Hispar	Karakorum	37.36	21.76	31.69	1.16	4.11	2.35	98.43		0.026	0.165	0.713	0.068		1.000	Poor
1438	201-2	Hispar	Karakorum	36.82	21.40	33.64	0.95	3.07	1.32	97.21		0.022	0.126	0.774	0.039		1.000	Poor
1438	204-2	Hispar	Karakorum	36.97	21.34	31.16	3.22	2.29	1.45	96.43		0.076	0.095	0.725	0.043		1.000	Poor
1438	206-2	Hispar	Karakorum	36.90	21.42	30.69	2.61	4.02	1.19	96.83		0.061	0.164	0.704	0.035		1.000	Poor
1438	212-2	Hispar	Karakorum	37.33	21.78	30.53	1.99	4.39	0.95	96.97		0.046	0.179	0.696	0.028		1.000	Poor
1438	219-2	Hispar	Karakorum	37.20	21.26	29.49	4.30	3.40	1.53	97.18		0.100	0.139	0.676	0.045		1.000	Poor
1438	224-2	Hispar	Karakorum	39.51	22.07	3.44	1.14	0.12	33.14	99.43	0.002	0.025		0.073	0.893	0.001	1.000	Superior
1438	225-2	Hispar	Karakorum	36.94	21.24	16.08	8.55	1.14	8.82	92.77		0.206	0.048	0.382	0.269		1.000	Poor
1438	246-2	Hispar	Karakorum	38.06	20.03	5.82	0.86	0.00	32.18	96.95		0.019		0.075	0.831	0.073	1.000	Excellent
1438	253-2	Hispar	Karakorum	37.88	22.47	30.28	4.13	3.59	1.32	99.67		0.093	0.143	0.676	0.038		1.000	Poor
1438	8-3	Hispar	Karakorum	36.84	21.42	34.25	0.31	3.36	1.86	98.04		0.007	0.136	0.780	0.054		1.000	Poor
1438	14-3	Hispar	Karakorum	37.17	21.62	32.31	1.07	2.16	3.41	97.74		0.025	0.088	0.739	0.100		1.000	Poor
1438	24-3	Hispar	Karakorum	36.66	21.10	33.67	1.08	3.98	1.41	97.90		0.025	0.161	0.766	0.041		1.000	Excellent
1438	34-3	Hispar	Karakorum	36.61	21.16	31.67	3.32	2.94	1.29	96.99		0.078	0.121	0.731	0.038		1.000	Poor
1438	36-3	Hispar	Karakorum	37.82	21.13	33.20	1.22	4.42	1.31	99.11		0.028	0.177	0.744	0.038		1.000	Fair
1438	38-3	Hispar	Karakorum	37.04	21.02	31.41	2.23	3.93	2.24	97.88		0.051	0.159	0.713	0.065		1.000	Fair
1438	39-3	Hispar	Karakorum	37.63	21.33	19.77	5.51	1.33	10.71	96.27		0.128	0.054	0.453	0.314		1.000	Poor
1438	45-3	Hispar	Karakorum	38.68	21.79	33.98	0.91	3.67	2.05	101.07		0.020	0.144	0.749	0.058		1.000	Poor
1438	46-3	Hispar	Karakorum	37.67	21.30	34.10	1.80	3.21	0.99	99.06		0.041	0.129	0.771	0.029		1.000	Poor
1438	49-3	Hispar	Karakorum	37.88	22.18	32.25	0.00	2.57	6.53	101.41			0.100	0.706	0.183		1.000	Good
1438	53-3	Hispar	Karakorum	38.11	21.93	37.95	0.42	3.71	0.85	102.97		0.009	0.144	0.815	0.024		1.000	Excellent
1438	55-3	Hispar	Karakorum	37.61	21.65	30.62	3.58	3.42	1.56	98.45		0.082	0.138	0.693	0.045		1.000	Poor
1438	56-3	Hispar	Karakorum	38.17	21.99	33.96	0.58	2.84	3.89	101.43		0.013	0.111	0.747	0.110		1.000	Poor
1438	63-3	Hispar	Karakorum	37.60	21.94	33.61	1.30	3.73	1.37	99.56		0.030	0.149	0.752	0.039		1.000	Poor
1438	69-3	Hispar	Karakorum	37.70	22.01	34.23	2.05	3.07	1.65	100.71		0.046	0.122	0.761	0.047		1.000	Poor
1438	75-3	Hispar	Karakorum	39.25	21.83	2.63	0.41	0.33	34.23	98.68		0.009	0.013	0.044	0.917	0.017	1.000	Superior
1438	78-3	Hispar	Karakorum	37.18	21.40	30.88	1.03	5.14	2.03	97.66		0.024	0.207	0.696	0.059		1.000	Fair
1438	85-3	Hispar	Karakorum	35.35	20.88	25.87	8.34	0.68	1.13	92.26		0.207	0.030	0.635	0.036		1.000	Poor
1438	87-3	Hispar	Karakorum	36.93	21.19	31.38	1.71	4.22	1.31	96.75		0.040	0.172	0.719	0.039		1.000	Poor
1438	93-3	Hispar	Karakorum	36.68	21.03	32.37	0.99	2.30	4.72	98.10		0.023	0.093	0.738	0.138		1.000	Excellent
1438	98-3	Hispar	Karakorum	38.98	20.17	4.57	1.54	0.32	32.85	98.45	0.009	0.034		0.052	0.833	0.070	1.000	Superior
1438	99-3	Hispar	Karakorum	36.88	20.60	30.77	3.07	3.61	1.26	96.19		0.072	0.149	0.713	0.037		1.000	Poor
1438	101-3	Hispar	Karakorum	37.30	22.22	23.83	9.48	1.21	0.47	94.51		0.228	0.051	0.567	0.014		1.000	Poor
1438	104-3	Hispar	Karakorum	37.70	21.77	33.93	0.90	4.01	1.75	100.07		0.020	0.159	0.754	0.050		1.000	Fair
1438	108-3	Hispar	Karakorum	38.62	22.25	33.13	2.39	2.92	3.04	102.36		0.053	0.114	0.723	0.085		1.000	Poor
4430	6-2	Domkar	Ladakh	37.77	20.29	31.10	6.24	1.10	0.63	97.14		0.148	0.046	0.728	0.019		1.000	Poor
4430	86-2	Domkar	Ladakh	38.69	6.67	24.39	0.32	0.00	29.07	99.15		0.007		0.148	0.164	0.534	1.000	Poor

Sample	Points	River/Dune	Domain	SiO_2	Al_2O_3	FeO	MnO	MgO	CaO	Total	Majorite	Spessartine	Pyrope	Almandine	Grossular	Andradite	Total	Quality
				wt%	wt%	wt%	wt%	wt%	wt%		$\{Mg_3\}[SiMg](Si_3)O_{12}$	$\{Mn_3\}[Al_2](Si_3)O_{12}$	$\{Mg_3\}[Al_2](Si_3)O_{12}$	$\{Fe_3\}[Al_2](Si_3)O_{12}$	$\{Ca_3\}[Al_2](Si_3)O_{12}$	$\{Ca_3\}[Fe_2](Si_3)O_{12}$		index
1439	74-1	Kandia	Kohistan	38.94	33.31	0.82	0.32	0.15	23.52	97.07		0.007	0.006	0.018	0.643		1.000	Poor
1439	79-1	Kandia	Kohistan	37.07	21.58	28.09	5.31	3.21	1.40	96.66		0.124	0.132	0.647	0.041		1.000	Poor
1439	141-1	Kandia	Kohistan	37.43	21.00	11.08	3.87	0.39	23.13	96.91		0.087	0.016	0.234	0.648	0.012	1.000	Excellent
1439	223-1	Kandia	Kohistan	39.96	33.53	1.53	0.35	0.00	23.16	98.53		0.008		0.032	0.625		1.000	Poor
1439	281-1	Kandia	Kohistan	38.84	33.24	1.28	0.08	0.42	23.86	97.71		0.002	0.016	0.027	0.647		1.000	Poor
1439	25-2	Kandia	Kohistan	44.55	10.04	12.50	0.59	14.47	10.30	92.45	0.413	0.013		0.279	0.181		1.000	Poor
1439	64-2	Kandia	Kohistan	38.54	33.30	0.30	0.21	0.20	23.66	96.21		0.005	0.008	0.006	0.651		1.000	Poor
1439	107-2	Kandia	Kohistan	39.58	33.02	1.08	0.22	0.19	23.32	97.41		0.005	0.007	0.023	0.635		1.000	Poor
1439	160-2	Kandia	Kohistan	36.19	30.12	1.37	0.17	0.24	19.21	87.30		0.004	0.010	0.033	0.584		1.000	Poor
1440	223-1	Swat	Kohistan	51.29	2.62	22.46	0.72	22.13	0.85	100.07	0.547	0.015		0.100		0.023	1.000	Poor
1440	39-2	Swat	Kohistan	38.12	21.12	24.79	2.44	4.73	8.47	99.68		0.054	0.185	0.521	0.213	0.025	1.000	Superior
1440	76-2	Swat	Kohistan	37.60	24.19	6.58	0.50	2.00	21.54	92.40		0.012	0.081	0.150	0.627		1.000	Poor
1440	230-2	Swat	Kohistan	38.87	19.65	5.38	0.64	0.39	33.13	98.06	0.010	0.014		0.058	0.826	0.087	1.000	Superior
4419	58-1	Zanskar	Himalaya	38.07	18.70	28.02	1.44	6.47	5.96	98.65	0.022	0.032	0.226	0.551	0.065	0.104	1.000	Superior
4419	66-1	Zanskar	Himalaya	37.66	18.67	31.10	7.30	1.90	1.23	97.87	0.028	0.172	0.041	0.704			1.000	Poor
4419	11-2	Zanskar	Himalaya	37.45	18.94	29.18	6.91	3.02	1.30	96.80	0.015	0.163	0.105	0.663			1.000	Poor
4419	14-2	Zanskar	Himalaya	38.04	18.28	33.45	4.64	2.24	1.08	97.72	0.034	0.109	0.048	0.741			1.000	Poor
4419	16-2	Zanskar	Himalaya	37.57	18.53	33.22	6.34	1.94	0.84	98.44	0.058	0.149		0.758			1.000	Fair
4419	17-2	Zanskar	Himalaya	37.56	18.61	30.56	5.61	3.61	1.64	97.59	0.090	0.131	0.028	0.703	0.044		1.000	Excellent
4419	18-2	Zanskar	Himalaya	38.36	19.41	32.78	3.03	4.08	1.85	99.52	0.066	0.069	0.076	0.736	0.041		1.000	Good
4419	38-2	Zanskar	Himalaya	37.92	17.86	22.17	6.65	1.24	11.84	97.69	0.015	0.154		0.485	0.224	0.032	1.000	Poor
4419	81-2	Zanskar	Himalaya	37.79	18.55	30.17	7.64	2.35	0.96	97.46	0.023	0.180	0.067	0.665			1.000	Poor
4419	98-2	Zanskar	Himalaya	37.09	17.94	33.59	5.04	2.31	0.94	96.91	0.064	0.120		0.770			1.000	Poor
4419	107-2	Zanskar	Himalaya	37.59	18.34	32.67	3.74	2.40	2.11	96.85	0.042	0.088	0.044	0.763	0.010		1.000	Poor
4419	120-2	Zanskar	Himalaya	36.96	18.21	32.50	5.53	1.98	1.11	96.28	0.050	0.132	0.016	0.761			1.000	Poor
4419	122-2	Zanskar	Himalaya	37.88	18.11	24.54	5.27	2.75	7.94	96.49	0.078	0.123		0.565	0.194		1.000	Poor
4419	123-2	Zanskar	Himalaya	37.62	18.82	33.91	1.33	2.81	3.05	97.54	0.055	0.031	0.042	0.782	0.062		1.000	Fair
4419	124-2	Zanskar	Himalaya	37.12	18.40	30.67	6.34	2.51	1.56	96.60	0.060	0.150	0.024	0.718	0.018		1.000	Poor
4419	127-2	Zanskar	Himalaya	38.19	18.27	33.29	1.97	3.64	2.35	97.70	0.083	0.046	0.038	0.764	0.039		1.000	Fair
4419	147-2	Zanskar	Himalaya	39.25	18.74	22.53	1.03	8.55	6.39	96.49	0.120	0.023	0.178	0.498	0.179	0.002	1.000	Excellent
4419	148-2	Zanskar	Himalaya	37.87	18.57	32.83	5.45	2.49	1.44	98.66	0.076	0.127	0.001	0.754	0.020		1.000	Fair
4419	160-2	Zanskar	Himalaya	37.82	17.92	31.60	5.14	3.41	1.47	97.36	0.105	0.121		0.731	0.025		1.000	Good
4419	166-2	Zanskar	Himalaya	38.25	18.55	32.90	4.74	2.63	1.14	98.20	0.031	0.111	0.066	0.727			1.000	Poor
4419	169-2	Zanskar	Himalaya	36.30	18.09	33.27	5.14	2.06	1.05	95.92	0.057	0.124		0.784		0.003	1.000	Fair
4419	178-2	Zanskar	Himalaya	37.43	18.76	31.65	6.45	2.05	1.30	97.64	0.034	0.152	0.039	0.731			1.000	Poor
4419	182-2	Zanskar	Himalaya	37.33	17.78	33.21	5.27	2.47	1.16	97.20	0.065	0.125		0.754			1.000	Poor
4419	184-2	Zanskar	Himalaya	36.94	18.37	31.29	8.03	0.92	0.86	96.41	0.006	0.193	0.031	0.698			1.000	Poor
4419	187-2	Zanskar	Himalaya	36.97	18.95	34.01	4.31	2.39	0.89	97.53	0.054	0.102	0.028	0.791	0.012		1.000	Good
4419	190-2	Zanskar	Himalaya	36.75	18.21	31.54	4.08	2.76	2.55	95.89	0.085	0.097		0.741	0.066		1.000	Fair
4419	208-2	Zanskar	Himalaya	36.97	18.48	35.89	2.22	2.38	1.19	97.12	0.074	0.053		0.838	0.022		1.000	Good
4419	221-2	Zanskar	Himalaya	37.32	18.58	39.23	0.77	2.52	1.54	99.97	0.044	0.018	0.044	0.832		0.045	1.000	Superior
4419	222-2	Zanskar	Himalaya	37.14	18.63	37.28	1.04	3.01	0.97	98.08	0.073	0.024	0.026	0.848	0.010	0.018	1.000	Excellent
4419	229-2	Zanskar	Himalaya	37.09	18.23	30.63	6.39	3.15	1.64	97.12	0.089	0.150	0.012	0.700	0.033	0.016	1.000	Superior
4419	259-2	Zanskar	Himalaya	37.32	18.91	30.33	6.76	2.43	1.55	97.31	0.032	0.159	0.058	0.705	0.007		1.000	Fair
4419	267-2	Zanskar	Himalaya	37.76	18.82	30.83	3.03	2.92	3.54	96.89	0.028	0.071	0.084	0.713	0.052		1.000	Poor
4419	281-2	Zanskar	Himalaya	37.39	19.01	32.30	7.17	1.89	1.34	99.10	0.052	0.167		0.742	0.014		1.000	Fair
4419	284-2	Zanskar	Himalaya	37.76	18.61	37.51	1.07	3.08	1.28	99.30	0.085	0.025	0.012	0.841	0.018	0.020	1.000	Superior
4419	291-2	Zanskar	Himalaya	36.80	18.40	31.99	6.44	2.34	0.97	96.94	0.069	0.153		0.749	0.009		1.000	Poor
4419	297-2	Zanskar	Himalaya	37.85	18.73	26.41	1.91	4.30	7.57	96.77	0.085	0.044	0.061	0.590	0.205	0.015	1.000	Excellent
4419	299-2	Zanskar	Himalaya	37.57	18.32	35.07	3.04	2.93	1.05	98.00	0.088	0.071		0.810	0.013		1.000	Good
4419	315-2	Zanskar	Himalaya	36.83	18.04	29.46	6.00	2.34	4.04	96.71	0.070	0.142		0.667	0.080	0.030	1.000	Good
4419	320-2	Zanskar	Himalaya	37.10	18.59	31.14	5.54	3.04	1.89	97.30	0.082	0.130	0.016	0.716	0.048	0.008	1.000	Superior
4419	321-2	Zanskar	Himalaya	38.48	19.09	26.99	5.61	3.96	4.08	98.22	0.051	0.129	0.091	0.611	0.083		1.000	Fair
4419	324-2	Zanskar	Himalaya	36.32	18.24	33.40	6.35	1.83	1.16	97.30	0.055	0.151	0.003	0.751		0.035	1.000	Superior
4419	326-2	Zanskar	Himalaya	37.02	17.98	34.56	3.42	2.02	1.33	96.33	0.062	0.082		0.816			1.000	Poor
4419	327-2	Zanskar	Himalaya	37.07	18.57	30.94	6.53	2.39	1.40	96.89	0.057	0.155	0.023	0.723	0.017		1.000	Poor
4419	345-2	Zanskar	Himalaya	37.41	18.77	31.27	6.79	2.07	0.94	97.25	0.015	0.161	0.067	0.699			1.000	Poor
4419	348-2	Zanskar	Himalaya	37.65	18.66	27.38	9.21	2.70	0.85	96.45		0.218	0.113	0.592			1.000	Poor
4419	377-2	Zanskar	Himalaya	37.01	18.84	36.52	0.72	2.70	1.66	97.45	0.074	0.017	0.013	0.847	0.047		1.000	Excellent
4419	379-2	Zanskar	Himalaya	38.36	18.70	25.31	2.13	4.14	8.69	97.33	0.104	0.049	0.027	0.569	0.247	0.004	1.000	Superior
4419	384-2	Zanskar	Himalaya	36.76	18.29	32.19	5.04	2.47	1.37	96.13	0.071	0.120	0.009	0.758	0.024		1.000	Fair
4419	391-2	Zanskar	Himalaya	36.82	18.45	34.83	4.84	1.76	1.39	98.08	0.049	0.114		0.793		0.022	1.000	Good
4419	395-2	Zanskar	Himalaya	37.56	18.35	33.53	3.30	3.30	1.44	97.48	0.093	0.077	0.013	0.775	0.032		1.000	Good
4419	398-2	Zanskar	Himalaya	37.60	19.27	34.00	2.08	4.49	1.34	98.79	0.050	0.048	0.115	0.749	0.009	0.029	1.000	Superior
4419	404-2	Zanskar	Himalaya	37.03	18.56	31.04	6.88	2.46	1.41	97.38	0.074	0.162		0.722	0.029		1.000	Good
4419	414-2	Zanskar	Himalaya	37.74	18.28	30.53	5.29	3.18	1.36	96.38	0.034	0.125	0.088	0.690			1.000	Poor
4419	425-2	Zanskar	Himalaya	38.34	18.22	27.60	1.52	3.00	10.22	98.90	0.079	0.035	0.014	0.579	0.235	0.058	1.000	Superior
4419	436-2	Zanskar	Himalaya	36.63	18.83	36.95	2.41	1.92	0.91	97.65	0.058	0.057		0.858	0.014	0.006	1.000	Superior
4419	447-2	Zanskar	Himalaya	37.19	18.68	33.82	2.49	3.63	1.33	97.14	0.085	0.058	0.036	0.781	0.038	0.002	1.000	Superior
4419	450-2	Zanskar	Himalaya	37.44	18.67	32.75	5.67	1.80	1.39	97.72	0.036	0.134	0.026	0.759			1.000	Poor
4419	455-2	Zanskar	Himalaya	37.18	18.76	31.43	5.91	1.82	1.31	96.40		0.141	0.076	0.717			1.000	Poor
4419	457-2	Zanskar	Himalaya	37.24	18.13	36.88	1.15	2.89	1.72	98.02	0.085	0.027	0.006	0.832	0.021	0.030	1.000	Superior
4419	465-2	Zanskar	Himalaya	37.30	18.70	35.23	2.40	2.21	1.18	97.01	0.024	0.057	0.061	0.807			1.000	Poor
4419	468-2	Zanskar	Himalaya	37.42	18.12	30.11	7.23	2.54	1.36	96.79	0.067	0.171	0.016	0.704	0.004		1.000	Poor
4419	469-2	Zanskar	Himalaya	37.76	18.29	31.58	5.92	2.12	1.64	97.32	0.039	0.140	0.036	0.726			1.000	Poor
4419	480-2	Zanskar	Himalaya	37.26	18.12	30.45	5.20	3.06	1.46	95.54	0.044	0.124	0.070	0.708			1.000	Poor
4419	484-2	Zanskar	Himalaya	36.90	18.12	27.59	10.58	1.94	0.72	95.86	0.040	0.254	0.029	0.626			1.000	Poor
4419	497-2	Zanskar	Himalaya	37.16	18.50	32.04	4.72	3.07	1.35	96.84	0.075	0.111	0.027	0.746	0.026		1.000	Fair
4419	526-2	Zanskar	Himalaya	36.49	18.19	36.88	2.31	1.67	1.74	97.29	0.046	0.055		0.846	0.001	0.028	1.000	Good
4419	540-2	Zanskar	Himalaya	37.22	18.40	29.61	7.52	3.04	1.24	97.03	0.086	0.177	0.011	0.689	0.028		1.000	Excellent
4419	559-2	Zanskar	Himalaya	36.78	18.13	29.20	8.17	1.90	1.60	95.78	0.053	0.196	0.010	0.693	0.011		1.000	Poor
4419	567-2	Zanskar	Himalaya	37.71	18.69	32.56	1.98	4.15	2.04	97.14	0.074	0.046	0.071	0.749	0.042		1.000	Good
4419	572-2	Zanskar	Himalaya	37.01	18.24	31.87	5.82	2.24	1.02	96.20	0.048	0.139	0.030	0.741			1.000	Poor
4419	578-2	Zanskar	Himalaya	36.99	18.89	28.65	6.51	3.90	1.75	96.70	0.069	0.153	0.069	0.658	0.045	0.007	1.000	Excellent
4419	593-2	Zanskar	Himalaya	37.20	17.86	36.56	1.62	1.78	1.35	96.38	0.056	0.039		0.854			1.000	Poor
4419	594-2	Zanskar	Himalaya	38.93	18.65	30.37	1.72	5.89	2.15	97.70	0.071	0.039	0.143	0.685	0.022		1.000	Poor
4419	614-2	Zanskar	Himalaya	37.18	18.75	30.49	6.04	2.33	1.27	96.05		0.144	0.098	0.691			1.000	Poor
4419	622-2	Zanskar	Himalaya	36.92	18.18	35.10	3.44	2.60	1.57	97.81	0.071	0.081	0.013	0.789	0.009	0.038	1.000	Superior
4419	628-2	Zanskar	Himalaya	38.11	18.22	29.93	2.06	2.59	6.72	97.65	0.070	0.048		0.685	0.149		1.000	Poor
4419	634-2	Zanskar	Himalaya	37.77	18.55	34.80	2.67	2.58	1.32	97.68	0.044	0.063	0.048	0.798			1.000	Poor
4419	638-2	Zanskar	Himalaya	37.21	18.47	33.86	3.65	2.46	1.25	96.90	0.054	0.086	0.031	0.792	0.004		1.000	Poor
4419	640-2	Zanskar	Himalaya	37.76	18.17	31.19	3.71	2.95	1.53	95.30		0.089	0.124	0.694			1.000	Poor
4419	678-2	Zanskar	Himalaya	37.46	19.37	31.56	4.73	2.99	1.59	97.70	0.020	0.110	0.096	0.727	0.010		1.000	Fair
4419	708-2	Zanskar	Himalaya	37.90	18.45	33.42	5.47	2.94	0.65	98.83	0.088	0.127		0.766	0.001		1.000	Good
4419	712-2	Zanskar	Himalaya	37.89	18.46	31.21	3.88	4.30	1.38	97.12	0.077	0.090	0.074	0.718	0.015		1.000	Fair
4419	727-2	Zanskar	Himalaya	37.11	18.39	31.52	6.02	2.33	1.65	97.00	0.072	0.142		0.736	0.029		1.000	Good
4419	728-2	Zanskar	Himalaya	36.89	18.89	29.84	2.08	3.13	6.83	97.66	0.016	0.048	0.106	0.631	0.125	0.074	1.000	Excellent
4419	729-2	Zanskar	Himalaya	37.56	19.01	35.81	1.36	3.98	1.18	98.90	0.058	0.031	0.084	0.793	0.004	0.030	1.000	Excellent
4419	734-2	Zanskar	Himalaya	36.75	18.30	34.59	2.32	3.27	1.00	96.24	0.090	0.055	0.017	0.808	0.026	0.004	1.000	Excellent
4419	739-2	Zanskar	Himalaya	37.67	18.38	29.37	5.59	2.96	3.16	97.14	0.078	0.131	0.019	0.679	0.070		1.000	Fair
4419	750-2	Zanskar	Himalaya	36.51	18.61	35.02	2.61	2.56	1.73	97.05	0.055	0.062	0.033	0.799	0.024	0.028	1.000	Superior
4419	760-2	Zanskar	Himalaya	36.79	18.53	36.15	2.64	1.83	1.68	97.61	0.050	0.062		0.837	0.014	0.009	1.000	Good
4419	766-2	Zanskar	Himalaya	36.85	18.56	35.84	1.57	2.32	1.64	96.77	0.067	0.037	0.007	0.839	0.035		1.000	Fair
4419	777-2	Zanskar	Himalaya	36.99	18.28	37.31	1.60	2.65	0.69	97.52	0.080	0.038		0.862	0.001	0.011	1.000	Superior
4419	779-2	Zanskar	Himalaya	36.77	18.99	33.71	3.89	2.16	1.23	96.76	0.028	0.092	0.053	0.790	0.006		1.000	Poor
4419	783-2	Zanskar	Himalaya	38.20	18.26	33.32	5.07	2.20	0.95	97.99	0.033	0.119	0.048	0.728			1.000	Poor
4419	795-2	Zanskar	Himalaya	37.23	18.38	28.82	1.17	3.10	6.89	95.60	0.092	0.028	0.006	0.670	0.200		1.000	Good
4419	797-2	Zanskar	Himalaya	37.72	19.17	29.95	5.99	3.00	1.62	97.44	0.007	0.140	0.114	0.682			1.000	Poor
4419	806-2	Zanskar	Himalaya	36.84	18.62	32.82	5.62	1.94	1.24	97.08	0.061	0.133		0.769	0.020		1.000	Good
4419	821-2	Zanskar	Himalaya	37.05	18.47	31.36	5.44	2.73	1.34	96.39	0.055	0.129	0.041	0.735	0.010		1.000	Poor
4419	825-2	Zanskar	Himalaya	37.62	19.08	32.91	1.55	4.84	3.52	99.51	0.012	0.035	0.177	0.676	0.013	0.088	1.000	Excellent
4419	827-2	Zanskar	Himalaya	37.42	18.96	32.69	1.26	4.10	3.46	97.88	0.055	0.029	0.093	0.722	0.068	0.033	1.000	Superior

Sample	Points	River/Dune	Domain	SiO_2	Al_2O_3	FeO	MnO	MgO	CaO	Total	Majorite	Spessartine	Pyrope	Almandine	Grossular	Andradite	Total	Quality
				wt%	wt%	wt%	wt%	wt%	wt%		$\{Mg_3\}[SiMg](Si_3)O_{12}$	$\{Mn_3\}[Al_2](Si_3)O_{12}$	$\{Mg_3\}[Al_2](Si_3)O_{12}$	$\{Fe_3\}[Al_2](Si_3)O_{12}$	$\{Ca_3\}[Al_2](Si_3)O_{12}$	$\{Ca_3\}[Fe_2](Si_3)O_{12}$		index
1426	1-1	Nandihar	Himalaya	37.36	21.02	34.05	1.41	3.89	1.00	98.72		0.032	0.157	0.770	0.029		1.000	Fair
1426	9-1	Nandihar	Himalaya	37.06	21.63	30.86	1.30	3.21	1.73	95.78		0.031	0.133	0.716	0.051		1.000	Poor
1426	10-1	Nandihar	Himalaya	37.24	20.76	33.49	1.79	3.30	1.30	97.89		0.041	0.135	0.766	0.038		1.000	Poor
1426	23-1	Nandihar	Himalaya	37.86	21.51	33.13	1.23	4.79	0.27	98.80		0.028	0.192	0.743	0.008		1.000	Poor
1426	32-1	Nandihar	Himalaya	38.35	20.94	34.45	0.70	2.79	2.69	99.92		0.016	0.112	0.772	0.077		1.000	Poor
1426	33-1	Nandihar	Himalaya	38.12	21.04	31.48	0.90	3.25	4.85	99.65		0.020	0.129	0.702	0.139		1.000	Fair
1426	68-1	Nandihar	Himalaya	36.03	21.41	31.53	3.48	1.91	2.04	96.39		0.082	0.079	0.735	0.061		1.000	Poor
1426	81-1	Nandihar	Himalaya	37.15	21.21	32.77	0.84	2.71	2.63	97.32		0.020	0.111	0.753	0.077		1.000	Poor
1426	85-1	Nandihar	Himalaya	37.53	21.65	34.53	2.30	2.69	1.07	99.75		0.053	0.108	0.778	0.031		1.000	Poor
1426	112-1	Nandihar	Himalaya	37.83	20.80	30.92	2.93	3.55	1.14	97.17		0.068	0.145	0.709	0.034		1.000	Poor
1426	114-1	Nandihar	Himalaya	37.68	21.10	33.97	1.34	3.82	1.21	99.13		0.031	0.153	0.765	0.035		1.000	Fair
1426	115-1	Nandihar	Himalaya	37.32	21.37	35.97	0.87	3.37	1.21	100.11		0.020	0.134	0.805	0.035		1.000	Excellent
1426	118-1	Nandihar	Himalaya	37.98	21.23	31.94	3.37	2.81	1.28	98.60		0.078	0.114	0.726	0.037		1.000	Poor
1426	120-1	Nandihar	Himalaya	38.10	21.52	32.72	1.20	4.78	2.02	100.32		0.027	0.188	0.722	0.057		1.000	Good
1426	121-1	Nandihar	Himalaya	36.53	21.07	34.66	1.82	2.94	1.55	98.58		0.042	0.119	0.788	0.045		1.000	Superior
1426	131-1	Nandihar	Himalaya	36.54	21.15	35.31	0.99	2.80	2.11	98.90		0.023	0.113	0.794	0.061		1.000	Superior
1426	138-1	Nandihar	Himalaya	37.89	21.12	36.88	0.42	3.88	0.46	100.65		0.010	0.154	0.820	0.009		1.000	Good
1426	142-1	Nandihar	Himalaya	37.45	21.65	31.72	0.95	4.61	2.16	98.53		0.022	0.184	0.711	0.062		1.000	Poor
1426	145-1	Nandihar	Himalaya	37.22	21.68	34.78	0.73	3.81	2.12	100.33		0.016	0.151	0.761	0.060		1.000	Excellent
1426	151-1	Nandihar	Himalaya	38.22	21.88	31.86	1.95	3.69	1.73	99.34		0.044	0.147	0.713	0.050		1.000	Poor
1426	157-1	Nandihar	Himalaya	38.07	20.76	28.39	2.50	2.14	7.21	99.07		0.057	0.086	0.638	0.205		1.000	Fair
1426	159-1	Nandihar	Himalaya	36.95	21.85	35.55	0.86	3.04	2.16	100.41		0.019	0.121	0.783	0.062		1.000	Excellent
1426	160-1	Nandihar	Himalaya	37.49	21.20	32.91	0.68	6.03	1.11	99.42		0.015	0.238	0.708	0.020	0.012	1.000	Superior
1426	161-1	Nandihar	Himalaya	37.34	21.27	36.37	0.32	3.60	0.66	99.56		0.007	0.144	0.818	0.019		1.000	Fair
1426	186-1	Nandihar	Himalaya	37.41	21.35	34.41	2.22	2.46	0.72	98.57		0.051	0.100	0.786	0.021		1.000	Poor
1426	189-1	Nandihar	Himalaya	36.23	21.41	33.54	1.32	3.05	2.08	97.63		0.031	0.125	0.768	0.061		1.000	Good
1426	223-1	Nandihar	Himalaya	38.31	21.59	28.82	0.69	9.12	1.59	100.12		0.015	0.350	0.577	0.017	0.027	1.000	Excellent
1426	229-1	Nandihar	Himalaya	37.21	21.69	34.12	1.54	3.82	1.19	99.57		0.035	0.153	0.764	0.034		1.000	Good
1426	234-1	Nandihar	Himalaya	37.27	20.83	34.26	0.62	4.87	1.13	98.97		0.014	0.195	0.758	0.019	0.013	1.000	Superior
1426	241-1	Nandihar	Himalaya	37.25	21.95	27.78	2.11	8.18	2.11	99.37		0.047	0.317	0.546	0.052	0.007	1.000	Good
1426	245-1	Nandihar	Himalaya	37.73	21.67	33.64	0.91	2.56	3.03	99.55		0.021	0.103	0.756	0.087		1.000	Poor
1426	249-1	Nandihar	Himalaya	37.83	21.37	27.01	4.31	3.12	4.68	98.32		0.098	0.125	0.609	0.135		1.000	Poor
1426	255-1	Nandihar	Himalaya	37.94	22.04	32.26	1.95	4.11	2.10	100.40		0.044	0.162	0.713	0.060		1.000	Poor
1426	261-1	Nandihar	Himalaya	37.77	21.35	32.76	0.83	3.45	2.07	98.24		0.019	0.139	0.743	0.060		1.000	Poor
1426	262-1	Nandihar	Himalaya	36.98	20.29	34.56	0.67	3.42	1.89	97.82	0.003	0.016	0.136	0.791	0.040		1.000	Good
1426	276-1	Nandihar	Himalaya	38.14	21.89	34.39	1.34	2.57	2.15	100.47		0.030	0.102	0.767	0.061		1.000	Poor
1426	280-1	Nandihar	Himalaya	38.40	20.50	33.74	1.52	3.31	1.05	98.53		0.035	0.134	0.767	0.031		1.000	Poor
1426	292-1	Nandihar	Himalaya	36.97	20.94	34.98	1.11	3.60	1.38	98.98		0.025	0.145	0.789	0.040	0.000	1.000	Superior
1426	301-1	Nandihar	Himalaya	37.43	21.28	33.79	0.63	3.57	2.20	98.90		0.014	0.143	0.761	0.064		1.000	Fair
1426	305-1	Nandihar	Himalaya	37.60	21.17	36.89	0.83	3.08	1.34	100.90	0.003	0.019	0.119	0.822	0.038		1.000	Excellent
1426	317-1	Nandihar	Himalaya	38.03	21.48	30.12	0.85	4.37	4.64	99.49		0.019	0.172	0.667	0.132		1.000	Fair
1426	323-1	Nandihar	Himalaya	37.65	21.53	35.95	0.82	3.42	1.72	101.09		0.018	0.135	0.795	0.049		1.000	Excellent
1426	334-1	Nandihar	Himalaya	38.63	21.63	33.59	0.66	2.89	4.16	101.55		0.015	0.113	0.738	0.117		1.000	Poor
1426	339-1	Nandihar	Himalaya	37.65	20.73	32.64	1.84	3.65	1.33	97.84		0.043	0.148	0.744	0.039		1.000	Poor
1426	357-1	Nandihar	Himalaya	36.67	21.22	37.57	0.47	3.23	1.11	100.26		0.011	0.129	0.811	0.029	0.003	1.000	Excellent
1426	358-1	Nandihar	Himalaya	37.50	20.89	32.69	3.15	2.88	0.90	98.01		0.073	0.118	0.749	0.026		1.000	Poor
1426	366-1	Nandihar	Himalaya	40.38	22.73	2.24	0.50	0.44	31.80	98.09		0.011	0.017	0.048	0.872		1.000	Poor
1426	369-1	Nandihar	Himalaya	38.24	21.60	32.41	0.65	3.63	4.66	101.19		0.014	0.142	0.710	0.131		1.000	Fair
1426	371-1	Nandihar	Himalaya	38.14	20.96	34.70	1.88	3.01	1.48	100.16		0.043	0.120	0.778	0.043		1.000	Fair
1426	376-1	Nandihar	Himalaya	38.71	21.35	32.83	0.60	6.22	1.02	100.73	0.000	0.013	0.242	0.716	0.014		1.000	Good
1426	392-1	Nandihar	Himalaya	37.73	20.97	30.04	0.77	2.76	6.54	98.80		0.018	0.110	0.674	0.188		1.000	Good
1426	395-1	Nandihar	Himalaya	37.79	21.14	37.83	0.53	3.35	0.63	101.28	0.007	0.012	0.124	0.840	0.017		1.000	Good
1426	405-1	Nandihar	Himalaya	37.56	21.06	33.82	1.58	4.60	1.03	99.65	0.006	0.036	0.175	0.754	0.029	0.001	1.000	Superior
1426	422-1	Nandihar	Himalaya	37.23	21.63	33.87	1.52	3.85	2.28	100.37		0.034	0.152	0.737	0.065		1.000	Excellent
1426	427-1	Nandihar	Himalaya	37.16	21.21	35.08	3.12	1.81	0.59	98.96		0.072	0.074	0.803	0.017		1.000	Poor
1426	432-1	Nandihar	Himalaya	37.31	21.26	31.58	1.40	1.02	6.77	99.34		0.032	0.041	0.713	0.196		1.000	Fair
1426	444-1	Nandihar	Himalaya	37.67	20.93	33.23	1.02	4.06	2.68	99.59	0.009	0.023	0.150	0.742	0.073		1.000	Excellent
1426	448-1	Nandihar	Himalaya	37.58	20.80	34.74	3.02	2.51	1.13	99.78		0.069	0.101	0.785	0.033		1.000	Fair
1426	453-1	Nandihar	Himalaya	37.76	22.13	33.64	1.13	3.47	2.37	100.51		0.025	0.137	0.745	0.067		1.000	Poor
1426	461-1	Nandihar	Himalaya	37.69	20.45	32.68	3.61	2.28	1.07	97.79		0.084	0.094	0.754	0.032		1.000	Poor
1426	479-1	Nandihar	Himalaya	37.44	21.63	36.27	0.50	2.59	1.65	100.08		0.011	0.104	0.814	0.048		1.000	Poor
1426	16-2	Nandihar	Himalaya	37.71	20.48	33.37	2.14	2.75	1.74	98.19		0.050	0.112	0.763	0.051		1.000	Poor
1426	28-2	Nandihar	Himalaya	37.82	21.18	34.35	1.31	3.68	1.56	99.90		0.030	0.147	0.768	0.045		1.000	Fair
1426	39-2	Nandihar	Himalaya	37.78	21.26	34.51	0.77	3.59	2.20	100.11		0.017	0.143	0.769	0.063		1.000	Good
1426	92-2	Nandihar	Himalaya	37.45	21.33	31.48	2.61	2.79	3.13	98.78		0.060	0.112	0.712	0.091		1.000	Poor
1426	98-2	Nandihar	Himalaya	38.18	21.08	31.06	4.09	2.26	1.71	98.38		0.095	0.092	0.709	0.050		1.000	Poor
1426	107-2	Nandihar	Himalaya	39.05	21.94	27.57	1.80	7.40	1.94	99.71		0.040	0.287	0.599	0.054		1.000	Fair
1426	122-2	Nandihar	Himalaya	37.70	21.71	32.66	3.49	2.27	1.55	99.38		0.080	0.092	0.739	0.045		1.000	Poor
1426	127-2	Nandihar	Himalaya	37.93	21.54	32.57	2.24	2.61	2.86	99.75		0.051	0.104	0.731	0.082		1.000	Poor
1426	130-2	Nandihar	Himalaya	39.11	21.34	33.78	0.96	4.67	1.76	101.62		0.021	0.182	0.737	0.044		1.000	Poor
1426	133-2	Nandihar	Himalaya	38.12	21.23	34.59	0.80	4.22	1.81	100.76		0.018	0.166	0.764	0.043		1.000	Good
1426	166-2	Nandihar	Himalaya	37.63	20.82	34.18	1.63	2.00	2.98	99.25		0.038	0.081	0.775	0.087		1.000	Fair
1426	168-2	Nandihar	Himalaya	37.90	21.24	34.43	1.01	3.98	1.03	99.59		0.023	0.159	0.771	0.030		1.000	Fair
1426	177-2	Nandihar	Himalaya	36.72	20.75	34.95	1.63	2.93	1.12	98.11		0.038	0.120	0.801	0.033		1.000	Good
1426	186-2	Nandihar	Himalaya	37.23	21.49	33.78	0.58	4.91	1.50	99.49		0.013	0.195	0.740	0.043		1.000	Superior
1426	188-2	Nandihar	Himalaya	37.91	21.24	31.49	2.20	3.51	2.16	98.51		0.050	0.141	0.712	0.063		1.000	Poor
1426	190-2	Nandihar	Himalaya	37.55	20.82	36.69	0.28	2.56	0.95	98.86		0.007	0.104	0.836	0.028		1.000	Poor
1426	192-2	Nandihar	Himalaya	38.08	20.91	28.41	5.71	2.61	0.88	96.59		0.134	0.108	0.659	0.026		1.000	Poor
1426	219-2	Nandihar	Himalaya	38.11	20.92	35.73	0.81	3.45	0.72	99.73		0.018	0.138	0.803	0.021		1.000	Fair
1426	227-2	Nandihar	Himalaya	38.15	20.79	35.06	1.92	3.14	1.35	100.40		0.044	0.125	0.784	0.030		1.000	Fair
1426	231-2	Nandihar	Himalaya	39.05	21.63	32.09	0.71	4.09	2.29	99.86		0.016	0.162	0.712	0.065		1.000	Poor
1426	256-2	Nandihar	Himalaya	37.42	20.59	36.34	2.70	1.24	1.00	99.31		0.063	0.051	0.833	0.029		1.000	Poor
1426	267-2	Nandihar	Himalaya	38.50	21.24	32.68	1.84	4.06	1.48	99.80		0.042	0.161	0.728	0.042		1.000	Poor
1426	269-2	Nandihar	Himalaya	39.99	21.56	2.24	0.49	0.34	32.78	97.40		0.011	0.013	0.048	0.907		1.000	Poor
1426	302-2	Nandihar	Himalaya	36.25	20.30	37.77	0.28	1.96	1.78	98.34		0.007	0.081	0.859	0.040	0.013	1.000	Superior
1426	306-2	Nandihar	Himalaya	38.14	21.14	28.57	0.98	2.93	7.06	98.81		0.022	0.117	0.639	0.202		1.000	Fair
1426	314-2	Nandihar	Himalaya	38.00	21.23	36.37	0.97	4.03	1.05	101.65		0.022	0.158	0.790	0.016	0.013	1.000	Excellent
1426	319-2	Nandihar	Himalaya	38.10	22.30	32.00	1.23	5.53	2.24	101.39		0.027	0.214	0.685	0.062		1.000	Good
1426	321-2	Nandihar	Himalaya	38.27	21.78	38.21	0.27	2.85	0.39	101.76		0.006	0.112	0.846	0.011		1.000	Poor
1426	326-2	Nandihar	Himalaya	37.74	21.41	35.29	2.13	3.14	1.10	100.81		0.048	0.125	0.786	0.031		1.000	Fair
1426	361-2	Nandihar	Himalaya	37.48	22.17	33.40	0.88	3.16	2.14	99.24		0.020	0.127	0.750	0.062		1.000	Poor
1426	371-2	Nandihar	Himalaya	37.95	21.52	31.64	0.85	3.68	2.85	98.49		0.019	0.148	0.713	0.082		1.000	Poor
1426	375-2	Nandihar	Himalaya	38.20	20.83	29.35	3.19	3.16	1.39	96.11		0.075	0.131	0.680	0.041		1.000	Poor
1426	380-2	Nandihar	Himalaya	37.40	21.04	32.90	1.32	2.44	2.21	97.31		0.031	0.100	0.758	0.065		1.000	Poor
1426	381-2	Nandihar	Himalaya	38.41	21.28	32.59	1.68	2.46	2.13	98.54		0.039	0.100	0.741	0.062		1.000	Poor
1426	385-2	Nandihar	Himalaya	37.67	21.96	32.95	1.67	3.50	1.64	99.38		0.038	0.140	0.739	0.047		1.000	Poor
1426	386-2	Nandihar	Himalaya	38.87	19.81	7.92	1.34	0.19	26.89	95.03		0.031	0.008	0.178	0.726		1.000	Poor
1426	398-2	Nandihar	Himalaya	38.15	21.85	35.46	1.54	3.62	1.35	101.97		0.034	0.142	0.778	0.038		1.000	Fair
1432	9-1	Astor	Nanga Parbat	38.49	21.44	26.81	2.20	4.86	6.86	100.67	0.000	0.048	0.188	0.572	0.176	0.015	1.000	Superior
1432	27-1	Astor	Nanga Parbat	38.10	21.64	29.27	1.49	4.58	5.70	100.78		0.033	0.178	0.623	0.153	0.006	1.000	Superior
1432	29-1	Astor	Nanga Parbat	36.46	21.54	27.53	1.82	2.53	8.58	98.47		0.041	0.101	0.589	0.247		1.000	Good
1432	44-1	Astor	Nanga Parbat	37.18	21.37	28.64	5.22	2.91	4.21	99.53		0.118	0.116	0.640	0.121		1.000	Superior
1432	72-1	Astor	Nanga Parbat	38.11	22.05	25.74	2.52	5.70	6.17	100.30		0.055	0.220	0.541	0.171		1.000	Excellent
1432	74-1	Astor	Nanga Parbat	38.35	21.07	28.15	1.12	4.56	6.21	99.45	0.002	0.025	0.177	0.621	0.159		1.000	Good
1432	109-1	Astor	Nanga Parbat	37.51	21.09	22.95	3.03	0.90	14.17	99.65		0.068	0.036	0.488	0.387	0.015	1.000	Superior
1432	185-1	Astor	Nanga Parbat	38.17	20.63	15.68	3.37	0.33	22.39	100.57		0.074	0.013	0.281	0.561	0.061	1.000	Excellent
1432	189-1	Astor	Nanga Parbat	38.25	21.65	25.18	1.21	6.34	7.71	100.34		0.026	0.243	0.502	0.191	0.022	1.000	Excellent
1432	196-1	Astor	Nanga Parbat	38.22	22.05	24.77	2.25	5.04	7.38	99.71		0.050	0.196	0.540	0.206		1.000	Excellent
1432	203-1	Astor	Nanga Parbat	38.21	22.15	26.88	2.06	3.11	9.38	101.79		0.045	0.120	0.563	0.260		1.000	Good
1432	223-1	Astor	Nanga Parbat	38.49	21.15	26.07	1.79	6.12	5.60	99.22	0.019	0.040	0.213	0.571	0.155		1.000	Excellent
1432	238-1	Astor	Nanga Parbat	38.71	22.09	25.78	2.20	5.29	6.65	100.72		0.048	0.204	0.557	0.184		1.000	Good
1432	269-1	Astor	Nanga Parbat	37.71	21.31	26.06	2.17	4.52	7.67	99.42		0.048	0.177	0.550	0.203	0.014	1.000	Superior
1432	284-1	Astor	Nanga Parbat	37.34	21.45	31.15	1.52	4.68	3.18	99.33		0.034	0.185	0.682	0.091		1.000	Superior
1432	285-1	Astor	Nanga Parbat	37.65	21.08	25.42	6.17	2.84	7.37	100.53		0.138	0.112	0.535	0.188	0.021	1.000	Superior
1432	307-1	Astor	Nanga Parbat	37.54	21.25	27.88	2.19	3.19	7.87	99.92		0.049	0.126	0.594	0.211	0.012	1.000	Superior
1432	339-1	Astor	Nanga Parbat	37.92	22.20	23.51	3.63	0.66	13.27	101.19		0.080	0.026	0.513	0.372		1.000	Excellent
1432	340-1	Astor	Nanga Parbat	37.41	21.20	25.65	1.33	3.77	9.10	98.47		0.030	0.149	0.556	0.252	0.007	1.000	Superior
1432	369-1	Astor	Nanga Parbat	37.44	21.21	30.68	1.58	5.20	2.47	98.59		0.036	0.207	0.685	0.071		1.000	Good
1432	387-1	Astor	Nanga Parbat	38.72	33.59	0.31	0.35	0.32	24.30	97.59		0.008	0.012	0.007	0.659		1.000	Poor
1432	391-1	Astor	Nanga Parbat	37.92	20.96	29.16	1.28	4.78	4.47	98.56		0.029	0.190	0.650	0.119		1.000	Fair
1432	451-1	Astor	Nanga Parbat	35.68	16.56	4.99	0.44	1.70	35.76	95.12					0.695	0.166	1.000	Poor
1432	452-1	Astor	Nanga Parbat	37.30	20.70	34.76	1.84	3.22	2.52	100.33		0.042	0.128	0.754	0.048	0.024	1.000	Superior
1432	461-1	Astor	Nanga Parbat	37.27	21.26	25.24	4.84	0.81	9.78	99.21		0.110	0.033	0.567	0.282		1.000	Good
1432	510-1	Astor	Nanga Parbat	38.16	21.57	24.53	2.73	5.44	6.78	99.21		0.061	0.213	0.536	0.189	0.001	1.000	Superior
1432	511-1	Astor	Nanga Parbat	37.99	21.72	26.87	2.70	4.38	6.80	100.46		0.060	0.170	0.571	0.188	0.002	1.000	Superior
1432	517-1	Astor	Nanga Parbat	37.87	20.72	25.93	1.79	4.59	7.75	98.65	0.010	0.040	0.168	0.562	0.201	0.019	1.000	Superior
1432	524-1	Astor	Nanga Parbat	37.89	21.22	25.52	1.42	2.38	10.73	99.16		0.032	0.094	0.566	0.303		1.000	Good
1432	3-2	Astor	Nanga Parbat	38.32	21.43	26.85	1.55	5.35	5.82	99.32		0.035	0.209	0.590	0.161		1.000	Good
1432	26-2	Astor	Nanga Parbat	36.90	21.14	35.46	1.49	3.22	2.28	100.49		0.034	0.128	0.757	0.054	0.011	1.000	Excellent
1432	47-2	Astor	Nanga Parbat	38.81	21.58	20.65	5.14	6.98	6.03	99.20		0.113	0.270	0.448	0.159		1.000	Excellent
1432	76-2	Astor	Nanga Parbat	38.21	21.38	26.75	2.99	4.79	5.88	100.01	0.004	0.066	0.182	0.583	0.160	0.005	1.000	Superior
1432	83-2	Astor	Nanga Parbat	37.33	21.56	25.20	1.45	5.65	6.96	98.15		0.033	0.223	0.534	0.197		1.000	Excellent
1432	104-2	Astor	Nanga Parbat	37.56	20.74	25.34	1.84	6.13	5.40	97.02	0.015	0.042	0.225	0.564	0.150	0.005	1.000	Superior
1432	208-2	Astor	Nanga Parbat	37.91	22.39	23.31	1.62	4.17	10.44	99.83		0.036	0.162	0.498	0.291		1.000	Excellent
1432	252-2	Astor	Nanga Parbat	37.76	21.07	24.07	1.31	2.35	13.03	99.59		0.029	0.092	0.505	0.345	0.022	1.000	Superior
1432	258-2	Astor	Nanga Parbat	37.95	21.21	19.46	10.59	1.88	10.27	101.35		0.235	0.073	0.397	0.264	0.024	1.000	Excellent
1432	272-2	Astor	Nanga Parbat	37.34	14.54	10.10	0.68	0.32	35.15	98.13			0.012		0.632	0.332	1.000	Good
1432	274-2	Astor	Nanga Parbat	37.88	21.94	33.38	1.02	5.15	2.30	101.67		0.022	0.199	0.698	0.064	0.001	1.000	Good
1432	293-2	Astor	Nanga Parbat	37.18	20.84	30.39	4.34	2.28	3.94	98.97		0.100	0.092	0.688	0.114		1.000	Good
1432	309-2	Astor	Nanga Parbat	36.79	21.49	27.09	2.77	3.07	6.65	97.87		0.063	0.124	0.611	0.192		1.000	Excellent
1432	324-2	Astor	Nanga Parbat	37.24	21.59	24.28	4.14	4.06	7.70	99.00		0.093	0.160	0.514	0.218		1.000	Excellent
1432	335-2	Astor	Nanga Parbat	37.72	21.34	24.03	2.90	1.01	13.86	100.85		0.064	0.039	0.495	0.372	0.017	1.000	Excellent
1432	370-2	Astor	Nanga Parbat	38.07	21.48	22.51	3.18	4.04	10.30	99.58		0.070	0.158	0.479	0.280	0.009	1.000	Superior
1432	371-2	Astor	Nanga Parbat	37.75	21.00	24.94	1.36	2.31	12.38	99.74		0.030	0.091	0.524	0.325	0.025	1.000	Superior
1432	380-2	Astor	Nanga Parbat	38.29	22.23	24.48	1.64	5.27	9.28	101.19		0.036	0.201	0.489	0.251	0.004	1.000	Good
1432	390-2	Astor	Nanga Parbat	39.06	19.87	3.89	0.55	0.39	36.39	100.14			0.015		0.848	0.122	1.000	Good
1432	409-2	Astor	Nanga Parbat	38.47	21.82	32.43	1.59	4.76	1.38	100.44		0.036	0.187	0.715	0.039		1.000	Poor
1432	417-2	Astor	Nanga Parbat	37.89	21.32	32.25	1.03	5.42	2.06	99.96		0.023	0.213	0.705	0.051	0.007	1.000	Superior
1432	430-2	Astor	Nanga Parbat	38.02	22.00	30.46	0.90	4.56	4.21	100.14		0.020	0.179	0.669	0.119		1.000	Good
1432	438-2	Astor	Nanga Parbat	38.24	21.83	25.25	2.14	5.63	5.47	98.57		0.048	0.221	0.557	0.155		1.000	Fair
1432	448-2	Astor	Nanga Parbat	38.55	21.33	28.77	0.89	4.58	7.34	101.46		0.020	0.176	0.597	0.176	0.028	1.000	Excellent
1432	471-2	Astor	Nanga Parbat	38.12	21.67	25.05	1.33	3.46	9.82	99.44		0.030	0.136	0.551	0.277		1.000	Good
1432	478-2	Astor	Nanga Parbat	39.38	22.30	25.59	2.51	5.92	6.28	101.98		0.054	0.225	0.545	0.171		1.000	Fair
1432	511-2	Astor	Nanga Parbat	38.59	21.47	24.88	2.87	4.45	6.76	99.03		0.064	0.175	0.549	0.191		1.000	Poor
1432	543-2	Astor	Nanga Parbat	38.68	22.11	14.59	12.01	5.01	9.29	101.68		0.260	0.191	0.283	0.244	0.010	1.000	Good
1432	548-2	Astor	Nanga Parbat	36.64	21.47	21.08	6.18	3.19	10.64	99.19		0.138	0.126	0.403	0.288	0.014	1.000	Good

Sample	Points	River/Dune	Domain	SiO_2	Al_2O_3	FeO	MnO	MgO	CaO	Total	Majorite	Spessartine	Pyrope	Almandine	Grossular	Andradite	Total	Quality
				wt%	wt%	wt%	wt%	wt%	wt%		$\{Mg_3\}[SiMg](Si_3)O_{12}$	$\{Mn_3\}[Al_2](Si_3)O_{12}$	$\{Mg_3\}[Al_2](Si_3)O_{12}$	$\{Fe_3\}[Al_2](Si_3)O_{12}$	$\{Ca_3\}[Al_2](Si_3)O_{12}$	$\{Ca_3\}[Fe_2](Si_3)O_{12}$		index
1462	89	Mankera	Thal	39.70	21.27	32.37	1.13	3.99	4.41	102.87		0.025	0.153	0.698	0.093		1.000	Poor
1462	93	Mankera	Thal	39.48	21.26	26.39	0.69	5.69	8.46	101.96	0.016	0.015	0.195	0.544	0.203	0.028	1.000	Excellent
1462	100	Mankera	Thal	40.22	21.70	25.35	1.66	7.27	5.48	101.68		0.036	0.275	0.538	0.125		1.000	Poor
1462	108	Mankera	Thal	39.26	23.14	23.68	0.76	4.13	13.47	104.43		0.016	0.153	0.447	0.358		1.000	Fair
1462	113	Mankera	Thal	39.04	22.08	36.16	1.29	4.02	1.73	104.33		0.028	0.153	0.770	0.045	0.002	1.000	Excellent
1462	115	Mankera	Thal	38.55	21.84	33.12	1.67	5.69	1.06	101.92		0.037	0.220	0.712	0.028	0.002	1.000	Excellent
1462	122	Mankera	Thal	40.42	22.37	31.00	0.90	5.73	3.47	103.90		0.019	0.215	0.654	0.094		1.000	Poor
1462	133	Mankera	Thal	39.22	21.59	28.90	2.11	6.35	1.68	99.86		0.047	0.248	0.633	0.047		1.000	Poor
1462	153	Mankera	Thal	39.85	21.48	24.65	3.30	6.93	5.78	101.99	0.033	0.071	0.218	0.521	0.154	0.003	1.000	Superior
1462	161	Mankera	Thal	39.82	22.52	21.74	0.69	9.38	8.11	102.26		0.015	0.346	0.410	0.192	0.023	1.000	Good
1462	171	Mankera	Thal	38.59	21.02	32.83	4.16	3.15	1.63	101.39		0.093	0.124	0.727	0.039		1.000	Poor
1462	186	Mankera	Thal	38.40	22.43	33.56	1.47	4.81	0.94	101.61		0.032	0.187	0.731	0.026		1.000	Poor
1462	202	Mankera	Thal	37.84	21.50	31.43	10.87	1.37	0.84	103.85		0.242	0.054	0.674	0.018	0.006	1.000	Excellent
1462	218	Mankera	Thal	34.54	18.09	13.67	0.97	0.89	15.61	83.77		0.025	0.041	0.354	0.518		1.000	Poor
1462	220	Mankera	Thal	38.51	22.13	31.45	3.18	3.30	4.40	102.96		0.070	0.127	0.676	0.122		1.000	Excellent
1462	225	Mankera	Thal	38.99	22.11	33.20	2.13	2.13	5.74	104.30		0.046	0.082	0.712	0.158		1.000	Fair
1462	235	Mankera	Thal	39.72	22.38	30.68	1.10	6.56	3.24	103.68		0.024	0.246	0.643	0.083	0.004	1.000	Excellent
1462	265	Mankera	Thal	38.98	21.74	32.23	1.28	4.59	3.00	101.81		0.028	0.178	0.700	0.084		1.000	Poor
1462	266	Mankera	Thal	40.06	21.44	28.75	2.57	4.01	6.09	102.92		0.056	0.153	0.616	0.146		1.000	Poor
1462	287	Mankera	Thal	39.00	22.18	33.06	1.23	6.67	1.41	103.55		0.026	0.252	0.671	0.025	0.013	1.000	Good
1462	359	Mankera	Thal	37.67	21.40	36.52	1.44	3.48	1.01	101.52		0.032	0.137	0.797	0.026	0.003	1.000	Excellent
1462	390	Mankera	Thal	38.21	21.74	31.56	6.09	3.12	1.33	102.05		0.136	0.122	0.694	0.038		1.000	Poor
1462	413	Mankera	Thal	36.76	21.30	35.38	2.11	3.96	1.15	100.65		0.048	0.157	0.740	0.021	0.011	1.000	Good
1462	417	Mankera	Thal	38.80	21.05	31.05	1.97	1.53	7.16	101.55		0.044	0.060	0.684	0.192		1.000	Poor
1462	426	Mankera	Thal	39.09	21.84	28.46	1.73	2.72	8.15	101.99		0.038	0.105	0.617	0.226		1.000	Poor
1462	483	Mankera	Thal	38.01	20.47	29.77	1.70	4.21	4.92	99.08	0.030	0.038	0.127	0.664	0.136		1.000	Excellent
1462	486	Mankera	Thal	38.84	20.50	33.89	3.46	0.86	4.84	102.39		0.078	0.034	0.750	0.098		1.000	Poor
1462	497	Mankera	Thal	37.92	21.47	32.19	6.76	3.42	1.01	102.78		0.150	0.133	0.680	0.016	0.013	1.000	Excellent
1462	532	Mankera	Thal	38.75	21.47	32.88	1.57	3.99	2.16	100.81		0.035	0.157	0.725	0.061		1.000	Poor
1462	533	Mankera	Thal	39.11	21.39	25.91	0.96	5.20	8.70	101.26	0.012	0.021	0.183	0.545	0.222	0.017	1.000	Excellent
1462	542	Mankera	Thal	38.52	21.54	33.49	2.17	4.94	0.99	101.64		0.048	0.192	0.731	0.023		1.000	Fair
1462	550	Mankera	Thal	38.24	21.29	32.00	1.22	4.53	3.94	101.21		0.027	0.176	0.685	0.093	0.018	1.000	Excellent
1462	551	Mankera	Thal	39.14	21.76	33.18	1.39	4.39	2.78	102.65		0.030	0.169	0.717	0.077		1.000	Fair
1462	554	Mankera	Thal	38.84	20.50	33.89	3.46	0.86	4.84	102.39		0.078	0.034	0.750	0.098		1.000	Poor
1462	563	Mankera	Thal	40.47	32.13	2.27	0.49	0.34	23.38	99.08		0.010	0.013	0.048	0.629		1.000	Poor
1462	569	Mankera	Thal	42.12	23.35	36.19	2.16	2.54	2.81	109.16		0.045	0.093	0.744	0.074		1.000	Poor
1462	576	Mankera	Thal	38.12	22.03	32.43	1.32	4.89	2.32	101.11		0.029	0.190	0.708	0.065		1.000	Good
1462	606	Mankera	Thal	39.81	20.91	27.43	4.11	0.72	9.93	102.91		0.091	0.028	0.596	0.246		1.000	Poor
1462	614	Mankera	Thal	40.90	22.18	20.88	0.89	8.40	10.24	103.48	0.009	0.019	0.295	0.408	0.239	0.030	1.000	Superior
1462	626	Mankera	Thal	41.80	22.15	24.71	0.68	8.54	7.36	105.24	0.047	0.014	0.247	0.501	0.190	0.002	1.000	Superior
1462	630	Mankera	Thal	38.08	21.19	36.75	2.03	3.18	1.91	103.14		0.045	0.124	0.771	0.026	0.027	1.000	Excellent
1462	641	Mankera	Thal	39.17	21.51	33.64	1.48	5.09	1.93	102.83	0.016	0.032	0.174	0.724	0.048		1.000	Good
1462	642	Mankera	Thal	38.48	21.47	35.56	1.33	3.39	2.38	102.60	0.010	0.029	0.119	0.776	0.066		1.000	Good
1462	643	Mankera	Thal	38.48	22.25	35.26	1.32	3.66	1.30	102.28		0.029	0.142	0.770	0.036		1.000	Poor
1462	646	Mankera	Thal	38.26	21.47	36.46	2.01	4.35	1.05	103.60		0.044	0.167	0.747	0.002	0.027	1.000	Good
1462	667	Mankera	Thal	37.57	21.73	32.78	2.52	4.26	1.70	100.56		0.056	0.168	0.721	0.048		1.000	Superior
1462	686	Mankera	Thal	38.47	21.46	31.12	2.77	4.07	2.63	100.52		0.062	0.160	0.687	0.074		1.000	Fair
1462	716	Mankera	Thal	41.26	19.15	5.19	0.78	0.00	36.26	102.64		0.016		0.022	0.801	0.096	1.000	Poor
1462	766	Mankera	Thal	39.05	22.19	32.47	1.63	4.80	2.85	102.99		0.035	0.184	0.697	0.078		1.000	Fair
1462	776	Mankera	Thal	39.77	20.62	23.90	1.59	5.75	10.04	101.67	0.038	0.034	0.168	0.486	0.240	0.034	1.000	Excellent
1462	787	Mankera	Thal	40.59	21.75	20.54	0.92	7.30	12.38	103.49		0.019	0.268	0.386	0.273	0.054	1.000	Excellent
1462	808	Mankera	Thal	39.58	22.19	25.45	0.52	10.62	3.20	101.57		0.011	0.396	0.497	0.060	0.025	1.000	Good
1462	821	Mankera	Thal	38.17	20.77	35.54	2.98	2.65	1.36	101.48	0.003	0.067	0.101	0.790	0.018		1.000	Poor
1462	850	Mankera	Thal	38.21	21.86	32.98	0.98	5.59	1.47	101.09		0.022	0.217	0.716	0.041		1.000	Excellent
1462	851	Mankera	Thal	39.05	20.65	26.94	1.38	3.68	9.11	100.82	0.045	0.031	0.083	0.587	0.250		1.000	Excellent
1462	867	Mankera	Thal	38.87	21.33	31.78	5.12	1.86	4.85	103.81	0.022	0.112	0.042	0.689	0.134	0.001	1.000	Excellent
1462	875	Mankera	Thal	39.90	20.57	3.57	0.62	0.20	35.16	100.02	0.000	0.013		0.036	0.869	0.060	1.000	Good
1462	895	Mankera	Thal	38.47	21.21	36.36	1.99	2.93	1.78	102.75	0.014	0.044	0.096	0.796	0.046		1.000	Good
1462	897	Mankera	Thal	39.45	22.57	26.16	0.46	6.44	7.91	102.99		0.010	0.241	0.526	0.207	0.006	1.000	Good
1462	906	Mankera	Thal	39.18	21.37	20.61	5.76	1.69	12.46	101.07		0.127	0.066	0.449	0.343		1.000	Poor
1462	912	Mankera	Thal	36.60	7.43	18.92	0.96	0.00	32.71	96.62		0.022		0.015	0.324	0.622	1.000	Good
1462	913	Mankera	Thal	38.15	21.05	34.93	2.39	3.03	1.75	101.29		0.054	0.120	0.774	0.039		1.000	Poor
1462	942	Mankera	Thal	38.04	21.10	33.91	2.31	3.82	1.67	100.85	0.003	0.052	0.147	0.751	0.038		1.000	Excellent
1462	951	Mankera	Thal	38.13	21.34	32.59	1.35	1.84	5.67	100.92		0.030	0.073	0.723	0.161		1.000	Fair
1462	963	Mankera	Thal	38.92	22.04	31.09	0.91	6.86	2.00	101.82		0.020	0.262	0.661	0.052	0.003	1.000	Excellent
1462	998	Mankera	Thal	39.45	22.05	27.58	0.62	6.10	5.78	101.59		0.013	0.233	0.590	0.158		1.000	Fair
1462	1011	Mankera	Thal	38.63	21.67	34.98	1.79	3.63	1.35	102.04		0.040	0.142	0.766	0.038		1.000	Poor
1462	1012	Mankera	Thal	38.47	21.68	28.50	1.45	2.54	9.12	101.77		0.032	0.098	0.615	0.249	0.005	1.000	Excellent
1462	1028	Mankera	Thal	38.04	21.10	33.91	2.31	3.82	1.67	100.85	0.003	0.052	0.147	0.751	0.038		1.000	Excellent
1462	1040	Mankera	Thal	38.91	21.40	31.53	0.86	1.47	9.54	103.70	0.003	0.019	0.052	0.663	0.240	0.023	1.000	Excellent
1462	1082	Mankera	Thal	38.67	21.87	33.48	1.24	4.52	2.42	102.21		0.027	0.175	0.726	0.067		1.000	Fair
1462	1084	Mankera	Thal	38.43	20.97	31.80	1.92	4.54	2.76	100.43	0.003	0.043	0.175	0.702	0.059		1.000	Good
1462	1089	Mankera	Thal	38.69	22.19	32.74	1.06	5.80	1.96	102.44		0.023	0.222	0.694	0.054		1.000	Excellent
1462	1091	Mankera	Thal	37.84	21.85	30.65	0.92	4.45	5.01	100.73		0.020	0.173	0.655	0.140		1.000	Excellent
1462	1095	Mankera	Thal	38.07	21.99	32.81	5.20	3.41	1.30	102.80		0.115	0.133	0.709	0.036		1.000	Excellent
1462	1127	Mankera	Thal	38.96	21.59	31.32	2.75	6.05	1.52	102.18	0.009	0.060	0.220	0.669	0.034	0.008	1.000	Excellent
1462	1197	Mankera	Thal	38.81	21.85	32.36	1.17	5.01	2.87	102.07		0.026	0.193	0.700	0.080		1.000	Fair
1462	1231	Mankera	Thal	38.28	21.66	33.41	2.17	5.18	1.36	102.06		0.048	0.200	0.707	0.028	0.010	1.000	Excellent
1462	1293	Mankera	Thal	39.02	21.73	23.29	1.03	6.44	9.87	101.38		0.022	0.244	0.456	0.237	0.031	1.000	Good
1462	1297	Mankera	Thal	37.74	22.16	34.47	4.23	2.72	2.04	103.37		0.093	0.106	0.726	0.057		1.000	Good
1462	1308	Mankera	Thal	38.92	21.68	34.19	1.12	2.48	4.61	103.00		0.025	0.096	0.743	0.128		1.000	Fair
1462	1311	Mankera	Thal	39.69	21.65	21.57	0.92	9.14	7.32	100.28	0.010	0.020	0.331	0.441	0.176	0.023	1.000	Superior
1462	1356	Mankera	Thal	38.23	21.21	35.18	1.00	3.82	1.98	101.42	0.007	0.022	0.140	0.774	0.050		1.000	Good
1462	1363	Mankera	Thal	38.35	21.11	29.71	8.40	2.74	1.30	101.61		0.189	0.108	0.658	0.034		1.000	Poor
1462	1383	Mankera	Thal	39.20	22.32	33.81	0.72	4.56	2.28	102.90		0.016	0.175	0.728	0.063		1.000	Poor
1463	1	Haidarabad	Thal	38.82	20.75	23.99	0.74	6.29	6.20	96.77		0.017	0.250	0.535	0.177		1.000	Poor
1463	5	Haidarabad	Thal	35.96	19.63	39.21	1.24	3.05	1.11	100.21		0.028	0.123	0.744		0.032	1.000	Good
1463	37	Haidarabad	Thal	35.84	30.25	2.44	0.55	0.28	22.21	91.57		0.013	0.011	0.055	0.646		1.000	Poor
1463	38	Haidarabad	Thal	35.39	29.62	1.63	0.53	0.20	22.10	89.47		0.013	0.008	0.038	0.657		1.000	Poor
1463	121	Haidarabad	Thal	35.25	20.19	34.97	3.48	3.80	1.18	98.87		0.080	0.154	0.672		0.034	1.000	Fair
1463	148	Haidarabad	Thal	36.44	19.97	33.43	1.08	3.74	4.70	99.36		0.025	0.150	0.668	0.070	0.065	1.000	Good
1463	214	Haidarabad	Thal	36.51	20.63	34.60	0.90	5.06	2.34	100.05		0.020	0.200	0.681	0.018	0.049	1.000	Good
1463	216	Haidarabad	Thal	36.54	20.05	29.04	2.67	4.52	7.23	100.05		0.060	0.178	0.522	0.120	0.085	1.000	Good
1463	285	Haidarabad	Thal	38.44	19.96	4.52	1.15	0.14	34.19	98.39		0.025	0.005	0.016	0.847	0.097	1.000	Excellent
1463	294	Haidarabad	Thal	35.88	20.36	35.28	0.61	3.80	4.53	100.46		0.014	0.150	0.660	0.061	0.068	1.000	Fair
1463	313	Haidarabad	Thal	36.32	19.49	28.21	0.70	3.07	11.23	99.03		0.016	0.122	0.509	0.223	0.098	1.000	Good
1463	375	Haidarabad	Thal	36.36	21.24	33.31	0.81	4.41	3.16	99.27		0.018	0.176	0.686	0.078	0.012	1.000	Good
1463	458	Haidarabad	Thal	36.34	20.58	33.21	2.24	6.11	2.00	100.46		0.050	0.239	0.599		0.056	1.000	Fair
1463	461	Haidarabad	Thal	37.96	20.77	22.50	0.94	7.89	8.54	98.61		0.021	0.305	0.421	0.180	0.058	1.000	Excellent
1463	502	Haidarabad	Thal	36.97	21.25	32.89	1.44	5.82	2.10	100.47		0.032	0.228	0.651	0.029	0.030	1.000	Good
1463	550	Haidarabad	Thal	35.96	20.22	26.98	13.17	2.34	1.51	100.18		0.302	0.094	0.529		0.044	1.000	Good
1463	612	Haidarabad	Thal	35.53	19.90	29.59	3.18	3.54	7.75	99.49		0.072	0.141	0.514	0.133	0.088	1.000	Fair
1463	646	Haidarabad	Thal	36.78	20.83	28.25	1.36	4.38	8.66	100.27		0.030	0.171	0.519	0.188	0.055	1.000	Good
1463	668	Haidarabad	Thal	37.39	18.39	6.90	0.62	0.16	35.99	99.46			0.006		0.762	0.189	1.000	Poor
1463	669	Haidarabad	Thal	35.22	19.89	39.18	1.06	3.50	0.70	99.56		0.024	0.142	0.721		0.020	1.000	Fair
1463	699	Haidarabad	Thal	36.76	20.76	35.76	0.37	4.77	2.57	100.97		0.008	0.187	0.700	0.022	0.050	1.000	Good
1463	711	Haidarabad	Thal	37.73	20.62	23.38	1.09	7.59	10.26	100.67		0.024	0.288	0.369	0.187	0.093	1.000	Fair
1463	727	Haidarabad	Thal	37.05	20.17	29.67	2.92	6.06	5.08	100.95		0.064	0.235	0.523	0.050	0.092	1.000	Good
1463	739	Haidarabad	Thal	35.90	20.29	35.09	1.81	5.07	1.86	100.02		0.041	0.201	0.645		0.053	1.000	Fair
1463	746	Haidarabad	Thal	35.55	20.84	39.09	3.54	1.27	0.75	101.05		0.081	0.051	0.808	0.000	0.021	1.000	Fair
1463	781	Haidarabad	Thal	36.51	20.15	34.12	1.89	5.22	3.04	100.94		0.042	0.205	0.628	0.002	0.084	1.000	Fair
1463	802	Haidarabad	Thal	36.10	21.09	37.72	1.47	2.98	1.27	100.63		0.033	0.119	0.778	0.019	0.018	1.000	Good
1463	808	Haidarabad	Thal	35.98	20.29	33.86	4.63	3.24	1.43	99.44		0.106	0.131	0.695		0.042	1.000	Good
1463	811	Haidarabad	Thal	35.61	20.01	26.75	1.74	0.74	13.42	98.27		0.040	0.030	0.505	0.329	0.061	1.000	Good
1463	819	Haidarabad	Thal	35.26	20.61	37.40	1.45	2.27	1.55	98.54		0.034	0.093	0.796	0.030	0.015	1.000	Good
1463	823	Haidarabad	Thal	36.38	20.58	37.63	1.18	2.62	1.59	99.97		0.027	0.106	0.804	0.020	0.026	1.000	Excellent
1463	844	Haidarabad	Thal	35.71	19.96	39.57	2.40	1.75	0.94	100.32		0.055	0.071	0.792		0.027	1.000	Good
1463	848	Haidarabad	Thal	36.00	19.55	35.54	6.02	2.77	0.71	100.59		0.138	0.112	0.642		0.021	1.000	Good
1463	905	Haidarabad	Thal	36.60	29.73	1.82	0.26	0.12	25.06	93.60		0.006	0.005	0.040	0.713		1.000	Poor
1463	912	Haidarabad	Thal	35.99	20.45	37.88	0.69	3.96	2.09	101.07		0.016	0.157	0.720		0.059	1.000	Poor
1463	913	Haidarabad	Thal	33.10	18.25	37.37	2.35	2.76	1.83	95.66		0.057	0.117	0.652		0.056	1.000	Poor
1463	940	Haidarabad	Thal	36.50	20.22	30.29	0.65	3.59	8.78	100.03		0.015	0.141	0.560	0.175	0.074	1.000	Good
1463	1023	Haidarabad	Thal	36.77	20.58	23.23	7.72	0.87	11.16	100.33		0.174	0.035	0.452	0.275	0.043	1.000	Good
1463	1097	Haidarabad	Thal	35.67	19.99	37.31	1.59	2.87	2.54	99.98		0.036	0.116	0.738	0.009	0.065	1.000	Good
1463	1113	Haidarabad	Thal	36.42	20.04	27.21	4.19	4.38	7.87	100.11		0.093	0.172	0.471	0.134	0.088	1.000	Fair
1463	1114	Haidarabad	Thal	35.44	21.02	34.33	2.04	5.34	2.30	100.47		0.046	0.210	0.614	0.013	0.052	1.000	Fair
1463	1182	Haidarabad	Thal	36.16	20.39	32.76	2.48	5.03	3.25	100.06		0.056	0.199	0.611	0.026	0.066	1.000	Fair
1463	1224	Haidarabad	Thal	36.56	20.76	28.47	2.78	3.34	7.45	99.35		0.063	0.133	0.566	0.176	0.036	1.000	Good
1463	1230	Haidarabad	Thal	35.17	19.15	38.81	2.84	2.62	1.64	100.24		0.065	0.106	0.679		0.048	1.000	Fair
1463	1232	Haidarabad	Thal	34.99	19.50	36.41	4.23	2.31	0.85	98.29		0.099	0.095	0.712		0.025	1.000	Good
1463	1244	Haidarabad	Thal	36.47	19.97	33.68	2.19	4.26	2.41	98.98		0.050	0.171	0.692	0.012	0.057	1.000	Excellent
1463	1250	Haidarabad	Thal	35.81	20.73	32.51	1.81	3.50	5.83	100.19		0.041	0.139	0.606	0.114	0.052	1.000	Fair
1463	1253	Haidarabad	Thal	36.78	19.80	32.69	0.86	4.81	4.63	99.57		0.019	0.191	0.636	0.051	0.081	1.000	Good
1463	1339	Haidarabad	Thal	35.18	19.95	31.14	9.49	2.80	1.56	100.12		0.217	0.113	0.550		0.045	1.000	Fair
1463	1442	Haidarabad	Thal	35.62	20.47	35.62	2.94	4.24	1.81	100.70		0.066	0.168	0.649		0.052	1.000	Fair
1463	1450	Haidarabad	Thal	36.70	19.85	40.26	0.88	1.17	1.57	100.43		0.020	0.048	0.886	0.001	0.045	1.000	Superior
1463	1476	Haidarabad	Thal	36.30	20.12	35.51	0.46	4.79	2.31	99.48		0.010	0.191	0.703	0.003	0.063	1.000	Good
1463	1488	Haidarabad	Thal	35.53	20.14	37.82	1.83	2.88	2.15	100.36		0.042	0.116	0.736		0.062	1.000	Fair
1463	1554	Haidarabad	Thal	36.72	20.52	33.12	1.67	2.03	6.35	100.41		0.038	0.081	0.680	0.141	0.041	1.000	Excellent
1463	1639	Haidarabad	Thal	37.53	20.67	25.64	0.84	5.40	9.97	100.05		0.019	0.209	0.469	0.212	0.065	1.000	Good
1463	1665	Haidarabad	Thal	36.41	20.60	35.90	0.55	3.06	3.15	99.66		0.013	0.123	0.754	0.060	0.030	1.000	Good
1463	1666	Haidarabad	Thal	37.29	20.66	25.32	0.97	8.56	6.44	99.24		0.021	0.329	0.434	0.102	0.076	1.000	Good
1463	1668	Haidarabad	Thal	37.48	20.69	24.33	0.81	6.10	9.99	99.41		0.018	0.236	0.441	0.214	0.064	1.000	Good
1463	1682	Haidarabad	Thal	37.41	20.37	24.46	0.98	7.45	9.12	99.78		0.021	0.286	0.404	0.160	0.091	1.000	Good
1463	1693	Haidarabad	Thal	35.22	20.05	36.96	2.81	2.39	1.97	99.39		0.065	0.097	0.741	0.004	0.054	1.000	Good

Sample	Points	River/Dune	Domain	SiO_2	Al_2O_3	FeO	MnO	MgO	CaO	Total	Majorite	Spessartine	Pyrope	Almandine	Grossular	Andradite	Total	Quality
				wt%	wt%	wt%	wt%	wt%	wt%		$\{Mg_3\}[SiMg](Si_3)O_{12}$	$\{Mn_3\}[Al_2](Si_3)O_{12}$	$\{Mg_3\}[Al_2](Si_3)O_{12}$	$\{Fe_3\}[Al_2](Si_3)O_{12}$	$\{Ca_3\}[Al_2](Si_3)O_{12}$	$\{Ca_3\}[Fe_2](Si_3)O_{12}$		index
1470	49	Muzaffarghar	Thal	38.25	20.65	32.19	1.97	6.31	1.13	100.50	0.006	0.044	0.238	0.674		0.032	1.000	Superior
1470	159	Muzaffarghar	Thal	40.39	20.08	17.24	0.77	8.84	12.73	100.05	0.050	0.016	0.265	0.325	0.287	0.057	1.000	Superior
1470	251	Muzaffarghar	Thal	38.54	19.02	29.61	3.23	3.01	4.44	97.85	0.009	0.075	0.111	0.676	0.056		1.000	Poor
1470	326	Muzaffarghar	Thal	39.29	19.36	27.56	5.12	2.40	6.76	100.49	0.047	0.115	0.033	0.613	0.149		1.000	Poor
1470	491	Muzaffarghar	Thal	37.16	18.31	35.30	0.86	2.62	3.37	97.62	0.080	0.020	0.001	0.799	0.075	0.025	1.000	Excellent
1470	629	Muzaffarghar	Thal	39.69	19.98	22.46	1.98	3.87	12.45	100.42	0.079	0.044	0.044	0.487	0.341		1.000	Excellent
1470	778	Muzaffarghar	Thal	38.81	22.29	10.48	0.95	0.58	23.04	96.14		0.021	0.023	0.233	0.657		1.000	Poor
1470	843	Muzaffarghar	Thal	39.47	19.62	18.77	0.97	8.81	11.04	98.68	0.034	0.021	0.291	0.351	0.226	0.077	1.000	Superior
1470	904	Muzaffarghar	Thal	38.45	19.93	30.21	1.25	6.69	2.47	99.00	0.049	0.028	0.198	0.655	0.050	0.020	1.000	Superior
1470	1054	Muzaffarghar	Thal	39.55	23.63	9.19	0.58	0.49	23.18	96.62		0.013	0.019	0.203	0.655		1.000	Poor
1470	1146	Muzaffarghar	Thal	37.66	19.45	32.84	1.58	5.48	1.90	98.90	0.025	0.036	0.185	0.699	0.000	0.054	1.000	Superior
1470	1240	Muzaffarghar	Thal	38.73	19.38	23.50	0.97	6.67	8.60	97.84	0.062	0.022	0.180	0.494	0.207	0.036	1.000	Superior
1470	1248	Muzaffarghar	Thal	38.14	18.27	21.36	3.08	2.09	14.78	97.72	0.058	0.070		0.446	0.353	0.052	1.000	Good
1470	1279	Muzaffarghar	Thal	38.19	19.69	33.99	1.55	5.30	1.22	99.93	0.045	0.035	0.150	0.735	0.005	0.030	1.000	Superior
1470	1312	Muzaffarghar	Thal	37.87	19.60	24.38	2.30	2.66	12.11	98.91	0.022	0.052	0.076	0.505	0.289	0.056	1.000	Superior
1470	1558	Muzaffarghar	Thal	37.01	19.36	33.08	2.46	3.65	2.59	98.16	0.028	0.057	0.112	0.728	0.037	0.039	1.000	Superior
1470	1644	Muzaffarghar	Thal	38.72	19.56	34.99	0.72	3.70	1.72	99.42	0.009	0.016	0.137	0.778			1.000	Poor
1470	1792	Muzaffarghar	Thal	37.16	19.05	36.46	0.83	3.27	1.23	98.00	0.065	0.019	0.048	0.832	0.027	0.009	1.000	Superior
1470	1822	Muzaffarghar	Thal	38.32	18.47	29.68	3.93	2.04	5.10	97.54	0.031	0.092	0.042	0.684	0.082		1.000	Poor
1470	2100	Muzaffarghar	Thal	38.15	19.48	35.23	0.88	4.14	1.94	99.83	0.065	0.020	0.078	0.781	0.043	0.012	1.000	Superior
1470	2182	Muzaffarghar	Thal	37.81	18.96	33.72	0.91	5.28	1.23	97.91	0.077	0.021	0.111	0.755	0.022	0.014	1.000	Superior
1470	2349	Muzaffarghar	Thal	39.15	19.83	30.25	1.83	6.71	1.38	99.16	0.041	0.041	0.211	0.669	0.007		1.000	Good
1470	2441	Muzaffarghar	Thal	36.86	19.01	29.83	3.73	1.02	6.84	97.28	0.021	0.088		0.689	0.155	0.004	1.000	Fair
1470	2445	Muzaffarghar	Thal	39.06	20.04	21.11	0.58	7.31	10.80	98.90	0.025	0.013	0.248	0.416	0.239	0.060	1.000	Superior
1470	2542	Muzaffarghar	Thal	38.04	18.98	30.55	2.46	4.30	3.62	97.96	0.085	0.057	0.060	0.693	0.100		1.000	Excellent
1470	2632	Muzaffarghar	Thal	38.18	18.50	23.59	12.59	0.69	5.73	99.28	0.001	0.292		0.539	0.063		1.000	Poor
1470	2641	Muzaffarghar	Thal	37.62	19.14	25.04	11.37	2.54	2.20	97.90	0.031	0.265	0.062	0.576	0.028		1.000	Fair
1470	2664	Muzaffarghar	Thal	39.00	15.95	7.75	0.29	0.54	35.43	98.97	0.014	0.006			0.722	0.251	1.000	Superior
1470	2665	Muzaffarghar	Thal	37.79	19.13	30.53	1.51	4.02	5.33	98.30	0.058	0.035	0.084	0.669	0.125	0.029	1.000	Superior
1470	2837	Muzaffarghar	Thal	36.44	19.19	31.24	3.63	3.09	3.55	97.15	0.016	0.085	0.106	0.688	0.057	0.049	1.000	Superior
1470	2876	Muzaffarghar	Thal	38.93	19.82	33.84	0.69	4.48	2.57	100.33	0.047	0.016	0.115	0.750	0.049		1.000	Fair
1470	3091	Muzaffarghar	Thal	36.25	18.68	34.25	1.24	4.30	1.63	96.36	0.017	0.029	0.155	0.732		0.049	1.000	Excellent
1470	3190	Muzaffarghar	Thal	40.31	29.00	2.84	0.31	0.16	24.72	97.35		0.007	0.006	0.061	0.680		1.000	Poor
1470	3195	Muzaffarghar	Thal	37.82	19.52	33.11	2.80	4.20	1.64	99.09	0.059	0.064	0.090	0.740	0.037	0.011	1.000	Superior
1470	3379	Muzaffarghar	Thal	38.39	19.22	32.96	1.18	5.45	2.52	99.72	0.058	0.027	0.138	0.705	0.032	0.040	1.000	Superior
1470	3401	Muzaffarghar	Thal	37.34	19.40	32.08	8.04	1.32	0.79	98.96	0.017	0.188	0.032	0.727			1.000	Fair
1470	3407	Muzaffarghar	Thal	38.04	19.31	30.34	1.39	6.98	1.35	97.40	0.068	0.032	0.189	0.672	0.024	0.015	1.000	Superior
1470	3429	Muzaffarghar	Thal	37.65	19.24	27.29	3.77	5.70	3.69	97.34	0.049	0.086	0.164	0.594	0.074	0.033	1.000	Superior
1470	3480	Muzaffarghar	Thal	38.48	19.25	35.41	1.26	2.50	2.28	99.18	0.008	0.029	0.091	0.806			1.000	Poor
1470	3785	Muzaffarghar	Thal	37.50	19.22	32.97	2.60	2.22	4.50	99.00	0.059	0.060	0.011	0.739	0.115	0.017	1.000	Superior
1470	4228	Muzaffarghar	Thal	37.29	19.34	33.42	2.27	3.59	2.20	98.11	0.055	0.053	0.073	0.755	0.052	0.012	1.000	Superior
1470	4273	Muzaffarghar	Thal	39.32	20.18	26.49	3.15	5.65	5.13	99.91	0.043	0.070	0.163	0.580	0.121		1.000	Fair
1470	4284	Muzaffarghar	Thal	38.15	19.17	34.19	3.51	3.59	0.90	99.51	0.073	0.080	0.048	0.773	0.015		1.000	Good
1470	4354	Muzaffarghar	Thal	37.27	19.75	24.92	12.11	1.55	4.22	99.81	0.028	0.278	0.026	0.547	0.096	0.027	1.000	Superior
1470	4406	Muzaffarghar	Thal	38.37	18.99	33.23	1.07	4.62	2.25	98.53	0.078	0.025	0.082	0.751	0.050		1.000	Good
1470	4451	Muzaffarghar	Thal	36.98	19.45	33.66	2.61	3.63	1.31	97.65	0.047	0.061	0.085	0.768	0.031	0.008	1.000	Superior
1470	4521	Muzaffarghar	Thal	37.51	19.87	33.60	1.95	4.67	1.36	98.95	0.028	0.044	0.150	0.738	0.013	0.027	1.000	Superior
1470	4577	Muzaffarghar	Thal	38.28	19.00	29.35	3.41	4.09	4.24	98.38	0.085	0.078	0.052	0.663	0.114		1.000	Excellent
1470	4937	Muzaffarghar	Thal	38.41	19.36	33.86	0.91	6.23	1.43	100.20	0.038	0.020	0.194	0.688		0.040	1.000	Superior
1470	4956	Muzaffarghar	Thal	38.23	20.16	35.45	0.73	3.53	2.18	100.27	0.034	0.017	0.096	0.792	0.048		1.000	Good
1470	5097	Muzaffarghar	Thal	38.58	19.66	31.23	4.94	2.83	1.67	98.91		0.114	0.115	0.710	0.006		1.000	Poor
1470	5292	Muzaffarghar	Thal	38.75	20.36	29.88	0.87	4.95	4.40	99.21	0.009	0.020	0.184	0.663	0.088		1.000	Fair
1470	5398	Muzaffarghar	Thal	37.10	19.41	24.72	0.89	3.82	11.43	97.36		0.020	0.153	0.494	0.248	0.081	1.000	Superior
1470	5406	Muzaffarghar	Thal	38.91	19.31	21.51	0.44	6.02	12.08	98.27	0.053	0.010	0.164	0.435	0.285	0.054	1.000	Superior
1470	5604	Muzaffarghar	Thal	37.88	19.65	22.08	0.93	5.75	12.28	98.58		0.021	0.224	0.402	0.247	0.097	1.000	Superior
1470	5623	Muzaffarghar	Thal	39.38	29.23	2.20	0.38	0.54	24.70	96.43		0.008	0.021	0.048	0.683		1.000	Poor
1470	5633	Muzaffarghar	Thal	38.26	19.35	27.89	4.46	6.90	2.31	99.17	0.033	0.100	0.228	0.574	0.002	0.064	1.000	Superior
1470	5740	Muzaffarghar	Thal	39.80	19.96	18.90	1.07	8.58	11.24	99.55	0.036	0.023	0.277	0.358	0.240	0.067	1.000	Superior
1470	5741	Muzaffarghar	Thal	38.30	19.43	34.72	2.60	2.29	2.62	99.97	0.038	0.060	0.042	0.785	0.042		1.000	Fair
1470	5827	Muzaffarghar	Thal	37.83	18.98	31.95	1.86	5.47	2.27	98.36	0.055	0.042	0.147	0.691	0.023	0.043	1.000	Superior
1470	5912	Muzaffarghar	Thal	38.05	19.36	24.37	0.55	2.76	14.22	99.31	0.012	0.012	0.093	0.481	0.317	0.085	1.000	Superior
1470	6049	Muzaffarghar	Thal	37.96	18.86	31.50	2.81	4.39	2.51	98.03	0.094	0.065	0.053	0.716	0.073		1.000	Superior
1470	6143	Muzaffarghar	Thal	38.47	19.42	33.23	3.80	3.38	1.82	100.13	0.060	0.086	0.056	0.746	0.033		1.000	Good
1470	6233	Muzaffarghar	Thal	37.86	19.62	33.06	2.43	4.32	2.32	99.61	0.041	0.055	0.118	0.720	0.036	0.031	1.000	Superior
1470	6341	Muzaffarghar	Thal	37.74	19.91	31.14	4.31	2.56	2.92	98.58		0.100	0.104	0.710	0.046		1.000	Poor
1470	6527	Muzaffarghar	Thal	37.75	19.48	33.14	2.05	3.78	1.95	98.15	0.038	0.047	0.102	0.755	0.034		1.000	Fair
1470	6765	Muzaffarghar	Thal	38.54	19.86	34.81	1.12	4.27	1.11	99.72	0.023	0.025	0.141	0.774			1.000	Fair
1474	14	Munda	Thal	38.84	21.58	28.19	0.90	3.41	7.68	100.60		0.020	0.133	0.617	0.215		1.000	Fair
1474	28	Munda	Thal	38.74	21.90	28.23	0.35	2.68	7.86	99.77		0.008	0.106	0.624	0.223		1.000	Poor
1474	39	Munda	Thal	39.58	22.44	31.17	0.26	4.86	1.55	99.86		0.006	0.191	0.687	0.044		1.000	Poor
1474	46	Munda	Thal	37.94	21.65	33.04	0.74	4.42	1.52	99.32		0.017	0.176	0.737	0.044		1.000	Poor
1474	55	Munda	Thal	39.02	21.91	28.47	2.67	1.79	7.00	100.86		0.060	0.070	0.628	0.198		1.000	Poor
1474	59	Munda	Thal	38.85	21.29	17.11	0.63	1.59	18.92	98.38		0.014	0.062	0.376	0.533		1.000	Fair
1474	77	Munda	Thal	40.82	32.60	1.50	0.12	0.16	24.23	99.43		0.003	0.006	0.031	0.648		1.000	Poor
1474	137	Munda	Thal	38.46	22.36	22.97	0.65	6.76	8.42	99.61		0.014	0.259	0.484	0.232		1.000	Excellent
1474	147	Munda	Thal	38.98	21.37	28.85	0.45	1.41	8.92	99.98		0.010	0.056	0.641	0.254		1.000	Poor
1474	167	Munda	Thal	37.03	21.73	28.96	0.60	6.25	3.23	97.79		0.014	0.248	0.632	0.092		1.000	Excellent
1474	178	Munda	Thal	39.39	21.95	30.13	0.43	6.85	1.17	99.91		0.010	0.266	0.657	0.033		1.000	Fair
1474	191	Munda	Thal	37.67	21.50	25.79	2.15	2.00	9.01	98.11		0.049	0.080	0.581	0.260		1.000	Poor
1474	195	Munda	Thal	39.11	23.33	19.31	0.50	6.15	12.27	100.67		0.011	0.232	0.408	0.332		1.000	Good
1474	228	Munda	Thal	39.05	21.49	21.26	9.14	1.31	2.56	94.80		0.218	0.055	0.501	0.077		1.000	Poor
1474	230	Munda	Thal	37.07	21.40	28.96	0.72	1.99	8.15	98.28		0.017	0.080	0.654	0.236		1.000	Fair
1474	231	Munda	Thal	37.81	21.57	33.30	1.58	2.50	1.49	98.26		0.037	0.102	0.760	0.044		1.000	Poor
1474	274	Munda	Thal	38.23	22.00	30.95	0.69	4.19	4.45	100.50		0.015	0.164	0.679	0.125		1.000	Fair
1474	297	Munda	Thal	38.06	21.03	32.07	2.63	2.74	1.60	98.14		0.061	0.112	0.732	0.047		1.000	Poor
1474	304	Munda	Thal	38.35	21.52	30.31	0.58	5.23	2.19	98.18		0.013	0.209	0.678	0.063		1.000	Poor
1474	326	Munda	Thal	38.55	21.25	24.28	0.99	3.21	10.90	99.18		0.022	0.126	0.535	0.307		1.000	Fair
1474	336	Munda	Thal	39.02	22.77	30.41	1.48	4.77	2.53	100.97		0.033	0.185	0.663	0.071		1.000	Poor
1474	419	Munda	Thal	38.11	21.53	32.27	0.86	4.24	1.40	98.40		0.020	0.170	0.727	0.040		1.000	Poor
1474	420	Munda	Thal	38.68	21.76	31.21	0.66	1.49	7.04	100.85		0.015	0.059	0.691	0.200		1.000	Poor
1474	459	Munda	Thal	36.95	21.40	33.00	2.46	3.04	0.95	97.80		0.057	0.124	0.756	0.028		1.000	Poor
1474	498	Munda	Thal	38.54	21.78	26.21	1.03	4.69	7.97	100.22		0.023	0.182	0.570	0.222		1.000	Good
1474	512	Munda	Thal	37.40	21.37	33.05	0.76	4.50	1.15	98.22		0.017	0.181	0.746	0.033		1.000	Poor
1474	516	Munda	Thal	38.14	21.55	31.82	0.86	4.34	2.83	99.53		0.019	0.172	0.707	0.081		1.000	Poor
1474	518	Munda	Thal	39.48	21.88	16.37	0.44	7.13	13.73	99.04	0.012	0.010	0.255	0.349	0.372		1.000	Superior
1474	532	Munda	Thal	37.58	21.25	34.43	0.61	3.41	2.02	99.31		0.014	0.137	0.774	0.058		1.000	Fair
1474	559	Munda	Thal	38.04	21.37	33.36	0.00	2.89	3.24	98.90			0.116	0.752	0.094		1.000	Poor
1474	605	Munda	Thal	36.97	21.29	32.90	1.38	4.23	1.44	98.20		0.032	0.171	0.744	0.042		1.000	Good
1474	609	Munda	Thal	38.51	21.85	32.55	0.75	3.91	2.06	99.63		0.017	0.155	0.725	0.059		1.000	Poor
1474	649	Munda	Thal	37.32	20.85	32.35	0.28	1.94	5.80	98.54		0.006	0.079	0.734	0.169		1.000	Fair
1474	722	Munda	Thal	41.34	23.08	13.01	0.44	15.18	7.42	100.47		0.009	0.547	0.251	0.177	0.015	1.000	Superior
1474	761	Munda	Thal	37.99	22.40	30.45	0.63	5.87	2.07	99.42		0.014	0.230	0.670	0.058		1.000	Fair
1474	847	Munda	Thal	38.39	21.89	30.93	0.55	4.38	3.94	100.08		0.012	0.172	0.681	0.111		1.000	Poor
1474	852	Munda	Thal	39.12	22.12	21.45	0.93	4.63	12.05	100.30		0.020	0.177	0.461	0.332		1.000	Good
1474	881	Munda	Thal	39.48	22.02	24.56	0.37	6.74	7.26	100.44		0.008	0.257	0.526	0.199		1.000	Excellent
1474	904	Munda	Thal	38.90	21.63	24.92	0.81	5.32	7.01	98.58		0.018	0.209	0.548	0.198		1.000	Poor
1474	911	Munda	Thal	37.91	22.07	32.11	0.59	4.49	1.19	98.37		0.013	0.180	0.722	0.034		1.000	Poor
1474	912	Munda	Thal	37.56	21.57	26.19	0.53	4.17	9.47	99.49		0.012	0.163	0.544	0.258	0.008	1.000	Excellent
1474	927	Munda	Thal	39.26	23.01	20.14	0.38	10.49	6.69	99.97		0.008	0.392	0.405	0.180		1.000	Excellent
1474	934	Munda	Thal	38.49	21.46	31.57	0.74	4.18	1.98	98.42		0.017	0.168	0.710	0.057		1.000	Poor
1474	937	Munda	Thal	38.02	32.20	1.74	0.35	0.59	23.92	96.83		0.008	0.023	0.037	0.656		1.000	Poor
1474	971	Munda	Thal	37.15	21.51	36.13	2.04	1.71	0.84	99.38		0.047	0.069	0.823	0.025		1.000	Poor
1474	1013	Munda	Thal	38.07	21.10	29.95	2.08	3.45	2.60	97.25		0.048	0.140	0.684	0.076		1.000	Poor
1474	1075	Munda	Thal	38.58	22.04	34.04	0.97	3.66	1.32	100.61		0.022	0.145	0.754	0.037		1.000	Poor
1474	1079	Munda	Thal	37.33	20.26	34.34	1.73	2.34	1.44	97.44		0.041	0.097	0.794	0.043		1.000	Poor
1474	1128	Munda	Thal	38.67	21.94	32.07	0.56	4.47	2.45	100.15		0.013	0.176	0.707	0.069		1.000	Poor
1474	1153	Munda	Thal	40.93	23.00	20.08	6.70	3.99	5.13	99.82		0.148	0.156	0.439	0.144		1.000	Poor
1474	1211	Munda	Thal	38.74	21.52	28.22	0.91	6.04	4.71	100.13		0.020	0.234	0.614	0.121		1.000	Fair
1474	1243	Munda	Thal	37.44	20.94	28.51	1.64	4.15	5.28	97.96		0.037	0.166	0.641	0.151		1.000	Good
1474	1269	Munda	Thal	38.86	21.26	23.66	1.16	4.89	8.76	98.60		0.026	0.192	0.521	0.247		1.000	Fair
1474	1334	Munda	Thal	39.09	21.86	27.52	0.91	2.01	8.61	99.99		0.020	0.079	0.609	0.244		1.000	Poor
1474	1362	Munda	Thal	39.22	21.19	18.68	0.52	6.12	13.34	99.07	0.026	0.011	0.199	0.395	0.358	0.010	1.000	Superior
1474	1406	Munda	Thal	40.68	32.63	1.81	0.24	0.27	23.94	99.57		0.005	0.010	0.038	0.640		1.000	Poor
1474	1410	Munda	Thal	38.28	21.92	31.44	1.85	5.39	1.62	100.51		0.041	0.211	0.689	0.046		1.000	Fair
1474	1419	Munda	Thal	37.74	22.05	27.90	3.45	1.37	5.48	97.99		0.080	0.056	0.636	0.160		1.000	Poor
1474	1463	Munda	Thal	37.75	22.00	33.54	0.35	4.51	1.21	99.36		0.008	0.179	0.748	0.035		1.000	Poor
1474	1484	Munda	Thal	38.29	21.10	24.88	1.05	3.46	9.10	97.88		0.024	0.138	0.556	0.261		1.000	Poor
1474	1515	Munda	Thal	39.44	21.18	24.60	1.17	2.01	11.43	99.82		0.026	0.079	0.542	0.323		1.000	Poor
1474	1608	Munda	Thal	38.48	21.78	20.34	0.40	6.26	10.51	97.77		0.009	0.244	0.444	0.294		1.000	Good
1474	1622	Munda	Thal	38.10	20.97	19.90	0.52	5.73	12.59	97.81		0.012	0.224	0.409	0.321	0.032	1.000	Superior
1474	1623	Munda	Thal	38.22	22.25	24.38	0.76	5.11	9.02	99.74		0.017	0.198	0.527	0.251		1.000	Superior
1474	1632	Munda	Thal	37.65	21.86	31.55	0.55	5.47	2.51	99.60		0.012	0.215	0.695	0.071		1.000	Superior
1474	1634	Munda	Thal	38.82	20.95	35.22	2.20	1.92	1.48	100.58		0.050	0.077	0.791	0.043		1.000	Poor
1474	1727	Munda	Thal	36.96	21.48	35.09	0.87	2.82	0.84	98.06		0.020	0.115	0.803	0.025		1.000	Poor
1474	1852	Munda	Thal	38.58	21.77	33.47	1.27	3.91	0.75	99.75		0.029	0.156	0.747	0.021		1.000	Poor
1474	1853	Munda	Thal	37.63	20.91	31.80	0.66	5.13	1.12	97.24		0.015	0.208	0.722	0.033		1.000	Poor
1474	1895	Munda	Thal	40.09	23.46	14.07	0.24	14.70	7.02	99.59		0.005	0.535	0.255	0.184		1.000	Good
1474	1972	Munda	Thal	38.15	21.61	25.03	2.93	6.80	3.71	98.23		0.065	0.267	0.552	0.105		1.000	Good

Appendix Table B5 SEM-EDS data and chemical calculations in epidote of Thal Desert and Upper Indus tributaries.

Sample	Points	River/Dune	Domain	SiO_2	Al_2O_3	FeO	MnO	MgO	CaO	La_2O_3	Ce_2O_3	Nd_2O_3	Total	Subgroup	Name
				wt%	wt%	wt%	wt%	wt%	wt%	wt%	wt%	wt%			
1749	17-1	Hushe	Karakorum	38.42	23.20	13.20	0.46	0.29	23.02				98.59	Clinozoisite	Epidote
1749	24-1	Hushe	Karakorum	38.61	22.02	13.06	0.38	0.34	22.65				97.06	Clinozoisite	Epidote
1749	36-1	Hushe	Karakorum	38.70	25.27	10.73	0.43	0.39	23.01				98.53	Clinozoisite	Epidote
1749	49-1	Hushe	Karakorum	38.06	24.85	10.52	0.24	0.24	23.74				97.65	Clinozoisite	Epidote
1749	94-1	Hushe	Karakorum	38.58	24.19	12.55	0.15	0.32	23.21				99.00	Clinozoisite	Epidote
1749	105-1	Hushe	Karakorum	38.33	24.02	12.00	0.42	0.32	22.80				97.89	Clinozoisite	Epidote
1749	122-1	Hushe	Karakorum	38.10	23.16	11.36	0.25	0.56	23.62				97.05	Clinozoisite	Epidote
1749	146-1	Hushe	Karakorum	38.55	25.72	10.52	0.41	0.45	22.74				98.39	Clinozoisite	Epidote
1749	169-1	Hushe	Karakorum	38.46	23.76	10.90	0.42	0.16	22.57				96.27	Clinozoisite	Clinozoisite
1749	186-1	Hushe	Karakorum	38.70	23.32	13.30	0.51	0.22	22.74				98.79	Clinozoisite	Epidote
1749	197-1	Hushe	Karakorum	38.22	20.81	16.33	0.16	0.59	22.09				98.20	Clinozoisite	Epidote
1749	215-1	Hushe	Karakorum	38.35	22.26	12.64	0.37	0.22	22.98				96.82	Clinozoisite	Clinozoisite
1749	236-1	Hushe	Karakorum	37.35	22.93	13.23	0.31	0.27	23.63				97.72	Clinozoisite	Epidote
1749	238-1	Hushe	Karakorum	37.16	21.18	13.25	0.37	0.26	24.80				97.02	Clinozoisite	Epidote
1749	240-1	Hushe	Karakorum	38.06	22.38	12.91	0.40	0.45	23.42				97.62	Clinozoisite	Epidote
1749	257-1	Hushe	Karakorum	38.79	22.12	13.30	0.32	0.00	22.89				97.42	Clinozoisite	Epidote
1749	276-1	Hushe	Karakorum	38.16	22.87	13.54	0.27	0.30	22.78				97.92	Clinozoisite	Epidote
1749	333-1	Hushe	Karakorum	37.84	24.53	11.18	0.33	0.32	22.58				96.78	Clinozoisite	Epidote
1749	341-1	Hushe	Karakorum	38.23	24.35	11.87	0.26	0.29	23.04				98.04	Clinozoisite	Epidote
1749	392-1	Hushe	Karakorum	37.76	24.60	10.45	0.45	0.00	23.16				96.42	Clinozoisite	Epidote
1749	398-1	Hushe	Karakorum	37.05	23.56	11.26	0.34	0.16	21.69				94.06	Clinozoisite	Epidote
1749	482-1	Hushe	Karakorum	38.90	24.79	11.27	0.22	0.18	23.13				98.49	Clinozoisite	Epidote
1749	488-1	Hushe	Karakorum	37.54	22.71	13.34	0.37	0.20	23.48				97.64	Clinozoisite	Epidote
1749	489-1	Hushe	Karakorum	38.20	27.74	7.68	0.16	0.54	23.75				98.07	Clinozoisite	Epidote
1749	503-1	Hushe	Karakorum	38.52	26.23	9.13	0.21	0.11	23.39				97.59	Clinozoisite	Epidote
1749	531-1	Hushe	Karakorum	37.52	23.39	11.90	0.70	0.30	22.59				96.40	Clinozoisite	Epidote
1749	536-1	Hushe	Karakorum	37.61	24.65	11.07	0.25	0.29	22.72				96.59	Clinozoisite	Epidote
1749	543-1	Hushe	Karakorum	38.89	22.53	13.76	0.32	0.14	23.20				98.84	Clinozoisite	Epidote
1749	588-1	Hushe	Karakorum	37.66	22.67	11.99	0.35	0.00	22.48				95.15	Clinozoisite	Epidote
1749	599-1	Hushe	Karakorum	37.57	24.65	12.22	0.28	0.19	22.87				97.78	Clinozoisite	Epidote
1749	610-1	Hushe	Karakorum	38.93	28.93	6.65	0.24	0.32	23.10				98.17	Clinozoisite	Clinozoisite
1749	616-1	Hushe	Karakorum	38.13	24.46	10.75	0.13	0.35	22.98				96.80	Clinozoisite	Epidote
1749	625-1	Hushe	Karakorum	37.54	24.44	11.56	0.35	0.00	22.54				96.43	Clinozoisite	Epidote
1749	631-1	Hushe	Karakorum	38.47	24.69	11.34	0.28	0.27	23.40				98.45	Clinozoisite	Epidote
1749	636-1	Hushe	Karakorum	37.82	23.93	11.98	0.38	0.26	23.21				97.58	Clinozoisite	Epidote
1749	677-1	Hushe	Karakorum	38.48	24.50	12.14	0.22	0.26	23.15				98.75	Clinozoisite	Epidote
1749	5-2	Hushe	Karakorum	37.26	21.56	13.44	0.36	0.24	24.60				97.46	Clinozoisite	Epidote
1749	23-2	Hushe	Karakorum	39.01	22.25	12.95	0.17	0.44	22.83				97.65	Clinozoisite	Epidote
1749	37-2	Hushe	Karakorum	37.96	23.27	11.66	0.38	0.30	22.61				96.18	Clinozoisite	Epidote
1749	58-2	Hushe	Karakorum	38.31	24.24	11.46	0.47	0.16	23.23				97.87	Clinozoisite	Epidote
1749	62-2	Hushe	Karakorum	38.38	23.00	11.10	0.65	0.41	22.59				96.13	Clinozoisite	Clinozoisite
1749	81-2	Hushe	Karakorum	36.64	24.52	12.09	0.28	0.28	23.07				96.88	Clinozoisite	Epidote
1749	110-2	Hushe	Karakorum	37.89	24.52	11.27	0.30	0.32	23.44				97.74	Clinozoisite	Epidote
1749	137-2	Hushe	Karakorum	36.89	23.65	9.92	0.25	0.40	21.20				92.31	Clinozoisite	Clinozoisite
1749	150-2	Hushe	Karakorum	38.63	24.08	11.49	0.40	0.36	21.94				96.90	Clinozoisite	Clinozoisite
1749	155-2	Hushe	Karakorum	38.18	24.04	12.11	0.48	0.45	22.40				97.66	Clinozoisite	Epidote
1749	156-2	Hushe	Karakorum	38.08	23.60	12.05	0.30	0.30	22.98				97.31	Clinozoisite	Epidote
1749	158-2	Hushe	Karakorum	38.71	24.36	11.03	0.33	0.20	22.92				97.55	Clinozoisite	Epidote
1749	181-2	Hushe	Karakorum	38.14	24.10	11.77	0.35	0.31	23.61				98.28	Clinozoisite	Epidote
1749	186-2	Hushe	Karakorum	38.95	24.52	11.13	0.16	0.16	22.87				97.79	Clinozoisite	Clinozoisite
1749	212-2	Hushe	Karakorum	38.88	26.22	9.79	0.35	0.31	22.87				98.42	Clinozoisite	Epidote
1749	215-2	Hushe	Karakorum	38.62	24.15	11.89	0.34	0.27	22.88				98.15	Clinozoisite	Epidote
1749	241-2	Hushe	Karakorum	37.91	25.19	10.13	0.29	0.37	23.23				97.12	Clinozoisite	Epidote
1749	269-2	Hushe	Karakorum	37.64	22.27	13.06	0.15	0.20	23.18				96.50	Clinozoisite	Epidote
1749	317-2	Hushe	Karakorum	37.77	22.45	13.08	0.38	0.32	24.09				98.09	Clinozoisite	Epidote
1749	371-2	Hushe	Karakorum	38.44	24.25	11.18	0.31	0.29	23.26				97.73	Clinozoisite	Epidote
1749	400-2	Hushe	Karakorum	38.88	23.84	11.08	0.27	0.25	22.56				96.88	Clinozoisite	Clinozoisite
1749	419-2	Hushe	Karakorum	38.09	23.14	12.26	0.22	0.11	22.45				96.27	Clinozoisite	Epidote
1749	420-2	Hushe	Karakorum	38.10	25.76	10.35	0.31	0.35	23.20				98.07	Clinozoisite	Epidote
1749	421-2	Hushe	Karakorum	38.64	24.75	10.80	0.31	0.47	22.41				97.38	Clinozoisite	Epidote
1749	435-2	Hushe	Karakorum	37.85	23.65	11.96	0.36	0.49	22.95				97.26	Clinozoisite	Epidote
1749	485-2	Hushe	Karakorum	38.72	24.82	11.58	0.42	0.55	22.17				98.26	Clinozoisite	Epidote
1749	508-2	Hushe	Karakorum	36.09	25.26	7.83	0.26	0.11	19.63				89.18	Clinozoisite	Clinozoisite
1749	568-2	Hushe	Karakorum	37.06	23.33	11.73	0.28	0.47	22.76				95.63	Clinozoisite	Epidote
1749	610-2	Hushe	Karakorum	38.38	26.24	10.09	0.33	0.24	22.77				98.05	Clinozoisite	Epidote
1749	645-2	Hushe	Karakorum	37.18	23.64	11.88	0.31	0.11	23.20				96.32	Clinozoisite	Epidote
1749	656-2	Hushe	Karakorum	37.25	24.18	11.49	0.39	0.46	22.26				96.03	Clinozoisite	Epidote
1749	697-2	Hushe	Karakorum	38.63	22.93	11.06	0.20	0.00	23.19				96.01	Clinozoisite	Clinozoisite
1749	740-2	Hushe	Karakorum	37.98	22.23	12.95	0.26	0.19	22.86				96.47	Clinozoisite	Epidote
1749	750-2	Hushe	Karakorum	38.10	21.94	12.79	0.30	0.14	23.03				96.30	Clinozoisite	Clinozoisite
1749	759-2	Hushe	Karakorum	38.19	23.09	12.30	0.40	0.22	22.70				96.90	Clinozoisite	Epidote
1749	785-2	Hushe	Karakorum	38.02	23.90	11.62	0.20	0.15	22.88				96.77	Clinozoisite	Epidote
1749	791-2	Hushe	Karakorum	38.65	24.00	10.88	0.35	0.10	22.44				96.42	Clinozoisite	Clinozoisite
1749	814-2	Hushe	Karakorum	38.53	21.58	14.82	0.35	0.49	22.31				98.08	Clinozoisite	Epidote
1749	820-2	Hushe	Karakorum	38.63	24.18	10.98	0.34	0.31	22.90				97.34	Clinozoisite	Epidote
1749	853-2	Hushe	Karakorum	37.91	26.86	9.42	0.33	0.54	22.33				97.39	Clinozoisite	Epidote
1749	862-2	Hushe	Karakorum	37.90	23.65	11.77	0.42	0.12	22.47				96.33	Clinozoisite	Epidote
1749	874-2	Hushe	Karakorum	36.07	23.40	9.35	0.31	0.50	18.98				88.61	Clinozoisite	Clinozoisite
1749	888-2	Hushe	Karakorum	37.88	26.91	8.38	0.51	0.49	23.07				97.24	Clinozoisite	Epidote
1749	931-2	Hushe	Karakorum	38.55	26.43	9.79	0.42	0.39	23.17				98.75	Clinozoisite	Epidote
1749	958-2	Hushe	Karakorum	38.17	24.32	10.63	0.42	0.29	22.92				96.75	Clinozoisite	Epidote
1749	967-2	Hushe	Karakorum	37.58	23.63	12.01	0.34	0.29	22.86				96.71	Clinozoisite	Epidote
1749	983-2	Hushe	Karakorum	38.89	24.13	11.30	0.46	0.22	22.79				97.79	Clinozoisite	Clinozoisite
1749	985-2	Hushe	Karakorum	37.72	23.69	11.65	0.53	0.00	22.92				96.51	Clinozoisite	Epidote
1749	997-2	Hushe	Karakorum	37.41	25.13	10.17	0.13	0.29	23.05				96.18	Clinozoisite	Epidote
1749	8-1	Hushe	Karakorum	34.86	20.10	13.54	0.49	0.81	18.25	2.76	4.35	1.80	96.96	Clinozoisite	Epidote
1749	35-1	Hushe	Karakorum	32.56	15.61	16.18	0.41	1.08	11.70	7.57	10.19	2.21	97.51	Allanite	Allanite-(Ce)
1749	60-1	Hushe	Karakorum	32.80	16.73	14.82	0.93	1.20	14.07	4.99	8.55	3.20	97.29	Allanite	Allanite-(Ce)
1749	173-1	Hushe	Karakorum	36.03	22.59	10.55	0.61	0.53	17.99	3.03	6.69	1.70	99.72	Clinozoisite	Epidote
1749	234-1	Hushe	Karakorum	35.09	18.78	13.41	0.33	0.24	18.69	3.12	6.23	2.49	98.38	Clinozoisite	Epidote
1749	248-1	Hushe	Karakorum	32.48	13.89	16.55	0.46	1.00	13.03	6.49	10.11	2.90	96.91	Allanite	Allanite-(Ce)
1749	264-1	Hushe	Karakorum	32.95	17.72	14.23	0.61	0.70	16.19	4.01	7.32	2.29	96.02	Clinozoisite	Epidote
1749	303-1	Hushe	Karakorum	32.23	15.21	15.29	0.55	0.90	12.48	6.64	10.06	2.44	95.80	Allanite	Allanite-(Ce)
1749	312-1	Hushe	Karakorum	34.03	18.96	12.74	0.70	0.92	14.70	3.02	6.62	2.47	94.16	Allanite	Epidote
1749	453-1	Hushe	Karakorum	33.11	17.94	13.05	0.94	0.65	11.66	6.13	10.27	3.61	97.36	Allanite	Allanite-(Ce)
1749	465-1	Hushe	Karakorum	33.65	19.18	12.75	0.68	0.58	14.15	6.04	8.87	2.50	98.40	Allanite	Allanite-(Ce)
1749	628-1	Hushe	Karakorum	32.55	15.16	14.80	0.53	1.19	13.62	8.10	10.06	2.00	98.01	Allanite	Allanite-(Ce)
1749	659-1	Hushe	Karakorum	33.79	17.84	13.24	0.62	0.54	14.50	4.72	7.28	2.46	94.99	Clinozoisite	Allanite-(Ce)
1749	679-1	Hushe	Karakorum	31.79	16.01	14.08	0.59	1.07	11.97	6.53	10.94	2.92	95.90	Allanite	Allanite-(Ce)
1749	64-2	Hushe	Karakorum	33.12	17.83	13.75	0.46	1.18	13.57	5.20	9.23	3.80	98.14	Allanite	Allanite-(Ce)
1749	204-2	Hushe	Karakorum	33.36	19.88	12.08	0.89	0.43	14.46	5.03	7.87	3.42	97.42	Allanite	Allanite-(Ce)
1749	234-2	Hushe	Karakorum	34.88	21.16	12.45	0.54	0.23	18.12	2.29	4.97	3.15	97.79	Clinozoisite	Epidote
1749	312-2	Hushe	Karakorum	33.48	17.39	13.77	0.54	1.09	14.34	5.61	8.15	2.81	97.18	Allanite	Allanite-(Ce)
1749	330-2	Hushe	Karakorum	31.92	14.68	15.89	0.76	1.03	12.05	7.50	9.94	2.30	96.07	Allanite	Allanite-(Ce)
1749	355-2	Hushe	Karakorum	34.42	19.60	14.09	0.46	0.74	16.06	4.29	7.17	1.80	98.63	Clinozoisite	Epidote
1749	387-2	Hushe	Karakorum	33.23	18.47	13.65	0.54	0.73	14.79	5.40	8.31	2.67	97.79	Allanite	Allanite-(Ce)
1749	620-2	Hushe	Karakorum	33.83	19.20	13.57	0.61	0.94	15.28	4.55	6.64	2.11	96.73	Clinozoisite	Epidote
1749	622-2	Hushe	Karakorum	33.23	20.04	13.84	0.98	0.83	14.41	4.55	6.78	3.59	98.25	Clinozoisite	Epidote
1749	658-2	Hushe	Karakorum	30.66	14.05	15.91	0.53	1.29	11.52	7.07	11.28	2.46	94.77	Allanite	Allanite-(Ce)
1749	734-2	Hushe	Karakorum	33.72	20.02	12.55	1.01	0.51	14.35	4.85	7.66	3.20	97.87	Allanite	Allanite-(Ce)
1749	819-2	Hushe	Karakorum	35.04	20.35	12.87	0.57	0.52	17.38	4.53	6.11	1.92	99.29	Clinozoisite	Epidote
1749	826-2	Hushe	Karakorum	32.87	16.94	13.51	0.53	0.96	14.18	5.62	9.37	3.15	97.13	Allanite	Allanite-(Ce)
1749	830-2	Hushe	Karakorum	34.88	20.08	12.22	0.46	0.56	17.20	4.48	5.50	1.29	96.67	Clinozoisite	Epidote
1749	911-2	Hushe	Karakorum	31.11	14.56	13.61	0.62	1.50	11.13	9.10	12.82	1.88	96.33	Allanite	Allanite-(Ce)
1749	955-2	Hushe	Karakorum	31.12	17.13	14.41	0.81	0.85	10.65	6.62	11.93	3.28	96.80	Allanite	Allanite-(Ce)
1749	956-2	Hushe	Karakorum	32.42	15.08	14.86	0.73	1.11	12.46	7.04	11.75	1.38	96.83	Allanite	Allanite-(Ce)
1749	961-2	Hushe	Karakorum	32.06	14.67	15.01	0.62	1.06	11.71	7.00	10.64	3.37	96.14	Allanite	Allanite-(Ce)

Sample	Points	River/Dune	Domain	SiO_2	Al_2O_3	FeO	MnO	MgO	CaO	La_2O_3	Ce_2O_3	Nd_2O_3	Total	Subgroup	Name
				wt%	wt%	wt%	wt%	wt%	wt%	wt%	wt%	wt%			
1748	443-1	Braldu	Karakorum	37.73	26.67	4.92	0.41	0.34	21.99				92.06	Clinozoisite	Clinozoisite
1748	457-1	Braldu	Karakorum	37.84	24.72	7.11	0.18	0.49	22.65				92.99	Clinozoisite	Clinozoisite
1748	461-1	Braldu	Karakorum	37.62	28.41	2.49	0.35	0.47	23.49				92.83	Clinozoisite	Clinozoisite
1748	470-1	Braldu	Karakorum	37.87	19.86	13.77	0.23	0.39	21.28				93.40	Clinozoisite	Epidote
1748	476-1	Braldu	Karakorum	49.91	3.38	6.74	0.10	12.73	22.96				95.82	Clinozoisite	Epidote
1748	478-1	Braldu	Karakorum	37.27	24.38	7.78	0.20	0.15	22.35				92.13	Clinozoisite	Clinozoisite
1748	479-1	Braldu	Karakorum	36.39	19.90	12.35	0.21	0.00	21.00				89.85	Clinozoisite	Epidote
1748	483-1	Braldu	Karakorum	36.28	20.58	13.60	0.25	0.36	19.43				90.50	Clinozoisite	Epidote
1748	484-1	Braldu	Karakorum	36.28	20.58	13.60	0.25	0.36	19.43				90.50	Clinozoisite	Epidote
1748	485-1	Braldu	Karakorum	37.06	21.65	12.81	0.00	0.38	21.19				93.09	Clinozoisite	Epidote
1748	496-1	Braldu	Karakorum	39.62	25.10	6.69	0.23	0.20	20.81				92.65	Clinozoisite	Clinozoisite
1748	497-1	Braldu	Karakorum	37.08	25.59	6.56	0.44	0.00	22.57				92.24	Clinozoisite	Clinozoisite
1748	499-1	Braldu	Karakorum	37.19	24.22	6.56	0.32	0.22	21.70				90.21	Clinozoisite	Clinozoisite
1748	506-1	Braldu	Karakorum	38.26	24.41	5.82	0.29	0.34	21.08				90.20	Clinozoisite	Clinozoisite
1748	524-1	Braldu	Karakorum	37.62	24.96	6.14	0.38	0.43	21.42				90.95	Clinozoisite	Clinozoisite
1748	527-1	Braldu	Karakorum	36.60	19.60	11.41	0.37	0.16	18.71				86.85	Clinozoisite	Epidote
1748	575-1	Braldu	Karakorum	37.15	22.50	8.86	0.40	0.38	20.23				89.52	Clinozoisite	Clinozoisite
1748	604-1	Braldu	Karakorum	39.46	25.37	5.89	0.25	0.14	22.78				93.89	Clinozoisite	Clinozoisite
1748	615-1	Braldu	Karakorum	37.44	28.83	2.16	0.24	0.23	22.12				91.02	Clinozoisite	Clinozoisite
1748	623-1	Braldu	Karakorum	37.64	21.80	11.42	0.36	0.22	22.75				94.19	Clinozoisite	Clinozoisite
1748	627-1	Braldu	Karakorum	37.85	25.76	6.39	0.34	0.31	22.16				92.81	Clinozoisite	Clinozoisite
1748	704-1	Braldu	Karakorum	39.21	29.98	0.75	0.20	0.27	23.51				93.92	Clinozoisite	Clinozoisite
1748	15-2	Braldu	Karakorum	37.74	22.90	7.92	0.28	0.28	21.72				90.84	Clinozoisite	Clinozoisite
1748	30-2	Braldu	Karakorum	38.21	25.27	5.68	0.22	0.20	21.95				91.53	Clinozoisite	Clinozoisite
1748	38-2	Braldu	Karakorum	38.44	29.26	4.62	0.19	0.16	22.97				95.64	Clinozoisite	Clinozoisite
1748	43-2	Braldu	Karakorum	38.44	25.69	5.90	0.39	0.37	22.79				93.58	Clinozoisite	Clinozoisite
1748	62-2	Braldu	Karakorum	37.92	24.03	7.81	0.30	0.29	22.05				92.40	Clinozoisite	Clinozoisite
1748	76-2	Braldu	Karakorum	38.54	26.50	4.46	0.32	0.48	22.82				93.12	Clinozoisite	Clinozoisite
1748	82-2	Braldu	Karakorum	36.52	19.35	13.88	0.31	0.32	21.68				92.06	Clinozoisite	Epidote
1748	86-2	Braldu	Karakorum	37.96	24.74	7.95	0.33	0.17	21.50				92.65	Clinozoisite	Clinozoisite
1748	89-2	Braldu	Karakorum	36.84	19.26	13.34	0.31	0.11	20.87				90.73	Clinozoisite	Epidote
1748	127-2	Braldu	Karakorum	37.46	25.19	6.50	0.25	0.30	22.07				91.77	Clinozoisite	Clinozoisite
1748	140-2	Braldu	Karakorum	38.54	25.62	4.96	0.30	0.23	22.37				92.02	Clinozoisite	Clinozoisite
1748	143-2	Braldu	Karakorum	39.03	25.08	4.97	0.26	0.16	22.79				92.29	Clinozoisite	Clinozoisite
1748	149-2	Braldu	Karakorum	36.35	23.16	7.58	0.27	0.39	20.43				88.18	Clinozoisite	Clinozoisite
1748	172-2	Braldu	Karakorum	37.10	20.71	10.78	0.25	0.11	21.72				90.67	Clinozoisite	Clinozoisite
1748	178-2	Braldu	Karakorum	38.64	26.30	5.34	0.30	0.24	22.50				93.32	Clinozoisite	Clinozoisite
1748	181-2	Braldu	Karakorum	37.90	24.10	8.62	0.29	0.38	22.16				93.45	Clinozoisite	Clinozoisite
1748	219-2	Braldu	Karakorum	38.43	23.38	10.03	0.27	0.31	21.64				94.06	Clinozoisite	Clinozoisite
1748	251-2	Braldu	Karakorum	37.03	19.18	13.92	0.57	0.33	21.99				93.02	Clinozoisite	Clinozoisite
1748	290-2	Braldu	Karakorum	38.03	25.69	5.77	0.16	0.21	20.81				90.67	Clinozoisite	Clinozoisite
1748	292-2	Braldu	Karakorum	36.65	21.96	10.22	0.10	0.09	21.19				90.21	Clinozoisite	Clinozoisite
1748	293-2	Braldu	Karakorum	36.69	21.13	10.83	0.31	0.22	19.82				89.00	Clinozoisite	Epidote
1748	294-2	Braldu	Karakorum	37.71	26.34	5.61	0.17	0.15	21.20				91.18	Clinozoisite	Clinozoisite
1748	312-2	Braldu	Karakorum	38.07	24.84	7.36	0.32	0.31	21.83				92.73	Clinozoisite	Clinozoisite
1748	329-2	Braldu	Karakorum	37.19	22.11	11.59	0.27	0.16	22.03				93.35	Clinozoisite	Clinozoisite
1748	334-2	Braldu	Karakorum	38.00	24.60	6.81	0.16	0.32	21.28				91.17	Clinozoisite	Clinozoisite
1748	340-2	Braldu	Karakorum	37.77	20.31	13.01	0.34	0.11	22.09				93.63	Clinozoisite	Epidote
1748	355-2	Braldu	Karakorum	38.38	24.43	7.55	0.33	0.13	23.23				94.05	Clinozoisite	Clinozoisite
1748	367-2	Braldu	Karakorum	37.14	19.89	14.72	0.19	0.00	22.17				94.11	Clinozoisite	Epidote
1748	371-2	Braldu	Karakorum	37.69	26.31	5.05	0.32	0.25	22.97				92.59	Clinozoisite	Clinozoisite
1748	379-2	Braldu	Karakorum	38.65	26.93	4.28	0.25	0.16	22.95				93.22	Clinozoisite	Clinozoisite
1748	409-2	Braldu	Karakorum	37.33	19.71	13.17	0.44	0.29	21.19				92.13	Clinozoisite	Epidote
1748	425-2	Braldu	Karakorum	37.64	24.13	7.13	0.17	1.18	19.89				90.14	Clinozoisite	Clinozoisite
1748	426-2	Braldu	Karakorum	37.58	26.13	5.48	0.24	0.46	21.17				91.06	Clinozoisite	Clinozoisite
1748	432-2	Braldu	Karakorum	37.68	24.59	6.85	0.35	0.00	21.49				90.96	Clinozoisite	Clinozoisite
1748	433-2	Braldu	Karakorum	37.06	25.17	5.49	0.22	0.38	21.95				90.27	Clinozoisite	Clinozoisite
1748	447-2	Braldu	Karakorum	37.33	24.51	7.15	0.30	0.30	20.94				90.53	Clinozoisite	Clinozoisite
1748	471-2	Braldu	Karakorum	35.29	19.30	10.12	0.28	0.22	17.66				82.87	Clinozoisite	Epidote
1748	482-2	Braldu	Karakorum	35.61	23.57	4.97	0.26	0.36	18.72				83.49	Clinozoisite	Clinozoisite
1748	505-2	Braldu	Karakorum	37.34	21.65	10.02	0.25	0.29	21.75				91.30	Clinozoisite	Clinozoisite
1748	518-2	Braldu	Karakorum	37.57	23.45	7.65	0.31	0.00	22.08				91.06	Clinozoisite	Clinozoisite
1748	523-2	Braldu	Karakorum	36.88	24.40	7.44	0.25	0.38	22.96				92.31	Clinozoisite	Epidote
1748	545-2	Braldu	Karakorum	38.11	22.75	9.06	0.31	0.21	22.22				92.66	Clinozoisite	Clinozoisite
1748	571-2	Braldu	Karakorum	37.21	18.60	15.49	0.22	0.21	21.31				93.04	Clinozoisite	Epidote
1748	586-2	Braldu	Karakorum	39.22	27.78	4.46	0.37	0.36	22.63				94.82	Clinozoisite	Clinozoisite
1748	591-2	Braldu	Karakorum	38.62	19.32	13.88	0.40	0.09	22.15				94.46	Clinozoisite	Epidote
1748	633-2	Braldu	Karakorum	37.05	21.53	11.10	0.12	0.29	20.90				90.99	Clinozoisite	Epidote
1748	637-2	Braldu	Karakorum	37.27	19.88	12.30	0.17	0.00	20.55				90.17	Clinozoisite	Epidote
1748	658-2	Braldu	Karakorum	37.97	27.68	4.61	0.40	0.16	22.24				93.06	Clinozoisite	Clinozoisite
1748	663-2	Braldu	Karakorum	36.75	27.03	4.26	0.48	0.09	20.86				89.47	Clinozoisite	Clinozoisite
1748	697-2	Braldu	Karakorum	37.25	25.28	6.53	0.17	0.36	23.06				92.65	Clinozoisite	Clinozoisite
1748	706-2	Braldu	Karakorum	37.32	19.82	13.68	0.34	0.21	21.77				93.14	Clinozoisite	Epidote
1748	709-2	Braldu	Karakorum	37.14	19.02	15.87	0.28	0.17	21.58				94.06	Clinozoisite	Epidote
1748	718-2	Braldu	Karakorum	37.36	20.31	13.56	0.30	0.00	21.44				92.97	Clinozoisite	Epidote
1748	747-2	Braldu	Karakorum	37.03	21.37	10.54	0.27	0.22	21.11				90.54	Clinozoisite	Clinozoisite
1748	767-2	Braldu	Karakorum	36.18	20.60	12.13	0.39	0.19	20.77				90.26	Clinozoisite	Epidote
1748	769-2	Braldu	Karakorum	37.63	21.30	11.24	0.36	0.44	22.37				93.34	Clinozoisite	Clinozoisite
1748	787-2	Braldu	Karakorum	36.62	22.12	11.09	0.31	0.16	21.71				92.01	Clinozoisite	Clinozoisite
1748	794-2	Braldu	Karakorum	36.97	22.99	9.43	0.24	0.00	22.25				91.88	Clinozoisite	Clinozoisite
1748	818-2	Braldu	Karakorum	36.83	19.29	13.83	0.45	0.30	20.94				91.64	Clinozoisite	Epidote
1748	835-2	Braldu	Karakorum	36.03	21.33	11.33	0.35	0.26	20.68				89.98	Clinozoisite	Clinozoisite
1748	520-1	Braldu	Karakorum	32.52	16.68	9.24	0.43	1.36	11.40	4.63	8.22	3.83	88.31	Allanite	Dissakisite-(Ce)
1748	552-1	Braldu	Karakorum	30.85	15.60	10.44	0.44	1.09	8.99	5.07	9.11	4.04	85.63	Allanite	Dissakisite-(Ce)
1748	620-1	Braldu	Karakorum	32.97	15.77	13.36	0.58	1.11	11.84	5.73	9.58	1.49	92.43	Allanite	Allanite-(Ce)
1748	642-1	Braldu	Karakorum	32.09	17.62	10.83	0.41	0.45	10.86	6.09	10.64	3.04	92.03	Allanite	Dissakisite-(Ce)
1748	42-2	Braldu	Karakorum	31.52	15.10	12.66	0.74	0.22	9.53	6.87	11.39	3.91	91.94	Allanite	Epidote
1748	52-2	Braldu	Karakorum	36.44	20.13	13.53	0.23	0.31	22.21	0.23	0.64	0.21	93.93	Clinozoisite	Epidote
1748	136-2	Braldu	Karakorum	32.72	15.45	12.80	0.85	0.93	10.47	6.20	10.33	2.72	92.47	Allanite	Allanite-(Ce)
1748	170-2	Braldu	Karakorum	32.26	15.87	12.74	0.34	0.74	10.47	6.32	10.18	4.22	93.14	Allanite	Allanite-(Ce)
1748	186-2	Braldu	Karakorum	33.10	12.84	15.08	0.62	0.90	11.60	7.04	11.81	2.11	95.10	Allanite	Allanite-(Ce)
1748	236-2	Braldu	Karakorum	34.82	22.00	7.06	0.31	0.31	16.03	3.37		3.32	87.22	Clinozoisite	Epidote
1748	306-2	Braldu	Karakorum	33.16	14.87	13.24	0.80	1.63	10.51	5.97	11.08	2.99	94.25	Allanite	Allanite-(Ce)
1748	323-2	Braldu	Karakorum	33.90	19.02	10.22	0.31	0.50	13.83	4.19	9.11	2.57	93.65	Allanite	Allanite-(Ce)
1748	338-2	Braldu	Karakorum	34.05	19.49	10.01	0.45	0.79	13.89	3.59	7.16	3.29	92.72	Allanite	Allanite-(Ce)
1748	430-2	Braldu	Karakorum	34.80	17.77	12.45	0.67	0.39	15.71	3.98	6.66	1.97	94.40	Allanite	Epidote
1748	546-2	Braldu	Karakorum	33.63	14.75	14.03	0.41	1.24	13.00	5.60	8.68	2.44	93.78	Allanite	Allanite-(Ce)
1748	560-2	Braldu	Karakorum	32.75	15.77	14.42	0.84	1.02	10.53	6.74	10.82	3.79	96.68	Allanite	Allanite-(Ce)
1748	589-2	Braldu	Karakorum	34.73	19.05	10.10	0.42	0.86	12.90	3.64	7.95	3.15	92.80	Allanite	Dissakisite-(Ce)
1748	805-2	Braldu	Karakorum	34.52	20.06	9.57	0.50	0.68	14.75	4.38	6.59	2.18	93.23	Allanite	Allanite-(Ce)

Sample	Points	River/Dune	Domain	SiO_2	Al_2O_3	FeO	MnO	MgO	CaO	La_2O_3	Ce_2O_3	Nd_2O_3	Total	Subgroup	Name
				wt%	wt%	wt%	wt%	wt%	wt%	wt%	wt%	wt%			
1437	52-1	Upper Hunza	Karakorum	39.97	27.88	6.80	0.50	0.26	23.88				99.29	Clinozoisite	Clinozoisite
1437	63-1	Upper Hunza	Karakorum	40.32	27.06	8.49	0.40	0.35	24.29				100.91	Clinozoisite	Epidote
1437	70-1	Upper Hunza	Karakorum	40.31	28.69	5.77	0.17	0.24	24.04				99.22	Clinozoisite	Clinozoisite
1437	91-1	Upper Hunza	Karakorum	39.43	25.23	8.21	0.44	0.48	22.83				96.62	Clinozoisite	Clinozoisite
1437	100-1	Upper Hunza	Karakorum	39.04	21.57	14.98	0.40	0.39	22.97				99.35	Clinozoisite	Epidote
1437	104-1	Upper Hunza	Karakorum	39.93	26.26	9.02	0.30	0.21	24.01				99.73	Clinozoisite	Clinozoisite
1437	153-1	Upper Hunza	Karakorum	39.52	22.84	13.47	0.30	0.27	23.40				99.80	Clinozoisite	Clinozoisite
1437	160-1	Upper Hunza	Karakorum	39.93	27.23	9.66	0.29	0.46	22.74				100.31	Clinozoisite	Epidote
1437	174-1	Upper Hunza	Karakorum	39.41	24.70	12.55	0.25	0.14	22.92				99.97	Clinozoisite	Epidote
1437	190-1	Upper Hunza	Karakorum	41.09	26.71	8.09	0.34	0.21	23.89				100.33	Clinozoisite	Clinozoisite
1437	191-1	Upper Hunza	Karakorum	40.14	26.04	8.64	0.48	0.00	23.61				98.91	Clinozoisite	Clinozoisite
1437	193-1	Upper Hunza	Karakorum	41.33	32.78	0.64	0.28	0.29	24.08				99.40	Clinozoisite	Clinozoisite
1437	194-1	Upper Hunza	Karakorum	40.02	26.06	8.62	0.43	0.42	23.53				99.08	Clinozoisite	Clinozoisite
1437	195-1	Upper Hunza	Karakorum	39.53	27.52	8.69	0.23	0.28	23.25				99.50	Clinozoisite	Epidote
1437	196-1	Upper Hunza	Karakorum	39.77	25.79	8.74	0.36	0.29	22.94				97.89	Clinozoisite	Clinozoisite
1437	198-1	Upper Hunza	Karakorum	40.99	26.38	9.54	0.30	0.34	23.57				101.12	Clinozoisite	Clinozoisite
1437	222-1	Upper Hunza	Karakorum	41.15	26.66	9.07	0.32	0.16	23.56				100.92	Clinozoisite	Clinozoisite
1437	226-1	Upper Hunza	Karakorum	44.22	13.35	19.08	0.23	8.30	11.90				97.08	Clinozoisite	Clinozoisite
1437	229-1	Upper Hunza	Karakorum	40.73	26.23	8.83	0.30	0.00	24.04				100.13	Clinozoisite	Clinozoisite
1437	232-1	Upper Hunza	Karakorum	40.24	26.45	9.10	0.30	0.25	22.98				99.32	Clinozoisite	Clinozoisite
1437	251-1	Upper Hunza	Karakorum	39.09	26.62	7.95	0.36	0.37	23.90				98.29	Clinozoisite	Epidote
1437	258-1	Upper Hunza	Karakorum	40.84	25.95	9.05	0.33	0.25	23.49				99.91	Clinozoisite	Clinozoisite
1437	341-1	Upper Hunza	Karakorum	41.90	26.42	9.80	0.35	0.08	22.61				101.16	Clinozoisite	Clinozoisite
1437	342-1	Upper Hunza	Karakorum	39.95	26.29	8.88	0.39	0.11	23.35				98.97	Clinozoisite	Clinozoisite
1437	346-1	Upper Hunza	Karakorum	40.73	27.68	6.68	0.28	0.10	22.97				98.44	Clinozoisite	Clinozoisite
1437	359-1	Upper Hunza	Karakorum	39.90	26.69	9.71	0.35	0.35	23.31				100.31	Clinozoisite	Epidote
1437	361-1	Upper Hunza	Karakorum	40.93	26.13	8.93	0.26	0.31	23.23				99.79	Clinozoisite	Clinozoisite
1437	368-1	Upper Hunza	Karakorum	40.64	22.99	13.96	0.37	0.45	22.33				100.74	Clinozoisite	Epidote
1437	371-1	Upper Hunza	Karakorum	40.47	29.86	5.44	0.31	0.12	23.86				100.06	Clinozoisite	Clinozoisite
1437	372-1	Upper Hunza	Karakorum	40.58	25.61	9.58	0.17	0.18	24.08				100.20	Clinozoisite	Clinozoisite
1437	386-1	Upper Hunza	Karakorum	40.59	27.06	9.32	0.37	0.09	23.47				100.90	Clinozoisite	Clinozoisite
1437	15-2	Upper Hunza	Karakorum	39.74	27.66	6.79	0.26	0.08	22.99				97.52	Clinozoisite	Clinozoisite
1437	31-2	Upper Hunza	Karakorum	39.68	24.27	10.71	0.33	0.41	22.76				98.16	Clinozoisite	Clinozoisite
1437	34-2	Upper Hunza	Karakorum	40.15	26.26	8.55	0.21	0.33	23.03				98.53	Clinozoisite	Clinozoisite
1437	83-2	Upper Hunza	Karakorum	40.28	26.11	9.23	0.33	0.10	23.29				99.34	Clinozoisite	Clinozoisite
1437	89-2	Upper Hunza	Karakorum	39.29	23.35	13.20	0.41	0.32	22.50				99.07	Clinozoisite	Clinozoisite
1437	94-2	Upper Hunza	Karakorum	39.91	25.06	10.50	0.25	0.00	23.23				98.95	Clinozoisite	Clinozoisite
1437	97-2	Upper Hunza	Karakorum	39.86	21.88	14.32	0.45	0.33	22.63				99.47	Clinozoisite	Epidote
1437	100-2	Upper Hunza	Karakorum	39.43	22.23	14.18	0.25	0.36	22.37				98.82	Clinozoisite	Epidote
1437	110-2	Upper Hunza	Karakorum	39.75	26.58	10.18	0.31	0.39	23.28				100.49	Clinozoisite	Epidote
1437	127-2	Upper Hunza	Karakorum	40.02	26.63	8.77	0.54	0.39	22.48				98.83	Clinozoisite	Clinozoisite
1437	137-2	Upper Hunza	Karakorum	40.14	27.10	8.77	0.36	0.40	23.53				100.30	Clinozoisite	Epidote
1437	138-2	Upper Hunza	Karakorum	41.61	27.94	7.99	0.24	0.13	23.78				101.69	Clinozoisite	Clinozoisite
1437	140-2	Upper Hunza	Karakorum	40.01	26.52	9.50	0.38	0.16	23.45				100.02	Clinozoisite	Clinozoisite
1437	157-2	Upper Hunza	Karakorum	40.35	25.54	10.92	0.36	0.29	23.04				100.50	Clinozoisite	Clinozoisite
1437	184-2	Upper Hunza	Karakorum	40.34	26.29	8.68	0.34	0.32	23.08				99.05	Clinozoisite	Clinozoisite
1437	206-2	Upper Hunza	Karakorum	40.09	22.56	13.74	0.35	0.31	22.60				99.65	Clinozoisite	Epidote
1437	210-2	Upper Hunza	Karakorum	39.45	26.00	9.48	0.36	0.00	23.71				99.00	Clinozoisite	Epidote
1437	225-2	Upper Hunza	Karakorum	39.10	25.00	9.71	0.25	0.13	23.06				97.25	Clinozoisite	Clinozoisite
1437	229-2	Upper Hunza	Karakorum	39.36	26.78	7.09	0.50	0.00	23.43				97.16	Clinozoisite	Clinozoisite
1437	234-2	Upper Hunza	Karakorum	40.02	26.74	8.21	0.25	0.35	22.87				98.44	Clinozoisite	Clinozoisite
1437	236-2	Upper Hunza	Karakorum	39.77	25.93	9.72	0.39	0.37	22.62				98.80	Clinozoisite	Clinozoisite
1437	237-2	Upper Hunza	Karakorum	39.85	25.73	10.04	0.39	0.12	22.69				98.82	Clinozoisite	Clinozoisite
1437	242-2	Upper Hunza	Karakorum	40.36	28.55	4.98	0.26	0.19	23.73				98.07	Clinozoisite	Clinozoisite
1437	243-2	Upper Hunza	Karakorum	39.16	23.27	11.97	0.36	0.15	23.11				98.02	Clinozoisite	Clinozoisite
1437	248-2	Upper Hunza	Karakorum	39.63	25.91	9.74	0.56	0.29	23.34				99.47	Clinozoisite	Epidote
1437	249-2	Upper Hunza	Karakorum	39.29	27.15	8.44	0.35	0.50	23.76				99.49	Clinozoisite	Epidote
1437	259-2	Upper Hunza	Karakorum	39.31	22.66	13.29	0.39	0.15	23.29				99.09	Clinozoisite	Clinozoisite
1437	260-2	Upper Hunza	Karakorum	40.03	24.76	11.63	0.23	0.13	23.56				100.34	Clinozoisite	Clinozoisite
1437	265-2	Upper Hunza	Karakorum	41.07	26.60	9.07	0.44	0.26	23.68				101.12	Clinozoisite	Clinozoisite
1437	269-2	Upper Hunza	Karakorum	40.55	27.19	8.10	0.50	0.11	23.60				100.05	Clinozoisite	Clinozoisite
1437	272-2	Upper Hunza	Karakorum	39.43	26.32	9.67	0.43	0.13	22.86				98.84	Clinozoisite	Epidote
1437	282-2	Upper Hunza	Karakorum	40.53	26.89	6.70	0.34	0.38	22.95				97.79	Clinozoisite	Clinozoisite
1437	289-2	Upper Hunza	Karakorum	38.12	23.07	12.66	0.45	0.38	22.85				97.53	Clinozoisite	Epidote
1437	292-2	Upper Hunza	Karakorum	40.70	27.27	8.17	0.10	0.00	23.00				99.24	Clinozoisite	Clinozoisite
1437	307-2	Upper Hunza	Karakorum	40.37	26.24	8.69	0.38	0.10	22.87				98.65	Clinozoisite	Clinozoisite
1437	308-2	Upper Hunza	Karakorum	39.60	23.88	13.33	0.34	0.22	23.11				100.48	Clinozoisite	Epidote
1437	334-2	Upper Hunza	Karakorum	39.75	27.67	6.53	0.38	0.20	23.89				98.42	Clinozoisite	Clinozoisite
1437	337-2	Upper Hunza	Karakorum	39.40	25.34	9.57	0.25	0.23	23.37				98.16	Clinozoisite	Clinozoisite
1437	338-2	Upper Hunza	Karakorum	40.30	25.94	10.35	0.37	0.35	23.00				100.31	Clinozoisite	Clinozoisite
1437	341-2	Upper Hunza	Karakorum	40.06	26.67	9.24	0.23	0.38	22.83				99.41	Clinozoisite	Clinozoisite
1437	344-2	Upper Hunza	Karakorum	40.14	26.28	10.12	0.48	0.26	23.36				100.64	Clinozoisite	Epidote
1437	352-2	Upper Hunza	Karakorum	40.95	28.57	7.20	0.30	0.00	23.86				100.88	Clinozoisite	Clinozoisite
1437	356-2	Upper Hunza	Karakorum	39.79	28.28	6.45	0.34	0.40	24.46				99.72	Clinozoisite	Clinozoisite
1437	360-2	Upper Hunza	Karakorum	40.10	22.79	12.73	0.34	0.13	22.52				98.61	Clinozoisite	Epidote
1437	366-2	Upper Hunza	Karakorum	39.68	21.84	15.66	0.32	0.33	23.26				101.09	Clinozoisite	Epidote
1437	394-2	Upper Hunza	Karakorum	38.28	26.36	8.22	0.29	0.23	24.47				97.85	Clinozoisite	Epidote
1437	400-2	Upper Hunza	Karakorum	39.94	25.48	10.35	0.25	0.08	23.20				99.30	Clinozoisite	Clinozoisite
1437	426-2	Upper Hunza	Karakorum	39.91	25.01	11.08	0.40	0.56	22.66				99.62	Clinozoisite	Clinozoisite
1437	429-2	Upper Hunza	Karakorum	48.72	7.14	16.73	0.41	12.54	11.78				97.32	Clinozoisite	Clinozoisite
1437	432-2	Upper Hunza	Karakorum	40.02	24.13	11.76	0.32	0.34	23.12				99.69	Clinozoisite	Clinozoisite
1437	435-2	Upper Hunza	Karakorum	40.17	26.39	9.22	0.31	0.54	23.40				100.03	Clinozoisite	Clinozoisite
1437	436-2	Upper Hunza	Karakorum	40.03	26.90	8.61	0.39	0.44	23.35				99.72	Clinozoisite	Clinozoisite
1437	446-2	Upper Hunza	Karakorum	40.08	26.39	10.23	0.41	0.18	22.64				99.93	Clinozoisite	Clinozoisite
1437	34-1	Upper Hunza	Karakorum	37.49	19.94	13.11	0.57	0.59	17.81	4.57	6.85	1.90	102.83	Clinozoisite	Epidote
1437	68-1	Upper Hunza	Karakorum	33.95	18.77	12.94	0.78	0.73	9.97	6.35	10.87	3.80	98.16	Allanite	Dissakisite-(Ce)
1437	236-1	Upper Hunza	Karakorum	34.46	17.06	13.13	0.86	1.05	11.28	5.37	11.75	3.86	98.82	Allanite	Allanite-(Ce)
1437	310-1	Upper Hunza	Karakorum	33.88	17.58	13.28	0.85	0.21	10.35	6.48	13.93	4.26	100.82	Allanite	Epidote
1437	334-1	Upper Hunza	Karakorum	34.71	19.20	13.26	0.46	0.17	10.69	5.95	11.47	4.72	100.63	Allanite	Dissakisite-(Ce)
1437	49-2	Upper Hunza	Karakorum	33.92	17.24	14.71	0.71	0.85	11.86	5.33	9.65	3.15	97.42	Allanite	Allanite-(Ce)
1437	96-2	Upper Hunza	Karakorum	33.07	12.13	16.82	0.64	1.34	9.72	7.62	13.56	3.15	98.05	Allanite	Ferriallanite-(Ce)
1437	283-2	Upper Hunza	Karakorum	32.33	12.38	17.66	0.59	0.97	9.23	9.71	14.30	1.16	98.33	Allanite	Ferriallanite-(Ce)
1437	386-2	Upper Hunza	Karakorum	34.34	17.96	13.02	0.56	0.00	11.17	5.61	12.62	4.26	99.54	Allanite	Epidote
1437	388-2	Upper Hunza	Karakorum	32.74	15.40	14.24	0.26	1.54	10.16	7.25	14.08	2.47	98.14	Allanite	Allanite-(Ce)
1437	398-2	Upper Hunza	Karakorum	33.21	11.68	18.67	1.09	0.89	10.07	5.22	12.24	4.43	97.50	Allanite	Ferriallanite-(Ce)
1437	406-2	Upper Hunza	Karakorum	33.96	11.81	17.06	0.50	1.70	9.51	8.99	13.29	2.34	99.16	Allanite	Ferriallanite-(Ce)
1437	450-2	Upper Hunza	Karakorum	34.66	15.94	15.36	0.58	0.64	13.26	6.72	10.91	2.47	100.54	Allanite	Allanite-(Ce)

Sample	Points	River/Dune	Domain	SiO_2	Al_2O_3	FeO	MnO	MgO	CaO	La_2O_3	Ce_2O_3	Nd_2O_3	Total	Subgroup	Name
				wt%	wt%	wt%	wt%	wt%	wt%	wt%	wt%	wt%			
1438	2-1	Hispar	Karakorum	38.09	27.08	7.11	0.45	0.17	23.19				96.09	Clinozoisite	Clinozoisite
1438	13-1	Hispar	Karakorum	35.71	20.34	13.62	0.17	0.32	22.40				92.56	Clinozoisite	Epidote
1438	17-1	Hispar	Karakorum	35.79	20.65	13.38	0.26	0.38	22.44				92.90	Clinozoisite	Epidote
1438	18-1	Hispar	Karakorum	36.95	23.60	10.71	0.28	0.10	22.17				93.81	Clinozoisite	Epidote
1438	28-1	Hispar	Karakorum	37.01	23.62	10.27	0.22	0.26	22.60				93.98	Clinozoisite	Epidote
1438	42-1	Hispar	Karakorum	35.80	26.24	6.14	0.26	0.36	22.87				91.67	Clinozoisite	Clinozoisite
1438	43-1	Hispar	Karakorum	38.32	25.67	9.73	0.29	0.22	22.79				97.02	Clinozoisite	Epidote
1438	53-1	Hispar	Karakorum	36.22	26.46	6.96	0.37	0.11	22.48				92.60	Clinozoisite	Clinozoisite
1438	61-1	Hispar	Karakorum	39.20	29.38	6.14	0.52	0.36	22.94				98.54	Clinozoisite	Clinozoisite
1438	64-1	Hispar	Karakorum	38.42	24.19	10.51	0.35	0.28	22.27				96.02	Clinozoisite	Clinozoisite
1438	73-1	Hispar	Karakorum	39.65	25.61	11.00	0.36	0.18	22.81				99.61	Clinozoisite	Epidote
1438	79-1	Hispar	Karakorum	36.15	22.32	11.99	0.52	0.20	22.17				93.35	Clinozoisite	Epidote
1438	81-1	Hispar	Karakorum	36.47	23.26	10.93	0.34	0.23	21.40				92.63	Clinozoisite	Epidote
1438	91-1	Hispar	Karakorum	35.44	23.76	10.26	0.30	0.19	21.83				91.78	Clinozoisite	Epidote
1438	95-1	Hispar	Karakorum	36.31	24.76	8.75	0.27	0.00	22.74				92.83	Clinozoisite	Epidote
1438	128-1	Hispar	Karakorum	36.82	22.58	12.33	0.53	0.29	22.96				95.51	Clinozoisite	Epidote
1438	166-1	Hispar	Karakorum	37.48	26.93	6.30	0.50	0.00	22.23				93.44	Clinozoisite	Clinozoisite
1438	174-1	Hispar	Karakorum	37.52	26.20	8.36	0.55	0.20	22.45				95.28	Clinozoisite	Epidote
1438	180-1	Hispar	Karakorum	37.82	29.11	5.84	0.44	0.36	23.51				97.08	Clinozoisite	Clinozoisite
1438	194-1	Hispar	Karakorum	38.52	30.40	4.00	0.29	0.61	23.18				97.00	Clinozoisite	Clinozoisite
1438	195-1	Hispar	Karakorum	38.06	26.93	7.97	0.32	0.41	22.29				95.98	Clinozoisite	Clinozoisite
1438	199-1	Hispar	Karakorum	36.13	21.24	13.60	0.28	0.31	22.30				93.86	Clinozoisite	Epidote
1438	208-1	Hispar	Karakorum	36.69	23.71	11.18	0.30	0.38	22.22				94.48	Clinozoisite	Epidote
1438	209-1	Hispar	Karakorum	37.79	26.68	7.61	0.38	0.27	22.53				95.26	Clinozoisite	Clinozoisite
1438	220-1	Hispar	Karakorum	38.89	26.73	8.18	0.37	0.23	23.37				97.77	Clinozoisite	Epidote
1438	3-2	Hispar	Karakorum	38.37	27.85	6.18	0.30	0.28	23.21				96.19	Clinozoisite	Clinozoisite
1438	13-2	Hispar	Karakorum	53.11	0.91	6.12	0.85	14.66	23.03				98.68	Clinozoisite	Clinozoisite
1438	14-2	Hispar	Karakorum	38.28	23.29	10.55	0.32	0.14	21.61				94.19	Clinozoisite	Clinozoisite
1438	30-2	Hispar	Karakorum	37.93	24.10	9.48	0.40	0.22	22.04				94.17	Clinozoisite	Clinozoisite
1438	57-2	Hispar	Karakorum	37.36	23.94	11.11	0.58	0.22	22.22				95.43	Clinozoisite	Epidote
1438	58-2	Hispar	Karakorum	36.98	23.99	10.47	0.21	0.39	22.40				94.44	Clinozoisite	Epidote
1438	87-2	Hispar	Karakorum	39.04	29.75	4.08	0.11	0.24	22.97				96.19	Clinozoisite	Clinozoisite
1438	89-2	Hispar	Karakorum	36.59	21.07	13.02	0.21	0.00	21.54				92.43	Clinozoisite	Epidote
1438	95-2	Hispar	Karakorum	38.85	26.04	8.60	0.44	0.00	23.06				96.99	Clinozoisite	Clinozoisite
1438	97-2	Hispar	Karakorum	36.71	21.44	13.76	0.41	0.11	22.30				94.73	Clinozoisite	Epidote
1438	109-2	Hispar	Karakorum	38.97	27.59	6.87	0.47	0.34	22.69				96.93	Clinozoisite	Clinozoisite
1438	110-2	Hispar	Karakorum	37.99	28.21	5.31	0.15	0.37	23.59				95.62	Clinozoisite	Clinozoisite
1438	126-2	Hispar	Karakorum	37.11	24.27	11.17	0.36	0.27	22.28				95.46	Clinozoisite	Epidote
1438	137-2	Hispar	Karakorum	38.03	27.46	7.35	0.51	0.23	22.38				95.96	Clinozoisite	Clinozoisite
1438	142-2	Hispar	Karakorum	37.24	24.32	9.23	0.39	0.00	22.96				94.14	Clinozoisite	Epidote
1438	149-2	Hispar	Karakorum	37.03	22.98	12.92	0.33	0.29	21.93				95.48	Clinozoisite	Epidote
1438	155-2	Hispar	Karakorum	38.36	26.02	7.80	0.44	0.20	22.80				95.62	Clinozoisite	Epidote
1438	157-2	Hispar	Karakorum	38.01	26.11	7.63	0.33	0.23	22.35				94.66	Clinozoisite	Clinozoisite
1438	162-2	Hispar	Karakorum	37.47	23.28	11.92	0.37	0.30	22.56				95.90	Clinozoisite	Epidote
1438	170-2	Hispar	Karakorum	37.26	23.07	11.68	0.49	0.23	22.51				95.24	Clinozoisite	Epidote
1438	171-2	Hispar	Karakorum	37.15	19.90	14.25	0.50	0.24	22.20				94.24	Clinozoisite	Epidote
1438	191-2	Hispar	Karakorum	37.65	27.20	7.16	0.47	0.39	22.64				95.51	Clinozoisite	Clinozoisite
1438	192-2	Hispar	Karakorum	37.17	21.68	13.41	0.26	0.10	22.00				94.62	Clinozoisite	Epidote
1438	200-2	Hispar	Karakorum	37.24	26.40	7.14	0.43	0.21	22.53				93.95	Clinozoisite	Clinozoisite
1438	218-2	Hispar	Karakorum	37.17	23.78	10.39	0.26	0.56	22.57				94.73	Clinozoisite	Epidote
1438	223-2	Hispar	Karakorum	37.07	24.51	9.49	0.14	0.23	22.73				94.17	Clinozoisite	Epidote
1438	227-2	Hispar	Karakorum	36.50	21.93	12.56	0.22	0.23	22.64				94.08	Clinozoisite	Epidote
1438	228-2	Hispar	Karakorum	37.98	29.01	5.06	0.28	0.10	22.96				95.39	Clinozoisite	Clinozoisite
1438	233-2	Hispar	Karakorum	37.53	29.64	5.33	0.32	0.29	23.22				96.33	Clinozoisite	Clinozoisite
1438	256-2	Hispar	Karakorum	38.54	27.00	7.32	0.31	0.16	22.40				95.73	Clinozoisite	Clinozoisite
1438	262-2	Hispar	Karakorum	38.15	27.05	6.84	0.43	0.23	22.61				95.31	Clinozoisite	Clinozoisite
1438	263-2	Hispar	Karakorum	38.64	32.87	0.76	0.22	0.28	23.33				96.10	Clinozoisite	Clinozoisite
1438	264-2	Hispar	Karakorum	36.72	26.64	6.34	0.28	0.39	23.03				93.40	Clinozoisite	Clinozoisite
1438	10-3	Hispar	Karakorum	37.95	27.47	7.65	0.52	0.39	22.80				96.78	Clinozoisite	Clinozoisite
1438	16-3	Hispar	Karakorum	36.86	23.99	10.73	0.22	0.47	23.10				95.37	Clinozoisite	Epidote
1438	21-3	Hispar	Karakorum	38.32	27.74	6.56	0.31	0.19	23.06				96.18	Clinozoisite	Clinozoisite
1438	22-3	Hispar	Karakorum	36.99	21.30	14.46	0.23	0.28	21.87				95.13	Clinozoisite	Epidote
1438	26-3	Hispar	Karakorum	37.49	24.41	9.75	0.30	0.31	22.71				94.97	Clinozoisite	Epidote
1438	28-3	Hispar	Karakorum	37.95	25.64	8.77	0.20	0.64	23.06				96.26	Clinozoisite	Epidote
1438	31-3	Hispar	Karakorum	38.35	27.97	6.22	0.22	0.26	22.53				95.55	Clinozoisite	Clinozoisite
1438	47-3	Hispar	Karakorum	38.02	24.05	10.98	0.33	0.42	21.89				95.69	Clinozoisite	Epidote
1438	48-3	Hispar	Karakorum	38.47	25.96	8.92	0.25	0.13	22.40				96.13	Clinozoisite	Epidote
1438	60-3	Hispar	Karakorum	37.57	27.09	6.92	0.28	0.00	22.79				94.65	Clinozoisite	Clinozoisite
1438	61-3	Hispar	Karakorum	37.25	21.25	14.13	0.29	0.35	22.02				95.29	Clinozoisite	Epidote
1438	64-3	Hispar	Karakorum	37.44	26.19	8.97	0.31	0.46	22.61				95.98	Clinozoisite	Epidote
1438	66-3	Hispar	Karakorum	37.65	22.37	12.45	0.56	0.50	21.65				95.18	Clinozoisite	Epidote
1438	67-3	Hispar	Karakorum	37.03	22.32	12.43	0.54	0.21	22.07				94.60	Clinozoisite	Epidote
1438	72-3	Hispar	Karakorum	44.77	10.57	13.92	0.14	10.60	11.60				91.60	Clinozoisite	Ferriepidote
1438	73-3	Hispar	Karakorum	36.49	21.83	12.77	0.33	0.35	22.16				93.93	Clinozoisite	Epidote
1438	77-3	Hispar	Karakorum	36.79	23.74	11.54	0.45	0.27	22.07				94.86	Clinozoisite	Epidote
1438	79-3	Hispar	Karakorum	36.39	21.65	13.17	0.42	0.37	21.95				93.95	Clinozoisite	Epidote
1438	80-3	Hispar	Karakorum	37.43	24.72	10.69	0.23	0.45	22.49				96.01	Clinozoisite	Epidote
1438	86-3	Hispar	Karakorum	37.61	22.65	12.05	0.55	0.31	22.72				95.89	Clinozoisite	Epidote
1438	90-3	Hispar	Karakorum	37.43	22.93	11.38	0.27	0.38	21.93				94.32	Clinozoisite	Epidote
1438	97-3	Hispar	Karakorum	37.66	26.44	6.42	0.17	0.30	22.71				93.70	Clinozoisite	Clinozoisite
1438	103-3	Hispar	Karakorum	38.52	30.13	4.90	0.17	0.33	23.45				97.50	Clinozoisite	Clinozoisite
1438	110-3	Hispar	Karakorum	37.16	22.13	14.14	0.27	0.25	21.94				95.89	Clinozoisite	Epidote
1438	167-1	Hispar	Karakorum	29.42	18.07	10.23	0.61	0.62	13.09				72.04	Clinozoisite	Epidote
1438	145-2	Hispar	Karakorum	32.48	21.45	7.27	0.26	0.36	16.91				78.73	Clinozoisite	Clinozoisite
1438	164-2	Hispar	Karakorum	29.32	12.68	13.90	0.45	1.20	12.56				70.11	Clinozoisite	Epidote
4426	36-1	Stagmo	Ladakh	38.77	23.94	10.48	0.21	0.71	23.06				97.17	Clinozoisite	Epidote
4426	139-1	Stagmo	Ladakh	39.26	22.66	12.87	0.21	0.36	22.25				97.61	Clinozoisite	Epidote
4426	240-1	Stagmo	Ladakh	38.33	21.40	13.50	0.17	0.36	22.59				96.35	Clinozoisite	Epidote
4426	253-1	Stagmo	Ladakh	38.15	21.86	14.42	0.17	0.35	22.00				96.95	Clinozoisite	Epidote
4426	150-2	Stagmo	Ladakh	39.17	22.75	13.58	0.28	0.13	22.34				98.25	Clinozoisite	Epidote
4426	199-2	Stagmo	Ladakh	38.80	22.16	13.08	0.23	0.57	22.62				97.46	Clinozoisite	Epidote
4426	301-2	Stagmo	Ladakh	32.88	13.00	15.55	0.46	1.70	10.34	7.75	13.89	4.08	99.65	Allanite	Ferriallanite-(Ce)
4430	36-1	Domkar	Ladakh	38.10	24.25	11.57	0.54	0.43	20.49				95.38	Clinozoisite	Clinozoisite
4430	121-1	Domkar	Ladakh	38.82	24.65	10.83	0.49	0.26	20.99				96.04	Clinozoisite	Clinozoisite
4430	122-1	Domkar	Ladakh	37.31	25.00	10.95	0.37	0.21	20.87				94.71	Clinozoisite	Epidote
4430	137-1	Domkar	Ladakh	38.92	24.54	10.96	0.67	0.59	20.10				95.78	Clinozoisite	Clinozoisite
4430	160-1	Domkar	Ladakh	37.52	23.34	11.35	0.49	0.00	20.67				93.37	Clinozoisite	Clinozoisite
4430	181-1	Domkar	Ladakh	38.13	24.76	10.41	0.34	0.15	21.16				94.95	Clinozoisite	Clinozoisite
4430	197-1	Domkar	Ladakh	37.88	20.35	14.74	0.37	0.56	19.81				93.71	Clinozoisite	Epidote
4430	201-1	Domkar	Ladakh	46.95	8.56	14.45	0.25	13.68	10.96				94.85	Clinozoisite	Epidote
4430	273-1	Domkar	Ladakh	38.20	22.24	12.94	0.29	0.12	19.91				93.70	Clinozoisite	Epidote
4430	286-1	Domkar	Ladakh	39.35	23.44	12.72	0.52	0.50	20.76				97.29	Clinozoisite	Epidote
4430	298-1	Domkar	Ladakh	38.21	22.69	12.99	0.36	0.30	20.46				95.01	Clinozoisite	Epidote
4430	316-1	Domkar	Ladakh	37.71	22.90	12.06	0.54	0.36	20.59				94.16	Clinozoisite	Clinozoisite
4430	321-1	Domkar	Ladakh	38.02	22.45	13.85	0.49	0.53	20.42				95.76	Clinozoisite	Epidote
4430	78-2	Domkar	Ladakh	38.13	23.05	13.35	0.45	0.00	20.24				95.22	Clinozoisite	Epidote
4430	96-2	Domkar	Ladakh	38.45	24.58	10.21	0.41	0.42	21.34				95.41	Clinozoisite	Clinozoisite
4430	165-2	Domkar	Ladakh	38.93	24.11	10.18	0.17	0.00	21.24				94.63	Clinozoisite	Clinozoisite
4430	169-2	Domkar	Ladakh	37.79	24.41	10.79	0.60	0.09	20.33				94.01	Clinozoisite	Clinozoisite
4430	238-2	Domkar	Ladakh	46.72	8.34	17.60	0.57	11.89	10.46				95.58	Clinozoisite	Clinozoisite
4430	249-2	Domkar	Ladakh	38.41	25.27	9.57	0.28	0.34	20.62				94.49	Clinozoisite	Clinozoisite
4430	268-2	Domkar	Ladakh	38.24	22.50	13.08	0.67	0.00	20.29				94.78	Clinozoisite	Epidote
4430	275-2	Domkar	Ladakh	38.41	22.97	13.32	0.45	0.50	20.16				95.81	Clinozoisite	Epidote
4430	276-2	Domkar	Ladakh	38.14	22.41	12.04	0.46	0.31	20.59				93.95	Clinozoisite	Epidote
4430	298-2	Domkar	Ladakh	37.84	22.56	11.85	0.28	0.30	20.14				92.97	Clinozoisite	Epidote
4430	303-2	Domkar	Ladakh	39.75	23.90	12.51	0.42	0.18	20.89				97.65	Clinozoisite	Epidote
4430	320-2	Domkar	Ladakh	38.77	20.35	13.55	0.52	0.28	20.17				93.64	Clinozoisite	Epidote

Sample	Points	River/Dune	Domain	SiO_2	Al_2O_3	FeO	MnO	MgO	CaO	La_2O_3	Ce_2O_3	Nd_2O_3	Total	Subgroup	Name
				wt%	wt%	wt%	wt%	wt%	wt%	wt%	wt%	wt%			
1439	14-1	Kandia	Kohistan	36.02	28.01	4.88	0.23	0.09	21.94				91.17	Clinozoisite	Clinozoisite
1439	15-1	Kandia	Kohistan	38.48	28.25	5.96	0.19	0.33	22.66				95.87	Clinozoisite	Clinozoisite
1439	17-1	Kandia	Kohistan	36.35	23.38	11.46	0.38	0.15	22.47				94.19	Clinozoisite	Epidote
1439	21-1	Kandia	Kohistan	37.99	23.45	11.46	0.40	0.00	21.85				95.15	Clinozoisite	Clinozoisite
1439	27-1	Kandia	Kohistan	38.17	29.43	5.53	0.48	0.41	23.52				97.54	Clinozoisite	Clinozoisite
1439	28-1	Kandia	Kohistan	38.92	33.07	1.07	0.20	0.37	23.76				97.39	Clinozoisite	Clinozoisite
1439	29-1	Kandia	Kohistan	36.93	26.55	7.92	0.22	0.38	23.19				95.19	Clinozoisite	Epidote
1439	37-1	Kandia	Kohistan	37.77	27.40	5.31	0.34	0.19	23.10				94.11	Clinozoisite	Clinozoisite
1439	39-1	Kandia	Kohistan	37.93	26.10	8.86	0.37	0.41	22.92				96.59	Clinozoisite	Epidote
1439	41-1	Kandia	Kohistan	37.63	27.24	7.76	0.44	0.13	22.92				96.12	Clinozoisite	Clinozoisite
1439	43-1	Kandia	Kohistan	37.20	24.31	11.63	0.36	0.25	21.58				95.33	Clinozoisite	Epidote
1439	44-1	Kandia	Kohistan	38.02	25.35	9.49	0.35	0.45	21.94				95.60	Clinozoisite	Epidote
1439	45-1	Kandia	Kohistan	38.10	28.64	6.13	0.31	0.30	22.75				96.23	Clinozoisite	Clinozoisite
1439	49-1	Kandia	Kohistan	37.56	27.33	8.14	0.34	0.17	22.69				96.23	Clinozoisite	Clinozoisite
1439	54-1	Kandia	Kohistan	38.02	31.60	3.51	0.29	0.16	23.18				96.76	Clinozoisite	Clinozoisite
1439	59-1	Kandia	Kohistan	35.91	31.65	0.22	0.21	0.21	21.67				89.87	Clinozoisite	Clinozoisite
1439	62-1	Kandia	Kohistan	37.67	25.66	10.02	0.42	0.16	22.86				96.79	Clinozoisite	Epidote
1439	66-1	Kandia	Kohistan	36.49	29.20	3.43	0.35	0.17	21.73				91.37	Clinozoisite	Clinozoisite
1439	70-1	Kandia	Kohistan	34.89	27.36	4.98	0.37	0.34	21.70				89.64	Clinozoisite	Clinozoisite
1439	76-1	Kandia	Kohistan	34.75	22.81	8.49	0.35	0.32	20.61				87.33	Clinozoisite	Epidote
1439	81-1	Kandia	Kohistan	36.65	27.91	5.61	0.34	0.27	21.08				91.86	Clinozoisite	Clinozoisite
1439	82-1	Kandia	Kohistan	35.07	26.17	5.13	0.25	0.11	21.56				88.29	Clinozoisite	Clinozoisite
1439	84-1	Kandia	Kohistan	35.46	29.35	2.82	0.48	0.51	21.00				89.62	Clinozoisite	Clinozoisite
1439	158-1	Kandia	Kohistan	35.48	29.12	2.30	0.13	0.28	21.50				88.81	Clinozoisite	Clinozoisite
1439	174-1	Kandia	Kohistan	36.15	23.95	9.13	0.46	0.42	21.04				91.15	Clinozoisite	Epidote
1439	176-1	Kandia	Kohistan	40.14	29.33	1.34	0.37	0.26	18.79				90.23	Clinozoisite	Clinozoisite
1439	178-1	Kandia	Kohistan	35.51	28.60	4.07	0.53	0.19	21.24				90.14	Clinozoisite	Clinozoisite
1439	181-1	Kandia	Kohistan	35.71	31.07	1.27	0.13	0.82	22.09				91.09	Clinozoisite	Clinozoisite
1439	182-1	Kandia	Kohistan	36.20	31.04	0.75	0.29	0.22	22.20				90.70	Clinozoisite	Clinozoisite
1439	183-1	Kandia	Kohistan	36.95	26.01	7.65	0.45	0.26	21.33				92.65	Clinozoisite	Clinozoisite
1439	196-1	Kandia	Kohistan	36.89	31.97	0.46	0.13	0.19	21.94				91.58	Clinozoisite	Clinozoisite
1439	200-1	Kandia	Kohistan	35.62	23.28	9.01	0.31	0.00	21.46				89.68	Clinozoisite	Epidote
1439	201-1	Kandia	Kohistan	36.62	28.61	4.63	0.25	0.46	21.71				92.28	Clinozoisite	Clinozoisite
1439	203-1	Kandia	Kohistan	36.96	28.26	4.47	0.34	0.22	21.54				91.79	Clinozoisite	Clinozoisite
1439	206-1	Kandia	Kohistan	35.82	25.75	6.94	0.26	0.20	21.25				90.22	Clinozoisite	Clinozoisite
1439	215-1	Kandia	Kohistan	36.55	23.59	11.64	0.55	0.28	20.95				93.56	Clinozoisite	Epidote
1439	218-1	Kandia	Kohistan	37.84	25.92	8.62	0.37	0.44	22.57				95.76	Clinozoisite	Epidote
1439	221-1	Kandia	Kohistan	38.15	25.58	9.70	0.42	0.24	21.63				95.72	Clinozoisite	Epidote
1439	225-1	Kandia	Kohistan	37.68	26.51	8.61	0.46	0.34	22.50				96.10	Clinozoisite	Epidote
1439	226-1	Kandia	Kohistan	37.59	23.70	11.33	0.27	0.21	22.54				95.64	Clinozoisite	Epidote
1439	228-1	Kandia	Kohistan	38.30	30.75	2.35	0.19	0.00	23.37				94.96	Clinozoisite	Clinozoisite
1439	230-1	Kandia	Kohistan	37.69	30.05	3.93	0.13	0.26	22.58				94.64	Clinozoisite	Clinozoisite
1439	237-1	Kandia	Kohistan	36.73	26.28	6.01	0.34	0.31	19.46				89.13	Clinozoisite	Clinozoisite
1439	242-1	Kandia	Kohistan	35.76	28.83	4.19	0.42	0.26	21.89				91.35	Clinozoisite	Clinozoisite
1439	244-1	Kandia	Kohistan	36.69	26.10	6.31	0.37	0.00	21.15				90.62	Clinozoisite	Clinozoisite
1439	248-1	Kandia	Kohistan	34.20	22.37	11.04	0.32	0.20	20.80				88.93	Clinozoisite	Epidote
1439	249-1	Kandia	Kohistan	34.43	22.86	8.41	0.34	0.00	20.40				86.44	Clinozoisite	Epidote
1439	252-1	Kandia	Kohistan	35.54	26.05	6.11	0.31	0.50	21.35				89.86	Clinozoisite	Clinozoisite
1439	269-1	Kandia	Kohistan	35.34	22.89	10.10	0.49	0.43	20.89				90.14	Clinozoisite	Epidote
1439	278-1	Kandia	Kohistan	33.85	21.21	10.96	0.34	0.00	20.51				86.87	Clinozoisite	Epidote
1439	282-1	Kandia	Kohistan	35.19	23.99	8.13	0.13	0.30	21.09				88.83	Clinozoisite	Epidote
1439	289-1	Kandia	Kohistan	35.73	29.36	1.03	0.27	0.36	21.88				88.63	Clinozoisite	Clinozoisite
1439	20-2	Kandia	Kohistan	35.34	24.85	8.08	0.48	0.44	20.70				89.89	Clinozoisite	Epidote
1439	21-2	Kandia	Kohistan	35.21	28.98	3.19	0.31	0.37	21.88				89.94	Clinozoisite	Clinozoisite
1439	45-2	Kandia	Kohistan	36.19	26.26	5.49	0.28	0.00	21.62				89.84	Clinozoisite	Clinozoisite
1439	48-2	Kandia	Kohistan	35.56	29.94	2.32	0.25	0.31	21.43				89.81	Clinozoisite	Clinozoisite
1439	49-2	Kandia	Kohistan	35.11	25.68	6.57	0.38	0.00	21.37				89.11	Clinozoisite	Clinozoisite
1439	56-2	Kandia	Kohistan	36.73	26.28	6.01	0.34	0.31	19.46				89.13	Clinozoisite	Clinozoisite
1439	66-2	Kandia	Kohistan	35.02	28.97	1.66	0.15	0.26	21.62				87.68	Clinozoisite	Clinozoisite
1439	67-2	Kandia	Kohistan	35.58	27.71	4.49	0.19	0.37	21.16				89.50	Clinozoisite	Clinozoisite
1439	68-2	Kandia	Kohistan	35.66	30.52	1.70	0.16	0.00	21.23				89.27	Clinozoisite	Clinozoisite
1439	69-2	Kandia	Kohistan	35.50	27.56	4.62	0.30	0.38	21.48				89.84	Clinozoisite	Clinozoisite
1439	71-2	Kandia	Kohistan	36.43	29.23	4.00	0.32	0.19	21.28				91.45	Clinozoisite	Clinozoisite
1439	74-2	Kandia	Kohistan	36.19	26.30	5.97	0.30	0.28	20.50				89.54	Clinozoisite	Clinozoisite
1439	76-2	Kandia	Kohistan	34.95	20.32	11.43	0.33	0.34	20.82				88.19	Clinozoisite	Clinozoisite
1439	91-2	Kandia	Kohistan	35.02	25.67	6.99	0.40	0.18	20.90				89.16	Clinozoisite	Clinozoisite
1439	97-2	Kandia	Kohistan	34.95	22.56	10.14	0.49	0.35	20.12				88.61	Clinozoisite	Epidote
1439	98-2	Kandia	Kohistan	34.50	26.55	5.98	0.33	0.41	21.44				89.21	Clinozoisite	Clinozoisite
1439	104-2	Kandia	Kohistan	35.22	28.22	3.80	0.38	0.10	21.03				88.75	Clinozoisite	Clinozoisite
1439	105-2	Kandia	Kohistan	34.75	24.49	7.18	0.00	0.00	20.85				87.27	Clinozoisite	Clinozoisite
1439	113-2	Kandia	Kohistan	35.17	21.78	11.19	0.39	0.42	20.09				89.04	Clinozoisite	Epidote
1439	118-2	Kandia	Kohistan	34.09	25.52	5.82	0.36	0.26	21.16				87.21	Clinozoisite	Clinozoisite
1439	123-2	Kandia	Kohistan	35.14	26.76	5.29	0.33	0.00	20.88				88.40	Clinozoisite	Clinozoisite
1439	170-2	Kandia	Kohistan	47.96	3.18	10.24	0.37	15.92	11.82				89.49	Clinozoisite	Clinozoisite
1439	174-2	Kandia	Kohistan	35.14	27.93	3.60	0.37	0.36	20.95				88.35	Clinozoisite	Clinozoisite
1439	177-2	Kandia	Kohistan	35.97	31.65	0.41	0.24	0.15	21.95				90.37	Clinozoisite	Clinozoisite
1439	181-2	Kandia	Kohistan	35.30	25.67	6.94	0.35	0.25	20.87				89.38	Clinozoisite	Clinozoisite
1439	183-2	Kandia	Kohistan	35.72	28.98	3.58	0.27	0.34	21.20				90.09	Clinozoisite	Clinozoisite
1439	187-2	Kandia	Kohistan	35.58	24.11	8.96	0.31	0.13	21.16				90.25	Clinozoisite	Epidote
1439	188-2	Kandia	Kohistan	35.38	27.92	3.36	0.17	0.42	21.50				88.75	Clinozoisite	Clinozoisite
1439	189-2	Kandia	Kohistan	34.37	21.95	10.12	0.39	0.23	21.44				88.50	Clinozoisite	Epidote
1439	193-2	Kandia	Kohistan	34.27	23.13	9.68	0.28	0.12	20.20				87.68	Clinozoisite	Epidote
1439	200-2	Kandia	Kohistan	35.12	26.39	7.30	0.36	0.46	21.01				90.64	Clinozoisite	Clinozoisite
1439	202-2	Kandia	Kohistan	35.93	31.28	0.28	0.17	0.22	22.18				90.06	Clinozoisite	Clinozoisite
1439	206-2	Kandia	Kohistan	35.67	25.46	5.61	0.35	0.00	21.62				88.71	Clinozoisite	Clinozoisite
1439	209-2	Kandia	Kohistan	33.65	24.32	6.23	0.35	0.13	21.13				85.81	Clinozoisite	Clinozoisite
1439	211-2	Kandia	Kohistan	35.79	26.88	5.53	0.23	0.21	21.51				90.15	Clinozoisite	Clinozoisite
1439	214-2	Kandia	Kohistan	35.44	26.76	5.87	0.30	0.26	21.29				89.92	Clinozoisite	Clinozoisite
1439	219-2	Kandia	Kohistan	36.16	22.80	8.70	0.38	0.13	20.17				88.34	Clinozoisite	Clinozoisite
1439	221-2	Kandia	Kohistan	36.33	31.93	0.63	0.28	0.42	21.92				91.51	Clinozoisite	Clinozoisite
1439	224-2	Kandia	Kohistan	37.49	26.75	6.45	0.29	0.11	21.15				92.24	Clinozoisite	Clinozoisite
1439	225-2	Kandia	Kohistan	35.92	31.17	1.11	0.24	0.31	21.68				90.43	Clinozoisite	Clinozoisite
1439	229-2	Kandia	Kohistan	35.89	25.73	5.38	0.14	0.14	20.90				88.18	Clinozoisite	Clinozoisite
1439	232-2	Kandia	Kohistan	47.38	2.93	12.62	0.32	13.12	10.50				86.87	Clinozoisite	Clinozoisite
1439	233-2	Kandia	Kohistan	35.53	25.81	7.04	0.26	0.14	21.33				90.11	Clinozoisite	Clinozoisite
1439	236-2	Kandia	Kohistan	36.60	29.22	2.38	0.41	0.08	21.51				90.20	Clinozoisite	Clinozoisite
1439	237-2	Kandia	Kohistan	35.09	25.52	6.57	0.23	0.49	20.90				88.80	Clinozoisite	Clinozoisite
1439	240-2	Kandia	Kohistan	35.56	23.89	8.00	0.23	0.43	20.28				88.39	Clinozoisite	Clinozoisite
1439	241-2	Kandia	Kohistan	34.13	22.13	9.61	0.38	0.19	20.38				86.82	Clinozoisite	Epidote

Sample	Points	River/Dune	Domain	SiO_2	Al_2O_3	FeO	MnO	MgO	CaO	La_2O_3	Ce_2O_3	Nd_2O_3	Total	Subgroup	Name
				wt%	wt%	wt%	wt%	wt%	wt%	wt%	wt%	wt%			
1440	12-1	Swat	Kohistan	38.40	27.04	7.98	0.63	0.16	22.97				97.18	Clinozoisite	Clinozoisite
1440	26-1	Swat	Kohistan	38.66	27.09	7.12	0.75	0.00	22.35				95.97	Clinozoisite	Clinozoisite
1440	63-1	Swat	Kohistan	38.68	23.29	11.15	0.23	0.24	22.00				95.59	Clinozoisite	Clinozoisite
1440	67-1	Swat	Kohistan	42.66	14.56	12.54	0.64	11.58	11.22				93.20	Clinozoisite	Clinozoisite
1440	80-1	Swat	Kohistan	38.27	22.89	11.56	0.77	0.26	21.89				95.64	Clinozoisite	Clinozoisite
1440	134-1	Swat	Kohistan	39.68	29.35	4.09	0.26	0.24	23.22				96.84	Clinozoisite	Clinozoisite
1440	154-1	Swat	Kohistan	39.63	33.21	1.33	0.65	0.52	23.69				99.03	Clinozoisite	Clinozoisite
1440	183-1	Swat	Kohistan	38.68	23.54	12.11	0.46	0.29	21.69				96.77	Clinozoisite	Clinozoisite
1440	211-1	Swat	Kohistan	38.33	26.22	8.05	0.39	0.37	22.56				95.92	Clinozoisite	Epidote
1440	212-1	Swat	Kohistan	38.90	29.58	3.61	0.61	0.45	23.23				96.38	Clinozoisite	Clinozoisite
1440	256-1	Swat	Kohistan	39.31	23.34	10.40	0.76	0.18	21.08				95.07	Clinozoisite	Epidote
1440	3-2	Swat	Kohistan	38.29	23.05	11.45	0.66	0.51	21.60				95.56	Clinozoisite	Clinozoisite
1440	23-2	Swat	Kohistan	39.25	27.70	6.06	0.39	0.14	22.93				96.47	Clinozoisite	Clinozoisite
1440	38-2	Swat	Kohistan	38.36	26.06	7.47	0.53	0.49	23.03				95.94	Clinozoisite	Epidote
1440	50-2	Swat	Kohistan	36.63	21.09	12.87	0.58	0.47	21.55				93.19	Clinozoisite	Epidote
1440	54-2	Swat	Kohistan	39.20	29.01	4.42	0.34	0.49	22.46				95.92	Clinozoisite	Clinozoisite
1440	114-2	Swat	Kohistan	37.52	22.83	12.74	0.82	0.19	22.30				96.40	Clinozoisite	Epidote
1440	132-2	Swat	Kohistan	37.73	24.97	9.71	1.45	0.37	21.56				95.79	Clinozoisite	Epidote
1440	134-2	Swat	Kohistan	38.70	24.73	10.24	0.64	0.20	22.87				97.38	Clinozoisite	Epidote
1440	135-2	Swat	Kohistan	38.51	25.25	9.74	0.75	0.33	21.63				96.21	Clinozoisite	Clinozoisite
1440	183-2	Swat	Kohistan	37.58	24.27	11.42	0.54	0.16	22.19				96.16	Clinozoisite	Epidote
1440	216-2	Swat	Kohistan	37.83	22.46	11.97	0.85	0.00	21.59				94.70	Clinozoisite	Clinozoisite
1440	250-2	Swat	Kohistan	40.17	26.56	7.61	0.55	0.39	22.83				98.11	Clinozoisite	Clinozoisite
1440	254-2	Swat	Kohistan	38.88	24.01	11.56	0.62	0.18	21.94				97.19	Clinozoisite	Clinozoisite
1440	286-2	Swat	Kohistan	37.38	22.46	12.58	0.58	0.26	21.90				95.16	Clinozoisite	Epidote
1440	319-2	Swat	Kohistan	38.31	24.95	9.40	0.56	0.17	22.70				96.09	Clinozoisite	Epidote
1440	329-2	Swat	Kohistan	38.44	25.45	9.08	0.73	0.11	22.14				95.95	Clinozoisite	Clinozoisite
1440	336-2	Swat	Kohistan	38.45	25.75	9.64	0.66	0.26	22.51				97.27	Clinozoisite	Epidote
1440	343-2	Swat	Kohistan	38.97	23.69	11.91	0.61	0.39	22.87				98.44	Clinozoisite	Epidote
4419	3-1	Zanskar	Himalaya	38.77	23.02	10.66	0.29	0.24	24.61				97.59	Clinozoisite	Epidote
4419	17-1	Zanskar	Himalaya	38.32	21.91	13.46	0.16	0.35	24.02				98.22	Clinozoisite	Epidote
4419	18-1	Zanskar	Himalaya	39.31	23.17	10.54	0.28	0.34	24.70				98.34	Clinozoisite	Clinozoisite
4419	20-1	Zanskar	Himalaya	38.00	19.64	16.19	0.36	0.29	23.32				97.80	Clinozoisite	Epidote
4419	25-1	Zanskar	Himalaya	39.39	21.64	13.04	0.32	0.27	23.69				98.35	Clinozoisite	Clinozoisite
4419	34-1	Zanskar	Himalaya	51.84	6.02	11.35	0.47	16.68	12.30				98.66	Clinozoisite	Clinozoisite
4419	49-1	Zanskar	Himalaya	38.59	20.72	15.82	0.46	0.64	24.28				100.51	Clinozoisite	Epidote
4419	99-1	Zanskar	Himalaya	37.83	20.12	14.13	0.45	0.11	24.37				97.01	Clinozoisite	Epidote
4419	134-1	Zanskar	Himalaya	38.73	21.33	14.73	0.37	0.23	23.94				99.33	Clinozoisite	Epidote
4419	140-1	Zanskar	Himalaya	38.80	23.87	9.58	0.22	0.11	24.03				96.61	Clinozoisite	Clinozoisite
4419	158-1	Zanskar	Himalaya	39.31	19.70	15.64	0.31	0.00	23.20				98.16	Clinozoisite	Epidote
4419	213-1	Zanskar	Himalaya	38.31	20.41	14.73	0.43	0.12	23.33				97.33	Clinozoisite	Epidote
4419	226-1	Zanskar	Himalaya	38.96	19.70	14.99	0.43	0.44	24.10				98.62	Clinozoisite	Epidote
4419	8-2	Zanskar	Himalaya	39.27	19.76	14.14	0.47	0.29	23.03				96.96	Clinozoisite	Epidote
4419	26-2	Zanskar	Himalaya	37.41	20.68	14.98	0.23	0.13	23.84				97.27	Clinozoisite	Epidote
4419	72-2	Zanskar	Himalaya	40.08	25.41	7.90	0.29	0.24	24.41				98.33	Clinozoisite	Clinozoisite
4419	115-2	Zanskar	Himalaya	38.44	19.00	15.43	0.46	0.26	23.18				96.77	Clinozoisite	Clinozoisite
4419	117-2	Zanskar	Himalaya	38.38	21.79	13.61	0.50	0.26	24.17				98.71	Clinozoisite	Epidote
4419	125-2	Zanskar	Himalaya	39.06	19.84	15.55	0.26	0.17	23.40				98.28	Clinozoisite	Epidote
4419	146-2	Zanskar	Himalaya	38.81	19.86	15.26	0.30	0.18	23.70				98.11	Clinozoisite	Epidote
4419	157-2	Zanskar	Himalaya	37.70	19.91	15.09	0.47	0.88	23.02				97.07	Clinozoisite	Epidote
4419	164-2	Zanskar	Himalaya	38.73	20.70	14.52	0.35	0.26	24.95				99.51	Clinozoisite	Epidote
4419	219-2	Zanskar	Himalaya	38.17	19.84	15.84	0.56	0.00	23.58				97.99	Clinozoisite	Epidote
4419	237-2	Zanskar	Himalaya	37.95	20.40	14.35	0.39	0.20	24.65				97.94	Clinozoisite	Epidote
4419	238-2	Zanskar	Himalaya	39.30	20.57	14.22	0.49	0.00	23.92				98.50	Clinozoisite	Epidote
4419	252-2	Zanskar	Himalaya	39.10	21.30	15.12	0.64	0.34	23.36				99.86	Clinozoisite	Epidote
4419	254-2	Zanskar	Himalaya	38.75	20.43	14.37	0.41	0.16	24.63				98.75	Clinozoisite	Epidote
4419	268-2	Zanskar	Himalaya	38.72	20.03	16.18	0.47	0.42	23.90				99.72	Clinozoisite	Epidote
4419	283-2	Zanskar	Himalaya	39.20	22.50	12.56	0.46	0.34	23.98				99.04	Clinozoisite	Clinozoisite
4419	301-2	Zanskar	Himalaya	36.97	22.49	12.35	0.27	0.29	24.36				96.73	Clinozoisite	Epidote
4419	303-2	Zanskar	Himalaya	39.79	20.97	12.89	0.58	0.40	22.75				97.38	Clinozoisite	Epidote
4419	367-2	Zanskar	Himalaya	38.06	20.11	15.19	0.41	0.20	23.68				97.65	Clinozoisite	Epidote
4419	369-2	Zanskar	Himalaya	39.84	20.68	15.18	0.32	0.38	23.48				99.88	Clinozoisite	Epidote
4419	376-2	Zanskar	Himalaya	38.74	20.74	13.50	0.29	0.00	24.60				97.87	Clinozoisite	Clinozoisite
4419	381-2	Zanskar	Himalaya	38.39	22.11	12.54	0.47	0.29	23.83				97.63	Clinozoisite	Epidote
4419	382-2	Zanskar	Himalaya	39.34	22.08	12.21	0.47	0.47	24.47				99.04	Clinozoisite	Clinozoisite
4419	400-2	Zanskar	Himalaya	39.10	20.16	14.49	0.45	0.21	23.95				98.36	Clinozoisite	Clinozoisite
4419	409-2	Zanskar	Himalaya	37.96	21.76	12.81	0.54	0.22	24.01				97.30	Clinozoisite	Epidote
4419	416-2	Zanskar	Himalaya	38.90	20.79	13.76	0.45	0.26	23.41				97.57	Clinozoisite	Epidote
4419	417-2	Zanskar	Himalaya	38.51	20.59	14.30	0.45	0.17	24.13				98.15	Clinozoisite	Epidote
4419	428-2	Zanskar	Himalaya	37.86	18.87	34.10	3.46	2.50	2.22				99.01	Clinozoisite	Epidote
4419	439-2	Zanskar	Himalaya	38.65	20.60	14.35	0.48	0.43	23.18				97.69	Clinozoisite	Epidote
4419	441-2	Zanskar	Himalaya	38.92	20.85	14.48	0.38	0.16	24.08				98.87	Clinozoisite	Epidote
4419	458-2	Zanskar	Himalaya	38.72	20.01	14.03	0.45	0.17	23.71				97.09	Clinozoisite	Epidote
4419	482-2	Zanskar	Himalaya	37.87	20.69	14.89	0.45	0.12	24.20				98.22	Clinozoisite	Epidote
4419	495-2	Zanskar	Himalaya	37.89	20.48	15.16	0.27	0.24	23.58				97.62	Clinozoisite	Epidote
4419	498-2	Zanskar	Himalaya	38.65	21.16	14.10	0.36	0.18	23.61				98.06	Clinozoisite	Clinozoisite
4419	529-2	Zanskar	Himalaya	38.03	21.17	14.59	0.27	0.00	24.05				98.11	Clinozoisite	Epidote
4419	560-2	Zanskar	Himalaya	39.00	20.83	13.06	0.84	0.35	22.88				96.96	Clinozoisite	Epidote
4419	570-2	Zanskar	Himalaya	38.80	24.18	9.32	0.40	0.10	23.87				96.67	Clinozoisite	Clinozoisite
4419	656-2	Zanskar	Himalaya	38.83	20.13	14.98	0.47	0.16	24.45				99.02	Clinozoisite	Epidote
4419	657-2	Zanskar	Himalaya	38.41	19.72	13.44	0.37	0.11	24.71				96.76	Clinozoisite	Epidote
4419	667-2	Zanskar	Himalaya	38.91	20.60	14.79	0.52	0.27	24.26				99.35	Clinozoisite	Epidote
4419	672-2	Zanskar	Himalaya	38.40	20.35	14.28	0.41	0.36	23.92				97.72	Clinozoisite	Epidote
4419	675-2	Zanskar	Himalaya	38.57	26.08	6.78	0.49	0.50	24.22				96.64	Clinozoisite	Clinozoisite
4419	692-2	Zanskar	Himalaya	38.77	21.65	13.82	0.41	0.29	24.26				99.20	Clinozoisite	Epidote
4419	697-2	Zanskar	Himalaya	39.18	22.48	11.07	0.37	0.29	23.97				97.36	Clinozoisite	Clinozoisite
4419	740-2	Zanskar	Himalaya	38.87	20.29	14.20	0.21	0.32	23.57				97.46	Clinozoisite	Epidote
4419	744-2	Zanskar	Himalaya	38.76	21.46	13.94	0.35	0.27	24.46				99.24	Clinozoisite	Epidote
4419	780-2	Zanskar	Himalaya	37.43	21.24	13.07	0.17	0.64	24.27				96.82	Clinozoisite	Epidote
4419	817-2	Zanskar	Himalaya	38.72	24.34	9.13	0.61	0.15	24.28				97.23	Clinozoisite	Epidote
4419	832-2	Zanskar	Himalaya	38.89	20.81	14.47	0.42	0.51	24.75				99.85	Clinozoisite	Epidote
4419	838-2	Zanskar	Himalaya	39.01	21.30	14.23	0.27	0.16	24.53				99.50	Clinozoisite	Epidote
4419	33-1	Zanskar	Himalaya	33.26	15.11	13.29	0.73	1.80	11.34	7.48	11.84	3.23	98.08	Allanite	Allanite-(Ce)
4419	179-1	Zanskar	Himalaya	34.34	16.71	13.54	0.87	0.90	13.53	5.52	8.99	3.64	98.04	Allanite	Allanite-(Ce)
4419	217-2	Zanskar	Himalaya	34.09	16.10	14.12	0.66	0.96	14.44	5.34	9.91	3.41	99.03	Allanite	Allanite-(Ce)
4419	241-1	Zanskar	Himalaya	32.46	13.67	15.70	0.56	1.33	12.05	8.12	12.79	3.06	99.74	Allanite	Allanite-(Ce)
4419	613-2	Zanskar	Himalaya	35.15	20.19	12.59	0.42	0.40	17.85	3.09	6.18	3.35	99.22	Clinozoisite	Epidote
4419	623-2	Zanskar	Himalaya	34.85	16.46	13.00	0.42	1.55	13.66	7.53	10.50	3.01	100.98	Allanite	Allanite-(Ce)
4419	413-2	Zanskar	Himalaya	33.79	16.18	14.11	0.84	1.12	12.14	6.76	10.02	3.89	98.85	Allanite	Allanite-(Ce)

Sample	Points	River/Dune	Domain	SiO_2	Al_2O_3	FeO	MnO	MgO	CaO	La_2O_3	Ce_2O_3	Nd_2O_3	Total	Subgroup	Name
				wt%	wt%	wt%	wt%	wt%	wt%	wt%	wt%	wt%			
1432	10-1	Astor	Nanga Parbat	37.88	28.26	5.91	0.33	0.00	23.85				96.23	Clinozoisite	Clinozoisite
1432	17-1	Astor	Nanga Parbat	38.04	25.98	10.16	0.43	0.22	23.49				98.32	Clinozoisite	Epidote
1432	19-1	Astor	Nanga Parbat	37.57	26.24	9.29	0.35	0.51	23.93				97.90	Clinozoisite	Epidote
1432	38-1	Astor	Nanga Parbat	38.74	25.13	10.74	0.30	0.56	23.64				99.09	Clinozoisite	Epidote
1432	45-1	Astor	Nanga Parbat	37.99	25.87	9.58	0.36	0.28	24.54				98.61	Clinozoisite	Epidote
1432	48-1	Astor	Nanga Parbat	38.50	28.12	7.23	0.27	0.39	23.24				97.75	Clinozoisite	Clinozoisite
1432	64-1	Astor	Nanga Parbat	38.28	25.66	10.78	0.46	0.40	22.56				98.14	Clinozoisite	Epidote
1432	71-1	Astor	Nanga Parbat	38.34	28.92	6.80	0.35	0.40	24.17				98.98	Clinozoisite	Clinozoisite
1432	89-1	Astor	Nanga Parbat	39.26	27.74	6.13	0.22	0.36	24.12				97.85	Clinozoisite	Clinozoisite
1432	90-2	Astor	Nanga Parbat	38.19	25.88	10.29	0.30	0.34	24.06				99.05	Clinozoisite	Epidote
1432	91-1	Astor	Nanga Parbat	38.42	26.37	8.87	0.46	0.28	23.73				98.14	Clinozoisite	Epidote
1432	93-1	Astor	Nanga Parbat	38.05	26.56	9.20	0.30	0.10	23.71				97.94	Clinozoisite	Epidote
1432	106-1	Astor	Nanga Parbat	38.54	27.97	7.92	0.30	0.20	24.53				99.47	Clinozoisite	Epidote
1432	117-1	Astor	Nanga Parbat	38.09	27.37	7.39	0.35	0.29	23.95				97.42	Clinozoisite	Epidote
1432	137-1	Astor	Nanga Parbat	38.14	28.48	6.80	0.23	0.51	24.42				98.58	Clinozoisite	Clinozoisite
1432	139-1	Astor	Nanga Parbat	38.20	26.93	7.91	0.27	0.41	24.58				98.29	Clinozoisite	Epidote
1432	152-1	Astor	Nanga Parbat	38.21	26.98	8.69	0.21	0.38	23.50				97.97	Clinozoisite	Epidote
1432	153-1	Astor	Nanga Parbat	38.48	27.95	6.86	0.29	0.40	24.65				98.63	Clinozoisite	Clinozoisite
1432	157-1	Astor	Nanga Parbat	38.41	26.49	8.47	0.19	0.30	25.04				98.89	Clinozoisite	Epidote
1432	159-1	Astor	Nanga Parbat	37.94	24.94	11.09	0.31	0.26	23.81				98.34	Clinozoisite	Epidote
1432	164-1	Astor	Nanga Parbat	38.39	25.84	10.24	0.37	0.34	23.75				98.92	Clinozoisite	Epidote
1432	175-1	Astor	Nanga Parbat	38.19	25.89	9.79	0.19	0.22	23.79				98.07	Clinozoisite	Epidote
1432	176-1	Astor	Nanga Parbat	37.62	25.97	8.72	0.34	0.25	24.39				97.29	Clinozoisite	Epidote
1432	188-1	Astor	Nanga Parbat	39.00	32.49	1.81	0.20	0.47	24.04				98.01	Clinozoisite	Clinozoisite
1432	200-1	Astor	Nanga Parbat	37.66	26.58	9.19	0.33	0.15	23.47				97.38	Clinozoisite	Epidote
1432	202-1	Astor	Nanga Parbat	37.98	25.57	9.66	0.27	0.38	23.31				97.17	Clinozoisite	Epidote
1432	217-1	Astor	Nanga Parbat	37.93	26.93	8.15	0.30	0.65	23.63				97.58	Clinozoisite	Epidote
1432	220-1	Astor	Nanga Parbat	38.30	28.40	7.09	0.24	0.35	24.64				99.02	Clinozoisite	Clinozoisite
1432	224-1	Astor	Nanga Parbat	38.39	27.14	8.39	0.32	0.49	23.70				98.44	Clinozoisite	Epidote
1432	239-1	Astor	Nanga Parbat	35.35	26.76	6.21	0.27	0.43	20.95				89.97	Clinozoisite	Clinozoisite
1432	241-1	Astor	Nanga Parbat	38.45	23.13	11.99	0.48	0.12	23.44				97.61	Clinozoisite	Epidote
1432	309-1	Astor	Nanga Parbat	38.61	26.21	10.34	0.34	0.11	23.84				99.45	Clinozoisite	Epidote
1432	315-1	Astor	Nanga Parbat	37.61	26.16	10.05	0.25	0.10	23.86				98.04	Clinozoisite	Epidote
1432	318-1	Astor	Nanga Parbat	37.35	26.37	8.07	0.20	0.17	23.93				96.10	Clinozoisite	Epidote
1432	319-1	Astor	Nanga Parbat	38.22	24.78	10.84	0.44	0.41	24.10				98.80	Clinozoisite	Epidote
1432	321-1	Astor	Nanga Parbat	37.93	25.26	11.42	0.31	0.25	23.68				98.84	Clinozoisite	Epidote
1432	322-1	Astor	Nanga Parbat	38.32	26.41	8.26	0.31	0.24	23.75				97.29	Clinozoisite	Epidote
1432	342-1	Astor	Nanga Parbat	38.62	26.47	9.23	0.24	0.47	24.08				99.10	Clinozoisite	Epidote
1432	347-1	Astor	Nanga Parbat	39.19	28.88	5.11	0.27	0.19	24.16				97.80	Clinozoisite	Clinozoisite
1432	359-1	Astor	Nanga Parbat	38.75	28.03	7.10	0.28	0.30	23.79				98.26	Clinozoisite	Clinozoisite
1432	361-1	Astor	Nanga Parbat	38.07	26.66	8.78	0.29	0.28	23.82				97.90	Clinozoisite	Epidote
1432	379-1	Astor	Nanga Parbat	37.67	27.58	7.98	0.28	0.33	24.31				98.15	Clinozoisite	Epidote
1432	403-1	Astor	Nanga Parbat	37.49	28.05	9.10	0.50	0.38	23.45				98.98	Clinozoisite	Epidote
1432	415-1	Astor	Nanga Parbat	37.96	27.35	6.76	0.13	0.00	23.24				95.45	Clinozoisite	Clinozoisite
1432	428-1	Astor	Nanga Parbat	37.48	24.76	10.07	0.24	0.24	24.20				96.99	Clinozoisite	Epidote
1432	432-1	Astor	Nanga Parbat	37.71	24.00	11.75	0.38	0.42	23.79				98.03	Clinozoisite	Epidote
1432	438-1	Astor	Nanga Parbat	38.44	26.97	8.01	0.27	0.26	23.57				97.52	Clinozoisite	Epidote
1432	441-1	Astor	Nanga Parbat	37.99	25.10	10.70	0.32	0.18	23.58				97.87	Clinozoisite	Epidote
1432	449-1	Astor	Nanga Parbat	38.72	27.64	7.69	0.31	0.22	24.14				98.72	Clinozoisite	Epidote
1432	460-1	Astor	Nanga Parbat	37.78	26.10	8.97	0.31	0.26	23.95				97.37	Clinozoisite	Epidote
1432	462-1	Astor	Nanga Parbat	39.05	31.04	2.56	0.41	0.17	24.93				98.17	Clinozoisite	Clinozoisite
1432	470-1	Astor	Nanga Parbat	38.59	25.27	9.77	0.59	0.22	22.81				97.24	Clinozoisite	Epidote
1432	479-1	Astor	Nanga Parbat	38.33	28.05	7.54	0.30	0.15	24.57				98.94	Clinozoisite	Epidote
1432	514-1	Astor	Nanga Parbat	37.24	27.71	7.40	0.21	0.30	23.94				96.79	Clinozoisite	Epidote
1432	528-1	Astor	Nanga Parbat	37.99	24.03	11.37	0.40	0.30	23.57				97.66	Clinozoisite	Epidote
1432	530-1	Astor	Nanga Parbat	36.47	27.81	5.46	0.33	0.51	21.78				92.36	Clinozoisite	Clinozoisite
1432	57-2	Astor	Nanga Parbat	37.06	27.03	8.10	0.27	0.48	23.28				96.22	Clinozoisite	Epidote
1432	74-2	Astor	Nanga Parbat	37.94	26.10	9.02	0.28	0.26	23.96				97.56	Clinozoisite	Epidote
1432	84-2	Astor	Nanga Parbat	37.79	26.79	8.46	0.34	0.37	23.79				97.55	Clinozoisite	Epidote
1432	94-2	Astor	Nanga Parbat	38.62	26.65	9.02	0.31	0.27	24.66				99.53	Clinozoisite	Epidote
1432	124-2	Astor	Nanga Parbat	38.16	25.37	11.41	0.20	0.21	23.42				98.76	Clinozoisite	Epidote
1432	169-2	Astor	Nanga Parbat	38.41	26.28	8.59	0.23	0.17	24.07				97.75	Clinozoisite	Epidote
1432	194-2	Astor	Nanga Parbat	41.13	17.04	16.71	0.13	8.67	11.28				94.96	Clinozoisite	Epidote
1432	198-2	Astor	Nanga Parbat	39.12	27.83	7.05	0.50	0.38	24.25				99.13	Clinozoisite	Clinozoisite
1432	200-2	Astor	Nanga Parbat	37.69	26.74	8.39	0.31	0.13	23.80				97.06	Clinozoisite	Epidote
1432	220-2	Astor	Nanga Parbat	38.26	25.28	11.10	0.33	0.00	23.87				98.85	Clinozoisite	Epidote
1432	243-2	Astor	Nanga Parbat	37.84	26.69	8.64	0.34	0.30	24.04				97.86	Clinozoisite	Epidote
1432	256-2	Astor	Nanga Parbat	37.19	27.62	7.69	0.27	0.14	23.89				96.80	Clinozoisite	Epidote
1432	288-2	Astor	Nanga Parbat	37.22	27.07	7.78	0.23	0.00	23.67				95.96	Clinozoisite	Epidote
1432	305-2	Astor	Nanga Parbat	38.31	29.33	6.08	0.24	0.34	24.37				98.67	Clinozoisite	Clinozoisite
1432	315-2	Astor	Nanga Parbat	41.58	29.11	8.24	0.30	0.43	23.29				102.96	Clinozoisite	Clinozoisite
1432	318-2	Astor	Nanga Parbat	38.31	27.51	6.73	0.30	0.32	23.65				96.83	Clinozoisite	Clinozoisite
1432	385-2	Astor	Nanga Parbat	37.49	25.67	8.53	0.37	0.41	23.13				95.60	Clinozoisite	Epidote
1432	392-2	Astor	Nanga Parbat	38.13	31.40	2.83	0.35	0.36	23.78				96.86	Clinozoisite	Clinozoisite
1432	395-2	Astor	Nanga Parbat	38.23	26.04	9.05	0.27	0.38	22.93				96.91	Clinozoisite	Epidote
1432	416-2	Astor	Nanga Parbat	38.19	25.91	9.68	0.29	0.25	23.96				98.29	Clinozoisite	Epidote
1432	428-2	Astor	Nanga Parbat	38.05	29.41	4.87	0.24	0.44	23.46				96.48	Clinozoisite	Clinozoisite
1432	437-2	Astor	Nanga Parbat	38.89	27.34	9.00	0.37	0.40	23.82				99.82	Clinozoisite	Epidote
1432	439-2	Astor	Nanga Parbat	38.17	26.91	7.35	0.24	0.17	23.82				96.66	Clinozoisite	Clinozoisite
1432	440-2	Astor	Nanga Parbat	37.41	25.94	9.40	0.28	0.55	23.65				97.23	Clinozoisite	Epidote
1432	447-2	Astor	Nanga Parbat	37.63	28.76	7.11	0.39	0.35	24.21				98.45	Clinozoisite	Clinozoisite
1432	487-2	Astor	Nanga Parbat	37.76	25.86	9.25	0.21	0.30	23.95				97.32	Clinozoisite	Epidote
1432	501-2	Astor	Nanga Parbat	37.09	26.45	8.75	0.39	0.47	23.17				96.31	Clinozoisite	Epidote
1432	516-2	Astor	Nanga Parbat	38.25	31.77	1.80	0.33	0.18	24.66				97.00	Clinozoisite	Clinozoisite
1432	540-2	Astor	Nanga Parbat	37.74	26.97	7.96	0.27	0.24	23.71				96.90	Clinozoisite	Epidote
1432	550-2	Astor	Nanga Parbat	39.14	27.55	8.22	0.30	0.44	23.08				98.74	Clinozoisite	Clinozoisite
1432	556-2	Astor	Nanga Parbat	37.51	24.82	10.70	0.28	0.24	24.07				97.61	Clinozoisite	Epidote

Sample	Points	River/Dune	Domain	SiO_2	Al_2O_3	FeO	MnO	MgO	CaO	La_2O_3	Ce_2O_3	Nd_2O_3	Total	Subgroup	Name
				wt%	wt%	wt%	wt%	wt%	wt%	wt%	wt%	wt%			
1462	47	Mankera	Thal	38.99	26.46	8.50	0.76	0.37	21.82				96.90	Clinozoisite	Clinozoisite
1462	48	Mankera	Thal	37.67	22.53	12.77	0.71	0.22	21.33				95.23	Clinozoisite	Clinozoisite
1462	49	Mankera	Thal	41.25	28.41	5.53	0.24	0.33	22.21				97.97	Clinozoisite	Clinozoisite
1462	58	Mankera	Thal	37.99	20.88	13.95	0.53	0.37	21.90				95.62	Clinozoisite	Epidote
1462	70	Mankera	Thal	38.81	24.88	10.30	1.00	0.30	21.98				97.27	Clinozoisite	Clinozoisite
1462	73	Mankera	Thal	36.94	25.23	8.43	0.66	0.55	23.21				95.02	Clinozoisite	Epidote
1462	75	Mankera	Thal	51.88	3.06	14.30	0.57	14.21	11.88				95.90	Clinozoisite	Epidote
1462	85	Mankera	Thal	39.96	25.94	8.83	0.37	0.33	22.15				97.58	Clinozoisite	Clinozoisite
1462	105	Mankera	Thal	37.71	26.72	7.54	0.58	0.38	22.44				95.37	Clinozoisite	Clinozoisite
1462	111	Mankera	Thal	39.35	31.46	2.93	0.38	0.21	23.50				97.83	Clinozoisite	Clinozoisite
1462	118	Mankera	Thal	38.99	24.93	9.84	0.60	0.00	22.20				96.56	Clinozoisite	Clinozoisite
1462	120	Mankera	Thal	38.93	23.60	11.93	0.50	0.16	21.84				96.96	Clinozoisite	Clinozoisite
1462	137	Mankera	Thal	38.17	24.63	9.71	0.59	0.46	22.09				95.65	Clinozoisite	Epidote
1462	139	Mankera	Thal	38.50	23.19	12.51	0.55	0.00	22.82				97.57	Clinozoisite	Epidote
1462	144	Mankera	Thal	39.97	30.73	4.78	0.86	0.09	22.77				99.20	Clinozoisite	Clinozoisite
1462	164	Mankera	Thal	39.98	27.02	8.22	0.40	0.48	23.36				99.46	Clinozoisite	Clinozoisite
1462	181	Mankera	Thal	39.33	27.18	8.27	0.87	0.21	22.19				98.05	Clinozoisite	Clinozoisite
1462	185	Mankera	Thal	38.56	23.97	10.41	0.90	0.16	22.44				96.44	Clinozoisite	Clinozoisite
1462	189	Mankera	Thal	39.21	25.40	10.08	0.77	0.00	22.33				97.79	Clinozoisite	Clinozoisite
1462	200	Mankera	Thal	38.52	24.90	9.86	0.65	0.00	22.11				96.04	Clinozoisite	Clinozoisite
1462	236	Mankera	Thal	38.73	26.76	8.05	0.58	0.12	22.91				97.15	Clinozoisite	Epidote
1462	240	Mankera	Thal	38.71	24.60	10.11	0.69	0.20	22.09				96.40	Clinozoisite	Clinozoisite
1462	245	Mankera	Thal	38.09	29.28	4.95	0.43	0.41	22.78				95.94	Clinozoisite	Clinozoisite
1462	247	Mankera	Thal	39.29	23.52	11.61	0.33	0.24	21.82				96.81	Clinozoisite	Epidote
1462	257	Mankera	Thal	37.95	23.24	11.40	0.57	0.00	22.08				95.24	Clinozoisite	Clinozoisite
1462	258	Mankera	Thal	38.16	23.17	12.43	0.58	0.33	22.24				96.91	Clinozoisite	Epidote
1462	267	Mankera	Thal	37.65	24.90	9.90	0.56	0.38	22.35				95.74	Clinozoisite	Epidote
1462	269	Mankera	Thal	39.63	32.18	2.05	0.27	0.36	23.20				97.69	Clinozoisite	Clinozoisite
1462	271	Mankera	Thal	38.50	25.93	9.59	0.70	0.00	21.79				96.51	Clinozoisite	Epidote
1462	275	Mankera	Thal	37.92	22.53	12.38	0.62	0.19	21.84				95.48	Clinozoisite	Clinozoisite
1462	278	Mankera	Thal	37.04	22.66	11.86	0.74	0.37	21.73				94.40	Clinozoisite	Epidote
1462	300	Mankera	Thal	38.95	26.60	9.02	0.92	0.43	22.16				98.08	Clinozoisite	Epidote
1462	304	Mankera	Thal	38.29	24.71	11.11	0.69	0.21	21.87				96.88	Clinozoisite	Epidote
1462	307	Mankera	Thal	37.23	24.15	10.55	0.69	0.23	22.20				95.05	Clinozoisite	Epidote
1462	318	Mankera	Thal	38.24	23.79	11.22	0.94	0.40	22.32				96.91	Clinozoisite	Epidote
1462	319	Mankera	Thal	38.12	25.89	8.49	0.44	0.29	22.57				95.80	Clinozoisite	Epidote
1462	323	Mankera	Thal	39.05	31.57	2.92	0.62	0.00	22.31				96.47	Clinozoisite	Clinozoisite
1462	327	Mankera	Thal	39.75	32.87	0.65	0.52	0.37	23.68				97.84	Clinozoisite	Clinozoisite
1462	547	Mankera	Thal	40.56	25.00	11.03	0.65	0.60	21.94				99.78	Clinozoisite	Clinozoisite
1462	555	Mankera	Thal	36.16	22.99	12.70	0.67	0.00	21.73				94.25	Clinozoisite	Epidote
1462	578	Mankera	Thal	38.76	23.26	12.52	0.98	0.26	21.81				97.59	Clinozoisite	Clinozoisite
1462	580	Mankera	Thal	40.10	25.01	11.03	0.79	0.38	22.66				99.97	Clinozoisite	Clinozoisite
1462	583	Mankera	Thal	37.98	23.40	12.17	0.55	0.42	22.00				96.52	Clinozoisite	Epidote
1462	593	Mankera	Thal	38.26	24.08	11.43	0.68	0.42	22.23				97.10	Clinozoisite	Epidote
1462	597	Mankera	Thal	37.65	26.61	8.50	0.91	0.17	22.53				96.37	Clinozoisite	Epidote
1462	603	Mankera	Thal	39.77	26.95	8.07	0.57	0.29	21.71				97.36	Clinozoisite	Clinozoisite
1462	604	Mankera	Thal	38.72	25.82	9.50	0.94	0.53	21.90				97.41	Clinozoisite	Epidote
1462	615	Mankera	Thal	39.57	25.84	9.70	0.70	0.42	22.07				98.30	Clinozoisite	Clinozoisite
1462	621	Mankera	Thal	38.94	22.62	12.63	0.76	0.12	22.19				97.26	Clinozoisite	Epidote
1462	627	Mankera	Thal	39.20	33.91	0.79	0.47	0.21	22.96				97.54	Clinozoisite	Clinozoisite
1462	651	Mankera	Thal	38.23	25.35	9.57	0.79	0.44	21.02				95.40	Clinozoisite	Clinozoisite
1462	665	Mankera	Thal	38.78	30.08	5.02	0.54	0.22	23.11				97.75	Clinozoisite	Clinozoisite
1462	670	Mankera	Thal	37.81	26.90	8.93	0.75	0.17	22.06				96.62	Clinozoisite	Epidote
1462	690	Mankera	Thal	37.99	22.82	12.00	0.56	0.20	22.50				96.07	Clinozoisite	Epidote
1462	709	Mankera	Thal	36.64	21.97	11.55	1.34	0.32	20.51				92.33	Clinozoisite	Clinozoisite
1462	720	Mankera	Thal	38.73	25.20	10.61	0.89	0.27	21.19				96.89	Clinozoisite	Clinozoisite
1462	724	Mankera	Thal	39.25	23.63	11.91	0.69	0.32	21.83				97.63	Clinozoisite	Clinozoisite
1462	733	Mankera	Thal	40.21	29.30	5.17	0.46	0.44	24.02				99.60	Clinozoisite	Clinozoisite
1462	745	Mankera	Thal	38.74	26.75	8.74	0.49	0.00	22.20				96.92	Clinozoisite	Clinozoisite
1462	749	Mankera	Thal	38.51	24.07	11.75	0.84	0.23	22.14				97.54	Clinozoisite	Epidote
1462	763	Mankera	Thal	38.04	23.24	10.66	0.63	0.20	21.73				94.50	Clinozoisite	Clinozoisite
1462	765	Mankera	Thal	38.41	27.89	7.02	0.64	0.79	22.31				97.06	Clinozoisite	Clinozoisite
1462	767	Mankera	Thal	30.30	22.48	20.43	0.50	21.91	0.42				96.04	Clinozoisite	Clinozoisite
1462	771	Mankera	Thal	37.70	7.70	18.16	1.08	0.00	29.92				94.56	Clinozoisite	Clinozoisite
1462	791	Mankera	Thal	37.80	24.22	10.18	0.77	0.11	22.53				95.61	Clinozoisite	Epidote
1462	802	Mankera	Thal	37.46	21.48	12.42	0.58	0.61	21.79				94.34	Clinozoisite	Clinozoisite
1462	826	Mankera	Thal	38.94	24.60	10.00	0.84	0.18	22.04				96.60	Clinozoisite	Clinozoisite
1462	988	Mankera	Thal	37.05	25.21	8.43	0.66	0.57	21.32				93.24	Clinozoisite	Epidote
1462	1022	Mankera	Thal	37.66	22.96	11.82	0.56	0.22	22.56				95.78	Clinozoisite	Epidote
1462	1027	Mankera	Thal	38.09	23.30	11.14	0.79	0.10	21.42				94.84	Clinozoisite	Clinozoisite
1462	1045	Mankera	Thal	39.89	32.13	1.40	0.50	0.41	23.17				97.50	Clinozoisite	Clinozoisite
1462	1058	Mankera	Thal	37.28	24.45	11.29	0.64	0.28	21.67				95.61	Clinozoisite	Epidote
1462	1065	Mankera	Thal	39.91	25.58	8.58	0.62	0.37	21.63				96.69	Clinozoisite	Clinozoisite
1462	1068	Mankera	Thal	38.93	24.34	10.61	0.66	0.00	22.99				97.53	Clinozoisite	Clinozoisite
1462	1076	Mankera	Thal	38.21	24.91	10.24	0.93	0.28	21.94				96.51	Clinozoisite	Epidote
1462	1077	Mankera	Thal	39.00	25.16	9.84	0.69	0.00	22.26				96.95	Clinozoisite	Clinozoisite
1462	1079	Mankera	Thal	38.93	25.13	10.45	0.58	0.45	22.26				97.80	Clinozoisite	Epidote
1462	1103	Mankera	Thal	39.00	27.15	5.75	0.43	0.45	22.89				95.67	Clinozoisite	Clinozoisite
1462	1109	Mankera	Thal	38.29	26.27	9.28	0.48	0.27	22.58				97.17	Clinozoisite	Epidote
1462	1118	Mankera	Thal	39.55	27.26	7.69	0.66	0.34	22.45				97.95	Clinozoisite	Clinozoisite
1462	1124	Mankera	Thal	38.93	23.57	12.70	0.92	0.30	22.74				99.16	Clinozoisite	Epidote
1462	1130	Mankera	Thal	27.97	22.94	20.42	0.47	20.12	0.28				92.20	Clinozoisite	Epidote
1462	1134	Mankera	Thal	39.48	30.72	3.52	0.73	0.30	23.09				97.84	Clinozoisite	Clinozoisite
1462	1143	Mankera	Thal	39.04	27.76	6.59	0.55	0.22	22.25				96.41	Clinozoisite	Clinozoisite
1462	1156	Mankera	Thal	37.73	23.16	11.68	0.35	0.32	22.20				95.44	Clinozoisite	Epidote
1462	1158	Mankera	Thal	39.22	25.16	10.05	0.46	0.42	22.51				97.82	Clinozoisite	Clinozoisite
1462	1160	Mankera	Thal	39.09	23.58	11.90	0.58	0.50	22.31				97.96	Clinozoisite	Clinozoisite
1462	1172	Mankera	Thal	39.98	31.80	1.66	0.27	0.12	23.44				97.27	Clinozoisite	Clinozoisite
1462	1176	Mankera	Thal	39.24	29.10	4.26	0.27	0.25	23.27				96.39	Clinozoisite	Clinozoisite
1462	1192	Mankera	Thal	37.28	24.78	9.65	0.54	0.28	22.61				95.14	Clinozoisite	Epidote
1462	1200	Mankera	Thal	38.05	23.65	10.82	0.93	0.00	22.37				95.82	Clinozoisite	Clinozoisite
1462	1205	Mankera	Thal	37.86	24.88	10.06	0.54	0.42	22.54				96.30	Clinozoisite	Epidote
1462	1207	Mankera	Thal	38.97	27.44	7.09	0.63	0.52	23.18				97.83	Clinozoisite	Clinozoisite
1462	1208	Mankera	Thal	38.68	25.00	10.51	0.49	0.17	22.42				97.27	Clinozoisite	Epidote
1462	1219	Mankera	Thal	37.18	23.33	10.89	0.71	0.30	22.40				94.81	Clinozoisite	Epidote
1462	1261	Mankera	Thal	37.65	22.80	12.21	0.46	0.18	21.43				94.73	Clinozoisite	Clinozoisite
1462	1272	Mankera	Thal	38.05	24.69	9.83	0.36	0.00	21.60				94.53	Clinozoisite	Clinozoisite
1462	1290	Mankera	Thal	38.32	25.52	9.99	0.68	0.27	22.62				97.40	Clinozoisite	Epidote
1462	1291	Mankera	Thal	38.59	24.95	8.34	0.78	0.10	22.16				94.92	Clinozoisite	Clinozoisite
1462	1296	Mankera	Thal	38.01	21.39	31.68	1.60	4.57	2.79				100.04	Clinozoisite	Clinozoisite

Sample	Points	River/Dune	Domain	SiO_2	Al_2O_3	FeO	MnO	MgO	CaO	La_2O_3	Ce_2O_3	Nd_2O_3	Total	Subgroup	Name
				wt%	wt%	wt%	wt%	wt%	wt%	wt%	wt%	wt%			
1463	9	Haidarabad	Thal	38.27	25.97	9.37	0.61	0.38	22.72				97.32	Clinozoisite	Epidote
1463	20	Haidarabad	Thal	40.27	24.61	11.46	0.48	0.00	21.69				98.51	Clinozoisite	Epidote
1463	36	Haidarabad	Thal	39.88	26.07	9.31	0.47	0.32	21.91				97.96	Clinozoisite	Clinozoisite
1463	84	Haidarabad	Thal	39.67	25.04	10.71	0.61	0.21	21.07				97.31	Clinozoisite	Clinozoisite
1463	118	Haidarabad	Thal	38.82	26.06	9.01	0.55	0.41	22.82				97.67	Clinozoisite	Epidote
1463	124	Haidarabad	Thal	39.91	29.10	5.55	0.35	0.38	23.21				98.50	Clinozoisite	Clinozoisite
1463	128	Haidarabad	Thal	39.14	31.48	2.17	0.49	0.32	22.72				96.32	Clinozoisite	Clinozoisite
1463	153	Haidarabad	Thal	38.37	24.74	11.14	0.61	0.24	22.54				97.64	Clinozoisite	Epidote
1463	207	Haidarabad	Thal	38.56	29.04	6.26	0.39	0.40	23.11				97.76	Clinozoisite	Clinozoisite
1463	211	Haidarabad	Thal	38.07	25.68	9.59	0.72	0.00	23.95				98.01	Clinozoisite	Epidote
1463	226	Haidarabad	Thal	38.73	26.75	8.03	0.40	0.45	23.13				97.49	Clinozoisite	Epidote
1463	234	Haidarabad	Thal	40.99	26.89	8.10	0.27	0.40	20.82				97.47	Clinozoisite	Clinozoisite
1463	275	Haidarabad	Thal	40.42	27.17	8.41	0.41	0.28	23.02				99.71	Clinozoisite	Clinozoisite
1463	288	Haidarabad	Thal	38.62	26.14	9.40	0.92	0.00	22.81				97.89	Clinozoisite	Epidote
1463	299	Haidarabad	Thal	38.93	22.54	12.51	0.81	0.19	22.05				97.03	Clinozoisite	Epidote
1463	345	Haidarabad	Thal	39.19	29.27	5.28	0.44	0.00	23.46				97.64	Clinozoisite	Clinozoisite
1463	351	Haidarabad	Thal	38.60	24.11	11.07	0.60	0.36	22.30				97.04	Clinozoisite	Clinozoisite
1463	358	Haidarabad	Thal	38.47	24.70	10.77	0.61	0.00	23.26				97.81	Clinozoisite	Epidote
1463	378	Haidarabad	Thal	39.40	26.01	9.12	0.66	0.10	21.12				96.41	Clinozoisite	Clinozoisite
1463	385	Haidarabad	Thal	38.05	26.04	8.65	0.40	0.40	22.44				95.98	Clinozoisite	Epidote
1463	418	Haidarabad	Thal	38.34	28.69	5.67	0.39	0.40	22.89				96.38	Clinozoisite	Clinozoisite
1463	420	Haidarabad	Thal	37.59	22.01	12.26	0.48	0.47	21.46				94.27	Clinozoisite	Clinozoisite
1463	443	Haidarabad	Thal	37.22	25.74	9.60	0.55	0.55	22.51				96.17	Clinozoisite	Epidote
1463	475	Haidarabad	Thal	39.23	25.52	10.50	0.47	0.21	22.48				98.41	Clinozoisite	Clinozoisite
1463	492	Haidarabad	Thal	40.12	28.32	6.01	0.49	0.14	23.16				98.24	Clinozoisite	Clinozoisite
1463	505	Haidarabad	Thal	39.38	26.13	8.09	0.44	0.11	23.66				97.81	Clinozoisite	Clinozoisite
1463	517	Haidarabad	Thal	38.08	25.99	11.36	0.88	0.00	22.73				99.04	Clinozoisite	Epidote
1463	529	Haidarabad	Thal	38.35	25.51	10.44	1.31	0.18	22.29				98.08	Clinozoisite	Epidote
1463	545	Haidarabad	Thal	37.43	26.50	9.67	0.31	0.08	23.58				97.57	Clinozoisite	Epidote
1463	561	Haidarabad	Thal	38.66	26.94	9.60	0.65	0.20	22.58				98.63	Clinozoisite	Epidote
1463	566	Haidarabad	Thal	38.20	26.75	9.79	0.64	0.14	22.59				98.11	Clinozoisite	Epidote
1463	567	Haidarabad	Thal	38.57	23.22	13.88	0.74	0.39	23.14				99.94	Clinozoisite	Epidote
1463	579	Haidarabad	Thal	39.20	30.07	4.07	0.59	0.38	23.43				97.74	Clinozoisite	Clinozoisite
1463	580	Haidarabad	Thal	38.79	26.12	8.28	0.69	0.58	23.02				97.48	Clinozoisite	Epidote
1463	596	Haidarabad	Thal	38.44	23.87	12.25	0.47	0.12	22.61				97.76	Clinozoisite	Epidote
1463	610	Haidarabad	Thal	37.20	24.32	11.77	0.57	0.00	23.23				97.09	Clinozoisite	Epidote
1463	627	Haidarabad	Thal	39.62	30.76	3.49	0.32	0.00	23.17				97.36	Clinozoisite	Clinozoisite
1463	635	Haidarabad	Thal	39.32	32.07	2.86	0.27	0.25	23.53				98.30	Clinozoisite	Clinozoisite
1463	641	Haidarabad	Thal	36.85	25.09	11.36	0.75	0.11	22.74				96.90	Clinozoisite	Epidote
1463	649	Haidarabad	Thal	38.26	27.07	9.50	0.95	0.34	23.25				99.37	Clinozoisite	Epidote
1463	651	Haidarabad	Thal	38.40	24.44	11.47	0.81	0.30	22.23				97.65	Clinozoisite	Epidote
1463	670	Haidarabad	Thal	40.07	27.02	8.36	0.30	0.26	22.30				98.31	Clinozoisite	Clinozoisite
1463	692	Haidarabad	Thal	37.02	25.65	10.26	0.64	0.15	23.61				97.33	Clinozoisite	Epidote
1463	694	Haidarabad	Thal	38.62	29.57	5.45	0.63	0.36	24.13				98.76	Clinozoisite	Clinozoisite
1463	722	Haidarabad	Thal	38.20	25.50	10.61	0.58	0.16	23.54				98.59	Clinozoisite	Epidote
1463	747	Haidarabad	Thal	39.63	31.87	2.00	0.47	0.00	23.90				97.87	Clinozoisite	Clinozoisite
1463	771	Haidarabad	Thal	39.41	26.90	8.76	0.60	0.26	23.05				98.98	Clinozoisite	Epidote
1463	804	Haidarabad	Thal	37.97	22.12	14.23	0.46	0.20	21.90				96.88	Clinozoisite	Epidote
1463	821	Haidarabad	Thal	38.30	24.50	10.73	0.47	0.18	21.73				95.91	Clinozoisite	Clinozoisite
1463	853	Haidarabad	Thal	39.08	25.81	9.31	0.38	0.27	22.84				97.69	Clinozoisite	Clinozoisite
1463	854	Haidarabad	Thal	37.76	26.32	9.65	0.50	0.28	22.85				97.36	Clinozoisite	Epidote
1463	900	Haidarabad	Thal	39.68	23.73	12.13	0.70	0.00	22.01				98.25	Clinozoisite	Epidote
1463	916	Haidarabad	Thal	50.08	1.89	12.15	0.56	10.24	22.94				97.86	Clinozoisite	Epidote
1463	918	Haidarabad	Thal	38.53	28.45	6.45	0.42	0.37	23.67				97.89	Clinozoisite	Clinozoisite
1463	960	Haidarabad	Thal	37.83	24.99	10.12	0.44	0.34	23.86				97.58	Clinozoisite	Epidote
1463	971	Haidarabad	Thal	38.21	22.69	13.27	0.60	0.25	22.85				97.87	Clinozoisite	Epidote
1463	972	Haidarabad	Thal	39.12	25.41	11.41	0.47	0.16	23.13				99.70	Clinozoisite	Epidote
1463	982	Haidarabad	Thal	38.66	26.81	8.31	0.34	0.09	23.62				97.83	Clinozoisite	Epidote
1463	1000	Haidarabad	Thal	39.20	27.74	7.47	0.42	0.20	23.41				98.44	Clinozoisite	Clinozoisite
1463	1015	Haidarabad	Thal	40.74	31.79	2.69	0.44	0.00	22.97				98.63	Clinozoisite	Clinozoisite
1463	1020	Haidarabad	Thal	38.99	25.37	10.97	0.58	0.21	22.94				99.06	Clinozoisite	Epidote
1463	1063	Haidarabad	Thal	38.04	26.16	10.61	0.42	0.21	21.94				97.38	Clinozoisite	Epidote
1463	1065	Haidarabad	Thal	38.85	29.61	4.75	0.64	0.13	23.49				97.47	Clinozoisite	Clinozoisite
1463	1082	Haidarabad	Thal	38.98	23.17	13.33	0.83	0.43	22.12				98.86	Clinozoisite	Epidote
1463	1103	Haidarabad	Thal	38.47	27.68	8.90	0.83	0.52	22.53				98.93	Clinozoisite	Epidote
1463	1111	Haidarabad	Thal	39.43	30.18	5.73	0.64	0.29	23.52				99.79	Clinozoisite	Clinozoisite
1463	1115	Haidarabad	Thal	39.52	25.26	12.16	0.39	0.22	22.55				100.10	Clinozoisite	Epidote
1463	1117	Haidarabad	Thal	40.46	31.60	2.17	0.60	0.31	23.36				98.50	Clinozoisite	Clinozoisite
1463	1122	Haidarabad	Thal	38.33	27.21	8.87	0.57	0.30	24.12				99.40	Clinozoisite	Epidote
1463	1136	Haidarabad	Thal	39.56	27.57	8.84	0.27	0.28	23.62				100.14	Clinozoisite	Epidote
1463	1173	Haidarabad	Thal	38.47	27.12	8.41	0.58	0.25	24.12				98.95	Clinozoisite	Epidote
1463	1238	Haidarabad	Thal	39.67	32.23	1.61	0.46	0.46	24.31				98.74	Clinozoisite	Clinozoisite
1463	1248	Haidarabad	Thal	37.67	24.86	10.96	0.49	0.00	23.20				97.18	Clinozoisite	Epidote
1463	1325	Haidarabad	Thal	39.63	27.17	9.34	0.47	0.11	23.51				100.23	Clinozoisite	Epidote
1463	1347	Haidarabad	Thal	38.14	27.21	7.62	0.32	0.00	23.45				96.74	Clinozoisite	Clinozoisite
1463	1362	Haidarabad	Thal	39.54	24.34	12.13	0.81	0.59	22.67				100.08	Clinozoisite	Epidote
1463	1410	Haidarabad	Thal	38.79	26.88	9.50	0.57	0.24	23.46				99.44	Clinozoisite	Epidote
1463	1427	Haidarabad	Thal	40.30	27.87	7.45	0.59	0.37	23.85				100.43	Clinozoisite	Clinozoisite
1463	1432	Haidarabad	Thal	38.25	22.77	12.79	0.80	0.51	22.36				97.48	Clinozoisite	Epidote
1463	1445	Haidarabad	Thal	39.08	32.34	1.95	0.35	0.26	23.88				97.86	Clinozoisite	Clinozoisite
1463	1447	Haidarabad	Thal	38.07	25.60	9.57	0.57	0.00	22.43				96.24	Clinozoisite	Epidote
1463	1455	Haidarabad	Thal	38.43	25.54	9.75	0.17	0.16	22.61				96.66	Clinozoisite	Epidote
1463	1466	Haidarabad	Thal	38.39	22.01	13.88	0.34	0.37	23.02				98.01	Clinozoisite	Epidote
1463	1486	Haidarabad	Thal	39.52	27.29	8.68	0.78	0.24	22.80				99.31	Clinozoisite	Epidote
1463	1506	Haidarabad	Thal	38.86	26.75	9.11	0.65	0.46	24.01				99.84	Clinozoisite	Epidote
1463	1542	Haidarabad	Thal	37.97	22.78	14.96	0.56	0.28	23.26				99.81	Clinozoisite	Epidote
1463	1551	Haidarabad	Thal	38.68	27.45	8.06	0.34	0.36	24.05				98.94	Clinozoisite	Epidote
1463	1572	Haidarabad	Thal	39.23	28.80	5.87	0.54	0.28	23.65				98.37	Clinozoisite	Clinozoisite
1463	1577	Haidarabad	Thal	37.77	23.42	12.53	0.58	0.20	23.43				97.93	Clinozoisite	Epidote
1463	1587	Haidarabad	Thal	38.62	21.97	14.27	0.36	0.28	22.90				98.40	Clinozoisite	Epidote
1463	1603	Haidarabad	Thal	38.09	23.55	12.78	0.78	0.32	22.76				98.28	Clinozoisite	Epidote
1463	1622	Haidarabad	Thal	38.01	25.40	10.05	0.50	0.40	23.46				97.82	Clinozoisite	Epidote
1463	1629	Haidarabad	Thal	39.52	27.69	7.89	0.54	0.43	23.81				99.88	Clinozoisite	Clinozoisite
1463	1634	Haidarabad	Thal	37.89	24.99	10.47	0.50	0.33	24.24				98.42	Clinozoisite	Epidote
1463	1638	Haidarabad	Thal	38.68	22.65	15.27	0.70	0.28	23.02				100.60	Clinozoisite	Epidote
1463	1644	Haidarabad	Thal	39.56	25.51	9.68	0.53	0.11	22.61				98.00	Clinozoisite	Clinozoisite
1463	1654	Haidarabad	Thal	42.32	26.73	6.93	0.44	0.15	23.43				100.00	Clinozoisite	Clinozoisite
1463	1657	Haidarabad	Thal	39.59	28.80	6.42	0.51	0.33	23.58				99.23	Clinozoisite	Clinozoisite
1463	1667	Haidarabad	Thal	40.02	32.54	1.75	0.32	0.31	24.21				99.15	Clinozoisite	Clinozoisite

Sample	Points	River/Dune	Domain	SiO_2	Al_2O_3	FeO	MnO	MgO	CaO	La_2O_3	Ce_2O_3	Nd_2O_3	Total	Subgroup	Name
				wt%	wt%	wt%	wt%	wt%	wt%	wt%	wt%	wt%			
1470	13	Muzaffarghar	Thal	38.72	27.02	6.83	0.22	0.58	23.95				97.32	Clinozoisite	Clinozoisite
1470	48	Muzaffarghar	Thal	40.14	23.37	12.37	0.33	0.22	23.18				99.61	Clinozoisite	Clinozoisite
1470	101	Muzaffarghar	Thal	44.04	12.39	19.85	0.32	9.11	11.86				97.57	Clinozoisite	Clinozoisite
1470	234	Muzaffarghar	Thal	40.26	21.83	13.98	0.32	0.20	23.20				99.79	Clinozoisite	Epidote
1470	289	Muzaffarghar	Thal	38.08	22.73	13.08	0.22	0.34	23.11				97.56	Clinozoisite	Epidote
1470	318	Muzaffarghar	Thal	39.37	22.32	13.97	0.42	0.21	22.40				98.69	Clinozoisite	Epidote
1470	423	Muzaffarghar	Thal	39.98	27.54	5.38	0.36	0.22	24.39				97.87	Clinozoisite	Clinozoisite
1470	517	Muzaffarghar	Thal	39.15	23.46	10.54	0.13	0.19	23.63				97.10	Clinozoisite	Clinozoisite
1470	588	Muzaffarghar	Thal	39.31	24.67	9.79	0.24	0.20	24.61				98.82	Clinozoisite	Epidote
1470	689	Muzaffarghar	Thal	38.07	20.12	15.43	0.21	0.26	23.76				97.85	Clinozoisite	Epidote
1470	701	Muzaffarghar	Thal	39.61	25.45	8.17	0.22	0.22	24.40				98.07	Clinozoisite	Clinozoisite
1470	749	Muzaffarghar	Thal	39.66	25.64	8.99	0.25	0.13	23.89				98.56	Clinozoisite	Clinozoisite
1470	789	Muzaffarghar	Thal	39.72	23.45	11.17	0.21	0.20	23.45				98.20	Clinozoisite	Clinozoisite
1470	790	Muzaffarghar	Thal	38.81	27.67	6.90	0.29	0.36	24.41				98.44	Clinozoisite	Clinozoisite
1470	845	Muzaffarghar	Thal	38.67	27.31	5.37	0.22	0.12	24.93				96.62	Clinozoisite	Clinozoisite
1470	886	Muzaffarghar	Thal	39.76	23.25	11.48	0.25	0.29	23.44				98.47	Clinozoisite	Clinozoisite
1470	976	Muzaffarghar	Thal	39.26	25.62	9.50	0.31	0.25	24.25				99.19	Clinozoisite	Epidote
1470	1073	Muzaffarghar	Thal	38.24	22.70	12.91	0.36	0.24	23.75				98.20	Clinozoisite	Epidote
1470	1128	Muzaffarghar	Thal	39.46	24.24	11.20	0.23	0.13	23.26				98.52	Clinozoisite	Clinozoisite
1470	1130	Muzaffarghar	Thal	39.38	21.14	14.65	0.18	0.22	23.52				99.09	Clinozoisite	Epidote
1470	1131	Muzaffarghar	Thal	38.64	22.28	14.51	0.40	0.42	23.05				99.30	Clinozoisite	Epidote
1470	1188	Muzaffarghar	Thal	39.00	24.04	10.71	0.37	0.19	22.62				96.93	Clinozoisite	Clinozoisite
1470	1263	Muzaffarghar	Thal	38.64	24.87	10.40	0.38	0.36	23.47				98.12	Clinozoisite	Epidote
1470	1276	Muzaffarghar	Thal	39.15	22.41	13.63	0.66	0.24	23.48				99.57	Clinozoisite	Epidote
1470	1300	Muzaffarghar	Thal	39.41	23.63	11.39	0.28	0.17	23.46				98.34	Clinozoisite	Clinozoisite
1470	1303	Muzaffarghar	Thal	37.37	20.89	14.52	0.24	0.26	23.59				96.87	Clinozoisite	Epidote
1470	1355	Muzaffarghar	Thal	39.76	25.01	9.54	0.26	0.44	23.77				98.78	Clinozoisite	Clinozoisite
1470	1390	Muzaffarghar	Thal	38.80	21.43	13.61	0.22	0.49	23.82				98.37	Clinozoisite	Epidote
1470	1418	Muzaffarghar	Thal	37.22	21.10	16.07	0.29	0.42	23.29				98.39	Clinozoisite	Epidote
1470	1448	Muzaffarghar	Thal	40.22	26.16	8.49	0.29	0.28	24.30				99.74	Clinozoisite	Clinozoisite
1470	1586	Muzaffarghar	Thal	39.09	24.74	9.40	0.52	0.18	23.81				97.74	Clinozoisite	Clinozoisite
1470	1589	Muzaffarghar	Thal	39.08	19.95	11.89	0.26	1.99	22.48				95.65	Clinozoisite	Clinozoisite
1470	1597	Muzaffarghar	Thal	39.56	25.80	8.13	0.28	0.37	24.27				98.41	Clinozoisite	Clinozoisite
1470	1640	Muzaffarghar	Thal	39.77	24.36	11.06	0.29	0.23	24.65				100.36	Clinozoisite	Epidote
1470	1643	Muzaffarghar	Thal	38.89	23.22	13.06	0.28	0.23	23.55				99.23	Clinozoisite	Epidote
1470	1722	Muzaffarghar	Thal	38.42	24.91	8.98	0.27	0.30	23.82				96.70	Clinozoisite	Epidote
1470	1730	Muzaffarghar	Thal	39.94	28.87	3.28	0.12	0.09	24.80				97.10	Clinozoisite	Clinozoisite
1470	1764	Muzaffarghar	Thal	39.39	25.77	8.75	0.31	0.28	23.94				98.44	Clinozoisite	Epidote
1470	1791	Muzaffarghar	Thal	39.91	24.93	8.94	0.33	0.34	23.17				97.62	Clinozoisite	Clinozoisite
1470	1875	Muzaffarghar	Thal	38.84	24.35	9.99	0.22	0.43	23.67				97.50	Clinozoisite	Epidote
1470	1925	Muzaffarghar	Thal	38.67	24.60	10.98	0.33	0.36	23.12				98.06	Clinozoisite	Epidote
1470	1970	Muzaffarghar	Thal	39.33	21.38	15.07	0.20	0.48	23.59				100.05	Clinozoisite	Epidote
1470	1989	Muzaffarghar	Thal	40.53	30.13	3.26	0.18	0.46	23.78				98.34	Clinozoisite	Clinozoisite
1470	1992	Muzaffarghar	Thal	38.91	22.01	13.36	0.43	0.14	23.33				98.18	Clinozoisite	Clinozoisite
1470	2041	Muzaffarghar	Thal	38.65	21.66	15.12	0.24	0.29	22.84				98.80	Clinozoisite	Epidote
1470	2047	Muzaffarghar	Thal	39.23	22.77	11.59	0.31	0.00	23.35				97.25	Clinozoisite	Clinozoisite
1470	2053	Muzaffarghar	Thal	39.11	24.29	10.19	0.43	0.23	23.32				97.57	Clinozoisite	Clinozoisite
1470	2067	Muzaffarghar	Thal	39.73	23.32	12.26	0.16	0.28	22.85				98.60	Clinozoisite	Clinozoisite
1470	2076	Muzaffarghar	Thal	39.00	22.65	14.40	0.40	0.39	23.15				99.99	Clinozoisite	Epidote
1470	2107	Muzaffarghar	Thal	39.27	24.94	10.32	0.26	0.26	23.14				98.19	Clinozoisite	Clinozoisite
1470	2135	Muzaffarghar	Thal	39.99	24.65	10.97	0.43	0.12	24.14				100.30	Clinozoisite	Clinozoisite
1470	2142	Muzaffarghar	Thal	41.01	30.58	0.56	0.18	0.12	25.14				97.59	Clinozoisite	Clinozoisite
1470	2186	Muzaffarghar	Thal	38.91	22.69	12.11	0.20	0.46	23.23				97.60	Clinozoisite	Clinozoisite
1470	2233	Muzaffarghar	Thal	39.74	28.40	4.72	0.28	0.49	24.89				98.52	Clinozoisite	Clinozoisite
1470	2254	Muzaffarghar	Thal	39.98	23.59	11.17	0.17	0.33	23.38				98.62	Clinozoisite	Clinozoisite
1470	2280	Muzaffarghar	Thal	39.47	24.34	11.28	0.32	0.66	23.64				99.71	Clinozoisite	Epidote
1470	2348	Muzaffarghar	Thal	39.44	22.87	11.87	0.38	0.24	23.33				98.13	Clinozoisite	Clinozoisite
1470	2375	Muzaffarghar	Thal	38.02	20.89	16.07	0.42	0.28	23.61				99.29	Clinozoisite	Epidote
1470	2380	Muzaffarghar	Thal	39.35	24.91	9.68	0.26	0.27	24.03				98.50	Clinozoisite	Clinozoisite
1470	2416	Muzaffarghar	Thal	39.28	25.64	8.56	0.27	0.43	23.89				98.07	Clinozoisite	Epidote
1470	2454	Muzaffarghar	Thal	38.75	22.58	14.23	0.25	0.52	23.29				99.62	Clinozoisite	Epidote
1470	2510	Muzaffarghar	Thal	39.19	19.48	15.56	0.00	0.26	23.20				97.69	Clinozoisite	Epidote
1470	2537	Muzaffarghar	Thal	54.02	2.43	16.14	0.48	14.16	12.16				99.39	Clinozoisite	Epidote
1470	101	Muzaffarghar	Thal	43.71	12.37	20.31	0.34	9.66	10.63				97.02	Clinozoisite	Epidote
1470	2121	Muzaffarghar	Thal	38.09	21.07	14.56	0.17	0.25	22.84				96.98	Clinozoisite	Epidote
1470	2614	Muzaffarghar	Thal	39.31	22.25	13.55	0.13	0.45	22.97				98.66	Clinozoisite	Epidote
1470	2706	Muzaffarghar	Thal	39.80	25.76	9.74	0.10	0.36	22.70				98.46	Clinozoisite	Clinozoisite
1470	2770	Muzaffarghar	Thal	37.84	22.32	12.37	0.15	0.18	23.60				96.46	Clinozoisite	Epidote
1470	2771	Muzaffarghar	Thal	45.75	26.09	3.56	0.07	0.30	22.04				97.81	Clinozoisite	Clinozoisite
1470	2808	Muzaffarghar	Thal	39.47	29.56	3.20	0.20	0.31	23.84				96.58	Clinozoisite	Clinozoisite
1470	3048	Muzaffarghar	Thal	39.56	24.95	10.74	0.20	0.08	23.44				98.97	Clinozoisite	Clinozoisite
1470	3055	Muzaffarghar	Thal	39.50	26.35	9.51	0.11	0.13	23.44				99.04	Clinozoisite	Epidote
1470	3064	Muzaffarghar	Thal	38.68	23.48	11.30	0.06	0.20	23.41				97.13	Clinozoisite	Clinozoisite
1470	3071	Muzaffarghar	Thal	38.64	23.37	12.65	0.13	0.39	22.64				97.82	Clinozoisite	Epidote
1470	3249	Muzaffarghar	Thal	38.54	24.94	10.03	0.11	0.20	22.82				96.64	Clinozoisite	Epidote
1470	3251	Muzaffarghar	Thal	40.08	25.55	9.74	0.14	0.28	23.47				99.26	Clinozoisite	Clinozoisite
1470	3364	Muzaffarghar	Thal	38.95	23.97	12.16	0.18	0.27	22.40				97.93	Clinozoisite	Clinozoisite
1470	3640	Muzaffarghar	Thal	38.21	22.45	13.53	0.20	0.25	22.67				97.31	Clinozoisite	Epidote
1470	3713	Muzaffarghar	Thal	37.40	21.39	14.78	0.18	0.18	22.85				96.78	Clinozoisite	Epidote
1470	3919	Muzaffarghar	Thal	39.64	26.81	7.99	0.18	0.17	24.35				99.14	Clinozoisite	Epidote
1470	3974	Muzaffarghar	Thal	40.31	30.99	2.74	0.07	0.27	24.59				98.97	Clinozoisite	Clinozoisite
1470	4007	Muzaffarghar	Thal	46.24	8.45	19.29	0.15	9.84	11.67				95.64	Clinozoisite	Clinozoisite
1470	4152	Muzaffarghar	Thal	39.70	23.48	12.13	0.20	0.10	23.29				98.90	Clinozoisite	Clinozoisite
1470	4193	Muzaffarghar	Thal	39.43	22.65	13.38	0.22	0.00	22.75				98.43	Clinozoisite	Epidote
1470	4194	Muzaffarghar	Thal	39.06	23.84	13.81	0.27	0.40	21.90				99.28	Clinozoisite	Epidote
1470	4325	Muzaffarghar	Thal	39.17	24.38	11.75	0.21	0.23	23.21				98.95	Clinozoisite	Epidote
1470	4327	Muzaffarghar	Thal	39.85	26.79	8.52	0.12	0.35	22.64				98.27	Clinozoisite	Clinozoisite
1470	4339	Muzaffarghar	Thal	39.81	24.77	9.70	0.12	0.00	22.55				96.95	Clinozoisite	Clinozoisite
1470	4512	Muzaffarghar	Thal	39.23	25.24	10.70	0.21	0.39	23.18				98.95	Clinozoisite	Epidote
1470	4538	Muzaffarghar	Thal	39.22	28.77	5.64	0.00	0.52	23.03				97.18	Clinozoisite	Clinozoisite
1470	4795	Muzaffarghar	Thal	40.70	27.08	7.39	0.17	0.00	22.88				98.22	Clinozoisite	Clinozoisite
1470	4887	Muzaffarghar	Thal	40.63	27.99	6.04	0.14	0.42	23.67				98.89	Clinozoisite	Clinozoisite
1470	5433	Muzaffarghar	Thal	39.32	23.07	12.45	0.09	0.21	23.06				98.20	Clinozoisite	Clinozoisite
1470	5641	Muzaffarghar	Thal	39.64	25.05	11.02	0.12	0.28	22.64				98.75	Clinozoisite	Clinozoisite
1470	5726	Muzaffarghar	Thal	39.29	25.38	9.72	0.11	0.26	24.25				99.01	Clinozoisite	Epidote
1470	5833	Muzaffarghar	Thal	39.66	26.71	7.47	0.09	0.27	23.88				98.08	Clinozoisite	Clinozoisite
1470	5920	Muzaffarghar	Thal	39.88	31.92	1.28	0.13	0.30	24.94				98.45	Clinozoisite	Clinozoisite
1470	5994	Muzaffarghar	Thal	40.27	27.88	5.59	0.08	0.27	24.36				98.45	Clinozoisite	Clinozoisite
1470	6263	Muzaffarghar	Thal	40.67	27.88	6.24	0.17	0.30	23.15				98.41	Clinozoisite	Clinozoisite

Sample	Points	River/Dune	Domain	SiO_2	Al_2O_3	FeO	MnO	MgO	CaO	La_2O_3	Ce_2O_3	Nd_2O_3	Total	Subgroup	Name
				wt%	wt%	wt%	wt%	wt%	wt%	wt%	wt%	wt%			
1474	2	Munda	Thal	39.46	30.87	3.54	0.39	0.35	22.85				97.46	Clinozoisite	Clinozoisite
1474	3	Munda	Thal	38.85	26.24	9.60	0.43	0.22	22.67				98.01	Clinozoisite	Epidote
1474	6	Munda	Thal	37.68	21.98	11.52	0.33	0.00	21.74				93.25	Clinozoisite	Clinozoisite
1474	13	Munda	Thal	39.68	24.53	11.27	0.24	0.17	22.69				98.58	Clinozoisite	Clinozoisite
1474	18	Munda	Thal	38.12	25.26	9.95	0.31	0.32	22.53				96.49	Clinozoisite	Epidote
1474	19	Munda	Thal	39.90	24.24	12.57	0.40	0.15	22.83				100.09	Clinozoisite	Clinozoisite
1474	106	Munda	Thal	37.88	26.06	9.98	0.52	0.34	23.21				97.99	Clinozoisite	Epidote
1474	107	Munda	Thal	39.97	27.06	8.83	0.41	0.58	22.92				99.77	Clinozoisite	Epidote
1474	111	Munda	Thal	40.62	33.19	1.11	0.25	0.40	24.44				100.01	Clinozoisite	Clinozoisite
1474	121	Munda	Thal	38.54	27.60	7.64	0.26	0.12	23.06				97.22	Clinozoisite	Clinozoisite
1474	128	Munda	Thal	39.12	27.61	7.78	0.33	0.43	22.57				97.84	Clinozoisite	Clinozoisite
1474	131	Munda	Thal	38.10	25.15	10.84	0.17	0.36	22.45				97.07	Clinozoisite	Epidote
1474	133	Munda	Thal	54.45	2.22	8.90	0.47	18.09	12.78				96.91	Clinozoisite	Epidote
1474	145	Munda	Thal	38.95	28.92	5.92	0.32	0.16	23.38				97.65	Clinozoisite	Clinozoisite
1474	152	Munda	Thal	39.25	26.98	7.39	0.43	0.00	22.78				96.83	Clinozoisite	Clinozoisite
1474	154	Munda	Thal	39.28	27.10	7.70	0.23	0.32	22.48				97.11	Clinozoisite	Clinozoisite
1474	165	Munda	Thal	37.82	20.66	14.93	0.29	0.17	21.54				95.41	Clinozoisite	Epidote
1474	180	Munda	Thal	38.46	23.54	11.92	0.33	0.17	22.93				97.35	Clinozoisite	Epidote
1474	181	Munda	Thal	40.18	27.24	8.55	0.39	0.33	22.72				99.41	Clinozoisite	Clinozoisite
1474	185	Munda	Thal	38.56	25.97	10.39	0.47	0.27	21.72				97.38	Clinozoisite	Epidote
1474	189	Munda	Thal	44.88	27.09	5.56	0.18	0.25	19.32				97.28	Clinozoisite	Clinozoisite
1474	196	Munda	Thal	37.50	26.67	8.56	0.29	0.37	21.84				95.23	Clinozoisite	Clinozoisite
1474	209	Munda	Thal	39.39	29.45	5.08	0.24	0.00	23.35				97.51	Clinozoisite	Clinozoisite
1474	226	Munda	Thal	37.88	24.99	11.43	0.26	0.00	22.71				97.27	Clinozoisite	Epidote
1474	253	Munda	Thal	40.94	33.57	1.05	0.27	0.40	23.41				99.64	Clinozoisite	Clinozoisite
1474	266	Munda	Thal	37.66	24.29	11.27	0.24	0.12	23.62				97.20	Clinozoisite	Epidote
1474	268	Munda	Thal	39.22	23.46	11.89	0.38	0.34	22.53				97.82	Clinozoisite	Clinozoisite
1474	272	Munda	Thal	38.89	22.84	11.63	0.33	0.42	23.16				97.27	Clinozoisite	Clinozoisite
1474	483	Munda	Thal	38.75	26.21	9.14	0.31	0.17	23.31				97.89	Clinozoisite	Epidote
1474	497	Munda	Thal	40.09	31.04	2.94	0.17	0.29	23.02				97.55	Clinozoisite	Clinozoisite
1474	499	Munda	Thal	40.36	30.58	3.33	0.20	0.25	22.66				97.38	Clinozoisite	Clinozoisite
1474	500	Munda	Thal	38.81	23.90	11.10	0.26	0.00	22.19				96.26	Clinozoisite	Clinozoisite
1474	517	Munda	Thal	38.59	24.22	11.06	0.21	0.33	22.62				97.03	Clinozoisite	Epidote
1474	520	Munda	Thal	39.48	25.03	11.09	0.32	0.18	22.55				98.65	Clinozoisite	Clinozoisite
1474	530	Munda	Thal	39.08	28.44	6.83	0.21	0.18	22.45				97.19	Clinozoisite	Clinozoisite
1474	531	Munda	Thal	40.31	25.84	9.60	0.30	0.14	23.23				99.42	Clinozoisite	Clinozoisite
1474	535	Munda	Thal	37.50	24.29	5.70	0.21	2.48	22.25				92.43	Clinozoisite	Epidote
1474	539	Munda	Thal	38.49	24.38	10.73	0.18	0.24	23.02				97.04	Clinozoisite	Epidote
1474	562	Munda	Thal	38.05	24.48	10.88	0.20	0.30	23.07				96.98	Clinozoisite	Epidote
1474	563	Munda	Thal	40.31	27.96	6.69	0.18	0.00	22.72				97.86	Clinozoisite	Clinozoisite
1474	572	Munda	Thal	40.13	27.47	7.89	0.39	0.22	22.80				98.90	Clinozoisite	Clinozoisite
1474	585	Munda	Thal	40.19	25.11	10.06	0.20	0.53	23.47				99.56	Clinozoisite	Clinozoisite
1474	587	Munda	Thal	38.26	27.14	8.39	0.38	0.29	22.42				96.88	Clinozoisite	Clinozoisite
1474	596	Munda	Thal	38.60	23.18	11.78	0.24	0.34	23.08				97.22	Clinozoisite	Clinozoisite
1474	613	Munda	Thal	38.89	27.65	6.80	0.18	0.22	22.86				96.60	Clinozoisite	Clinozoisite
1474	627	Munda	Thal	38.43	23.40	11.53	0.51	0.31	23.01				97.19	Clinozoisite	Epidote
1474	884	Munda	Thal	40.15	29.24	5.34	0.29	0.33	23.56				98.91	Clinozoisite	Clinozoisite
1474	885	Munda	Thal	54.53	2.24	13.42	0.41	15.54	12.17				98.31	Clinozoisite	Clinozoisite
1474	913	Munda	Thal	38.57	25.21	10.25	0.44	0.32	22.01				96.80	Clinozoisite	Epidote
1474	914	Munda	Thal	38.06	24.17	10.68	0.31	0.51	22.79				96.52	Clinozoisite	Epidote
1474	916	Munda	Thal	39.34	23.32	12.27	0.43	0.14	22.86				98.36	Clinozoisite	Clinozoisite
1474	917	Munda	Thal	38.30	22.52	12.91	0.25	0.20	22.69				96.87	Clinozoisite	Epidote
1474	923	Munda	Thal	38.92	23.86	11.80	0.44	0.49	22.08				97.59	Clinozoisite	Clinozoisite
1474	931	Munda	Thal	38.71	28.44	7.91	0.46	0.53	22.62				98.67	Clinozoisite	Clinozoisite
1474	933	Munda	Thal	36.85	24.04	11.14	0.27	0.23	22.28				94.81	Clinozoisite	Epidote
1474	942	Munda	Thal	37.52	24.91	10.84	0.23	0.22	22.61				96.33	Clinozoisite	Epidote
1474	947	Munda	Thal	38.10	22.32	13.37	0.32	0.12	22.44				96.67	Clinozoisite	Epidote
1474	963	Munda	Thal	39.00	24.99	10.67	0.30	0.20	22.73				97.89	Clinozoisite	Clinozoisite
1474	969	Munda	Thal	40.23	25.97	9.22	0.20	0.26	22.85				98.73	Clinozoisite	Clinozoisite
1474	972	Munda	Thal	38.63	23.98	11.30	0.28	0.31	22.03				96.53	Clinozoisite	Clinozoisite
1474	981	Munda	Thal	38.00	24.64	10.07	0.21	0.26	22.13				95.31	Clinozoisite	Epidote
1474	986	Munda	Thal	39.02	23.11	12.31	0.37	0.21	22.67				97.69	Clinozoisite	Clinozoisite
1474	988	Munda	Thal	39.71	32.39	1.54	0.14	0.09	23.31				97.18	Clinozoisite	Clinozoisite
1474	994	Munda	Thal	39.85	23.09	12.12	0.24	0.41	22.27				97.98	Clinozoisite	Epidote
1474	1001	Munda	Thal	37.07	24.56	10.56	0.36	0.00	22.66				95.21	Clinozoisite	Epidote
1474	1006	Munda	Thal	38.35	24.55	10.73	0.45	0.40	22.14				96.62	Clinozoisite	Epidote
1474	1010	Munda	Thal	39.52	24.78	11.80	0.47	0.31	22.83				99.71	Clinozoisite	Epidote
1474	1015	Munda	Thal	39.55	26.15	9.46	0.35	0.15	22.11				97.77	Clinozoisite	Clinozoisite
1474	1019	Munda	Thal	39.35	32.04	3.56	0.26	0.35	23.70				99.26	Clinozoisite	Clinozoisite
1474	1028	Munda	Thal	39.14	30.61	2.99	0.39	0.26	23.98				97.37	Clinozoisite	Clinozoisite
1474	1036	Munda	Thal	39.78	24.18	11.40	0.49	0.22	22.55				98.62	Clinozoisite	Clinozoisite
1474	1043	Munda	Thal	38.94	26.81	8.35	0.32	0.29	22.95				97.66	Clinozoisite	Epidote
1474	1089	Munda	Thal	40.14	23.44	13.17	0.20	0.16	22.56				99.67	Clinozoisite	Epidote
1474	1093	Munda	Thal	38.06	23.72	11.92	0.41	0.19	21.91				96.21	Clinozoisite	Epidote
1474	1343	Munda	Thal	41.59	28.49	7.46	0.29	0.49	22.55				100.87	Clinozoisite	Clinozoisite
1474	1367	Munda	Thal	39.21	25.36	10.41	0.43	0.32	22.13				97.86	Clinozoisite	Clinozoisite
1474	1395	Munda	Thal	39.13	25.00	10.30	0.25	0.58	22.69				97.95	Clinozoisite	Clinozoisite
1474	1399	Munda	Thal	38.73	26.15	8.98	0.23	0.61	22.54				97.24	Clinozoisite	Epidote
1474	1409	Munda	Thal	39.97	31.85	1.71	0.19	0.30	23.78				97.80	Clinozoisite	Clinozoisite
1474	1418	Munda	Thal	39.35	26.34	8.26	0.10	0.67	22.06				96.78	Clinozoisite	Clinozoisite
1474	1422	Munda	Thal	39.52	29.78	5.07	0.20	0.35	23.36				98.28	Clinozoisite	Clinozoisite
1474	1435	Munda	Thal	38.83	27.94	6.91	0.27	0.54	23.42				97.91	Clinozoisite	Clinozoisite
1474	1442	Munda	Thal	39.38	26.83	8.30	0.26	0.29	23.03				98.09	Clinozoisite	Clinozoisite
1474	1445	Munda	Thal	39.05	24.71	11.48	0.39	0.26	23.07				98.96	Clinozoisite	Epidote
1474	1451	Munda	Thal	39.60	31.56	3.85	0.29	0.42	23.67				99.39	Clinozoisite	Clinozoisite
1474	1460	Munda	Thal	38.77	25.74	9.78	0.16	0.23	22.68				97.36	Clinozoisite	Epidote
1474	1478	Munda	Thal	39.31	28.09	6.73	0.19	0.26	23.35				97.93	Clinozoisite	Clinozoisite
1474	1494	Munda	Thal	39.14	28.80	5.61	0.50	0.39	22.01				96.45	Clinozoisite	Clinozoisite
1474	1497	Munda	Thal	39.84	26.17	9.93	0.52	0.30	22.21				98.97	Clinozoisite	Clinozoisite
1474	1499	Munda	Thal	38.77	23.92	12.19	0.33	0.14	22.53				97.88	Clinozoisite	Epidote
1474	1500	Munda	Thal	38.15	20.86	14.44	0.35	0.64	22.22				96.66	Clinozoisite	Epidote
1474	1502	Munda	Thal	38.93	24.84	9.63	0.40	0.00	23.15				96.95	Clinozoisite	Clinozoisite
1474	1519	Munda	Thal	39.97	28.89	6.08	0.12	0.31	22.91				98.28	Clinozoisite	Clinozoisite
1474	1926	Munda	Thal	38.91	25.44	10.48	0.27	0.27	22.79				98.16	Clinozoisite	Epidote
1474	1939	Munda	Thal	37.90	23.23	12.48	0.11	0.34	22.67				96.73	Clinozoisite	Epidote
1474	1940	Munda	Thal	37.19	24.05	10.07	0.22	0.00	21.81				93.34	Clinozoisite	Clinozoisite
1474	1950	Munda	Thal	38.52	27.28	8.09	0.44	0.23	22.69				97.25	Clinozoisite	Clinozoisite
1474	1963	Munda	Thal	40.31	31.46	3.17	0.14	0.41	22.88				98.37	Clinozoisite	Clinozoisite
1474	1965	Munda	Thal	39.14	27.16	7.18	0.32	0.47	22.86				97.13	Clinozoisite	Clinozoisite
1474	1995	Munda	Thal	39.11	29.07	5.60	0.30	0.44	23.01				97.53	Clinozoisite	Clinozoisite

Appendix Table B6 SEM-EDS data and chemical calculations in pyroxene of Thal Desert and Upper Indus tributaries.

Sample	Points	River/Dune	Domain	SiO_2	TiO_2	Al_2O_3	FeO	MnO	MgO	CaO	K_2O	Na_2O	Total	Mg#	En	Fs	Wo	En/Fs	Name
				wt%	wt%	wt%	wt%	wt%	wt%	wt%	wt%	wt%							
1749	6-1	Hushe	Karakorum	53.63	0.45	1.60	7.22	0.32	14.86	22.56	0.35	1.13	102.12	91	42	12	46	3.5	ferrian diopside
1749	42-1	Hushe	Karakorum	42.97	1.23	10.81	18.24	0.38	9.64	11.82	1.77	1.17	98.03	66	34	37	30	0.9	aluminian ferrian subsilicic augite
1749	78-1	Hushe	Karakorum	53.80	0.29	1.55	4.91	0.29	15.48	23.73	0.13	0.32	100.50	86	44	8	48	5.3	diopside
1749	113-1	Hushe	Karakorum	42.94	0.41	10.18	18.07	0.45	9.55	10.60	1.08	1.25	94.54	60	35	38	28	0.9	aluminian ferrian subsilicic augite
1749	170-1	Hushe	Karakorum	54.78	0.00	0.64	1.15	0.26	18.65	25.05	0.21	0.38	101.12	100	50	2	48	23.3	diopside
1749	241-1	Hushe	Karakorum	43.38	0.96	12.12	18.55	0.47	8.80	11.48	2.05	1.37	99.17	63	------------------------				aluminian ferrian sodian subsilicic unusual pyroxene
1749	249-1	Hushe	Karakorum	53.31	0.27	0.64	2.14	0.23	18.10	24.25	0.36	0.51	99.81	100	49	4	47	13.4	diopside
1749	293-1	Hushe	Karakorum	54.46	0.36	0.67	2.51	0.28	17.98	23.77	0.24	0.48	100.76	100	49	4	47	11.4	diopside
1749	297-1	Hushe	Karakorum	54.50	0.45	1.24	3.96	0.17	16.43	24.94	0.40	0.53	102.61	98	45	6	49	7.1	ferrian diopside
1749	305-1	Hushe	Karakorum	43.30	0.85	11.96	17.77	0.41	9.33	11.70	1.51	1.30	98.11	63	33	37	30	0.9	aluminian ferrian subsilicic augite
1749	350-1	Hushe	Karakorum	54.15	0.27	0.43	4.28	0.39	15.90	24.34	0.19	0.11	100.07	88	44	7	49	6.1	diopside
1749	420-1	Hushe	Karakorum	54.16	0.33	0.57	3.52	0.35	16.54	22.91	0.20	0.38	98.97	89	47	6	47	7.6	diopside
1749	427-1	Hushe	Karakorum	52.09	0.48	0.64	13.42	0.52	9.35	22.32	0.22	0.45	99.48	55	28	24	48	1.2	diopside
1749	448-1	Hushe	Karakorum	52.76	0.16	0.71	3.13	0.18	17.51	23.97	0.10	0.65	99.16	100	48	5	47	9.3	diopside
1749	473-1	Hushe	Karakorum	54.19	0.23	0.86	6.08	0.29	14.77	23.18	0.23	0.76	100.59	86	42	10	48	4.1	diopside
1749	511-1	Hushe	Karakorum	54.93	0.24	0.75	2.50	0.23	17.75	24.51	0.19	0.46	101.57	100	48	4	48	11.5	diopside
1749	581-1	Hushe	Karakorum	52.64	0.35	1.06	8.50	0.52	13.16	22.75	0.23	0.53	99.74	77	38	15	47	2.6	diopside
1749	617-1	Hushe	Karakorum	54.44	0.30	1.40	1.83	0.24	17.78	24.27	0.26	0.56	101.08	100	49	3	48	15.2	diopside
1749	649-1	Hushe	Karakorum	54.08	0.24	0.83	7.30	0.46	13.92	21.75	0.21	0.78	99.56	77	41	13	46	3.2	diopside
1749	12-2	Hushe	Karakorum	53.28	0.32	0.93	7.70	0.17	14.35	24.20	0.27	0.34	101.57	84	40	12	48	3.2	diopside
1749	72-2	Hushe	Karakorum	52.63	0.42	0.88	10.99	0.37	11.18	23.83	0.31	0.36	100.97	67	32	18	49	1.8	diopside
1749	87-2	Hushe	Karakorum	54.65	0.50	0.60	1.49	0.31	18.90	25.23	0.21	0.14	102.04	100	50	3	48	18.5	diopside
1749	236-2	Hushe	Karakorum	53.30	0.57	1.14	7.96	0.31	14.33	23.48	0.27	0.55	101.90	84	40	13	47	3.1	diopside
1749	274-2	Hushe	Karakorum	55.37	0.43	0.00	1.03	0.32	19.71	24.73	0.26	0.18	102.03	100	52	2	46	25.8	diopside
1749	289-2	Hushe	Karakorum	55.26	0.22	0.71	1.61	0.12	18.92	24.16	0.16	0.34	101.51	100	51	3	47	19.4	diopside
1749	331-2	Hushe	Karakorum	54.16	0.25	0.34	3.21	0.28	16.93	25.00	0.14	0.53	100.83	100	46	5	49	8.6	diopside
1749	349-2	Hushe	Karakorum	44.12	1.20	10.94	17.15	0.54	10.10	11.70	1.50	1.17	98.42	64	36	35	30	1.0	aluminian ferrian subsilicic augite
1749	368-2	Hushe	Karakorum	54.94	0.00	0.65	3.01	0.00	16.98	24.71	0.14	0.17	100.60	92	47	5	49	10.1	diopside
1749	396-2	Hushe	Karakorum	53.39	0.49	0.42	5.39	0.28	15.35	24.75	0.30	0.68	101.05	97	42	9	49	4.8	ferrian wollastonite
1749	412-2	Hushe	Karakorum	42.62	1.02	10.30	17.44	0.42	10.12	11.86	1.74	1.40	96.90	74	------------------------				aluminian ferrian sodian subsilicic unusual pyroxene
1749	424-2	Hushe	Karakorum	55.26	0.47	0.31	1.87	0.35	18.90	24.38	0.21	0.43	102.18	100	50	3	47	15.0	diopside
1749	452-2	Hushe	Karakorum	43.20	1.25	9.94	15.63	0.33	10.57	11.69	1.64	1.27	95.52	71	38	32	30	1.2	aluminian ferrian subsilicic augite
1749	496-2	Hushe	Karakorum	41.80	1.08	10.98	15.69	0.45	9.58	10.45	1.55	1.34	92.93	65	37	35	29	1.1	aluminian ferrian sodian subsilicic augite
1749	538-2	Hushe	Karakorum	52.51	0.20	0.64	4.03	0.35	16.22	23.04	0.18	0.32	97.49	93	46	7	47	6.6	diopside
1749	549-2	Hushe	Karakorum	53.43	0.27	0.73	8.53	0.30	13.23	21.41	0.14	1.06	99.10	76	39	15	46	2.7	diopside
1749	602-2	Hushe	Karakorum	52.54	0.44	0.39	11.21	0.18	11.74	23.52	0.19	0.55	100.76	70	34	18	48	1.8	diopside
1749	657-2	Hushe	Karakorum	54.37	0.42	0.75	2.79	0.33	17.30	24.69	0.25	0.53	101.45	100	47	5	48	9.8	diopside
1749	659-2	Hushe	Karakorum	43.70	1.29	9.26	17.32	0.67	10.39	11.29	1.63	1.89	97.43	75	36	35	28	1.0	aluminian ferrian sodian subsilicic augite
1749	666-2	Hushe	Karakorum	54.15	0.10	0.56	3.15	0.20	17.20	24.64	0.25	0.00	100.26	95	47	5	48	9.1	diopside
1749	716-2	Hushe	Karakorum	55.30	0.13	1.29	2.24	0.17	17.77	23.80	0.09	0.95	101.74	100	49	4	47	13.0	diopside
1749	735-2	Hushe	Karakorum	43.69	0.95	10.18	17.22	0.41	10.51	11.40	1.78	1.47	97.61	73	37	35	29	1.1	aluminian ferrian sodian subsilicic augite
1749	763-2	Hushe	Karakorum	41.78	1.15	11.90	18.97	0.38	8.01	12.27	1.72	0.97	97.16	57	------------------------				aluminian ferrian subsilicic unusual pyroxene
1749	764-2	Hushe	Karakorum	42.44	0.89	12.27	18.37	0.53	9.32	11.39	1.67	1.49	98.38	68	------------------------				aluminian ferrian sodian subsilicic unusual pyroxene
1749	842-2	Hushe	Karakorum	53.96	0.39	0.26	2.41	0.35	18.23	24.45	0.35	0.20	100.60	100	49	4	47	11.7	diopside
1749	843-2	Hushe	Karakorum	42.35	0.75	11.94	17.13	0.47	9.48	11.60	1.36	0.94	96.01	62	34	36	30	1.0	aluminian ferrian subsilicic augite
1749	848-2	Hushe	Karakorum	54.98	0.37	0.30	4.08	0.36	16.27	23.99	0.14	0.26	100.74	88	45	7	48	6.5	diopside
1749	858-2	Hushe	Karakorum	54.98	0.51	0.00	1.34	0.28	18.64	24.70	0.32	0.28	101.05	100	50	2	48	20.4	diopside
1749	924-2	Hushe	Karakorum	54.23	0.43	0.81	2.49	0.37	17.81	24.06	0.39	0.62	101.22	100	48	4	47	11.0	diopside
1749	940-2	Hushe	Karakorum	40.51	0.63	14.42	16.70	0.21	10.24	11.57	0.89	2.18	97.35	86	------------------------				aluminian ferrian sodian subsilicic unusual pyroxene
1749	989-2	Hushe	Karakorum	52.87	0.24	1.23	5.66	0.43	15.28	23.86	0.37	0.22	100.15	90	43	10	48	4.5	diopside
1749	1009-2	Hushe	Karakorum	51.85	0.49	0.36	13.73	0.21	9.42	23.44	0.33	0.23	100.06	56	28	23	49	1.2	diopside
1749	1018-2	Hushe	Karakorum	55.16	0.35	0.26	0.60	0.18	19.20	24.25	0.23	0.22	100.45	100	52	1	47	43.6	diopside
1748	8-1	Braldu	Karakorum	52.42	0.37	0.66	5.52	0.13	13.90	24.13	0.28	0.44	97.84	85	40	9	50	4.4	wollastonite
1748	11-1	Braldu	Karakorum	49.39	1.14	3.57	9.46	0.22	12.13	22.19	0.12	0.72	98.94	78	36	16	48	2.2	aluminian ferrian diopside
1748	29-1	Braldu	Karakorum	47.94	1.16	4.44	8.51	0.23	12.36	22.33	0.31	0.62	97.90	86	37	15	48	2.5	aluminian ferrian diopside
1748	34-1	Braldu	Karakorum	54.02	0.19	0.63	6.20	0.10	13.15	25.12	0.19	0.22	99.81	79	38	10	52	3.7	wollastonite
1748	44-1	Braldu	Karakorum	54.25	0.47	0.58	6.40	0.32	13.62	23.99	0.17	0.84	100.64	81	39	11	50	3.6	diopside
1748	52-1	Braldu	Karakorum	50.26	0.99	2.93	8.37	0.19	12.43	21.92	0.24	0.72	98.04	77	38	15	48	2.6	aluminian diopside
1748	59-1	Braldu	Karakorum	43.17	0.90	11.41	18.88	0.26	8.25	11.23	0.80	1.46	96.38	51	30	40	30	0.8	aluminian ferrian sodian subsilicic augite
1748	73-1	Braldu	Karakorum	50.92	0.27	0.57	11.45	0.27	10.51	23.38	0.16	0.00	97.53	62	31	19	50	1.6	diopside
1748	77-1	Braldu	Karakorum	51.67	0.24	0.85	15.09	0.16	8.29	22.81	0.21	0.73	100.05	52	25	26	49	1.0	hedenbergite
1748	91-1	Braldu	Karakorum	51.70	0.45	0.94	20.65	0.43	5.65	13.88	0.17	4.77	98.63	47	------------------------				aegirine-augite
1748	112-1	Braldu	Karakorum	50.09	1.32	3.91	6.52	0.25	12.85	24.17	0.20	0.42	99.73	84	38	11	51	3.4	aluminian wollastonite
1748	118-1	Braldu	Karakorum	53.60	0.20	0.47	8.89	0.17	11.92	24.65	0.27	0.25	100.43	71	34	15	51	2.3	wollastonite
1748	134-1	Braldu	Karakorum	51.02	0.26	0.61	14.55	0.31	8.99	22.65	0.19	0.14	98.73	52	27	25	48	1.1	diopside
1748	188-1	Braldu	Karakorum	53.54	0.32	0.45	6.69	0.21	13.27	24.06	0.27	0.20	99.03	78	39	11	50	3.4	wollastonite
1748	196-1	Braldu	Karakorum	52.95	0.36	0.26	4.07	0.17	16.18	24.68	0.15	0.31	99.12	96	45	7	49	6.8	diopside
1748	199-1	Braldu	Karakorum	53.62	0.15	0.47	1.72	0.14	16.36	25.26	0.14	0.67	98.52	100	46	3	51	15.6	wollastonite
1748	247-1	Braldu	Karakorum	54.30	0.24	0.39	1.57	0.13	16.75	24.95	0.18	0.31	98.82	96	47	3	50	17.5	wollastonite
1748	252-1	Braldu	Karakorum	53.27	0.36	1.09	8.09	0.30	12.97	22.10	0.15	1.24	99.58	79	39	14	47	2.8	diopside
1748	257-1	Braldu	Karakorum	46.44	1.79	5.90	9.26	0.26	10.26	23.08	0.33	0.76	98.09	80	32	17	52	1.9	aluminian ferrian wollastonite
1748	272-1	Braldu	Karakorum	55.44	0.36	0.00	0.92	0.12	17.32	24.41	0.10	0.10	98.76	97	49	2	49	29.6	diopside
1748	332-1	Braldu	Karakorum	53.88	0.35	0.31	0.89	0.11	16.90	24.20	0.20	0.29	97.13	97	48	2	50	30.1	diopside
1748	337-1	Braldu	Karakorum	51.06	0.55	1.89	7.17	0.17	13.57	21.28	0.18	0.56	96.44	78	41	12	46	3.3	diopside
1748	347-1	Braldu	Karakorum	52.41	0.20	1.20	7.92	0.25	12.09	22.90	0.14	0.39	97.50	73	36	14	50	2.6	diopside
1748	364-1	Braldu	Karakorum	50.53	0.58	2.37	8.27	0.19	11.99	22.92	0.19	0.56	97.58	76	36	14	50	2.5	aluminian diopside
1748	388-1	Braldu	Karakorum	51.69	0.31	0.72	11.51	0.23	10.36	23.59	0.22	0.36	99.01	63	31	19	50	1.6	wollastonite
1748	404-1	Braldu	Karakorum	52.02	0.53	0.40	11.82	0.27	10.33	23.86	0.36	0.39	99.97	64	30	20	50	1.5	wollastonite
1748	406-1	Braldu	Karakorum	55.27	0.31	0.25	3.76	0.18	14.99	24.29	0.23	0.30	99.59	88	43	6	50	6.8	wollastonite
1748	422-1	Braldu	Karakorum	52.88	0.41	0.82	12.36	0.23	10.98	21.82	0.25	0.21	99.97	61	33	21	46	1.6	diopside
1748	423-1	Braldu	Karakorum	50.67	0.38	1.01	18.05	0.13	6.76	22.88	0.11	0.33	100.31	41	20	31	49	0.7	hedenbergite
1748	436-1	Braldu	Karakorum	53.40	0.42	0.53	9.50	0.15	11.61	24.25	0.09	0.19	100.14	69	34	16	51	2.1	wollastonite
1748	445-1	Braldu	Karakorum	54.19	0.24	0.55	1.80	0.16	16.77	25.37	0.26	0.50	99.83	100	46	3	50	15.1	wollastonite
1748	452-1	Braldu	Karakorum	54.79	0.11	0.40	0.93	0.07	16.70	24.71	0.06	0.32	98.10	97	48	2	51	29.7	wollastonite
1748	480-1	Braldu	Karakorum	54.03	0.00	0.92	7.38	0.15	12.27	22.34	0.18	1.51	98.77	77	38	13	49	2.9	sodian diopside
1748	501-1	Braldu	Karakorum	54.33	0.31	2.35	3.65	0.08	15.14	22.62	0.36	1.60	100.44	98	45	6	49	7.2	sodian diopside
1748	510-1	Braldu	Karakorum	51.51	0.41	0.44	14.57	0.15	8.52	23.45	0.26	0.50	99.81	53	25	25	50	1.0	wollastonite
1748	536-1	Braldu	Karakorum	48.59	1.45	3.81	6.76	0.10	13.25	21.82	0.20	0.64	96.62	85	40	12	48	3.4	aluminian diopside
1748	553-1	Braldu	Karakorum	53.04	0.45	0.71	3.91	0.24	15.06	23.16	0.00	0.25	96.82	87	44	7	49	6.5	diopside
1748	560-1	Braldu	Karakorum	50.43	1.04	3.84	7.28	0.19	12.36	24.23	0.30	0.56	100.22	83	36	12	51	2.9	aluminian wollastonite
1748	572-1	Braldu	Karakorum	50.96	0.86	2.15	9.77	0.25	11.58	23.08	0.23	0.61	99.49	73	34	17	49	2.1	diopside
1748	587-1	Braldu	Karakorum	54.15	0.35	0.36	0.62	0.11	17.54	25.34	0.20	0.28	98.95	100	49	1	50	42.6	wollastonite
1748	606-1	Braldu	Karakorum	53.25	0.52	1.32	8.83	0.26	12.03	23.52	0.14	0.44	100.31	71	35	15	50	2.4	diopside
1748	612-1	Braldu	Karakorum	54.20	0.00	0.44	0.74	0.04	17.08	24.08	0.00	0.36	96.94	98	49	1	50	39.0	diopside
1748	640-1	Braldu	Karakorum	51.61	0.30	0.81	13.31	0.19	9.92	23.52	0.27	0.11	100.04	58	29	22	49	1.3	diopside
1748	643-1	Braldu	Karakorum	55.61	0.29	0.42	0.58	0.12	17.03	24.70	0.20	0.22	99.19	98	48	1	50	43.3	wollastonite
1748	651-1	Braldu	Karakorum	46.60	1.12	7.17	3.65	0.17	13.42	25.28	0.26	0.32	97.97	100	40	6	54	6.2	aluminian ferrian subsilicic wollastonite
1748	669-1	Braldu	Karakorum	51.26	0.44	0.78	15.13	0.23	9.22	22.69	0.16	0.25	100.16	53	27	25	48	1.1	diopside
1748	672-1	Braldu	Karakorum	45.72	1.94	7.14	9.42	0.15	10.07	23.20	0.31	0.28	98.22	74	31	17	52	1.9	aluminian wollastonite
1748	688-1	Braldu	Karakorum	51.26	0.22	0.90	14.59	0.15	9.10	23.62	0.22	0.37	100.44	57	26	24	49	1.1	diopside
1748	702-1	Braldu	Karakorum	54.11	0.52	0.67	6.36	0.24	14.78	23.06	0.19	0.43	100.36	81	42	11	47	4.0	diopside
1748	708-1	Braldu	Karakorum	52.63	0.36	0.60	11.56	0.27	11.29	23.41	0.29	0.27	100.69	65	32	19	48	1.7	diopside
1748	712-1	Braldu	Karakorum	51.79	0.41	0.94	7.27	0.32	12.78	23.89	0.24	0.51	98.15	81	37	12	50	3.0	wollastonite
1748	714-1	Braldu	Karakorum	50.49	0.28	0.96	19.74	0.50	6.46	18.08	0.07	2.91	99.49	50	------------------------				aegirine-augite
1748	719-1	Braldu	Karakorum	46.37	1.73	7.50	9.42	0.20	10.48	23.47	0.20	0.41	99.77	77	32	16	52	1.9	aluminian ferrian subsilicic wollastonite
1748	733-1	Braldu	Karakorum	48.89	0.70	3.69	9.73	0.23	10.96	22.55	0.25	0.82	97.82	77	33	17	49	2.0	aluminian ferrian diopside
1748	734-1	Braldu	Karakorum	45.77	1.19	6.71	10.36	0.16	10.71	22.20	0.19	0.50	97.79	79	33	18	49	1.8	aluminian ferrian diopside
1748	12-2	Braldu	Karakorum	54.02	0.28	0.19	2.17	0.20	16.44	24.26	0.23	0.73	98.53	99	47	4	50	12.4	diopside
1748	32-2	Braldu	Karakorum	46.10	1.47	7.20	8.01	0.19	10.98	22.32	0.07	0.62	96.96	80	35	15	51	2.4	aluminian wollastonite
1748	77-2	Braldu	Karakorum	48.47	1.40	5.91	8.38	0.22	11.74	23.00	0.33	0.76	100.22	84	35	15	50	2.4	aluminian ferrian diopside
1748	91-2	Braldu	Karakorum	54.38	0.33	0.33	1.02	0.11	16.90	24.80	0.19	0.28	98.34	97	48	2	50	26.6	wollastonite
1748	106-2	Braldu	Karakorum	55.14	0.36	0.83	2.17	0.12	16.22	24.20	0.22	0.39	99.67	93	46	4	50	12.6	diopside
1748	122-2	Braldu	Karakorum	51.73	0.42	0.88	12.05	0.36	10.26	21.75	0.28	0.46	98.19	60	31	21	48	1.5	diopside
1748	123-2	Braldu	Karakorum	55.39	0.00	1.13	0.73	0.05	16.68	25.16	0.15	0.74	100.02	99	47	1	51	38.1	wollastonite
1748	129-2	Braldu	Karakorum	50.77	0.62	1.79	7.86	0.22	12.68	23.78	0.40	0.60	98.72	85	37	13	50	2.8	ferrian wollastonite
1748	133-2	Braldu	Karakorum	54.85	0.37	0.78	1.15	0.13	17.19	25.19	0.39	0.52	100.58	100	48	2	50	23.8	wollastonite
1748	134-2	Braldu	Karakorum	55.39	0.24	0.35	1.10	0.05	16.51	25.31	0.32	0.25	99.52	96	47	2	51	25.6	wollastonite
1748	138-2	Braldu	Karakorum	53.15	0.28	1.36	7.57	0.21	12.97	24.85	0.10	0.26	100.74	76	37	12	51	3.0	wollastonite
1748	144-2	Braldu	Karakorum	54.65	0.35	0.33	1.33	0.15	16.88	25.47	0.10	0.34	99.61	97	47	2	51	20.3	wollastonite
1748	185-2	Braldu	Karakorum	44.75	1.81	7.45	8.92	0.20	10.79	22.64	0.09	0.52	97.19	83	34	16	51	2.1	aluminian ferrian subsilicic wollastonite
1748	188-2	Braldu	Karakorum	52.95	0.25	0.55	3.37	0.11	15.59	24.51	0.23	0.61	98.16	98	44	6	50	8.0	wollastonite
1748	189-2	Braldu	Karakorum	52.52	0.36	1.17	11.86	0.33	10.81	22.53	0.34	0.44	100.37	62	32	20	48	1.6	diopside
1748	238-2	Braldu	Karakorum	54.31	0.00	0.61	1.15	0.08	17.55	23.98	0.00	0.24	97.93	96	49	2	49	25.4	diopside
1748	240-2	Braldu	Karakorum	53.37	0.22	0.45	2.56	0.12	16.86	24.17	0.25	0.35	98.35	98	47	4	49	11.2	diopside
1748	305-2	Braldu	Karakorum	53.97	0.31	0.39	0.59	0.08	17.79	23.74	0.26	0.43	97.58	100	50	1	48	47.2	diopside
1748	330-2	Braldu	Karakorum	55.51	0.19	1.28	0.85	0.03	17.36	24.24	0.22	0.65	100.33	97	49	1	49	35.2	diopside
1748	339-2	Braldu	Karakorum	47.26	1.39	5.92	7.82	0.06	12.35	22.22	0.14	0.53	97.71	84	38	14	49	2.8	aluminian ferrian diopside
1748	360-2	Braldu	Karakorum	53.75	0.29	0.59	4.70	0.11	15.25	23.92	0.21	0.43	99.24	87	43	8	49	5.7	diopside
1748	364-2	Braldu	Karakorum	54.58	0.35	0.42	0.56	0.10	17.98	23.71	0.39	0.41	98.50	100	51	1	48	48.4	diopside
1748	386-2	Braldu	Karakorum	53.42	0.42	0.41	8.24	0.24	12.97	20.46	0.30	1.55	98.02	78	40	15	45	2.7	sodian diopside
1748	393-2	Braldu	Karakorum	50.68	0.38	0.26	15.55	0.24	8.23	22.57	0.26	0.15	98.32	49	25	27	49	0.9	hedenbergite
1748	511-2	Braldu	Karakorum	50.95	0.62	0.34	9.10	0.26	12.86	21.91	0.26	0.45	96.75	76	38	16	47	2.4	diopside
1748	512-2	Braldu	Karakorum	53.16	0.37	0.98	3.58	0.15	15.72	22.59	0.38	0.39	97.33	89	46	6	48	7.5	diopside
1748	532-2	Braldu	Karakorum	52.66	0.21	0.89	10.39	0.35	12.00	22.37	0.23	0.42	99.53	68	35	18	47	2.0	diopside
1748	538-2	Braldu	Karakorum	46.38	1.33	6.30	9.29	0.19	11.81	21.99	0.21	0.36	97.86	81	36	16	48	2.2	aluminian ferrian diopside
1748	549-2	Braldu	Karakorum	47.45	1.16	4.60	8.55	0.14	12.41	22.52	0.17	0.80	97.81	90	37	15	48	2.5	aluminian ferrian diopside
1748	554-2	Braldu	Karakorum	52.42	0.42	0.73	9.86	0.30	12.93	22.72	0.27	0.58	100.23	76	37	16	47	2.3	diopside
1748	563-2	Braldu	Karakorum	52.81	0.24	0.58	6.76	0.19	14.08	22.67	0.21	0.36	97.90	79	41	11	48	3.6	diopside
1748	583-2	Braldu	Karakorum	52.00	0.42	0.65	9.68	0.22	12.42	23.33	0.19	0.11	99.01	71	36	16	48	2.2	diopside
1748	596-2	Braldu	Karakorum	52.16	0.63	1.60	7.45	0.22	13.25	23.65	0.39	0.43	99.79	81	38	12	49	3.1	diopside
1748	601-2	Braldu	Karakorum	55.28	0.21	0.94	1.14	0.11	16.97	23.30	0.20	0.55	98.71	96	49	2	49	24.2	diopside
1748	602-2	Braldu	Karakorum	50.46	0.79	3.04	8.67	0.31	12.03	22.67	0.30	0.62	98.90	77	36	15	49	2.4	aluminian diopside
1748	615-2	Braldu	Karakorum	54.37	0.39	0.59	1.32	0.15	17.87	23.62	0.28	0.35	98.93	98	50	2	48	21.6	diopside
1748	649-2	Braldu	Karakorum	51.99	0.40	0.62	8.67	0.19	12.32	21.45	0.31	0.27	96.21	72	38	15	47	2.5	diopside
1748	683-2	Braldu	Karakorum	55.06	0.00	0.26	0.88	0.08	17.78	23.71	0.00	0.36	98.12	97	50	2	48	33.0	diopside
1748	733-2	Braldu	Karakorum	52.53	0.46	0.76	7.78	0.32	13.07	23.32	0.17	0.00	98.41	75	38	13	49	2.9	diopside
1748	747-2	Braldu	Karakorum	53.21	0.36	0.36	2.89	0.15	16.62	23.96	0.15	0.43	98.12	97	47	5	48	9.7	diopside
1748	759-2	Braldu	Karakorum	50.73	0.34	0.26	17.68	0.17	6.64	22.84	0.32	0.13	99.12	40	20	30	50	0.7	hedenbergite
1748	764-2	Braldu	Karakorum	40.91	2.15	11.27	12.88	0.21	7.75	22.90	0.12	0.61	98.79	76	25	23	52	1.1	aluminian ferrian subsilicic wollastonite
1748	771-2	Braldu	Karakorum	46.58	1.52	5.95	10.39	0.18	10.61	21.50	0.37	0.71	97.82	76	33	19	48	1.8	aluminian ferrian diopside
1748	782-2	Braldu	Karakorum	46.40	1.03	5.48	10.34	0.21	10.36	21.30	0.34	0.59	96.05	73	33	19	48	1.8	aluminian ferrian diopside
1748	802-2	Braldu	Karakorum	46.76	1.37	5.99	9.79	0.15	10.35	21.91	0.22	0.58	97.12	72	33	18	50	1.9	aluminian diopside
1748	809-2	Braldu	Karakorum	53.01	0.31	0.95	2.71	0.07	16.16	22.70	0.32	0.40	96.62	91	47	5	48	10.4	diopside

Sample	Points	River/Dune	Domain	SiO_2	TiO_2	Al_2O_3	FeO	MnO	MgO	CaO	K_2O	Na_2O	Total	Mg#	En	Fs	Wo	En/Fs	Name
				wt%	wt%	wt%	wt%	wt%	wt%	wt%	wt%	wt%							
1437	6-1	Upper Hunza	Karakorum	42.53	1.12	11.47	20.29	0.62	8.64	11.16	1.48	2.31	99.63	71	------	------	------		aluminian ferrian sodian subsilicic unusual pyroxene
1437	17-1	Upper Hunza	Karakorum	53.76	0.34	0.83	4.87	0.17	14.24	24.83	0.26	0.56	99.86	87	41	8	51	5.0	wollastonite
1437	20-1	Upper Hunza	Karakorum	52.16	0.26	0.87	10.22	0.61	11.52	22.69	0.18	0.62	99.13	70	34	18	48	1.9	diopside
1437	45-1	Upper Hunza	Karakorum	50.27	0.36	0.91	18.07	0.47	6.39	22.70	0.29	0.14	99.62	39	19	31	49	0.6	hedenbergite
1437	56-1	Upper Hunza	Karakorum	51.81	0.40	0.96	10.90	0.50	12.61	20.35	0.15	0.45	98.13	68	37	19	43	2.0	augite
1437	75-1	Upper Hunza	Karakorum	54.25	0.41	0.78	15.31	0.65	27.28	0.70	0.19	0.37	99.92	79	74	24	1	3.0	(clino)enstatite
1437	120-1	Upper Hunza	Karakorum	52.73	0.28	0.62	12.09	0.73	12.10	22.03	0.19	0.52	101.31	69	34	20	45	1.7	diopside
1437	130-1	Upper Hunza	Karakorum	53.57	0.35	0.69	11.02	0.60	11.87	22.45	0.28	0.64	101.47	68	34	19	47	1.8	diopside
1437	169-1	Upper Hunza	Karakorum	53.13	0.42	0.63	10.88	0.66	11.85	23.12	0.26	0.46	101.41	69	34	19	48	1.8	diopside
1437	199-1	Upper Hunza	Karakorum	43.68	1.40	7.10	25.74	0.46	5.11	10.44	1.29	2.11	97.33	35	19	54	27	0.3	aluminian ferrian sodian augite
1437	201-1	Upper Hunza	Karakorum	44.92	1.22	5.55	31.78	0.61	2.65	9.80	0.89	1.56	98.98	15	10	65	25	0.1	aluminian ferrian sodian augite
1437	204-1	Upper Hunza	Karakorum	53.24	0.64	0.78	9.84	0.63	12.99	22.00	0.19	0.68	100.99	73	37	17	46	2.2	diopside
1437	233-1	Upper Hunza	Karakorum	52.58	0.23	0.45	13.82	0.66	10.52	21.48	0.15	0.62	100.50	59	31	24	45	1.3	diopside
1437	264-1	Upper Hunza	Karakorum	52.89	0.28	0.59	8.06	0.51	12.97	23.65	0.35	0.27	99.59	76	37	14	49	2.7	diopside
1437	270-1	Upper Hunza	Karakorum	52.88	0.30	1.22	13.00	0.54	9.76	23.24	0.19	0.32	101.45	57	29	22	49	1.3	diopside
1437	292-1	Upper Hunza	Karakorum	53.17	0.57	0.42	11.05	0.70	10.95	22.83	0.33	1.01	101.02	69	32	19	48	1.7	diopside
1437	318-1	Upper Hunza	Karakorum	52.72	0.46	0.90	8.50	0.49	14.58	21.92	0.28	0.29	100.15	80	41	14	45	2.9	augite
1437	365-1	Upper Hunza	Karakorum	52.77	0.46	0.91	10.06	0.60	11.88	23.03	0.32	0.00	100.03	68	35	17	48	2.0	diopside
1437	369-1	Upper Hunza	Karakorum	53.08	0.32	1.25	5.61	0.28	14.85	23.00	0.23	0.52	99.14	86	43	10	48	4.5	diopside
1437	385-1	Upper Hunza	Karakorum	52.85	0.13	0.32	9.69	0.75	11.74	23.74	0.00	0.18	99.40	68	34	17	49	2.0	diopside
1437	21-2	Upper Hunza	Karakorum	52.77	0.13	0.59	13.01	0.51	10.73	21.85	0.29	0.37	100.25	60	32	22	46	1.4	diopside
1437	32-2	Upper Hunza	Karakorum	50.86	0.33	0.58	18.81	0.55	5.84	22.33	0.20	0.00	99.48	36	18	33	49	0.5	hedenbergite
1437	47-2	Upper Hunza	Karakorum	53.11	0.28	0.96	10.89	0.27	11.77	23.48	0.19	0.45	101.41	68	34	18	48	1.9	diopside
1437	52-2	Upper Hunza	Karakorum	52.27	0.30	0.61	12.70	0.61	11.22	22.32	0.09	0.58	100.71	65	32	22	46	1.5	diopside
1437	109-2	Upper Hunza	Karakorum	54.31	0.59	1.19	2.80	0.73	15.96	23.94	0.34	0.24	100.10	91	45	6	49	8.0	diopside
1437	116-2	Upper Hunza	Karakorum	52.48	0.59	4.33	12.13	0.41	16.33	11.64	0.39	0.78	99.09	71	51	22	26	2.3	aluminian augite
1437	120-2	Upper Hunza	Karakorum	51.59	0.17	0.73	13.26	0.37	9.16	22.81	0.21	0.12	98.41	55	28	23	49	1.2	diopside
1437	124-2	Upper Hunza	Karakorum	51.89	0.17	0.67	16.18	0.44	9.43	19.88	0.21	0.44	99.31	51	29	28	43	1.0	augite
1437	149-2	Upper Hunza	Karakorum	53.66	0.25	0.86	10.61	0.61	11.37	23.24	0.16	0.65	101.41	66	33	18	49	1.8	diopside
1437	153-2	Upper Hunza	Karakorum	55.63	0.26	1.50	1.49	0.49	16.93	24.24	0.26	0.19	100.99	95	48	3	49	15.2	diopside
1437	161-2	Upper Hunza	Karakorum	53.01	0.43	1.38	8.77	0.57	13.04	22.76	0.13	0.48	100.56	74	38	15	47	2.5	diopside
1437	209-2	Upper Hunza	Karakorum	53.78	0.34	0.57	11.71	0.58	11.73	22.29	0.23	0.25	101.49	64	34	20	46	1.7	diopside
1437	264-2	Upper Hunza	Karakorum	53.23	0.41	1.05	11.01	0.65	12.51	21.89	0.15	0.89	101.79	73	36	19	45	1.9	diopside
1437	273-2	Upper Hunza	Karakorum	52.68	0.55	0.68	12.24	0.89	10.59	22.96	0.24	0.63	101.47	64	31	21	48	1.4	diopside
1437	275-2	Upper Hunza	Karakorum	50.87	0.64	4.11	2.11	0.19	16.67	24.31	0.10	0.14	99.15	100	47	4	49	12.8	aluminian diopside
1437	303-2	Upper Hunza	Karakorum	52.92	0.49	1.06	11.85	0.62	11.72	20.54	0.19	0.54	99.94	64	35	21	44	1.7	augite
1437	310-2	Upper Hunza	Karakorum	52.91	0.30	0.36	14.64	0.31	9.42	21.95	0.18	0.20	100.26	53	28	25	47	1.1	diopside
1437	314-2	Upper Hunza	Karakorum	51.94	0.52	0.98	10.68	0.77	12.05	21.76	0.28	0.51	99.50	70	35	19	46	1.9	diopside
1437	357-2	Upper Hunza	Karakorum	52.40	0.62	2.86	1.16	0.11	16.46	24.71	0.12	0.26	98.69	98	47	2	51	23.1	aluminian wollastonite
1437	364-2	Upper Hunza	Karakorum	53.69	0.17	0.85	6.59	0.44	14.74	21.94	0.25	0.44	99.11	80	43	11	46	3.7	diopside
1437	369-2	Upper Hunza	Karakorum	43.24	1.64	8.42	23.97	0.54	6.47	10.73	1.50	1.69	98.19	44	23	49	28	0.5	aluminian ferrian sodian subsilicic augite
1437	412-2	Upper Hunza	Karakorum	44.70	0.74	10.84	18.19	0.66	9.02	11.56	1.46	1.90	99.06	63	32	38	30	0.9	aluminian ferrian sodian subsilicic augite
1437	416-2	Upper Hunza	Karakorum	39.77	1.06	20.68	2.16	0.17	0.11	35.30	0.27	0.00	99.52	9	0	5	95	0.1	aluminian subsilicic wollastonite
1437	425-2	Upper Hunza	Karakorum	51.44	0.56	1.75	6.45	0.39	15.20	21.65	0.26	0.72	98.42	91	44	11	45	4.0	ferrian diopside
1437	445-2	Upper Hunza	Karakorum	52.51	0.00	1.03	9.64	0.26	12.61	21.85	0.07	0.26	98.24	70	37	16	46	2.3	diopside
1438	5-1	Hispar	Karakorum	53.14		0.56	9.71	0.30	12.30	23.77			99.76	69	35	16	49	2.2	diopside
1438	19-1	Hispar	Karakorum	53.97		0.73	10.10	0.41	12.37	23.54			101.12	69	35	17	48	2.1	diopside
1438	27-1	Hispar	Karakorum	54.90		0.68	2.83	0.19	16.91	25.13			100.65	91	46	5	49	10.0	diopside
1438	38-1	Hispar	Karakorum	54.34		0.49	3.18	0.26	16.42	25.24			99.93	90	45	5	50	8.5	diopside
1438	100-1	Hispar	Karakorum	54.57		0.33	3.79	0.79	15.70	24.49			99.67	88	44	7	49	6.1	diopside
1438	113-1	Hispar	Karakorum	52.69		0.77	12.28	0.47	11.27	23.11			100.58	62	32	20	47	1.6	diopside
1438	124-1	Hispar	Karakorum	54.19		1.22	5.53	0.39	16.01	22.99			100.35	84	45	9	46	4.8	diopside
1438	130-1	Hispar	Karakorum	53.98		0.54	10.13	0.34	12.41	23.82			101.21	69	35	17	48	2.1	diopside
1438	179-1	Hispar	Karakorum	55.26		0.36	2.89	0.33	16.91	25.27			101.02	91	46	5	49	9.3	diopside
1438	202-1	Hispar	Karakorum	53.50		0.56	10.09	0.39	12.25	23.92			100.71	68	35	17	49	2.1	diopside
1438	5-2	Hispar	Karakorum	52.52		0.63	13.20	0.48	10.50	23.57			100.89	59	30	22	48	1.4	diopside
1438	10-2	Hispar	Karakorum	53.53		0.53	9.86	0.42	12.56	23.46			100.35	69	36	16	48	2.2	diopside
1438	38-2	Hispar	Karakorum	53.18		0.43	10.87	0.34	11.88	23.86			100.56	66	34	18	49	1.9	diopside
1438	59-2	Hispar	Karakorum	53.23		0.27	10.93	0.41	11.85	24.06			100.75	66	33	18	49	1.9	diopside
1438	102-2	Hispar	Karakorum	48.05		6.64	17.96	0.31	10.67	11.83			95.45	51	36	35	29	1.0	aluminian augite
1438	108-2	Hispar	Karakorum	55.03		0.79	3.02	0.19	17.09	24.53			100.65	91	47	5	48	9.5	diopside
1438	141-2	Hispar	Karakorum	55.29		0.51	2.89	0.26	16.95	25.42			101.32	91	46	5	49	9.6	diopside
1438	156-2	Hispar	Karakorum	53.39		0.67	11.16	0.35	12.41	23.13			101.11	66	35	18	47	1.9	diopside
1438	197-2	Hispar	Karakorum	55.13		1.00	5.29	0.07	15.55	24.95			101.99	84	43	8	49	5.2	diopside
1438	266-2	Hispar	Karakorum	50.38		0.26	24.84	0.18	3.35	22.76			101.78	19	10	42	48	0.2	hedenbergite
1438	11-3	Hispar	Karakorum	53.74		0.81	6.68	0.16	14.29	24.60			100.27	79	40	11	49	3.7	diopside
1438	12-3	Hispar	Karakorum	53.37		0.43	11.47	0.33	11.63	23.47			100.70	64	33	19	48	1.8	diopside
4426	74-1	Stagmo	Ladakh	49.97	0.78	5.50	14.37	0.14	13.84	11.81	0.81	0.74	97.95	63	45	27	28	1.7	aluminian augite
4426	205-1	Stagmo	Ladakh	52.20	0.39	1.83	10.03	0.25	13.51	21.45	0.23	0.51	100.40	75	39	17	44	2.3	augite
4426	217-1	Stagmo	Ladakh	53.26	0.71	1.36	9.01	0.35	12.76	22.64	0.33	0.53	100.96	72	37	15	47	2.4	diopside
4426	229-1	Stagmo	Ladakh	52.11	0.61	0.82	9.52	0.36	12.95	21.85	0.26	0.79	99.28	77	38	16	46	2.3	diopside
4426	245-1	Stagmo	Ladakh	52.45	0.42	1.38	10.24	0.23	13.70	21.53	0.10	0.58	100.63	76	39	17	44	2.3	augite
4426	280-1	Stagmo	Ladakh	53.04	0.44	0.57	9.98	0.40	12.66	21.39	0.14	0.37	99.00	69	37	17	45	2.2	diopside
4426	283-1	Stagmo	Ladakh	52.44	0.33	0.67	10.58	0.36	13.35	21.53	0.25	0.78	100.29	78	38	18	44	2.2	ferrian augite
4426	329-1	Stagmo	Ladakh	52.55	0.71	2.25	4.43	0.25	16.30	22.36	0.22	0.45	99.52	91	47	8	46	6.2	diopside
4426	343-2	Stagmo	Ladakh	52.98	0.48	0.54	9.69	0.24	13.52	22.17	0.19	0.73	100.53	77	39	16	45	2.4	diopside
4426	31-2	Stagmo	Ladakh	51.17	0.52	0.82	10.08	0.34	12.53	21.97	0.26	0.68	98.38	76	37	17	46	2.1	ferrian diopside
4426	102-2	Stagmo	Ladakh	51.90	0.27	1.52	8.55	0.31	13.26	22.24	0.10	0.49	98.65	76	39	15	47	2.7	diopside
4426	192-2	Stagmo	Ladakh	53.88	0.23	0.91	10.48	0.30	11.88	21.79	0.14	0.57	100.17	67	35	18	47	2.0	diopside
4426	211-2	Stagmo	Ladakh	52.98	0.42	0.51	9.86	0.47	12.71	22.08	0.39	0.54	99.97	72	37	17	46	2.2	diopside
4426	261-2	Stagmo	Ladakh	46.25	1.28	7.61	16.71	0.32	10.98	11.59	0.84	1.22	96.80	59	38	33	29	1.1	aluminian ferrian augite
4426	312-2	Stagmo	Ladakh	53.01	0.44	0.62	9.65	0.36	13.07	21.98	0.07	0.24	99.46	71	38	16	46	2.3	diopside
4430	3-1	Domkar	Ladakh	52.81	0.51	1.31	9.83	0.65	12.73	21.30	0.20	0.71	100.04	71	38	17	45	2.2	diopside
4430	17-1	Domkar	Ladakh	54.07	0.14	0.91	6.91	0.49	14.04	23.61	0.25	0.39	100.83	80	40	12	48	3.4	diopside
4430	25-1	Domkar	Ladakh	54.96	0.09	1.77	12.55	0.52	29.45	0.73	0.22	0.32	100.63	84	79	20	1	4.0	(clino)enstatite
4430	71-1	Domkar	Ladakh	53.99	0.15	0.94	10.55	0.83	12.68	21.28	0.14	0.79	101.35	70	37	19	45	2.0	augite
4430	76-1	Domkar	Ladakh	53.10	0.44	1.21	11.36	0.66	13.05	21.14	0.21	0.56	101.73	71	37	19	43	1.9	augite
4430	80-1	Domkar	Ladakh	51.67	0.82	2.99	8.97	0.43	14.39	20.18	0.22	0.56	100.24	78	42	15	42	2.7	aluminian augite
4430	103-1	Domkar	Ladakh	53.32	0.34	0.53	13.99	0.66	8.31	23.88	0.13	0.42	101.59	51	25	24	51	1.0	wollastonite
4430	116-1	Domkar	Ladakh	45.73	1.54	8.64	17.95	0.42	11.56	10.73	0.93	0.94	98.46	59	39	35	26	1.1	aluminian ferrian augite
4430	126-1	Domkar	Ladakh	43.66	0.72	9.94	21.20	0.52	8.81	11.92	1.19	1.48	99.44	59	30	41	29	0.7	aluminian ferrian sodian subsilicic augite
4430	244-1	Domkar	Ladakh	51.56	0.20	1.15	24.84	0.43	18.69	1.87	0.11	0.11	98.97	57	55	41	4	1.3	(clino)enstatite
4430	245-1	Domkar	Ladakh	52.58	0.52	1.23	22.13	0.73	21.26	1.32	0.20	0.20	100.16	64	61	37	3	1.7	(clino)enstatite
4430	336-1	Domkar	Ladakh	39.26	0.65	16.38	7.34	0.51	0.24	35.16	0.22	0.00	99.75	33	------	------	------		aluminian ferrian subsilicic esseneite
4430	15-2	Domkar	Ladakh	54.06	0.52	1.17	9.61	0.59	13.56	20.97	0.28	0.56	101.31	72	39	17	44	2.4	augite
4430	30-2	Domkar	Ladakh	48.54	1.70	7.56	16.43	0.55	11.30	11.83	0.97	1.10	99.97	56	39	32	29	1.2	aluminian augite
4430	55-2	Domkar	Ladakh	47.36	1.09	7.07	14.99	0.85	13.48	11.55	0.85	1.40	98.65	73	44	29	27	1.5	aluminian ferrian sodian augite
4430	62-2	Domkar	Ladakh	51.79	0.37	0.43	26.90	0.92	17.51	0.94	0.08	0.32	99.26	54	52	46	2	1.1	(clino)enstatite
4430	151-2	Domkar	Ladakh	52.76	0.39	0.77	10.02	0.92	12.88	21.01	0.26	0.37	99.37	70	38	18	44	2.1	augite
4430	152-2	Domkar	Ladakh	46.54	0.93	9.25	17.20	0.55	10.76	11.83	0.78	1.08	98.93	57	37	34	29	1.1	aluminian augite
4430	171-2	Domkar	Ladakh	45.27	2.00	9.42	15.42	0.50	11.72	11.44	1.20	1.51	98.47	69	41	31	28	1.3	aluminian ferrian sodian subsilicic augite
4430	173-2	Domkar	Ladakh	52.63	0.87	1.25	10.95	0.54	12.51	21.83	0.26	0.59	101.43	70	36	19	45	1.9	diopside
4430	252-2	Domkar	Ladakh	47.14	1.65	8.29	15.80	0.54	12.55	11.48	0.89	0.95	99.30	63	42	31	28	1.4	aluminian augite
4430	259-2	Domkar	Ladakh	45.93	1.18	8.37	17.76	0.60	10.47	11.89	0.98	1.13	98.31	58	36	35	29	1.0	aluminian ferrian augite
4430	294-2	Domkar	Ladakh	44.26	1.18	9.65	17.82	0.60	10.52	12.46	1.42	0.92	98.82	65	35	35	30	1.0	aluminian ferrian subsilicic augite
1439	47-1	Kandia	Kohistan	48.96		4.16	9.60	0.25	11.91	21.12			95.99	69	37	17	47	2.2	aluminian diopside
1439	135-1	Kandia	Kohistan	49.23		3.44	11.15	0.20	10.93	20.55			95.50	64	34	20	46	1.7	aluminian diopside
1439	171-1	Kandia	Kohistan	49.21		4.24	10.18	0.22	11.42	21.17			96.45	67	35	18	47	2.0	aluminian diopside
1439	180-1	Kandia	Kohistan	50.97		1.36	25.55	0.41	18.83	0.81			97.93	57	55	43	2	1.3	(clino)enstatite
1439	195-1	Kandia	Kohistan	41.87		13.30	17.49	0.25	8.74	10.75			92.40	47	33	38	29	0.9	aluminian subsilicic augite
1439	247-1	Kandia	Kohistan	51.14		2.11	24.74	0.29	19.52	1.04			98.84	58	57	41	2	1.4	(clino)enstatite
1439	257-1	Kandia	Kohistan	50.44		1.01	27.17	0.52	18.04	0.85			98.04	55	53	45	2	1.2	(clino)enstatite
1439	320-1	Kandia	Kohistan	51.70		0.94	6.33	0.10	13.49	23.47			96.04	79	40	11	50	3.7	diopside
1439	333-1	Kandia	Kohistan	48.28		2.67	8.83	0.16	12.04	20.40			92.38	71	38	16	46	2.4	aluminian diopside
1439	54-2	Kandia	Kohistan	52.72		0.79	7.66	0.10	13.00	23.75			98.02	75	38	13	50	3.0	diopside
1439	103-2	Kandia	Kohistan	51.04		1.35	25.71	0.33	19.08	0.89			98.39	57	56	43	2	1.3	(clino)enstatite
1439	119-2	Kandia	Kohistan	50.25		1.27	28.25	0.31	17.93	0.94			98.96	55	52	46	2	1.1	(clino)enstatite
1439	130-2	Kandia	Kohistan	48.45		3.59	10.11	0.15	11.64	20.83			94.77	67	36	18	46	2.0	aluminian diopside
1439	172-2	Kandia	Kohistan	49.64		2.77	11.86	0.13	11.31	20.63			96.33	63	34	20	45	1.7	aluminian diopside
1439	212-2	Kandia	Kohistan	49.61		3.61	8.71	0.18	12.49	21.02			95.62	72	38	15	46	2.5	aluminian diopside

Sample	Points	River/Dune	Domain	SiO_2	TiO_2	Al_2O_3	FeO	MnO	MgO	CaO	K_2O	Na_2O	Total	Mg#	En	Fs	Wo	En/Fs	Name
				wt%	wt%	wt%	wt%	wt%	wt%	wt%	wt%	wt%							
1440	14-1	Swat	Kohistan	51.63		1.79	9.78	0.46	13.04	21.66			98.36	70	38	17	45	2.3	diopside
1440	17-1	Swat	Kohistan	50.57		3.00	14.10	0.36	12.94	17.27			98.25	62	39	24	37	1.6	aluminian augite
1440	18-1	Swat	Kohistan	51.74		1.27	25.10	0.46	20.29	0.60			99.46	60	58	41	1	1.4	(clino)enstatite
1440	19-1	Swat	Kohistan	51.96		1.76	23.66	0.43	20.87	0.35			99.03	61	60	39	1	1.5	(clino)enstatite
1440	20-1	Swat	Kohistan	51.24		2.53	9.91	0.26	12.82	21.02			97.79	70	38	17	45	2.2	aluminian augite
1440	24-1	Swat	Kohistan	51.24		1.98	9.46	0.19	13.21	21.65			97.71	71	39	16	46	2.4	diopside
1440	30-1	Swat	Kohistan	49.97		3.19	10.59	0.27	12.08	21.26			97.35	67	36	18	46	2.0	aluminian diopside
1440	32-1	Swat	Kohistan	52.05		1.90	23.75	0.44	21.41	0.84			100.40	63	60	38	2	1.6	(clino)enstatite
1440	40-1	Swat	Kohistan	50.28		3.42	9.26	0.32	12.90	21.17			97.35	71	39	16	45	2.4	aluminian diopside
1440	43-1	Swat	Kohistan	50.93		1.66	23.83	0.41	20.53	0.93			98.28	62	59	39	2	1.5	(clino)enstatite
1440	49-1	Swat	Kohistan	50.82		2.64	11.09	0.23	12.61	20.88			98.28	67	37	19	44	2.0	aluminian augite
1440	51-1	Swat	Kohistan	51.13		1.90	25.28	0.49	19.76	0.75			99.31	59	57	42	2	1.4	(clino)enstatite
1440	53-1	Swat	Kohistan	50.43		3.34	9.09	0.26	13.34	21.17			97.63	72	39	16	45	2.5	aluminian diopside
1440	59-1	Swat	Kohistan	50.94		2.47	9.57	0.26	12.87	21.58			97.68	71	38	16	46	2.3	aluminian diopside
1440	61-1	Swat	Kohistan	50.78		2.86	10.28	0.17	12.83	21.03			97.95	69	38	17	45	2.2	aluminian augite
1440	62-1	Swat	Kohistan	50.97		1.54	25.86	0.51	19.10	0.78			98.75	57	55	43	2	1.3	(clino)enstatite
1440	113-1	Swat	Kohistan	50.54		3.46	9.28	0.26	12.74	21.62			97.91	71	38	16	46	2.4	aluminian diopside
1440	116-1	Swat	Kohistan	51.43		1.57	21.95	0.49	21.80	0.78			98.02	65	62	36	2	1.7	(clino)enstatite
1440	118-1	Swat	Kohistan	51.32		2.20	23.18	0.42	21.15	0.64			98.90	63	61	38	1	1.6	(clino)enstatite
1440	119-1	Swat	Kohistan	51.96		1.95	22.88	0.40	21.13	1.84			100.15	63	59	37	4	1.6	(clino)enstatite
1440	125-1	Swat	Kohistan	50.62		2.63	8.83	0.08	13.29	21.58			97.04	73	39	15	46	2.7	aluminian diopside
1440	127-1	Swat	Kohistan	51.43		2.05	9.37	0.26	13.20	21.84			98.15	72	38	16	46	2.4	diopside
1440	131-1	Swat	Kohistan	51.41		2.04	24.07	0.38	20.34	0.65			98.90	60	59	40	1	1.5	(clino)enstatite
1440	132-1	Swat	Kohistan	50.97		1.76	10.45	0.35	13.65	20.90			98.06	72	39	17	43	2.3	augite
1440	140-1	Swat	Kohistan	49.82		3.40	10.67	0.24	12.64	20.09			96.86	68	38	18	43	2.1	aluminian augite
1440	142-1	Swat	Kohistan	50.60		1.36	26.10	0.41	19.19	0.82			98.49	58	55	43	2	1.3	(clino)enstatite
1440	144-1	Swat	Kohistan	51.25		1.77	25.40	0.43	19.81	0.49			99.14	59	57	42	1	1.4	(clino)enstatite
1440	145-1	Swat	Kohistan	51.74		1.22	23.39	0.44	21.53	0.85			99.18	64	61	38	2	1.6	(clino)enstatite
1440	146-1	Swat	Kohistan	49.87		3.69	10.34	0.17	12.97	20.15			97.18	69	39	18	43	2.2	aluminian augite
1440	148-1	Swat	Kohistan	50.61		2.64	10.69	0.29	12.38	21.09			97.71	67	37	18	45	2.0	aluminian augite
1440	156-1	Swat	Kohistan	51.06		2.64	10.50	0.21	12.34	21.16			97.90	68	37	18	45	2.1	aluminian diopside
1440	157-1	Swat	Kohistan	51.84		1.38	9.40	0.48	13.53	21.86			98.49	72	39	16	45	2.4	diopside
1440	158-1	Swat	Kohistan	51.44		2.19	23.12	0.39	21.22	0.98			99.34	63	60	38	2	1.6	(clino)enstatite
1440	160-1	Swat	Kohistan	50.87		1.02	25.83	0.81	18.74	1.14			98.42	57	54	43	2	1.3	(clino)enstatite
1440	169-1	Swat	Kohistan	51.46		1.77	22.62	0.34	21.65	0.60			98.45	64	62	37	1	1.7	(clino)enstatite
1440	170-1	Swat	Kohistan	51.05		2.64	8.54	0.26	13.08	22.18			97.75	73	39	15	47	2.6	aluminian diopside
1440	172-1	Swat	Kohistan	50.78		2.91	10.37	0.18	12.58	21.13			97.95	68	37	18	45	2.1	aluminian diopside
1440	174-1	Swat	Kohistan	50.76		1.95	26.14	0.52	18.74	0.79			98.90	56	55	44	2	1.3	(clino)enstatite
1440	180-1	Swat	Kohistan	51.74		1.95	23.80	0.42	21.25	0.73			99.89	63	60	38	1	1.6	(clino)enstatite
1440	181-1	Swat	Kohistan	49.72		3.11	10.12	0.16	11.97	21.82			96.90	68	36	17	47	2.1	aluminian diopside
1440	182-1	Swat	Kohistan	50.90		1.55	24.52	0.40	20.45	0.76			98.58	61	58	40	2	1.5	(clino)enstatite
1440	184-1	Swat	Kohistan	50.29		3.09	9.84	0.25	12.50	21.60			97.58	69	37	17	46	2.2	aluminian diopside
1440	185-1	Swat	Kohistan	51.65		1.40	22.88	0.49	21.10	0.80			98.32	62	61	38	2	1.6	(clino)enstatite
1440	186-1	Swat	Kohistan	50.68		2.41	10.24	0.24	12.98	21.74			98.29	71	38	17	45	2.2	aluminian diopside
1440	187-1	Swat	Kohistan	51.31		2.24	9.89	0.34	12.68	21.79			98.25	70	37	17	46	2.2	aluminian diopside
1440	190-1	Swat	Kohistan	50.68		2.47	13.64	0.33	13.62	17.75			98.50	65	40	23	37	1.7	aluminian augite
1440	195-1	Swat	Kohistan	49.84		3.29	9.59	0.27	12.70	21.15			96.84	70	38	17	45	2.3	aluminian diopside
1440	196-1	Swat	Kohistan	49.85		3.11	10.46	0.19	12.37	20.75			96.72	68	37	18	45	2.1	aluminian augite
1440	199-1	Swat	Kohistan	51.25		1.77	25.23	0.33	19.78	0.78			99.13	59	57	41	2	1.4	(clino)enstatite
1440	201-1	Swat	Kohistan	50.28		3.03	10.97	0.27	12.70	19.95			97.21	67	38	19	43	2.0	aluminian augite
1440	206-1	Swat	Kohistan	51.69		1.60	22.28	0.37	22.08	0.69			98.71	65	63	36	1	1.7	(clino)enstatite
1440	261-1	Swat	Kohistan	50.24		3.13	6.84	0.16	14.82	21.66			96.86	82	43	11	45	3.8	aluminian diopside
1440	262-1	Swat	Kohistan	52.71		1.62	7.82	0.30	14.47	22.02			98.93	77	42	13	45	3.2	diopside
1440	264-1	Swat	Kohistan	51.25		2.24	9.95	0.26	12.97	21.50			98.17	70	38	17	45	2.3	aluminian diopside
1440	265-1	Swat	Kohistan	51.09		2.80	9.94	0.26	12.52	21.27			97.88	69	37	17	46	2.2	aluminian diopside
1440	274-1	Swat	Kohistan	51.67		2.20	9.80	0.25	12.85	21.76			98.53	70	38	17	46	2.3	diopside
1440	276-1	Swat	Kohistan	51.38		1.91	25.74	0.49	19.83	0.83			100.18	59	56	42	2	1.3	(clino)enstatite
1440	278-1	Swat	Kohistan	50.90		2.65	9.06	0.29	12.97	21.47			97.35	72	39	16	46	2.5	aluminian diopside
1440	279-1	Swat	Kohistan	51.43		1.93	9.23	0.30	13.30	20.95			97.14	72	39	16	45	2.5	augite
1440	26-2	Swat	Kohistan	50.68		1.72	25.43	0.43	20.05	0.80			99.11	60	57	41	2	1.4	(clino)enstatite
1440	28-2	Swat	Kohistan	51.01		2.03	24.95	0.39	19.82	0.84			99.04	59	57	41	2	1.4	(clino)enstatite
1440	30-2	Swat	Kohistan	49.88		4.85	11.96	0.21	15.09	11.27			93.26	69	50	23	27	2.2	aluminian augite
1440	31-2	Swat	Kohistan	51.30		0.96	25.03	0.39	21.83	0.85			100.36	65	59	39	2	1.5	ferrian (clino)enstatite
1440	32-2	Swat	Kohistan	50.86		1.54	24.13	0.44	20.17	0.80			97.94	61	58	40	2	1.5	(clino)enstatite
1440	34-2	Swat	Kohistan	51.56		1.96	9.83	0.26	12.93	21.81			98.34	70	38	17	46	2.3	diopside
1440	42-2	Swat	Kohistan	50.96		2.11	10.33	0.27	12.60	21.57			97.84	68	37	17	46	2.1	diopside
1440	53-2	Swat	Kohistan	52.59		0.63	8.53	0.43	12.77	23.63			98.58	73	37	14	49	2.5	diopside
1440	57-2	Swat	Kohistan	50.65		2.94	12.06	0.30	15.34	17.47			98.75	72	44	20	36	2.2	aluminian augite
1440	58-2	Swat	Kohistan	51.59		1.16	9.60	0.35	13.89	21.62			98.21	74	40	16	44	2.5	augite
1440	59-2	Swat	Kohistan	52.15		1.95	22.83	0.37	21.72	0.69			99.70	63	62	37	1	1.7	(clino)enstatite
1440	60-2	Swat	Kohistan	51.26		1.30	11.53	0.30	13.12	20.18			97.69	67	38	19	42	2.0	augite
1440	62-2	Swat	Kohistan	50.87		3.30	9.45	0.30	12.85	20.99			97.76	71	38	16	45	2.3	aluminian diopside
1440	75-2	Swat	Kohistan	52.30		1.16	25.44	0.42	19.72	0.74			99.78	58	57	42	2	1.4	(clino)enstatite
1440	77-2	Swat	Kohistan	50.99		1.58	24.46	0.45	19.75	0.87			98.10	59	57	41	2	1.4	(clino)enstatite
1440	78-2	Swat	Kohistan	51.49		1.03	24.94	0.68	20.22	0.87			99.23	60	57	41	2	1.4	(clino)enstatite
1440	83-2	Swat	Kohistan	51.19		2.23	8.81	0.32	12.45	22.45			97.45	72	37	15	48	2.4	aluminian diopside
1440	85-2	Swat	Kohistan	51.60		1.53	23.88	0.47	20.09	0.62			98.18	60	59	40	1	1.5	(clino)enstatite
1440	87-2	Swat	Kohistan	51.18		1.73	23.01	0.31	20.98	0.52			97.74	62	61	38	1	1.6	(clino)enstatite
1440	90-2	Swat	Kohistan	50.71		1.76	24.98	0.39	20.01	0.84			98.70	60	57	41	2	1.4	(clino)enstatite
1440	94-2	Swat	Kohistan	50.62		2.38	20.99	0.38	21.83	0.62			96.82	66	64	35	1	1.8	aluminian (clino)enstatite
1440	164-2	Swat	Kohistan	51.11		1.94	25.03	0.48	18.92	0.69			98.17	57	56	42	1	1.3	(clino)enstatite
1440	166-2	Swat	Kohistan	51.20		2.48	9.55	0.29	13.16	22.15			98.82	72	38	16	46	2.4	aluminian diopside
1440	167-2	Swat	Kohistan	52.71		1.54	23.83	0.33	20.53	0.82			99.77	61	59	39	2	1.5	(clino)enstatite
1440	173-2	Swat	Kohistan	51.36		1.92	9.89	0.27	12.99	21.78			98.21	70	38	17	46	2.3	diopside
1440	174-2	Swat	Kohistan	51.68		2.71	8.73	0.14	13.14	21.71			98.12	73	39	15	46	2.6	aluminian diopside
1440	178-2	Swat	Kohistan	50.52		2.90	10.92	0.35	11.88	21.18			97.74	66	36	19	46	1.9	aluminian diopside
1440	180-2	Swat	Kohistan	51.29		3.45	12.30	0.24	13.28	18.82			99.38	66	39	21	40	1.9	aluminian augite
1440	185-2	Swat	Kohistan	51.48		2.45	22.54	0.35	21.96	0.66			99.44	65	62	36	1	1.7	aluminian (clino)enstatite
1440	189-2	Swat	Kohistan	51.62		1.54	24.14	0.33	20.43	0.62			98.67	60	59	40	1	1.5	(clino)enstatite
1440	190-2	Swat	Kohistan	51.19		2.36	22.28	0.33	21.32	0.66			98.15	63	62	37	1	1.7	aluminian (clino)enstatite
1440	193-2	Swat	Kohistan	51.65		1.41	24.79	0.45	20.70	0.91			99.91	61	58	40	2	1.5	(clino)enstatite
1440	194-2	Swat	Kohistan	51.01		2.85	8.79	0.28	12.77	22.34			98.03	72	38	15	47	2.5	aluminian diopside
1440	207-2	Swat	Kohistan	51.79		1.32	25.14	0.39	20.46	0.76			99.86	60	58	41	2	1.4	(clino)enstatite
1440	305-2	Swat	Kohistan	50.04		3.05	10.32	0.21	12.35	21.51			97.48	69	37	18	46	2.1	aluminian diopside
1440	306-2	Swat	Kohistan	51.18		1.81	23.94	0.46	20.86	0.85			99.09	62	59	39	2	1.5	(clino)enstatite
1440	309-2	Swat	Kohistan	51.08		1.10	26.30	0.46	18.70	0.86			98.50	56	54	44	2	1.2	(clino)enstatite
1440	312-2	Swat	Kohistan	50.84		1.87	25.10	0.46	19.13	0.74			98.14	58	56	42	2	1.3	(clino)enstatite
1440	315-2	Swat	Kohistan	51.88		1.26	24.29	0.45	20.22	0.65			98.76	60	58	40	1	1.5	(clino)enstatite
1440	327-2	Swat	Kohistan	50.76		3.68	9.68	0.18	13.44	20.28			98.02	71	40	16	43	2.4	aluminian augite
1440	328-2	Swat	Kohistan	51.07		1.08	25.29	0.41	20.58	0.64			99.07	61	58	41	1	1.4	(clino)enstatite

Sample	Points	River/Dune	Domain	SiO_2	TiO_2	Al_2O_3	FeO	MnO	MgO	CaO	K_2O	Na_2O	Total	Mg#	En	Fs	Wo	En/Fs	Name
				wt%	wt%	wt%	wt%	wt%	wt%	wt%	wt%	wt%							
4419	21-1	Zanskar	Himalaya	53.64	0.20	1.76	2.77	0.17	16.88	23.93	0.00	0.33	99.68	94	47	5	48	10.2	diopside
4419	30-1	Zanskar	Himalaya	53.82	0.29	1.25	0.62	0.08	17.42	24.26	0.26	0.46	98.46	100	49	1	49	44.2	diopside
4419	43-1	Zanskar	Himalaya	54.31	0.32	0.40	3.79	0.21	16.50	23.68	0.23	0.34	99.78	91	46	6	48	7.3	diopside
4419	52-1	Zanskar	Himalaya	54.65	0.39	0.82	3.01	0.29	16.31	24.85	0.33	0.59	101.24	97	45	5	50	8.8	diopside
4419	73-1	Zanskar	Himalaya	52.24	0.32	1.13	13.33	0.18	10.05	23.14	0.21	0.20	100.80	57	29	22	49	1.3	diopside
4419	81-1	Zanskar	Himalaya	54.19	0.33	0.23	4.39	0.20	16.18	24.41	0.23	0.21	100.38	90	45	7	48	6.3	diopside
4419	172-1	Zanskar	Himalaya	54.23	0.31	0.56	2.42	0.37	16.86	24.30	0.26	0.42	99.72	97	47	4	49	10.8	diopside
4419	176-1	Zanskar	Himalaya	52.66	0.36	0.62	12.51	0.22	10.71	23.03	0.34	0.42	100.86	62	31	21	48	1.5	diopside
4419	210-1	Zanskar	Himalaya	52.18	0.28	0.25	10.93	0.44	11.42	23.20	0.15	0.35	99.20	67	33	19	48	1.8	diopside
4419	214-1	Zanskar	Himalaya	52.60	0.43	0.54	10.21	0.28	12.16	23.07	0.30	0.30	99.89	70	35	17	48	2.1	diopside
4419	217-1	Zanskar	Himalaya	42.42	0.47	13.78	21.56	0.11	6.28	10.73	0.72	1.81	97.89	42	24	46	29	0.5	aluminian ferrian sodian subsilicic augite
4419	218-1	Zanskar	Himalaya	63.57	0.83	17.78	0.58	0.12	0.25	0.43	13.71	1.16	98.41	43	--------	--------	--------		aluminian unusual pyroxene
4419	232-1	Zanskar	Himalaya	52.37	0.98	2.09	9.35	0.17	15.46	18.67	0.24	0.60	99.93	77	45	16	39	2.9	augite
4419	240-1	Zanskar	Himalaya	53.56	0.44	0.78	1.44	0.18	17.53	24.91	0.26	0.33	99.45	100	48	3	49	19.1	diopside
4419	51-2	Zanskar	Himalaya	53.96	0.27	0.82	9.33	0.25	12.22	23.18	0.24	0.62	100.89	70	36	16	49	2.3	diopside
4419	61-2	Zanskar	Himalaya	51.20	0.53	0.77	14.88	0.28	8.96	21.34	0.25	0.56	98.77	52	27	26	47	1.1	diopside
4419	68-2	Zanskar	Himalaya	53.40	0.48	0.53	8.84	0.21	13.45	23.17	0.21	0.35	100.65	75	38	14	47	2.6	diopside
4419	93-2	Zanskar	Himalaya	52.56	0.14	0.71	11.42	0.14	11.67	23.36	0.20	0.39	100.59	68	33	19	48	1.8	diopside
4419	96-2	Zanskar	Himalaya	53.14	0.35	0.51	14.09	0.35	9.85	21.55	0.24	1.46	101.52	62	29	24	46	1.2	ferrian sodian diopside
4419	101-2	Zanskar	Himalaya	51.95	0.32	0.39	11.69	0.25	10.58	23.47	0.18	0.37	99.21	63	31	20	49	1.6	diopside
4419	108-2	Zanskar	Himalaya	52.95	0.45	1.18	10.52	0.22	11.69	22.27	0.27	0.49	100.04	66	35	18	47	1.9	diopside
4419	134-2	Zanskar	Himalaya	53.27	0.44	0.77	8.15	0.19	13.12	22.69	0.18	0.88	99.68	77	38	14	48	2.8	diopside
4419	137-2	Zanskar	Himalaya	53.64	0.53	0.88	10.19	0.26	12.03	23.72	0.42	0.35	102.02	69	34	17	49	2.1	diopside
4419	144-2	Zanskar	Himalaya	54.64	0.33	0.57	6.74	0.26	14.56	23.70	0.35	0.00	101.15	79	41	11	48	3.7	diopside
4419	161-2	Zanskar	Himalaya	52.29	0.18	1.16	12.56	0.36	11.16	21.94	0.26	0.58	100.50	65	33	21	46	1.5	diopside
4419	203-2	Zanskar	Himalaya	53.27	0.56	0.54	9.26	0.34	12.34	23.46	0.44	0.00	100.20	70	36	16	49	2.3	diopside
4419	215-2	Zanskar	Himalaya	53.42	0.30	1.61	5.68	0.10	15.19	23.96	0.17	0.45	100.87	88	43	9	48	4.7	diopside
4419	218-2	Zanskar	Himalaya	52.66	0.65	3.27	12.62	0.35	9.46	18.79	0.29	2.53	100.63	64	31	24	45	1.3	aluminian sodian augite
4419	246-2	Zanskar	Himalaya	52.03	0.22	0.33	14.09	0.41	9.08	22.88	0.11	0.44	99.58	53	27	24	49	1.1	diopside
4419	255-2	Zanskar	Himalaya	53.11	0.33	0.54	12.22	0.36	10.78	22.62	0.13	0.84	100.93	64	32	21	48	1.5	diopside
4419	269-2	Zanskar	Himalaya	53.45	0.26	0.53	5.10	0.31	14.74	24.11	0.28	0.49	99.26	88	42	9	49	4.9	diopside
4419	271-2	Zanskar	Himalaya	52.17	0.33	0.24	9.47	0.18	12.71	22.88	0.30	0.87	99.16	80	37	16	48	2.3	ferrian diopside
4419	280-2	Zanskar	Himalaya	50.23	0.35	2.62	10.30	0.30	11.97	22.04	0.28	1.13	99.22	83	35	18	47	2.0	aluminian ferrian diopside
4419	309-2	Zanskar	Himalaya	52.52	0.37	1.03	10.12	0.33	12.37	22.01	0.31	0.83	99.88	74	36	17	46	2.1	diopside
4419	329-2	Zanskar	Himalaya	52.27	0.48	0.64	12.41	0.32	10.19	22.40	0.28	0.24	99.23	59	30	21	48	1.4	diopside
4419	337-2	Zanskar	Himalaya	51.81	0.45	0.39	11.92	0.33	10.54	22.35	0.23	0.47	98.50	62	31	21	48	1.5	diopside
4419	338-2	Zanskar	Himalaya	51.03	0.42	0.20	13.39	0.23	9.39	23.56	0.19	0.12	98.53	56	28	23	50	1.2	diopside
4419	366-2	Zanskar	Himalaya	52.19	0.36	1.72	12.87	0.40	9.93	20.91	0.21	1.64	100.25	65	31	23	46	1.3	ferrian sodian diopside
4419	370-2	Zanskar	Himalaya	54.29	0.32	1.06	3.50	0.22	16.03	24.43	0.20	0.20	100.25	89	45	6	49	7.7	diopside
4419	378-2	Zanskar	Himalaya	54.11	0.18	0.40	4.18	0.27	15.77	24.72	0.13	0.30	100.06	90	44	7	49	6.3	diopside
4419	403-2	Zanskar	Himalaya	53.32	0.27	1.58	9.95	0.22	12.09	22.34	0.07	1.01	100.84	71	36	17	47	2.1	diopside
4419	430-2	Zanskar	Himalaya	54.33	0.15	0.71	8.14	0.16	13.70	22.96	0.12	0.19	100.45	75	39	13	47	2.9	diopside
4419	431-2	Zanskar	Himalaya	54.41	0.16	0.54	4.42	0.16	15.49	24.37	0.29	0.26	100.11	87	44	7	49	6.0	diopside
4419	432-2	Zanskar	Himalaya	54.81	0.29	0.41	2.95	0.31	16.25	25.11	0.16	0.44	100.73	94	45	5	50	8.9	diopside
4419	435-2	Zanskar	Himalaya	54.58	0.49	0.39	5.95	0.37	14.13	23.95	0.16	0.49	100.50	81	40	10	49	4.0	diopside
4419	451-2	Zanskar	Himalaya	52.68	0.15	1.09	10.93	0.26	12.20	23.04	0.17	0.36	100.89	70	35	18	47	1.9	diopside
4419	453-2	Zanskar	Himalaya	52.20	0.40	0.35	16.32	0.13	7.96	23.03	0.14	0.17	100.69	47	24	27	49	0.9	hedenbergite
4419	460-2	Zanskar	Himalaya	52.79	0.44	1.89	7.31	0.29	13.93	23.77	0.24	0.33	100.99	81	39	12	48	3.3	diopside
4419	466-2	Zanskar	Himalaya	51.87	0.22	1.05	13.41	0.16	10.20	23.50	0.20	0.40	101.02	62	29	22	49	1.3	diopside
4419	508-2	Zanskar	Himalaya	54.65	0.16	0.86	2.14	0.13	16.43	25.01	0.16	0.46	100.01	95	46	4	50	12.9	wollastonite
4419	518-2	Zanskar	Himalaya	50.63	0.53	0.24	16.47	0.33	7.12	23.11	0.26	0.46	99.15	45	21	28	50	0.8	wollastonite
4419	531-2	Zanskar	Himalaya	52.52	0.38	2.46	9.85	0.39	11.25	19.70	0.14	2.25	98.94	75	36	18	45	2.0	aluminian ferrian sodian diopside
4419	537-2	Zanskar	Himalaya	52.02	0.32	0.43	13.57	0.23	10.28	23.29	0.19	0.43	100.77	61	30	22	48	1.3	diopside
4419	554-2	Zanskar	Himalaya	53.65	0.08	0.24	4.90	0.13	15.54	24.53	0.21	0.31	99.58	91	43	8	49	5.5	diopside
4419	563-2	Zanskar	Himalaya	50.65	0.62	1.55	17.41	0.73	6.64	19.87	0.35	1.78	99.61	46	21	33	46	0.7	ferrian sodian hedenbergite
4419	584-2	Zanskar	Himalaya	51.67	0.30	0.20	15.25	0.17	9.05	22.91	0.08	0.37	100.00	53	26	25	48	1.0	diopside
4419	617-2	Zanskar	Himalaya	52.48	0.38	1.67	25.92	0.25	19.86	0.77	0.20	0.00	101.53	58	57	42	2	1.4	(clino)enstatite
4419	626-2	Zanskar	Himalaya	54.20	0.28	0.72	3.59	0.17	16.58	24.16	0.10	0.20	100.00	90	46	6	48	7.9	diopside
4419	641-2	Zanskar	Himalaya	52.94	0.25	1.21	9.26	0.28	13.46	22.38	0.29	0.67	100.74	78	39	15	46	2.5	diopside
4419	681-2	Zanskar	Himalaya	55.66	0.20	1.10	0.72	0.14	17.77	24.84	0.16	0.44	101.02	98	49	1	49	36.8	diopside
4419	687-2	Zanskar	Himalaya	52.14	0.30	0.99	14.20	0.18	10.82	21.63	0.33	0.65	101.24	63	31	23	45	1.3	diopside
4419	706-2	Zanskar	Himalaya	52.74	0.47	2.42	2.28	0.17	16.46	23.64	0.15	0.24	98.57	93	47	4	49	12.0	aluminian diopside
4419	734-2	Zanskar	Himalaya	54.42	0.37	1.52	3.90	0.19	15.26	25.02	0.39	0.48	101.55	91	43	6	51	6.6	wollastonite
4419	738-2	Zanskar	Himalaya	53.42	0.42	1.34	7.61	0.17	13.54	23.71	0.27	0.91	101.40	84	39	12	49	3.1	diopside
4419	757-2	Zanskar	Himalaya	50.54	0.60	1.36	12.58	0.39	10.12	21.89	0.33	1.07	98.88	68	31	22	47	1.4	ferrian diopside
4419	786-2	Zanskar	Himalaya	48.57	0.70	5.24	17.30	0.38	12.40	12.52	0.81	0.98	98.90	63	40	32	29	1.2	aluminian ferrian augite
4419	796-2	Zanskar	Himalaya	51.66	0.75	3.31	6.29	0.16	14.91	21.83	0.36	0.49	99.77	86	44	11	46	4.1	aluminian diopside
4419	799-2	Zanskar	Himalaya	51.77	0.38	1.94	11.84	0.19	11.24	21.37	0.15	1.26	100.14	71	34	20	46	1.7	ferrian diopside
4419	834-2	Zanskar	Himalaya	51.87	0.28	1.02	11.95	0.18	11.87	22.73	0.17	0.84	100.91	74	34	19	47	1.7	ferrian diopside
4419	836-2	Zanskar	Himalaya	52.35	0.55	3.35	6.24	0.12	16.16	21.36	0.27	0.58	100.98	90	46	10	44	4.5	aluminian augite
1426	7-1	Nandihar	Himalaya	52.09	0.45	1.42	10.70	0.19	11.87	21.66	0.16	0.33	98.86	66	35	18	46	1.9	diopside
1426	63-1	Nandihar	Himalaya	50.77	0.44	0.66	32.95	0.55	13.36	0.82	0.28	0.34	100.18	42	41	57	2	0.7	(clino)ferrosilite
1426	86-1	Nandihar	Himalaya	49.80	1.51	3.94	11.21	0.37	13.71	17.33	0.27	0.72	98.85	72	42	20	38	2.1	aluminian augite
1426	95-1	Nandihar	Himalaya	51.76	0.60	1.90	10.79	0.33	12.61	21.18	0.21	0.58	99.97	71	37	18	45	2.0	augite
1426	97-1	Nandihar	Himalaya	52.83	0.34	1.92	10.85	0.09	11.76	20.38	0.22	0.45	98.84	66	36	19	45	1.9	diopside
1426	281-1	Nandihar	Himalaya	45.56	1.45	10.54	17.52	0.23	9.98	13.24	0.97	1.46	100.95	62	34	34	32	1.0	aluminian ferrian sodian subsilicic augite
1426	293-1	Nandihar	Himalaya	53.43	0.56	1.47	10.95	0.43	12.83	21.67	0.28	0.59	102.21	70	37	18	45	2.0	augite
1426	325-1	Nandihar	Himalaya	49.13	1.73	4.09	15.41	0.50	13.70	15.81	0.11	0.76	101.25	68	40	26	33	1.5	aluminian ferrian augite
1426	344-1	Nandihar	Himalaya	51.29	0.40	4.01	22.43	0.85	20.24	0.14	0.14	0.00	99.49	62	61	39	0	1.5	aluminian (clino)enstatite
1426	370-1	Nandihar	Himalaya	50.67	0.31	3.35	23.46	0.61	19.48	0.36	0.43	0.37	99.04	61	59	41	1	1.4	aluminian (clino)enstatite
1426	381-1	Nandihar	Himalaya	50.19	0.29	3.37	23.18	0.51	20.45	0.40	0.24	0.43	99.07	64	60	39	1	1.5	aluminian (clino)enstatite
1426	388-1	Nandihar	Himalaya	53.49	0.29	1.68	9.46	0.46	13.27	21.56	0.23	0.71	101.14	74	39	16	45	2.4	diopside
1426	391-1	Nandihar	Himalaya	52.72	0.36	1.82	8.81	0.32	12.88	22.35	0.33	0.62	100.22	75	38	15	47	2.5	diopside
1426	401-1	Nandihar	Himalaya	52.55	0.53	1.71	14.90	0.29	24.55	1.93	0.11	0.20	96.76	75	71	25	4	2.9	(clino)enstatite
1426	423-1	Nandihar	Himalaya	52.64	0.54	1.05	8.75	0.28	13.23	22.60	0.29	0.83	100.19	80	38	15	47	2.6	diopside
1426	434-1	Nandihar	Himalaya	52.02	0.99	4.65	8.58	0.42	16.90	16.88	0.15	0.42	101.00	78	50	15	36	3.3	aluminian augite
1426	6-2	Nandihar	Himalaya	51.85	0.41	3.13	22.03	0.81	20.57	0.33	0.12	0.37	99.63	62	61	38	1	1.6	aluminian (clino)enstatite
1426	7-2	Nandihar	Himalaya	52.33	0.76	1.85	15.47	0.53	17.13	12.02	0.13	0.28	100.49	67	49	26	25	1.9	augite
1426	37-2	Nandihar	Himalaya	54.39	0.41	0.58	5.40	0.24	15.63	23.26	0.19	0.83	100.94	90	44	9	47	4.9	diopside
1426	50-2	Nandihar	Himalaya	49.80	0.92	5.43	10.64	0.40	12.24	18.71	0.32	1.32	99.78	75	38	19	42	2.0	aluminian ferrian augite
1426	71-2	Nandihar	Himalaya	54.07	0.30	0.34	8.47	0.59	12.57	24.45	0.15	0.00	100.93	73	36	14	50	2.5	diopside
1426	77-2	Nandihar	Himalaya	51.71	0.60	3.83	23.17	0.59	20.58	0.48	0.29	0.41	101.67	63	60	39	1	1.5	aluminian (clino)enstatite
1426	97-2	Nandihar	Himalaya	42.15	2.00	12.97	19.59	0.09	7.47	11.41	1.99	1.41	99.07	54	--------	--------	--------		aluminian ferrian sodian subsilicic unusual pyroxene
1426	275-2	Nandihar	Himalaya	54.26	0.48	1.99	1.66	0.50	17.29	24.50	0.27	0.68	101.63	100	48	3	49	14.1	diopside
1426	281-2	Nandihar	Himalaya	52.67	0.54	2.00	12.82	0.42	10.83	21.21	0.41	0.71	101.61	62	32	22	45	1.5	diopside
1426	287-2	Nandihar	Himalaya	52.40	1.20	1.64	11.92	0.46	16.63	16.29	0.27	0.52	101.33	76	47	20	33	2.4	augite
1426	327-2	Nandihar	Himalaya	52.38	0.63	2.25	7.66	0.34	14.14	21.76	0.19	0.49	99.84	78	41	13	46	3.1	diopside
1426	339-2	Nandihar	Himalaya	48.12	1.14	6.08	12.20	0.31	13.20	16.37	0.52	1.92	99.87	88	41	22	37	1.9	aluminian ferrian sodian augite
1426	354-2	Nandihar	Himalaya	51.03	0.90	4.36	9.82	0.44	15.06	17.73	0.17	0.69	100.21	77	45	17	38	2.6	aluminian augite
1426	355-2	Nandihar	Himalaya	50.37	1.77	4.04	12.42	0.34	13.93	15.49	0.17	0.61	99.15	67	43	22	35	1.9	aluminian augite
1426	358-2	Nandihar	Himalaya	42.77	1.15	12.08	15.58	0.52	10.11	10.49	0.92	1.86	95.49	67	38	34	28	1.1	aluminian ferrian sodian subsilicic augite
1426	403-2	Nandihar	Himalaya	52.90	0.50	0.93	11.46	0.32	11.99	22.50	0.24	0.74	101.57	70	34	19	47	1.8	diopside
1426	414-2	Nandihar	Himalaya	51.09	0.16	3.54	21.34	0.67	21.73	0.40	0.23	0.32	99.48	67	63	36	1	1.8	aluminian (clino)enstatite
1426	421-2	Nandihar	Himalaya	41.14	1.30	13.58	19.79	0.23	7.63	11.13	1.86	1.69	98.35	61	--------	--------	--------		aluminian ferrian sodian subsilicic unusual pyroxene
1426	427-2	Nandihar	Himalaya	51.16	0.54	1.63	8.78	0.37	12.87	22.15	0.16	0.52	98.19	76	38	15	47	2.5	diopside
1426	12-2	Nandihar	Himalaya	47.36	0.86	9.88	14.09	0.24	12.03	11.24	0.85	1.47	98.02	64	43	29	29	1.5	aluminian sodian augite
1426	102-1	Nandihar	Himalaya	51.55	0.64	1.81	14.95	0.51	14.46	17.26	0.22	0.45	101.85	70	41	24	35	1.7	ferrian augite
1426	148-1	Nandihar	Himalaya	40.13	0.63	15.02	14.40	0.25	10.68	11.48	1.42	2.18	96.19	99	--------	--------	--------		aluminian ferrian sodian subsilicic unusual pyroxene
1426	139-2	Nandihar	Himalaya	52.94	0.65	1.25	9.83	0.33	12.99	23.39	0.23	0.75	102.36	79	37	16	47	2.3	ferrian diopside
1426	118-2	Nandihar	Himalaya	51.08	1.23	3.53	15.98	0.51	13.82	15.85	0.25	0.49	102.73	64	40	27	33	1.5	aluminian augite
1426	153-2	Nandihar	Himalaya	52.03	0.59	2.70	11.44	0.44	12.54	20.58	0.31	0.78	101.41	71	37	20	44	1.9	aluminian augite
1426	156-1	Nandihar	Himalaya	54.07	0.20	1.16	0.62	0.33	17.45	25.34	0.09	0.38	99.63	100	48	1	50	32.5	wollastonite
1426	162-2	Nandihar	Himalaya	50.74	0.40	3.42	25.75	0.48	19.88	0.32	0.20	0.10	101.28	60	57	42	1	1.4	aluminian (clino)enstatite
1426	174-1	Nandihar	Himalaya	44.16	0.89	10.66	19.87	0.21	9.01	11.63	0.74	1.74	98.91	57	31	39	29	0.8	aluminian ferrian sodian subsilicic augite
1426	159-2	Nandihar	Himalaya	51.97	0.39	2.71	10.73	0.34	12.07	22.67	0.12	0.61	101.62	72	35	18	47	1.9	aluminian diopside
1426	183-2	Nandihar	Himalaya	47.37	1.21	4.88	14.03	0.37	11.14	16.78	0.28	0.61	96.66	62	36	26	39	1.4	aluminian augite
1426	180-1	Nandihar	Himalaya	50.24	1.07	3.84	14.21	0.48	14.97	16.02	0.14	0.40	101.37	71	43	24	33	1.8	aluminian augite
1426	174-2	Nandihar	Himalaya	42.06	1.31	11.54	18.95	0.49	9.03	10.25	0.91	2.31	96.83	66	--------	--------	--------		subsilicic aegirine-augite
1426	185-2	Nandihar	Himalaya	54.71	0.36	0.65	2.56	0.49	16.28	25.08	0.17	0.51	100.81	96	45	5	50	9.5	wollastonite
1426	187-1	Nandihar	Himalaya	51.49	0.67	1.06	14.86	0.60	11.50	22.18	0.32	0.55	103.23	69	32	24	44	1.3	ferrian diopside
1426	187-2	Nandihar	Himalaya	51.86	0.42	2.37	12.61	0.43	12.25	21.58	0.18	0.89	102.59	74	35	21	44	1.7	aluminian ferrian augite
1426	191-1	Nandihar	Himalaya	51.11	0.59	3.57	26.25	0.48	19.87	0.43	0.24	0.15	102.70	60	56	43	1	1.3	aluminian (clino)enstatite
1426	199-1	Nandihar	Himalaya	52.41	0.43	1.07	13.39	0.32	11.43	22.62	0.33	0.37	102.37	66	32	22	46	1.5	diopside
1426	198-2	Nandihar	Himalaya	51.15	0.38	3.39	24.97	0.60	20.57	0.30	0.14	0.14	101.64	62	59	41	1	1.4	aluminian (clino)enstatite
1426	199-2	Nandihar	Himalaya	49.31	0.71	4.08	15.48	0.58	10.18	20.24	0.48	1.12	102.19	69	30	27	43	1.1	aluminian ferrian augite
1426	202-1	Nandihar	Himalaya	51.77	0.45	3.47	23.03	0.59	22.59	0.13	0.15	0.31	102.48	68	63	37	0	1.7	aluminian ferrian (clino)enstatite
1426	209-2	Nandihar	Himalaya	52.65	0.83	3.11	12.09	0.40	15.98	15.98	0.20	0.64	101.89	73	46	20	33	2.3	aluminian augite
1426	221-2	Nandihar	Himalaya	50.94	0.81	3.09	13.87	0.52	11.28	20.77	0.40	0.71	102.39	67	33	24	44	1.4	aluminian ferrian augite
1426	254-2	Nandihar	Himalaya	38.26	0.14	20.01	32.19	0.94	2.44	8.23	0.21	0.00	102.42	13	--------	--------	--------		aluminian subsilicic unusual pyroxene
1426	262-2	Nandihar	Himalaya	51.78	0.65	2.11	11.40	0.52	12.64	22.72	0.41	0.61	102.85	78	35	19	46	1.9	ferrian diopside
1426	265-2	Nandihar	Himalaya	49.64	1.07	3.36	15.35	0.37	11.26	19.58	0.31	0.79	101.74	66	33	26	41	1.3	aluminian ferrian augite
1426	258-2	Nandihar	Himalaya	51.51	0.45	3.80	25.37	0.63	19.88	0.48	0.18	0.35	102.66	61	57	42	1	1.4	aluminian (clino)enstatite
1426	256-1	Nandihar	Himalaya	50.70	0.43	4.49	23.50	0.53	20.79	0.32	0.06	0.27	101.08	63	60	39	1	1.5	aluminian (clino)enstatite
1426	272-2	Nandihar	Himalaya	51.61	0.29	3.06	26.22	0.70	19.62	0.14	0.06	0.00	101.70	57	56	43	0	1.3	aluminian (clino)enstatite
1426	274-2	Nandihar	Himalaya	52.42	0.52	2.30	11.82	0.23	11.40	23.08	0.08	0.36	102.19	65	33	19	48	1.7	aluminian diopside

Sample	Points	River/Dune	Domain	SiO_2	TiO_2	Al_2O_3	FeO	MnO	MgO	CaO	K_2O	Na_2O	Total	Mg#	En	Fs	Wo	En/Fs	Name
				wt%	wt%	wt%	wt%	wt%	wt%	wt%	wt%	wt%							
1432	18-1	Astor	Nanga Parbat	51.91	0.52	0.61	4.49	0.32	15.14	25.51	0.28		98.78	94	42	7	51	5.6	wollastonite
1432	36-1	Astor	Nanga Parbat	42.93	0.70	13.56	19.67	0.46	8.13	11.43	0.95	1.02	98.86	50	29	41	30	0.7	aluminian ferrian subsilicic augite
1432	62-1	Astor	Nanga Parbat	48.43	0.78	3.00	11.50	0.48	10.77	24.81	0.19		99.97	75	30	19	50	1.6	aluminian ferrian wollastonite
1432	68-1	Astor	Nanga Parbat	49.81	0.34	2.16	13.19	0.39	9.61	24.40	0.14		100.04	62	28	22	50	1.3	wollastonite
1432	103-1	Astor	Nanga Parbat	43.71	0.66	14.64	18.08	1.02	10.19	10.37	0.81	1.84	101.30	66	36	38	26	1.0	aluminian ferrian sodian subsilicic augite
1432	104-1	Astor	Nanga Parbat	51.17	0.38	0.62	8.63	0.86	12.68	25.77	0.20		100.30	84	35	15	51	2.4	ferrian wollastonite
1432	135-1	Astor	Nanga Parbat	41.25	0.60	15.77	17.71	0.67	8.74	11.07	0.74	1.71	98.25	63	-----	-----	-----		aluminian ferrian sodian subsilicic unusual pyroxene
1432	162-1	Astor	Nanga Parbat	51.72	0.75	0.98	4.85	0.47	14.63	25.64	0.13		99.18	91	41	8	51	4.9	wollastonite
1432	171-1	Astor	Nanga Parbat	49.50	0.54	0.76	14.32	0.46	9.50	25.90	0.25		101.24	67	26	23	51	1.1	ferrian wollastonite
1432	235-1	Astor	Nanga Parbat	53.09	0.68	0.65	3.16	0.39	15.84	26.87	0.40		101.08	100	43	5	52	7.9	wollastonite
1432	316-1	Astor	Nanga Parbat	52.43	0.56	0.77	3.37	0.45	15.79	26.01	0.15		99.52	97	43	6	51	7.4	wollastonite
1432	317-1	Astor	Nanga Parbat	51.60	0.34	1.45	5.45	0.39	14.88	24.72	0.17		99.00	90	41	9	49	4.5	diopside
1432	343-1	Astor	Nanga Parbat	50.75	0.35	1.19	28.99	0.47	17.31	1.14	0.11		100.32	53	50	48	2	1.0	(clino)enstatite
1432	345-1	Astor	Nanga Parbat	43.03	1.08	10.86	21.42	1.07	9.29	11.59	1.85	1.77	101.95	73	-----	-----	-----		aluminian ferrian sodian subsilicic unusual pyroxene
1432	401-1	Astor	Nanga Parbat	51.12	0.30	0.85	12.67	0.57	10.63	25.51	0.17		101.83	69	29	20	50	1.4	ferrian wollastonite
1432	473-1	Astor	Nanga Parbat	53.46	0.48	0.72	7.18	0.35	13.59	24.80	0.00	0.41	101.01	80	38	12	50	3.2	wollastonite
1432	523-1	Astor	Nanga Parbat	51.85	0.37	0.52	3.79	0.37	14.90	25.55	0.21		97.57	93	42	7	52	6.4	wollastonite
1432	527-1	Astor	Nanga Parbat	51.81	0.43	0.60	21.10	0.66	5.02	23.54	0.22	0.35	103.73	31	15	36	50	0.4	hedenbergite
1432	69-2	Astor	Nanga Parbat	52.03	0.55	0.70	6.00	0.71	13.24	24.95	0.34		98.52	81	38	11	51	3.5	wollastonite
1432	153-2	Astor	Nanga Parbat	51.49	0.28	0.20	8.77	0.26	12.75	25.86	0.17		99.77	81	35	14	51	2.5	ferrian wollastonite
1432	162-2	Astor	Nanga Parbat	55.29	0.19	0.63	2.08	0.26	15.88	26.22	0.12	0.29	100.95	93	44	4	52	12.1	wollastonite
1432	166-2	Astor	Nanga Parbat	54.95	0.32	1.05	7.24	0.75	13.15	23.79	0.17	0.41	101.84	76	38	13	49	2.9	diopside
1432	201-2	Astor	Nanga Parbat	51.02	0.47	0.39	20.39	0.66	5.99	22.58	0.13	0.24	101.86	35	18	35	48	0.5	hedenbergite
1432	207-2	Astor	Nanga Parbat	54.09	0.36	0.73	5.16	0.47	14.36	24.47	0.28	0.42	100.35	84	41	9	50	4.5	wollastonite
1432	238-2	Astor	Nanga Parbat	42.24	1.02	10.94	23.00	0.36	6.23	12.08	1.51	1.22	98.61	44	22	47	31	0.5	aluminian ferrian subsilicic augite
1432	391-2	Astor	Nanga Parbat	55.33	0.31	0.30	3.68	0.23	15.42	25.43	0.17	0.29	101.16	88	43	6	51	7.0	wollastonite
1432	401-2	Astor	Nanga Parbat	54.96	0.45	1.26	2.79	0.35	15.92	25.42	0.28	0.29	101.72	92	44	5	51	9.0	wollastonite
1432	403-2	Astor	Nanga Parbat	48.29	0.43	0.72	21.81	0.44	5.09	23.96	0.24		100.98	35	15	36	49	0.4	ferrian wollastonite
1432	449-2	Astor	Nanga Parbat	55.47	0.33	0.99	4.14	0.34	14.68	25.08	0.15	0.37	101.55	86	42	7	51	5.8	wollastonite
1432	486-2	Astor	Nanga Parbat	41.30	1.28	12.70	23.89	0.57	4.97	11.83	1.90	1.04	99.48	37	-----	-----	-----		aluminian ferrian subsilicic unusual pyroxene
1432	509-2	Astor	Nanga Parbat	54.76	0.21	1.70	5.41	0.26	13.91	24.16	0.11	0.59	101.11	82	40	9	50	4.4	wollastonite
1432	527-2	Astor	Nanga Parbat	50.79	0.31	0.38	7.95	0.68	13.32	25.10	0.15		98.69	86	37	13	50	2.7	ferrian wollastonite
1432	542-2	Astor	Nanga Parbat	51.40	0.36	1.35	5.01	0.52	14.41	24.61	0.20		97.87	88	41	9	50	4.6	wollastonite
1462	18	Mankera	Thal	53.28		2.79	9.80	0.17	13.68	22.67			102.40	71	38	16	46	2.4	aluminian diopside
1462	91	Mankera	Thal	54.16		2.49	2.25	0.19	15.46	24.07			98.62	92	45	4	51	11.3	aluminian wollastonite
1462	119	Mankera	Thal	53.09		0.53	8.63	0.27	12.74	24.01			99.27	72	36	14	49	2.6	diopside
1462	138	Mankera	Thal	52.10		4.83	8.67	0.14	11.31	20.05			97.09	70	37	16	47	2.3	aluminian diopside
1462	178	Mankera	Thal	51.60		2.03	5.18	0.13	14.80	22.91			96.66	84	43	9	48	5.0	diopside
1462	195	Mankera	Thal	50.98		2.56	26.17	0.37	19.35	0.64			100.08	58	56	43	1	1.3	aluminian (clino)enstatite
1462	230	Mankera	Thal	54.83		0.38	4.67	0.23	15.96	25.30			101.36	86	43	7	49	5.8	diopside
1462	272	Mankera	Thal	53.45		2.04	11.63	0.24	12.89	21.91			102.16	66	37	19	45	1.9	augite
1462	294	Mankera	Thal	51.88		4.32	5.37	0.19	15.39	23.30			100.46	86	44	9	47	4.9	aluminian diopside
1462	301	Mankera	Thal	53.05		1.48	11.20	0.32	12.32	22.48			100.85	66	35	19	46	1.9	diopside
1462	329	Mankera	Thal	54.91		0.69	25.53	0.56	21.39	1.06			104.15	60	58	40	2	1.5	(clino)enstatite
1462	368	Mankera	Thal	56.27		1.66	2.84	0.15	17.97	25.02			103.91	92	48	4	48	10.7	diopside
1462	421	Mankera	Thal	52.59		3.66	7.03	0.19	14.99	23.27			101.74	81	42	11	47	3.7	aluminian diopside
1462	429	Mankera	Thal	53.32		2.87	25.19	0.55	21.37	0.62			103.92	61	59	40	1	1.5	aluminian (clino)enstatite
1462	437	Mankera	Thal	54.18		2.97	10.45	0.25	13.75	22.74			104.35	70	38	17	45	2.3	aluminian diopside
1462	528	Mankera	Thal	53.92		1.45	11.70	0.18	11.65	24.23			103.13	64	33	19	49	1.7	diopside
1462	545	Mankera	Thal	54.76		0.85	24.69	0.45	22.02	0.95			103.72	62	60	38	2	1.6	(clino)enstatite
1462	573	Mankera	Thal	52.73		2.21	10.60	0.20	13.22	21.84			100.80	69	38	17	45	2.2	augite
1462	581	Mankera	Thal	52.74		2.44	23.73	0.31	21.32	0.65			101.19	62	60	38	1	1.6	aluminian (clino)enstatite
1462	592	Mankera	Thal	54.75		0.59	3.15	0.17	16.77	24.86			100.29	90	46	5	49	9.0	diopside
1462	600	Mankera	Thal	49.84		3.64	25.92	0.40	18.19	1.55			99.55	57	53	43	3	1.2	aluminian (clino)enstatite
1462	659	Mankera	Thal	51.27		2.18	9.13	0.21	13.68	21.65			98.12	73	40	15	45	2.6	diopside
1462	682	Mankera	Thal	50.84		2.92	7.45	0.14	14.44	22.04			97.83	79	42	12	46	3.4	aluminian diopside
1462	702	Mankera	Thal	52.57		0.71	8.34	0.50	13.01	23.40			98.53	74	37	14	48	2.6	diopside
1462	706	Mankera	Thal	50.75		3.34	9.12	0.15	14.54	19.78			97.68	74	43	15	42	2.8	aluminian augite
1462	737	Mankera	Thal	53.85		1.12	4.19	0.20	15.75	24.59			99.71	87	44	7	49	6.4	diopside
1462	754	Mankera	Thal	53.02		0.44	10.71	0.30	12.88	22.44			99.80	68	37	18	46	2.1	diopside
1462	755	Mankera	Thal	53.17		0.75	8.70	0.21	12.53	24.28			99.64	72	36	14	50	2.5	diopside
1462	768	Mankera	Thal	50.83		3.70	9.95	0.24	12.91	21.67			99.31	70	38	17	46	2.3	aluminian diopside
1462	809	Mankera	Thal	50.74		3.69	9.65	0.16	12.37	21.67			98.27	70	37	16	47	2.2	aluminian diopside
1462	813	Mankera	Thal	51.13		3.71	10.77	0.17	12.38	19.31			97.47	67	38	19	43	2.0	aluminian augite
1462	831	Mankera	Thal	54.06		1.93	22.93	0.37	23.34	0.74			103.37	66	63	35	1	1.8	(clino)enstatite
1462	896	Mankera	Thal	50.85		2.22	27.55	0.39	18.66	0.75			100.42	56	54	45	2	1.2	(clino)enstatite
1462	905	Mankera	Thal	50.99		4.09	5.78	0.17	31.41	0.67			93.10	93	89	9	1	9.4	aluminian (clino)enstatite
1462	916	Mankera	Thal	53.81		2.19	10.65	0.16	13.33	22.99			103.13	69	37	17	46	2.2	diopside
1462	917	Mankera	Thal	56.00		1.13	2.42	0.13	17.98	25.17			102.82	93	48	4	48	12.6	diopside
1462	940	Mankera	Thal	52.32		4.36	11.80	0.32	11.61	22.29			102.70	64	34	20	47	1.7	aluminian diopside
1462	950	Mankera	Thal	52.19		4.46	9.89	0.23	13.81	21.52			102.10	71	40	16	44	2.4	aluminian augite
1462	967	Mankera	Thal	51.40		3.48	5.56	0.16	15.34	23.75			99.69	89	43	9	48	4.8	aluminian diopside
1462	968	Mankera	Thal	53.41		1.23	21.27	0.53	23.38	0.66			100.47	67	65	34	1	1.9	(clino)enstatite
1462	979	Mankera	Thal	54.29		2.00	4.31	0.20	16.89	24.71			102.40	91	45	7	48	6.7	diopside
1462	992	Mankera	Thal	54.10		1.42	10.65	0.47	12.28	24.07			102.98	67	34	17	48	2.0	diopside
1462	1014	Mankera	Thal	54.86		0.89	5.89	0.22	15.25	24.77			101.87	82	42	9	49	4.4	diopside
1462	1015	Mankera	Thal	52.25		0.71	11.16	0.19	11.17	23.88			99.37	64	32	18	49	1.8	diopside
1462	1037	Mankera	Thal	53.51		1.22	5.38	0.19	15.07	23.99			99.36	83	43	9	49	4.8	diopside
1462	1039	Mankera	Thal	52.21		1.48	8.10	0.11	14.08	22.66			98.64	76	40	13	47	3.1	diopside
1462	1041	Mankera	Thal	51.64		1.72	6.29	0.29	14.43	23.51			97.89	82	41	11	48	3.9	diopside
1462	1047	Mankera	Thal	54.03		1.12	12.24	0.17	29.56	0.72			97.85	83	80	19	1	4.2	(clino)enstatite
1462	1050	Mankera	Thal	52.56		2.51	8.93	0.33	11.90	21.91			98.15	70	36	16	48	2.3	aluminian diopside
1462	1069	Mankera	Thal	52.85		1.58	22.44	0.47	22.50	0.55			100.38	65	63	36	1	1.8	(clino)enstatite
1462	1078	Mankera	Thal	49.31		1.93	30.40	0.52	15.80	0.77			98.74	49	47	51	2	0.9	(clino)ferrosilite
1462	1080	Mankera	Thal	53.16		2.20	4.75	0.18	16.08	23.63			100.01	87	45	8	47	5.8	diopside
1462	1138	Mankera	Thal	52.01		1.42	8.94	0.30	13.39	22.56			98.62	73	38	15	47	2.6	diopside
1462	1154	Mankera	Thal	56.00		0.22	0.61	0.10	19.29	25.56			101.78	100	51	1	48	48.3	diopside
1462	1166	Mankera	Thal	50.71		3.30	24.47	0.26	20.04	0.34			99.12	60	59	41	1	1.4	aluminian (clino)enstatite
1462	1167	Mankera	Thal	52.15		4.30	8.65	0.09	11.46	22.38			99.02	70	35	15	50	2.3	aluminian diopside
1462	1171	Mankera	Thal	52.31		1.39	10.00	0.15	11.54	23.98			99.36	67	33	17	50	2.0	diopside
1462	1212	Mankera	Thal	52.25		2.51	23.69	0.35	21.39	0.70			100.89	62	60	38	1	1.6	aluminian (clino)enstatite
1462	1216	Mankera	Thal	53.53		1.87	3.48	0.12	16.78	23.91			99.69	90	47	6	48	8.3	diopside
1462	1226	Mankera	Thal	49.63		3.98	10.03	0.21	12.38	21.64			97.87	70	37	17	46	2.2	aluminian diopside
1462	1284	Mankera	Thal	53.72		1.44	29.12	0.56	18.95	0.81			104.61	54	52	46	2	1.1	(clino)enstatite
1462	1299	Mankera	Thal	55.07		2.36	22.45	0.32	23.76	1.18			105.13	66	64	34	2	1.9	(clino)enstatite
1462	1313	Mankera	Thal	46.04		0.56	2.95	0.24	13.19	24.22			87.19	99	41	6	54	7.4	wollastonite
1462	1324	Mankera	Thal	54.13		0.67	12.12	0.35	11.60	24.46			103.34	63	32	19	49	1.7	diopside
1462	1326	Mankera	Thal	54.59		1.07	22.22	0.49	23.56	1.12			103.05	66	63	34	2	1.8	(clino)enstatite
1462	1341	Mankera	Thal	54.79		0.68	26.20	0.54	21.03	0.82			104.05	59	57	41	2	1.4	(clino)enstatite

Sample	Points	River/Dune	Domain	SiO_2	TiO_2	Al_2O_3	FeO	MnO	MgO	CaO	K_2O	Na_2O	Total	Mg#	En	Fs	Wo	En/Fs	Name
				wt%	wt%	wt%	wt%	wt%	wt%	wt%	wt%	wt%							
1463	8	Haidarabad	Thal	52.31	0.22	2.00	18.69	0.30	23.95	0.66	0.12	0.31	98.55	71	68	30	1	2.2	(clino)enstatite
1463	35	Haidarabad	Thal	50.50	0.45	2.82	20.93	0.44	21.99	0.78	0.25	0.44	98.60	69	64	35	2	1.8	aluminian ferrian (clino)enstatite
1463	65	Haidarabad	Thal	49.69	0.16	1.95	4.46	0.41	19.11	15.97	0.07	0.26	92.08	91	57	8	34	7.0	augite
1463	74	Haidarabad	Thal	49.23	0.59	1.13	16.55	0.39	22.09	2.23	0.20	0.27	92.67	73	67	29	5	2.3	(clino)enstatite
1463	87	Haidarabad	Thal	49.87	0.46	0.69	8.01	0.31	12.76	22.08	0.24	0.38	94.81	79	38	14	48	2.7	diopside
1463	89	Haidarabad	Thal	48.80	0.00	2.35	17.39	0.30	22.72	0.41	0.00	0.14	92.11	71	69	30	1	2.3	aluminian (clino)enstatite
1463	93	Haidarabad	Thal	49.48	1.04	3.52	6.66	0.35	14.89	20.74	0.16	0.66	97.52	90	44	12	44	3.8	aluminian ferrian augite
1463	134	Haidarabad	Thal	49.33	0.55	4.78	9.88	0.36	11.87	20.30	0.31	1.07	98.44	78	37	18	45	2.1	aluminian ferrian diopside
1463	150	Haidarabad	Thal	49.59	0.43	3.65	8.57	0.43	12.90	20.95	0.15	0.84	97.51	82	39	15	46	2.6	aluminian ferrian diopside
1463	204	Haidarabad	Thal	51.12	0.59	2.01	21.56	0.41	21.59	1.04	0.46	0.20	98.98	67	62	36	2	1.8	(clino)enstatite
1463	276	Haidarabad	Thal	52.85	0.55	1.73	17.49	0.32	24.67	0.98	0.29	0.35	99.23	74	70	28	2	2.5	(clino)enstatite
1463	277	Haidarabad	Thal	47.40	0.59	7.23	20.41	0.46	8.53	11.10	0.73	0.95	97.39	43	30	42	28	0.7	aluminian augite
1463	281	Haidarabad	Thal	52.21	0.23	2.47	18.02	0.49	25.04	0.94	0.22	0.29	99.91	76	69	29	2	2.4	aluminian ferrian (clino)enstatite
1463	284	Haidarabad	Thal	53.41	0.26	0.00	1.85	0.31	17.90	24.53	0.32	0.35	98.92	100	49	3	48	14.6	diopside
1463	320	Haidarabad	Thal	49.06	4.44	2.80	8.25	0.37	11.86	20.07	0.44	1.26	98.55	72	38	16	46	2.5	aluminian titanian diopside
1463	355	Haidarabad	Thal	52.01	0.54	1.50	9.80	0.41	14.03	20.74	0.32	0.86	100.21	81	40	17	43	2.4	ferrian augite
1463	394	Haidarabad	Thal	51.52	0.32	2.29	7.20	0.20	14.08	20.94	0.17	0.91	97.63	83	42	12	45	3.4	aluminian diopside
1463	411	Haidarabad	Thal	49.77	1.03	2.91	7.65	0.36	15.01	18.54	0.34	0.66	96.28	83	46	14	41	3.3	aluminian augite
1463	413	Haidarabad	Thal	53.10	0.42	1.43	1.11	0.27	18.70	23.12	0.34	0.61	99.11	100	52	2	46	23.9	diopside
1463	416	Haidarabad	Thal	51.37	0.75	1.90	10.53	0.33	13.39	19.37	0.23	0.58	98.46	71	40	18	42	2.2	augite
1463	484	Haidarabad	Thal	50.54	0.70	1.88	10.61	0.30	13.70	19.67	0.27	0.55	98.20	76	40	18	42	2.2	augite
1463	576	Haidarabad	Thal	51.18	0.32	2.36	22.24	0.54	21.93	0.80	0.14	0.19	99.71	67	62	36	2	1.7	aluminian (clino)enstatite
1463	586	Haidarabad	Thal	53.51	0.33	2.26	3.87	0.25	17.32	22.54	0.22	0.30	100.60	93	48	6	45	7.5	diopside
1463	597	Haidarabad	Thal	51.41	0.29	2.35	21.64	0.53	21.21	0.83	0.29	0.30	98.86	65	62	36	2	1.7	aluminian (clino)enstatite
1463	600	Haidarabad	Thal	48.08	1.04	8.75	8.65	0.38	10.72	19.98	0.24	2.08	99.93	87	36	17	48	2.1	aluminian ferrian sodian diopside
1463	606	Haidarabad	Thal	52.11	0.33	2.99	7.76	0.23	14.85	20.40	0.23	0.61	99.51	81	44	13	43	3.3	aluminian augite
1463	640	Haidarabad	Thal	52.06	0.36	1.76	7.09	0.30	14.20	21.76	0.15	1.02	98.69	87	42	12	46	3.4	diopside
1463	652	Haidarabad	Thal	53.66	0.70	1.89	16.01	0.42	26.31	0.64	0.30	0.32	100.25	77	73	26	1	2.9	(clino)enstatite
1463	659	Haidarabad	Thal	54.18	0.49	0.57	3.41	0.26	16.93	23.93	0.00	0.52	100.30	95	47	6	48	8.2	diopside
1463	685	Haidarabad	Thal	51.45	0.85	2.60	7.22	0.38	15.09	21.64	0.31	0.36	99.92	85	43	12	45	3.5	aluminian augite
1463	687	Haidarabad	Thal	51.39	0.37	2.41	22.07	0.40	20.73	0.72	0.22	0.09	98.41	63	61	37	2	1.6	aluminian (clino)enstatite
1463	689	Haidarabad	Thal	50.53	0.38	2.44	25.34	0.73	19.25	0.75	0.29	0.45	100.16	61	56	43	2	1.3	aluminian ferrian (clino)enstatite
1463	703	Haidarabad	Thal	49.47	0.78	6.19	5.78	0.33	14.72	22.66	0.24	0.77	100.95	100	43	10	47	4.3	aluminian ferrian diopside
1463	706	Haidarabad	Thal	52.17	0.40	0.71	13.29	0.41	9.19	22.97	0.24	0.23	99.61	55	28	23	49	1.2	diopside
1463	719	Haidarabad	Thal	49.98	0.75	4.02	9.74	0.41	12.89	21.04	0.24	1.16	100.24	85	38	17	45	2.3	aluminian ferrian augite
1463	742	Haidarabad	Thal	50.28	0.38	2.41	23.76	0.51	19.63	0.85	0.32	0.16	98.32	61	58	40	2	1.4	aluminian (clino)enstatite
1463	752	Haidarabad	Thal	52.14	0.13	0.92	22.16	0.10	21.44	0.76	0.00	0.40	98.04	64	62	36	2	1.7	(clino)enstatite
1463	756	Haidarabad	Thal	50.62	0.75	1.30	23.40	0.60	18.37	2.12	0.23	0.31	97.70	59	55	40	5	1.4	(clino)enstatite
1463	770	Haidarabad	Thal	51.08	0.48	2.54	22.56	0.45	20.41	0.71	0.09	0.26	98.59	62	60	38	2	1.6	aluminian (clino)enstatite
1463	783	Haidarabad	Thal	51.82	0.79	3.61	9.12	0.30	12.86	20.98	0.23	0.71	100.41	73	39	16	45	2.4	aluminian diopside
1463	812	Haidarabad	Thal	51.00	0.55	3.76	7.61	0.28	14.13	20.37	0.08	0.87	98.66	82	43	13	44	3.2	aluminian augite
1463	814	Haidarabad	Thal	52.72	0.44	1.57	7.53	0.31	18.66	17.56	0.23	0.18	99.20	85	52	12	35	4.2	augite
1463	907	Haidarabad	Thal	52.71	0.31	1.06	9.26	0.85	13.23	21.20	0.21	0.89	99.73	77	39	17	45	2.3	augite
1463	909	Haidarabad	Thal	51.40	0.33	2.82	22.75	0.53	20.82	0.82	0.10	0.46	100.04	64	60	38	2	1.6	aluminian (clino)enstatite
1463	919	Haidarabad	Thal	55.91	0.36	1.86	10.41	0.37	17.91	13.70	0.26	0.39	101.18	75	53	18	29	3.0	augite
1463	998	Haidarabad	Thal	49.56	0.31	3.91	10.20	0.33	11.38	21.24	0.19	1.04	98.17	76	35	18	47	1.9	aluminian ferrian diopside
1463	1008	Haidarabad	Thal	52.53	0.45	1.44	10.19	0.53	12.84	22.12	0.25	0.44	100.79	73	37	17	46	2.1	diopside
1463	1019	Haidarabad	Thal	51.23	0.38	2.46	9.77	0.41	12.63	20.76	0.30	0.68	98.62	74	38	17	45	2.2	aluminian augite
1463	1026	Haidarabad	Thal	51.20	0.41	0.87	24.29	0.69	18.92	1.64	0.24	0.18	98.46	59	55	41	3	1.3	(clino)enstatite
1463	1071	Haidarabad	Thal	55.23	0.27	0.47	3.08	0.22	17.31	24.15	0.33	0.27	101.35	94	47	5	48	9.3	diopside
1463	1077	Haidarabad	Thal	51.45	0.18	1.68	25.47	0.55	20.17	0.79	0.30	0.12	100.72	61	57	41	2	1.4	(clino)enstatite
1463	1092	Haidarabad	Thal	50.81	0.38	2.05	23.19	0.50	21.59	0.78	0.31	0.26	99.87	67	61	38	2	1.6	ferrian (clino)enstatite
1463	1143	Haidarabad	Thal	52.27	0.16	1.11	9.67	0.51	10.89	23.17	0.14	0.53	98.46	67	33	17	50	1.9	wollastonite
1463	1146	Haidarabad	Thal	51.34	0.41	2.51	24.75	0.44	20.20	0.89	0.21	0.16	100.92	61	58	40	2	1.4	aluminian (clino)enstatite
1463	1161	Haidarabad	Thal	52.41	0.47	3.98	7.31	0.13	12.97	21.22	0.18	1.24	99.92	78	40	13	47	3.1	aluminian diopside
1463	1236	Haidarabad	Thal	52.06	0.43	1.88	9.25	0.33	12.75	21.19	0.39	0.00	98.28	71	38	16	46	2.4	diopside
1463	1308	Haidarabad	Thal	51.35	0.41	1.69	22.00	0.43	22.01	0.85	0.29	0.37	99.40	68	63	36	2	1.7	ferrian (clino)enstatite
1463	1323	Haidarabad	Thal	52.91	0.49	0.90	9.67	0.30	12.07	22.81	0.26	0.92	100.32	74	35	16	48	2.2	diopside
1463	1418	Haidarabad	Thal	51.22	0.75	4.23	8.06	0.28	12.86	20.77	0.40	0.66	99.23	75	40	14	46	2.7	aluminian diopside
1463	1503	Haidarabad	Thal	53.29	0.41	0.87	8.92	0.38	13.89	22.51	0.17	0.18	100.62	74	39	15	46	2.7	diopside
1463	1556	Haidarabad	Thal	52.09	0.35	2.67	9.36	0.40	13.10	21.41	0.36	0.23	99.97	72	39	16	45	2.4	aluminian diopside
1463	1602	Haidarabad	Thal	53.47	0.68	0.99	3.51	0.29	15.78	23.60	0.52	0.53	99.37	94	45	6	49	7.4	diopside
1463	1651	Haidarabad	Thal	51.33	0.36	2.28	20.23	0.46	23.04	0.70	0.26	0.26	98.90	70	66	33	1	2.0	(clino)enstatite
1463	1687	Haidarabad	Thal	43.18	0.47	29.18	3.66	0.12	0.38	20.19	0.61	1.45	99.24	16	------------------------				aluminian sodian subsilicic unusual pyroxene
1470	230	Muzaffarghar	Thal	51.84	0.19	0.57	12.17	0.30	11.07	24.58	0.00	0.25	100.97	68	31	20	49	1.6	wollastonite
1470	295	Muzaffarghar	Thal	51.25	0.43	2.00	10.11	0.77	13.20	22.17	0.28	0.79	100.99	84	37	17	45	2.2	ferrian diopside
1470	344	Muzaffarghar	Thal	54.84	0.61	0.68	2.52	0.24	16.35	24.85	0.28	0.21	100.57	92	46	4	50	10.5	diopside
1470	375	Muzaffarghar	Thal	50.67	0.21	2.57	11.53	0.35	11.69	22.34	0.18	0.55	100.08	73	34	19	47	1.8	aluminian ferrian diopside
1470	392	Muzaffarghar	Thal	50.82	0.35	0.51	11.42	0.41	11.65	24.62	0.18	0.26	100.23	76	32	18	49	1.8	ferrian wollastonite
1470	395	Muzaffarghar	Thal	50.87	0.67	3.83	8.61	0.20	13.54	21.76	0.23	0.79	100.49	83	40	14	46	2.7	aluminian ferrian diopside
1470	490	Muzaffarghar	Thal	51.14	0.81	1.44	11.84	1.01	12.27	21.32	0.29	0.66	100.79	74	35	21	44	1.7	ferrian augite
1470	612	Muzaffarghar	Thal	51.72	0.41	2.34	21.37	0.35	22.05	0.99	0.39	0.26	99.87	68	63	35	2	1.8	aluminian (clino)enstatite
1470	666	Muzaffarghar	Thal	53.06	0.18	0.22	1.49	0.32	17.38	26.05	0.33	0.24	99.28	100	47	3	50	16.9	wollastonite
1470	696	Muzaffarghar	Thal	50.49	0.57	3.54	10.01	0.40	12.11	22.05	0.15	0.63	99.95	75	36	17	47	2.1	aluminian diopside
1470	698	Muzaffarghar	Thal	50.66	0.21	3.00	25.65	0.41	19.44	0.80	0.22	0.42	100.80	61	56	42	2	1.3	aluminian ferrian (clino)enstatite
1470	760	Muzaffarghar	Thal	50.31	0.52	2.98	24.58	0.89	19.49	0.89	0.29	0.33	100.28	62	57	42	2	1.4	aluminian (clino)enstatite
1470	773	Muzaffarghar	Thal	50.84	0.29	4.22	17.15	0.57	25.84	0.46	0.20	0.09	99.66	78	72	28	1	2.6	aluminian ferrian (clino)enstatite
1470	801	Muzaffarghar	Thal	53.70	0.19	0.49	4.59	0.39	15.48	25.50	0.32	0.30	100.95	95	42	8	50	5.5	wollastonite
1470	851	Muzaffarghar	Thal	50.69	0.74	1.97	10.42	1.00	12.16	22.46	0.26	0.48	100.18	76	35	18	46	1.9	ferrian diopside
1470	958	Muzaffarghar	Thal	49.30	0.81	3.60	9.79	0.70	12.89	22.08	0.26	0.84	100.28	88	37	17	46	2.2	aluminian ferrian diopside
1470	1002	Muzaffarghar	Thal	49.93	0.69	5.26	9.19	0.27	11.71	22.43	0.21	1.44	101.13	87	35	16	49	2.2	aluminian ferrian sodian diopside
1470	1006	Muzaffarghar	Thal	49.35	0.54	2.55	26.83	0.35	19.93	0.85	0.24	0.29	100.92	63	56	43	2	1.3	aluminian ferrian (clino)enstatite
1470	1214	Muzaffarghar	Thal	51.95	0.36	1.96	4.25	0.56	16.04	24.78	0.13	0.28	100.31	100	44	7	49	5.9	ferrian diopside
1470	1280	Muzaffarghar	Thal	52.13	0.55	0.40	24.51	0.57	21.20	1.06	0.21	0.29	100.92	64	59	39	2	1.5	ferrian (clino)enstatite
1470	1313	Muzaffarghar	Thal	54.92	0.24	0.75	4.78	0.31	15.42	23.77	0.19	0.48	100.87	85	44	8	48	5.4	diopside
1470	1314	Muzaffarghar	Thal	52.09	0.47	0.99	12.42	0.79	12.26	22.05	0.16	0.36	101.59	69	35	21	45	1.7	diopside
1470	1487	Muzaffarghar	Thal	52.41	0.75	1.55	20.77	0.45	22.72	0.95	0.19	0.26	100.04	68	64	34	2	1.9	(clino)enstatite
1470	1559	Muzaffarghar	Thal	51.57	0.60	1.45	11.61	0.56	12.00	22.00	0.29	0.42	100.49	70	35	20	46	1.8	diopside
1470	1607	Muzaffarghar	Thal	53.15	0.22	0.32	0.99	0.19	18.68	25.17	0.14	0.32	99.20	100	50	2	48	27.9	diopside
1470	1611	Muzaffarghar	Thal	51.44	0.57	1.43	9.81	0.41	13.42	22.17	0.23	0.74	100.22	82	38	16	45	2.3	ferrian diopside
1470	1627	Muzaffarghar	Thal	52.51	0.46	0.83	5.93	0.33	14.16	24.02	0.21	0.46	98.90	86	41	10	49	4.0	diopside
1470	1703	Muzaffarghar	Thal	49.84	0.25	3.40	26.30	0.37	18.83	0.80	0.22	0.30	100.32	60	55	44	2	1.3	aluminian ferrian (clino)enstatite
1470	1800	Muzaffarghar	Thal	49.89	0.58	2.40	26.22	0.27	18.94	0.84	0.24	0.34	99.71	60	55	43	2	1.3	aluminian ferrian (clino)enstatite
1470	1832	Muzaffarghar	Thal	51.32	0.76	3.61	9.21	0.29	12.34	21.97	0.23	0.75	100.48	75	37	16	47	2.3	aluminian diopside
1470	1866	Muzaffarghar	Thal	50.12	0.67	3.39	12.03	0.55	12.33	20.42	0.30	0.94	100.76	77	36	21	43	1.7	aluminian ferrian augite
1470	1870	Muzaffarghar	Thal	50.63	0.81	2.98	10.54	0.25	12.10	21.38	0.19	0.51	99.38	70	36	18	46	2.0	aluminian diopside
1470	1974	Muzaffarghar	Thal	50.89	0.45	0.77	30.55	0.60	15.82	1.58	0.28	0.00	100.94	49	46	51	3	0.9	(clino)ferrosilite
1470	1988	Muzaffarghar	Thal	51.75	0.41	1.78	6.78	0.30	14.67	23.28	0.24	0.50	99.71	90	41	11	47	3.7	ferrian diopside
1470	2079	Muzaffarghar	Thal	50.79	0.56	2.18	24.90	0.42	20.41	0.77	0.30	0.47	100.81	64	58	40	2	1.4	ferrian (clino)enstatite
1470	2125	Muzaffarghar	Thal	51.09	0.57	1.63	26.03	0.47	19.82	0.92	0.13	0.00	100.66	59	56	42	2	1.3	(clino)enstatite
1470	2276	Muzaffarghar	Thal	50.77	0.52	2.51	20.94	0.41	22.08	0.96	0.23	0.46	98.88	69	64	34	2	1.8	aluminian ferrian (clino)enstatite
1470	2413	Muzaffarghar	Thal	51.63	0.45	2.24	22.63	0.38	21.84	0.70	0.11	0.27	100.26	66	62	37	1	1.7	(clino)enstatite
1470	2451	Muzaffarghar	Thal	52.07	0.42	1.60	22.44	0.29	22.11	0.55	0.28	0.20	99.97	66	63	36	1	1.7	(clino)enstatite
1470	2570	Muzaffarghar	Thal	51.08	0.76	3.73	8.37	0.32	13.08	22.52	0.18	0.72	100.76	81	38	14	47	2.7	aluminian diopside
1470	2603	Muzaffarghar	Thal	52.63	0.23	2.44	20.11	0.17	24.44	0.85	0.13	0.00	101.01	71	67	31	2	2.1	aluminian (clino)enstatite
1470	2636	Muzaffarghar	Thal	47.96	1.37	9.51	7.47	0.14	10.43	20.61	0.11	1.10	98.69	71	35	14	50	2.4	aluminian wollastonite
1470	2647	Muzaffarghar	Thal	53.17	0.64	3.42	1.97	0.35	15.90	24.06	0.17	0.90	100.58	100	46	4	50	12.1	aluminian wollastonite
1470	2726	Muzaffarghar	Thal	48.55	0.64	5.53	11.65	0.19	10.74	20.93	0.25	0.76	99.22	70	33	20	46	1.6	aluminian ferrian diopside
1470	2732	Muzaffarghar	Thal	53.00	0.50	1.34	10.54	0.41	13.62	21.39	0.20	0.38	101.38	72	39	17	44	2.2	augite
1470	2795	Muzaffarghar	Thal	52.09	0.38	2.44	20.02	0.44	23.85	0.71	0.25	0.18	100.37	71	67	32	1	2.1	aluminian (clino)enstatite
1470	3045	Muzaffarghar	Thal	52.76	0.72	1.81	5.64	0.22	14.56	24.41	0.23	0.46	100.81	88	41	9	50	4.4	diopside
1470	3088	Muzaffarghar	Thal	53.16	0.35	1.02	8.25	0.26	13.55	23.49	0.00	0.63	100.72	79	38	14	48	2.8	diopside
1470	3144	Muzaffarghar	Thal	50.61	0.77	3.63	9.93	0.30	12.04	21.82	0.20	0.65	99.95	73	36	17	47	2.1	aluminian diopside
1470	3162	Muzaffarghar	Thal	52.55	0.17	0.27	10.39	0.29	11.70	23.80	0.13	0.37	99.68	69	34	17	49	2.0	diopside
1470	3174	Muzaffarghar	Thal	51.74	0.71	1.92	8.11	0.25	14.69	22.03	0.25	0.28	99.98	82	42	13	45	3.1	augite
1470	3179	Muzaffarghar	Thal	50.61	0.48	3.06	10.87	0.41	12.71	21.53	0.14	0.71	100.52	78	37	18	45	2.0	aluminian ferrian augite
1470	3183	Muzaffarghar	Thal	52.90	0.50	1.14	18.59	0.41	25.00	1.12	0.19	0.00	99.85	73	69	29	2	2.3	(clino)enstatite
1470	3366	Muzaffarghar	Thal	51.48	0.27	1.91	22.50	0.40	22.68	0.64	0.27	0.37	100.52	70	63	36	1	1.8	ferrian (clino)enstatite
1470	3542	Muzaffarghar	Thal	53.01	0.49	1.35	8.70	0.28	13.10	23.62	0.20	0.52	101.26	77	37	14	48	2.6	diopside
1470	3545	Muzaffarghar	Thal	48.95	0.40	2.13	27.95	0.57	17.59	1.13	0.11	0.00	98.83	55	51	47	2	1.1	(clino)enstatite
1470	3552	Muzaffarghar	Thal	50.71	0.10	2.37	22.59	0.19	20.93	0.85	0.13	0.26	98.12	65	61	37	2	1.6	aluminian (clino)enstatite
1470	3573	Muzaffarghar	Thal	50.59	0.33	1.01	25.99	0.50	18.46	1.17	0.08	0.16	98.30	57	54	44	2	1.2	(clino)enstatite
1470	3811	Muzaffarghar	Thal	52.99	0.54	1.95	4.56	0.22	15.80	24.15	0.25	0.38	100.85	93	44	7	48	5.9	diopside
1470	3837	Muzaffarghar	Thal	51.72	0.62	0.56	13.05	0.37	10.32	23.62	0.19	0.31	100.76	62	30	22	49	1.4	diopside
1470	3864	Muzaffarghar	Thal	52.04	0.62	1.04	11.76	0.42	12.68	21.69	0.20	0.48	100.94	71	36	19	44	1.9	augite
1470	4001	Muzaffarghar	Thal	50.54	0.54	1.41	24.95	0.42	19.79	0.94	0.24	0.00	98.83	60	57	41	2	1.4	(clino)enstatite
1470	4090	Muzaffarghar	Thal	43.32	1.35	13.26	17.26	0.35	10.14	11.64	1.11	1.90	100.34	71	36	35	29	1.0	aluminian ferrian sodian subsilicic augite
1470	4172	Muzaffarghar	Thal	50.92	0.23	1.55	26.16	0.29	18.65	0.88	0.08	0.25	99.03	57	55	43	2	1.3	(clino)enstatite
1470	4287	Muzaffarghar	Thal	52.42	0.39	0.72	5.98	0.47	14.35	23.12	0.24	0.37	98.06	84	41	10	48	4.0	diopside
1470	4455	Muzaffarghar	Thal	50.07	0.22	2.84	26.70	0.43	18.55	0.86	0.27	0.25	100.20	58	54	44	2	1.2	aluminian ferrian (clino)enstatite
1470	4460	Muzaffarghar	Thal	50.43	0.40	2.30	25.02	0.34	18.96	0.75	0.23	0.24	98.68	59	56	42	2	1.3	aluminian (clino)enstatite
1470	4515	Muzaffarghar	Thal	54.24	0.18	0.91	4.93	0.60	15.13	23.87	0.24	0.59	100.68	89	43	9	48	4.9	diopside
1470	4581	Muzaffarghar	Thal	44.80	1.39	11.91	14.33	0.28	12.18	12.39	0.67	1.60	99.55	74	42	28	30	1.5	aluminian ferrian sodian subsilicic augite
1470	4698	Muzaffarghar	Thal	54.08	0.31	0.69	3.34	0.21	16.50	24.21	0.09	0.29	99.72	92	46	6	48	8.3	diopside
1470	4803	Muzaffarghar	Thal	50.92	0.31	2.27	12.05	0.38	12.20	21.48	0.20	0.43	100.25	71	35	20	45	1.7	aluminian augite
1470	4819	Muzaffarghar	Thal	53.98	0.43	1.67	4.62	0.43	14.53	24.47	0.33	0.27	100.74	85	42	8	50	5.1	wollastonite
1470	4844	Muzaffarghar	Thal	50.89	0.72	3.42	10.44	0.22	12.40	21.57	0.32	0.81	100.79	76	37	18	46	2.1	aluminian ferrian diopside
1470	4850	Muzaffarghar	Thal	51.76	0.42	1.85	24.26	0.60	20.73	0.71	0.20	0.45	100.99	64	59	40	1	1.5	(clino)enstatite
1470	4927	Muzaffarghar	Thal	53.90	0.45	0.83	1.48	0.23	16.99	24.69	0.19	0.46	99.20	100	48	3	50	17.6	diopside
1470	5033	Muzaffarghar	Thal	48.68	2.48	5.52	6.88	0.30	14.38	22.61	0.18	0.62	101.64	92	41	12	47	3.6	aluminian ferrian diopside
1470	5036	Muzaffarghar	Thal	49.60	0.72	1.43	25.64	0.48	19.35	0.86	0.31	0.34	98.73	62	56	42	2	1.3	ferrian (clino)enstatite
1470	5102	Muzaffarghar	Thal	51.51	0.59	1.16	13.56	0.35	9.81	22.92	0.23	0.33	100.48	58	29	23	48	1.3	diopside
1470	5115	Muzaffarghar	Thal	55.22	0.00	0.16	1.95	0.05	16.95	25.42	0.06	0.00	99.81	94	47	3	50	15.1	wollastonite
1470	5282	Muzaffarghar	Thal	50.77	0.88	3.59	9.31	0.27	12.60	22.27	0.35	0.50	100.54	77	37	16	47	2.3	aluminian diopside
1470	5309	Muzaffarghar	Thal	52.89	0.68	1.49	18.74	0.45	25.15	0.86	0.33	0.24	100.83	75	69	29	2	2.3	ferrian (clino)enstatite
1470	5405	Muzaffarghar	Thal	52.24	0.32	2.46	19.60	0.37	24.13	0.86	0.17	0.26	100.40	72	67	31	2	2.2	aluminian (clino)enstatite
1470	5521	Muzaffarghar	Thal	46.19	1.08	7.60	16.25	0.24	10.42	16.21	1.02	0.92	99.94	67	33	30	37	1.1	aluminian ferrian subsilicic augite
1470	5640	Muzaffarghar	Thal	50.19	0.36	2.41	27.55	0.39	18.46	0.92	0.19	0.21	100.68	58	53	45	2	1.2	aluminian ferrian (clino)enstatite
1470	6065	Muzaffarghar	Thal	52.71	0.40	2.42	5.27	0.31	16.05	23.19	0.14	0.45	100.94	93	45	9	46	5.1	aluminian diopside
1470	6315	Muzaffarghar	Thal	51.59	0.51	3.22	5.30	0.27	15.27	23.83	0.11	0.28	100.37	92	43	9	48	4.9	aluminian diopside
1470	6399	Muzaffarghar	Thal	54.41	0.30	0.78	1.86	0.09	16.96	26.11	0.15	0.23	100.88	100	46	3	51	15.5	wollastonite
1470	6511	Muzaffarghar	Thal	52.40	0.26	2.41	20.71	0.31	22.13	0.78	0.15	0.00	99.16	66	64	34	2	1.9	aluminian (clino)enstatite
1470	6517	Muzaffarghar	Thal	49.61	0.56	2.15	26.84	0.63	18.35	0.97	0.21	0.33	99.65	59	53	45	2	1.2	ferrian (clino)enstatite
1470	6659	Muzaffarghar	Thal	52.80	0.52	2.28	2.22	0.28	15.87	25.07	0.29	0.33	99.66	98	45	4	51	11.3	wollastonite

Sample	Points	River/Dune	Domain	SiO_2	TiO_2	Al_2O_3	FeO	MnO	MgO	CaO	K_2O	Na_2O	Total	Mg#	En	Fs	Wo	En/Fs	Name
				wt%	wt%	wt%	wt%	wt%	wt%	wt%	wt%	wt%							
1474	16	Munda	Thal	51.46	0.46	3.39	24.89	0.55	19.41	0.82	0.23	0.10	101.31	58	57	42	2	1.4	aluminian (clino)enstatite
1474	74	Munda	Thal	53.30	0.53	1.82	2.19	0.58	16.45	24.39	0.21	0.69	100.17	100	46	4	49	10.5	diopside
1474	87	Munda	Thal	52.56	0.66	2.17	3.61	0.31	16.33	23.76	0.35	0.22	99.97	95	46	6	48	7.4	diopside
1474	100	Munda	Thal	50.78	0.76	2.64	8.68	0.44	14.19	21.22	0.22	0.80	99.71	86	41	15	44	2.8	aluminian ferrian augite
1474	109	Munda	Thal	51.70	0.24	1.78	26.32	0.73	19.13	0.78	0.09	0.10	100.86	57	55	44	2	1.3	(clino)enstatite
1474	156	Munda	Thal	52.86	0.35	2.16	8.85	0.23	12.58	22.62	0.22	0.70	100.57	74	37	15	48	2.5	diopside
1474	157	Munda	Thal	51.94	0.57	2.04	8.75	0.39	14.48	21.60	0.40	0.64	100.78	85	41	15	44	2.8	ferrian augite
1474	159	Munda	Thal	52.59	0.38	1.24	4.22	0.17	15.57	24.28	0.37	0.34	99.15	95	44	7	49	6.3	diopside
1474	166	Munda	Thal	51.76	0.24	1.76	9.84	0.13	11.48	22.49	0.34	0.84	98.89	72	35	17	49	2.1	diopside
1474	169	Munda	Thal	50.29	0.54	5.24	6.37	0.39	15.32	22.51	0.16	0.52	101.33	96	43	11	46	4.0	aluminian ferrian diopside
1474	188	Munda	Thal	53.31	0.50	1.04	9.91	0.23	11.95	23.39	0.27	0.47	101.07	69	35	17	49	2.1	diopside
1474	198	Munda	Thal	56.06	0.22	0.50	0.98	0.16	18.37	24.43	0.00	0.37	101.07	97	50	2	48	28.7	diopside
1474	201	Munda	Thal	51.96	0.45	1.55	22.88	0.52	20.97	0.80	0.19	0.00	99.31	62	60	38	2	1.6	(clino)enstatite
1474	204	Munda	Thal	52.65	0.28	0.85	8.44	0.37	12.97	24.19	0.29	0.39	100.42	79	37	14	49	2.6	diopside
1474	229	Munda	Thal	53.91	0.35	3.02	12.67	0.32	29.15	0.54	0.20	0.38	100.54	85	79	20	1	4.0	aluminian (clino)enstatite
1474	235	Munda	Thal	53.01	0.00	0.66	9.65	0.36	12.35	23.63	0.21	0.37	100.24	72	35	16	49	2.2	diopside
1474	255	Munda	Thal	52.34	0.27	1.48	25.20	0.42	19.12	0.64	0.12	0.25	99.84	57	56	42	1	1.3	(clino)enstatite
1474	283	Munda	Thal	45.08	0.45	14.01	14.34	0.17	11.12	11.67	0.26	1.41	98.52	62	40	29	30	1.4	aluminian sodian subsilicic augite
1474	310	Munda	Thal	52.28	0.35	1.72	8.99	0.40	13.33	21.60	0.26	0.64	99.57	77	39	15	45	2.5	diopside
1474	313	Munda	Thal	52.01	0.77	1.74	8.85	0.55	14.13	20.95	0.35	0.73	100.10	81	41	15	44	2.7	augite
1474	384	Munda	Thal	52.35	0.40	1.30	6.93	0.41	14.83	22.43	0.12	0.54	99.30	85	42	12	46	3.6	diopside
1474	400	Munda	Thal	50.32	0.35	2.38	20.63	0.48	22.48	0.80	0.31	0.43	98.18	72	64	34	2	1.9	aluminian ferrian (clino)enstatite
1474	406	Munda	Thal	49.75	0.39	1.91	25.62	0.53	18.44	0.76	0.31	0.15	97.87	58	55	44	2	1.3	(clino)enstatite
1474	415	Munda	Thal	49.86	0.99	6.11	10.96	0.38	13.05	17.43	0.22	1.00	99.99	72	41	20	39	2.1	aluminian augite
1474	453	Munda	Thal	52.43	0.51	1.38	10.06	0.31	12.92	20.53	0.24	0.66	99.04	70	39	17	44	2.2	augite
1474	463	Munda	Thal	53.52	0.18	0.97	17.11	0.23	26.27	0.87	0.15	0.21	99.53	76	72	27	2	2.7	(clino)enstatite
1474	477	Munda	Thal	51.13	0.56	3.35	10.24	0.37	12.55	21.23	0.28	0.51	100.22	73	37	18	45	2.1	aluminian diopside
1474	489	Munda	Thal	40.57	0.32	33.18	0.85	0.16	0.31	23.63	0.31	0.33	99.67	39	--------	--------	--------		aluminian subsilicic unusual pyroxene
1474	490	Munda	Thal	51.72	0.22	3.33	9.81	0.39	13.36	21.03	0.25	0.71	100.82	78	39	17	44	2.3	aluminian augite
1474	508	Munda	Thal	51.84	0.49	2.68	20.84	0.44	21.94	0.78	0.33	0.41	99.75	67	64	35	2	1.8	aluminian (clino)enstatite
1474	521	Munda	Thal	51.57	0.55	1.19	23.49	0.88	20.85	0.91	0.19	0.35	99.99	64	59	39	2	1.5	(clino)enstatite
1474	554	Munda	Thal	53.64	0.29	0.48	7.32	0.36	13.22	24.58	0.27	0.33	100.51	78	38	12	50	3.1	wollastonite
1474	564	Munda	Thal	53.53	0.44	3.18	4.90	0.33	16.24	22.13	0.23	0.78	101.75	92	46	8	45	5.5	aluminian diopside
1474	582	Munda	Thal	53.81	0.49	0.81	3.49	0.33	16.48	24.02	0.43	0.22	100.09	94	46	6	48	7.7	diopside
1474	593	Munda	Thal	50.70	0.30	2.19	25.06	0.50	17.96	1.75	0.31	0.47	99.25	58	54	43	4	1.3	(clino)enstatite
1474	613	Munda	Thal	51.29	0.49	2.73	11.38	0.49	12.00	21.34	0.14	0.87	100.73	73	35	20	45	1.8	aluminian ferrian diopside
1474	614	Munda	Thal	52.82	0.39	0.87	8.96	0.57	13.11	21.96	0.30	1.28	100.24	84	38	16	46	2.5	ferrian diopside
1474	646	Munda	Thal	50.28	0.24	2.53	22.09	0.42	21.80	0.71	0.23	0.60	98.91	70	62	36	1	1.7	aluminian ferrian (clino)enstatite
1474	692	Munda	Thal	51.91	0.34	2.07	9.29	0.30	13.81	21.84	0.17	0.74	100.47	82	40	15	45	2.6	ferrian augite
1474	719	Munda	Thal	52.37	0.56	3.04	10.86	0.34	12.24	20.54	0.25	0.81	101.00	68	37	19	44	1.9	aluminian augite
1474	724	Munda	Thal	53.80	0.42	1.63	12.80	0.29	28.65	0.97	0.19	0.27	99.03	83	78	20	2	3.9	(clino)enstatite
1474	758	Munda	Thal	52.75	0.27	1.79	21.16	0.49	22.48	0.86	0.30	0.43	100.53	68	64	34	2	1.9	(clino)enstatite
1474	781	Munda	Thal	52.96	0.36	2.58	4.28	0.24	16.44	22.31	0.38	0.40	99.94	92	47	7	46	6.5	aluminian diopside
1474	786	Munda	Thal	50.44	0.45	4.39	7.93	0.29	12.31	21.47	0.24	1.10	98.61	81	38	14	48	2.7	aluminian diopside
1474	796	Munda	Thal	53.32	0.37	1.01	2.96	0.29	17.43	22.93	0.24	0.36	98.92	97	49	5	46	9.5	diopside
1474	815	Munda	Thal	53.35	0.43	1.63	19.60	0.29	23.60	1.43	0.09	0.42	100.82	70	66	31	3	2.1	(clino)enstatite
1474	821	Munda	Thal	54.53	0.25	0.86	3.30	0.37	16.65	23.13	0.25	0.00	99.33	90	47	6	47	8.1	diopside
1474	824	Munda	Thal	54.64	0.63	2.18	11.72	0.45	16.41	12.32	0.26	0.56	99.17	71	51	21	28	2.4	augite
1474	865	Munda	Thal	52.82	0.55	1.55	4.98	0.36	15.15	23.41	0.31	0.00	99.12	84	43	9	48	5.1	diopside
1474	925	Munda	Thal	50.43	0.77	3.81	8.98	0.31	12.93	21.64	0.36	0.70	99.92	81	38	15	46	2.5	aluminian ferrian diopside
1474	932	Munda	Thal	51.95	0.00	0.70	27.49	0.29	18.02	0.78	0.00	0.29	99.53	54	53	46	2	1.2	(clino)enstatite
1474	941	Munda	Thal	51.87	0.42	2.48	20.58	0.51	23.21	0.64	0.18	0.41	100.30	71	65	33	1	2.0	aluminian ferrian (clino)enstatite
1474	1004	Munda	Thal	50.05	0.52	1.66	22.93	0.40	20.99	0.86	0.27	0.35	98.03	66	60	38	2	1.6	ferrian (clino)enstatite
1474	1009	Munda	Thal	51.87	0.00	1.10	23.07	0.30	21.19	0.65	0.38	0.00	98.56	63	61	38	1	1.6	(clino)enstatite
1474	1023	Munda	Thal	51.85	0.38	2.01	9.63	0.42	13.78	20.80	0.30	0.64	99.80	78	40	16	43	2.4	augite
1474	1024	Munda	Thal	49.48	0.96	7.65	8.06	0.15	10.89	20.33	0.23	1.97	99.72	81	36	15	49	2.4	aluminian ferrian sodian diopside
1474	1064	Munda	Thal	51.59	0.38	2.82	9.10	0.18	12.86	21.04	0.41	0.65	99.03	75	39	16	46	2.5	aluminian diopside
1474	1077	Munda	Thal	51.57	0.52	7.47	6.63	0.33	20.30	11.32	0.30	1.72	100.15	94	63	12	25	5.2	aluminian ferrian sodian augite
1474	1094	Munda	Thal	52.24	0.22	2.65	22.01	0.53	21.92	0.88	0.22	0.38	101.03	67	62	36	2	1.7	aluminian (clino)enstatite
1474	1100	Munda	Thal	50.69	0.84	4.56	8.60	0.34	13.13	21.99	0.20	0.93	101.26	84	39	15	47	2.6	aluminian ferrian diopside
1474	1106	Munda	Thal	54.53	0.15	1.97	5.96	0.29	34.47	0.27	0.24	0.29	98.17	98	90	9	1	9.8	ferrian (clino)enstatite
1474	1113	Munda	Thal	51.50	0.58	2.49	9.22	0.33	13.56	21.38	0.37	0.81	100.23	82	40	16	45	2.5	aluminian ferrian augite
1474	1120	Munda	Thal	54.12	0.33	1.44	3.91	0.33	17.54	22.43	0.21	0.64	100.94	97	49	7	45	7.4	augite
1474	1125	Munda	Thal	51.28	0.80	4.52	10.90	0.35	13.50	19.21	0.33	0.79	101.68	74	40	19	41	2.1	aluminian augite
1474	1158	Munda	Thal	50.97	0.60	4.72	10.30	0.15	12.07	20.66	0.22	0.92	100.61	72	37	18	45	2.1	aluminian diopside
1474	1167	Munda	Thal	50.07	0.46	1.02	25.91	0.54	17.49	1.38	0.26	0.23	97.35	56	52	45	3	1.2	(clino)enstatite
1474	1171	Munda	Thal	52.02	0.41	1.83	3.81	0.32	16.95	22.18	0.37	0.43	98.32	98	48	7	45	7.3	ferrian diopside
1474	1193	Munda	Thal	50.93	0.75	3.60	13.72	0.34	13.58	17.03	0.16	0.74	100.85	68	40	23	36	1.7	aluminian augite
1474	1194	Munda	Thal	51.52	0.00	2.71	20.47	0.12	22.02	0.71	0.13	0.42	98.11	67	65	34	1	1.9	aluminian (clino)enstatite
1474	1202	Munda	Thal	48.64	0.73	4.25	11.86	0.37	10.63	20.85	0.35	0.82	98.50	71	33	21	46	1.5	aluminian ferrian diopside
1474	1206	Munda	Thal	50.12	0.42	2.92	22.20	0.26	20.80	0.98	0.14	0.45	98.28	66	61	37	2	1.7	aluminian (clino)enstatite
1474	1255	Munda	Thal	51.54	0.56	2.81	20.74	0.45	22.39	0.78	0.24	0.47	99.98	69	64	34	2	1.9	aluminian (clino)enstatite
1474	1300	Munda	Thal	55.05	0.28	1.43	2.59	0.24	17.55	23.08	0.21	0.91	101.34	100	49	4	46	11.0	diopside
1474	1301	Munda	Thal	52.60	0.55	2.52	8.04	0.41	13.75	22.65	0.32	0.51	101.36	80	40	14	47	2.9	aluminian diopside
1474	1319	Munda	Thal	51.43	0.48	2.17	9.69	0.32	16.03	19.78	0.29	0.47	100.66	86	45	16	40	2.9	ferrian augite
1474	1360	Munda	Thal	50.67	1.04	4.58	8.65	0.50	12.42	21.66	0.26	0.75	100.51	76	37	16	47	2.4	aluminian diopside
1474	1431	Munda	Thal	49.95	0.63	2.93	8.81	0.39	13.31	21.11	0.40	0.99	98.50	88	40	15	45	2.6	aluminian ferrian diopside
1474	1437	Munda	Thal	51.39	0.33	1.32	24.13	0.65	20.73	0.68	0.12	0.62	99.98	65	59	40	1	1.5	ferrian (clino)enstatite
1474	1438	Munda	Thal	54.13	0.51	1.82	2.01	0.22	16.67	24.33	0.32	0.57	100.57	98	47	4	49	13.3	diopside
1474	1439	Munda	Thal	50.03	1.14	3.23	7.48	0.37	13.56	22.43	0.37	0.55	99.15	86	40	13	47	3.1	aluminian ferrian diopside
1474	1450	Munda	Thal	51.97	0.65	1.29	9.40	0.59	12.82	22.51	0.31	0.50	100.05	76	37	16	47	2.3	diopside
1474	1455	Munda	Thal	51.72	0.91	2.62	4.63	0.33	15.91	23.26	0.34	0.44	100.16	96	45	8	47	5.7	aluminian ferrian diopside
1474	1465	Munda	Thal	51.33	0.13	2.11	8.87	0.28	13.56	21.35	0.32	0.29	98.23	77	40	15	45	2.6	diopside
1474	1468	Munda	Thal	53.58	0.28	1.67	3.46	0.06	17.51	23.85	0.21	0.46	101.09	100	48	5	47	8.8	ferrian diopside
1474	1469	Munda	Thal	53.05	0.39	1.36	20.18	0.42	23.70	0.83	0.20	0.14	100.28	69	66	32	2	2.1	(clino)enstatite
1474	1473	Munda	Thal	50.35	0.82	3.17	12.72	0.66	14.11	17.38	0.21	0.48	99.90	72	41	22	37	1.9	aluminian augite
1474	1493	Munda	Thal	52.10	0.45	1.21	11.31	0.36	14.17	20.58	0.36	0.20	100.75	74	40	18	42	2.2	augite
1474	1520	Munda	Thal	56.48	0.13	0.27	1.57	0.19	18.19	24.35	0.13	0.24	101.55	95	50	3	48	18.4	diopside
1474	1533	Munda	Thal	51.80	0.19	2.76	9.88	0.24	12.98	20.25	0.23	0.84	99.16	74	39	17	44	2.3	aluminian augite
1474	1583	Munda	Thal	50.71	0.54	1.05	25.55	0.67	18.87	1.09	0.26	0.17	98.90	59	55	43	2	1.3	(clino)enstatite
1474	1636	Munda	Thal	50.40	0.53	3.13	8.15	0.20	13.52	21.00	0.32	0.79	98.04	83	41	14	45	2.9	aluminian ferrian diopside
1474	1637	Munda	Thal	50.75	0.53	4.45	8.44	0.34	12.61	21.36	0.10	1.18	99.77	81	38	15	47	2.6	aluminian ferrian diopside
1474	1869	Munda	Thal	50.88	0.44	3.47	9.19	0.29	13.12	21.46	0.18	0.87	99.90	81	39	16	46	2.5	aluminian ferrian diopside
1474	1877	Munda	Thal	50.48	0.49	1.18	13.49	0.52	9.55	23.34	0.36	0.56	99.97	64	28	23	49	1.2	ferrian diopside
1474	1879	Munda	Thal	52.27	0.40	3.10	5.26	0.28	15.69	23.03	0.09	0.49	100.60	92	44	9	47	5.0	aluminian diopside
1474	1910	Munda	Thal	51.75	0.41	3.86	4.87	0.33	15.35	22.39	0.24	0.55	99.76	91	45	8	47	5.3	aluminian diopside
1474	1935	Munda	Thal	52.08	0.38	2.44	13.10	0.30	9.89	18.81	0.19	2.42	99.62	67	32	24	44	1.3	aluminian ferrian sodian augite
1474	1943	Munda	Thal	51.44	0.61	1.88	24.29	0.61	20.29	0.94	0.18	0.33	100.57	62	58	40	2	1.5	(clino)enstatite
1474	1969	Munda	Thal	51.32	0.58	0.82	24.55	0.63	19.45	1.24	0.29	0.17	99.06	60	56	41	3	1.4	(clino)enstatite
1474	2010	Munda	Thal	50.60	0.55	4.03	9.17	0.36	12.35	21.70	0.16	0.85	99.77	78	37	16	47	2.3	aluminian diopside

Appendix Table B7 Summary of amphibole data of samples in Thal Desert and Upper Indus tributaries.

RIVER SAND SAMPLES (end-member source-rock domains)			actinolite	clino-ferro-suenoite	cummingtonite	edenite	ferri-sadanagaite	ferri-tschermakite	ferro-actinolite	ferro-ferri-hornblende	ferro-hornblende	ferro-pargasite	ferro-rootname4	ferro-sadanagaite	ferro-taramite	ferro-tschermakite	grunerite	hastingsite	magnesio-ferri-hornblende	magnesio-hastingsite	magnesio-hornblende	pargasite	potassic-ferro-pargasite	potassic-hastingsite	potassic-magnesio-hastingsite	potassic-pargasite	sadanagaite	Ti-rich hastingsite	Ti-rich magnesio-ferri-hornblende	Ti-rich magnesio-hastingsite	Ti-rich pargasite	Ti-rich potassic-pargasite	tremolite	tschermakite	
S1749	Hushe	Karakorum	2.0	0.0	1.0	1.0	0.0	0.0	0.0	0.0	0.0	7.8	0.0	0.0	0.0	0.0	0.0	0.0	8.8	23.5	9.8	43.1	1.0	0.0	2.0	0.0	0.0	0.0	0.0	0.0	0.0	0.0	0.0	0.0	100.0
S1748	Braldu	Karakorum	11.0	0.0	1.0	1.0	0.0	0.0	1.0	0.0	6.0	4.0	0.0	0.0	0.0	1.0	0.0	0.0	6.0	4.0	43.0	12.0	6.0	0.0	1.0	1.0	0.0	0.0	0.0	0.0	0.0	0.0	2.0	0.0	100.0
S1437	Hunza	Northern Karakorum	7.2	0.0	1.0	1.0	0.0	0.0	0.0	3.1	10.3	6.2	0.0	0.0	0.0	0.0	1.0	0.0	20.6	6.2	20.6	7.2	12.4	1.0	0.0	2.1	0.0	0.0	0.0	0.0	0.0	0.0	0.0	0.0	100.0
S1438	Hispar	Southern Karakorum	18.8	0.0	3.0	0.0	0.0	0.0	0.0	0.0	2.0	5.9	0.0	1.0	0.0	0.0	1.0	0.0	19.8	4.0	28.7	12.9	2.0	0.0	0.0	1.0	0.0	0.0	0.0	0.0	0.0	0.0	0.0	0.0	100.0
S4426	Stagmo	Ladakh arc	2.0	0.0	0.0	0.0	0.0	0.0	0.0	0.0	0.0	1.0	0.0	0.0	0.0	0.0	0.0	1.0	47.0	3.0	33.0	13.0	0.0	0.0	0.0	0.0	0.0	0.0	0.0	0.0	0.0	0.0	0.0	0.0	100.0
S4430	Domkar	Ladakh arc	4.0	0.0	1.0	0.0	0.0	0.0	0.0	1.0	0.0	0.0	0.0	1.0	0.0	0.0	0.0	0.0	77.0	13.0	2.0	0.0	0.0	0.0	0.0	0.0	0.0	0.0	1.0	0.0	0.0	0.0	0.0	0.0	100.0
S1439	Kandia	Kohistan arc	20.0	0.0	1.0	2.9	0.0	1.0	0.0	0.0	0.0	1.0	1.0	3.8	0.0	0.0	0.0	0.0	10.5	6.7	13.3	37.1	0.0	0.0	0.0	0.0	0.0	0.0	0.0	0.0	1.0	0.0	0.0	1.0	100.0
S1440	Swat	Kohistan arc	3.0	0.0	5.0	1.0	1.0	1.0	0.0	1.0	0.0	0.0	0.0	0.0	0.0	0.0	0.0	0.0	33.7	20.8	6.9	26.7	0.0	0.0	0.0	0.0	0.0	0.0	0.0	0.0	0.0	0.0	0.0	0.0	100.0
S4419	Zanskar	Greater+Tethys Himalaya	6.3	1.1	2.1	0.0	0.0	0.0	0.0	0.0	3.2	14.7	0.0	2.1	0.0	0.0	0.0	4.2	7.4	7.4	24.2	16.8	5.3	1.1	1.1	2.1	1.1	0.0	0.0	0.0	0.0	0.0	0.0	0.0	100.0
S1426	Nandihar Khwar	Greater Himalaya	4.0	0.0	1.0	1.0	0.0	1.0	0.0	1.0	2.0	13.0	0.0	0.0	0.0	0.0	0.0	5.0	8.0	21.0	17.0	22.0	1.0	0.0	0.0	0.0	1.0	1.0	0.0	0.0	0.0	0.0	1.0	0.0	100.0
S1432	Astor	Nanga Parbat	2.0	0.0	0.0	0.0	1.0	3.0	0.0	1.0	2.0	3.0	0.0	0.0	0.0	0.0	0.0	1.0	8.0	4.0	30.0	31.0	1.0	1.0	1.0	0.0	0.0	0.0	0.0	0.0	0.0	0.0	0.0	11.0	100.0
EOLIAN SAND SAMPLES (sediment sink)																																			
S1462	Mankera	Thal Desert	6.8	0.0	2.9	0.0	0.0	1.0	0.0	1.9	1.9	2.9	0.0	1.9	0.0	0.0	0.0	0.0	17.5	0.0	39.8	15.5	1.0	0.0	1.0	0.0	1.0	0.0	0.0	0.0	0.0	0.0	1.0	3.9	100.0
S1463	Haidarabad	Thal Desert	9.0	0.0	2.0	1.0	0.0	2.0	0.0	0.0	0.0	2.0	0.0	3.0	1.0	0.0	1.0	3.0	27.0	20.0	7.0	10.0	1.0	0.0	1.0	1.0	5.0	0.0	0.0	2.0	1.0	0.0	1.0	0.0	100.0
S1470	Muzaffarghar	Thal Desert	12.0	0.0	0.0	2.0	0.0	0.0	0.0	1.0	0.0	6.0	0.0	7.0	0.0	0.0	0.0	2.0	4.0	4.0	31.0	25.0	1.0	0.0	0.0	2.0	0.0	0.0	0.0	0.0	1.0	1.0	1.0	0.0	100.0
S1474	Munda	Thal Desert	9.0	0.0	3.0	0.0	0.0	0.0	1.0	0.0	1.0	3.0	0.0	1.0	0.0	0.0	1.0	0.0	11.0	2.0	36.0	26.0	1.0	0.0	0.0	1.0	0.0	0.0	0.0	0.0	0.0	0.0	2.0	2.0	100.0
AVERAGE SPECTRA FOR DISTINCT TECTONIC DOMAINS																																			
		Karakorum	9.8	0.0	1.5	0.8	0.0	0.0	0.3	0.8	4.5	6.0	0.0	0.3	0.0	0.3	0.5	0.0	13.8	9.5	25.5	19.0	5.3	0.3	0.8	1.0	0.0	0.0	0.0	0.0	0.0	0.0	0.5	0.0	100.0
		Ladakh	3.0	0.0	0.5	0.0	0.0	0.0	0.0	0.5	0.0	0.5	0.0	0.5	0.0	0.0	0.0	0.5	62.0	8.0	17.5	6.5	0.0	0.0	0.0	0.0	0.0	0.0	0.5	0.0	0.0	0.0	0.0	0.0	100.0
		Kohistan	11.7	0.0	2.9	1.9	0.5	1.0	0.0	0.5	0.0	0.5	0.5	1.9	0.0	0.0	0.0	0.0	21.8	13.6	10.2	32.0	0.0	0.0	0.0	0.0	0.0	0.0	0.0	0.0	0.5	0.0	0.0	0.5	100.0
		Himalaya	5.1	0.5	1.5	0.5	0.0	0.5	0.0	0.5	2.6	13.8	0.0	1.0	0.0	0.0	0.0	4.6	7.7	14.4	20.5	19.5	3.1	0.5	0.5	1.0	1.0	0.5	0.0	0.0	0.0	0.0	0.5	0.0	100.0
		Nanga Parbat	2.0	0.0	0.0	0.0	1.0	3.0	0.0	1.0	2.0	3.0	0.0	0.0	0.0	0.0	0.0	1.0	8.0	4.0	30.0	31.0	1.0	1.0	1.0	0.0	0.0	0.0	0.0	0.0	0.0	0.0	0.0	11.0	100.0
		Thal Desert	9.2	0.0	2.0	0.7	0.0	0.7	0.2	0.7	0.7	3.5	0.0	3.2	0.2	0.0	0.5	1.2	14.9	6.5	28.5	19.1	1.0	0.0	0.5	1.0	1.5	0.0	0.0	0.5	0.5	0.2	1.2	1.5	100.0

Appendix Table B8 Summary of garnet data of samples in Thal Desert and Upper Indus tributaries.

RIVER SAND SAMPLES (end-member source-rock domains)			**majorite**	**spessartine**	**pyrope**	**almandine**	**grossular**	**andradite**	
S1749	Hushe	Karakorum	0.0	15.9	7.8	60.6	14.0	1.7	100.0
S1748	Braldu	Karakorum	0.7	8.5	9.4	73.4	6.4	1.6	100.0
S1437	Hunza	Northern Karakorum	1.3	3.8	2.5	38.4	45.5	8.4	100.0
S1438	Hispar	Southern Karakorum	0.0	5.7	12.8	69.2	12.1	0.2	100.0
S4426	Stagmo	Ladakh arc	no garnet grains						
S4430	Domkar	Ladakh arc	0.0	8.7	2.6	48.8	10.2	29.8	100.0
S1439	Kandia	Kohistan arc	6.1	3.7	2.8	19.0	68.2	0.2	100.0
S1440	Swat	Kohistan arc	15.7	2.7	7.5	23.4	47.0	3.8	100.0
S4419	Zanskar	Greater+Tethys Himalaya	5.8	10.5	4.1	75.2	3.4	0.9	100.0
S1426	Nandihar Khwar	Greater Himalaya	0.0	3.5	13.8	74.4	8.1	0.1	100.0
S1432	Astor	Nanga Parbat	0.1	5.7	14.9	53.3	24.3	1.8	100.0
EOLIAN SAND SAMPLES (sediment sink)									
S1462	Mankera	Thal Desert	0.4	4.6	15.7	63.9	13.8	1.5	100.0
S1463	Haidarabad	Thal Desert	0.0	5.2	15.2	60.9	13.1	5.6	100.0
S1470	Muzaffarghar	Thal Desert	3.8	5.8	11.2	62.8	13.8	2.6	100.0
S1474	Munda	Thal Desert	0.1	2.7	17.3	62.1	17.7	0.1	100.0
AVERAGE SPECTRA FOR DISTINCT TECTONIC DOMAINS									
		Karakorum	0.3	8.2	10.5	67.8	12.0	1.2	100.0
		Ladakh	0.0	8.7	2.6	48.8	10.2	29.8	100.0
		Kohistan	9.4	3.4	4.4	20.5	60.9	1.4	100.0
		Himalaya	2.9	7.0	8.9	74.8	5.8	0.5	100.0
		Nanga Parbat	0.1	5.7	14.9	53.3	24.3	1.8	100.0
		Thal Desert	1.1	4.6	14.9	62.6	14.6	2.3	100.0

Appendix Table B9 Summary of epidote data of samples in Thal Desert and Upper Indus tributaries.

RIVER SAND SAMPLES (end-member source-rock domains)			**allanite-(Ce)**	**clinozoisite**	**dissakisite-(Ce)**	**epidote**	**ferriallanite-(Ce)**	**ferriepidote**	
S1749	Hushe	Karakorum	17.9	12.0	0.0	70.1	0.0	0.0	100.0
S1748	Braldu	Karakorum	10.0	58.0	4.0	28.0	0.0	0.0	100.0
S1437	Hunza	Northern Karakorum	4.1	62.9	2.1	26.8	4.1	0.0	100.0
S1438	Hispar	Southern Karakorum	0.0	41.2	0.0	57.6	0.0	1.2	100.0
S4426	Stagmo	Ladakh arc	0.0	0.0	0.0	85.7	14.3	0.0	100.0
S4430	Domkar	Ladakh arc	0.0	44.0	0.0	56.0	0.0	0.0	100.0
S1439	Kandia	Kohistan arc	0.0	73.7	0.0	26.3	0.0	0.0	100.0
S1440	Swat	Kohistan arc	0.0	58.6	0.0	41.4	0.0	0.0	100.0
S4419	Zanskar	Greater+Tethys Himalaya	8.6	20.0	0.0	71.4	0.0	0.0	100.0
S1426	Nandihar Khwar	Greater Himalaya	0.0	93.8	0.0	6.3	0.0	0.0	100.0
S1432	Astor	Nanga Parbat	0.0	27.6	0.0	72.4	0.0	0.0	100.0
EOLIAN SAND SAMPLES (sediment sink)									
S1462	Mankera	Thal Desert	0.0	60.0	0.0	40.0	0.0	0.0	100.0
S1463	Haidarabad	Thal Desert	0.0	39.4	0.0	60.6	0.0	0.0	100.0
S1470	Muzaffarghar	Thal Desert	0.0	55.6	0.0	44.4	0.0	0.0	100.0
S1474	Munda	Thal Desert	0.0	62.0	0.0	38.0	0.0	0.0	100.0
AVERAGE SPECTRA FOR DISTINCT TECTONIC DOMAINS									
		Karakorum	8.8	42.1	1.5	46.4	1.0	0.3	100.0
		Ladakh	0.0	34.4	0.0	62.5	3.1	0.0	100.0
		Kohistan	0.0	70.3	0.0	29.7	0.0	0.0	100.0
		Himalaya	7.0	33.7	0.0	59.3	0.0	0.0	100.0
		Nanga Parbat	0.0	27.6	0.0	72.4	0.0	0.0	100.0
		Thal Desert	0.0	54.3	0.0	45.7	0.0	0.0	100.0

Appendix Table B10 Summary of pyroxene data of samples in Thal Desert and Upper Indus tributaries.

			(clino) enstatite	(clino) ferrosilite	aegirine-augite	aluminian (clino) enstatite	aluminian augite	aluminian diopside	aluminian ferrian (clino) enstatite	aluminian ferrian augite	aluminian ferrian diopside	aluminian ferrian sodian augite	aluminian ferrian sodian diopside	aluminian ferrian sodian subsilicic augite	aluminian ferrian sodian subsilicic unusual pyroxene	aluminian ferrian subsilicic augite	aluminian ferrian subsilicic esseneite	aluminian ferrian subsilicic unusual pyroxene	aluminian ferrian subsilicic wollastonite	aluminian ferrian wollastonite	aluminian sodian augite	aluminian sodian subsilicic augite	aluminian sodian subsilicic unusual pyroxene	aluminian subsilicic augite	aluminian subsilicic unusual pyroxene	aluminian subsilicic wollastonite	aluminian titanian diopside	aluminian unusual pyroxene	aluminian wollastonite	augite	diopside	ferrian (clino)enstatite	ferrian augite	ferrian diopside	ferrian sodian diopside	ferrian sodian hedenbergite	ferrian wollastonite	hedenbergite	sodian diopside	subsilicic aegirine-augite	wollastonite	
RIVER SAND SAMPLES (end-member source-rock domains																																										
S1749	Hushe	Karakorum	0.0	0.0	0.0	0.0	0.0	0.0	0.0	0.0	0.0	0.0	0.0	5.8	7.7	11.5	0.0	1.9	0.0	0.0	0.0	0.0	0.0	0.0	0.0	0.0	0.0	0.0	0.0	0.0	67.3	0.0	0.0	3.8	0.0	0.0	1.9	0.0	0.0	0.0	0.0	100.0
S1748	Braldu	Karakorum	0.0	0.0	2.0	0.0	0.0	5.0	0.0	0.0	9.9	0.0	0.0	1.0	0.0	0.0	0.0	0.0	4.0	1.0	0.0	0.0	0.0	0.0	0.0	0.0	0.0	0.0	4.0	0.0	42.6	0.0	0.0	0.0	0.0	0.0	1.0	4.0	3.0	0.0	22.8	100.0
S1437	Hunza	Northern Karakorum	2.2	0.0	0.0	0.0	2.2	2.2	0.0	0.0	0.0	4.4	0.0	4.4	2.2	0.0	0.0	0.0	0.0	0.0	0.0	0.0	0.0	0.0	0.0	2.2	0.0	0.0	2.2	8.9	60.0	0.0	0.0	2.2	0.0	0.0	0.0	4.4	0.0	0.0	2.2	100.0
S1438	Hispar	Southern Karakorum	0.0	0.0	0.0	0.0	4.5	0.0	0.0	0.0	0.0	0.0	0.0	0.0	0.0	0.0	0.0	0.0	0.0	0.0	0.0	0.0	0.0	0.0	0.0	0.0	0.0	0.0	0.0	0.0	90.9	0.0	0.0	0.0	0.0	0.0	0.0	4.5	0.0	0.0	0.0	100.0
S4426	Stagmo	Ladakh arc	0.0	0.0	0.0	0.0	6.7	0.0	0.0	6.7	0.0	0.0	0.0	0.0	0.0	0.0	0.0	0.0	0.0	0.0	0.0	0.0	0.0	0.0	0.0	0.0	0.0	0.0	0.0	13.3	60.0	0.0	6.7	6.7	0.0	0.0	0.0	0.0	0.0	0.0	0.0	100.0
S4430	Domkar	Ladakh arc	17.4	0.0	0.0	0.0	17.4	0.0	0.0	8.7	0.0	4.3	0.0	8.7	0.0	4.3	4.3	0.0	0.0	0.0	0.0	0.0	0.0	0.0	0.0	0.0	0.0	0.0	0.0	17.4	13.0	0.0	0.0	0.0	0.0	0.0	0.0	0.0	0.0	0.0	4.3	100.0
S1439	Kandia	Kohistan arc	33.3	0.0	0.0	0.0	0.0	46.7	0.0	0.0	0.0	0.0	0.0	0.0	0.0	0.0	0.0	0.0	0.0	0.0	0.0	0.0	0.0	6.7	0.0	0.0	0.0	0.0	0.0	0.0	13.3	0.0	0.0	0.0	0.0	0.0	0.0	0.0	0.0	0.0	0.0	100.0
S1440	Swat	Kohistan arc	43.0	0.0	0.0	3.0	14.0	25.0	0.0	0.0	0.0	0.0	0.0	0.0	0.0	0.0	0.0	0.0	0.0	0.0	0.0	0.0	0.0	0.0	0.0	0.0	0.0	0.0	0.0	4.0	10.0	1.0	0.0	0.0	0.0	0.0	0.0	0.0	0.0	0.0	0.0	100.0
S4419	Zanskar	Greater+Tethys Himalaya	1.4	0.0	0.0	0.0	1.4	2.9	0.0	1.4	1.4	0.0	1.4	1.4	0.0	0.0	0.0	0.0	0.0	0.0	1.4	0.0	0.0	0.0	0.0	0.0	0.0	1.4	0.0	1.4	68.6	0.0	0.0	5.7	2.9	1.4	0.0	1.4	0.0	0.0	4.3	100.0
S1426	Nandihar Khwar	Greater Himalaya	1.5	1.5	0.0	18.5	13.8	3.1	1.5	9.2	0.0	1.5	0.0	4.6	4.6	0.0	0.0	0.0	0.0	0.0	1.5	0.0	0.0	0.0	1.5	0.0	0.0	0.0	0.0	6.2	20.0	0.0	1.5	4.6	0.0	0.0	0.0	0.0	0.0	1.5	3.1	100.0
S1432	Astor	Nanga Parbat	3.0	0.0	0.0	0.0	0.0	0.0	0.0	0.0	0.0	0.0	0.0	3.0	6.1	6.1	0.0	3.0	0.0	3.0	0.0	0.0	0.0	0.0	0.0	0.0	0.0	0.0	0.0	0.0	6.1	0.0	0.0	0.0	0.0	0.0	18.2	6.1	0.0	0.0	45.5	100.0
EOLIAN SAND SAMPLES (sediment sink)																																										
S1462	Mankera	Thal Desert	16.7	1.5	0.0	10.6	4.5	19.7	0.0	0.0	0.0	0.0	0.0	0.0	0.0	0.0	0.0	0.0	0.0	0.0	0.0	0.0	0.0	0.0	0.0	0.0	0.0	0.0	1.5	3.0	40.9	0.0	0.0	0.0	0.0	0.0	0.0	0.0	0.0	0.0	1.5	100.0
S1463	Haidarabad	Thal Desert	15.6	0.0	0.0	12.5	9.4	7.8	4.7	3.1	6.3	0.0	1.6	0.0	0.0	0.0	0.0	0.0	0.0	0.0	0.0	0.0	1.6	0.0	0.0	0.0	1.6	0.0	0.0	9.4	20.3	3.1	1.6	0.0	0.0	0.0	0.0	0.0	0.0	0.0	1.6	100.0
S1470	Muzaffarghar	Thal Desert	11.1	1.1	0.0	8.9	1.1	8.9	8.9	2.2	6.7	0.0	1.1	2.2	0.0	1.1	0.0	0.0	0.0	0.0	0.0	0.0	0.0	0.0	0.0	0.0	0.0	0.0	2.2	3.3	18.9	6.7	1.1	5.6	0.0	0.0	1.1	0.0	0.0	0.0	7.8	100.0
S1474	Munda	Thal Desert	17.0	0.0	0.0	7.0	7.0	11.0	3.0	2.0	11.0	2.0	1.0	0.0	0.0	0.0	0.0	0.0	0.0	0.0	0.0	1.0	0.0	0.0	1.0	0.0	0.0	0.0	0.0	6.0	20.0	3.0	3.0	4.0	0.0	0.0	0.0	0.0	0.0	0.0	1.0	100.0
AVERAGE SPECTRA FOR DISTINCT TECTONIC DOMAINS																																										
		Karakorum	0.5	0.0	0.9	0.0	0.9	2.7	0.0	0.0	4.5	0.9	0.0	2.7	2.3	2.7	0.0	0.5	1.8	0.5	0.0	0.0	0.0	0.0	0.0	0.5	0.0	0.0	2.3	1.8	56.8	0.0	0.0	1.4	0.0	0.0	0.9	3.2	1.4	0.0	10.9	100.0
		Ladakh	10.5	0.0	0.0	0.0	13.2	0.0	0.0	7.9	0.0	2.6	0.0	5.3	0.0	2.6	2.6	0.0	0.0	0.0	0.0	0.0	0.0	0.0	0.0	0.0	0.0	0.0	0.0	15.8	31.6	0.0	2.6	2.6	0.0	0.0	0.0	0.0	0.0	0.0	2.6	100.0
		Kohistan	41.7	0.0	0.0	2.6	12.2	27.8	0.0	0.0	0.0	0.0	0.0	0.0	0.0	0.0	0.0	0.0	0.0	0.0	0.0	0.0	0.0	0.9	0.0	0.0	0.0	0.0	0.0	3.5	10.4	0.9	0.0	0.0	0.0	0.0	0.0	0.0	0.0	0.0	0.0	100.0
		Himalaya	1.5	0.7	0.0	8.9	7.4	3.0	0.7	5.2	0.7	0.7	0.7	3.0	2.2	0.0	0.0	0.0	0.0	0.0	1.5	0.0	0.0	0.0	0.7	0.0	0.0	0.7	0.0	3.7	45.2	0.0	0.7	5.2	1.5	0.7	0.0	0.7	0.0	0.7	3.7	100.0
		Nanga Parbat	3.0	0.0	0.0	0.0	0.0	0.0	0.0	0.0	0.0	0.0	0.0	3.0	6.1	6.1	0.0	3.0	0.0	3.0	0.0	0.0	0.0	0.0	0.0	0.0	0.0	0.0	0.0	0.0	6.1	0.0	0.0	0.0	0.0	0.0	18.2	6.1	0.0	0.0	45.5	100.0
		Thal Desert	15.0	0.6	0.0	9.4	5.3	11.6	4.4	1.9	6.6	0.6	0.9	0.6	0.0	0.3	0.0	0.0	0.0	0.0	0.0	0.3	0.3	0.0	0.3	0.0	0.3	0.0	0.9	5.3	24.1	3.4	1.6	2.8	0.0	0.0	0.3	0.0	0.0	0.0	3.1	100.0

Appendix Table C1 Detailed information of samples in Thal Desert and Upper Indus tributaries.

Sample	River bars	Location	Country	Collected by	Year	Latitude	Longitude	Tectonic domain
	End members							
S1749	Hushe	downstream Charakusa	Pakistan	Mike Searle	2001	35°30'55" N	76°24'23" E	Karakorum
S1748	Braldu	downstream Baltoro	Pakistan	Mike Searle	2001	35°40'14" N	76°06'58" E	Karakorum
S1437	Hunza	Altit	Pakistan	Giacomo Ghielmi, Filippo Lazzati	2001	36°18'52" N	74°41'07" E	Northern+Central Karakorum
S1438	Hispar	Nagar	Pakistan	Giacomo Ghielmi, Filippo Lazzati	2001	36°17'57" N	74°40'33" E	Southern Karakorum
S4426	Stagmo	Stagmo	India	Jan Blöthe, Henry Munack	2011	34°07'00" N	77°42'00" E	Ladakh arc
S4430	Domkar	Domkar	India	Jan Blöthe, Henry Munack	2011	34°23'27" N	76°46'21" E	Ladakh arc
S1439	Kandia	Halil	Pakistan	Giacomo Ghielmi, Filippo Lazzati	2001	35°26'46" N	73°12'31" E	Kohistan arc
S1440	Swat	Fatepur	Pakistan	Giacomo Ghielmi, Filippo Lazzati	2001	35°03'16" N	72°28'30" E	Kohistan arc
S4419	Zanskar	Rumbak	India	Jan Blöthe, Henry Munack	2011	34°08'34" N	77°17'04" E	Greater+Tethys Himalaya
S1426	Nandihar Khwar	Daut	Pakistan	Giacomo Ghielmi, Filippo Lazzati	2001	34°46'16" N	72°55'50" E	Greater Himalaya
S1432	Astor	Bunji	Pakistan	Giacomo Ghielmi, Filippo Lazzati	2001	35°34'27" N	74°39'12" E	Nanga Parbat
S1454	Soan	Trap	Pakistan	Giacomo Ghielmi, Filippo Lazzati	2001	33°03'34" N	71°55'29" E	Potwar Plateau
	Indus River							
S1447	Indus	Kushalgar	Pakistan	Giacomo Ghielmi, Filippo Lazzati	2001	33°28'53" N	71°54'38" E	
S1455	Indus	Kalabagh	Pakistan	Giacomo Ghielmi, Filippo Lazzati	2001	32°54'42" N	71°31'30" E	
S1461	Indus	Dhera Ismail Khan	Pakistan	Giacomo Ghielmi, Filippo Lazzati	2001	31°45'31" N	70°56'12" E	
	Desert dunes							
S1462	Thal	Mankera	Pakistan	Giacomo Ghielmi, Filippo Lazzati	2001	31°23'47" N	71°25'27" E	
S1463	Thal	Haidarabad	Pakistan	Giacomo Ghielmi, Filippo Lazzati	2001	31°20'42" N	71°42'12" E	
S1470	Thal	Muzaffarghar	Pakistan	Giacomo Ghielmi, Filippo Lazzati	2001	30°04'18" N	71°08'40" E	
S1474	Thal	Munda	Pakistan	Giacomo Ghielmi, Filippo Lazzati	2001	30°34'56" N	71°15'16" E	

Appendix Table C2 Petrography of samples in Thal Desert and Upper Indus tributaries.

	Site	Sample	Operator	GSZ	Q	F	Lv	Lc	Lp	Lh	Lm	Lu	total	Qp/Q	P/F	Rcd/Rc	Rmb/Rm	MI*	% mica	% biotite/mica	% HM
End members				(mm)																	
Hushe	downstream Charakusa	S1749	G. Vezzoli	207	55	41	0	2	0	0	3	0	100.0	6	59	n.d.	5	405	6%	67%	2%
Braldu	downstream Baltoro	S1748	G. Vezzoli	184	50	26	0	18	0.3	0	6	0	100.0	0	48	66	9	350	3%	86%	3%
Hunza	Altit	S1437	G. Vezzoli	222	23	23	0	18	13	0	24	0	100.0	16	67	61	5	247	1%	n.d.	3%
Hispar	Nagar	S1438	G. Vezzoli	353	58	31	0	5	1	0	5	0	100.0	3	56	60	17	381	5%	63%	9%
Stagmo	Stagmo	S4426	A.Resentini	164	41	57	0	0.4	0	0	1	0	100.0	5	82	0	44	456	9%	71%	21%
Domkar	Domkar	S4430	A.Resentini	351	47	50	0	0.2	1	0	2	0	100.0	18	68	n.d.	22	403	2%	75%	13%
Kandia	Halil	S1439	G. Vezzoli	260	32	18	0	2	0	0	48	0	100.0	17	88	n.d.	65	320	4%	n.d.	29%
Swat	Fatepur	S1440	G. Vezzoli	380	26	47	2	0	0.5	0	21	3	100.0	14	82	n.d.	55	339	3%	100%	23%
Zanskar	Rumbak	S4419	A.Resentini	223	49	15	0.3	29	1	0	6	0.3	100.0	3	60	13	11	356	1%	n.d.	11%
Nandihar Khwar	Daut	S1426	G. Vezzoli	308	59	25	0	0	0	0	16	0	100.0	37	58	n.d.	9	411	6%	31%	6%
Astor	Bunji	S1432	G. Vezzoli	308	67	30	0	0	0	0	3	0	100.0	18	50	n.d.	13	390	13%	85%	19%
Soan	Trap	S1454	G. Vezzoli	178	48	18	1	11	10	4	9	0	100.0	9	43	17	24	192	1%	n.d.	6%
Indus River																					
Indus	Kushalgar	S1447	G. Vezzoli	179	42	22	0	9	6	1	21	0.4	100.0	16	68	55	18	292	6%	87%	12%
Indus	Kalabagh	S1455	G. Vezzoli	138	43	16	1	15	11	1	11	1	100.0	9	45	25	14	253	3%	29%	10%
Indus	Dhera Ismail Khan	S1461	G. Vezzoli	249	45	24	2	12	4	3	11	0.4	100.0	10	49	42	24	296	3%	n.d.	16%
Desert dunes																					
Thal	Mankera	S1462	G. Vezzoli	199	39	34	1	5	1	1	18	1	100.0	13	49	50	29	317	1%	n.d.	15%
Thal	Haidarabad	S1463	G. Vezzoli	243	35	33	1	7	2	0.4	22	0.4	100.0	6	43	56	41	283	1%	n.d.	15%
Thal	Muzaffarghar	S1470	G. Vezzoli	218	30	34	3	8	2	0	23	0	100.0	11	59	21	31	294	1%	n.d.	19%
Thal	Munda	S1474	G. Vezzoli	153	43	36	0.4	7	5	0	9	0.4	100.0	8	53	41	24	273	2%	n.d.	12%

Appendix Table C3 Heavy minerals of samples in Thal Desert and Upper Indus tributaries.

	Site	Sample	Operator	HMC	tHMC	zircon	tourmaline	rutile	titanite	apatite	epidote	garnet	chloritoid	staurolite	andalusite	kyanite	sillimanite	amphibole	clinopyroxene	enstatite	hypersthene	olivine	Cr-spinel	other tHM		% transparent	% opaque	% turbid		ZTR	HCI	MMI
End members																																
Hushe	downstream Charakusa	S1749	S. Andò	4.8	2.5	6	1	0	10	0	11	2	0	0	0	0	1	67	1	0	0	0	0	0	100.0	94%	3%	3%	100%	7	6	n.d.
Braldu	downstream Baltoro	S1748	S. Andò	6.5	4.5	5	0.5	0.5	3	0	34	6	0	0.5	0	0	0.5	46	2	1	0	0	0	0.5	100.0	87%	5%	7%	100%	6	17	n.d.
Hunza	Altit	S1437	S. Andò	2.9	1.5	1	4	0	4	0	20	2	0	0.5	0	0	0	66	2	0	0	0	0	0	100.0	71%	3%	26%	100%	5	7	n.d.
Hispar	Nagar	S1438	S. Andò	8.7	6.7	2	0.5	0	9	0.5	21	21	0	1	0	0	0	41	3	0	0	0	0	0	100.0	80%	6%	14%	100%	3	24	n.d.
Stagmo	Stagmo	S4426	W.Liang, M.Limonta	12.6	12.0	0.5	0	0	3	1	2	0.5	0	0	0	0	0	90	3	0	0	0	0	0	100.0	95%	5%	0%	100%	0	0	n.d.
Domkar	Domkar	S4430	W.Liang, M.Limonta	9.7	8.1	0.5	1	0	2	0.5	7	0.5	0	0	0	0	0	86	0.5	0	1	0	0	0	100.0	84%	16%	0%	100%	2	1	n.d.
Kandia	Halil	S1439	S. Andò	44.2	33.4	0	0	0	0	0	38	0	0	0	0	0	0	60	1	0.5	0	0	0	0	100.0	76%	1%	23%	100%	0	46	n.d.
Swat	Fatepur	S1440	S. Andò	31.4	27.5	0	0	1	0	0	8	0.5	0	0	0	0	0	67	8	0	15	0	0	0	100.0	89%	6%	5%	100%	1	6	n.d.
Zanskar	Rumbak	S4419	W.Liang, M.Limonta	4.8	4.6	1	4	0	1	4	12	14	0	1	0	0	22	31	10	0	0	0	0	0.4	100.0	97%	3%	0%	100%	6	9	98
Nandihar Khwar	Daut	S1426	S. Andò	4.8	4.0	0	2	0.5	0	0	10	26	0	1	0	6	1	47	0	2	4	0	0.5	0.5	100.0	90%	1%	9%	100%	2	10	69
Astor	Bunji	S1432	S. Andò	17.9	16.9	0.4	0	0.4	0	0	19	7	0	0	0	0	0	71	1	0.4	0	0	0	0	100.0	97%	1%	2%	100%	1	3	n.d.
Soan	Trap	S1454	S. Andò	5.0	3.8	0	3	0	0	0	76	5	0	0	0	0	0	16	0	0	0	0	0	0	100.0	77%	7%	15%	100%	3	10	n.d.
Indus River																																
Indus	Kushalgar	S1447	P. Paparella	12.2	9.8	0	0	0	1	0	17	9	0	2	0	0.4	0.4	60	7	1	3	0	0	0	100.0	81%	8%	11%	100%	0	20	48
Indus	Kalabagh	S1455	S. Andò	8.7	6.7	1	2	0.5	2	0	30	8	1	2	0	1	0	44	4	1	2	0.5	0	1.0	100.0	79%	13%	8%	100%	3	11	33
Indus	Dhera Ismail Khan	S1461	P. Paparella	27.7	22.9	0.5	0	0.5	4	0	22	29	0	1	0	0.5	0	40	0.5	0	2	0	0	0	100.0	86%	8%	5%	100%	1	17	n.d.
Desert dunes																																
Thal	Mankera	S1462	S. Andò	21.2	15.3	0	0.5	1	1	0	15	11	0	0.5	0	0.5	0.5	64	2	0	4	0	0	0	100.0	77%	8%	15%	100%	1	12	n.d.
Thal	Haidarabad	S1463	P. Paparella	24.2	18.6	0.4	1	0	1	0	16	14	0	2	0	0.4	0	55	7	0	3	0.4	0	0	100.0	77%	10%	13%	100%	1	7	n.d.
Thal	Muzaffarghar	S1470	S. Andò	26.4	17.7	2	1	0.5	1	0	20	13	0.5	2	0	1	0.5	45	5	0	6	0.5	0	0	100.0	69%	13%	18%	100%	4	10	48
Thal	Munda	S1474	P. Paparella	12.3	10.0	0	0	0.5	1	0	18	9	0	0	0	0.5	0.5	60	8	0	3	0	0	0	100.0	84%	6%	10%	100%	0	5	n.d.

Appendix Table C4 Chemistry of samples in Thal Desert and Upper Indus tributaries.

					Method	LF200	LF200	LF200	LF200	LF200	LF200	LF200	LF200	LF200	LF200	LF200	LF200	LF200	LF200	LF200	LF200	LF200	LF200	LF200
					Analyte	SiO_2	Al_2O_3	Fe_2O_3	MgO	CaO	Na_2O	K_2O	TiO_2	P_2O_5	MnO	LOI	Sum	Rb	Cs	Be	Sr	Ba	Sc	Y
						%	%	%	%	%	%	%	%	%	%	%	%	ppm	ppm	ppm	ppm	ppm	ppm	ppm
End member	River/Desert	Locality	Sample	% class	MDL	0.01	0.01	0.04	0.01	0.01	0.01	0.01	0.01	0.01	0.01	-5.1	0.01	0.1	0.1	1	0.5	1	1	0.1
KARAKORUM	Hispar	Nagar	S1438	94%	63-2000 wet	70.0	12.7	3.8	1.2	4.2	2.5	2.1	0.4	0.1	0.1	2.5	99.80	63	2.3	2	278	448	11	41
LADAKH	Domkar	Domkar	S4430	98%	63-2000 wet	67.5	14.9	4.7	1.2	3.7	4.0	2.1	0.5	0.1	0.1	1.2	99.88	59	2.1	<1	331	358	9	16
KOHISTAN	Kandia	Halil	S1439	90%	63-2000 wet	54.7	16.3	7.7	5.1	8.4	2.7	0.8	1.0	0.2	0.1	2.7	99.78	25	1.7	<1	387	163	25	21
KOHISTAN	Swat	Fatepur	S1440	97%	63-2000 wet	57.1	16.4	7.8	4.3	7.2	3.2	0.9	1.0	0.1	0.1	1.7	99.80	25	1.1	<1	370	157	21	17
HIMALAYA	Zanskar	Rumbak	S4419	98%	63-2000 wet	63.8	10.0	2.2	1.4	9.8	1.9	2.0	0.3	0.2	0.1	8.2	99.86	68	2.9	<1	400	528	6	27
HIMALAYA	Nandihar	Daut	S1426	99%	63-2000 wet	76.7	11.5	2.4	0.8	1.4	2.2	2.9	0.3	0.1	0.0	1.6	99.93	126	4.3	2	111	378	5	12
NANGA PARBAT	Astor	Bunji	S1432	93%	63-2000 wet	69.0	14.1	3.8	1.9	4.0	2.8	2.6	0.4	0.1	0.1	1.0	99.87	111	2.9	2	249	431	10	20
POTWAR PLATEAU	Soan	Trap	S1454	95%	63-2000 wet	73.0	8.5	3.1	1.1	5.5	1.6	1.7	0.6	0.1	0.1	4.8	99.89	60	2.1	<1	191	291	6	18
	Indus	Kushalgar	S1447	98%	63-2000 wet	63.2	12.3	5.1	2.6	6.3	2.2	1.9	0.7	0.1	0.1	5.2	99.82	76	3.1	4	258	322	12	26
	Indus	Kalabagh	S1455	93%	63-2000 wet	62.7	11.5	4.7	2.5	7.1	2.0	1.9	0.7	0.1	0.1	6.5	99.82	76	3.3	<1	251	348	10	27
	Indus	Dhera Ismail Khan	S1461	97%	63-2000 wet	61.4	11.9	6.0	2.9	7.6	2.0	1.6	0.9	0.2	0.2	5.1	99.80	57	2.1	<1	279	301	16	39
	THAL	Mankera	S1462	100%	62-250 wet	64.4	13.3	5.5	2.7	5.9	2.4	1.7	0.7	0.1	0.1	3.2	99.84	59	1.7	4	284	316	15	28
	THAL	Haidarabad	S1463	96%	63-2000 wet	63.7	13.5	5.8	2.7	6.1	2.4	1.6	0.7	0.1	0.1	3.0	99.82	54	1.5	2	286	304	16	27
	THAL	Muzaffarghar	S1470	100%	63-2000 wet	57.7	12.7	8.3	3.5	8.0	2.2	1.4	1.1	0.2	0.2	4.5	99.74	49	1.6	2	263	263	19	44
	THAL	Munda	S1474	100%	62-250 wet	70.6	12.7	3.1	1.7	4.3	2.6	2.0	0.4	0.1	0.1	2.3	99.89	69	1.8	3	266	382	9	16

LF200	LF200	LF200	LF200	LF200	LF200	LF200	LF200	LF200	LF200	LF200	LF200	LF200	LF200	LF200	LF200	LF200	LF200	LF200	LF200	LF200	LF200	AQ200	LF200	LF200	LF200	AQ200	AQ200	AQ200	AQ200	AQ200	AQ200
La	Ce	Pr	Nd	Sm	Eu	Gd	Tb	Dy	Ho	Er	Tm	Yb	Lu	Th	U	Zr	Hf	V	Nb	Ta	Cr	Mo	W	Co	Ni	Cu	Ag	Au	Zn	Cd	Hg
ppm	ppm	ppm	ppm	ppm	ppm	ppm	ppm	ppm	ppm	ppm	ppm	ppm	ppm	ppm	ppm	ppm	ppm	ppm	ppm	ppm	ppm	ppm	ppm	ppm	ppm	ppm	ppm	ppb	ppm	ppm	ppm
0.1	0.1	0.02	0.3	0.05	0.02	0.05	0.01	0.05	0.02	0.03	0.01	0.05	0.01	0.2	0.1	0.1	0.1	8	0.1	0.1	14	0.1	0.5	0.2	20	0.1	0.1	0.5	1	0.1	0.01
117	219	23	77	13	1.3	9	1.3	7	1.5	5	0.7	5	0.8	56	6	395	11	48	13	1.3	82	0.3	15	7	<20	30	<0.1	3.7	30	0.1	<0.01
30	55	6	22	4	1.0	3	0.5	3	0.6	2	0.3	2	0.3	11	2	157	4	87	5	0.5	14	0.2	1	8	<20	8	<0.1	2.0	29	<0.1	<0.01
17	33	4	16	4	1.1	4	0.6	4	0.7	2	0.3	2	0.3	6	1	113	3	203	8	0.4	130	<0.1	1	25	73	31	<0.1	1.3	54	<0.1	<0.01
12	24	3	12	3	0.9	3	0.5	3	0.7	2	0.3	2	0.3	3	1	110	3	207	4	0.3	96	0.2	1	25	43	32	<0.1	2.8	41	<0.1	<0.01
55	99	11	37	6	1.4	5	0.8	5	0.9	3	0.4	3	0.4	14	3	186	5	34	11	1.0	27	0.3	1	5	<20	7	<0.1	1.5	27	<0.1	<0.01
18	38	4	16	3	0.9	3	0.4	2	0.5	1	0.2	1	0.2	9	2	113	4	47	7	0.5	27	0.4	2	6	<20	10	<0.1	0.6	41	<0.1	<0.01
29	57	7	25	5	0.9	4	0.6	3	0.7	2	0.3	2	0.3	14	3	134	4	71	6	0.5	55	0.2	1	11	<20	12	<0.1	0.9	34	<0.1	<0.01
29	55	6	23	4	0.8	3	0.5	3	0.6	2	0.3	2	0.3	10	2	216	6	74	9	0.8	137	0.2	1	6	21	7	<0.1	0.8	39	<0.1	<0.01
42	83	9	33	6	1.1	5	0.8	4	1.0	3	0.4	3	0.4	16	3	306	8	108	12	1.0	109	0.4	2	11	33	11	<0.1	3.2	44	<0.1	<0.01
49	95	10	38	7	1.2	6	0.9	5	0.9	3	0.4	3	0.4	20	4	323	8	98	13	1.2	130	0.2	2	11	31	12	<0.1	1.5	55	<0.1	<0.01
82	147	16	57	9	1.4	8	1.2	7	1.4	5	0.6	5	0.7	29	4	254	7	113	15	1.6	157	0.2	1	11	21	7	<0.1	1.4	35	<0.1	<0.01
40	75	8	30	6	1.1	5	0.8	5	1.0	3	0.5	3	0.4	16	2	195	5	120	9	0.7	123	0.2	6	12	22	9	<0.1	0.8	28	<0.1	<0.01
42	79	9	33	6	1.1	5	0.8	5	0.9	3	0.4	3	0.5	17	2	213	6	129	9	0.7	130	0.1	2	12	31	9	<0.1	0.5	49	<0.1	<0.01
84	162	18	64	11	1.5	9	1.4	8	1.6	5	0.7	5	0.7	38	5	524	13	187	16	1.5	212	0.2	2	14	40	9	<0.1	1.2	27	<0.1	<0.01
23	43	5	19	3	0.8	3	0.5	3	0.5	2	0.3	2	0.2	9	2	106	3	70	5	0.6	55	<0.1	1	8	21	7	<0.1	0.6	42	<0.1	<0.01

LF200	AQ200	LF200	AQ200	AQ200	AQ200	AQ200	AQ200	TC000	TC000																						
Ga	Tl	Sn	Pb	As	Sb	Bi	Se	TOT/C	TOT/S	CIA	CIW	PIA	WIP	CIX	CIA/WIP	$\alpha^{Al}Mg$	$\alpha^{Al}Ca$	$\alpha^{Al}Na$	$\alpha^{Al}K$	$\alpha^{Al}Rb$	$\alpha^{Al}Cs$	$\alpha^{Al}Be$	$\alpha^{Al}Sr$	$\alpha^{Al}Ba$	LaN/YbN	LaN/SmN	GdN/HoN	HoN/YbN	Eu/Eu*	Ce/Ce*	MREE/ MREE*
ppm	ppm	ppm	ppm	ppm	ppm	ppm	ppm	%	%																						
0.5	0.1	1	0.1	0.5	0.1	0.1	0.5	0.02	0.02																						
13	0.1	2	8	40	<0.1	0.2	<0.5	0.5	0.20	48	53	48	54	67	0.9	1.6	0.8	1.2	1.3	1.3	1.6	1.0	1.0	1.1	17.0	5.7	1.7	1.0	0.37	0.98	0.74
13	<0.1	<1	4	3	<0.1	<0.1	<0.5	0.1	<0.02	49	53	49	67	63	0.7	1.8	1.0	0.9	1.5	1.6	2.1	4.5	1.0	1.6	10.8	4.9	1.5	1.0	0.87	0.95	1.06
18	<0.1	<1	3	3	0.1	<0.1	<0.5	0.1	<0.02	45	46	44	66	76	0.7	0.5	0.5	1.4	4.2	4.2	2.8	5.0	0.9	3.8	5.5	2.8	1.4	1.0	0.94	0.93	1.43
16	<0.1	<1	3	2	<0.1	<0.1	<0.5	0.1	<0.02	46	48	46	67	73	0.7	0.6	0.6	1.2	3.5	4.2	4.4	5.0	1.0	4.0	4.2	2.4	1.2	1.1	0.95	0.92	1.42
10	<0.1	2	4	5	0.2	0.2	<0.5	2.2	<0.02	31	33	28	63	65	0.5	1.1	0.3	1.2	1.0	0.9	1.0	3.1	0.5	0.7	14.2	5.7	1.6	1.0	0.75	0.94	0.99
12	0.2	2	4	2	<0.1	0.3	<0.5	0.1	<0.02	56	66	59	50	63	1.1	2.1	2.1	1.2	0.8	0.6	0.8	0.9	2.3	1.2	11.5	3.5	1.7	1.3	0.83	0.97	1.39
15	0.2	2	3	4	<0.1	0.2	<0.5	0.1	<0.02	50	55	50	63	66	0.8	1.1	0.9	1.2	1.1	0.8	1.4	1.1	1.2	1.3	11.1	3.9	1.6	1.1	0.66	0.95	1.12
8	<0.1	1	6	2	0.1	0.1	<0.5	1.0	<0.02	37	41	35	45	66	0.8	1.2	0.4	1.3	1.0	0.9	1.2	2.6	1.0	1.1	10.3	4.4	1.6	0.9	0.66	0.96	1.03
13	0.1	3	7	5	0.1	0.1	<0.5	1.1	<0.02	42	45	41	59	68	0.7	0.7	0.5	1.3	1.3	1.0	1.2	0.5	1.0	1.5	10.7	4.2	1.4	1.1	0.61	0.97	1.02
13	0.1	2	7	4	0.1	0.1	<0.5	1.4	<0.02	39	42	37	59	68	0.7	0.7	0.4	1.3	1.2	1.0	1.0	3.5	1.0	1.3	11.6	4.4	1.7	0.9	0.60	0.96	1.02
12	<0.1	2	5	3	<0.1	0.1	<0.5	1.2	<0.02	39	41	38	59	70	0.7	0.6	0.4	1.4	1.6	1.3	1.7	3.6	0.9	1.5	11.9	5.4	1.5	0.9	0.51	0.93	0.86
14	<0.1	2	5	3	<0.1	0.1	<0.5	0.5	<0.02	45	48	44	58	70	0.8	0.8	0.6	1.3	1.6	1.4	2.3	0.5	1.0	1.6	9.5	4.6	1.3	1.0	0.64	0.95	1.02
14	<0.1	1	4	3	0.1	0.1	<0.5	0.5	<0.02	45	48	44	59	70	0.8	0.8	0.6	1.3	1.7	1.6	2.7	1.0	1.0	1.7	9.7	4.6	1.5	0.9	0.62	0.94	0.99
14	<0.1	3	5	3	0.2	0.2	<0.5	1.0	<0.02	40	42	39	61	71	0.6	0.6	0.4	1.4	1.8	1.7	2.4	1.0	1.1	1.9	12.6	4.6	1.6	1.0	0.46	0.96	0.91
12	<0.1	1	4	2	<0.1	0.1	<0.5	0.4	<0.02	48	52	47	57	66	0.8	1.1	0.8	1.1	1.3	1.2	2.1	0.6	1.0	1.3	9.7	4.1	1.5	1.0	0.74	0.94	1.09

Appendix Table C5 Nd isotopes in Thal Desert sand.

Desert dunes	Site	Sample	$^{143}Nd/^{144}Nd$	ppm	ε_{Nd}
Thal	Mankera	1462	0.511963	2	-13.17
Thal	Haidarabad	1463	0.512459	6	-3.49
Thal	Muzaffarghar	1470	0.512192	4	-8.70
Thal	Munda	1474	0.512077	7	-10.94

Appendix Table C6 Petrography and Heavy mineral data used for fixing model calculation.

Sample	Group	GSZ	Qz	KF	P	Lvm	Lc	Lsm	Lh	Lmf	Lmb	Lu	Mica	HM		MI*	tHMC	ZTR	Ttn	Ep	Gt	HgM	Amp	CPX	OPX	&tHM	
S1462	Thal	199	33	15	14	2	4	3	1	9	3	1	1	15	100.0	318	14.3	1	1	15	11	1	64	2	4	0	100.0
S1463	Thal	243	29	16	12	3	6	4	0	7	7	0	1	15	100.0	284	18.5	1	1	16	14	2	55	7	3	0	100.0
S1474	Thal	153	37	14	16	1	6	6	0	3	2	0	2	12	100.0	271	9.7	0	1	18	9	1	60	8	3	0	100.0
S1470	Thal	218	24	11	16	5	6	4	0	10	5	0	1	19	100.0	299	17.1	4	1	20	13	4	45	5	6	1	100.0
S4421	Ladakh	328	48	15	24	0	0	1	0	4	1	0	4	3	100.0	392	3.0	3	2	7	1	0	75	6	2	5	100.0
S4211	Ladakh	154	39	14	24	0	0	1	0	1	0	0	9	12	100.0	450	5.2	1	3	14	0	0	75	2	1	2	100.0
S1677	Himalaya	110	48	11	11	0	13	1	0	4	1	0	8	3	100.0	393	3.4	13	2	7	10	22	41	4	0	0	100.0
S4430	Ladakh	351	40	14	29	0	0	0	0	1	0	0	2	13	100.0	403	8.1	2	2	7	0	0	86	0	1	0	100.0
S4432	Ladakh	293	35	10	28	0	4	2	0	4	1	0	3	12	100.0	369	11.1	0	2	11	1	1	76	4	0	4	100.0
S4215	Himalaya	160	38	7	9	0	22	0	0	3	1	0	10	10	100.0	417	4.2	3	4	19	11	4	53	0	0	5	100.0
S1749	Karakorum	207	51	15	22	0	2	0	0	2	0	0	6	2	100.0	405	1.4	7	10	11	2	1	67	1	0	0	100.0
W 21	Upper Indus	319	35	21	21	0	6	4	1	6	0	0	3	2	100.0	336	4.0	4	7	22	13	6	43	4	1	0	100.0
S1748	Karakorum	184	47	13	12	0	17	1	0	4	1	0	3	3	100.0	350	3.6	6	3	34	6	1	46	2	1	0	100.0
W 23	Karakorum	108	43	18	14	0	7	0	0	2	0	0	10	6	100.0	n.d.	2.1	7	8	8	14	4	48	11	0	0	100.0
S1433	Upper Indus	410	47	15	15	1	6	3	0	2	3	0	6	3	100.0	330	2.1	0	0	16	7	7	62	6	2	0	100.0
S1435	Kohistan	360	27	12	14	1	8	16	0	5	5	1	4	8	100.0	288	14.9	0	0	8	3	0	78	7	3	0	100.0
S1437	Karakorum	222	22	7	15	0	17	19	0	15	1	0	1	3	100.0	241	1.0	5	4	20	2	0	66	2	0	0	100.0
S1438	Karakorum	353	50	12	15	0	4	1	0	3	2	0	5	9	100.0	390	6.4	3	9	21	21	1	41	3	0	0	100.0
S1436	Karakorum	335	35	9	13	1	12	13	1	6	2	0	4	4	100.0	270	3.8	1	3	22	7	5	53	8	0	0	100.0
S1434	Kohistan	333	42	8	14	0	12	14	0	6	1	0	3	0	100.0	231	1.5	1	0	24	2	0	70	2	0	0	100.0
S1432	Nanga Parbat	308	46	10	10	0	0	0	0	0	2	0	13	19	100.0	390	16.5	1	0	19	7	0	71	1	0	0	100.0
SED 15	Nanga Parbat	392	41	25	24	0	2	0	0	1	0	0	6	1	100.0	452	0.6	0	0	0	0	18	64	18	0	0	100.0
95 P W 26	Nanga Parbat	358	37	12	17	0	1	0	0	8	0	0	22	3	100.0	432	0.2	4	3	9	8	1	67	7	3	0	100.0
W 27	Nanga Parbat	311	35	16	15	0	3	0	0	1	0	0	13	15	100.0	437	10.6	0	4	10	18	1	59	7	0	0	100.0
S1431	Upper Indus	191	44	16	14	1	4	4	0	3	2	0	9	4	100.0	329	3.8	2	7	20	9	3	53	4	1	0	100.0
S1439	Kohistan	260	22	1	10	2	1	0	0	3	28	0	4	29	100.0	320	33.2	0	0	38	0	0	60	1	0	0	100.0
S1428	Upper Indus	252	40	12	17	1	8	5	0	3	2	0	5	6	100.0	300	6.0	0	1	12	12	1	58	4	11	0	100.0
S1426	Himalaya	308	52	9	13	0	0	0	0	13	0	0	6	6	100.0	411	3.8	2	0	10	26	8	47	0	6	1	100.0
S1427	Upper Indus	219	36	13	12	1	10	3	0	3	5	0	6	11	100.0	305	15.1	3	1	15	13	6	52	7	1	2	100.0
S1443	Kabul	152	33	7	6	0	12	17	0	8	2	0	7	8	100.0	214	5.7	1	0	24	12	2	55	5	0	0	100.0
S1444	Kabul	112	34	8	9	0	10	10	0	12	2	0	6	6	100.0	227	4.7	1	0	23	7	3	57	5	4	0	100.0
S1440	Kohistan	380	20	6	29	2	0	3	0	4	8	2	3	23	100.0	339	27.2	1	0	8	0	0	67	9	14	0	100.0
S1441	Kohistan	290	25	5	28	2	0	6	0	4	7	0	4	18	100.0	265	19.4	1	0	19	0	0	77	2	1	0	100.0
S1442	Kohistan	144	27	8	19	0	4	5	0	3	5	0	5	24	100.0	293	24.4	0	0	21	3	0	68	1	7	0	100.0
S1445	Kabul	105	38	4	10	1	11	7	0	11	2	0	9	8	100.0	267	5.9	0	2	18	3	2	66	6	1	0	100.0
S1446	Indus	193	33	9	13	2	7	6	0	15	2	1	3	9	100.0	305	7.3	0	0	16	2	3	68	6	3	0	100.0
S1447	Indus	179	35	6	12	1	7	8	1	10	3	0	6	12	100.0	292	9.7	0	1	17	9	3	60	7	4	0	100.0
S1455	Indus	138	38	8	6	1	13	13	1	5	1	1	3	10	100.0	251	6.6	3	2	30	8	3	44	4	3	2	100.0
S1448	Potwar Plateau	228	50	5	4	2	10	17	3	4	3	0	0	3	100.0	210	2.3	4	1	74	15	0	4	0	1	0	100.0
S1454	Potwar Plateau	178	45	9	7	2	10	12	4	2	3	0	1	6	100.0	192	3.7	3	0	76	5	0	16	0	0	0	100.0
S1458	West Pakistan	120	29	5	5	1	27	16	3	9	1	1	2	1	100.0	147	1.0	3	1	30	6	2	41	11	3	2	100.0
S1459	West Pakistan	280	16	1	5	10	16	13	5	0	2	16	0	16	100.0	n.d.	14.1	1	0	44	0	0	15	15	15	11	100.0
S1457	West Pakistan	135	22	4	6	7	21	13	3	5	4	4	0	12	100.0	154	14.6	1	0	32	13	1	7	26	11	9	100.0
S1456	West Pakistan	150	42	5	5	1	17	14	3	3	2	3	1	4	100.0	255	3.2	0	0	36	0	0	55	4	2	1	100.0
S1461	Indus	249	36	10	9	1	9	5	3	4	3	0	3	16	100.0	296	21.9	1	4	22	29	2	40	0	2	0	100.0
S1460	West Pakistan	167	45	2	3	3	18	15	5	4	1	1	0	1	100.0	172	0.2	18	1	30	18	2	6	14	2	9	100.0
S1472	West Pakistan	306	42	4	7	2	21	11	2	6	3	0	0	2	100.0	204	3.9	5	1	52	20	0	19	1	1	0	100.0
S1482	West Pakistan	86	41	6	5	0	17	5	0	8	1	0	9	7	100.0	261	1.3	2	0	26	5	1	61	1	2	0	100.0
S1483	West Pakistan	101	31	3	3	0	46	10	2	5	0	0	0	0	100.0	160	0.2	15	2	43	15	1	6	12	0	6	100.0
S1484	West Pakistan	259	7	1	1	0	86	3	2	1	0	0	0	0	100.0	n.d.	0.1	16	1	47	17	2	9	1	0	5	100.0
S1473	Indus	235	34	9	14	3	10	7	0	7	4	1	4	7	100.0	281	9.0	1	0	30	9	3	47	3	4	1	100.0
S1471	Indus	206	38	8	10	2	10	7	1	5	3	0	4	11	100.0	289	6.7	0	0	28	7	3	57	3	1	0	100.0
S1449	Punjab	259	45	3	2	4	11	14	2	5	4	0	1	8	100.0	216	8.9	4	1	55	30	2	7	1	0	0	100.0
S1453	Punjab	260	39	5	5	5	14	17	2	7	3	0	1	3	100.0	223	4.6	1	1	29	45	1	18	2	1	0	100.0
S1464	Punjab	122	37	10	7	3	13	7	1	9	4	0	3	7	100.0	251	4.4	2	1	41	7	2	42	4	2	0	100.0
S1469	Punjab	296	45	11	11	1	9	12	0	5	3	0	2	2	100.0	242	2.5	5	0	37	2	4	49	1	1	0	100.0
S1475	Punjab	194	48	6	7	0	9	12	1	10	2	0	3	4	100.0	262	5.1	3	1	25	34	2	30	3	1	0	100.0
S1477	Punjab	91	60	6	3	0	2	17	0	6	0	0	3	2	100.0	219	0.4	11	0	53	9	3	19	3	0	2	100.0
S1467	Punjab	286	55	10	6	1	7	8	0	4	1	0	4	3	100.0	266	5.3	10	0	8	36	15	26	1	1	0	100.0
S1478	Punjab	156	52	9	5	1	11	10	1	3	1	0	6	1	100.0	233	1.0	13	3	20	17	6	39	1	1	0	100.0
S1479	Punjab	160	50	6	11	3	8	5	0	7	3	0	5	2	100.0	244	7.3	2	4	24	31	1	31	4	3	0	100.0
7A	Kamlial	260	21	10	13	10	5	12	1	5	14	4	4	1	100.0	214	0.5	10	2	46	41	0	0	0	0	1	100.0
5.5A	Kamlial	215	21	7	15	13	5	14	1	9	9	1	3	0	100.0	207	0.2	3	3	52	41	0	0	0	0	1	100.0
5A	Kamlial	320	26	6	5	9	8	20	2	14	5	2	3	1	100.0	172	0.1	10	0	32	51	7	0	0	0	1	100.0
4.5A	Kamlial	150	24	4	17	19	2	10	4	2	14	0	2	3	100.0	n.d.	0.3	7	5	47	31	3	4	0	0	2	100.0
3.5A	Kamlial	140	30	7	13	10	5	13	0	8	6	1	5	2	100.0	184	0.3	9	0	41	49	0	1	0	0	0	100.0
2A	Kamlial	195	29	9	16	14	3	12	3	4	6	1	3	2	100.0	242	0.2	8	2	37	51	0	0	0	0	2	100.0
1.5A	Kamlial	225	27	2	15	17	3	13	0	8	8	0	5	1	100.0	192	0.2	6	3	46	36	3	3	0	0	4	100.0
1A	Kamlial	230	24	8	25	19	0	12	1	2	6	1	3	1	100.0	n.d.	0.1	9	0	12	73	0	2	0	0	4	100.0
S1481	Indus final	157	40	8	10	2	12	7	0	9	3	0	2	8	100.0	258	9.1	3	3	24	13	3	51	2	1	0	100.0
S1486	Indus final	116	44	11	10	2	7	8	0	9	2	0	3	4	100.0	281	6.0	1	5	31	12	2	47	1	1	0	100.0
S1489	Indus final	119	44	6	8	2	10	6	1	3	4	0	4	13	100.0	257	8	2	1	17	6	3	61	6	1	0	100.0
S1502	Indus final	134	31	5	9	1	13	7	1	9	4	0	2	20	100.0	270	19	5	3	21	17	6	41	4	3	1	100.0
S1480	Indus final	111	44	11	9	1	10	6	0	8	1	0	5	6	100.0	265											0.0
S1485	Indus final	268	44	14	12	2	6	6	1	6	1	0	5	3	100.0	286											0.0
S1487	Indus final	204	43	7	10	1	8	5	0	8	3	0	4	12	100.0	265											0.0
S1488	Indus final	135	42	8	11	1	12	4	0	7	3	0	2	10	100.0	274											0.0
S1500	Indus delta	115	40	9	10	1	9	7	0	8	2	0	3	10	100.0	236	1.9	2	1	24	11	3	55	3	1	0	100.0
S1490	Indus delta	106	47	7	9	1	15	5	0	6	2	0	4	3	100.0	257	2.0	4	1	35	12	3	44	2	0	0	100.0
KB 5,2	Delta core	100	40	10	12	1	11	2	0	6	0	0	15	3	100.0	243	2.4	5	2	30	2	2	52	4	3	0	100.0
TH 10,8	Delta core	130	38	11	15	3	9	3	0	7	3	0	10	2	100.0	252	3.5	2	0	23	13	2	48	8	2	0	100.0
KB 20,1	Delta core	90	46	10	10	1	13	3	0	7	0	0	7	2	100.0	254	2.3	4	3	28	4	3	51	5	2	2	100.0
KB 23.2	Delta core	80	40	10	10	0	8	4	0	7	0	0	19	1	100.0	255	0.2	3	2	21	5	6	54	4	1	3	100.0
KB 26,2	Delta core	75	36	8	8	1	9	1	0	3	0	0	32	2	100.0	254	0.3	2	4	28	5	3	53	4	1	0	100.0
KB 30,1	Delta core	70	37	11	8	2	9	2	0	4	1	0	25	1	100.0	255	0.4	3	1	29	3	0	50	8	3	1	100.0
KB 34.4	Delta core	170	41	5	15	3	8	8	1	6	2	0	12	0	100.0	252	2.7	3	1	27	11	4	45	6	1	0	100.0
KB 40,5	Delta core	125	39	12	14	3	5	3	0	7	2	0	12	3	100.0	226	3.3	2	3	35	4	1	54	0	0	0	100.0
KB 41.2	Delta core	115	46	8	14	3	4	3	0	8	2	0	9	2	100.0	238	3.2	3	1	26	4	1	62	1	1	0	100.0
6H5	Indus Fan																4.2	1	2	23	2	0	62	5	1	3	100.0
15H5	Indus Fan		49	5	9	1	14	2	0	4	1	0	10	4		283	5.0	2	3	25	7	5	50	3	0	5	100.0
25F3	Indus Fan																1.3	1	3	20	2	2	67	2	0	5	100.0
65F2	Indus Fan																0.5	3	2	21	1	1	68	0	0	3	100.0
6Rcc	Indus Fan																2.0	2	3	28	6	1	50	5	0	2	100.0
14Rcc	Indus Fan																2.4	0	2	32	1	1	60	1	0	2	100.0
21Rcc	Indus Fan																1.6	0	1	30	1	0	60	3	0	4	100.0
26Rcc	Indus Fan																4.8	0	2	39	5	1	49	1	0	2	100.0

Appendix Table C7 U-Pb zircon ages in samples of Thal Desert and upper Indus tributaries.

Sample S1749 Hushe River @ downstream Charakusa (Karakorum)   68 grains analysed   55 concordant ages

	concentrations			isotopic ratios						ages						discordance		preferred age	
grain	U [ppm]	Pb [ppm]	Th/U	Pb207/Pb206	2σ 76	Pb207/U235	2σ 75	Pb206/U238	2σ 68	age 206/238	2σ age 68	age 207/235	2σ age 75	age 207/206	2σ age 76	Δ 68-75 [%]	Δ 68-76 [%]	age	2σ age
S1749_001	1196.95242	10.7	1.0	0.05022	0.00098	0.12868	0.00261	0.01863	0.00027	119	1.68	122.9	2.35	205.1	44.47	-3.2	-42.0	119	1.68
S1749_002	4450.24953	10.7	1.4	0.1026	0.00206	0.04843	0.00097	0.00343	5.00E-05	22.1	0.34	48	0.94	1671.7	36.68	-54.0	-98.7		
S1749_003	362.021032	65.5	0.4	0.11231	0.00132	5.67443	0.08049	0.36727	0.00489	2016.6	23.05	1927.5	12.25	1837.1	21.12	4.6	9.8	1837.1	21.12
S1749_004	1762.81412	92.5	0.6	0.06495	0.00077	0.96948	0.01379	0.10851	0.00143	664.1	8.31	688.2	7.11	772.6	24.73	-3.5	-14.0	664.1	8.31
S1749_005	665.33595	54.3	2.3	0.0595	0.00079	0.67954	0.01042	0.08302	0.00111	514.1	6.62	526.5	6.3	585.5	28.66	-2.4	-12.2	514.1	6.62
S1749_006	2392.27411	150.3	0.2	0.07006	8.00E-04	1.36023	0.01892	0.14113	0.00185	851	10.44	872	8.14	930.2	23.23	-2.4	-8.5	851	10.44
S1749_007	3510.95172	5.3	0.5	0.04614	0.00249	0.01968	0.00101	0.0031	7.00E-05	20	0.45	19.8	1.01	4.7	124.97	1.0	325.5	20	0.45
S1749_008	22567.6084	34.5	0.2	0.07532	0.00133	0.02951	0.00054	0.00285	4.00E-05	18.3	0.26	29.5	0.54	1077	34.98	-38.0	-98.3		
S1749_009	290.269115	25.0	0.6	0.10114	0.00162	1.50393	0.02584	0.10809	0.00156	661.7	9.05	932	10.48	1645.1	29.34	-29.0	-59.8		
S1749_010	17231.875	33.7	0.5	0.04662	0.00068	0.02629	0.00043	0.0041	6.00E-05	26.4	0.35	26.3	0.42	29.6	34.05	0.4	-10.8	26.4	0.35
S1749_011	211.994298	60.4	1.3	0.11375	0.00151	5.4798	0.08421	0.35018	0.00487	1935.4	23.25	1897.4	13.2	1860.2	23.77	2.0	4.0	1860.2	23.77
S1749_012	1288.27304	108.2	0.6	0.0676	0.00079	1.30835	0.01849	0.14069	0.00185	848.5	10.46	849.4	8.13	856.4	24.12	-0.1	-0.9	848.5	10.46
S1749_013	1436.66905	14.9	0.5	0.05339	0.00107	0.1258	0.00262	0.01713	0.00025	109.5	1.57	120.3	2.36	345.2	44.92	-9.0	-68.3	109.5	1.57
S1749_014	1139.87703	2.7	0.8	0.04757	0.00167	0.02255	0.00077	0.00345	6.00E-05	22.2	0.38	22.6	0.77	77.3	82.2	-1.8	-71.3	22.2	0.38
S1749_015	6095.65142	12.0	1.6	0.19514	0.00499	0.1024	0.00234	0.00381	7.00E-05	24.5	0.47	99	2.16	2786	41.28	-75.3	-99.1		
S1749_016	6849.04654	52.0	1.3	0.05092	0.00084	0.08318	0.00148	0.01187	0.00016	76.1	1.04	81.1	1.39	237.2	37.68	-6.2	-67.9	76.1	1.04
S1749_017	2948.35146	6.2	0.9	0.05689	0.0023	0.02552	0.00098	0.00326	6.00E-05	21	0.41	25.6	0.97	486.5	87.44	-18.0	-95.7		
S1749_018	1695.95438	66.9	0.1	0.06921	0.00083	1.05225	0.0151	0.11052	0.00146	675.8	8.48	730	7.47	905	24.57	-7.4	-25.3	675.8	8.48
S1749_019	518.570667	69.0	0.6	0.15839	0.00185	5.85021	0.0824	0.26849	0.00358	1533.1	18.17	1953.9	12.21	2438.6	19.61	-21.5	-37.1		
S1749_020	2084.06702	13.1	0.4	0.0547	0.00093	0.12018	0.0022	0.01597	0.00022	102.1	1.41	115.2	1.99	400.1	37.27	-11.4	-74.5	102.1	1.41
S1749_021	1312.73392	76.6	0.7	0.06589	8.00E-04	1.00732	0.01453	0.11113	0.00147	679.3	8.52	707.5	7.35	802.8	25.15	-4.0	-15.4	679.3	8.52
S1749_022	1237.72055	58.0	0.5	0.06472	0.00086	0.65368	0.01003	0.07342	0.00099	456.7	5.92	510.7	6.16	765.1	27.9	-10.6	-40.3	456.7	5.92
S1749_023	828.408487	52.7	0.9	0.06416	0.00083	0.96221	0.01445	0.10902	0.00146	667	8.47	684.4	7.47	746.9	27.01	-2.5	-10.7	667	8.47
S1749_024	1609.52594	382.7	0.5	0.16121	0.00179	9.87322	0.13525	0.44519	0.00583	2373.8	25.98	2423	12.63	2468.4	18.58	-2.0	-3.8	2468.4	18.58
S1749_025	4406.21994	13.7	0.1	0.0516	0.00116	0.03446	0.00079	0.00486	7.00E-05	31.2	0.46	34.4	0.77	267.7	50.73	-9.3	-88.3	31.2	0.46
S1749_026	4954.14367	50.2	0.6	0.04907	0.00064	0.12246	0.00185	0.01814	0.00024	115.9	1.52	117.3	1.68	151.2	30.24	-1.2	-23.3	115.9	1.52
S1749_027	1823.15096	44.7	0.4	0.05625	0.00073	0.33428	0.00504	0.0432	0.00058	272.6	3.55	292.8	3.84	461.7	28.69	-6.9	-41.0	272.6	3.55
S1749_028	556.07735	34.7	0.4	0.06365	0.00097	0.76563	0.01286	0.08744	0.00121	540.4	7.15	577.3	7.4	730	31.93	-6.4	-26.0	540.4	7.15
S1749_029	554.446625	27.3	0.4	0.06362	0.00089	0.77506	0.01227	0.08856	0.0012	547	7.11	582.7	7.02	728.9	29.35	-6.1	-25.0	547	7.11
S1749_030	5096.01677	9.7	0.7	0.04882	0.00098	0.02199	0.00046	0.00327	5.00E-05	21.1	0.3	22.1	0.45	139.1	46.42	-4.5	-84.8	21.1	0.3
S1749_031	3828.94316	5.6	0.1	0.05685	0.00225	0.02513	0.00095	0.00321	6.00E-05	20.7	0.4	25.2	0.94	485.2	85.74	-17.9	-95.7		
S1749_032	5547.7277	149.4	0.4	0.0609	0.00071	0.41493	0.00584	0.04952	0.00065	311.6	3.99	352.4	4.19	635.8	24.78	-11.6	-51.0	311.6	3.99
S1749_033	2190.06417	28.1	1.8	0.04761	0.00074	0.11205	0.00192	0.01711	0.00023	109.4	1.48	107.8	1.75	78.9	37.27	1.5	38.7	109.4	1.48
S1749_034	722.411338	7.5	1.2	0.06696	0.00241	0.14177	0.00487	0.01539	3.00E-04	98.5	1.88	134.6	4.33	836.5	73.37	-26.8	-88.2		
S1749_035	12789.7791	30.1	2.2	0.05127	0.00098	0.02297	0.00046	0.00326	5.00E-05	21	0.3	23.1	0.45	252.8	43.31	-9.1	-91.7	21	0.3
S1749_036	2335.19873	22.3	0.5	0.04883	0.00075	0.11936	0.00202	0.01777	0.00024	113.5	1.53	114.5	1.83	139.7	35.64	-0.9	-18.8	113.5	1.53
S1749_037	1262.18143	56.8	0.2	0.06142	0.00076	0.87867	0.01291	0.10399	0.00138	637.8	8.06	640.3	6.98	653.9	26.48	-0.4	-2.5	637.8	8.06
S1749_038	3077.17877	9.8	0.2	0.04544	0.0012	0.03739	0.00099	0.00598	9.00E-05	38.4	0.58	37.3	0.97	0.1	30.53	2.9	38300.0	38.4	0.58
S1749_039	1373.07076	11.2	0.4	0.04996	0.00093	0.12316	0.00242	0.01792	0.00025	114.5	1.6	117.9	2.19	193.2	42.72	-2.9	-40.7	114.5	1.6
S1749_040	1586.69578	81.3	0.7	0.06292	0.00077	0.76789	0.01113	0.08872	0.00117	548	6.95	578.5	6.39	705.4	25.7	-5.3	-22.3	548	6.95
S1749_041	1842.71967	43.3	0.2	0.06031	0.00083	0.39935	0.00628	0.04813	0.00065	303	3.99	341.2	4.55	614.7	29.58	-11.2	-50.7	303	3.99
S1749_042	17059.0181	23.6	0.3	0.04607	0.00069	0.01914	0.00032	0.00302	4.00E-05	19.4	0.26	19.3	0.32	0.1	36.87	0.5	19300.0	19.4	0.26
S1749_043	3416.36965	24.5	0.6	0.04841	0.00073	0.10654	0.00178	0.016	0.00022	102.3	1.38	102.8	1.64	119.5	35.21	-0.5	-14.4	102.3	1.38
S1749_044	1865.54982	103.8	0.7	0.06546	0.00078	1.11783	0.016	0.12413	0.00164	754.3	9.4	761.9	7.67	789.2	24.82	-1.0	-4.4	754.3	9.4
S1749_045	5200.3832	8.5	1.5	0.04503	0.00153	0.02022	0.00068	0.00326	5.00E-05	21	0.34	20.3	0.67	0.1	26.15	3.4	20900.0	21	0.34
S1749_046	810.470508	46.2	0.6	0.06496	0.00084	0.90381	0.01359	0.10114	0.00135	621.1	7.92	653.8	7.25	773.1	26.92	-5.0	-19.7	621.1	7.92
S1749_047	1009.419	4.1	0.7	0.0522	0.00206	0.04715	0.00179	0.00657	0.00012	42.2	0.8	46.8	1.73	294.2	87.38	-9.8	-85.7	42.2	0.8
S1749_048	10223.0173	26.0	3.3	0.07276	0.0012	0.03076	0.00054	0.00307	4.00E-05	19.8	0.28	30.8	0.53	1007.2	33.09	-35.7	-98.0		
S1749_049	596.845485	5.5	0.5	0.05154	0.00125	0.1259	0.00308	0.01775	0.00027	113.5	1.7	120.4	2.78	265.2	54.67	-5.7	-57.2	113.5	1.7
S1749_050	3052.71789	35.9	1.8	0.04909	0.00072	0.11412	0.00187	0.0169	0.00023	108	1.45	109.7	1.7	152.2	33.9	-1.5	-29.0	108	1.45
S1749_051	4582.33828	10.1	1.4	0.04857	0.00184	0.02077	0.00076	0.00311	6.00E-05	20	0.37	20.9	0.76	127.2	86.96	-4.3	-84.3	20	0.37
S1749_052	1118.6776	31.6	0.5	0.06394	0.00096	0.46891	0.00781	0.0533	0.00073	334.8	4.48	390.4	5.4	739.8	31.54	-14.2	-54.7		
S1749_053	4595.38409	8.9	1.0	0.05072	0.00106	0.02325	5.00E-04	0.00333	5.00E-05	21.4	0.31	23.3	0.5	228	47.6	-8.2	-90.6	21.4	0.31
S1749_054	673.489577	5.3	0.0	0.04864	0.00113	0.11021	0.0026	0.01647	0.00025	105.3	1.56	106.2	2.38	130.7	53.75	-0.8	-19.4	105.3	1.56
S1749_055	600.106935	23.1	0.5	0.0632	0.00103	0.62019	0.01098	0.07134	0.001	444.2	6.02	490	6.88	714.8	34.36	-9.3	-37.9	444.2	6.02
S1749_056	2248.77028	19.7	0.4	0.05166	0.00085	0.12702	0.00226	0.01787	0.00025	114.2	1.56	121.4	2.03	270.3	37.16	-5.9	-57.8	114.2	1.56
S1749_057	588.691858	50.9	0.4	0.07331	0.00092	1.73802	0.02567	0.17232	0.0023	1024.9	12.67	1022.7	9.52	1022.7	25.11	0.2	0.2	1024.9	12.67
S1749_058	637.613619	39.9	0.7	0.06514	0.00086	1.1161	0.01708	0.12454	0.00168	756.6	9.61	761.1	8.2	778.9	27.57	-0.6	-2.9	756.6	9.61
S1749_059	2543.93157	25.2	0.8	0.05162	0.00077	0.12516	0.00208	0.01762	0.00024	112.6	1.52	119.7	1.88	268.6	33.89	-5.9	-58.1	112.6	1.52
S1749_060	26929.7987	73.6	2.2	0.05694	0.001	0.02429	0.00045	0.0031	4.00E-05	20	0.28	24.4	0.45	488.7	38.63	-18.0	-95.9		
S1749_061	37110.4172	216.8	0.3	0.04859	0.00059	0.10334	0.0015	0.01546	2.00E-04	98.9	1.3	99.9	1.38	127.9	28.42	-1.0	-22.7	98.9	1.3
S1749_062	1037.14133	57.4	0.7	0.07184	9.00E-04	1.29008	0.01907	0.13053	0.00174	790.9	9.94	841.3	8.45	981.5	25.33	-6.0	-19.4	790.9	9.94
S1749_063	1549.1891	11.9	0.5	0.04703	0.00098	0.10715	0.00232	0.01656	0.00024	105.9	1.5	103.4	2.13	50.3	48.16	2.4	110.5	105.9	1.5
S1749_064	1343.7177	92.1	1.4	0.06698	9.00E-04	0.96229	0.01488	0.10443	0.00141	640.3	8.23	684.5	7.7	837.2	27.78	-6.5	-23.5	640.3	8.23
S1749_065	1113.78543	9.6	0.4	0.05002	0.00097	0.12115	0.00247	0.01761	0.00025	112.5	1.59	116.1	2.23	195.9	44.67	-3.1	-42.6	112.5	1.59
S1749_066	1648.66335	5.9	0.8	0.04587	0.00116	0.04221	0.00108	0.00669	1.00E-04	43	0.65	42	1.05	0.1	50.39	2.4	42900.0	43	0.65
S1749_068	1632.35609	3.0	1.1	0.11229	0.00299	0.05667	0.00143	0.00367	6.00E-05	23.6	0.41	56	1.37	1836.7	47.43	-57.9	-98.7		

Sample S1437 Upper Hunza River @ Altit (Northern Karakorum)   45 grains analysed   38 concordant ages

	concentrations			isotopic ratios						ages						discordance		preferred age	
grain	U [ppm]	Pb [ppm]	Th/U	Pb207/Pb206	2σ 76	Pb207/U235	2σ 75	Pb206/U238	2σ 68	age 206/238	2σ age 68	age 207/235	2σ age 75	age 207/206	2σ age 76	Δ 68-75 [%]	Δ 68-76 [%]	age	2σ age
S1437_001	1407.8	7.5	0.9	0.06033	0.00126	0.13883	0.00291	0.01672	0.00024	106.9	1.5	132	2.59	615.4	44.37	-19.015	-82.6		
S1437_002	3669.8	10.1	0.6	0.05147	0.001	0.06901	0.00136	0.00974	0.00013	62.5	0.85	67.8	1.3	262.1	43.87	-7.817	-76.2	62.5	0.85
S1437_003	695.1	3.7	1.3	0.05047	0.00175	0.11651	0.00392	0.01678	0.00028	107.2	1.76	111.9	3.57	216.9	78.25	-4.200	-50.6	107.2	1.76
S1437_004	384.9	16.9	0.9	0.06765	0.00109	1.38367	0.02366	0.14865	0.00201	893.4	11.28	882	10.08	857.8	33.18	1.293	4.2	893.4	11.28
S1437_005	3100.4	8.3	0.7	0.0485	0.00101	0.06392	0.00135	0.00958	0.00013	61.4	0.85	62.9	1.29	123.9	48.36	-2.385	-50.4	61.4	0.85
S1437_006	2332.7	12.2	1.1	0.04861	0.00092	0.11531	0.00224	0.01724	0.00023	110.2	1.48	110.8	2.04	128.8	43.78	-0.542	-14.4	110.2	1.48
S1437_007	2209.0	9.3	0.7	0.04811	0.00099	0.10983	0.00229	0.01659	0.00023	106.1	1.45	105.8	2.09	104.9	47.74	0.284	1.1	106.1	1.45
S1437_008	492.8	17.8	0.6	0.05828	0.00123	0.84714	0.01811	0.10565	0.00154	647.4	8.96	623.1	9.95	539.5	46.2	3.900	20.0	647.4	8.96
S1437_009	1924.3	9.7	1.2	0.0719	0.00187	0.18161	0.00456	0.01836	0.00029	117.3	1.85	169.4	3.92	983.1	52.06	-30.756	-88.1		
S1437_010	2385.7	10.4	1.3	0.05164	0.00104	0.11692	0.00239	0.01645	0.00023	105.2	1.45	112.3	2.17	269.7	45.47	-6.322	-61.0	105.2	1.45
S1437_011	2501.5	12.0	0.9	0.04849	0.00092	0.11498	0.00224	0.01723	0.00023	110.1	1.48	110.5	2.04	123.2	43.97	-0.362	-10.6	110.1	1.48
S1437_012	561.6	3.3	0.9	0.08778	0.00405	0.23719	0.01004	0.01964	0.00047	125.4	2.97	216.1	8.24	1377.7	86.15	-41.971	-90.9		
S1437_013	473.2	2.4	1.0	0.04661	0.00176	0.12045	0.00441	0.01878	0.00032	120	2.05	115.5	4	29.1	88.21	3.896	312.4	120	2.05
S1437_014	3481.3	15.1	0.8	0.0454	0.00193	0.05541	0.00228	0.00887	0.00016	56.9	1.02	54.8	2.19	0.1	65.25	3.832	56800.0	56.9	1.02
S1437_015	1484.4	7.4	0.8	0.04771	0.00107	0.12933	0.00292	0.0197	0.00028	125.8	1.76	123.5	2.63	84.1	53.36	1.862	49.6	125.8	1.76
S1437_016	498.7	9.2	0.8	0.05453	0.0011	0.47633	0.00979	0.06348	0.00089	396.8	5.4	395.6	6.73	393.1	44.35	0.303	0.9	396.8	5.4
S1437_017	176.7	3.1	1.3	0.0552	0.00179	0.45742	0.01451	0.06022	0.00101	377	6.14	382.5	10.11	420.1	70.53	-1.438	-10.3	377	6.14
S1437_018	759.9	2.0	1.2	0.05112	0.00212	0.0676	0.0027	0.00961	0.00017	61.7	1.11	66.4	2.57	246.4	92.64	-7.078	-75.0	61.7	1.11
S1437_019	648.0	1.6	1.0	0.0496	0.00244	0.06855	0.00324	0.01004	2.00E-04	64.4	1.27	67.3	3.08	176.3	110.67	-4.309	-63.5	64.4	1.27
S1437_020	5024.7	27.9	0.7	0.04926	0.00087	0.12003	0.0022	0.01771	0.00024	113.2	1.5	115.1	1.99	160.2	40.66	-1.651	-29.3	113.2	1.5
S1437_021	785.4	3.0	1.8	0.04932	0.00176	0.07716	0.00267	0.01137	0.00019	72.9	1.21	75.5	2.52	163.1	81.26	-3.444	-55.3	72.9	1.21
S1437_022	875.7	4.6	0.5	0.04852	0.00129	0.13545	0.00355	0.02029	3.00E-04	129.5	1.92	129	3.18	124.6	61.31	0.388	3.9	129.5	1.92
S1437_023	659.7	4.5	1.2	0.12622	0.00339	0.32002	0.00795	0.01843	0.00033	117.7	2.09	281.9	6.11	2045.9	46.68	-58.248	-94.2		
S1437_024	4616.3	83.8	0.2	0.05878	0.00075	0.67316	0.00972	0.08323	0.00106	515.4	6.3	522.6	5.9	559.1	27.71	-1.378	-7.8	515.4	6.3
S1437_025	886.1	13.6	0.2	0.0437	0.00116	0.1029	0.00272	0.01711	0.00025	109.4	1.59	99.4	2.51	0.1	0	10.060	109300.0	109.4	1.59
S1437_026	2717.5	54.3	2.0	0.06164	0.00084	0.71673	0.01078	0.0845	0.00109	522.9	6.47	548.7	6.38	661.7	28.87	-4.702	-21.0	522.9	6.47
S1437_027	6721.2	18.5	3.7	0.05218	0.00118	0.0662	0.0015	0.00922	0.00013	59.2	0.85	65.1	1.43	293.5	50.92	-9.063	-79.8	59.2	0.85
S1437_028	828.6	6.5	2.1	0.04945	0.00122	0.12876	0.00315	0.01892	0.00028	120.9	1.76	123	2.83	169.3	56.4	-1.707	-28.6	120.9	1.76
S1437_030	971.9	10.4	0.7	0.0618	0.00134	0.38766	0.00844	0.04559	0.00067	287.4	4.11	332.7	6.18	667	45.89	-13.616	-56.9		
S1437_031	563.5	2.2	0.6	0.05182	0.00193	0.12369	0.00446	0.01735	3.00E-04	110.9	1.92	118.4	4.03	277.6	83.13	-6.334	-60.1	110.9	1.92
S1437_032	4791.0	10.6	0.9	0.04824	0.00099	0.06396	0.00133	0.00964	0.00013	61.8	0.86	63	1.27	110.9	47.79	-1.905	-44.3	61.8	0.86
S1437_033	1877.1	9.7	1.6	0.07535	0.0028	0.09834	0.00342	0.00948	0.00019	60.9	1.2	95.2	3.16	1078	72.95	-36.029	-94.4		
S1437_034	1329.3	8.8	1.5	0.05088	0.00137	0.1217	0.00328	0.01738	0.00025	111.1	1.62	116.6	2.97	235.5	61.17	-4.717	-52.8	111.1	1.62
S1437_035	1023.0	8.2	0.9	0.04765	0.00172	0.10991	0.00386	0.01676	0.00028	107.2	1.79	105.9	3.53	81.3	84.34	1.228	31.9	107.2	1.79
S1437_036	1633.7	8.1	1.1	0.04946	0.00107	0.12335	0.00269	0.01813	0.00026	115.8	1.62	118.1	2.43	169.6	49.63	-1.948	-31.7	115.8	1.62
S1437_037	1653.3	9.3	0.3	0.04705	0.00152	0.13097	0.00416	0.02023	0.00032	129.1	2.03	125	3.73	51.5	75.74	3.280	150.7	129.1	2.03
S1437_038	1888.9	43.3	0.4	0.05755	8.00E-04	0.74665	0.0114	0.0943	0.00122	580.9	7.18	566.3	6.63	512.2	30.45	2.578	13.4	580.9	7.18
S1437_039	16100.9	27.5	2.1	0.04823	0.00084	0.06807	0.00124	0.01026	0.00014	65.8	0.88	66.9	1.18	110.5	40.62	-1.644	-40.5	65.8	0.88
S1437_040	50920.1	141.4	7.2	0.04929	0.00076	0.05039	0.00083	0.00743	1.00E-04	47.7	0.62	49.9	0.8	161.8	35.56	-4.409	-70.5	47.7	0.62
S1437_041	991.6	2.1	0.6	0.04909	0.00197	0.06809	0.00264	0.01008	0.00018	64.7	1.13	66.9	2.51	152	91.24	-3.288	-57.4	64.7	1.13
S1437_042	2334.6	3.3	0.8	0.04757	0.00184	0.05768	0.00215	0.00881	0.00016	56.6	1	56.9	2.07	77	90.13	-0.527	-26.5	56.6	1
S1437_043	2770.5	12.3	1.2	0.04949	0.00093	0.11448	0.00222	0.01681	0.00023	107.5	1.46	110.1	2.02	171.3	43.31	-2.361	-37.2	107.5	1.46
S1437_044	2252.2	15.0	0.9	0.0496	0.00185	0.09725	0.0035	0.01425	0.00025	91.2	1.6	94.2	3.24	176.4	84.71	-3.185	-48.3	91.2	1.6
S1437_045	527.737	8.2	0.4	0.04296	0.00117	0.09594	0.00023	0.01623	0.00263	103.8	1.49	93	2.43	0.1	0	11.613	103700.0	103.8	1.49

Sample S1748 Braldu River @ downstream Baltoro (Karakorum) 154 grains analysed 124 concordant ages

	concentrations			isotopic ratios						ages						discordance		preferred age	
grain	U [ppm]	Pb [ppm]	Th/U	Pb207/Pb206	2σ 76	Pb207/U235	2σ 75	Pb206/U238	2σ 68	age 206/238	2σ age 68	age 207/235	2σ age 75	age 207/206	2σ age 76	Δ 68-75 [%]	Δ 68-76 [%]	age	2σ age
S1748_001	4623.1	43.4	0.2	0.04765	0.00064	0.11429	0.00175	0.01744	0.00023	111.4	1.5	109.9	1.6	81.2	32.5	1.4	37.2	111.4	1.5
S1748_002	432.1	142.9	0.7	0.20152	0.00218	15.16426	0.20264	0.54706	0.00713	2813.0	29.7	2825.6	12.7	2838.5	17.5	-0.4	-0.9	2838.5	17.5
S1748_003	552.8	40.4	0.8	0.06522	0.00083	1.22055	0.01797	0.13605	0.00180	822.3	10.2	810.0	8.2	781.4	26.5	1.5	5.2	822.3	10.2
S1748_004	1495.4	2.9	0.8	0.06660	0.00310	0.03225	0.00141	0.00352	0.00008	22.7	0.5	32.2	1.4	825.4	94.2	-29.5	-97.2		
S1748_005	1479.1	80.5	0.1	0.06849	0.00084	1.21362	0.01749	0.12882	0.00169	781.1	9.7	806.9	8.0	883.4	25.2	-3.2	-11.6	781.1	9.7
S1748_006	138.6	9.5	0.6	0.06195	0.00142	1.03906	0.02416	0.12193	0.00188	741.7	10.8	723.4	12.0	672.4	48.2	2.5	10.3	741.7	10.8
S1748_007	712.6	146.0	0.2	0.16311	0.00176	8.37449	0.11166	0.37325	0.00484	2044.7	22.7	2272.4	12.1	2488.2	18.1	-10.0	-17.8	2488.2	18.1
S1748_008	1461.1	11.1	0.5	0.05453	0.00098	0.13099	0.00248	0.01746	0.00024	111.6	1.5	125.0	2.2	393.0	39.6	-10.7	-71.6	111.6	1.5
S1748_009	994.7	72.3	0.3	0.06963	0.00081	1.47417	0.02048	0.15392	0.00201	922.9	11.2	919.8	8.4	917.4	23.6	0.3	0.6	922.9	11.2
S1748_010	575.7	9.4	0.6	0.04453	0.00107	0.10058	0.00244	0.01642	0.00024	105.0	1.5	97.3	2.3	0.1	0.0	7.9	104900.0	105.0	1.5
S1748_011	1423.6	92.0	0.4	0.07139	0.00081	1.64441	0.02261	0.16747	0.00218	998.1	12.0	987.4	8.7	968.5	23.0	1.1	3.1	998.1	12.0
S1748_012	660.4	46.0	0.9	0.06945	0.00086	1.49175	0.02167	0.15616	0.00206	935.4	11.5	927.0	8.8	912.1	25.4	0.9	2.6	935.4	11.5
S1748_013	1899.8	74.1	0.8	0.06905	0.00080	0.96146	0.01336	0.10122	0.00132	621.6	7.7	684.1	6.9	900.3	23.7	-9.1	-31.0	621.6	7.7
S1748_014	1925.9	12.1	0.6	0.05019	0.00090	0.12809	0.00243	0.01855	0.00026	118.5	1.6	122.4	2.2	203.7	41.1	-3.2	-41.8	118.5	1.6
S1748_015	3029.9	43.0	0.3	0.05957	0.00101	0.23687	0.00428	0.02891	0.00040	183.7	2.5	215.9	3.5	588.1	36.5	-14.9	-68.8	183.7	2.5
S1748_016	1285.0	8.2	0.6	0.05140	0.00105	0.12521	0.00263	0.01771	0.00025	113.2	1.6	119.8	2.4	258.9	46.3	-5.5	-56.3	113.2	1.6
S1748_017	371.8	70.5	1.3	0.15727	0.00178	9.01166	0.12391	0.41656	0.00551	2244.9	25.1	2339.2	12.6	2426.5	19.1	-4.0	-7.5	2426.5	19.1
S1748_018	2636.9	24.8	0.8	0.04819	0.00071	0.12754	0.00208	0.01924	0.00026	122.8	1.6	121.9	1.9	108.8	34.5	0.7	12.9	122.8	1.6
S1748_019	384.9	27.8	1.5	0.06564	0.00092	1.20061	0.01894	0.13297	0.00180	804.8	10.2	800.9	8.7	795.0	29.2	0.5	1.2	804.8	10.2
S1748_020	609.9	27.0	0.7	0.07543	0.00126	1.14966	0.02052	0.11080	0.00158	677.4	9.2	777.1	9.7	1080.1	33.3	-12.8	-37.3	677.4	9.2
S1748_021	2630.4	28.3	0.7	0.04976	0.00070	0.12554	0.00199	0.01834	0.00024	117.2	1.5	120.1	1.8	183.8	32.5	-2.4	-36.2	117.2	1.5
S1748_022	2596.1	32.2	1.0	0.05653	0.00085	0.13019	0.00215	0.01674	0.00023	107.0	1.4	124.3	1.9	472.6	33.2	-13.9	-77.4		
S1748_023	238.1	2.9	0.3	0.05094	0.00188	0.17928	0.00640	0.02559	0.00047	162.9	2.9	167.4	5.5	238.0	83.0	-2.7	-31.6	162.9	2.9
S1748_024	203.8	15.2	0.5	0.06673	0.00103	1.24982	0.02112	0.13617	0.00188	823.0	10.7	823.3	9.5	829.2	31.9	0.0	-0.7	823.0	10.7
S1748_025	670.2	138.6	0.5	0.13135	0.00148	6.87477	0.09440	0.38049	0.00501	2078.6	23.4	2095.4	12.2	2116.1	19.7	-0.8	-1.8	2116.1	19.7
S1748_026	2516.2	335.7	0.2	0.16129	0.00177	7.02007	0.09446	0.31641	0.00412	1772.2	20.2	2114.0	12.0	2469.3	18.4	-16.2	-28.2		
S1748_027	1298.1	11.9	0.7	0.05935	0.00102	0.14586	0.00266	0.01787	0.00025	114.2	1.6	138.2	2.4	580.1	37.0	-17.4	-80.3		
S1748_028	2615.7	124.4	0.4	0.06501	0.00075	1.03171	0.01437	0.11537	0.00150	703.9	8.7	719.8	7.2	774.6	24.2	-2.2	-9.1	703.9	8.7
S1748_029	184.3	57.4	1.1	0.16221	0.00185	10.68735	0.14826	0.47898	0.00638	2522.8	27.8	2496.3	12.9	2478.8	19.2	1.1	1.8	2478.8	19.2
S1748_030	1418.7	8.8	0.4	0.04996	0.00113	0.11955	0.00273	0.01739	0.00026	111.2	1.6	114.7	2.5	193.3	51.6	-3.1	-42.5	111.2	1.6
S1748_031	1154.6	74.8	0.7	0.06601	0.00077	1.17407	0.01646	0.12930	0.00169	783.9	9.6	788.5	7.7	806.7	24.4	-0.6	-2.8	783.9	9.6
S1748_032	17404.7	44.3	5.4	0.05696	0.00152	0.02564	0.00067	0.00327	0.00005	21.1	0.3	25.7	0.7	489.4	58.3	-17.9	-95.7		
S1748_033	2782.0	119.2	0.1	0.06423	0.00072	0.98142	0.01338	0.11109	0.00144	679.1	8.4	694.3	6.9	749.1	23.5	-2.2	-9.3	679.1	8.4
S1748_034	1788.9	100.7	0.8	0.06499	0.00075	1.07835	0.01491	0.12063	0.00157	734.2	9.0	742.8	7.3	773.9	23.9	-1.2	-5.1	734.2	9.0
S1748_035	479.4	16.6	0.4	0.06263	0.00104	0.53029	0.00940	0.06156	0.00086	385.1	5.2	432.0	6.2	695.6	34.9	-10.9	-44.6	385.1	5.2
S1748_036	1844.4	9.0	0.1	0.06243	0.00139	0.10578	0.00237	0.01232	0.00019	78.9	1.2	102.1	2.2	689.0	46.9	-22.7	-88.5		
S1748_037	254.4	14.1	0.8	0.06670	0.00107	1.28538	0.02238	0.14010	0.00196	845.2	11.1	839.2	10.0	828.3	33.2	0.7	2.0	845.2	11.1
S1748_038	728.9	71.2	1.9	0.08155	0.00097	2.38310	0.03379	0.21244	0.00280	1241.8	14.9	1237.5	10.1	1234.7	23.2	0.3	0.6	1234.7	23.2
S1748_039	414.2	0.7	0.9	0.05385	0.00341	0.03015	0.00181	0.00407	0.00010	26.2	0.7	30.2	1.8	364.8	136.6	-13.2	-92.8		
S1748_040	549.6	3.1	0.8	0.04961	0.00164	0.12352	0.00400	0.01810	0.00030	115.6	1.9	118.3	3.6	176.6	75.3	-2.3	-34.5	115.6	1.9
S1748_041	476.2	24.7	0.4	0.06170	0.00092	0.91089	0.01498	0.10733	0.00146	657.2	8.5	657.5	8.0	663.6	31.5	0.0	-1.0	657.2	8.5
S1748_042	712.6	35.2	0.8	0.06650	0.00087	1.24884	0.01873	0.13653	0.00182	825.0	10.3	822.9	8.5	822.0	27.0	0.3	0.4	825.0	10.3
S1748_043	812.1	9.2	0.3	0.05713	0.00106	0.29759	0.00576	0.03787	0.00054	239.6	3.3	264.5	4.5	496.2	40.2	-9.4	-51.7	239.6	3.3
S1748_044	1257.3	33.8	0.9	0.06267	0.00085	0.69598	0.01069	0.08073	0.00108	500.5	6.4	536.4	6.4	697.1	28.6	-6.7	-28.2	500.5	6.4
S1748_045	3972.4	120.5	0.9	0.05791	0.00066	0.68356	0.00945	0.08580	0.00111	530.7	6.6	528.9	5.7	526.2	25.2	0.3	0.9	530.7	6.6
S1748_046	1443.2	43.3	0.2	0.06636	0.00095	0.63835	0.01021	0.06994	0.00095	435.8	5.7	501.3	6.3	817.6	29.8	-13.1	-46.7		
S1748_047	1542.7	9.4	0.7	0.05003	0.00100	0.11469	0.00236	0.01667	0.00024	106.5	1.5	110.2	2.2	196.4	45.6	-3.4	-45.8	106.5	1.5
S1748_048	2723.3	3.9	0.2	0.05741	0.00158	0.02633	0.00071	0.00333	0.00005	21.5	0.3	26.4	0.7	506.9	59.9	-18.6	-95.8		
S1748_049	27688.1	84.4	11.2	0.14126	0.00187	0.06100	0.00090	0.00314	0.00004	20.2	0.3	60.1	0.9	2242.7	22.7	-66.4	-99.1		
S1748_050	373.4	34.5	1.3	0.06706	0.00089	1.35244	0.02059	0.14661	0.00196	881.9	11.0	868.6	8.9	839.7	27.5	1.5	5.0	881.9	11.0
S1748_051	2560.2	40.1	0.7	0.05174	0.00071	0.17025	0.00263	0.02392	0.00032	152.4	2.0	159.6	2.3	273.9	31.0	-4.5	-44.4	152.4	2.0
S1748_052	11211.2	35.9	4.9	0.06226	0.00094	0.02421	0.00040	0.00283	0.00004	18.2	0.3	24.3	0.4	683.1	32.0	-25.1	-97.3		
S1748_053	2287.9	144.3	0.2	0.06604	0.00074	0.98201	0.01338	0.10809	0.00140	661.7	8.2	694.6	6.9	807.8	23.2	-4.7	-18.1	661.7	8.2
S1748_054	5135.2	49.2	0.4	0.04785	0.00061	0.11078	0.00164	0.01683	0.00022	107.6	1.4	106.7	1.5	90.8	30.8	0.8	18.5	107.6	1.4
S1748_055	582.2	6.9	0.4	0.06171	0.00161	0.14663	0.00377	0.01727	0.00028	110.4	1.8	138.9	3.3	664.1	55.1	-20.5	-83.4		
S1748_056	3907.2	39.5	0.6	0.04806	0.00064	0.11448	0.00175	0.01732	0.00023	110.7	1.5	110.1	1.6	102.2	31.3	0.5	8.3	110.7	1.5
S1748_057	138.6	7.7	0.5	0.07203	0.00139	0.89757	0.01794	0.09058	0.00134	559.0	7.9	650.4	9.6	987.2	38.5	-14.1	-43.4		
S1748_058	606.6	67.7	0.4	0.08020	0.00093	2.34050	0.03274	0.21216	0.00278	1240.3	14.8	1224.7	10.0	1201.8	22.8	1.3	3.2	1201.8	22.8
S1748_059	1348.6	68.2	0.7	0.06410	0.00076	0.92274	0.01309	0.10464	0.00137	641.6	8.0	663.8	6.9	745.1	25.0	-3.3	-13.9	641.6	8.0
S1748_060	455.0	36.7	0.5	0.07221	0.00092	1.61974	0.02393	0.16308	0.00217	973.9	12.0	977.9	9.3	991.7	25.6	-0.4	-1.8	973.9	12.0
S1748_061	2072.7	194.8	0.7	0.13847	0.00159	3.76966	0.05219	0.19791	0.00261	1164.1	14.1	1586.3	11.1	2208.1	19.8	-26.6	-47.3		
S1748_062	4362.2	43.1	1.0	0.05213	0.00074	0.13994	0.00223	0.01951	0.00026	124.6	1.7	133.0	2.0	291.2	32.2	-6.3	-57.2	124.6	1.7
S1748_063	4636.2	296.3	0.4	0.06479	0.00071	1.11999	0.01506	0.12568	0.00163	763.2	9.3	763.0	7.2	767.4	22.8	0.0	-0.5	763.2	9.3
S1748_064	1046.9	53.8	0.5	0.06628	0.00097	0.92960	0.01512	0.10197	0.00139	625.9	8.1	667.4	8.0	815.1	30.4	-6.2	-23.2	625.9	8.1
S1748_065	952.3	7.9	1.1	0.04895	0.00109	0.10973	0.00249	0.01630	0.00024	104.2	1.5	105.7	2.3	145.6	51.4	-1.4	-28.4	104.2	1.5
S1748_066	1369.8	42.3	0.3	0.07537	0.00100	1.13417	0.01724	0.10939	0.00147	669.2	8.5	769.7	8.2	1078.5	26.5	-13.1	-38.0		
S1748_067	1567.1	13.2	1.6	0.04809	0.00092	0.11685	0.00233	0.01766	0.00025	112.9	1.6	112.2	2.1	103.7	44.4	0.6	8.9	112.9	1.6
S1748_068	2769.0	70.1	0.1	0.09261	0.00131	1.36273	0.02148	0.10697	0.00147	655.2	8.6	873.0	9.2	1479.8	26.7	-24.9	-55.7		
S1748_069	549.6	36.3	0.3	0.06998	0.00088	1.66103	0.02446	0.17256	0.00229	1026.2	12.6	993.8	9.3	927.7	25.7	3.3	10.6	1026.2	12.6
S1748_070	287.0	12.4	0.6	0.06641	0.00109	1.14072	0.02025	0.12486	0.00176	758.5	10.1	772.9	9.6	819.4	34.1	-1.9	-7.4	758.5	10.1
S1748_071	1394.3	8.6	0.9	0.05019	0.00104	0.12222	0.00261	0.01770	0.00025	113.1	1.6	117.1	2.4	203.8	47.5	-3.4	-44.5	113.1	1.6
S1748_072	2062.9	97.3	0.5	0.11306	0.00127	2.31038	0.03151	0.14856	0.00194	892.9	10.9	1215.5	9.7	1849.1	20.1	-26.5	-51.7		
S1748_073	5914.6	6.1	1.0	0.05210	0.00124	0.02427	0.00058	0.00339	0.00005	21.8	0.3	24.4	0.6	289.8	53.6	-10.7	-92.5	21.8	0.3
S1748_074	2208.0	118.2	1.1	0.07135	0.00081	1.40404	0.01939	0.14305	0.00187	861.9	10.5	890.6	8.2	967.5	23.1	-3.2	-10.9	861.9	10.5
S1748_075	334.3	17.0	1.0	0.06685	0.00103	1.33598	0.02262	0.14529	0.00201	874.5	11.3	861.5	9.8	833.0	31.8	1.5	5.0	874.5	11.3
S1748_076	1309.5	20.5	0.3	0.06814	0.00123	0.46749	0.00882	0.04988	0.00071	313.8	4.4	389.5	6.1	872.7	36.9	-19.4	-64.0		
S1748_077	8072.1	48.3	0.2	0.04823	0.00061	0.12608	0.00186	0.01900	0.00025	121.4	1.6	120.6	1.7	110.5	29.6	0.7	9.9	121.4	1.6
S1748_078	833.3	14.5	0.2	0.05632	0.00132	0.28094	0.00666	0.03626	0.00055	229.6	3.4	251.4	5.3	464.2	51.7	-8.7	-50.5	229.6	3.4
S1748_079	1347.0	22.5	0.2	0.06262	0.00108	0.60874	0.01115	0.07067	0.00100	440.2	6.0	482.8	7.0	695.5	36.3	-8.8	-36.7	440.2	6.0
S1748_080	761.5	7.4	0.0	0.05185	0.00134	0.18391	0.00472	0.02578	0.00040	164.1	2.5	171.4	4.1	279.0	57.9	-4.3	-41.2	164.1	2.5
S1748_081	388.1	13.5	0.7	0.05800	0.00097	0.75606	0.01356	0.09476	0.00132	583.6	7.8	571.7	7.8	529.5	36.5	2.1	10.2	583.6	7.8
S1748_082	993.1	8.0	0.5	0.05043	0.00103	0.12121	0.00256	0.01747	0.00025	111.7	1.6	116.2	2.3	214.7	46.7	-3.9	-48.0	111.7	1.6
S1748_083	1880.2	3.4	0.8	0.05159	0.00158	0.02337	0.00070	0.00329	0.00005	21.2	0.4	23.5	0.7	267.4	68.9	-9.8	-92.1	21.2	0.4
S1748_084	2089.0	133.7	0.6	0.07121	0.00088	0.84876	0.01230	0.08665	0.00114	535.7	6.8	624.0	6.8	963.5	24.7	-14.2	-44.4		
S1748_085	2994.0	30.5	0.8	0.04811	0.00069	0.10648	0.00171	0.01609	0.00021	102.9	1.4	102.7	1.6	104.8	33.4	0.2	-1.8	102.9	1.4
S1748_086	745.2	60.2	0.6	0.06615	0.00087	1.04985	0.01584	0.11537	0.00154	703.9	8.9	728.8	7.9	811.2	27.2	-3.4	-13.2	703.9	8.9
S1748_087	5376.5	8.9	0.5	0.07956	0.00142	0.03129	0.00058	0.00286	0.00004	18.4	0.3	31.3	0.6	1186.1	34.9	-41.2	-98.4		
S1748_088	812.1	66.5	0.5	0.06619	0.00079	1.23367	0.01755	0.13549	0.00178	819.1	10.1	816.0	8.0	812.5	24.8	0.4	0.8	819.1	10.1
S1748_089	376.7	20.7	0.5	0.06610	0.00094	1.18335	0.01894	0.13015	0.00177	788.7	10.1	792.9	8.8	809.4	29.6	-0.5	-2.6	788.7	10.1
S1748_090	1596.5	15.2	0.6	0.04780	0.00085	0.11686	0.00221	0.01777	0.00025	113.6	1.6	112.2	2.0	88.4	42.8	1.2	28.5	113.6	1.6
S1748_091	1355.1	88.7	1.0	0.06528	0.00077	1.20116	0.01699	0.13376	0.00175	809.3	10.0	801.1	7.8	783.4	24.7	1.0	3.3	809.3	10.0
S1748_093	6876.8	56.7	1.2	0.04744	0.00061	0.09285	0.00139	0.01423	0.00019	91.1	1.2	90.2	1.3	70.8	31.0	1.0	28.7	91.1	1.2
S1748_094	3160.3	102.3	0.5	0.05801	0.00067	0.63630	0.00889	0.07974	0.00104	494.5	6.2	500.0	5.5	529.8	25.6	-1.1	-6.7	494.5	6.2
S1748_095	1322.5	2.1	0.9	0.05032	0.00195	0.02432	0.00091	0.00351	0.00006	22.6	0.4	24.4	0.9	210.0	87.3	-7.4	-89.2	22.6	0.4
S1748_096	64.8	3.6	22.0	0.04146	0.00178	0.01991	0.00084	0.00349	0.00006	22.5	0.4	20.0	0.8	0.1	0.0	12.5	22400.0	22.5	0.4
S1748_097	769.7	4.5	0.9	0.05625	0.00165	0.12735	0.00366	0.01646	0.00027	105.2	1.7	121.7	3.3	461.4	64.2	-13.6	-77.2		
S1748_098	2025.4	74.0	0.2	0.06512	0.00077	1.13832	0.01605	0.12708	0.00167	771.2	9.5	771.7	7.6	778.1	24.5	-0.1	-0.9	771.2	9.5
S1748_099	1355.1	173.4	0.5	0.11156	0.00123	5.36256	0.07284	0.34945	0.00456	1932.0	21.8	1878.9	11.6	1824.9	19.9	2.8	5.9	1824.9	19.9
S1748_100	746.9	15.5	0.2	0.06114	0.00109	0.63843	0.01200	0.07592	0.00108	471.7	6.5	501.3	7.4	644.0	37.8	-5.9	-26.8	471.7	6.5
S1748_101	826.8	29.2	0.6	0.06498	0.00088	0.98266	0.01521	0.10993	0.00148	672.3	8.6	695.0	7.8	773.8	28.3	-3.3	-13.1	672.3	8.6
S1748_102	2987.5	108.1	1.5	0.08059	0.00094	1.16272	0.01634	0.10488	0.00138	642.9	8.0	783.2	7.7	1211.5	22.9	-17.9	-46.9		
S1748_103	1112.2	5.4	0.2	0.04571	0.00113	0.10513	0.00262	0.01672	0.00025	106.9	1.6	101.5	2.4	0.1	41.1	5.3	106800.0	106.9	1.6
S1748_104	257.7	2.9	1.2	0.05245	0.00185	0.17918	0.00615	0.02483	0.00043	158.1	2.7	167.4	5.3	305.0	78.2	-5.6	-48.2	158.1	2.7
S1748_105	1157.8	1.5	1.4	0.07335	0.00319	0.03068	0.00126	0.00304	0.00006	19.6	0.4	30.7	1.2	1023.5	85.7	-36.2	-98.1		
S1748_106	3665.9	24.1	0.3	0.05107	0.00074	0.11929	0.00192	0.01698	0.00023	108.5	1.4	114.4	1.8	244.0	32.9	-5.2	-55.5	108.5	1.4
S1748_107	691.4	3.5	0.5	0.05125	0.00151	0.12179	0.00353	0.01728	0.00028	110.4	1.8	116.7	3.2	252.1	66.2	-5.4	-56.2	110.4	1.8
S1748_108	10979.7	19.4	2.2	0.05196	0.00137	0.02121	0.00055	0.00297	0.00005	19.1	0.3	21.3	0.6	283.6	59.0	-10.3	-93.3	19.1	0.3
S1748_109	606.6	27.2	1.0	0.06608	0.00092	1.21646	0.01920	0.13382	0.00181	809.6	10.3	808.2	8.8	808.9	29.0	0.2	0.1	809.6	10.3
S1748_110	3873.0	162.0	0.0	0.06758	0.00076	1.35097	0.01850	0.14532	0.00189	874.7	10.7	868.0	8.0	855.7	23.0	0.8	2.2	874.7	10.7
S1748_111	1903.1	124.8	1.6	0.06339	0.00074	1.04679	0.01467	0.12005	0.00157	730.9	9.0	727.3	7.3	721.2	24.5	0.5	1.3	730.9	9.0
S1748_112	838.2	12.6	1.1	0.05025	0.00093	0.18401	0.00357	0.02662	0.00037	169.4	2.4	171.5	3.1	206.6	42.2	-1.2	-18.0	169.4	2.4
S1748_113	1593.2	17.8	0.3	0.04670	0.00092	0.11662	0.00240	0.01815	0.00026	116.0	1.6	112.0	2.2	33.9	46.0	3.6	242.2	116.0	1.6
S1748_114	1433.4	86.1	0.5	0.06499	0.00077	0.90492	0.01287	0.10122	0.00133	621.6	7.8	654.4	6.9	773.9	24.9	-5.0	-19.7	621.6	7.8
S1748_115	1596.5	124.7	0.2	0.10898	0.00124	2.71629	0.03750	0.18118	0.00238	1073.4	13.0	1332.9	10.3	1782.5	20.6	-19.5	-39.8		
S1748_116	981.7	190.3	0.4	0.11323	0.00125	5.09775	0.06938	0.32729	0.00427	1825.2	20.7	1835.7	11.6	1851.8	19.8	-0.6	-1.4	1851.8	19.8
S1748_117	1973.2	139.9	0.1	0.07722	0.00088	1.61189	0.02230	0.15173	0.00198	910.7	11.1	974.8	8.7	1127.0	22.5	-6.6	-19.2	910.7	11.1
S1748_118	2627.1	69.6	0.9	0.06219	0.00077	0.44448	0.00646	0.05196	0.00069	326.5	4.2	373.4	4.5	680.6	26.2	-12.6	-52.0	326.5	4.2
S1748_119	4611.7	8.7	0.7	0.04642	0.00097	0.02468	0.00053	0.00386	0.00006	24.9	0.4	24.8	0.5	19.5	48.9	0.4	27.7	24.9	0.4
S1748_120	768.1	63.1	2.1	0.06314	0.00080	1.06427	0.01572	0.12254	0.00163	745.1	9.3	735.9	7.7	712.9	26.6	1.3	4.5	745.1	9.3
S1748_121	1629.1	11.0	0.6	0.04844	0.00091	0.11794	0.00233	0.01770	0.00025	113.1	1.6	113.2	2.1	121.0	43.9	-0.1	-6.5	113.1	1.6
S1748_122	20315.6	738.0	0.7	0.06749	0.00073	1.26689	0.01708	0.13646	0.00177	824.6	10.0	831.0	7.7	852.9	22.4	-0.8	-3.3	824.6	10.0
S1748_123	4882.4	4.1	0.7	0.04846	0.00138	0.01808	0.00051	0.00271	0.00004	17.5	0.3	18.2	0.5	121.9	65.8	-3.8	-85.6	17.5	0.3
S1748_125	6483.8	8.3	0.6	0.04887	0.00158	0.01801	0.00057	0.00268	0.00005	17.2	0.3	18.1	0.6	141.5	74.3	-5.0	-87.8	17.2	0.3
S1748_126	7630.2	9.4	0.4	0.04640	0.00092	0.02375	0.00049	0.00372	0.00005	23.9	0.3	23.8	0.5	18.2	46.7	0.4	31.3	23.9	0.3
S1748_127	1347.0	11.0	1.1	0.04924	0.00096	0.11684	0.00237	0.01725	0.00024	110.2	1.6	112.2	2.2	159.5	44.8	-1.8	-30.9	110.2	1.6
S1748_128	25962.8	18.3	0.0	0.04726	0.00073	0.01601	0.00027	0.00246	0.00003	15.9	0.2	16.1	0.3	61.9	35.7	-1.2	-74.3	15.9	0.2
S1748_129	2022.1	106.3	0.3	0.07093	0.00081	1.60241	0.02232	0.16422	0.00215	980.2	11.9	971.2	8.7	955.5	23.3	0.9	2.6	980.2	11.9
S1748_130	1668.2	95.1	0.6	0.07126	0.00083	1.60218	0.02249	0.16345	0.00215	975.9	11.9	971.1	8.8	964.8	23.3	0.5	1.2	975.9	11.9
S1748_131	1107.3	2.3	1.0	0.05574	0.00229	0.03242	0.00128	0.00423	0.00008	27.2	0.5	32.4	1.3	441.8	88.9	-16.0	-93.8		
S1748_132	523.5	99.4	1.2	0.17052	0.00192	11.13681	0.15401	0.47476	0.00628	2504.4	27.5	2534.6	12.9	2562.8	18.8	-1.2	-2.3	2562.8	18.8
S1748_133	952.3	6.6	0.3	0.04955	0.00109	0.12165	0.00273	0.01785	0.00026	114.0	1.7	116.6	2.5	174.0	50.6	-2.2	-34.5	114.0	1.7
S1748_134	1606.3	87.3	0.3	0.06714	0.00078	1.30233	0.01832	0.14101	0.00185	850.4	10.5	846.7	8.1	842.1	24.1	0.4	1.0	850.4	10.5
S1748_135	326.1	25.0	0.7	0.06998	0.00098	1.55106	0.02465	0.16112	0.00220	963.0	12.2	950.9	9.8	927.8	28.6	1.3	3.8	963.0	12.2
S1748_136	605.0	22.8	0.8	0.05667	0.00084	0.70350	0.01164	0.09025	0.00123	557.0	7.3	540.9	6.9	477.8	32.9	3.0	16.6	557.0	7.3
S1748_137	2951.6	37.0	0.4	0.04952	0.00067	0.17663	0.00272	0.02593	0.00034	165.0	2.2	165.2	2.4	172.6	31.1	-0.1	-4.4	165.0	2.2
S1748_138	1320.9	111.7	0.7	0.07301	0.00084	1.64996	0.02306	0.16427	0.00215	980.5	11.9	989.5	8.8	1014.3	23.2	-0.9	-3.3	980.5	11.9
S1748_139	849.6	10.7	0.6	0.06318	0.00138	0.16281	0.00359	0.01873	0.00028	119.6	1.8	153.2	3.1	714.2	45.7	-21.9	-83.3		
S1748_140	1166.0	100.2	0.8	0.06486	0.00076	1.15666	0.01631	0.12963	0.00170	785.7	9.7	780.4	7.7	770.0	24.4	0.7	2.0	785.7	9.7
S1748_141	2623.8	143.1	0.5	0.06433	0.00080	0.72187	0.01055	0.08158	0.00108	505.5	6.4	551.8	6.2	752.3	26.0	-8.4	-32.8	505.5	6.4
S1748_142	1669.9	67.7	0.2	0.06366	0.00078	0.69659	0.01006	0.07954	0.00105	493.4	6.3	536.7	6.0	730.4	25.6	-8.1	-32.4	493.4	6.3
S1748_143	1195.3	92.5	0.4	0.06896	0.00085	1.40931	0.02058	0.14856	0.00197	892.9	11.1	892.9	8.7	897.5	25.3	0.0	-0.5	892.9	11.1
S1748_144	1407.3	206.3	0.7	0.12185	0.00135	6.19677	0.08476	0.36970	0.00484	2028.0	22.8	2004.0	12.0	1983.4	19.7	1.2	2.2	1983.4	19.7
S1748_145	989.9	29.0	0.8	0.05814	0.00082	0.63465	0.01007	0.07935	0.00107	492.3	6.4	499.0	6.3	534.5	31.0	-1.3	-7.9	492.3	6.4
S1748_146	962.1	2.7	0.9	0.17890	0.00975	0.09100	0.00414	0.00370	0.00013	23.8	0.8	88.4	3.9	2642.7	87.7	-73.1	-99.1		
S1748_147	738.7	183.5	0.8	0.16768	0.00186	10.56073	0.14451	0.45783	0.00601	2430.0	26.6	2485.3	12.7	2534.6	18.5	-2.2	-4.1	2534.6	18.5
S1748_148	2111.8	107.4	0.7	0.06554	0.00082	1.12337	0.01653	0.12460	0.00166	757.0	9.5	764.6	7.9	791.6	26.1	-1.0	-4.4	757.0	9.5
S1748_149	1234.5	244.5	0.5	0.16205	0.00179	10.91789	0.14886	0.48977	0.00641	2569.7	27.7	2516.2	12.7	2477.1	18.5	2.1	3.7	2477.1	18.5
S1748_150	295.2	13.6	0.7	0.07097	0.00114	1.35116	0.02363	0.13839	0.00195	835.6	11.1	868.1	10.2	956.6	32.6	-3.7	-12.6		
S1748_151	1030.6	6.7	0.7	0.04874	0.00111	0.11897	0.00275	0.01774	0.00026	113.4	1.7	114.1	2.5	135.4	52.6	-0.6	-16.2	113.4	1.7
S1748_152	805.6	46.9	0.6	0.07797	0.00096	1.89657	0.02768	0.17682	0.00236	1049.6	12.9	1079.9	9.7	1146.1	24.4	-2.8	-8.4	1049.6	12.9
S1748_153	52.2	2.4	0.8	0.06442	0.00211	1.21156	0.03897	0.13671	0.00254	826.0	14.4	805.9	17.9	755.5	67.7	2.5	9.3	826.0	14.4
S1748_154	10645.4	69.8	1.6	0.04972	0.00063	0.11336	0.00168	0.01657	0.00022	106.0	1.4	109.0	1.5	181.8	29.3	-2.8	-41.7	106.0	1.4

Sample S1438 Hispar River @ Nagar (Central Karakorum) 458 grains analysed 359 concordant ages

grain	concentrations U [ppm]	Pb [ppm]	Th/U	isotopic ratios Pb207/Pb206	2σ 76	Pb207/U235	2σ 75	Pb206/U238	2σ 68	ages age 206/238	2σ age 68	age 207/235	2σ age 75	age 207/206	2σ age 76	discordance Δ 68-75 [%]	Δ 68-76 [%]	preferred age age	2σ age
S1438_001	1186.6	9.0	1.0	0.05174	0.00255	0.04247	0.00207	0.00597	1.00E-04	38.3	0.6	42.2	2.0	274.0	108.9	-9.2	-86.0	38.3	0.61
S1438_002	3676.8	77.0	1.5	0.05858	0.00096	0.1374	0.00243	0.01705	0.00022	109.0	1.4	130.7	2.2	551.4	35.5	-16.6	-80.2		
S1438_003	2956.2	450.4	0.6	0.07039	0.00082	1.45445	0.01978	0.15017	0.00185	901.9	10.4	911.7	8.2	939.8	23.8	-1.1	-4.0	901.9	10.38
S1438_004	70367.4	351.4	0.8	0.05882	0.00072	0.05003	7.00E-04	0.00618	8.00E-05	39.7	0.5	49.6	0.7	560.6	26.4	-20.0	-92.9		
S1438_005	2607.2	37.6	0.2	0.05462	0.00136	0.1277	0.00324	0.01699	0.00023	108.6	1.4	122.0	2.9	396.6	54.5	-11.0	-72.6	108.6	1.43
S1438_006	1301.7	20.4	0.1	0.04982	0.00124	0.11616	0.00295	0.01694	0.00022	108.3	1.4	111.6	2.7	186.8	56.9	-3.0	-42.0	108.3	1.42
S1438_007	2937.3	97.6	0.1	0.09868	0.00134	0.51806	0.00783	0.03816	0.00048	241.4	3.0	423.9	5.2	1599.3	25.2	-43.1	-84.9		
S1438_008	2350.6	15.6	0.8	0.06725	0.0019	0.05545	0.00157	0.00599	8.00E-05	38.5	0.5	54.8	1.5	845.6	57.6	-29.7	-95.4		
S1438_009	1837.5	27.3	0.4	0.04877	0.00117	0.12236	0.00301	0.01823	0.00024	116.5	1.5	117.2	2.7	137.0	55.5	-0.6	-15.0	116.5	1.51
S1438_010	11413.5	165.1	0.3	0.04886	0.00066	0.11325	0.00171	0.01685	0.00021	107.7	1.3	108.9	1.6	141.3	31.4	-1.1	-23.8	107.7	1.33
S1438_011	1158.3	8.7	0.6	0.04773	0.00198	0.11428	0.00473	0.0174	0.00026	111.2	1.6	109.9	4.3	84.8	96.7	1.2	31.1	111.2	1.64
S1438_012	4118.3	87.1	0.1	0.06013	0.00119	0.35858	0.00743	0.04334	0.00056	273.5	3.5	311.2	5.6	608.2	42.4	-12.1	-55.0	273.5	3.46
S1438_013	3337.3	19.4	1.1	0.04896	0.00137	0.03938	0.00112	0.00585	8.00E-05	37.6	0.5	39.2	1.1	146.1	64.4	-4.1	-74.3	37.6	0.5
S1438_014	1407.3	91.2	0.2	0.06352	0.00092	0.62574	0.00994	0.0716	9.00E-04	445.8	5.4	493.4	6.2	725.7	30.3	-9.6	-38.6	445.8	5.39
S1438_015	1641.3	22.0	0.3	0.04795	0.00123	0.11348	0.00296	0.0172	0.00023	109.9	1.4	109.1	2.7	95.5	60.7	0.7	15.1	109.9	1.44
S1438_016	679.1	45.0	0.4	0.06581	0.0015	0.62284	0.01451	0.06878	0.00092	428.8	5.5	491.6	9.1	800.5	46.9	-12.8	-46.4	428.8	5.52
S1438_017	820.6	14.5	0.7	0.0826	0.00214	0.19674	0.00512	0.01731	0.00024	110.6	1.5	182.4	4.4	1259.8	49.7	-39.4	-91.2		
S1438_018	1488.5	150.2	0.6	0.06408	0.00085	0.96331	0.01443	0.10927	0.00136	668.5	7.9	685.0	7.5	744.2	28.0	-2.4	-10.2	668.5	7.91
S1438_019	1407.3	113.0	0.4	0.06713	0.00109	0.70451	0.01229	0.07628	0.00097	473.9	5.8	541.5	7.3	841.7	33.4	-12.5	-43.7	473.9	5.8
S1438_020	264.1	40.1	0.4	0.07425	0.00131	1.75976	0.03283	0.17225	0.00222	1024.5	12.2	1030.8	12.1	1048.4	35.1	-0.6	-2.3	1024.5	12.21
S1438_021	5661.5	1774.6	0.2	0.16706	0.00184	8.67441	0.11336	0.3774	0.00465	2064.1	21.8	2304.4	11.9	2528.4	18.4	-10.4	-18.4	2528.4	18.37
S1438_022	5944.4	32.4	0.8	0.04921	0.0011	0.04005	0.00092	0.00592	8.00E-05	38.0	0.5	39.9	0.9	157.7	51.3	-4.8	-75.9	38.0	0.49
S1438_023	571.6	18.4	0.4	0.05673	0.0021	0.25002	0.00918	0.03203	0.00047	203.3	3.0	226.6	7.5	480.4	80.3	-10.3	-57.7	203.3	2.96
S1438_024	4244.7	67.4	1.0	0.05196	0.00105	0.11588	0.00244	0.01621	0.00021	103.7	1.3	111.3	2.2	283.5	45.6	-6.8	-63.4	103.7	1.32
S1438_025	945.1	216.8	0.5	0.10801	0.0013	4.25386	0.05901	0.28626	0.00356	1622.8	17.8	1684.5	11.4	1766.0	21.8	-3.7	-8.1	1766.0	21.84
S1438_026	609.3	8.9	0.4	0.04989	0.00187	0.114	0.00426	0.01661	0.00024	106.2	1.5	109.6	3.9	189.8	84.9	-3.1	-44.0	106.2	1.52
S1438_027	1569.6	74.8	0.3	0.06998	0.00145	0.69223	0.01488	0.07189	0.00095	447.5	5.7	534.1	8.9	927.9	42.1	-16.2	-51.8		
S1438_028	871.6	5.0	1.4	0.05751	0.00305	0.04423	0.00231	0.00559	9.00E-05	35.9	0.6	43.9	2.3	510.9	112.8	-18.2	-93.0		
S1438_029	3708.9	19.1	0.6	0.05629	0.00146	0.04631	0.00122	0.00598	8.00E-05	38.4	0.5	46.0	1.2	463.0	56.9	-16.5	-91.7		
S1438_030	2135.5	15.2	2.0	0.05751	0.00223	0.04312	0.00166	0.00545	8.00E-05	35.0	0.5	42.9	1.6	510.7	83.4	-18.4	-93.1		
S1438_031	3597.6	34.7	0.2	0.05181	0.0012	0.12655	0.00301	0.01775	0.00023	113.4	1.5	121.0	2.7	277.1	52.0	-6.3	-59.1	113.4	1.48
S1438_032	9102.5	61.0	1.8	0.05462	0.00102	0.04453	0.00088	0.00593	8.00E-05	38.1	0.5	44.2	0.9	396.8	41.2	-13.8	-90.4		
S1438_033	999.9	68.6	0.6	0.07738	0.0012	1.0898	0.01828	0.10237	0.0013	628.3	7.6	748.4	8.9	1131.0	30.5	-16.0	-44.4		
S1438_034	16927.8	68.1	0.2	0.05011	0.00082	0.04066	0.00072	0.0059	7.00E-05	37.9	0.5	40.5	0.7	200.1	37.5	-6.4	-81.1	37.9	0.48
S1438_035	241.5	66.9	0.7	0.14218	0.00204	7.04245	0.11087	0.36001	0.00463	1982.2	22.0	2116.8	14.0	2253.9	24.5	-6.4	-12.1	2253.9	24.51
S1438_036	1260.2	12.8	0.7	0.05132	0.00166	0.12139	0.00394	0.01719	0.00024	109.9	1.5	116.3	3.6	255.4	72.6	-5.5	-57.0	109.9	1.52
S1438_037	771.6	2.8	0.7	0.05221	0.00399	0.04441	0.00334	0.00618	0.00012	39.7	0.8	44.1	3.3	294.8	165.1	-10.0	-86.5	39.7	0.78
S1438_038	2150.6	119.7	0.7	0.06513	0.00095	0.88086	0.01409	0.09829	0.00124	604.4	7.3	641.4	7.6	778.7	30.2	-5.8	-22.4	604.4	7.26
S1438_039	49968.4	462.4	0.5	0.04847	0.00063	0.09626	0.00143	0.01443	0.00018	92.4	1.1	93.3	1.3	122.3	30.5	-1.0	-24.4	92.4	1.14
S1438_040	7487.6	21.8	0.2	0.05556	0.00132	0.04397	0.00107	0.00575	8.00E-05	37.0	0.5	43.7	1.0	434.4	51.9	-15.3	-91.5		
S1438_041	13167.9	51.9	3.0	0.05056	0.00132	0.03938	0.00105	0.00566	8.00E-05	36.4	0.5	39.2	1.0	220.7	59.4	-7.1	-83.5	36.4	0.49
S1438_042	862.1	50.3	0.4	0.07893	0.00153	1.57692	0.03198	0.14521	0.00191	874.1	10.8	961.2	12.6	1170.4	38.0	-9.1	-25.3	874.1	10.76
S1438_043	286.8	26.9	1.2	0.07034	0.00161	1.44169	0.0339	0.14897	0.00201	895.2	11.3	906.4	14.1	938.4	46.3	-1.2	-4.6	895.2	11.27
S1438_044	1962.0	4.6	0.8	0.06774	0.00377	0.05702	0.00311	0.00612	0.00011	39.3	0.7	56.3	3.0	860.5	111.3	-30.2	-95.4		
S1438_045	684.8	31.3	0.6	0.05853	0.00122	0.65088	0.0141	0.08082	0.00106	501.0	6.3	509.0	8.7	549.8	44.7	-1.6	-8.9	501.0	6.3
S1438_046	2903.4	29.5	0.4	0.05037	0.00116	0.12128	0.00287	0.0175	0.00023	111.8	1.5	116.2	2.6	211.9	52.3	-3.8	-47.2	111.8	1.45
S1438_047	754.6	4.2	1.1	0.15238	0.00689	0.13672	0.00588	0.00652	0.00013	41.9	0.8	130.1	5.3	2372.8	75.1	-67.8	-98.2		
S1438_048	1226.2	11.2	0.1	0.04838	0.00157	0.10377	0.00339	0.01559	0.00022	99.7	1.4	100.3	3.1	117.9	74.8	-0.6	-15.4	99.7	1.38
S1438_049	960.2	8.7	0.3	0.05006	0.00183	0.11365	0.00415	0.0165	0.00024	105.5	1.5	109.3	3.8	197.9	82.9	-3.5	-46.7	105.5	1.51
S1438_050	645.2	6.6	0.8	0.05106	0.00239	0.11649	0.0054	0.01658	0.00026	106.0	1.7	111.9	4.9	243.7	104.4	-5.3	-56.5	106.0	1.65
S1438_051	1273.4	32.5	0.7	0.29749	0.00652	0.90548	0.01924	0.02212	0.00034	141.1	2.2	654.7	10.3	3457.2	33.6	-78.4	-95.9		
S1438_052	3276.9	298.8	0.3	0.07039	0.00085	1.33001	0.01867	0.13733	0.00171	829.5	9.7	858.9	8.1	939.8	24.7	-3.4	-11.7	829.5	9.69
S1438_053	594.3	7.3	0.6	0.04893	0.00211	0.11309	0.00485	0.0168	0.00026	107.4	1.6	108.8	4.4	144.5	98.4	-1.3	-25.7	107.4	1.62
S1438_054	467.9	3.5	0.6	0.06618	0.00389	0.17309	0.00998	0.01901	0.00036	121.4	2.3	162.1	8.6	812.0	118.4	-25.1	-85.0		
S1438_055	324.5	4.8	0.7	0.07979	0.00371	0.20512	0.00935	0.01868	0.00032	119.3	2.0	189.4	7.9	1191.8	89.0	-37.0	-90.0		
S1438_056	3941.0	166.5	0.2	0.05844	0.00077	0.7217	0.01077	0.08976	0.00112	554.1	6.6	551.7	6.4	546.4	28.6	0.4	1.4	554.1	6.64
S1438_057	211.3	15.1	1.6	0.08658	0.00248	1.09276	0.03135	0.09173	0.00133	565.8	7.9	749.8	15.2	1351.3	54.3	-24.5	-58.1		
S1438_058	1282.8	138.1	0.5	0.0688	0.00093	1.2897	0.01961	0.13625	0.00171	823.4	9.7	841.2	8.7	892.7	27.7	-2.1	-7.8	823.4	9.7
S1438_059	2639.2	93.8	0.5	0.06688	0.00111	0.48703	0.0087	0.05293	0.00068	332.5	4.1	402.9	5.9	834.0	34.3	-17.5	-60.1		
S1438_060	460.3	31.9	0.5	0.0644	0.00135	0.89922	0.01962	0.1015	0.00134	623.2	7.8	651.3	10.5	754.6	43.8	-4.3	-17.4	623.2	7.84
S1438_061	441.4	22.0	0.2	0.06146	0.00154	0.58732	0.015	0.06946	0.00094	432.9	5.7	469.2	9.6	655.3	52.9	-7.7	-33.9	432.9	5.68
S1438_062	573.5	54.0	0.6	0.0658	0.00111	1.14702	0.02078	0.1267	0.00162	769.0	9.3	775.8	9.8	800.0	35.0	-0.9	-3.9	769.0	9.3
S1438_063	1439.4	17.5	0.5	0.06556	0.00166	0.1517	0.0039	0.01682	0.00023	107.5	1.5	143.4	3.4	792.3	52.2	-25.0	-86.4		
S1438_064	1780.9	109.3	0.4	0.06487	0.001	0.66614	0.01124	0.07464	0.00095	464.0	5.7	518.4	6.9	770.1	32.3	-10.5	-39.7	464.0	5.68
S1438_065	1113.1	18.3	1.4	0.18705	0.00418	0.53922	0.01198	0.02095	0.00031	133.7	1.9	437.9	7.9	2716.4	36.4	-69.5	-95.1		
S1438_066	1243.2	18.4	0.9	0.04827	0.00139	0.11361	0.00331	0.01711	0.00023	109.3	1.5	109.3	3.0	112.5	66.5	0.0	-2.8	109.3	1.48
S1438_067	1663.9	20.2	0.6	0.04906	0.00131	0.11209	0.00304	0.01661	0.00022	106.2	1.4	107.9	2.8	150.8	61.2	-1.6	-29.6	106.2	1.41
S1438_068	1001.7	12.6	0.7	0.0513	0.00178	0.11878	0.00413	0.01683	0.00024	107.6	1.5	114.0	3.7	254.1	77.9	-5.6	-57.7	107.6	1.53
S1438_069	432.0	35.0	0.7	0.06795	0.00132	1.05252	0.02139	0.11259	0.00147	687.7	8.5	730.1	10.6	867.0	39.7	-5.8	-20.7	687.7	8.53
S1438_070	1320.6	15.3	0.5	0.05122	0.0015	0.12225	0.00362	0.01735	0.00024	110.9	1.5	117.1	3.3	250.9	66.1	-5.3	-55.8	110.9	1.51
S1438_071	3095.8	175.0	0.2	0.05907	0.00078	0.64472	0.00963	0.07933	0.00099	492.1	5.9	505.2	5.9	569.7	28.4	-2.6	-13.6	492.1	5.93
S1438_072	7887.6	1631.5	0.2	0.11431	0.00129	4.84536	0.06475	0.30809	0.00383	1731.3	18.9	1792.8	11.3	1869.0	20.2	-3.4	-7.4	1869.0	20.19
S1438_073	371.6	34.9	0.5	0.15049	0.00327	2.02114	0.04445	0.09761	0.00139	600.4	8.2	1122.6	14.9	2351.6	36.7	-46.5	-74.5		
S1438_074	760.3	269.2	1.1	0.16246	0.00193	9.64899	0.13356	0.43169	0.00541	2313.3	24.4	2401.9	12.7	2481.4	19.9	-3.7	-6.8	2481.4	19.9
S1438_075	1348.9	16.2	0.5	0.0566	0.00155	0.13079	0.00363	0.0168	0.00023	107.4	1.5	124.8	3.3	475.2	59.7	-13.9	-77.4		
S1438_076	19585.9	65.0	0.1	0.05481	0.00095	0.043	8.00E-04	0.0057	7.00E-05	36.7	0.5	42.7	0.8	404.4	38.2	-14.1	-90.9		
S1438_077	9140.2	135.9	1.4	0.04859	0.00074	0.1173	0.00195	0.01755	0.00022	112.1	1.4	112.6	1.8	128.1	35.3	-0.4	-12.5	112.1	1.4
S1438_078	230.2	1.7	0.9	0.21796	0.01458	0.21955	0.01347	0.00732	0.00022	47.0	1.4	201.5	11.2	2965.7	103.9	-76.7	-98.4		
S1438_079	594.3	8.2	0.4	0.34535	0.01656	1.54002	0.06555	0.03241	0.00087	205.6	5.4	946.5	26.2	3686.6	71.3	-78.3	-94.4		
S1438_080	1273.4	5.1	0.3	0.05861	0.00267	0.04829	0.00217	0.00599	1.00E-04	38.5	0.6	47.9	2.1	552.5	96.5	-19.6	-93.0		
S1438_081	2263.8	10.1	0.9	0.04901	0.00193	0.03941	0.00155	0.00584	9.00E-05	37.6	0.6	39.2	1.5	148.2	89.7	-4.1	-74.6	37.6	0.55
S1438_082	3616.5	55.9	1.2	0.06391	0.00152	0.14452	0.00352	0.01644	0.00022	105.1	1.4	137.1	3.1	738.5	49.5	-23.3	-85.8		
S1438_083	356.6	21.5	0.6	0.05815	0.00142	0.67157	0.01677	0.08394	0.00113	519.6	6.7	521.7	10.2	535.0	53.0	-0.4	-2.9	519.6	6.72
S1438_084	381.1	27.8	0.4	0.06902	0.00159	1.21036	0.02858	0.12747	0.00172	773.4	9.9	805.4	13.1	899.3	46.7	-4.0	-14.0	773.4	9.85
S1438_085	2377.0	74.3	0.1	0.05753	0.00089	0.54222	0.0092	0.06851	0.00087	427.2	5.3	439.9	6.1	511.4	34.1	-2.9	-16.5	427.2	5.25
S1438_086	2463.8	56.5	0.4	0.06486	0.00108	0.44045	0.00787	0.04936	0.00063	310.6	3.9	370.6	5.5	769.7	34.5	-16.2	-59.6		
S1438_087	2195.9	22.7	0.4	0.04925	0.00123	0.11853	0.00303	0.01749	0.00023	111.8	1.5	113.7	2.8	159.5	57.4	-1.7	-29.9	111.8	1.48
S1438_088	2790.2	241.7	0.4	0.07609	0.00096	1.86229	0.02701	0.1779	0.00223	1055.5	12.2	1067.8	9.6	1097.4	25.1	-1.2	-3.8	1055.5	12.22
S1438_089	464.1	155.9	1.2	0.16952	0.00211	10.91575	0.15641	0.46803	0.00593	2474.9	26.0	2516.0	13.3	2552.9	20.7	-1.6	-3.1	2552.9	20.71
S1438_090	1039.5	11.0	0.4	0.05271	0.00178	0.12167	0.00413	0.01678	0.00024	107.2	1.5	116.6	3.7	316.5	75.2	-8.1	-66.1	107.2	1.52
S1438_091	1237.6	8.4	0.3	0.04966	0.00194	0.09814	0.00382	0.01436	0.00021	91.9	1.4	95.1	3.5	178.9	88.6	-3.4	-48.6	91.9	1.35
S1438_092	956.5	54.5	1.5	0.07107	0.00133	0.9842	0.01938	0.10066	0.00131	618.3	7.7	695.8	9.9	959.4	37.7	-11.1	-35.6	618.3	7.7
S1438_093	852.7	71.2	1.3	0.07094	0.00116	1.57175	0.02782	0.16105	0.00207	962.6	11.5	959.1	11.0	955.6	33.2	0.4	0.7	962.6	11.5
S1438_094	992.3	6.1	1.1	0.05114	0.00242	0.12115	0.00569	0.01722	0.00027	110.1	1.7	116.1	5.2	247.0	105.5	-5.2	-55.4	110.1	1.73
S1438_095	1324.3	16.2	1.1	0.04831	0.00149	0.10986	0.00342	0.01653	0.00023	105.7	1.5	105.8	3.1	114.7	71.3	-0.1	-7.8	105.7	1.45
S1438_096	1375.3	475.7	0.7	0.15927	0.0019	8.91897	0.12431	0.40704	0.00511	2201.4	23.4	2329.7	12.7	2447.9	20.1	-5.5	-10.1	2447.9	20.07
S1438_097	2273.3	17.5	0.1	0.04902	0.00131	0.11232	0.00306	0.01666	0.00022	106.5	1.4	108.1	2.8	148.7	61.6	-1.5	-28.4	106.5	1.43
S1438_098	996.1	11.3	0.4	0.0979	0.00351	0.23323	0.0082	0.01732	0.00028	110.7	1.8	212.9	6.8	1584.6	65.5	-48.0	-93.0		
S1438_099	2631.7	37.0	0.4	0.04981	0.00144	0.12743	0.00374	0.0186	0.00026	118.8	1.6	121.8	3.4	186.1	66.1	-2.5	-36.2	118.8	1.62
S1438_100	2045.0	183.6	0.3	0.07518	0.00109	1.8957	0.03039	0.18328	0.00233	1084.9	12.7	1079.6	10.7	1073.3	28.7	0.5	1.1	1084.9	12.7
S1438_101	2318.5	24.6	0.6	0.07754	0.00164	0.19624	0.00429	0.0184	0.00025	117.5	1.6	181.9	3.6	1135.1	41.5	-35.4	-89.6		
S1438_102	7057.5	23.6	0.4	0.04662	0.00127	0.0376	0.00104	0.00586	8.00E-05	37.7	0.5	37.5	1.0	29.5	62.9	0.5	27.8	37.7	0.51
S1438_103	452.8	29.4	0.3	0.0645	0.00139	1.16423	0.02596	0.1312	0.00175	794.7	10.0	783.9	12.2	758.0	44.7	1.4	4.8	794.7	9.96
S1438_104	929.9	13.8	0.1	0.04203	0.00178	0.0983	0.00024	0.017	0.00418	108.7	3.9	95.2	1.5	0.1	0.0	14.2	108600.0	108.7	3.87
S1438_105	460.3	6.0	0.6	0.096	0.00359	0.66044	0.02425	0.05001	0.00082	314.6	5.0	514.9	14.8	1547.7	68.7	-38.9	-79.7		
S1438_106	428.2	71.3	0.5	0.16971	0.00238	7.77922	0.12123	0.33318	0.00432	1853.8	20.9	2205.8	14.0	2554.8	23.3	-16.0	-27.4		
S1438_107	671.6	7.8	0.9	0.07656	0.00286	0.17779	0.00656	0.01688	0.00026	107.9	1.7	166.2	5.7	1109.8	72.8	-35.1	-90.3		
S1438_108	431.9	6.8	0.6	0.0411	0.00313	0.09047	0.00687	0.016	0.00026	102.3	1.7	87.9	6.4	0.1	0.0	16.4	102200.0	102.3	1.65
S1438_109	609.3	30.4	0.5	0.05865	0.00125	0.73055	0.01616	0.09054	0.0012	558.7	7.1	556.9	9.5	554.2	45.7	0.3	0.8	558.7	7.07
S1438_110	801.8	3.9	1.1	0.07124	0.0038	0.05695	0.00297	0.00581	1.00E-04	37.3	0.7	56.2	2.9	964.4	105.2	-33.6	-96.1		
S1438_111	941.4	103.9	0.7	0.06772	0.001	1.31734	0.02157	0.14138	0.0018	852.5	10.2	853.3	9.5	860.1	30.4	-0.1	-0.9	852.5	10.17
S1438_112	807.4	11.0	1.2	0.07012	0.00226	0.16898	0.00544	0.01752	0.00026	111.9	1.6	158.5	4.7	931.8	64.7	-29.4	-88.0	111.9	1.63
S1438_113	2043.1	9.1	0.6	0.06324	0.00265	0.04962	0.00205	0.0057	9.00E-05	36.7	0.6	49.2	2.0	716.4	86.5	-25.4	-94.9		
S1438_114	1779.0	19.8	0.3	0.04885	0.00129	0.11757	0.00317	0.01749	0.00024	111.8	1.5	112.9	2.9	140.5	60.8	-1.0	-20.4		
S1438_115	4380.5	20.1	0.6	0.08546	0.00193	0.07404	0.00171	0.0063	9.00E-05	40.5	0.6	72.5	1.6	1326.0	43.1	-44.1	-96.9		
S1438_117	620.7	8.4	0.8	0.06333	0.00261	0.15182	0.00618	0.01743	0.00027	111.4	1.7	143.5	5.5	719.2	85.0	-22.4	-84.5		
S1438_118	2724.1	14.1	0.5	0.12374	0.00358	0.10284	0.00295	0.00604	9.00E-05	38.8	0.6	99.4	2.7	2010.8	50.4	-61.0	-98.1		
S1438_119	1152.7	99.5	0.7	0.07584	0.00113	1.22054	0.02001	0.11697	0.00149	713.1	8.6	810.0	9.2	1090.9	29.4	-12.0	-34.6	713.1	8.62
S1438_120	1245.1	112.9	0.2	0.07911	0.0011	1.48315	0.02311	0.13627	0.00173	823.5	9.8	923.5	9.5	1174.9	27.2	-10.8	-29.9	823.5	9.82
S1438_121	2333.6	31.5	0.5	0.04856	0.00108	0.12441	0.00287	0.01862	0.00024	118.9	1.6	119.1	2.6	126.7	51.4	-0.2	-6.2	118.9	1.55
S1438_122	1162.1	15.1	0.7	0.05445	0.00159	0.13866	0.00409	0.01851	0.00026	118.2	1.6	131.8	3.7	389.5	63.9	-10.3	-69.7	118.2	1.63
S1438_123	41164.0	371.6	0.4	0.21951	0.00277	0.22613	0.00327	0.00749	1.00E-04	48.1	0.6	207.0	2.7	2977.1	20.2	-76.8	-98.4		
S1438_124	1813.0	8.6	1.7	0.05207	0.00226	0.04161	0.00179	0.00581	9.00E-05	37.3	0.6	41.4	1.8	288.4	96.0	-9.9	-87.1	37.3	0.57
S1438_125	15201.6	62.6	0.6	0.05285	0.00093	0.04134	0.00078	0.00569	7.00E-05	36.5	0.5	41.1	0.8	322.4	39.3	-11.2	-88.7	36.5	0.47
S1438_126	196.2	61.4	2.8	0.09842	0.00171	3.98018	0.07399	0.29396	0.00389	1661.3	19.4	1630.2	15.1	1594.3	32.1	1.9	4.2	1594.3	32.14
S1438_127	2777.0	138.4	0.1	0.0604	0.00086	0.62234	0.00991	0.07489	0.00095	465.5	5.7	491.3	6.2	618.1	30.4	-5.3	-24.7	465.5	5.7
S1438_128	886.7	11.7	0.6	0.09773	0.00265	0.26563	0.00721	0.01976	0.00029	126.1	1.8	239.2	5.8	1581.3	49.8	-47.3	-92.0		
S1438_129	2062.0	22.8	0.8	0.05589	0.00138	0.13174	0.00334	0.01713	0.00023	109.5	1.5	125.7	3.0	447.6	53.9	-12.9	-75.5	109.5	1.47
S1438_130	1535.6	39.7	0.7	0.09401	0.00177	0.65278	0.01291	0.05047	0.00067	317.4	4.1	510.2	7.9	1508.4	35.1	-37.8	-79.0		
S1438_131	1752.6	20.4	0.5	0.05535	0.00141	0.13451	0.00349	0.01766	0.00024	112.9	1.5	128.1	3.1	426.3	55.2	-11.9	-73.5	112.9	1.52
S1438_132	1880.9	18.0	0.3	0.04785	0.00132	0.11359	0.00319	0.01725	0.00023	110.3	1.5	109.2	2.9	91.0	65.0	1.0	21.2	110.3	1.49
S1438_133	1058.3	117.0	1.6	0.07098	0.00111	1.44598	0.02473	0.14808	0.0019	890.2	10.7	908.2	10.3	956.7	31.3	-2.0	-7.0	890.2	10.69
S1438_134	1109.3	68.4	0.7	0.06277	0.00104	0.79746	0.01433	0.09234	0.00119	569.4	7.0	595.4	8.1	700.5	35.0	-4.4	-18.7	569.4	7.02
S1438_135	1703.5	14.9	0.5	0.04632	0.00156	0.11037	0.00374	0.01732	0.00025	110.7	1.6	106.3	3.4	14.5	78.0	4.1	663.4	110.7	1.55
S1438_136	3329.7	670.1	1.3	0.15243	0.00183	6.88857	0.09698	0.32848	0.00414	1831.0	20.1	2097.2	12.5	2373.4	20.3	-12.7	-22.9	2373.4	20.32
S1438_137	7715.9	77.4	1.6	0.04857	0.00087	0.11226	0.00216	0.0168	0.00022	107.4	1.4	108.0	2.0	127.2	41.7	-0.6	-15.6	107.4	1.37
S1438_138	1750.7	169.9	1.1	0.0733	0.00101	1.71747	0.02665	0.1703	0.00216	1013.8	11.9	1015.1	10.0	1022.3	27.6	-0.1	-0.8	1013.8	11.92
S1438_139	1284.7	54.8	0.2	0.06667	0.00127	0.87471	0.01763	0.09537	0.00125	587.2	7.4	638.1	9.6	827.4	39.3	-8.0	-29.0	587.2	7.38
S1438_140	3261.8	20.6	0.1	0.04788	0.00128	0.11786	0.00321	0.01789	0.00024	114.3	1.5	113.1	2.9	92.1	63.1	1.1	24.1	114.3	1.54
S1438_141	3348.6	36.0	0.5	0.04791	0.00107	0.11488	0.00267	0.01743	0.00023	111.4	1.5	110.4	2.4	93.5	53.4	0.9	19.1	111.4	1.46
S1438_142	396.2	3.9	0.7	0.05276	0.00304	0.1281	0.0073	0.01765	0.00031	112.8	1.9	122.4	6.6	318.4	125.8	-7.8	-64.6	112.8	1.93
S1438_143	992.3	6.1	0.9	0.05225	0.00262	0.14475	0.00717	0.02014	0.00033	128.5	2.1	137.3	6.4	296.3	110.4	-6.4	-56.6	128.5	2.09
S1438_144	2633.6	4.7	1.0	0.05177	0.00437	0.04146	0.00344	0.00582	0.00013	37.4	0.8	41.3	3.4	275.4	182.4	-9.4	-86.4	37.4	0.82
S1438_145	701.8	36.6	0.3	0.071	0.00131	1.61522	0.03176	0.16537	0.00218	986.6	12.0	976.1	12.3	957.3	37.4	1.1	3.1	986.6	12.03
S1438_146	947.0	75.7	0.3	0.07325	0.00113	1.28144	0.02166	0.12716	0.00163	771.6	9.4	837.5	9.6	1020.9	30.8	-7.9	-24.4	771.6	9.35
S1438_147	684.8	7.2	0.6	0.04983	0.00221	0.12217	0.00539	0.01782	0.00028	113.9	1.8	117.0	4.9	187.2	100.2	-2.6	-39.2	113.9	1.75
S1438_148	194.3	10.4	0.9	0.0663	0.00221	0.71177	0.02373	0.07804	0.00116	484.4	6.9	545.8	14.1	815.8	68.2	-11.2	-40.6	484.4	6.92

Sample S1438 Hispar River @ Nagar (Central Karakorum) 458 grains analysed 359 concordant ages

grain	concentrations U [ppm]	Pb [ppm]	Th/U	isotopic ratios Pb207/Pb206	2σ 76	Pb207/U235	2σ 75	Pb206/U238	2σ 68	ages age 206/238	2σ age 68	age 207/235	2σ age 75	age 207/206	2σ age 76	discordance Δ 68-75 [%]	Δ 68-76 [%]	preferred age age	2σ age
S1438_149	948.9	69.7	0.4	0.07172	0.00113	1.58757	0.0274	0.16089	0.00207	961.7	11.5	965.3	10.8	978.1	31.8	-0.4	-1.7	961.7	11.52
S1438_150	5097.4	438.7	0.7	0.08498	0.0011	2.17107	0.03236	0.18569	0.00235	1098.0	12.8	1171.8	10.4	1315.1	25.0	-6.3	-16.5	1098.0	12.8
S1438_151	762.2	6.0	0.6	0.04851	0.00229	0.11747	0.00551	0.0176	0.00028	112.5	1.8	112.8	5.0	124.1	107.5	-0.3	-9.3	112.5	1.75
S1438_152	9021.4	60.1	0.2	0.04994	0.00099	0.1203	0.00252	0.01751	0.00023	111.9	1.5	115.3	2.3	192.0	45.5	-2.9	-41.7	111.9	1.45
S1438_153	1181.0	11.5	0.5	0.04747	0.00179	0.11269	0.00425	0.01725	0.00025	110.3	1.6	108.4	3.9	72.3	88.1	1.8	52.6	110.3	1.61
S1438_154	281.1	107.5	0.7	0.19899	0.00268	14.83617	0.22675	0.54193	0.00702	2791.5	29.4	2804.8	14.5	2817.9	21.8	-0.5	-0.9	2817.9	21.83
S1438_155	4148.5	57.7	0.4	0.05607	0.00166	0.13273	0.00397	0.01721	0.00024	110.0	1.5	126.5	3.6	454.9	64.6	-13.0	-75.8		
S1438_156	147.1	58.5	1.4	0.16299	0.00244	10.3777	0.17135	0.46281	0.00611	2451.9	26.9	2469.1	15.3	2486.9	25.0	-0.7	-1.4	2486.9	25
S1438_157	1888.4	394.9	0.5	0.15613	0.00193	6.44815	0.09291	0.3002	0.0038	1692.3	18.9	2038.9	12.7	2414.2	20.8	-17.0	-29.9		
S1438_158	2810.9	141.1	0.0	0.0582	0.00083	0.63177	0.01009	0.07891	0.00101	489.6	6.0	497.2	6.3	536.7	31.4	-1.5	-8.8	489.6	6.01
S1438_159	2614.7	28.6	0.3	0.04997	0.00113	0.11741	0.00275	0.01708	0.00023	109.2	1.4	112.7	2.5	193.7	51.7	-3.1	-43.6	109.2	1.44
S1438_160	477.3	45.8	0.5	0.07382	0.0013	1.35929	0.02562	0.13384	0.00175	809.8	10.0	871.6	11.0	1036.6	35.1	-7.1	-21.9	809.8	9.96
S1438_161	273.5	3.8	0.4	0.11989	0.00514	0.31795	0.01322	0.01928	0.00035	123.1	2.2	280.3	10.2	1954.5	74.6	-56.1	-93.7		
S1438_162	2265.7	8.9	0.3	0.04847	0.00183	0.0405	0.00153	0.00607	9.00E-05	39.0	0.6	40.3	1.5	122.4	86.4	-3.2	-68.1	39.0	0.57
S1438_163	743.3	376.6	0.4	0.31965	0.00422	30.16421	0.45517	0.68594	0.00896	3367.1	34.3	3492.2	14.8	3568.1	20.2	-3.6	-5.6	3568.1	20.18
S1438_164	8081.9	335.6	0.1	0.05779	0.00075	0.55506	0.00831	0.06981	0.00088	435.0	5.3	448.3	5.4	521.7	28.5	-3.0	-16.6	435.0	5.33
S1438_165	366.0	35.0	1.2	0.08163	0.00163	1.30371	0.02721	0.1161	0.00156	708.1	9.0	847.4	12.0	1236.5	38.3	-16.4	-42.7	112.6	1.5
S1438_166	1999.7	32.6	1.7	0.05093	0.00124	0.12349	0.0031	0.01763	0.00024	112.6	1.5	118.2	2.8	237.5	55.3	-4.7	-52.6	113.9	1.59
S1438_167	1179.1	13.4	0.5	0.04833	0.00154	0.11848	0.00381	0.01782	0.00025	113.9	1.6	113.7	3.5	115.5	73.6	0.2	-1.4	117.9	1.51
S1438_168	7042.4	69.6	0.1	0.04934	0.00087	0.12534	0.00237	0.01846	0.00024	117.9	1.5	119.9	2.1	164.0	40.5	-1.7	-28.1		
S1438_169	5914.3	21.9	0.6	0.04828	0.00127	0.03994	0.00107	0.00601	8.00E-05	38.7	0.5	39.8	1.1	112.9	60.8	-2.8	-65.7	38.7	0.52
S1438_170	828.2	60.7	0.4	0.06459	0.00109	1.12129	0.02048	0.1262	0.00164	766.1	9.4	763.6	9.8	760.9	35.2	0.3	0.7	766.1	9.38
S1438_171	1977.1	531.7	0.4	0.16643	0.00207	8.38684	0.12172	0.36629	0.00465	2011.9	21.9	2273.8	13.2	2522.1	20.7	-11.5	-20.2	2522.1	20.74
S1438_172	39.6	2.8	1.6	0.06063	0.00449	0.85727	0.0625	0.10278	0.00211	630.7	12.4	628.6	34.2	626.0	152.1	0.3	0.8	630.7	12.35
S1438_173	1769.6	88.4	0.4	0.05944	0.00094	0.72859	0.01264	0.0891	0.00115	550.2	6.8	555.7	7.4	583.3	33.9	-1.0	-5.7	550.2	6.79
S1438_174	7104.7	52.1	0.7	0.04795	0.00095	0.11691	0.00246	0.01772	0.00023	113.2	1.5	112.3	2.2	95.8	47.6	0.8	18.2	113.2	1.47
S1438_175	945.1	7.5	1.2	0.06217	0.00269	0.16162	0.00694	0.0189	3.00E-04	120.7	1.9	152.1	6.1	680.1	90.0	-20.6	-82.3		
S1438_177	1373.4	12.4	0.6	0.04964	0.00164	0.12399	0.00414	0.01816	0.00026	116.0	1.6	118.7	3.7	178.0	75.5	-2.3	-34.8	116.0	1.64
S1438_178	830.1	40.0	0.4	0.06775	0.00127	1.12904	0.02248	0.12113	0.0016	737.1	9.2	767.3	10.7	861.0	38.4	-3.9	-14.4	737.1	9.18
S1438_179	1558.3	70.5	0.4	0.06786	0.00114	1.04639	0.01908	0.11209	0.00146	684.8	8.5	727.1	9.5	864.3	34.5	-5.8	-20.8	684.8	8.45
S1438_180	690.5	37.9	0.5	0.07169	0.00136	1.15027	0.0232	0.11662	0.00155	711.1	8.9	777.4	11.0	977.3	38.3	-8.5	-27.2	711.1	8.92
S1438_181	630.1	3.8	0.7	0.04932	0.00319	0.12092	0.00772	0.01782	0.00032	113.9	2.0	115.9	7.0	163.0	144.4	-1.7	-30.1	113.9	2.03
S1438_182	1484.7	210.4	0.2	0.11032	0.00149	4.28828	0.06593	0.28255	0.00362	1604.2	18.2	1691.1	12.7	1804.7	24.3	-5.1	-11.1	1804.7	24.29
S1438_183	1099.8	8.3	0.7	0.04999	0.00204	0.12151	0.00494	0.01767	0.00027	112.9	1.7	116.4	4.5	194.4	92.1	-3.0	-41.9	112.9	1.69
S1438_184	32827.4	136.2	1.0	0.13135	0.00218	0.12226	0.00219	0.00677	9.00E-05	43.5	0.6	117.1	2.0	2116.1	28.9	-62.9	-97.9		
S1438_185	2175.2	94.1	0.4	0.06135	0.00099	0.78154	0.0138	0.0926	0.0012	570.9	7.1	586.4	7.9	651.6	34.2	-2.6	-12.4	570.9	7.06
S1438_186	1788.4	320.3	0.2	0.14793	0.00189	7.94538	0.11789	0.39042	0.00498	2124.8	23.1	2224.8	13.4	2322.1	21.8	-4.5	-8.5	2322.1	21.79
S1438_187	4544.6	14.3	2.8	0.05468	0.0029	0.04059	0.00212	0.0054	9.00E-05	34.7	0.6	40.4	2.1	399.1	114.2	-14.1	-91.3		
S1438_188	1896.0	77.4	0.7	0.06417	0.00122	0.90107	0.01817	0.10207	0.00135	626.5	7.9	652.3	9.7	747.2	39.6	-4.0	-16.2	626.5	7.88
S1438_189	2201.6	14.9	0.6	0.04749	0.00148	0.12303	0.00387	0.01883	0.00026	120.3	1.7	117.8	3.5	73.0	73.0	2.1	64.8	120.3	1.67
S1438_190	3686.3	9.5	0.4	0.06467	0.0024	0.06001	0.00222	0.00674	1.00E-04	43.3	0.7	59.2	2.1	763.7	76.3	-26.9	-94.3		
S1438_191	771.6	6.1	0.8	0.07081	0.00291	0.18387	0.00748	0.01888	3.00E-04	120.5	1.9	171.4	6.4	951.8	82.0	-29.7	-87.3		
S1438_192	488.6	32.6	0.3	0.07152	0.0014	1.56572	0.03242	0.15912	0.00212	951.9	11.8	956.7	12.8	972.4	39.5	-0.5	-2.1	951.9	11.81
S1438_193	179.2	10.5	0.5	0.07492	0.00221	1.86609	0.05555	0.18105	0.00267	1072.7	14.6	1069.1	19.7	1066.4	58.2	0.3	0.6	1072.7	14.55
S1438_194	2467.6	17.3	0.9	0.05978	0.00165	0.14489	0.00406	0.01762	0.00025	112.6	1.6	137.4	3.6	595.1	59.1	-18.0	-81.1		
S1438_195	750.8	60.1	0.3	0.06535	0.00111	1.13818	0.02103	0.1266	0.00165	768.4	9.5	771.6	10.0	785.7	35.4	-0.4	-2.2	768.4	9.45
S1438_196	1635.6	129.3	0.5	0.07839	0.00115	1.25132	0.02048	0.11603	0.00149	707.7	8.6	824.0	9.2	1156.8	28.7	-14.1	-38.8		
S1438_197	1654.5	105.1	0.5	0.06172	0.00109	0.83104	0.01586	0.09788	0.00128	602.0	7.5	614.2	8.8	664.3	37.5	-2.0	-9.4	602.0	7.52
S1438_198	1107.4	4.5	0.9	0.0598	0.00312	0.05029	0.00259	0.00611	0.00011	39.3	0.7	49.8	2.5	596.5	109.2	-21.1	-93.4		
S1438_199	786.7	12.2	0.9	0.05106	0.00216	0.1323	0.00556	0.01883	0.00029	120.3	1.9	126.2	5.0	243.7	94.4	-4.7	-50.6	120.3	1.85
S1438_200	996.1	12.4	0.9	0.05159	0.00175	0.12191	0.00417	0.01718	0.00025	109.8	1.6	116.8	3.8	267.1	76.2	-6.0	-58.9	109.8	1.57
S1438_201	715.0	8.0	0.5	0.04673	0.00211	0.11006	0.00495	0.01712	0.00027	109.4	1.7	106.0	4.5	35.5	105.1	3.2	208.2	109.4	1.69
S1438_202	1448.9	5.9	0.6	0.0483	0.0023	0.0392	0.00185	0.0059	9.00E-05	37.9	0.6	39.0	1.8	114.0	108.6	-2.8	-66.8	37.9	0.6
S1438_203	8489.4	35.7	0.5	0.04926	0.00108	0.04026	0.00092	0.00594	8.00E-05	38.2	0.5	40.1	0.9	160.1	50.3	-4.7	-76.1	38.2	0.51
S1438_204	601.8	23.8	0.3	0.05662	0.00189	0.36491	0.01224	0.04685	0.00069	295.2	4.2	315.9	9.1	475.9	72.9	-6.6	-38.0	295.2	4.22
S1438_205	716.9	3.3	0.7	0.05634	0.00467	0.04702	0.00382	0.00607	0.00014	39.0	0.9	46.7	3.7	464.9	174.6	-16.5	-91.6		
S1438_206	443.3	5.0	1.1	0.35722	0.01137	0.4564	0.01332	0.00929	0.00018	59.6	1.2	381.8	9.3	3738.1	47.6	-84.4	-98.4		
S1438_207	607.5	3.2	1.0	0.0737	0.00415	0.06419	0.00354	0.00633	0.00012	40.7	0.8	63.2	3.4	1033.4	109.9	-35.6	-96.1		
S1438_208	1160.2	141.0	0.5	0.07155	0.00105	1.58058	0.02608	0.16058	0.00207	960.0	11.5	962.6	10.3	973.2	29.7	-0.3	-1.4	960.0	11.5
S1438_209	822.5	90.3	0.5	0.06997	0.0011	1.49164	0.02594	0.15495	0.00201	928.7	11.2	927.0	10.6	927.6	32.0	0.2	0.1	928.7	11.23
S1438_210	1147.0	43.9	0.3	0.05628	0.00179	0.4032	0.01291	0.05207	0.00075	327.2	4.6	344.0	9.3	462.8	69.2	-4.9	-29.3	327.2	4.61
S1438_211	498.0	41.4	0.6	0.06853	0.0014	1.2413	0.02673	0.13166	0.00177	797.4	10.1	819.5	12.1	884.6	41.8	-2.7	-9.9	797.4	10.07
S1438_212	1101.7	6.3	0.6	0.04993	0.00415	0.04321	0.00352	0.00629	0.00014	40.4	0.9	43.0	3.4	191.8	182.4	-6.0	-78.9	40.4	0.88
S1438_214	915.0	332.7	0.8	0.16956	0.00238	9.09144	0.1446	0.38974	0.00507	2121.6	23.5	2347.2	14.6	2553.3	23.3	-9.6	-16.9	2553.3	23.32
S1438_215	3644.8	106.5	0.3	0.06733	0.00109	0.48961	0.00872	0.05286	0.00069	332.1	4.2	404.6	5.9	847.9	33.4	-17.9	-60.8		
S1438_216	1073.4	182.0	0.4	0.10752	0.00149	4.07584	0.0644	0.27554	0.00355	1568.9	17.9	1649.5	12.9	1757.9	25.1	-4.9	-10.8	1757.9	25.1
S1438_217	699.9	10.4	0.7	0.05405	0.0042	0.12613	0.00961	0.01696	0.00036	108.4	2.3	120.6	8.7	372.8	165.6	-10.1	-70.9	108.4	2.31
S1438_218	4955.9	21.0	0.9	0.04732	0.00132	0.03949	0.00113	0.00607	8.00E-05	39.0	0.5	39.3	1.1	64.9	65.7	-0.8	-39.9	39.0	0.54
S1438_219	4606.9	22.2	1.2	0.05049	0.00139	0.04135	0.00116	0.00595	8.00E-05	38.3	0.5	41.1	1.1	217.5	62.4	-6.8	-82.4	38.3	0.53
S1438_220	577.3	181.8	0.8	0.16673	0.00229	10.39245	0.16303	0.45309	0.00586	2409.0	26.0	2470.4	14.5	2525.0	22.9	-2.5	-4.6	2525.0	22.87
S1438_221	7159.4	81.1	0.9	0.05191	0.00096	0.1155	0.00229	0.01617	0.00021	103.4	1.3	111.0	2.1	281.5	41.8	-6.8	-63.3	103.4	1.34
S1438_222	311.3	3.9	1.0	0.05056	0.00306	0.12575	0.00752	0.01808	0.00032	115.5	2.0	120.3	6.8	221.0	134.3	-4.0	-47.7	115.5	2.04
S1438_223	3439.1	209.9	0.5	0.05951	0.00086	0.76254	0.01246	0.09315	0.0012	574.1	7.1	575.5	7.2	585.6	31.1	-0.2	-2.0	574.1	7.07
S1438_224	1328.1	8.8	1.4	0.23455	0.00645	0.24659	0.00656	0.00764	0.00013	49.1	0.8	223.8	5.3	3083.3	43.2	-78.1	-98.4		
S1438_225	1903.5	183.9	0.5	0.06547	0.00103	1.08472	0.01884	0.12043	0.00156	733.0	9.0	745.9	9.2	789.6	32.6	-1.7	-7.2	733.0	8.99
S1438_226	1709.2	140.3	0.4	0.08079	0.00119	1.72193	0.02851	0.15493	0.002	928.5	11.2	1016.7	10.6	1216.3	28.7	-8.7	-23.7	928.5	11.19
S1438_227	1720.5	10.5	0.6	0.05126	0.00181	0.12944	0.00459	0.01836	0.00027	117.3	1.7	123.6	4.1	252.3	79.2	-5.1	-53.5	117.3	1.7
S1438_228	1958.2	83.2	0.7	0.06852	0.00113	1.44512	0.02609	0.1533	0.002	919.4	11.2	907.8	10.8	884.4	33.7	1.3	4.0	919.4	11.2
S1438_229	1001.7	44.6	0.8	0.07003	0.00149	1.24442	0.02767	0.12916	0.00175	783.1	10.0	820.9	12.5	929.3	43.0	-4.6	-15.7	783.1	9.99
S1438_230	145.3	6.1	0.5	0.07407	0.00279	1.71833	0.06436	0.16863	0.00271	1004.6	14.9	1015.4	24.0	1043.4	74.1	-1.1	-3.7	1004.6	14.93
S1438_231	4578.6	237.7	0.7	0.07553	0.00117	1.76209	0.03041	0.16959	0.00221	1009.9	12.2	1031.6	11.2	1082.6	30.9	-2.1	-6.7	1009.9	12.16
S1438_232	1445.1	17.4	1.1	0.05144	0.0025	0.12326	0.00595	0.01742	0.00028	111.3	1.8	118.0	5.4	260.5	107.9	-5.7	-57.3	111.3	1.79
S1438_233	1156.4	43.3	0.5	0.06783	0.00153	1.30349	0.03052	0.13969	0.00191	842.9	10.8	847.3	13.5	863.3	46.0	-0.5	-2.4	842.9	10.81
S1438_234	569.7	2.1	0.7	0.05032	0.00428	0.04367	0.00366	0.00631	0.00013	40.5	0.8	43.4	3.6	209.8	186.0	-6.7	-80.7	40.5	0.84
S1438_235	2090.3	191.4	0.5	0.06614	0.00098	1.2693	0.0211	0.1395	0.0018	841.9	10.2	832.1	9.4	810.8	30.6	1.2	3.8	841.9	10.2
S1438_236	2184.6	107.7	0.2	0.05979	0.00094	0.68135	0.01191	0.08284	0.00108	513.0	6.4	527.6	7.2	595.3	34.5	-2.8	-13.8	513.0	6.4
S1438_237	1226.2	44.9	0.2	0.06714	0.00167	0.79237	0.0203	0.08578	0.00119	530.6	7.1	592.5	11.5	842.2	51.1	-10.4	-37.0	530.6	7.09
S1438_238	1450.7	177.5	0.8	0.0796	0.00117	2.32413	0.03845	0.21225	0.00275	1240.8	14.6	1219.7	11.7	1187.0	28.7	1.7	4.5	1187.0	28.71
S1438_239	1697.9	30.5	1.9	0.06876	0.00219	0.17386	0.00556	0.01838	0.00027	117.4	1.7	162.8	4.8	891.5	64.5	-27.9	-86.8		
S1438_240	505.6	2.7	0.7	0.04861	0.00359	0.12095	0.00882	0.01809	0.00035	115.6	2.2	115.9	8.0	129.1	165.2	-0.3	-10.5	115.6	2.2
S1438_241	135.8	33.7	1.5	0.10384	0.00203	4.5286	0.09378	0.31702	0.00435	1775.2	21.3	1736.2	17.2	1693.8	35.6	2.2	4.8	1693.8	35.61
S1438_242	3671.2	38.6	0.1	0.06127	0.0012	0.45324	0.00945	0.05377	0.00072	337.6	4.4	379.5	6.6	648.8	41.6	-11.0	-48.0	337.6	4.37
S1438_243	696.1	5.9	1.2	0.04932	0.00246	0.12415	0.00615	0.0183	3.00E-04	116.9	1.9	118.8	5.6	162.9	112.7	-1.6	-28.2	116.9	1.89
S1438_244	6353.8	57.2	0.1	0.04724	0.00093	0.10844	0.00227	0.01669	0.00022	106.7	1.4	104.5	2.1	60.7	46.6	2.1	75.8	106.7	1.4
S1438_245	930.1	65.8	0.1	0.0642	0.0011	1.09843	0.02053	0.12436	0.00163	755.6	9.4	752.6	9.9	748.3	35.8	0.4	1.0	755.6	9.36
S1438_246	1186.6	42.3	0.7	0.06189	0.00132	0.66156	0.01486	0.07771	0.00105	482.4	6.3	515.6	9.1	670.2	45.2	-6.4	-28.0	482.4	6.27
S1438_247	239.6	13.5	1.0	0.0617	0.00204	0.9588	0.03196	0.11297	0.00168	689.9	9.7	682.7	16.6	663.6	69.4	1.1	4.0	689.9	9.73
S1438_248	562.2	39.5	0.5	0.06439	0.0013	0.94837	0.02026	0.10706	0.00144	655.6	8.4	677.3	10.6	754.6	42.0	-3.2	-13.1	655.6	8.36
S1438_249	2554.4	12.7	1.1	0.05095	0.00176	0.04235	0.00147	0.00604	9.00E-05	38.8	0.6	42.1	1.4	238.4	77.6	-7.8	-83.7	38.8	0.56
S1438_250	516.9	141.1	2.0	0.09883	0.00151	3.93126	0.06711	0.28914	0.00378	1637.2	18.9	1620.1	13.8	1602.2	28.2	1.1	2.2	1602.2	28.24
S1438_251	741.0	47.9	1.1	0.07995	0.00095	1.23667	0.01723	0.11245	0.00145	686.9	8.4	817.4	7.8	1195.6	23.3	-16.0	-42.5		
S1438_252	425.8	3.7	0.7	0.05489	0.00149	0.12643	0.00337	0.01674	0.00026	107.0	1.7	120.9	3.0	407.7	58.8	-11.5	-73.8	107.0	1.66
S1438_253	8874.1	69.4	0.3	0.04821	0.00057	0.11362	0.00157	0.01713	0.00022	109.5	1.4	109.3	1.4	109.7	27.4	0.2	-0.2	109.5	1.39
S1438_254	462.6	28.0	1.6	0.06076	0.00084	0.83222	0.01284	0.09956	0.00131	611.9	7.7	614.8	7.1	630.7	29.5	-0.5	-3.0	611.9	7.71
S1438_255	4485.2	529.9	0.5	0.09556	0.001	3.39239	0.04372	0.25805	0.00326	1479.8	16.7	1502.6	10.1	1539.2	19.5	-1.5	-3.9	1539.2	19.5
S1438_256	1864.9	313.1	1.1	0.1076	0.00114	4.75969	0.06181	0.32154	0.00408	1797.3	19.9	1777.8	10.9	1759.2	19.1	1.1	2.2	1759.2	19.14
S1438_257	11746.1	508.6	0.1	0.1848	0.00193	2.23504	0.02876	0.08792	0.00111	543.2	6.6	1192.1	9.0	2696.4	17.2	-54.4	-79.9		
S1438_258	769.7	70.8	0.8	0.07184	0.00082	1.55707	0.02122	0.15756	0.00202	943.2	11.3	953.3	8.4	981.3	23.2	-1.1	-3.9	943.2	11.26
S1438_259	2071.6	22.7	1.6	0.0487	0.00075	0.11728	0.00196	0.01751	0.00023	111.9	1.5	112.6	1.8	133.4	35.7	-0.6	-16.1	111.9	1.47
S1438_260	4204.7	334.5	0.5	0.07127	0.00075	1.51112	0.01958	0.15412	0.00195	924.0	10.9	934.9	7.9	965.2	21.4	-1.2	-4.3	924.0	10.89
S1438_261	851.6	8.4	1.0	0.04759	0.00099	0.11505	0.00245	0.01757	0.00025	112.3	1.6	110.6	2.2	78.2	49.5	1.5	43.6	112.3	1.57
S1438_262	2925.3	37.8	1.8	0.05499	0.00079	0.13069	0.00207	0.01728	0.00023	110.4	1.4	124.7	1.9	411.6	31.6	-11.5	-73.2	110.4	1.44
S1438_263	745.1	144.1	0.9	0.16133	0.00171	7.84649	0.10222	0.35354	0.00451	1951.5	21.5	2213.6	11.7	2469.7	17.8	-11.8	-21.0	2469.7	17.82
S1438_264	1713.4	16.2	1.2	0.04945	0.00091	0.11685	0.00225	0.01718	0.00024	109.8	1.5	112.2	2.0	169.3	42.6	-2.1	-35.1	109.8	1.5
S1438_265	3975.4	26.5	0.3	0.05304	0.00073	0.12123	0.00186	0.01662	0.00022	106.2	1.4	116.2	1.7	330.3	30.8	-8.6	-67.8	106.2	1.38
S1438_266	15609.0	138.3	1.0	0.05038	0.00056	0.1169	0.00156	0.01687	0.00021	107.8	1.4	112.3	1.4	212.4	25.6	-4.0	-49.2	107.8	1.36
S1438_267	1160.7	11.0	1.3	0.05558	0.00102	0.13389	0.00256	0.01751	0.00024	111.9	1.5	127.6	2.3	435.3	40.0	-12.3	-74.3	111.9	1.54
S1438_268	2245.6	822.0	0.7	0.30309	0.00313	27.4307	0.35187	0.65788	0.00832	3258.9	32.4	3399.0	12.6	3486.1	15.9	-4.1	-6.5	3486.1	15.9
S1438_269	3123.8	8.7	0.4	0.04655	0.00116	0.03731	0.00093	0.00583	8.00E-05	37.5	0.5	37.2	0.9	25.9	57.8	0.8	44.8	37.5	0.54
S1438_270	3662.2	71.3	0.4	0.06707	0.00078	0.43581	0.00599	0.04723	0.00061	297.5	3.7	367.3	4.2	840.1	24.1	-19.0	-64.6		
S1438_271	3170.9	70.9	1.6	0.05145	0.00065	0.2483	0.0036	0.03508	0.00045	222.3	2.8	225.2	2.9	260.9	28.7	-1.3	-14.8	222.3	2.82
S1438_272	1621.3	12.8	0.6	0.04888	0.00085	0.11738	0.00216	0.01746	0.00024	111.6	1.5	112.7	2.0	142.1	40.5	-1.0	-21.5	111.6	1.5
S1438_273	4753.3	250.2	0.3	0.06355	0.00068	0.97032	0.01264	0.11099	0.00141	678.5	8.2	688.6	6.5	726.7	22.4	-1.5	-6.6	678.5	8.16
S1438_274	2902.8	143.9	0.2	0.06427	0.00072	0.99282	0.01335	0.11229	0.00143	686.1	8.3	700.2	6.8	750.5	23.5	-2.0	-8.6	686.1	8.31
S1438_275	2463.0	34.8	0.2	0.04299	0.00065	0.09419	0.00157	0.01593	0.00021	101.9	1.3	91.4	1.5	0.1	0.0	11.5	101800.0	101.9	1.32
S1438_276	2165.8	101.4	0.3	0.0678	0.00075	0.91224	0.01219	0.09781	0.00125	601.6	7.3	658.2	6.5	862.3	22.9	-8.6	-30.2	601.6	7.32
S1438_277	1361.3	13.5	0.7	0.07382	0.00116	0.18431	0.00309	0.01815	0.00025	116.0	1.6	171.8	2.7	1036.5	31.5	-32.5	-88.8		
S1438_278	4460.6	165.4	0.4	0.05974	0.00065	0.69481	0.00917	0.08455	0.00107	523.2	6.4	535.7	5.5	594.0	23.4	-2.3	-11.9	523.2	6.4
S1438_279	900.7	9.0	1.1	0.04964	0.00099	0.11888	0.00244	0.01741	0.00024	111.3	1.6	114.1	2.2	178.1	46.0	-2.5	-37.5	111.3	1.55
S1438_280	203746.0	274.8	0.5	0.07299	0.00078	0.06347	0.00083	0.00632	8.00E-05	40.6	0.5	62.5	0.8	1013.8	21.4	-35.0	-96.0		
S1438_281	1381.8	8.6	0.7	0.04948	0.00103	0.12094	0.00256	0.01777	0.00025	113.5	1.6	115.9	2.3	170.8	47.7	-2.1	-33.5	113.5	1.59
S1438_282	3328.6	94.3	0.5	0.06487	0.00073	1.13936	0.01534	0.12766	0.00163	774.5	9.3	772.2	7.3	770.3	23.5	0.3	0.5	774.5	9.32
S1438_283	640.7	2.2	0.9	0.04775	0.00188	0.11819	0.00453	0.01799	0.00032	115.0	2.0	113.4	4.1	85.7	91.9	1.4	34.2	115.0	2.03
S1438_284	4599.8	63.9	0.3	0.05989	0.00074	0.54288	0.00774	0.0659	0.00085	411.4	5.2	440.3	5.1	599.4	26.4	-6.6	-31.4	411.4	5.15
S1438_285	16597.7	49.3	0.2	0.0496	0.00061	0.12654	0.00181	0.01855	0.00024	118.5	1.5	121.0	1.6	176.1	28.6	-2.1	-32.7	118.5	1.51
S1438_286	2149.4	6.0	0.9	0.04987	0.00131	0.12093	0.00316	0.01763	0.00027	112.6	1.7	115.9	2.9	188.9	60.0	-2.8	-40.4	112.6	1.69
S1438_287	1082.9	21.9	0.4	0.06954	0.00095	1.57129	0.02402	0.16425	0.00219	980.4	12.1	958.9	9.5	914.8	27.7	2.2	7.2	980.4	12.1
S1438_288	3668.4	227.0	0.4	0.0746	0.00079	1.72087	0.02244	0.16768	0.00213	999.3	11.7	1016.3	8.4	1057.5	21.6	-1.7	-5.5	999.3	11.74
S1438_289	6734.9	20.6	0.4	0.05097	0.00075	0.04331	7.00E-04	0.00618	8.00E-05	39.7	0.5	43.0	0.7	239.4	33.7	-7.7	-83.4	39.7	0.52
S1438_290	1723.6	13.2	0.6	0.04779	9.00E-04	0.11559	0.00226	0.01758	0.00024	112.4	1.5	111.1	2.1	88.0	44.8	1.2	27.7	112.4	1.54
S1438_291	12562.9	237.9	1.2	0.057	0.00062	0.47287	0.00623	0.06031	0.00077	377.5	4.7	393.2	4.3	490.8	24.0	-4.0	-23.1	377.5	4.65
S1438_292	597.7	55.7	1.0	0.07368	0.00087	1.71819	0.02389	0.16951	0.00219	1009.4	12.1	1015.3	8.9	1032.8	23.4	-0.6	-2.3	1009.4	12.08
S1438_293	22589.5	33.8	0.3	0.05012	0.00072	0.04535	0.00072	0.00658	9.00E-05	42.3	0.6	45.0	0.7	200.6	33.2	-6.0	-78.9	42.3	0.55
S1438_294	6651.0	37.9	0.2	0.04843	0.00063	0.1118	0.00166	0.01678	0.00022	107.3	1.4	107.6	1.5	120.5	30.5	-0.3	-11.0	107.3	1.38
S1438_295	2497.4	20.0	0.2	0.05215	0.00078	0.18382	0.003	0.02562	0.00034	163.1	2.1	171.3	2.6	291.8	33.8	-4.8	-44.1	163.1	2.13
S1438_296	6958.0	18.5	1.0	0.06309	0.001	0.05299	9.00E-04	0.00611	8.00E-05	39.2	0.5	52.4	0.9	711.2	33.4	-25.2	-94.5		
S1438_297	3523.0	71.2	0.3	0.06091	0.00071	0.96946	0.01332	0.11569	0.00148	705.7	8.6	688.2	6.9	636.2	24.8	2.5	10.9	705.7	8.58

Sample S1438 Hispar River @ Nagar (Central Karakorum) 458 grains analysed 359 concordant ages

	concentrations			isotopic ratios						ages						discordance		preferred age	
grain	U [ppm]	Pb [ppm]	Th/U	Pb207/Pb206	2σ 76	Pb207/U235	2σ 75	Pb206/U238	2σ 68	age 206/238	2σ age 68	age 207/235	2σ age 75	age 207/206	2σ age 76	Δ 68-75 [%]	Δ 68-76 [%]	age	2σ age
S1438_298	1156.6	34.9	1.0	0.11375	0.00178	0.72673	0.01203	0.04644	0.00065	292.6	4.0	554.6	7.1	1860.1	28.1	-47.2	-84.3		
S1438_299	1314.2	6.0	1.3	0.04633	0.00118	0.13385	0.0034	0.021	0.00031	134.0	2.0	127.6	3.0	14.9	59.3	5.0	799.3	134.0	1.98
S1438_300	4040.9	171.0	0.2	0.07073	0.00078	1.3103	0.01744	0.13467	0.00172	814.4	9.8	850.3	7.7	949.6	22.4	-4.2	-14.2	814.4	9.76
S1438_301	2522.0	34.7	0.6	0.05722	0.00079	0.31946	0.00493	0.04058	0.00053	256.5	3.3	281.5	3.8	499.5	30.3	-8.9	-48.6	256.5	3.3
S1438_303	2427.8	7.9	0.6	0.04705	0.00103	0.03952	0.00088	0.00611	9.00E-05	39.2	0.6	39.4	0.9	51.4	51.8	-0.5	-23.7	39.2	0.56
S1438_304	1136.1	9.8	0.2	0.04766	0.00088	0.11725	0.00225	0.01788	0.00025	114.3	1.6	112.6	2.1	81.7	44.0	1.5	39.9	114.3	1.55
S1438_305	1117.7	3.9	1.0	0.05227	0.00151	0.04276	0.00121	0.00595	9.00E-05	38.2	0.6	42.5	1.2	297.4	64.4	-10.1	-87.2	38.2	0.6
S1438_306	1207.8	25.7	0.2	0.06116	0.00103	0.41467	0.00736	0.04929	0.00068	310.2	4.2	352.2	5.3	644.8	35.6	-11.9	-51.9	310.2	4.16
S1438_307	4904.8	15.2	0.8	0.04951	0.00083	0.03999	0.00071	0.00587	8.00E-05	37.7	0.5	39.8	0.7	171.9	38.6	-5.3	-78.1	37.7	0.51
S1438_308	4006.1	13.7	0.6	0.04776	0.00097	0.03603	0.00075	0.00548	8.00E-05	35.3	0.5	35.9	0.7	86.5	48.5	-1.7	-59.2	35.3	0.49
S1438_309	2231.3	13.5	0.4	0.05896	0.00101	0.13709	0.00247	0.0169	0.00023	108.1	1.5	130.5	2.2	565.5	36.8	-17.2	-80.9		
S1438_310	4743.1	16.3	0.7	0.04784	0.00078	0.0384	0.00067	0.00584	8.00E-05	37.5	0.5	38.3	0.7	90.4	39.0	-2.1	-58.5	37.5	0.5
S1438_311	5748.2	22.1	0.6	0.0777	0.00108	0.06653	0.00102	0.00622	8.00E-05	40.0	0.5	65.4	1.0	1139.3	27.4	-38.8	-96.5		
S1438_312	1367.4	24.7	0.5	0.05566	0.00077	0.25754	0.00398	0.03364	0.00044	213.3	2.8	232.7	3.2	438.4	30.1	-8.3	-51.3	213.3	2.75
S1438_313	4188.3	13.5	0.4	0.0479	0.00083	0.04026	0.00073	0.00611	8.00E-05	39.3	0.5	40.1	0.7	93.1	41.4	-2.0	-57.8	39.3	0.53
S1438_314	8184.2	69.7	0.2	0.05074	0.00059	0.12362	0.00171	0.01771	0.00023	113.2	1.4	118.3	1.5	229.0	26.8	-4.3	-50.6	113.2	1.43
S1438_315	2542.5	9.3	1.0	0.04803	0.00098	0.04069	0.00085	0.00616	9.00E-05	39.6	0.6	40.5	0.8	101.0	47.6	-2.2	-60.8	39.6	0.55
S1438_316	1291.7	52.2	0.4	0.0678	0.00094	0.59143	0.0091	0.06341	0.00084	396.3	5.1	471.8	5.8	862.5	28.4	-16.0	-54.1		
S1438_317	11948.8	44.2	1.7	0.05084	0.00066	0.03972	0.00059	0.00568	7.00E-05	36.5	0.5	39.5	0.6	233.7	29.8	-7.6	-84.4	36.5	0.47
S1438_318	837.3	7.3	0.7	0.05129	0.00115	0.11558	0.00261	0.01638	0.00024	104.7	1.5	111.1	2.4	253.9	50.6	-5.8	-58.8	104.7	1.51
S1438_319	1776.9	19.6	0.8	0.05022	0.00077	0.12128	0.00202	0.01755	0.00023	112.2	1.5	116.2	1.8	205.3	35.1	-3.4	-45.3	112.2	1.48
S1438_320	724.7	39.4	0.5	0.0621	0.00077	0.90106	0.01298	0.10548	0.00137	646.4	8.0	652.3	6.9	677.5	26.4	-0.9	-4.6	646.4	7.99
S1438_321	1887.4	86.6	0.4	0.06588	0.00078	0.90216	0.01257	0.09954	0.00128	611.7	7.5	652.9	6.7	802.6	24.6	-6.3	-23.8	611.7	7.52
S1438_322	777.9	2.9	1.6	0.04622	0.00175	0.03814	0.00141	0.006	1.00E-04	38.6	0.7	38.0	1.4	8.9	87.5	1.6	333.7	38.6	0.66
S1438_323	4605.9	15.2	0.4	0.05224	0.00085	0.04511	0.00078	0.00628	8.00E-05	40.3	0.5	44.8	0.8	295.8	36.5	-10.0	-86.4	40.3	0.54
S1438_324	3361.3	129.2	0.2	0.08994	0.00098	1.04552	0.01378	0.0845	0.00108	522.9	6.4	726.7	6.8	1424.1	20.6	-28.0	-63.3		
S1438_325	2812.7	134.3	0.4	0.06465	0.00071	0.91575	0.01215	0.10297	0.00131	631.8	7.7	660.1	6.4	762.8	22.9	-4.3	-17.2	631.8	7.66
S1438_326	1537.4	55.9	0.7	0.05939	0.00078	0.45698	0.0068	0.05593	0.00073	350.9	4.5	382.2	4.7	581.4	28.3	-8.2	-39.6	350.9	4.46
S1438_327	10583.4	156.0	0.3	0.07606	0.00085	0.27113	0.00365	0.02591	0.00033	164.9	2.1	243.6	2.9	1096.6	22.3	-32.3	-85.0		
S1438_328	139.2	11.8	1.2	0.0688	0.00121	1.31336	0.0243	0.13876	0.00197	837.7	11.2	851.6	10.7	892.8	35.9	-1.6	-6.2	837.7	11.18
S1438_329	1254.9	4.4	0.6	0.16621	0.0034	0.16037	0.00311	0.00701	0.00011	45.1	0.7	151.0	2.7	2519.8	34.0	-70.1	-98.2		
S1438_330	1770.7	32.5	0.7	0.05631	0.00094	0.2942	0.00523	0.03798	0.00052	240.3	3.2	261.9	4.1	463.9	37.0	-8.2	-48.2	240.3	3.22
S1438_331	640.7	32.5	0.4	0.06418	0.00082	1.18418	0.01738	0.13411	0.00175	811.3	10.0	793.3	8.1	747.7	26.8	2.3	8.5	811.3	9.97
S1438_332	7029.7	9.7	1.0	0.04962	0.00121	0.04279	0.00104	0.00627	9.00E-05	40.3	0.6	42.5	1.0	177.1	56.0	-5.2	-77.2	40.3	0.6
S1438_333	1013.3	40.7	0.9	0.0644	0.00084	1.13425	0.01687	0.12803	0.00168	776.6	9.6	769.8	8.0	754.7	27.3	0.9	2.9	776.6	9.61
S1438_334	3414.5	17.9	0.6	0.05138	0.00084	0.12742	0.00223	0.01803	0.00024	115.2	1.5	121.8	2.0	257.7	37.1	-5.4	-55.3	115.2	1.54
S1438_335	1539.4	76.9	0.6	0.06869	0.00078	1.05488	0.01434	0.11164	0.00143	682.2	8.3	731.3	7.1	889.4	23.4	-6.7	-23.3	682.2	8.3
S1438_336	4608.0	241.6	0.2	0.07067	0.00075	1.15855	0.01513	0.11917	0.00151	725.8	8.7	781.3	7.1	947.9	21.6	-7.1	-23.4	725.8	8.71
S1438_337	2126.9	17.5	1.0	0.04957	8.00E-04	0.12529	0.00216	0.01837	0.00025	117.4	1.6	119.9	2.0	175.0	37.0	-2.1	-32.9	117.4	1.56
S1438_338	58818.8	504.3	1.2	0.38884	0.00412	0.49503	0.00641	0.00925	0.00012	59.4	0.8	408.3	4.4	3866.5	15.9	-85.5	-98.5		
S1438_339	2028.7	12.4	0.5	0.04722	0.00083	0.1151	0.00213	0.01772	0.00024	113.2	1.5	110.6	1.9	59.9	41.7	2.4	89.0	113.2	1.52
S1438_340	569.1	32.6	0.6	0.07516	0.00095	1.73552	0.02517	0.16785	0.0022	1000.2	12.2	1021.8	9.3	1072.8	25.1	-2.1	-6.8	1000.2	12.16
S1438_341	3424.8	670.3	0.2	0.13074	0.00136	6.2724	0.08086	0.34874	0.00442	1928.6	21.1	2014.6	11.3	2108.0	18.1	-4.3	-8.5	2108.0	18.13
S1438_342	2221.1	20.8	0.7	0.04969	0.00087	0.12431	0.00228	0.01818	0.00025	116.2	1.6	119.0	2.1	180.7	40.1	-2.4	-35.7	116.2	1.57
S1438_343	1230.3	76.3	0.9	0.0629	0.00073	0.96792	0.0133	0.11187	0.00144	683.6	8.3	687.4	6.9	704.7	24.4	-0.6	-3.0	683.6	8.33
S1438_344	1289.7	3.2	1.2	0.04967	0.00178	0.04239	0.00147	0.0062	0.00011	39.9	0.7	42.2	1.4	179.4	81.4	-5.5	-77.8	39.9	0.68
S1438_345	10178.1	20.2	0.5	0.04834	0.00074	0.04164	0.00069	0.00626	8.00E-05	40.2	0.5	41.4	0.7	116.1	35.7	-2.9	-65.4	40.2	0.53
S1438_346	249.7	6.6	0.2	0.06112	0.00126	0.95571	0.02024	0.11367	0.00168	694.0	9.7	681.1	10.5	643.3	43.8	1.9	7.9	694.0	9.72
S1438_347	313.2	15.6	0.5	0.06643	0.00114	1.27369	0.02309	0.13938	0.00196	841.2	11.1	834.0	10.3	819.8	35.3	0.9	2.6	841.2	11.1
S1438_348	1119.8	60.4	0.5	0.06618	0.00079	1.07449	0.01499	0.11802	0.00152	719.1	8.8	740.9	7.3	812.1	24.6	-2.9	-11.5	719.1	8.78
S1438_349	399.2	39.3	1.6	0.07192	0.00091	1.60288	0.02341	0.162	0.00213	967.9	11.8	971.3	9.1	983.8	25.7	-0.4	-1.6	967.9	11.8
S1438_350	1463.7	14.9	0.7	0.05157	0.00088	0.12104	0.00218	0.01706	0.00023	109.1	1.5	116.0	2.0	266.5	38.6	-5.9	-59.1	109.1	1.47
S1438_351	1322.4	5.0	0.4	0.08098	0.00187	0.06746	0.00153	0.00606	9.00E-05	38.9	0.6	66.3	1.5	1220.9	44.8	-41.3	-96.8		
S1438_352	4667.3	38.5	0.5	0.05012	0.00065	0.1135	0.00168	0.01646	0.00021	105.2	1.4	109.2	1.5	200.6	29.8	-3.7	-47.6	105.2	1.35
S1438_353	1469.8	14.1	1.0	0.04836	0.00084	0.11375	0.00209	0.0171	0.00023	109.3	1.5	109.4	1.9	116.9	40.4	-0.1	-6.5	109.3	1.47
S1438_354	1887.4	7.5	0.8	0.06408	0.0013	0.05486	0.00113	0.00622	9.00E-05	40.0	0.6	54.2	1.1	744.2	42.4	-26.2	-94.6		
S1438_355	3353.1	222.3	0.8	0.06504	7.00E-04	0.97239	0.01279	0.10868	0.00138	665.1	8.0	689.7	6.6	775.5	22.5	-3.6	-14.2	665.1	8.03
S1438_356	1748.2	17.9	0.3	0.04759	0.00082	0.11818	0.00216	0.01805	0.00024	115.3	1.6	113.4	2.0	78.0	41.2	1.7	47.8	115.3	1.55
S1438_357	2147.4	21.1	0.3	0.05572	0.00087	0.13322	0.00225	0.01738	0.00023	111.1	1.5	127.0	2.0	441.0	34.0	-12.5	-74.8	111.1	1.48
S1438_358	4790.2	20.5	0.7	0.05536	0.00101	0.04545	0.00086	0.00597	8.00E-05	38.4	0.5	45.1	0.8	426.5	39.5	-14.9	-91.0		
S1438_359	2403.3	213.9	1.0	0.06504	7.00E-04	1.17782	0.01554	0.13164	0.00167	797.2	9.5	790.3	7.2	775.7	22.6	0.9	2.8	797.2	9.54
S1438_360	739.0	213.2	0.6	0.16448	0.00174	9.79499	0.12794	0.43289	0.00553	2318.7	24.9	2415.7	12.0	2502.2	17.7	-4.0	-7.3	2502.2	17.74
S1438_361	3203.7	32.3	0.8	0.04941	0.00071	0.12178	0.00194	0.01792	0.00024	114.5	1.5	116.7	1.8	167.4	33.2	-1.9	-31.6	114.5	1.49
S1438_362	5658.1	435.7	0.1	0.18666	0.00195	3.62393	0.04688	0.14112	0.00179	851.0	10.1	1554.8	10.3	2713.0	17.2	-45.3	-68.6		
S1438_363	1375.6	14.2	0.8	0.05142	0.00089	0.12044	0.00219	0.01703	0.00023	108.8	1.5	115.5	2.0	259.7	39.2	-5.8	-58.1	108.8	1.47
S1438_364	571.1	48.6	0.7	0.06517	0.00084	1.22749	0.01812	0.13692	0.0018	827.2	10.2	813.2	8.3	779.7	26.9	1.7	6.1	827.2	10.19
S1438_365	1170.9	15.8	1.1	0.08878	0.00134	0.22479	0.00364	0.0184	0.00025	117.6	1.6	205.9	3.0	1399.5	28.6	-42.9	-91.6		
S1438_366	10935.5	40.7	0.3	0.05017	0.00068	0.04408	0.00067	0.00639	8.00E-05	41.0	0.5	43.8	0.7	202.8	31.3	-6.4	-79.8	41.0	0.53
S1438_367	204.7	8.8	0.5	0.0622	0.0015	0.70039	0.01688	0.08185	0.00128	507.2	7.6	539.0	10.1	681.0	50.7	-5.9	-25.5	507.2	7.61
S1438_368	816.8	8.4	0.8	0.05102	0.00107	0.12101	0.00258	0.01724	0.00025	110.2	1.6	116.0	2.3	241.8	47.5	-5.0	-54.4	110.2	1.56
S1438_369	2943.7	135.2	0.4	0.06424	0.00075	0.74739	0.01033	0.08457	0.00109	523.4	6.5	566.7	6.0	749.5	24.5	-7.6	-30.2	523.4	6.47
S1438_370	4380.8	313.0	0.3	0.07034	0.00076	1.23222	0.01625	0.12734	0.00162	772.7	9.3	815.4	7.4	938.3	22.0	-5.2	-17.6	772.7	9.27
S1438_371	3613.1	14.1	1.5	0.04883	0.00088	0.03881	0.00074	0.00578	8.00E-05	37.1	0.5	38.7	0.7	139.9	41.9	-4.1	-73.5	37.1	0.51
S1438_372	1903.8	34.7	0.5	0.0573	0.00079	0.25103	0.00386	0.03185	0.00042	202.1	2.6	227.4	3.1	502.4	30.0	-11.1	-59.8	202.1	2.61
S1438_373	1659.6	9.4	0.4	0.04027	0.00153	0.03245	0.00124	0.00586	0.00008	37.7	0.5	32.4	1.2	0.1	0.0	16.4	37600.0	37.7	0.54
S1438_374	978.5	11.3	0.9	0.04923	0.00097	0.11972	0.00244	0.01768	0.00025	113.0	1.6	114.8	2.2	158.8	45.5	-1.6	-28.8	113.0	1.57
S1438_375	1048.1	9.3	0.6	0.04907	0.00096	0.12025	0.00244	0.01782	0.00025	113.8	1.6	115.3	2.2	151.0	45.3	-1.3	-24.6	113.8	1.58
S1438_376	2874.1	90.4	0.3	0.06454	0.00078	0.90818	0.0128	0.10228	0.00132	627.8	7.7	656.1	6.8	759.5	25.2	-4.3	-17.3	627.8	7.74
S1438_377	1412.5	39.6	0.2	0.05758	8.00E-04	0.69096	0.01074	0.08723	0.00115	539.1	6.8	533.4	6.5	513.5	30.6	1.1	5.0	539.1	6.84
S1438_378	4421.7	13.7	0.5	0.04958	0.00085	0.04129	0.00075	0.00605	8.00E-05	38.9	0.5	41.1	0.7	175.2	39.5	-5.4	-77.8	38.9	0.53
S1438_379	12634.6	111.3	0.4	0.04785	0.00055	0.12095	0.00165	0.01837	0.00023	117.4	1.5	115.9	1.5	90.9	27.9	1.3	29.2	117.4	1.48
S1438_380	1238.5	210.3	1.9	0.09915	0.00107	3.84993	0.05088	0.28224	0.00361	1602.6	18.1	1603.3	10.7	1608.3	20.0	0.0	-0.4	1608.3	20.04
S1438_381	1518.9	79.3	0.9	0.06888	0.00092	0.65167	0.00981	0.06877	0.00091	428.7	5.5	509.5	6.0	895.2	27.3	-15.9	-52.1		
S1438_382	2775.8	197.2	0.7	0.10559	0.00115	2.63747	0.03492	0.18157	0.00232	1075.5	12.7	1311.2	9.8	1724.6	19.9	-18.0	-37.6		
S1438_383	11371.5	432.2	0.2	0.05916	0.00063	0.65426	0.00853	0.0804	0.00102	498.5	6.1	511.1	5.2	572.8	22.3	-2.5	-13.0	498.5	6.08
S1438_384	5138.2	338.8	0.1	0.07505	8.00E-04	1.55013	0.02026	0.15015	0.00191	901.8	10.7	950.5	8.1	1069.8	21.2	-5.1	-15.7	901.8	10.69
S1438_385	1310.1	81.3	0.4	0.07198	0.00082	1.51303	0.02063	0.15279	0.00196	916.6	11.0	935.7	8.3	985.5	23.0	-2.0	-7.0	916.6	10.98
S1438_386	691.9	26.0	1.0	0.05648	8.00E-04	0.60197	0.0095	0.07748	0.00103	481.0	6.1	478.5	6.0	470.5	31.4	0.5	2.2	481.0	6.14
S1438_387	945.8	6.8	0.5	0.05238	0.00113	0.12752	0.00279	0.0177	0.00026	113.1	1.6	121.9	2.5	301.9	48.3	-7.2	-62.5	113.1	1.62
S1438_388	700.1	7.6	0.7	0.04722	0.00106	0.11511	0.00262	0.01772	0.00026	113.2	1.6	110.6	2.4	59.7	53.2	2.4	89.6	113.2	1.62
S1438_389	1715.5	117.3	0.4	0.06396	0.00072	1.01224	0.01368	0.11504	0.00147	701.9	8.5	710.0	6.9	740.4	23.6	-1.1	-5.2	701.9	8.51
S1438_390	1439.1	79.8	0.2	0.06665	0.00077	0.95425	0.01308	0.10407	0.00134	638.2	7.8	680.3	6.8	826.8	23.9	-6.2	-22.8	638.2	7.81
S1438_391	9218.0	83.4	0.1	0.04923	0.00057	0.11499	0.00159	0.01698	0.00022	108.5	1.4	110.5	1.4	158.8	27.0	-1.8	-31.7	108.5	1.38
S1438_392	1289.7	10.0	0.3	0.04861	0.00093	0.11421	0.00226	0.01708	0.00024	109.2	1.5	109.8	2.1	128.9	44.2	-0.5	-15.3	109.2	1.5
S1438_393	4591.6	12.2	0.4	0.0479	0.00085	0.04115	0.00077	0.00625	9.00E-05	40.1	0.5	41.0	0.8	93.2	42.5	-2.2	-57.0	40.1	0.54
S1438_394	1514.8	20.1	1.8	0.04839	8.00E-04	0.12311	0.00219	0.01849	0.00025	118.1	1.6	117.9	2.0	118.6	38.7	0.2	-0.4	118.1	1.58
S1438_395	3684.7	11.3	0.3	0.04976	0.00092	0.04277	0.00082	0.00625	9.00E-05	40.2	0.6	42.5	0.8	183.6	42.3	-5.4	-78.1	40.2	0.55
S1438_396	2628.5	130.5	0.2	0.06521	0.00072	0.87542	0.01173	0.09758	0.00125	600.2	7.3	638.5	6.4	781.1	23.1	-6.0	-23.2	600.2	7.32
S1438_397	3367.4	12.9	0.7	0.0497	0.00113	0.04088	0.00093	0.00598	9.00E-05	38.4	0.6	40.7	0.9	181.0	51.9	-5.7	-78.8	38.4	0.56
S1438_398	1080.9	38.6	0.4	0.05888	0.00074	0.70302	0.01024	0.08679	0.00113	536.5	6.7	540.6	6.1	562.8	27.3	-0.8	-4.7	536.5	6.7
S1438_399	696.0	15.7	0.5	0.07055	0.00129	0.58975	0.01118	0.06076	0.00087	380.3	5.3	470.7	7.1	944.5	37.1	-19.2	-59.7		
S1438_400	865.9	7.2	0.7	0.06373	0.0013	0.15664	0.00325	0.01787	0.00026	114.2	1.6	147.8	2.9	732.5	42.6	-22.7	-84.4		
S1438_401	2505.6	227.2	0.3	0.07909	0.00085	2.13291	0.02807	0.19604	0.0025	1154.0	13.5	1159.5	9.1	1174.3	21.1	-0.5	-1.7	1174.3	21.11
S1438_402	3658.1	14.7	1.9	0.07281	0.00123	0.06017	0.00106	0.00601	8.00E-05	38.6	0.5	59.3	1.0	1008.5	33.8	-34.9	-96.2		
S1438_403	2696.0	95.7	0.3	0.08264	0.00095	0.72644	0.00993	0.0639	0.00082	399.3	5.0	554.5	5.8	1260.8	22.1	-28.0	-68.3		
S1438_404	139.2	55.0	1.5	0.1622	0.00187	10.68738	0.14774	0.47896	0.00636	2522.7	27.7	2496.3	12.8	2478.7	19.3	1.1	1.8	2478.7	19.32
S1438_405	2129.0	8.2	0.7	0.04846	0.00102	0.04026	0.00087	0.00604	9.00E-05	38.8	0.6	40.1	0.9	121.6	49.0	-3.2	-68.1	38.8	0.55
S1438_406	2663.3	26.7	0.2	0.04758	7.00E-04	0.11319	0.00184	0.01729	0.00023	110.5	1.5	108.9	1.7	77.8	35.5	1.5	42.0	110.5	1.45
S1438_407	186.3	17.2	0.5	0.07138	0.00104	1.50987	0.0243	0.15376	0.00208	922.0	11.7	934.4	9.8	968.3	29.5	-1.3	-4.8	922.0	11.65
S1438_408	970.3	11.2	0.8	0.04936	0.00094	0.11697	0.00232	0.01723	0.00024	110.1	1.5	112.3	2.1	164.9	44.1	-2.0	-33.2	110.1	1.52
S1438_409	1254.9	173.8	0.3	0.12416	0.00133	3.67004	0.04825	0.21487	0.00274	1254.7	14.6	1564.9	10.5	2016.8	18.9	-19.8	-37.8		
S1438_410	2933.5	147.2	0.2	0.05453	0.00063	0.62031	0.00853	0.08269	0.00106	512.2	6.3	490.0	5.3	392.9	25.5	4.5	30.4	512.2	6.3
S1438_411	779.9	3.3	1.3	0.05386	0.00181	0.04337	0.00141	0.00585	1.00E-04	37.6	0.6	43.1	1.4	365.2	73.7	-12.8	-89.7	37.6	0.63
S1438_412	448.3	5.6	0.8	0.04859	0.00129	0.11498	0.00303	0.0172	0.00026	109.9	1.7	110.5	2.8	128.2	61.4	-0.5	-14.3	109.9	1.67
S1438_413	960.1	174.2	1.0	0.11	0.0012	4.27724	0.05677	0.28265	0.00362	1604.7	18.2	1689.0	10.9	1799.4	19.7	-5.0	-10.8	1799.4	19.69
S1438_414	3787.1	218.4	0.4	0.06081	0.00066	0.80281	0.01061	0.09597	0.00122	590.8	7.2	598.4	6.0	632.4	23.1	-1.3	-6.6	590.8	7.19
S1438_415	771.7	8.1	0.5	0.05074	0.00108	0.12293	0.00267	0.01761	0.00025	112.5	1.6	117.7	2.4	229.1	48.5	-4.4	-50.9	112.5	1.59
S1438_416	571.1	48.0	0.4	0.06737	0.00086	1.22362	0.01788	0.13203	0.00173	799.4	9.9	811.4	8.2	849.2	26.2	-1.5	-5.9	799.4	9.85
S1438_417	853.6	8.8	0.5	0.05064	0.00099	0.12215	0.00247	0.01753	0.00025	112.0	1.6	117.0	2.2	224.7	44.7	-4.3	-50.2	112.0	1.56
S1438_418	2120.8	19.1	0.1	0.05621	0.00082	0.13093	0.00211	0.01693	0.00022	108.2	1.4	124.9	1.9	460.1	32.4	-13.4	-76.5		
S1438_419	425.8	15.2	1.7	0.06083	0.0011	0.80194	0.01517	0.09583	0.00135	589.9	8.0	597.9	8.6	633.1	38.4	-1.3	-6.8	589.9	7.96
S1438_420	1484.1	14.2	1.1	0.04842	0.00088	0.12103	0.0023	0.01817	0.00025	116.1	1.6	116.0	2.1	120.0	42.1	0.1	-3.3	116.1	1.58
S1438_421	8147.4	86.8	0.2	0.0482	0.00056	0.115	0.00159	0.01734	0.00022	110.9	1.4	110.5	1.5	108.9	27.2	0.4	1.8	110.9	1.41
S1438_422	5209.8	44.4	0.4	0.05326	0.00069	0.1261	0.00186	0.01721	0.00022	110.0	1.4	120.6	1.7	339.8	28.9	-8.8	-67.6	110.0	1.42
S1438_423	978.5	9.9	0.9	0.04776	0.00138	0.11485	0.00328	0.01748	0.00028	111.7	1.8	110.4	3.0	86.3	68.3	1.2	29.4	111.7	1.76
S1438_424	1332.6	45.5	0.3	0.05993	0.00078	0.74189	0.01103	0.08999	0.00118	555.5	7.0	563.5	6.4	601.0	28.0	-1.4	-7.6	555.5	6.97
S1438_425	2536.3	87.0	0.2	0.06176	7.00E-04	0.86167	0.01176	0.10142	0.0013	622.7	7.6	631.0	6.4	665.7	24.3	-1.3	-6.5	622.7	7.62
S1438_426	397.1	16.8	1.0	0.05913	0.00095	0.74947	0.01294	0.09213	0.00126	568.2	7.4	567.9	7.5	571.9	34.5	0.1	-0.6	568.2	7.43
S1438_428	114.6	21.9	1.4	0.16631	0.00213	11.05515	0.16462	0.48319	0.00677	2541.2	29.4	2527.8	13.9	2520.9	21.3	0.5	0.8	2520.9	21.34
S1438_429	601.8	2.6	0.5	0.09022	0.0026	0.33676	0.0093	0.02713	0.00047	172.6	3.0	294.7	7.1	1430.2	54.1	-41.4	-87.9		
S1438_430	1085.0	12.9	0.4	0.04981	0.00124	0.12274	0.00304	0.01791	0.00027	114.5	1.7	117.6	2.8	185.9	56.8	-2.6	-38.4	114.5	1.71
S1438_431	307.1	89.8	1.2	0.1642	0.00181	10.28743	0.13807	0.45543	0.00592	2419.4	26.2	2461.0	12.4	2499.3	18.5	-1.7	-3.2	2499.3	18.46
S1438_432	4968.3	14.2	1.2	0.05377	0.00095	0.04386	0.00081	0.00593	8.00E-05	38.1	0.5	43.6	0.8	361.3	38.8	-12.6	-89.5	38.1	0.52
S1438_433	499.5	7.5	0.2	0.06131	0.00147	0.23388	0.00557	0.02773	0.00043	176.3	2.7	213.4	4.6	650.2	50.7	-17.4	-72.9		
S1438_434	2472.9	5.9	0.4	0.04753	0.00111	0.04101	0.00096	0.00627	9.00E-05	40.3	0.6	40.8	0.9	75.4	55.2	-1.2	-46.6	40.3	0.59
S1438_435	562.9	6.7	0.5	0.07586	0.00152	0.3894	0.0079	0.03732	0.00055	236.2	3.4	333.9	5.8	1091.3	39.6	-29.3	-78.4		
S1438_437	675.5	47.5	0.4	0.08592	0.00107	2.001	0.02892	0.1693	0.00223	1008.2	12.3	1115.9	9.8	1336.3	24.0	-9.7	-24.6	1008.2	12.3
S1438_438	1216.0	13.6	0.4	0.04893	0.00087	0.11539	0.00216	0.01714	0.00023	109.6	1.5	110.9	2.0	144.3	41.1	-1.2	-24.0	109.6	1.49
S1438_439	380.8	23.5	0.9	0.06474	0.00099	0.87052	0.01443	0.09775	0.00133	601.2	7.8	635.9	7.8	765.8	31.8	-5.5	-21.5	601.2	7.79
S1438_440	1259.0	308.4	0.6	0.15801	0.00169	8.70627	0.11445	0.40052	0.00512	2171.4	23.6	2307.7	12.0	2434.5	18.0	-5.9	-10.8	2434.5	18
S1438_441	665.3	48.5	0.5	0.06886	0.00087	1.14915	0.01667	0.12131	0.00159	738.1	9.1	776.8	7.9	894.5	25.7	-5.0	-17.5	738.1	9.12
S1438_442	2481.1	9.2	0.9	0.07932	0.00143	0.06651	0.00123	0.0061	9.00E-05	39.2	0.6	65.4	1.2	1180.0	35.2	-40.1	-96.7		
S1438_443	2630.5	21.2	1.1	0.04718	0.00074	0.11543	0.00197	0.01778	0.00024	113.6	1.5	110.9	1.8	58.1	36.4	2.4	95.5	113.6	1.5
S1438_444	4919.1	15.1	0.2	0.04728	0.00084	0.03705	0.00069	0.0057	8.00E-05	36.6	0.5	36.9	0.7	62.8	42.1	-0.8	-41.7	36.6	0.5
S1438_445	818.8	28.1	0.7	0.06086	0.00082	0.80302	0.01219	0.09591	0.00126	590.4	7.4	598.5	6.9	634.2	28.7	-1.4	-6.9	590.4	7.43
S1438_446	847.5	5.9	0.6	0.05246	0.00124	0.13183	0.00312	0.01827	0.00027	116.7	1.7	125.7	2.8	305.7	52.7	-7.2	-61.8	116.7	1.71
S1438_447	1572.2	115.3	0.4	0.09901	0.00116	2.78972	0.03865	0.20481	0.00267	1201.1	14.3	1352.8	10.4	1605.6	21.7	-11.2	-25.2	1605.6	21.65
S1438_448	1232.3	12.9	0.2	0.04742	0.00087	0.11921	0.0023	0.01827	0.00025	116.7	1.6	114.4	2.1	69.9	43.9	2.0	67.0	116.7	1.59
S1438_449	1832.1	395.3	0.3	0.15845	0.00168	7.05075	0.09206	0.32346	0.00412	1806.6	20.1	2117.9	11.6	2439.2	17.8	-14.7	-25.9		
S1438_450	227.2	16.1	2.0	0.0607	0.00116	0.68116	0.01348	0.08157	0.00117	505.5	7.0	527.5	8.1	628.6	40.6	-4.2	-19.6	505.5	6.96
S1438_451	1469.8	68.3	0.5	0.06424	0.00077	0.93054	0.01313	0.1053	0.00136	645.4	8.0	667.9	6.9	749.4	25.2	-3.4	-13.9	645.4	7.95
S1438_452	2059.4	22.7	1.3	0.04718	0.00084	0.10764	0.00203	0.01658	0.00023	106.0	1.4	103.8	1.9	57.9	42.6	2.1	83.1	106.0	1.43
S1438_453	1866.9	75.4	0.4	0.05874	0.00069	0.48384	0.00671	0.05988	0.00077	374.9	4.7	400.7	4.6	557.4	25.3	-6.4	-32.7	374.9	4.68
S1438_454	530.2	32.0	0.5	0.06334	0.00086	0.92007	0.0141	0.1056	0.0014	647.1	8.2	662.4	7.5	719.5	28.6	-2.3	-10.1	647.1	8.15
S1438_455	3103.4	151.5	0.1	0.07049	0.00078	1.35509	0.01818	0.13973	0.00179	843.2	10.1	869.8	7.8	942.7	22.5	-3.1	-10.6	843.2	10.12
S1438_456	178.1	11.4	0.4	0.06844	0.00122	1.28787	0.02408	0.13678	0.00196	826.4	11.1	840.4	10.7	882.0	36.3	-1.7	-6.3	826.4	11.1
S1438_457	1666.3	99.9	0.3	0.06683	0.00082	0.91817	0.01317	0.09986	0.0013	613.6	7.6	661.4	7.0	832.6	25.5	-7.2	-26.3	613.6	7.62
S1438_458	878.2	93.3	0.4	0.07718	9.00E-04	1.72839	0.02396	0.16278	0.00211	972.2	11.7	1019.2	8.9	1125.9	23.1	-4.6	-13.7	972.2	11.68

Sample S4430 Domkar River @ Domkar (Ladakh batholith) 80 grains analysed 42 concordant ages

grain	concentrations U [ppm]	Pb [ppm]	Th/U	isotopic ratios Pb207/Pb206	2σ 76	Pb207/U235	2σ 75	Pb206/U238	2σ 68	ages age 206/238	2σ age 68	age 207/235	2σ age 75	age 207/206	2σ age 76	discordance Δ 68-75 [%]	Δ 68-76 [%]	preferred age age	2σ age
S4430_001	1819.9	10.4	1.1	0.08625	0.00154	0.09647	0.00177	0.00813	0.00012	52.2	0.7	93.5	1.6	1343.8	34.2	-44.2	-96.1		
S4430_002	6376.7	36.9	0.7	0.04761	0.00065	0.06235	0.00096	0.00952	0.00012	61.1	0.8	61.4	0.9	79.0	33.0	-0.5	-22.7	61.1	0.8
S4430_003	974.4	7.3	0.7	0.07638	0.00172	0.13560	0.00303	0.01290	0.00020	82.7	1.3	129.1	2.7	1105.1	44.4	-35.9	-92.5		
S4430_004	5209.8	44.0	3.5	0.15793	0.00205	0.19379	0.00281	0.00892	0.00012	57.2	0.8	179.9	2.4	2433.6	21.8	-68.2	-97.6		
S4430_005	1269.2	8.6	0.5	0.04776	0.00106	0.06371	0.00143	0.00970	0.00014	62.2	0.9	62.7	1.4	86.4	52.6	-0.8	-28.0	62.2	0.9
S4430_006	393.0	2.2	0.9	0.04993	0.00201	0.05550	0.00216	0.00808	0.00015	51.9	0.9	54.8	2.1	191.9	90.9	-5.3	-73.0	51.9	0.9
S4430_007	262.0	1.6	0.5	0.06295	0.00302	0.08064	0.00367	0.00931	0.00020	59.7	1.3	78.7	3.5	706.5	99.0	-24.1	-91.5		
S4430_008	577.3	4.1	0.8	0.05224	0.00147	0.07179	0.00199	0.00999	0.00016	64.1	1.0	70.4	1.9	296.1	62.8	-8.9	-78.4	64.1	1.0
S4430_009	681.7	4.9	0.8	0.04853	0.00138	0.06578	0.00185	0.00985	0.00015	63.2	1.0	64.7	1.8	125.3	65.8	-2.3	-49.6	63.2	1.0
S4430_012	419.7	2.8	0.8	0.05698	0.00189	0.07294	0.00234	0.00930	0.00016	59.7	1.0	71.5	2.2	490.3	72.1	-16.5	-87.8		
S4430_013	1240.5	7.4	0.5	0.04873	0.00113	0.06741	0.00157	0.01006	0.00015	64.5	0.9	66.2	1.5	134.8	53.4	-2.6	-52.2	64.5	0.9
S4430_014	1146.4	7.8	0.4	0.07503	0.00169	0.10383	0.00231	0.01006	0.00015	64.5	1.0	100.3	2.1	1069.3	44.5	-35.7	-94.0		
S4430_016	1836.2	14.6	1.5	0.04785	0.00092	0.06113	0.00122	0.00929	0.00013	59.6	0.8	60.3	1.2	90.7	46.1	-1.2	-34.3	59.6	0.8
S4430_017	1080.9	10.8	0.9	0.05199	0.00122	0.09171	0.00215	0.01282	0.00019	82.1	1.2	89.1	2.0	285.1	52.6	-7.9	-71.2	82.1	1.2
S4430_018	5478.0	21.3	0.3	0.04685	0.00076	0.04635	0.00081	0.00719	0.00010	46.2	0.6	46.0	0.8	41.3	37.8	0.4	11.9	46.2	0.6
S4430_019	233.4	2.4	2.1	0.08317	0.00415	0.10709	0.00505	0.00936	0.00021	60.1	1.3	103.3	4.6	1273.2	94.4	-41.8	-95.3		
S4430_020	511.8	3.1	0.9	0.06221	0.00196	0.07642	0.00233	0.00893	0.00015	57.3	1.0	74.8	2.2	681.5	65.8	-23.4	-91.6		
S4430_021	6043.0	24.9	0.1	0.05276	0.00082	0.06245	0.00106	0.00860	0.00011	55.2	0.7	61.5	1.0	318.4	35.1	-10.2	-82.7	55.2	0.7
S4430_022	425.8	3.4	2.1	0.06095	0.00207	0.08029	0.00263	0.00957	0.00017	61.4	1.1	78.4	2.5	637.6	71.5	-21.7	-90.4		
S4430_023	1545.5	11.6	1.0	0.05162	0.00114	0.09620	0.00215	0.01355	0.00020	86.7	1.3	93.3	2.0	268.6	49.7	-7.1	-67.7	86.7	1.3
S4430_024	513.8	4.2	1.8	0.05000	0.00161	0.06517	0.00206	0.00948	0.00016	60.8	1.0	64.1	2.0	195.0	73.3	-5.1	-68.8	60.8	1.0
S4430_025	671.4	4.6	1.1	0.04808	0.00141	0.06298	0.00183	0.00952	0.00015	61.1	1.0	62.0	1.8	103.4	68.0	-1.5	-40.9	61.1	1.0
S4430_026	1072.7	9.1	1.2	0.04765	0.00121	0.06300	0.00160	0.00961	0.00014	61.7	0.9	62.0	1.5	81.1	60.2	-0.5	-23.9	61.7	0.9
S4430_027	3602.9	26.1	1.4	0.08440	0.00148	0.08761	0.00159	0.00755	0.00011	48.5	0.7	85.3	1.5	1301.7	33.7	-43.1	-96.3		
S4430_028	1416.6	6.9	0.4	0.04895	0.00109	0.06567	0.00149	0.00975	0.00014	62.6	0.9	64.6	1.4	145.5	51.6	-3.1	-57.0	62.6	0.9
S4430_029	1543.5	10.7	0.4	0.05396	0.00097	0.09021	0.00170	0.01215	0.00017	77.9	1.1	87.7	1.6	369.1	40.1	-11.2	-78.9	77.9	1.1
S4430_030	1826.0	14.9	0.6	0.04832	0.00082	0.08697	0.00157	0.01308	0.00018	83.8	1.1	84.7	1.5	114.8	39.6	-1.1	-27.0	83.8	1.1
S4430_031	2438.1	16.5	0.9	0.04807	0.00081	0.06544	0.00118	0.00990	0.00013	63.5	0.9	64.4	1.1	102.7	39.5	-1.4	-38.2	63.5	0.9
S4430_032	2282.5	16.6	1.4	0.04956	0.00086	0.06405	0.00118	0.00939	0.00013	60.3	0.8	63.0	1.1	174.2	40.1	-4.3	-65.4	60.3	0.8
S4430_033	2129.0	12.9	1.2	0.04735	0.00090	0.05149	0.00102	0.00790	0.00011	50.7	0.7	51.0	1.0	66.6	45.0	-0.6	-23.9	50.7	0.7
S4430_034	657.1	4.5	0.8	0.04952	0.00136	0.06845	0.00186	0.01005	0.00016	64.4	1.0	67.2	1.8	172.5	62.7	-4.2	-62.7	64.4	1.0
S4430_035	5952.1	42.1	0.4	0.04101	0.00061	0.04362	0.00072	0.00773	0.00010	49.6	0.7	43.3	0.7	0.1	0.0	14.5	49500.0	49.6	0.7
S4430_036	34.8	4.2	0.3	0.72482	0.01828	6.80995	0.13376	0.06829	0.00163	425.9	9.8	2087.0	17.4	4780.7	35.7	-79.6	-91.1		
S4430_037	507.7	2.9	0.9	0.04832	0.00172	0.05281	0.00182	0.00794	0.00014	51.0	0.9	52.3	1.8	115.0	81.7	-2.5	-55.7	51.0	0.9
S4430_038	1042.0	9.0	0.5	0.07040	0.00136	0.12298	0.00243	0.01270	0.00018	81.3	1.2	117.8	2.2	940.1	39.0	-31.0	-91.4		
S4430_040	1564.0	11.3	0.7	0.05056	0.00094	0.06872	0.00134	0.00988	0.00014	63.4	0.9	67.5	1.3	220.9	42.7	-6.1	-71.3	63.4	0.9
S4430_041	419.7	3.4	1.4	0.06647	0.00218	0.08915	0.00281	0.00975	0.00017	62.5	1.1	86.7	2.6	821.3	67.2	-27.9	-92.4		
S4430_042	608.0	4.5	1.1	0.06162	0.00195	0.08194	0.00251	0.00967	0.00017	62.0	1.1	80.0	2.4	660.9	66.5	-22.5	-90.6		
S4430_043	454.5	2.9	0.6	0.05721	0.00196	0.07920	0.00262	0.01006	0.00018	64.5	1.1	77.4	2.5	499.0	74.2	-16.7	-87.1		
S4430_044	706.2	4.5	0.8	0.05961	0.00166	0.10607	0.00289	0.01293	0.00021	82.8	1.3	102.4	2.7	589.6	59.2	-19.1	-86.0		
S4430_046	1042.0	11.4	1.3	0.23396	0.00386	0.33306	0.00546	0.01035	0.00016	66.4	1.0	291.9	4.2	3079.4	26.1	-77.3	-97.8		
S4430_047	303.0	3.1	0.7	0.27103	0.00714	0.41605	0.00935	0.01116	0.00023	71.5	1.5	353.2	6.7	3312.0	40.7	-79.8	-97.8		
S4430_048	233.4	2.4	1.3	0.16628	0.00459	0.25679	0.00637	0.01123	0.00022	72.0	1.4	232.1	5.2	2520.6	45.7	-69.0	-97.1		
S4430_049	1033.8	8.4	0.7	0.06356	0.00125	0.11267	0.00227	0.01289	0.00019	82.5	1.2	108.4	2.1	726.9	41.2	-23.9	-88.7		
S4430_050	3277.4	21.0	0.2	0.06758	0.00097	0.09011	0.00143	0.00969	0.00013	62.2	0.8	87.6	1.3	855.7	29.7	-29.0	-92.7		
S4430_051	4745.1	33.2	0.6	0.04783	0.00068	0.08268	0.00131	0.01257	0.00017	80.5	1.1	80.7	1.2	89.8	34.2	-0.2	-10.4	80.5	1.1
S4430_052	1103.4	7.9	1.6	0.05043	0.00122	0.06542	0.00159	0.00943	0.00014	60.5	0.9	64.3	1.5	214.7	55.1	-5.9	-71.8	60.5	0.9
S4430_053	1101.3	6.9	0.8	0.04905	0.00117	0.06483	0.00155	0.00961	0.00014	61.6	0.9	63.8	1.5	150.2	54.8	-3.4	-59.0	61.6	0.9
S4430_054	603.9	4.2	1.4	0.05047	0.00166	0.05606	0.00180	0.00807	0.00013	51.8	0.9	55.4	1.7	216.8	74.3	-6.5	-76.1	51.8	0.9
S4430_055	12923.2	131.5	1.9	0.06856	0.00083	0.09849	0.00140	0.01044	0.00014	67.0	0.9	95.4	1.3	885.6	24.9	-29.8	-92.4		
S4430_056	4450.4	26.7	1.5	0.04702	0.00073	0.04997	0.00085	0.00773	0.00010	49.6	0.7	49.5	0.8	50.1	36.2	0.2	-1.0	49.6	0.7
S4430_057	374.6	2.1	0.8	0.05201	0.00205	0.05537	0.00211	0.00774	0.00014	49.7	0.9	54.7	2.0	286.0	87.6	-9.1	-82.6	49.7	0.9
S4430_058	1733.9	11.2	0.8	0.05348	0.00100	0.07092	0.00138	0.00964	0.00013	61.8	0.9	69.6	1.3	349.1	41.7	-11.2	-82.3	61.8	0.9
S4430_059	1451.4	10.5	1.1	0.05052	0.00101	0.06813	0.00141	0.00980	0.00014	62.9	0.9	66.9	1.3	218.9	45.7	-6.0	-71.3	62.9	0.9
S4430_060	577.3	4.0	0.5	0.04964	0.00140	0.06772	0.00188	0.00992	0.00016	63.6	1.0	66.5	1.8	178.1	64.3	-4.4	-64.3	63.6	1.0
S4430_061	268.2	2.3	0.7	0.14490	0.00462	0.20660	0.00589	0.01036	0.00022	66.5	1.4	190.7	5.0	2286.6	53.8	-65.1	-97.1		
S4430_062	605.9	5.8	0.7	0.07078	0.00190	0.12248	0.00321	0.01258	0.00020	80.6	1.3	117.3	2.9	951.2	54.1	-31.3	-91.5		
S4430_063	22958.0	291.1	1.0	0.22305	0.00247	0.42400	0.00568	0.01382	0.00018	88.5	1.1	358.9	4.1	3002.9	17.7	-75.3	-97.1		
S4430_064	1240.5	9.1	1.1	0.04638	0.00102	0.06089	0.00136	0.00954	0.00014	61.2	0.9	60.0	1.3	17.4	51.3	2.0	251.7	61.2	0.9
S4430_065	706.2	6.2	0.8	0.04881	0.00128	0.08954	0.00234	0.01333	0.00020	85.4	1.3	87.1	2.2	138.7	60.7	-2.0	-38.4	85.4	1.3
S4430_066	329.6	2.7	0.6	0.09284	0.00281	0.12906	0.00369	0.01010	0.00018	64.8	1.2	123.2	3.3	1484.4	56.5	-47.4	-95.6		
S4430_068	1367.4	9.0	0.8	0.05276	0.00107	0.06000	0.00125	0.00827	0.00012	53.1	0.8	59.2	1.2	318.4	45.5	-10.3	-83.3	53.1	0.8
S4430_069	1125.9	8.5	0.8	0.04838	0.00104	0.06625	0.00145	0.00995	0.00014	63.8	0.9	65.1	1.4	117.9	49.9	-2.0	-45.9	63.8	0.9
S4430_070	524.1	3.4	0.5	0.05756	0.00178	0.07692	0.00230	0.00971	0.00016	62.3	1.0	75.2	2.2	512.7	66.7	-17.2	-87.8		
S4430_071	554.8	5.2	0.7	0.04686	0.00145	0.08115	0.00247	0.01259	0.00020	80.6	1.3	79.2	2.3	41.7	72.6	1.8	93.3	80.6	1.3
S4430_072	1181.2	8.0	1.5	0.05096	0.00118	0.06413	0.00150	0.00915	0.00013	58.7	0.9	63.1	1.4	239.0	52.6	-7.0	-75.4	58.7	0.9
S4430_073	1981.6	11.7	0.5	0.05026	0.00093	0.06608	0.00127	0.00956	0.00013	61.3	0.9	65.0	1.2	206.8	42.2	-5.7	-70.4	61.3	0.9
S4430_074	947.8	7.1	0.7	0.06015	0.00127	0.08354	0.00178	0.01010	0.00015	64.8	0.9	81.5	1.7	609.0	44.9	-20.5	-89.4		
S4430_075	831.1	7.0	0.9	0.06815	0.00144	0.09430	0.00201	0.01006	0.00015	64.5	1.0	91.5	1.9	873.0	43.2	-29.5	-92.6		
S4430_076	274.3	2.1	0.9	0.08398	0.00300	0.11527	0.00388	0.00998	0.00019	64.0	1.2	110.8	3.5	1291.9	68.1	-42.2	-95.0		
S4430_077	4720.6	27.1	0.5	0.04905	0.00073	0.06100	0.00099	0.00904	0.00012	58.0	0.8	60.1	1.0	150.4	34.3	-3.5	-61.4	58.0	0.8
S4430_078	2325.5	15.4	1.0	0.04792	0.00089	0.05067	0.00098	0.00769	0.00011	49.4	0.7	50.2	1.0	94.4	44.4	-1.6	-47.7	49.4	0.7
S4430_079	5326.5	26.2	0.5	0.05756	0.00089	0.06028	0.00101	0.00761	0.00010	48.9	0.7	59.4	1.0	512.8	34.0	-17.7	-90.5		
S4430_080	419.7	4.4	1.0	0.10751	0.00250	0.20134	0.00452	0.01361	0.00022	87.2	1.4	186.3	3.8	1757.6	41.9	-53.2	-95.0		

Sample S1439 Kandia River @ Halil (Kohistan arc) 37 grains analysed 32 concordant ages

grain	concentrations U [ppm]	Pb [ppm]	Th/U	isotopic ratios Pb207/Pb206	2σ 76	Pb207/U235	2σ 75	Pb206/U238	2σ 68	ages age 206/238	2σ age 68	age 207/235	2σ age 75	age 207/206	2σ age 76	discordance Δ 68-75 [%]	Δ 68-76 [%]	preferred age age	2σ age
S1439_001	808.6	5.2	0.6	0.05088	0.00139	0.09295	0.00251	0.01328	0.00021	85.0	1.3	90.2	2.3	235.2	62.0	-5.8	-63.9	85.0	1.3
S1439_002	380.8	2.3	0.7	0.04974	0.00186	0.09066	0.0033	0.01325	0.00023	84.9	1.5	88.1	3.1	182.7	85.0	-3.6	-53.5	84.9	1.5
S1439_003	346.0	2.6	1.1	0.04832	0.00181	0.09096	0.0033	0.01369	0.00024	87.6	1.5	88.4	3.1	114.8	85.9	-0.9	-23.7	87.6	1.5
S1439_004	151.5	0.7	0.7	0.04985	0.00398	0.09353	0.0072	0.01364	0.00036	87.3	2.3	90.8	6.7	188.0	175.9	-3.9	-53.6	87.3	2.3
S1439_005	3715.5	17.7	0.3	0.04739	0.00074	0.07025	0.00119	0.01078	0.00014	69.1	0.9	68.9	1.1	68.6	37.4	0.3	0.7	69.1	0.9
S1439_006	296.8	2.0	1.1	0.04624	0.00215	0.08991	0.00404	0.01413	0.00027	90.5	1.7	87.4	3.8	9.9	108.2	3.5	814.1	90.5	1.7
S1439_007	444.2	3.2	0.6	0.05092	0.00169	0.08789	0.00285	0.01255	0.00021	80.4	1.3	85.5	2.7	237.4	74.7	-6.0	-66.1	80.4	1.3
S1439_008	214.9	1.7	0.9	0.08367	0.00301	0.16976	0.00573	0.01475	0.00029	94.4	1.8	159.2	5.0	1284.8	68.5	-40.7	-92.7		
S1439_009	663.3	4.2	0.6	0.05011	0.00195	0.08606	0.00324	0.01248	0.00023	80.0	1.5	83.8	3.0	200.2	88.1	-4.5	-60.0	80.0	1.5
S1439_010	341.9	2.4	0.9	0.0506	0.00186	0.09872	0.00353	0.01418	0.00025	90.8	1.6	95.6	3.3	222.4	83.1	-5.0	-59.2	90.8	1.6
S1439_011	939.6	7.0	1.3	0.04617	0.0011	0.09004	0.00216	0.01417	0.00021	90.7	1.3	87.5	2.0	6.6	56.0	3.7	1274.2	90.7	1.3
S1439_012	100.3	0.7	1.0	0.04686	0.00461	0.0809	0.00769	0.01255	0.00038	80.4	2.4	79.0	7.2	41.8	220.2	1.8	92.3	80.4	2.4
S1439_013	374.6	3.0	1.4	0.04639	0.0018	0.08931	0.00337	0.014	0.00025	89.6	1.6	86.9	3.2	17.8	90.8	3.1	403.4	89.6	1.6
S1439_014	1600.8	8.5	1.1	0.05043	0.00106	0.08292	0.00177	0.01195	0.00017	76.6	1.1	80.9	1.7	214.6	47.8	-5.3	-64.3	76.6	1.1
S1439_015	1046.1	11.5	1.2	0.04808	0.00094	0.09383	0.00189	0.01419	2.00E-04	90.8	1.3	91.1	1.8	103.1	45.4	-0.3	-11.9	90.8	1.3
S1439_016	133.1	35.7	0.8	0.16872	0.002	10.64065	0.14992	0.45844	0.00615	2432.7	27.2	2492.3	13.1	2545.0	19.7	-2.4	-4.4	2545.0	19.7
S1439_017	466.7	2.6	0.7	0.04823	0.00172	0.07722	0.00268	0.01164	2.00E-04	74.6	1.3	75.5	2.5	110.6	81.9	-1.2	-32.5	74.6	1.3
S1439_018	243.6	1.5	1.0	0.06847	0.00393	0.13213	0.00714	0.01403	0.00035	89.8	2.2	126.0	6.4	882.8	114.5	-28.7	-89.8		
S1439_019	448.3	2.4	1.2	0.05689	0.00245	0.11075	0.00457	0.01415	0.00028	90.6	1.8	106.7	4.2	486.7	92.9	-15.1	-81.4		
S1439_020	929.4	32.3	0.3	0.06571	0.00095	1.06116	0.01697	0.11738	0.00158	715.5	9.1	734.4	8.4	797.2	30.0	-2.6	-10.2	715.5	9.1
S1439_021	272.3	1.3	0.7	0.04585	0.00284	0.0896	0.00535	0.01421	0.00032	90.9	2.0	87.1	5.0	0.1	132.4	4.4	90800.0	90.9	2.0
S1439_022	196.5	1.7	1.1	0.11373	0.00566	0.25265	0.01126	0.01615	0.00044	103.3	2.8	228.7	9.1	1859.8	87.3	-54.8	-94.4		
S1439_023	401.2	2.4	0.9	0.05102	0.00193	0.09453	0.00347	0.01347	0.00024	86.3	1.5	91.7	3.2	241.5	85.1	-5.9	-64.3	86.3	1.5
S1439_024	243.6	2.0	1.4	0.0474	0.00219	0.0887	0.00393	0.0136	0.00027	87.1	1.7	86.3	3.7	69.0	106.9	0.9	26.2	87.1	1.7
S1439_025	86.0	0.4	0.5	0.0515	0.00684	0.08099	0.01036	0.01143	0.00045	73.3	2.9	79.1	9.7	263.5	279.4	-7.3	-72.2	73.3	2.9
S1439_026	493.3	3.7	1.3	0.04666	0.00163	0.08869	0.00303	0.01382	0.00023	88.5	1.5	86.3	2.8	31.5	81.6	2.5	181.0	88.5	1.5
S1439_027	477.0	3.7	1.3	0.04961	0.00179	0.09818	0.00343	0.01439	0.00025	92.1	1.6	95.1	3.2	176.6	81.9	-3.2	-47.8	92.1	1.6
S1439_028	409.4	2.1	0.7	0.04443	0.00199	0.08476	0.00368	0.01387	0.00026	88.8	1.7	82.6	3.4	0.1	19.6	7.5	88700.0	88.8	1.7
S1439_029	266.1	1.5	1.2	0.04845	0.00317	0.08546	0.00533	0.01282	0.00032	82.1	2.1	83.3	5.0	121.1	147.3	-1.4	-32.2	82.1	2.1
S1439_030	489.3	4.1	0.2	0.04632	0.00151	0.09419	0.00301	0.01478	0.00024	94.6	1.6	91.4	2.8	14.2	75.8	3.5	566.2	94.6	1.6
S1439_031	92.1	0.6	1.1	0.1469	0.00945	0.35892	0.02017	0.01776	0.00063	113.5	4.0	311.4	15.1	2310.2	106.4	-63.6	-95.1		
S1439_032	270.2	2.0	1.2	0.04808	0.00218	0.08617	0.00376	0.01303	0.00026	83.4	1.6	83.9	3.5	103.1	103.9	-0.6	-19.1	83.4	1.6
S1439_033	712.4	5.3	0.6	0.04894	0.00124	0.09727	0.00246	0.01445	0.00022	92.5	1.4	94.2	2.3	145.1	58.2	-1.8	-36.3	92.5	1.4
S1439_034	1193.4	9.1	0.6	0.04803	0.00098	0.08903	0.00187	0.01347	0.00019	86.3	1.2	86.6	1.7	100.5	47.6	-0.3	-14.1	86.3	1.2
S1439_035	294.8	3.2	1.0	0.04908	0.00188	0.09279	0.00344	0.01374	0.00024	88.0	1.6	90.1	3.2	151.7	87.2	-2.3	-42.0	88.0	1.6
S1439_036	196.5	1.3	0.7	0.04643	0.00304	0.09292	0.00588	0.01455	0.00033	93.1	2.1	90.2	5.5	20.0	150.1	3.2	365.5	93.1	2.1
S1439_037	141.2	1.0	0.8	0.05201	0.00401	0.09818	0.00724	0.01372	0.00038	87.8	2.4	95.1	6.7	285.9	167.0	-7.7	-69.3	87.8	2.4

Sample 1440 Swat River @ Fatepur (Kohistan arc) 72 grains analysed 28 concordant ages

grain	concentrations U [ppm]	Pb [ppm]	Th/U	isotopic ratios Pb207/Pb206	2σ 76	Pb207/U235	2σ 75	Pb206/U238	2σ 68	ages age 206/238	2σ age 68	age 207/235	2σ age 75	age 207/206	2σ age 76	discordance Δ 68-75 [%]	Δ 68-76 [%]	preferred age age	2σ age
S1440_001	477.892133	1.9	1.1	0.05667	0.00355	0.10251	0.00602	0.01315	0.00035	84.2	2.2	99.1	5.55	478.1	133.65	-15.0	-82.4		
S1440_002	224.144098	0.5	0.7	0.35097	0.03553	0.65418	0.04737	0.01355	0.001	86.8	6.37	511.1	29.08	3711.2	146.16	-83.0	-97.7		
S1440_003	365.820084	1.5	0.8	0.07758	0.00319	0.14696	0.00566	0.01377	0.00028	88.2	1.77	139.2	5.01	1136.1	79.81	-36.6	-92.2		
S1440_004	596.307883	1.9	1.6	0.06489	0.0056	0.08486	0.00682	0.00951	0.00033	61	2.11	82.7	6.38	770.9	171.87	-26.2	-92.1		
S1440_005	811.993713	5.0	1.2	0.06295	0.00173	0.12734	0.00338	0.01471	0.00023	94.1	1.44	121.7	3.04	706.4	57.32	-22.7	-86.7		
S1440_006	469.433865	2.7	1.1	0.15481	0.00402	0.32919	0.00773	0.01546	0.00028	98.9	1.75	288.9	5.91	2399.7	43.5	-65.8	-95.9		
S1440_008	215.68583	0.5	0.8	0.21333	0.01549	0.27878	0.01662	0.0095	0.00042	61	2.69	249.7	13.19	2931	112.83	-75.6	-97.9		
S1440_009	238.946066	0.6	0.8	0.05234	0.00556	0.09074	0.00924	0.0126	0.00043	80.7	2.72	88.2	8.6	300.5	225.46	-8.5	-73.1	80.7	2.72
S1440_010	135.332285	0.6	0.6	0.08392	0.00662	0.15007	0.01087	0.013	0.00045	83.3	2.87	142	9.6	1290.7	146.15	-41.3	-93.5		
S1440_011	302.383075	1.1	0.7	0.06303	0.00435	0.11393	0.0074	0.01314	0.00036	84.2	2.3	109.6	6.75	709.3	140.34	-23.2	-88.1		
S1440_012	444.059062	2.1	1.5	0.11708	0.00365	0.22656	0.00647	0.01407	0.00026	90.1	1.68	207.4	5.36	1912.1	54.97	-56.6	-95.3		
S1440_013	304.497642	3.2	1.0	0.09258	0.00533	0.19726	0.01026	0.01549	0.00045	99.1	2.83	182.8	8.7	1479.1	105.45	-45.8	-93.3		
S1440_014	380.622053	1.4	1.7	0.19065	0.00686	0.40676	0.01246	0.01551	0.00037	99.2	2.34	346.5	9	2747.8	57.93	-71.4	-96.4		
S1440_015	251.633468	2.2	0.8	0.09818	0.00578	0.19683	0.01043	0.01457	0.00043	93.3	2.75	182.4	8.85	1589.8	106.15	-48.8	-94.1		
S1440_016	835.253949	4.5	1.5	0.06468	0.00176	0.12102	0.00317	0.0136	0.00021	87.1	1.34	116	2.87	764	56.21	-24.9	-88.6		
S1440_018	293.924807	1.6	0.7	0.11374	0.00376	0.22825	0.00686	0.01459	0.00029	93.4	1.82	208.7	5.67	1860.1	58.58	-55.2	-95.0		
S1440_019	327.757879	2.2	1.3	0.06652	0.00264	0.12394	0.00466	0.01354	0.00026	86.7	1.62	118.6	4.21	822.7	80.73	-26.9	-89.5		
S1440_020	152.248821	1.3	1.0	0.07269	0.00598	0.14662	0.01112	0.01466	0.00052	93.8	3.32	138.9	9.85	1005.2	158.65	-32.5	-90.7		
S1440_021	452.517329	2.6	1.4	0.06086	0.00216	0.11671	0.00396	0.01394	0.00024	89.2	1.54	112.1	3.6	634.4	74.66	-20.4	-85.9		
S1440_022	274.893705	2.3	1.0	0.11389	0.00321	0.396	0.01034	0.02527	0.00045	160.9	2.81	338.7	7.52	1862.4	50.08	-52.5	-91.4		
S1440_023	287.581107	1.6	0.7	0.07594	0.00292	0.15394	0.00556	0.01474	0.00028	94.3	1.8	145.4	4.89	1093.4	75.1	-35.1	-91.4		
S1440_024	473.662999	2.4	0.8	0.15737	0.00416	0.2636	0.00625	0.01218	0.00022	78	1.4	237.6	5.02	2427.6	44.12	-67.2	-96.8		
S1440_025	384.851187	2.2	0.5	0.06395	0.0022	0.13762	0.0045	0.01564	0.00027	100.1	1.73	130.9	4.02	740.1	71.07	-23.5	-86.5		
S1440_026	247.404334	1.1	1.3	0.08586	0.00412	0.16103	0.00714	0.01363	0.00032	87.3	2.02	151.6	6.25	1335	90.04	-42.4	-93.5		
S1440_027	900.805525	3.9	1.2	0.04862	0.00162	0.09447	0.00305	0.01412	0.00023	90.4	1.44	91.7	2.83	129.7	76.62	-1.4	-30.3	90.4	1.44
S1440_028	219.914964	14.9	0.8	0.08204	0.00127	2.07048	0.03365	0.18345	0.00243	1085.8	13.25	1139.1	11.13	1246.5	29.78	-4.7	-12.9	1085.8	13.25
S1440_029	422.913392	2.3	1.4	0.06141	0.00239	0.11293	0.00419	0.01337	0.00024	85.6	1.55	108.6	3.82	653.6	81.39	-21.2	-86.9		
S1440_030	754.900405	3.6	1.0	0.04883	0.00172	0.09216	0.00314	0.01372	0.00023	87.8	1.44	89.5	2.92	139.7	80.87	-1.9	-37.2	87.8	1.44
S1440_031	706.265365	3.1	1.1	0.05839	0.00196	0.11384	0.00367	0.01417	0.00023	90.7	1.49	109.5	3.34	544.6	71.54	-17.2	-83.3		
S1440_032	560.360244	1.0	0.9	0.0499	0.00375	0.06012	0.00432	0.00876	0.00023	56.2	1.49	59.3	4.14	190.1	166.14	-5.2	-70.4	56.2	1.49
S1440_033	386.965754	2.2	1.3	0.06201	0.0024	0.11501	0.00424	0.01348	0.00024	86.3	1.55	110.5	3.86	674.4	80.54	-21.9	-87.2		
S1440_034	1234.9071	5.2	0.2	0.05765	0.00133	0.10494	0.00238	0.01323	0.00019	84.7	1.19	101.3	2.19	516	50.09	-16.4	-83.6		
S1440_035	255.862602	1.5	1.0	0.08121	0.00334	0.159	0.00611	0.01423	0.00029	91.1	1.84	149.8	5.35	1226.5	78.57	-39.2	-92.6		
S1440_036	188.196459	1.0	0.8	0.08724	0.00425	0.17141	0.00775	0.01428	0.00033	91.4	2.11	160.6	6.71	1365.7	90.99	-43.1	-93.3		
S1440_037	583.620481	2.5	0.7	0.05444	0.00197	0.09608	0.00335	0.01283	0.00022	82.2	1.4	93.2	3.1	389.2	78.7	-11.8	-78.9	82.2	1.4
S1440_038	287.581107	1.4	0.9	0.05941	0.00299	0.11429	0.00551	0.01398	0.00028	89.5	1.78	109.9	5.02	582.3	105.55	-18.6	-84.6		
S1440_039	277.008272	1.7	1.3	0.05371	0.00352	0.09729	0.00602	0.01317	0.00035	84.3	2.2	94.3	5.57	358.9	141.23	-10.6	-76.5	84.3	2.2
S1440_040	194.54016	0.9	0.8	0.05668	0.00364	0.09903	0.00611	0.0127	0.00029	81.3	1.86	95.9	5.64	478.5	136.78	-15.2	-83.0		
S1440_041	907.149226	3.0	0.7	0.04883	0.00205	0.08907	0.00358	0.01326	0.00024	84.9	1.55	86.6	3.34	139.6	95.65	-2.0	-39.2	84.9	1.55
S1440_042	363.705517	1.5	0.6	0.06682	0.00273	0.1154	0.00445	0.01255	0.00024	80.4	1.55	110.9	4.05	832.1	82.95	-27.5	-90.3		
S1440_043	642.828356	3.6	1.2	0.05397	0.0017	0.10451	0.00318	0.01407	0.00022	90.1	1.41	100.9	2.93	369.8	69.15	-10.7	-75.6	90.1	1.41
S1440_044	209.342129	1.2	1.0	0.05594	0.00329	0.10744	0.00609	0.01396	3.00E-04	89.4	1.88	103.6	5.59	449.6	125.99	-13.7	-80.1		
S1440_045	1450.59293	8.0	0.9	0.04682	0.00106	0.08568	0.00193	0.0133	0.00018	85.2	1.16	83.5	1.81	39.8	52.44	2.0	114.1	85.2	1.16
S1440_046	304.497642	2.0	1.2	0.11541	0.00382	0.22805	0.00694	0.01436	0.00027	91.9	1.75	208.6	5.74	1886.3	58.43	-55.9	-95.1		
S1440_047	697.807097	3.4	1.2	0.05147	0.00165	0.1002	0.0031	0.01415	0.00022	90.6	1.43	97	2.86	261.9	71.79	-6.6	-65.4	90.6	1.43
S1440_049	346.788981	1.4	0.9	0.04887	0.00277	0.08719	0.00477	0.01297	0.00027	83.1	1.7	84.9	4.45	141.4	128.01	-2.1	-41.2	83.1	1.7
S1440_050	425.027959	2.6	1.3	0.04664	0.00187	0.08622	0.00336	0.01344	0.00023	86	1.45	84	3.14	30.6	93.73	2.4	181.0	86	1.45
S1440_051	1133.40789	7.5	1.2	0.05022	0.00181	0.09984	0.00346	0.01445	0.00025	92.5	1.58	96.6	3.19	205.1	81.74	-4.2	-54.9	92.5	1.58
S1440_052	1165.1264	4.4	0.9	0.04896	0.00139	0.0912	0.00253	0.01354	2.00E-04	86.7	1.29	88.6	2.36	146	65.39	-2.1	-40.6	86.7	1.29
S1440_053	492.694102	2.7	1.2	0.06119	0.00228	0.11837	0.00422	0.01406	0.00025	90	1.59	113.6	3.83	646	78.2	-20.8	-86.1		
S1440_054	750.671271	4.0	1.0	0.04817	0.00147	0.08975	0.00267	0.01354	0.00021	86.7	1.32	87.3	2.49	107.4	70.66	-0.7	-19.3	86.7	1.32
S1440_055	173.394491	0.8	0.6	0.05817	0.00374	0.1099	0.00669	0.01373	0.00035	87.9	2.2	105.9	6.12	535.7	135.44	-17.0	-83.6		
S1440_057	890.23269	3.7	1.0	0.05003	0.0016	0.09159	0.00284	0.01331	0.00021	85.2	1.32	89	2.65	196.3	72.6	-4.3	-56.6	85.2	1.32
S1440_058	342.559848	1.6	0.9	0.05463	0.0026	0.10468	0.00479	0.01393	0.00027	89.2	1.7	101.1	4.4	397.1	102.82	-11.8	-77.5	89.2	1.7
S1440_059	78.2389775	0.3	0.8	0.07173	0.00736	0.13078	0.01269	0.01325	0.00049	84.9	3.11	124.8	11.4	978.2	196.19	-32.0	-91.3		
S1440_061	405.996856	2.0	1.0	0.05303	0.00221	0.09293	0.00371	0.01274	0.00023	81.6	1.47	90.2	3.45	330.1	91.56	-9.5	-75.3	81.6	1.47
S1440_062	539.214575	2.8	1.1	0.0497	0.0018	0.09525	0.00334	0.01393	0.00023	89.2	1.48	92.4	3.09	180.8	82.33	-3.5	-50.7	89.2	1.48
S1440_063	742.213003	2.4	0.7	0.04646	0.00463	0.08404	0.00792	0.01315	0.00047	84.2	3.02	81.9	7.42	21.3	223.53	2.8	295.3	84.2	3.02
S1440_064	353.132682	6.9	1.2	0.0487	0.00226	0.08872	0.00397	0.01324	0.00025	84.8	1.57	86.3	3.7	133.2	105.7	-1.7	-36.3	84.8	1.57
S1440_066	59.2078749	0.3	0.5	0.07104	0.00905	0.13828	0.0169	0.01415	0.00056	90.6	3.54	131.5	15.08	958.6	240.71	-31.1	-90.5	90.6	3.54
S1440_067	962.127967	4.8	0.8	0.07292	0.00175	0.14585	0.0034	0.01454	0.00022	93	1.37	138.2	3.02	1011.7	48.03	-32.7	-90.8		
S1440_068	947.325998	5.1	1.2	0.04907	0.00136	0.09502	0.00258	0.01407	0.00021	90.1	1.33	92.2	2.39	151.3	63.86	-2.3	-40.4	90.1	1.33
S1440_069	1006.53387	4.1	1.1	0.05405	0.00191	0.10577	0.00359	0.01422	0.00024	91	1.52	102.1	3.29	372.8	77.3	-10.9	-75.6	91	1.52
S1440_070	513.839771	2.5	1.4	0.05105	0.00205	0.10078	0.0039	0.01435	0.00025	91.8	1.62	97.5	3.59	243.3	90.05	-5.8	-62.3	91.8	1.62
S1440_071	589.964182	3.2	1.7	0.04821	0.00179	0.08772	0.00315	0.01323	0.00022	84.7	1.42	85.4	2.94	109.4	85.46	-0.8	-22.6	84.7	1.42
S1440_072	790.848043	4.1	0.9	0.04713	0.00141	0.08949	0.00261	0.0138	0.00021	88.4	1.33	87	2.43	55.2	70.29	1.6	60.1	88.4	1.33

Sample S1426 Nandihar Kwar River @ Daut (Greater Himalaya) 45 grains analysed 36 concordant ages

grain	concentrations U [ppm]	Pb [ppm]	Th/U	isotopic ratios Pb207/Pb206	2σ 76	Pb207/U235	2σ 75	Pb206/U238	2σ 68	ages age 206/238	2σ age 68	age 207/235	2σ age 75	age 207/206	2σ age 76	discordance Δ 68-75 [%]	Δ 68-76 [%]	preferred age age	2σ age
S1426_002	230	22	0.6	0.09573	0.00133	2.27258	0.03795	0.17257	0.00258	1026.3	14.16	1203.8	11.78	1542.5	25.83	-14.7	-33.5		
S1426_003	4762	22	0.3	0.06573	0.00074	1.09937	0.01642	0.12158	0.00173	739.7	9.96	753	7.94	797.8	23.35	-1.8	-7.3	739.7	9.96
S1426_004	5944	285	0.0	0.06663	0.00074	1.17811	0.01754	0.12853	0.00183	779.5	10.46	790.4	8.18	826.3	23.08	-1.4	-5.7	779.5	10.46
S1426_005	1779	351	0.4	0.06797	0.00079	1.54965	0.02352	0.16573	0.00237	988.6	13.13	950.4	9.37	867.6	23.81	4.0	13.9	988.6	13.13
S1426_006	1404	131	0.8	0.32521	0.00488	0.49218	0.011	0.00018		70.5	1.12	406.4	5.53	3594.6	22.83	-82.7	-98.0		
S1426_007	2349	12	0.7	0.06666	0.00076	1.36214	0.02056	0.14854	0.00212	892.8	11.92	872.8	8.84	827.2	23.72	2.3	7.9	892.8	11.92
S1426_008	755	179	0.3	0.05775	0.00132	0.27063	0.00642	0.03407	0.00055	215.9	3.45	243.2	5.13	520.1	49.51	-11.2	-58.5	215.9	3.45
S1426_009	496	15	0.7	0.0575	9.00E-04	0.68695	0.01242	0.08684	0.0013	536.8	7.68	531	7.47	510.5	34.32	1.1	5.2	536.8	7.68
S1426_010	849	21	1.2	0.06704	0.00083	1.30283	0.02045	0.14126	0.00204	851.8	11.53	847	9.02	839.1	25.48	0.6	1.5	851.8	11.53
S1426_012	4122	71	1.4	0.05406	0.00065	0.42255	0.00652	0.05681	0.00081	356.2	4.97	357.9	4.65	373.6	26.51	-0.5	-4.7	356.2	4.97
S1426_013	864	114	0.8	0.09528	0.00373	0.11205	0.00408	0.00855	0.00019	54.9	1.24	107.8	3.73	1533.6	71.93	-49.1	-96.4		
S1426_014	1377	136	0.3	0.11458	0.00129	4.86444	0.07286	0.3086	0.00442	1733.8	21.76	1796.1	12.61	1873.3	20.17	-3.5	-7.4	1873.3	20.17
S1426_015	1515	6	0.2	0.05604	0.00071	0.60422	0.00959	0.07837	0.00113	486.4	6.76	479.9	6.07	453.8	27.34	1.4	7.2	486.4	6.76
S1426_016	2062	188	0.6	0.16141	0.00186	7.09542	0.10732	0.31955	0.00461	1787.5	22.54	2123.5	13.46	2470.5	19.28	-15.8	-27.6		
S1426_017	1332	55	0.4	0.05592	7.00E-04	0.65795	0.01045	0.08553	0.00124	529	7.34	513.4	6.4	448.9	27.33	3.0	17.8	529	7.34
S1426_018	1355	258	1.1	0.07216	0.00084	1.60223	0.02435	0.1614	0.00231	964.5	12.85	971.1	9.5	990.5	23.4	-0.7	-2.6	964.5	12.85
S1426_019	3550	59	2.4	0.06785	0.00077	1.27751	0.01916	0.13687	0.00195	826.9	11.08	835.7	8.54	864	23.25	-1.1	-4.3	826.9	11.08
S1426_020	1070	156	1.7	0.06744	8.00E-04	1.42524	0.02198	0.15362	0.00221	921.2	12.35	899.6	9.2	851.5	24.58	2.4	8.2	921.2	12.35
S1426_021	2652	422	0.4	0.06801	0.00078	1.41658	0.02137	0.1514	0.00217	908.8	12.12	895.9	8.98	869	23.48	1.4	4.6	908.8	12.12
S1426_022	2264	121	0.7	0.06862	8.00E-04	1.36444	0.02074	0.14454	0.00207	870.3	11.67	873.8	8.91	887.3	23.77	-0.4	-1.9	870.3	11.67
S1426_023	1505	197	1.3	0.068	0.00084	1.34515	0.02112	0.1438	0.00208	866.1	11.72	865.5	9.15	868.6	25.35	0.1	-0.3	866.1	11.72
S1426_024	3156	154	1.0	0.05409	0.00072	0.40932	0.00669	0.05501	8.00E-04	345.2	4.88	348.4	4.82	374.7	29.72	-0.9	-7.9	345.2	4.88
S1426_025	5946	125	0.0	0.05682	0.00068	0.56343	0.00871	0.07208	0.00104	448.7	6.23	453.8	5.66	483.9	26.52	-1.1	-7.3	448.7	6.23
S1426_026	411	95	0.6	0.06847	0.00101	1.47992	0.02583	0.15711	0.00234	940.7	13.04	922.2	10.58	882.9	30.17	2.0	6.5	940.7	13.04
S1426_027	8386	230	2.1	0.06719	0.00075	1.21029	0.01808	0.13094	0.00187	793.2	10.65	805.3	8.31	843.6	23.11	-1.5	-6.0	793.2	10.65
S1426_028	1702	35	0.3	0.06843	8.00E-04	1.48196	0.02264	0.15743	0.00226	942.5	12.59	923	9.26	881.6	23.99	2.1	6.9	942.5	12.59
S1426_029	781	693	0.2	0.06601	0.00085	1.41908	0.02278	0.15627	0.00227	936	12.68	897	9.56	806.7	26.58	4.3	16.0	936	12.68
S1426_030	423	122	1.0	0.06644	0.00107	1.4212	0.02632	0.1555	0.00237	931.7	13.21	897.9	11.04	820.1	33.37	3.8	13.6	931.7	13.21
S1426_031	1172	45	0.3	0.06887	0.00095	1.1825	0.01984	0.12481	0.00184	758.2	10.55	792.5	9.23	894.9	28.35	-4.3	-15.3	758.2	10.55
S1426_032	521	29	0.6	0.16435	0.00187	11.78459	0.17775	0.52125	0.00751	2704.5	31.83	2587.4	14.12	2500.9	18.99	4.5	8.1	2500.9	18.99
S1426_033	8518	57	0.1	0.07451	0.00093	0.22827	0.0036	0.02227	0.00032	142	2.03	208.8	2.97	1054.9	25.18	-32.0	-86.5		
S1426_034	4480	147	0.0	0.05277	0.00104	0.11871	0.00253	0.01635	0.00025	104.6	1.6	113.9	2.3	318.8	44.26	-8.2	-67.2	104.6	1.6
S1426_035	7540	74	0.1	0.05739	0.00067	0.54032	0.00822	0.06844	0.00098	426.8	5.91	438.6	5.42	506	25.3	-2.7	-15.7	426.8	5.91
S1426_036	4343	33	0.1	0.06618	0.00076	0.8058	0.01224	0.08851	0.00127	546.7	7.51	600.1	6.88	812.1	23.98	-8.9	-32.7	546.7	7.51
S1426_037	483	163	3.9	0.06666	0.00136	0.3156	0.00685	0.03442	0.00055	218.1	3.4	278.5	5.29	827.1	41.96	-21.7	-73.6		
S1426_038	3264	158	0.1	0.05648	0.00068	0.5916	0.0092	0.07615	0.0011	473.1	6.56	471.9	5.87	470.4	26.73	0.3	0.6	473.1	6.56
S1426_040	1804	19	0.3	0.06375	0.00079	1.06868	0.01684	0.12187	0.00176	741.3	10.13	738.1	8.27	733.2	26.01	0.4	1.1	741.3	10.13
S1426_041	2877	120	0.4	0.05796	0.00084	0.48446	0.00837	0.06076	9.00E-04	380.2	5.45	401.1	5.72	528	31.87	-5.2	-28.0	380.2	5.45
S1426_042	2303	60	0.5	0.06647	0.00078	1.44642	0.02215	0.15818	0.00227	946.6	12.65	908.4	9.19	821.3	24.29	4.2	15.3	946.6	12.65
S1426_043	1947	77	1.0	0.05348	0.00073	0.51183	0.00852	0.06957	0.00102	433.5	6.12	419.7	5.72	349.2	30.43	3.3	24.1	433.5	6.12
S1426_044	958	52	2.2	0.06728	0.00085	1.46465	0.02329	0.15825	0.0023	947	12.79	915.9	9.6	846.4	25.94	3.4	11.9	947	12.79
S1426_045	947	135	0.8	0.10416	0.00126	4.72944	0.07366	0.33006	0.00481	1838.7	23.3	1772.5	13.05	1699.5	22.09	3.7	8.2	1699.5	22.09

Sample S1432 Astor River @ Bunji (Nanga Parbat) 190 grains analysed 120 concordant ages

	concentrations			isotopic ratios						ages						discordance		preferred age	
grain	U [ppm]	Pb [ppm]	Th/U	Pb207/Pb206	2σ 76	Pb207/U235	2σ 75	Pb206/U238	2σ 68	age 206/238	2σ age 68	age 207/235	2σ age 75	age 207/206	2σ age 76	Δ 68-75 [%]	Δ 68-76 [%]	age	2σ age
S1432_001	583.2	7.1	0.3	0.0563	0.0012	0.1269	0.0028	0.0164	0.0002	104.9	1.4	121.3	2.5	461.6	48.4	-13.5	-77.3		
S1432_003	4902.9	24.7	0.5	0.0489	0.0007	0.0665	0.0011	0.0099	0.0001	63.4	0.8	65.4	1.0	144.2	35.0	-3.1	-56.0	63.4	0.8
S1432_004	812.9	211.7	0.3	0.1144	0.0012	4.4893	0.0554	0.2854	0.0034	1618.5	17.1	1729.0	10.2	1869.6	19.2	-6.4	-13.4	1869.6	19.2
S1432_005	634.2	186.1	0.3	0.1155	0.0013	4.8106	0.0601	0.3027	0.0037	1704.8	18.0	1786.7	10.5	1888.0	19.5	-4.6	-9.7	1888.0	19.5
S1432_006	2183.4	165.9	0.1	0.1061	0.0012	1.3288	0.0168	0.0910	0.0011	561.6	6.5	858.4	7.3	1733.8	20.3	-34.6	-67.6		
S1432_007	1105.5	170.2	0.1	0.1129	0.0012	3.3536	0.0412	0.2160	0.0026	1260.7	13.7	1493.6	9.6	1846.0	19.1	-15.6	-31.7		
S1432_008	292.6	59.2	0.3	0.1166	0.0013	5.0582	0.0650	0.3153	0.0039	1766.8	18.9	1829.1	10.9	1904.9	20.2	-3.4	-7.2	1904.9	20.2
S1432_009	1439.3	13.1	0.6	0.0497	0.0009	0.0938	0.0017	0.0137	0.0002	87.8	1.1	91.1	1.6	183.1	41.9	-3.6	-52.0	87.8	1.1
S1432_010	653.9	148.4	0.6	0.1320	0.0014	6.2148	0.0769	0.3423	0.0041	1897.5	19.7	2006.5	10.8	2124.8	18.6	-5.4	-10.7	2124.8	18.6
S1432_011	2154.0	297.2	0.1	0.1151	0.0012	4.1760	0.0509	0.2637	0.0031	1508.6	16.0	1669.3	10.0	1881.9	18.8	-9.6	-19.8	1881.9	18.8
S1432_012	730.4	144.3	0.2	0.1190	0.0013	4.3073	0.0533	0.2631	0.0032	1505.7	16.1	1694.8	10.2	1941.4	19.1	-11.2	-22.4	1941.4	19.1
S1432_013	3336.0	226.4	0.1	0.1043	0.0011	1.7238	0.0211	0.1202	0.0014	731.5	8.2	1017.4	7.9	1701.6	19.4	-28.1	-57.0		
S1432_014	271.0	55.3	0.3	0.1135	0.0013	4.9458	0.0640	0.3168	0.0039	1773.9	19.0	1810.1	10.9	1856.2	20.5	-2.0	-4.4	1856.2	20.5
S1432_016	371.1	73.7	0.4	0.1134	0.0013	4.9292	0.0628	0.3161	0.0039	1770.8	18.9	1807.3	10.8	1853.7	20.1	-2.0	-4.5	1853.7	20.1
S1432_015	820.8	149.4	0.3	0.1155	0.0012	4.8891	0.0605	0.3077	0.0037	1729.2	18.2	1800.4	10.4	1887.9	19.2	-4.0	-8.4	1887.9	19.2
S1432_017	1466.8	143.3	0.2	0.1127	0.0013	2.4263	0.0308	0.1565	0.0019	937.1	10.6	1250.4	9.1	1843.7	20.1	-25.1	-49.2		
S1432_018	877.7	167.4	0.6	0.1146	0.0012	4.1264	0.0511	0.2618	0.0031	1498.8	16.1	1659.6	10.1	1873.6	19.2	-9.7	-20.0	1873.6	19.2
S1432_019	1786.8	95.9	0.3	0.1076	0.0012	1.2459	0.0158	0.0842	0.0010	521.1	6.0	821.6	7.1	1758.9	20.2	-36.6	-70.4		
S1432_020	616.5	164.5	0.6	0.1123	0.0013	4.2603	0.0544	0.2758	0.0034	1570.3	17.0	1685.7	10.5	1836.6	20.2	-6.8	-14.5	1836.6	20.2
S1432_021	1435.3	122.1	0.2	0.1002	0.0011	2.0761	0.0259	0.1507	0.0018	904.6	10.1	1141.0	8.6	1627.4	20.1	-20.7	-44.4		
S1432_022	765.8	163.7	0.2	0.1117	0.0012	4.8164	0.0604	0.3135	0.0038	1757.6	18.6	1787.8	10.5	1827.2	19.6	-1.7	-3.8	1827.2	19.6
S1432_023	699.0	103.4	0.2	0.1162	0.0013	4.4735	0.0560	0.2799	0.0034	1590.9	17.0	1726.1	10.4	1898.2	19.5	-7.8	-16.2	1898.2	19.5
S1432_024	993.5	132.8	0.1	0.1151	0.0012	4.3581	0.0541	0.2754	0.0033	1567.9	16.7	1704.4	10.3	1880.7	19.2	-8.0	-16.6	1880.7	19.2
S1432_025	2531.0	101.8	0.1	0.1470	0.0016	1.6687	0.0207	0.0826	0.0010	511.3	5.9	996.7	7.9	2310.7	18.5	-48.7	-77.9		
S1432_026	267.0	74.0	0.6	0.1609	0.0018	9.8453	0.1251	0.4447	0.0055	2371.8	24.4	2420.4	11.7	2465.4	18.6	-2.0	-3.8	2465.4	18.6
S1432_027	594.9	97.6	0.4	0.1158	0.0013	4.6324	0.0589	0.2908	0.0035	1645.4	17.7	1755.1	10.6	1892.5	19.9	-6.3	-13.1	1892.5	19.9
S1432_028	950.3	126.6	0.3	0.1382	0.0015	4.2431	0.0529	0.2232	0.0027	1298.8	14.2	1682.4	10.3	2204.6	18.7	-22.8	-41.1		
S1432_029	1203.6	103.9	0.2	0.1134	0.0013	2.5445	0.0324	0.1631	0.0020	974.1	11.0	1284.9	9.3	1854.5	20.1	-24.2	-47.5		
S1432_030	763.8	126.8	0.3	0.1148	0.0013	4.8670	0.0611	0.3083	0.0037	1732.2	18.4	1796.6	10.6	1876.2	19.5	-3.6	-7.7	1876.2	19.5
S1432_031	862.0	95.8	0.1	0.1124	0.0012	3.3095	0.0415	0.2140	0.0026	1250.0	13.7	1483.3	9.8	1838.9	19.7	-15.7	-32.0		
S1432_032	2104.9	115.6	0.1	0.1110	0.0012	1.6768	0.0209	0.1098	0.0013	671.7	7.7	999.8	7.9	1815.7	19.5	-32.8	-63.0		
S1432_033	730.4	139.9	0.3	0.1153	0.0012	4.7340	0.0589	0.2985	0.0036	1684.1	17.9	1773.3	10.4	1884.0	19.3	-5.0	-10.6	1884.0	19.3
S1432_034	559.6	66.3	0.2	0.1150	0.0013	3.6741	0.0470	0.2323	0.0028	1346.5	14.8	1565.7	10.2	1879.5	20.1	-14.0	-28.4		
S1432_035	479.1	94.8	0.5	0.1147	0.0013	5.0856	0.0643	0.3224	0.0039	1801.3	19.1	1833.7	10.7	1874.8	19.7	-1.8	-3.9	1874.8	19.7
S1432_036	2201.1	198.6	0.1	0.1155	0.0012	2.7654	0.0341	0.1740	0.0021	1034.1	11.5	1346.2	9.2	1888.1	19.0	-23.2	-45.2		
S1432_037	467.3	2.5	0.4	0.0498	0.0019	0.0763	0.0028	0.0111	0.0002	71.4	1.2	74.7	2.7	186.4	86.6	-4.4	-61.7	71.4	1.2
S1432_038	689.2	105.9	0.4	0.1147	0.0013	4.9236	0.0620	0.3120	0.0038	1750.6	18.6	1806.3	10.6	1875.2	19.6	-3.1	-6.6	1875.2	19.6
S1432_039	1046.6	106.9	0.1	0.1140	0.0012	3.0579	0.0383	0.1950	0.0024	1148.6	12.7	1422.2	9.6	1863.5	19.5	-19.2	-38.4		
S1432_040	1510.0	197.4	0.1	0.1132	0.0012	4.3334	0.0535	0.2783	0.0033	1582.8	16.9	1699.7	10.2	1851.1	19.1	-6.9	-14.5	1851.1	19.1
S1432_041	504.6	72.4	0.4	0.1146	0.0013	4.7235	0.0608	0.2997	0.0037	1689.9	18.2	1771.4	10.8	1872.9	20.2	-4.6	-9.8	1872.9	20.2
S1432_042	247.4	44.8	0.5	0.1138	0.0015	5.0123	0.0664	0.3203	0.0040	1791.1	19.5	1821.4	11.2	1860.2	21.1	-1.7	-3.7	1860.2	21.1
S1432_043	649.9	131.1	0.4	0.1138	0.0013	4.7491	0.0602	0.3033	0.0037	1707.7	18.3	1775.9	10.6	1861.1	19.8	-3.8	-8.2	1861.1	19.8
S1432_044	1360.7	39.1	0.0	0.1063	0.0013	0.9069	0.0121	0.0620	0.0008	387.9	4.7	655.4	6.5	1736.7	22.0	-40.8	-77.7		
S1432_045	579.2	72.9	0.4	0.1133	0.0013	4.7885	0.0614	0.3072	0.0038	1726.7	18.5	1782.9	10.8	1853.2	20.1	-3.2	-6.8	1853.2	20.1
S1432_046	881.6	167.7	0.4	0.1352	0.0015	6.4970	0.0808	0.3492	0.0042	1930.9	20.2	2045.5	11.0	2166.9	18.6	-5.6	-10.9	2166.9	18.6
S1432_047	824.7	139.3	0.2	0.1176	0.0013	4.8168	0.0623	0.2976	0.0037	1679.5	18.2	1787.8	10.9	1920.7	20.2	-6.1	-12.6	1920.7	20.2
S1432_048	1007.3	187.7	0.5	0.1143	0.0012	5.0866	0.0633	0.3234	0.0039	1806.5	19.0	1833.9	10.6	1869.0	19.2	-1.5	-3.3	1869.0	19.2
S1432_049	2016.5	102.9	0.1	0.1119	0.0013	2.7092	0.0349	0.1760	0.0022	1044.8	11.8	1331.0	9.6	1830.8	20.5	-21.5	-42.9		
S1432_050	1121.2	130.7	0.1	0.1161	0.0013	4.0504	0.0507	0.2537	0.0031	1457.4	15.8	1644.4	10.2	1896.4	19.3	-11.4	-23.1	1896.4	19.3
S1432_051	208.1	26.4	0.4	0.1164	0.0015	5.0314	0.0700	0.3141	0.0040	1761.0	19.7	1824.6	11.8	1902.0	22.4	-3.5	-7.4	1902.0	22.4
S1432_052	1089.8	88.3	5.8	0.1242	0.0014	2.6266	0.0344	0.1537	0.0019	921.7	10.6	1308.1	9.6	2017.6	20.5	-29.5	-54.3		
S1432_053	1421.6	87.1	0.3	0.1265	0.0014	2.2705	0.0287	0.1305	0.0016	790.5	9.0	1203.2	8.9	2049.9	19.4	-34.3	-61.4		
S1432_054	691.2	117.9	0.4	0.1151	0.0013	4.5810	0.0583	0.2892	0.0035	1637.6	17.6	1745.8	10.6	1881.9	19.8	-6.2	-13.0	1881.9	19.8
S1432_055	4443.5	568.5	0.1	0.1176	0.0012	4.7812	0.0588	0.2956	0.0035	1669.4	17.6	1781.6	10.3	1919.5	18.7	-6.3	-13.0	1919.5	18.7
S1432_056	1409.8	182.4	0.3	0.1097	0.0012	3.6974	0.0471	0.2449	0.0030	1412.1	15.5	1570.8	10.2	1795.0	20.1	-10.1	-21.3	1795.0	20.1
S1432_057	555.7	78.7	0.4	0.1205	0.0014	4.9309	0.0632	0.2974	0.0036	1678.6	18.1	1807.6	10.8	1963.5	19.8	-7.1	-14.5	1963.5	19.8
S1432_058	2464.2	323.5	0.2	0.1358	0.0014	5.8018	0.0717	0.3104	0.0037	1742.9	18.4	1946.7	10.7	2174.8	18.3	-10.5	-19.9	2174.8	18.3
S1432_059	449.6	69.1	0.8	0.1173	0.0013	4.4800	0.0582	0.2775	0.0034	1578.8	17.3	1727.3	10.8	1916.1	20.3	-8.6	-17.6	1916.1	20.3
S1432_060	2591.9	66.2	0.1	0.1051	0.0012	1.1332	0.0146	0.0784	0.0010	486.5	5.7	769.3	6.9	1715.4	20.7	-36.8	-71.6		
S1432_061	253.3	25.9	0.2	0.1138	0.0016	4.7661	0.0708	0.3044	0.0040	1713.0	19.9	1778.9	12.5	1861.1	24.5	-3.7	-8.0	1861.1	24.5
S1432_062	432.0	74.0	0.5	0.1133	0.0015	5.0728	0.0665	0.3255	0.0040	1816.3	19.6	1831.6	11.1	1852.9	20.7	-0.8	-2.0	1852.9	20.7
S1432_063	655.8	102.6	0.3	0.1169	0.0013	4.6704	0.0603	0.2904	0.0036	1643.4	17.8	1761.9	10.8	1909.4	20.1	-6.7	-13.9	1909.4	20.1
S1432_064	1040.7	125.6	0.2	0.1114	0.0012	4.1749	0.0527	0.2725	0.0033	1553.4	16.8	1669.1	10.3	1821.7	19.7	-6.9	-14.7	1821.7	19.7
S1432_065	873.8	110.5	0.4	0.1421	0.0016	5.9909	0.0761	0.3065	0.0038	1723.4	18.5	1974.5	11.1	2252.6	18.9	-12.7	-23.5	2252.6	18.9
S1432_066	363.3	61.7	0.3	0.1246	0.0015	5.0618	0.0676	0.2953	0.0037	1667.7	18.4	1829.7	11.3	2023.2	20.8	-8.9	-17.6	2023.2	20.8
S1432_067	1064.2	94.8	0.2	0.1175	0.0014	2.8562	0.0371	0.1768	0.0022	1049.2	11.9	1370.4	9.8	1917.8	20.4	-23.4	-45.3		
S1432_068	339.7	41.9	0.5	0.1124	0.0013	4.2312	0.0568	0.2735	0.0034	1558.7	17.3	1680.1	11.0	1839.1	21.4	-7.2	-15.2	1839.1	21.4
S1432_069	2483.9	65.2	0.1	0.1095	0.0012	0.9608	0.0124	0.0638	0.0008	398.7	4.7	683.7	6.4	1790.2	20.5	-41.7	-77.7		
S1432_070	235.6	1.6	0.8	0.0471	0.0030	0.0823	0.0050	0.0127	0.0003	81.3	1.8	80.3	4.7	55.2	144.9	1.2	47.3	81.3	1.8
S1432_071	960.2	135.2	0.3	0.1166	0.0013	5.0171	0.0636	0.3127	0.0038	1753.9	18.7	1822.2	10.7	1905.1	19.6	-3.7	-7.9	1905.1	19.6
S1432_072	2175.6	67.7	0.2	0.1204	0.0014	1.0118	0.0135	0.0611	0.0008	382.2	4.6	709.8	6.8	1962.3	21.2	-46.2	-80.5		
S1432_073	640.1	107.5	0.4	0.1190	0.0013	5.0570	0.0648	0.3089	0.0038	1735.3	18.7	1828.9	10.9	1941.0	19.8	-5.1	-10.6	1941.0	19.8
S1432_074	895.4	103.8	0.2	0.1145	0.0013	5.2493	0.0679	0.3334	0.0041	1854.6	19.9	1860.7	11.0	1871.2	20.2	-0.3	-0.9	1871.2	20.2
S1432_075	402.5	87.0	0.3	0.1455	0.0017	8.2045	0.1105	0.4099	0.0052	2214.5	23.8	2253.8	12.2	2293.4	20.3	-1.7	-3.4	2293.4	20.3
S1432_076	161.0	0.7	0.4	0.0547	0.0051	0.0841	0.0076	0.0112	0.0004	71.7	2.2	82.0	7.1	398.5	197.7	-12.6	-82.0	71.7	2.2
S1432_077	349.5	41.1	0.5	0.1166	0.0014	5.0693	0.0694	0.3161	0.0040	1770.4	19.6	1831.0	11.6	1904.4	21.8	-3.3	-7.0	1904.4	21.8
S1432_078	730.4	82.7	0.3	0.1155	0.0013	4.7424	0.0610	0.2984	0.0037	1683.2	18.2	1774.8	10.8	1888.0	20.0	-5.2	-10.8	1888.0	20.0
S1432_079	543.9	67.6	0.4	0.1137	0.0013	4.9942	0.0651	0.3194	0.0040	1786.7	19.3	1818.3	11.0	1858.6	20.4	-1.7	-3.9	1858.6	20.4
S1432_080	885.6	79.9	0.3	0.1121	0.0013	3.4021	0.0453	0.2206	0.0028	1285.1	14.5	1504.9	10.5	1833.4	21.2	-14.6	-29.9		
S1432_081	1910.5	124.5	0.2	0.1777	0.0020	5.1806	0.0656	0.2119	0.0026	1238.7	13.8	1849.4	10.8	2631.8	18.1	-33.0	-52.9		
S1432_082	577.3	79.3	0.5	0.1137	0.0014	5.1073	0.0673	0.3265	0.0041	1821.6	19.7	1837.3	11.2	1859.0	20.8	-0.9	-2.0	1859.0	20.8
S1432_083	314.2	34.8	0.5	0.1165	0.0015	4.9759	0.0692	0.3105	0.0040	1743.1	19.5	1815.2	11.8	1902.8	22.2	-4.0	-8.4	1902.8	22.2
S1432_084	683.3	56.3	0.3	0.1155	0.0013	4.4979	0.0591	0.2830	0.0035	1606.3	17.6	1730.6	10.9	1888.1	20.6	-7.2	-14.9	1888.1	20.6
S1432_085	1400.0	92.5	0.6	0.1173	0.0014	2.8404	0.0377	0.1760	0.0022	1045.3	12.0	1366.3	10.0	1915.0	21.0	-23.5	-45.4		
S1432_086	2395.5	117.5	0.5	0.1453	0.0016	3.1035	0.0393	0.1552	0.0019	930.1	10.6	1433.6	9.7	2291.7	18.8	-35.1	-59.4		
S1432_087	746.1	61.5	0.5	0.1349	0.0016	4.2845	0.0564	0.2308	0.0029	1338.7	15.0	1690.4	10.8	2162.9	20.1	-20.8	-38.1		
S1432_088	1280.2	97.7	0.1	0.1120	0.0013	2.9666	0.0383	0.1926	0.0024	1135.4	12.8	1399.1	9.8	1831.2	20.3	-18.8	-38.0		
S1432_089	677.4	92.3	0.4	0.1465	0.0017	6.3921	0.0828	0.3171	0.0039	1775.3	19.2	2031.2	11.4	2305.8	19.3	-12.6	-23.0	2305.8	19.3
S1432_090	4072.4	41.2	0.1	0.1339	0.0016	0.4376	0.0059	0.0238	0.0003	151.4	1.9	368.6	4.2	2149.1	21.2	-58.9	-93.0		
S1432_091	763.8	48.2	0.2	0.1140	0.0014	3.2896	0.0443	0.2097	0.0026	1227.3	14.0	1478.6	10.5	1864.3	21.5	-17.0	-34.2		
S1432_092	824.7	94.1	0.2	0.1158	0.0013	4.7386	0.0619	0.2974	0.0037	1678.3	18.3	1774.1	11.0	1892.5	20.4	-5.4	-11.3	1892.5	20.4
S1432_093	2120.6	60.3	0.2	0.1129	0.0013	1.5883	0.0209	0.1022	0.0013	627.4	7.4	965.6	8.2	1847.1	20.9	-35.0	-66.0		
S1432_094	598.9	49.6	0.3	0.1162	0.0014	5.0261	0.0679	0.3143	0.0040	1761.7	19.4	1823.7	11.5	1899.0	21.4	-3.4	-7.2	1899.0	21.4
S1432_095	1502.1	67.3	0.5	0.1216	0.0014	2.5364	0.0334	0.1517	0.0019	910.2	10.5	1282.5	9.6	1979.1	20.6	-29.0	-54.0		
S1432_096	677.4	48.3	0.5	0.1186	0.0015	5.2409	0.0729	0.3212	0.0041	1795.4	20.1	1859.3	11.9	1935.3	22.1	-3.4	-7.2	1935.3	22.1
S1432_097	541.9	79.0	0.4	0.1134	0.0014	4.6739	0.0628	0.2996	0.0038	1689.4	18.7	1762.6	11.2	1854.2	21.3	-4.2	-8.9	1854.2	21.3
S1432_099	198.3	27.4	0.8	0.1255	0.0018	5.7479	0.0873	0.3328	0.0045	1851.7	21.8	1938.6	13.1	2036.5	24.5	-4.5	-9.1	2036.5	24.5
S1432_100	453.6	2.4	0.6	0.0510	0.0022	0.0812	0.0033	0.0116	0.0002	74.2	1.4	79.3	3.1	239.7	95.8	-6.4	-69.0	74.2	1.4
S1432_101	1013.2	66.2	0.3	0.1117	0.0014	4.8547	0.0675	0.3158	0.0040	1768.9	19.8	1794.4	11.7	1827.9	22.4	-1.4	-3.2	1827.9	22.4
S1432_102	769.7	82.0	0.9	0.1115	0.0013	5.0700	0.0670	0.3306	0.0041	1841.2	19.9	1831.1	11.2	1823.4	20.8	0.6	1.0	1823.4	20.8
S1432_103	538.0	65.9	0.3	0.1150	0.0014	4.2694	0.0587	0.2698	0.0034	1539.8	17.4	1687.5	11.3	1880.0	21.9	-8.8	-18.1	1880.0	21.9
S1432_104	551.8	78.6	0.4	0.1117	0.0013	5.1320	0.0689	0.3340	0.0042	1857.8	20.3	1841.4	11.4	1826.7	21.3	0.9	1.7	1826.7	21.3
S1432_105	4066.5	56.4	0.3	0.1069	0.0014	0.4678	0.0065	0.0318	0.0004	201.8	2.5	389.6	4.5	1747.0	22.9	-48.2	-88.4		
S1432_106	820.8	170.2	0.9	0.1637	0.0018	10.3642	0.1327	0.4603	0.0057	2440.7	25.0	2467.9	11.9	2493.8	18.4	-1.1	-2.1	2493.8	18.4
S1432_107	1052.5	100.5	0.2	0.1136	0.0014	3.6878	0.0495	0.2360	0.0030	1365.8	15.4	1568.7	10.7	1857.4	21.3	-12.9	-26.5	1857.4	21.3
S1432_108	877.7	4.9	1.1	0.0655	0.0023	0.1042	0.0035	0.0116	0.0002	74.0	1.3	100.6	3.2	791.8	71.9	-26.4	-90.7		
S1432_109	3008.1	109.4	0.1	0.1446	0.0016	1.6873	0.0218	0.0848	0.0010	524.8	6.2	1003.8	8.2	2282.8	19.3	-47.7	-77.0		
S1432_110	392.7	40.0	0.6	0.1139	0.0015	4.5062	0.0648	0.2876	0.0037	1629.4	18.7	1732.1	12.0	1862.2	23.3	-5.9	-12.5	1862.2	23.3
S1432_111	538.0	54.1	0.4	0.1131	0.0014	3.9555	0.0544	0.2541	0.0032	1459.8	16.6	1625.1	11.1	1850.1	22.0	-10.2	-21.1	1850.1	22.0
S1432_112	1784.8	57.7	0.1	0.1117	0.0013	1.4452	0.0195	0.0941	0.0012	579.6	6.9	907.9	8.1	1826.5	21.7	-36.2	-68.3		
S1432_113	508.6	62.2	0.5	0.1143	0.0014	5.1094	0.0681	0.3249	0.0041	1813.6	19.8	1837.7	11.3	1868.7	20.9	-1.3	-2.9	1868.7	20.9
S1432_114	2102.9	158.8	0.3	0.1106	0.0013	2.4787	0.0324	0.1629	0.0020	972.9	11.1	1265.8	9.4	1809.0	20.6	-23.1	-46.2		
S1432_115	1409.8	70.7	0.1	0.1470	0.0018	2.4293	0.0333	0.1201	0.0015	731.3	8.8	1251.3	9.9	2311.1	21.1	-41.6	-68.4		
S1432_116	742.2	100.5	0.5	0.1130	0.0013	4.6771	0.0623	0.3008	0.0038	1695.1	18.6	1763.2	11.2	1848.5	21.0	-3.9	-8.3	1848.5	21.0
S1432_117	471.2	75.2	0.6	0.1485	0.0018	7.0028	0.0951	0.3428	0.0044	1900.2	21.0	2111.8	12.1	2328.3	20.4	-10.0	-18.4	2328.3	20.4
S1432_118	479.1	63.1	0.9	0.1129	0.0014	5.3394	0.0735	0.3439	0.0044	1905.3	21.0	1875.2	11.8	1845.7	21.9	1.6	3.2	1845.7	21.9
S1432_119	659.7	86.3	0.4	0.1135	0.0014	4.6497	0.0630	0.2979	0.0038	1680.7	18.6	1758.2	11.3	1855.4	21.5	-4.4	-9.4	1855.4	21.5
S1432_120	2697.9	50.8	0.3	0.1154	0.0014	1.0657	0.0147	0.0671	0.0009	418.7	5.1	736.6	7.2	1886.5	22.2	-43.2	-77.8		
S1432_121	881.6	54.5	0.7	0.1133	0.0014	3.6039	0.0496	0.2313	0.0029	1341.1	15.3	1550.4	10.9	1852.3	22.0	-13.5	-27.6		
S1432_122	598.9	50.3	0.7	0.1139	0.0014	5.2232	0.0713	0.3334	0.0042	1854.8	20.4	1856.4	11.6	1861.9	21.6	-0.1	-0.4	1861.9	21.6
S1432_123	1604.2	40.9	0.5	0.1117	0.0016	2.5785	0.0395	0.1677	0.0022	999.5	12.4	1294.5	11.2	1827.9	25.8	-22.8	-45.3		
S1432_124	724.5	50.1	0.5	0.1135	0.0014	4.2004	0.0573	0.2690	0.0034	1535.5	17.3	1674.1	11.2	1856.2	21.7	-8.3	-17.3	1856.2	21.7
S1432_125	1716.1	115.6	0.5	0.1680	0.0019	4.5507	0.0594	0.1969	0.0024	1158.7	13.2	1740.3	10.9	2537.4	18.9	-33.4	-54.3		
S1432_126	915.0	57.4	0.3	0.1101	0.0014	2.8178	0.0395	0.1860	0.0024	1099.8	12.9	1360.3	10.5	1800.8	22.8	-19.2	-38.9		
S1432_127	744.2	89.2	0.5	0.1139	0.0014	5.1753	0.0711	0.3303	0.0042	1839.8	20.3	1848.6	11.7	1862.1	21.8	-0.5	-1.2	1862.1	21.8
S1432_128	545.9	58.6	0.4	0.1115	0.0013	4.8368	0.0653	0.3153	0.0040	1766.6	19.4	1791.3	11.4	1823.9	21.4	-1.4	-3.1	1823.9	21.4
S1432_129	970.0	156.1	0.9	0.1578	0.0018	6.5281	0.0865	0.3006	0.0038	1694.2	18.7	2049.7	11.7	2432.6	19.5	-17.3	-30.4		
S1432_130	1871.2	97.7	0.3	0.1472	0.0017	2.8281	0.0372	0.1396	0.0017	842.4	9.8	1363.0	9.9	2314.0	19.6	-38.2	-63.6		
S1432_131	373.1	43.3	0.7	0.1140	0.0014	4.8167	0.0665	0.3070	0.0039	1725.9	19.3	1787.8	11.6	1864.6	22.0	-3.5	-7.4	1864.6	22.0
S1432_132	528.2	39.6	0.5	0.1200	0.0015	3.9596	0.0553	0.2398	0.0031	1385.7	16.0	1626.0	11.3	1956.2	22.1	-14.8	-29.2		
S1432_133	428.0	40.2	0.7	0.1138	0.0014	5.0741	0.0706	0.3241	0.0041	1809.7	20.2	1831.8	11.8	1860.7	22.2	-1.2	-2.7	1860.7	22.2
S1432_134	125.7	14.5	1.6	0.1177	0.0018	5.3423	0.0869	0.3298	0.0046	1837.6	22.4	1875.7	13.9	1921.7	26.9	-2.0	-4.4	1921.7	26.9
S1432_135	928.7	85.9	0.5	0.1143	0.0013	4.8299	0.0646	0.3072	0.0038	1727.1	19.0	1790.1	11.3	1868.0	21.0	-3.5	-7.5	1868.0	21.0
S1432_136	1727.9	92.5	0.4	0.1100	0.0013	3.0381	0.0413	0.2007	0.0025	1178.8	13.5	1417.2	10.4	1800.0	21.7	-16.8	-34.5		
S1432_137	924.8	80.9	0.2	0.1128	0.0013	5.0915	0.0678	0.3280	0.0041	1828.6	19.9	1834.7	11.3	1845.3	20.9	-0.3	-0.9	1845.3	20.9
S1432_138	1317.5	29.1	0.5	0.1124	0.0017	2.4026	0.0382	0.1553	0.0021	930.5	11.8	1243.4	11.4	1839.2	27.0	-25.2	-49.4		
S1432_139	1034.8	59.0	0.5	0.1124	0.0014	3.5721	0.0486	0.2309	0.0029	1339.3	15.2	1543.4	10.8	1839.0	21.6	-13.2	-27.2		
S1432_140	1394.1	160.2	0.4	0.1124	0.0013	4.6774	0.0613	0.3024	0.0037	1703.1	18.5	1763.2	11.0	1838.9	20.4	-3.4	-7.4	1838.9	20.4
S1432_141	428.0	31.0	0.4	0.1128	0.0015	4.4872	0.0645	0.2892	0.0038	1637.6	18.8	1728.6	11.9	1844.4	23.2	-5.3	-11.2	1844.4	23.2
S1432_142	1625.8	183.3	0.4	0.1096	0.0013	3.8840	0.0514	0.2577	0.0032	1477.8	16.4	1610.4	10.7	1792.0	20.9	-8.2	-17.5	1792.0	20.9
S1432_143	716.7	30.8	0.1	0.1144	0.0015	2.2506	0.0317	0.1429	0.0018	861.2	10.3	1197.0	9.9	1870.9	22.8	-28.1	-54.0		
S1432_145	2831.4	2.6	0.4	0.1108	0.0013	1.2551	0.0168	0.0823	0.0010	509.9	6.1	825.7	7.6	1813.0	21.3	-38.2	-71.9		
S1432_146	730.4	95.2	0.4	0.1143	0.0014	4.8073	0.0654	0.3058	0.0039	1719.9	19.0	1786.2	11.4	1868.2	21.4	-3.7	-7.9	1868.2	21.4
S1432_147	756.0	92.5	0.2	0.1130	0.0013	5.1789	0.0695	0.3330	0.0042	1852.8	20.2	1849.2	11.4	1848.8	21.0	0.2	0.2	1848.8	21.0
S1432_148	2745.0	94.3	0.5	0.0523	0.0007	0.3447	0.0050	0.0479	0.0006	301.6	3.7	300.7	3.8	298.4	29.7	0.3	1.1	301.6	3.7
S1432_149	2024.4	46.6	0.2	0.1267	0.0015	2.3309	0.0309	0.1337	0.0017	808.7	9.5	1221.7	9.4	2053.2	20.3	-33.8	-60.6		
S1432_150	1333.2	102.6	0.6	0.1136	0.0013	3.1918	0.0426	0.2041	0.0025	1197.4	13.6	1455.2	10.3	1858.4	20.9	-17.7	-35.6		
S1432_151	284.7	99.2	0.7	0.1253	0.0033	3.7310	0.0947	0.2165	0.0042	1263.3	22.1	1578.1	20.3	2032.3	45.6	-19.9	-37.8		
S1432_152	1093.7	18.9	0.5	0.1150	0.0014	4.6350	0.0622	0.2930	0.0037	1656.3	18.3	1755.6	11.2	1879.6	21.0	-5.7	-11.9	1879.6	21.0
S1432_154	632.3	80.9	1.1	0.1134	0.0014	5.2221	0.0710	0.3347	0.0042	1861.3	20.4	1856.2	11.6	1854.2	21.4	0.3	0.4	1854.2	21.4
S1432_155	612.6	54.7	0.8	0.1149	0.0014	5.3100	0.0742	0.3360	0.0043	1867.3	20.7	1870.5	11.9	1877.7	22.1	-0.2	-0.6	1877.7	22.1
S1432_156	987.7	92.6	0.6	0.1118	0.0013	4.2709	0.0580	0.2777	0.0035	1579.6	17.6	1687.8	11.2	1828.6	21.4	-6.4	-13.6	1828.6	21.4
S1432_157	1912.5	74.0	0.3	0.1125	0.0014	1.7737	0.0243	0.1146	0.0014	699.3	8.3	1035.9	8.9	1840.2	21.8	-32.5	-62.0		
S1432_158	4070.4	117.8	0.3	0.0989	0.0012	1.1594	0.0157	0.0852	0.0011	527.2	6.3	781.7	7.4	1603.0	22.1	-32.6	-67.1		
S1432_159	1081.9	111.1	0.8	0.1132	0.0013	4.4717	0.0603	0.2870	0.0036	1626.4	18.0	1725.7	11.2	1852.1	21.2	-5.8	-12.2	1852.1	21.2
S1432_160	1991.0	164.5	0.1	0.1184	0.0014	3.7113	0.0493	0.2278	0.0028	1323.1	14.9	1573.8	10.6	1932.0	20.5	-15.9	-31.5		
S1432_161	1722.0	160.6	0.7	0.1168	0.0014	4.6242	0.0616	0.2877	0.0036	1630.1	17.9	1753.6	11.1	1907.8	20.6	-7.0	-14.6	1907.8	20.6
S1432_162	661.7	75.3	0.8	0.1133	0.0014	4.8031	0.0656	0.3082	0.0039	1731.6	19.2	1785.4	11.5	1852.6	21.5	-3.0	-6.5	1852.6	21.5
S1432_164	559.6	52.4	0.9	0.1101	0.0014	5.2972	0.0741	0.3497	0.0045	1933.2	21.4	1868.4	12.0	1800.8	22.3	3.5	7.4	1800.8	22.3
S1432_165	439.8	30.0	0.7	0.1153	0.0015	5.2912	0.0770	0.3335	0.0044	1855.2	21.1	1867.4	12.4	1884.7	23.3	-0.7	-1.6	1884.7	23.3
S1432_166	714.7	86.5	0.5	0.1092	0.0014	4.6083	0.0664	0.3066	0.0040	1724.1	19.6	1750.8	12.0	1786.5	23.4	-1.5	-3.5	1786.5	23.4
S1432_167	7895.3	7.2	0.2	0.0734	0.0017	0.0271	0.0006	0.0027	0.0000	17.3	0.3	27.2	0.6	1024.5	47.4	-36.4	-98.3		
S1432_168	2371.9	104.1	0.6	0.1093	0.0013	2.5204	0.0341	0.1676	0.0021	998.8	11.6	1277.9	9.8	1787.7	21.5	-21.8	-44.1		
S1432_169	290.6	22.6	0.6	0.1376	0.0020	6.5763	0.1032	0.3473	0.0048	1921.5	23.1	2056.2	13.8	2197.6	24.8	-6.6	-12.6	2197.6	24.8
S1432_170	543.9	59.8	0.7	0.1125	0.0014	4.5981	0.0638	0.2972	0.0038	1677.3	18.8	1748.9	11.6	1839.3	22.0	-4.1	-8.8	1839.3	22.0
S1432_171	1453.0	208.4	0.4	0.1147	0.0014	4.7760	0.0646	0.3027	0.0038	1704.5	18.8	1780.7	11.4	1874.8	21.1	-4.3	-9.1	1874.8	21.1
S1432_172	373.1	40.6	0.6	0.1123	0.0015	5.2293	0.0782	0.3385	0.0045	1879.2	21.6	1857.4	12.7	1836.7	24.3	1.2	2.3	1836.7	24.3
S1432_173	488.9	36.8	0.7	0.1103	0.0016	5.0730	0.0799	0.3342	0.0046	1858.9	22.1	1831.6	13.4	1804.4	26.1	1.5	3.0	1804.4	26.1
S1432_174	6854.7	21.5	0.9	0.0476	0.0009	0.0483	0.0009	0.0074	0.0001	47.4	0.6	47.9	0.9	76.1	45.1	-1.0	-37.7	47.4	0.6
S1432_176	2108.8	117.9	0.0	0.1137	0.0014	2.9303	0.0397	0.1873	0.0024	1106.8	12.7	1389.8	10.3	1859.2	21.2	-20.4	-40.5		
S1432_177	1606.2	146.1	0.1	0.1150	0.0014	4.6532	0.0627	0.2941	0.0037	1662.0	18.3	1758.9	11.3	1879.6	21.0	-5.5	-11.6	1879.6	21.0
S1432_178	467.3	56.3	1.7	0.1143	0.0014	5.5833	0.0790	0.3550	0.0046	1958.3	21.7	1913.5	12.2	1869.0	22.4	2.3	4.8	1869.0	22.4
S1432_179	494.8	62.9	0.6	0.1097	0.0015	5.2561	0.0787	0.3483	0.0046	1926.5	22.1	1861.8	12.8	1793.9	24.4	3.5	7.4	1793.9	24.4
S1432_180	382.9	41.6	0.5	0.1166	0.0016	5.0150	0.0765	0.3126	0.0042	1753.3	20.6	1821.9	12.9	1904.8	24.8	-3.8	-8.0	1904.8	24.8
S1432_181	922.9	62.6	0.6	0.1153	0.0014	4.9623	0.0694	0.3129	0.0040	1755.1	19.6	1812.9	11.8	1883.7	22.0	-3.2	-6.8	1883.7	22.0
S1432_182	620.5	52.3	0.5	0.1157	0.0014	5.0982	0.0717	0.3204	0.0041	1791.5	20.0	1835.8	12.0	1890.1	22.2	-2.4	-5.2	1890.1	22.2
S1432_183	2118.6	62.2	0.3	0.1054	0.0014	1.4450	0.0208	0.0997	0.0013	612.5	7.5	907.8	8.6	1720.7	23.6	-32.5	-64.4		
S1432_184	854.1	59.2	0.4	0.1142	0.0015	4.2062	0.0622	0.2676	0.0035	1528.8	17.9	1675.2	12.1	1867.6	23.9	-8.7	-18.1	1867.6	23.9
S1432_185	351.5	38.6	0.7	0.1299	0.0017	5.8118	0.0834	0.3251	0.0042	1814.6	20.6	1948.2	12.4	2096.9	22.3	-6.9	-13.5	2096.9	22.3
S1432_186	337.7	34.1	0.8	0.1153	0.0017	5.4565	0.0870	0.3439	0.0048	1905.3	22.8	1893.8	13.7	1884.8	26.2	0.6	1.1	1884.8	26.2
S1432_187	814.9	83.7	1.7	0.1141	0.0014	4.1859	0.0584	0.2666	0.0034	1523.3	17.3	1671.3	11.4	1866.1	22.0	-8.9	-18.4	1866.1	22.0
S1432_188	1244.9	78.3	0.7	0.1132	0.0014	2.9965	0.0416	0.1924	0.0024	1134.3	13.2	1406.7	10.6	1851.2	21.9	-19.4	-38.7		
S1432_189	1195.8	78.0	0.5	0.1576	0.0020	4.8548	0.0692	0.2239	0.0029	1302.2	15.3	1794.4	12.0	2430.2	21.5	-27.4	-46.4		
S1432_190	1237.0	131.8	0.8	0.1109	0.0013	5.0165	0.0688	0.3288	0.0041	1832.5	20.1	1822.1	11.6	1814.0	21.6	0.6	1.0	1814.0	21.6

Sample S1447 Indus River @ Kushalgar 210 grains analysed 174 concordant ages

	concentrations			isotopic ratios						ages						discordance		preferred age	
grain	U [ppm]	Pb [ppm]	Th/U	Pb207/Pb206	2σ 76	Pb207/U235	2σ 75	Pb206/U238	2σ 68	age 206/238	2σ age 68	age 207/235	2σ age 75	age 207/206	2σ age 76	Δ 68-75 [%]	Δ 68-76 [%]	age	2σ age
S1447_001	2937.13351	111.8	0.7	0.05246	0.00086	1.01574	0.0175	0.14092	0.00179	849.9	10.13	711.8	8.81	305.3	36.69	19.402	178.4		
S1447_002	1101.68939	157.4	0.6	0.1127	0.00123	5.45075	0.06887	0.35199	0.00431	1944.1	20.57	1892.9	10.84	1843.3	19.65	2.705	5.5	1843.3	19.65
S1447_003	532.870874	3.5	0.9	0.05145	0.00162	0.11839	0.00362	0.01675	0.00027	107.1	1.68	113.6	3.29	261	70.81	-5.722	-59.0	107.1	1.68
S1447_004	13636.8423	41.0	1.0	0.04758	0.00072	0.03879	0.00062	0.00593	7.00E-05	38.1	0.48	38.6	0.6	77.7	36.11	-1.295	-51.0	38.1	0.48
S1447_005	1046.71065	8.5	0.5	0.05341	0.00158	0.13331	0.00381	0.01816	0.00029	116	1.82	127.1	3.41	346.4	65.51	-8.733	-66.5	116	1.82
S1447_006	439.829629	316.4	0.5	0.26613	0.00277	21.39784	0.2616	0.58513	0.00708	2969.6	28.8	3156.8	11.86	3283.4	16.23	-5.930	-9.6	3283.4	16.23
S1447_008	2116.68153	24.0	0.6	0.05084	0.00074	0.22768	0.00352	0.03259	0.00041	206.7	2.56	208.3	2.91	233.5	33.12	-0.768	-11.5	206.7	2.56
S1447_009	1471.7386	59.8	0.5	0.06413	0.00075	1.18735	0.01574	0.13473	0.00165	814.8	9.4	794.7	7.31	746.1	24.67	2.529	9.2	814.8	9.4
S1447_010	446.173629	0.9	1.1	0.04302	0.00378	0.04805	0.00407	0.00813	0.00022	52.2	1.41	47.7	3.95	0.1	38.78	9.434	52100.0	52.2	1.41
S1447_011	4804.29613	33.8	1.1	0.05368	0.00085	0.11824	0.00195	0.01603	0.00021	102.5	1.31	113.5	1.78	357.7	35.5	-9.692	-71.3	102.5	1.31
S1447_012	186.081892	0.8	0.8	0.04494	0.00928	0.06944	0.00928	0.01124	0.00049	72.1	3.15	68.2	8.81	0.1	250.87	5.718	72000.0	72.1	3.15
S1447_013	340.445281	11.0	0.3	0.05986	0.00108	0.81766	0.01515	0.09939	0.00135	610.9	7.9	606.7	8.46	598.7	38.76	0.692	2.0	610.9	7.9
S1447_014	615.338985	3.2	0.6	0.05022	0.00182	0.12289	0.00428	0.01781	0.00031	113.8	1.94	117.7	3.87	205.1	82.05	-3.314	-44.5	113.8	1.94
S1447_015	3892.91777	21.8	0.8	0.04728	0.00072	0.11868	0.0019	0.01827	0.00023	116.7	1.46	113.9	1.73	63	35.05	2.458	85.2	116.7	1.46
S1447_016	1069.97088	7.1	0.5	0.06108	0.00174	0.14602	0.004	0.0174	0.00028	111.2	1.75	138.4	3.55	642.2	60.07	-19.653	-82.7		
S1447_017	169.165357	0.5	0.5	0.04706	0.00643	0.06613	0.00869	0.01022	0.00041	65.6	2.64	65	8.28	52.1	297.6	0.923	25.9	65.6	2.64
S1447_018	615.338985	20.8	0.6	0.06383	0.00092	1.0244	0.01571	0.11679	0.00149	712.1	8.62	716.1	7.88	735.9	30.11	-0.559	-3.2	712.1	8.62
S1447_019	617.453552	124.6	0.5	0.18043	0.00192	11.30176	0.14041	0.4558	0.00557	2421	24.65	2548.3	11.59	2656.9	17.54	-4.995	-8.9	2656.9	17.54
S1447_020	1082.65828	192.8	0.4	0.14657	0.00161	9.7959	0.12481	0.48636	0.00602	2554.9	26.12	2415.8	11.74	2306.2	18.78	5.758	10.8	2306.2	18.78
S1447_021	653.401191	21.8	0.4	0.05888	0.00096	0.7746	0.01316	0.09573	0.00126	589.4	7.4	582.4	7.53	562.6	35.2	1.202	4.8	589.4	7.4
S1447_022	2019.41145	23.2	0.8	0.05019	0.00074	0.26074	0.00409	0.03781	0.00048	239.2	2.96	235.3	3.3	203.7	33.93	1.657	17.4	239.2	2.96
S1447_023	205.112995	0.9	0.6	0.0562	0.00507	0.10099	0.00858	0.01308	0.00044	83.7	2.82	97.7	7.92	459.4	189.23	-14.330	-81.8		
S1447_024	482.121267	2.5	0.8	0.05024	0.00198	0.11706	0.00442	0.01696	0.00031	108.4	1.94	112.4	4.02	205.9	89.06	-3.559	-47.4	108.4	1.94
S1447_025	243.1752	0.9	0.8	0.05024	0.0041	0.06104	0.00477	0.00884	0.00024	56.7	1.56	60.2	4.57	206.2	179.07	-5.814	-72.5	56.7	1.56
S1447_026	5413.29142	108.5	0.2	0.05949	0.00068	0.77709	0.01008	0.09505	0.00116	585.4	6.81	583.8	5.76	585	24.56	0.274	0.1	585.4	6.81
S1447_027	272.779138	0.3	0.6	0.05337	0.00827	0.05895	0.00871	0.00804	4.00E-04	51.6	2.53	58.2	8.35	344.3	317.17	-11.340	-85.0	51.6	2.53
S1447_028	587.849615	46.8	0.3	0.11442	0.00146	3.83665	0.05379	0.244	0.00314	1407.4	16.27	1600.5	11.29	1870.7	22.82	-12.065	-24.8	1870.7	22.82
S1447_029	613.224418	40.8	0.3	0.07062	0.001	1.88654	0.02879	0.19438	0.00251	1145.1	13.57	1076.4	10.13	946.5	28.81	6.382	21.0	946.5	28.81
S1447_030	4413.10125	49.8	0.1	0.05267	0.00077	0.25605	0.00398	0.03538	0.00045	224.1	2.78	231.5	3.21	314.5	32.86	-3.197	-28.7	224.1	2.78
S1447_031	1099.57482	42.3	1.5	0.06392	0.00098	0.95851	0.01551	0.10911	0.00142	667.6	8.26	682.5	8.04	739.1	32.24	-2.183	-9.7	667.6	8.26
S1447_032	1387.15593	41.9	0.4	0.05889	0.00096	0.76313	0.01299	0.0943	0.00124	580.9	7.3	575.8	7.48	562.9	35.29	0.886	3.2	580.9	7.3
S1447_033	2082.84846	143.6	0.1	0.11621	0.00126	5.30445	0.06656	0.33212	0.00405	1848.7	19.6	1869.6	10.72	1898.8	19.34	-1.118	-2.6	1898.8	19.34
S1447_034	238.946066	1.8	0.7	0.06489	0.00468	0.13133	0.00885	0.01473	0.00044	94.3	2.78	125.3	7.94	770.6	144.79	-24.741	-87.8		
S1447_035	4514.60046	16.0	0.5	0.04535	0.00094	0.06887	0.00144	0.01105	0.00015	70.8	0.95	67.6	1.36	0.1	12.64	4.734	70700.0	70.8	0.95
S1447_036	1932.7142	49.4	0.1	0.05965	0.00074	0.80864	0.01114	0.09864	0.00122	606.4	7.15	601.7	6.26	590.9	26.74	0.781	2.6	606.4	7.15
S1447_037	558.245677	2.8	0.4	0.06106	0.00243	0.14514	0.00548	0.0173	0.00033	110.5	2.08	137.6	4.86	641.4	83.38	-19.695	-82.8		
S1447_038	854.285052	22.0	0.3	0.06702	0.00106	0.82379	0.01355	0.08944	0.00117	552.2	6.94	610.2	7.54	838.3	32.51	-9.505	-34.1	552.2	6.94
S1447_039	1378.69766	26.3	0.3	0.0649	0.00094	1.31558	0.02037	0.14748	0.0019	886.8	10.67	852.6	8.93	771.2	30.24	4.011	15.0	886.8	10.67
S1447_040	1296.22955	47.5	0.2	0.05738	0.00095	0.68928	0.01186	0.08741	0.00115	540.2	6.82	532.4	7.13	505.6	35.83	1.465	6.8	540.2	6.82
S1447_041	598.42245	3.0	1.1	0.05061	0.00514	0.05843	0.00558	0.0084	0.00032	53.9	2.04	57.7	5.35	223.3	219.05	-6.586	-75.9	53.9	2.04
S1447_042	642.828356	41.6	0.5	0.07535	0.00105	1.75544	0.0263	0.1695	0.00218	1009.4	12.02	1029.2	9.69	1078	27.7	-1.924	-6.4	1009.4	12.02
S1447_043	1898.88113	8.4	0.5	0.09101	0.00166	0.13621	0.00247	0.01089	0.00015	69.8	0.96	129.7	2.21	1446.7	34.41	-46.184	-95.2		
S1447_044	1450.59293	4.2	1.2	0.04772	0.00145	0.07273	0.00216	0.01109	0.00017	71.1	1.09	71.3	2.04	84.4	71.55	-0.281	-15.8	71.1	1.09
S1447_045	238.946066	16.1	0.6	0.0731	0.00114	1.78818	0.02941	0.17798	0.00237	1055.9	12.98	1041.2	10.71	1016.8	31.39	1.412	3.8	1055.9	12.98
S1447_046	606.880718	22.7	0.6	0.06533	0.00101	0.78854	0.01282	0.08782	0.00114	542.7	6.78	590.3	7.28	784.9	32.29	-8.064	-30.9	542.7	6.78
S1447_047	985.388203	35.9	0.9	0.05865	0.00103	0.63497	0.01139	0.07877	0.00105	488.8	6.28	499.2	7.07	554.2	37.69	-2.083	-11.8	488.8	6.28
S1447_048	608.995285	39.8	0.5	0.07151	0.00098	1.89223	0.02808	0.19252	0.00246	1135	13.32	1078.4	9.86	972.1	27.7	5.249	16.8	972.1	27.7
S1447_049	554.016544	11.8	0.3	0.05833	0.0012	0.69451	0.01438	0.08664	0.00122	535.6	7.21	535.5	8.62	541.4	45.12	0.019	-1.1	535.6	7.21
S1447_050	401.767722	26.2	0.5	0.06708	0.00099	1.35636	0.02134	0.14712	0.00191	884.8	10.72	870.3	9.19	840.2	30.54	1.666	5.3	884.8	10.72
S1447_051	606.880718	14.7	0.6	0.06074	0.00105	0.77815	0.01383	0.09321	0.00125	574.5	7.34	584.4	7.9	630.1	36.78	-1.694	-8.8	574.5	7.34
S1447_052	3218.37091	32.2	0.1	0.05221	0.00102	0.19185	0.00379	0.02673	0.00036	170.1	2.27	178.2	3.23	294.7	44.08	-4.545	-42.3	170.1	2.27
S1447_053	767.587807	3.8	0.7	0.05319	0.00152	0.10414	0.00289	0.01424	0.00022	91.2	1.39	100.6	2.66	336.8	63.28	-9.344	-72.9	91.2	1.39
S1447_054	329.872446	2.3	1.3	0.06927	0.00627	0.13391	0.00488	0.01407	0.00026	90	1.67	127.6	4.37	906.7	77.38	-29.467	-90.1		
S1447_055	568.818512	9.6	0.4	0.08638	0.00175	1.17921	0.0236	0.09933	0.00147	610.5	8.59	790.9	11	1346.6	38.52	-22.809	-54.7		
S1447_056	811.993713	31.8	1.1	0.06892	0.00097	1.27669	0.01929	0.13477	0.00172	815	9.79	835.4	8.6	896.3	28.8	-2.442	-9.1	815	9.79
S1447_057	672.432293	3.3	1.1	0.04482	0.00192	0.08555	0.00353	0.01389	0.00025	88.9	1.61	83.3	3.3	0.1	36.05	6.723	88800.0	88.9	1.61
S1447_058	1818.52759	11.4	1.1	0.05129	0.00104	0.15512	0.00316	0.022	3.00E-04	140.3	1.89	146.4	2.77	253.8	45.92	-4.167	-44.7	140.3	1.89
S1447_059	560.360244	61.2	0.9	0.16627	0.00244	8.91726	0.14097	0.39019	0.00565	2123.7	26.18	2329.6	14.43	2520.4	24.46	-8.838	-15.7	2520.4	24.46
S1447_060	162.821656	40.0	1.7	0.16053	0.002	10.89611	0.15257	0.49382	0.00654	2587.2	28.2	2514.3	13.02	2461.2	20.86	2.899	5.1	2461.2	20.86
S1447_061	20970.1605	264.7	2.8	0.05386	0.00075	0.09506	0.00143	0.01284	0.00016	82.2	1.02	92.2	1.32	365	31.4	-10.846	-77.5	82.2	1.02
S1447_062	7633.58673	46.2	1.0	0.05042	0.00064	0.11148	0.00156	0.01609	2.00E-04	102.9	1.25	107.3	1.43	214.3	29.3	-4.101	-52.0	102.9	1.25
S1447_063	10877.3324	170.7	0.3	0.05167	0.00063	0.22992	0.00314	0.03237	4.00E-04	205.4	2.47	210.1	2.59	270.9	27.93	-2.237	-24.2	205.4	2.47
S1447_064	2017.29688	4.8	1.2	0.0497	0.00158	0.05035	0.00155	0.00737	0.00012	47.3	0.76	49.9	1.5	180.9	72.65	-5.210	-73.9	47.3	0.76
S1447_065	543.443709	1.6	1.3	0.04513	0.00275	0.04565	0.00268	0.00736	0.00016	47.3	1.02	45.3	2.6	0.1	92.25	4.415	47200.0	47.3	1.02
S1447_066	319.299611	5.6	0.3	0.07801	0.00179	0.91191	0.02049	0.08504	0.0013	526.1	7.71	658.1	10.88	1147.2	44.91	-20.058	-54.1		
S1447_067	528.64174	2.3	0.8	0.08107	0.00431	0.08682	0.00422	0.00779	2.00E-04	50	1.28	84.5	3.95	1223.1	100.97	-40.828	-95.9		
S1447_068	585.735048	4.0	1.3	0.05132	0.00209	0.0986	0.00383	0.01398	0.00026	89.5	1.65	95.5	3.54	255.2	91.05	-6.283	-64.9	89.5	1.65
S1447_069	1175.69923	64.8	2.0	0.06591	0.00086	1.1862	0.01687	0.13093	0.00164	793.2	9.34	794.2	7.84	803.6	26.97	-0.126	-1.3	793.2	9.34
S1447_070	1731.83034	3.8	0.8	0.04939	0.00201	0.04335	0.00168	0.00638	0.00012	41	0.74	43.1	1.64	166.5	92.18	-4.872	-75.4	41	0.74
S1447_071	270.664571	26.9	0.6	0.10932	0.00156	5.25432	0.08105	0.34967	0.00475	1933	22.69	1861.5	13.16	1788	25.79	3.841	8.1	1788	25.79
S1447_072	501.15237	3.4	1.1	0.05078	0.00213	0.12303	0.00493	0.01762	0.00033	112.6	2.08	117.8	4.46	231	93.99	-4.414	-51.3	112.6	2.08
S1447_073	12920.0041	64.9	2.1	0.04774	0.00068	0.08471	0.00129	0.01291	0.00016	82.7	1.03	82.6	1.21	85.4	34.42	0.121	-3.2	82.7	1.03
S1447_074	3499.60832	12.3	0.7	0.0503	0.00096	0.07679	0.00148	0.01111	0.00015	71.2	0.94	75.1	1.4	209	43.55	-5.193	-65.9	71.2	0.94
S1447_075	171.279924	2.2	0.6	0.29531	0.01757	0.74483	0.0336	0.01835	0.00078	117.2	4.94	565.2	19.56	3445.8	89.4	-79.264	-96.6		
S1447_076	710.494499	58.2	0.8	0.11268	0.00138	5.20754	0.07115	0.33621	0.00427	1868.4	20.61	1853.8	11.64	1843.1	21.92	0.788	1.4	1843.1	21.92
S1447_077	1148.20986	19.4	0.2	0.05522	0.00088	0.38772	0.00643	0.05107	0.00066	321.1	4.03	332.7	4.7	421.1	34.87	-3.487	-23.7	321.1	4.03
S1447_078	545.558276	3.0	0.7	0.04916	0.00194	0.11176	0.00424	0.01654	3.00E-04	105.7	1.89	107.6	3.87	155.3	90.09	-1.766	-31.9	105.7	1.89
S1447_079	22422.868	72.4	0.8	0.0466	0.00065	0.07012	0.00105	0.01094	0.00014	70.2	0.87	68.8	1	28.9	32.66	2.035	142.9	70.2	0.87
S1447_080	1651.4768	55.5	0.3	0.0666	8.00E-04	1.02821	0.01385	0.11231	0.00138	686.1	8.01	718	6.94	825.3	24.97	-4.443	-16.9	686.1	8.01
S1447_081	1351.20829	75.7	0.7	0.06944	9.00E-04	1.41209	0.02013	0.14794	0.00186	889.4	10.43	894	8.47	911.7	26.59	-0.515	-2.4	889.4	10.43
S1447_083	2493.07445	108.0	0.2	0.11222	0.00142	1.64855	0.02276	0.10686	0.00135	654.5	7.86	989	8.73	1835.7	22.74	-33.822	-64.3		
S1447_084	858.514186	43.6	0.3	0.07182	0.00099	1.65098	0.02454	0.16722	0.00214	996.8	11.79	989.9	9.4	980.9	27.79	0.697	1.6	996.8	11.79
S1447_085	6193.56663	116.3	0.2	0.06238	0.00074	0.91395	0.01217	0.10659	0.0013	652.9	7.6	659.2	6.46	687.1	25.1	-0.956	-5.0	652.9	7.6
S1447_086	697.807097	14.3	0.3	0.05788	0.00102	0.69492	0.01259	0.08733	0.00117	539.8	6.92	535.8	7.54	525.1	38.53	0.747	2.8	539.8	6.92
S1447_087	148.019687	1.4	1.0	0.37572	0.01818	1.31766	0.04698	0.02551	0.00095	162.4	5.95	853.5	20.58	3814.7	71.31	-80.972	-95.7		
S1447_088	312.95591	12.7	0.9	0.05946	0.00128	0.77521	0.01664	0.09485	0.00136	584.1	8.02	582.7	9.52	583.9	45.98	0.240	0.0	584.1	8.02
S1447_089	573.047646	3.9	0.3	0.09265	0.00225	0.31938	0.0074	0.02508	0.00039	159.7	2.48	281.4	5.7	1480.7	45.48	-43.248	-89.2		
S1447_090	6254.88907	44.1	2.6	0.08127	0.00133	0.19595	0.00327	0.01754	0.00023	112.1	1.47	181.7	2.78	1227.9	31.78	-38.305	-90.9		
S1447_092	1065.74175	3.8	0.7	0.04541	0.00135	0.111	0.00323	0.01778	0.00027	113.6	1.71	106.9	2.96	0.1	36.92	6.268	113500.0	113.6	1.71
S1447_093	2467.69964	405.7	0.3	0.14794	0.00159	9.80732	0.12269	0.48222	0.00587	2536.9	25.53	2416.8	11.53	2322.2	18.32	4.969	9.2	2322.2	18.32
S1447_094	847.941351	113.3	0.2	0.15178	0.00173	8.49527	0.11072	0.40714	0.00509	2201.8	23.31	2285.4	11.84	2366.1	19.33	-3.658	-6.9	2366.1	19.33
S1447_095	1059.39805	6.5	0.8	0.04685	0.00203	0.11703	0.00485	0.01817	0.00035	116.1	2.19	112.4	4.41	41.2	100.76	3.292	181.8	116.1	2.19
S1447_096	228.373232	4.7	0.9	0.05828	0.00182	0.79039	0.02397	0.09865	0.00166	606.5	9.75	591.4	13.59	539.7	67.38	2.553	12.4	606.5	9.75
S1447_097	1332.17718	4.7	0.9	0.04858	0.00373	0.05019	0.00364	0.00752	0.00022	48.3	1.41	49.7	3.52	127.4	171.54	-2.817	-62.1	48.3	1.41
S1447_098	393.309455	1.4	0.7	0.04913	0.00301	0.08629	0.00502	0.01278	3.00E-04	81.8	1.92	84	4.7	154	137.33	-2.619	-46.9	81.8	1.92
S1447_099	2529.02208	9.0	0.5	0.10667	0.00237	0.17944	0.00379	0.01224	0.00019	78.4	1.2	167.6	3.26	1743.4	40.11	-53.222	-95.5		
S1447_100	1270.85474	129.5	0.8	0.11025	0.00134	5.19087	0.07057	0.34246	0.00433	1898.5	20.79	1851.1	11.57	1803.6	21.87	2.561	5.3	1803.6	21.87
S1447_101	1672.62247	103.6	0.7	0.07419	9.00E-04	1.96332	0.02666	0.1925	0.00238	1134.9	12.89	1103	9.14	1046.5	24.34	2.892	8.4	1046.5	24.34
S1447_102	255.862602	5.9	0.6	0.06146	0.00167	0.9269	0.02468	0.1097	0.00177	671	10.29	666	13.01	655.4	57.38	0.751	2.4	671	10.29
S1447_103	1653.59136	60.4	0.3	0.06927	9.00E-04	1.14079	0.01615	0.1198	0.0015	729.4	8.61	772.9	7.66	906.7	26.43	-5.628	-19.6	729.4	8.61
S1447_104	1467.50947	16.1	0.2	0.05714	0.00089	0.54476	0.00892	0.06935	0.00089	432.2	5.38	441.6	5.86	496.3	34.18	-2.129	-12.9	432.2	5.38
S1447_105	2622.06303	4.1	0.3	0.04796	0.0015	0.03498	0.00106	0.00531	8.00E-05	34.1	0.53	34.9	1.04	96	73.33	-2.292	-64.5	34.1	0.53
S1447_106	854.285052	11.5	0.6	0.05649	0.00114	0.44874	0.00912	0.05778	8.00E-04	362.1	4.86	376.4	6.39	470.9	44.61	-3.799	-23.1	362.1	4.86
S1447_107	524.412606	2.5	0.7	0.41002	0.0161	0.65551	0.01877	0.01163	0.00036	74.5	2.28	511.9	11.51	3946.2	57.66	-85.446	-98.1		
S1447_108	302.383075	1.0	0.9	0.04188	0.00426	0.04993	0.00488	0.00867	0.00027	55.7	1.74	49.5	4.72	0.1	4.84	12.525	55600.0	55.7	1.74
S1447_109	1547.86301	30.6	0.1	0.06316	0.00082	0.74346	0.01054	0.08562	0.00106	529.6	6.32	564.4	6.14	713.7	27.31	-6.166	-25.8	529.6	6.32
S1447_110	822.566547	2.3	0.7	0.04853	0.0023	0.07586	0.00346	0.01137	0.00022	72.9	1.4	74.2	3.26	125.2	108.15	-1.752	-41.8	72.9	1.4
S1447_111	329.872446	4.0	0.8	0.41862	0.02065	1.36751	0.04833	0.02376	0.00092	151.4	5.79	875.1	20.73	3977.4	71.93	-82.699	-96.2		
S1447_112	2509.99098	4.6	0.1	0.04877	0.00131	0.05362	0.00141	0.008	0.00012	51.4	0.75	53	1.36	136.6	61.81	-3.019	-62.4	51.4	0.75
S1447_113	600.537017	14.1	0.3	0.06121	0.00109	0.92429	0.01688	0.10984	0.00148	671.8	8.62	664.6	8.91	646.5	37.81	1.083	3.9	671.8	8.62
S1447_115	63.4370088	2.1	0.6	0.06015	0.00239	1.22898	0.04744	0.14861	0.00294	893.2	16.48	813.9	21.61	608.9	83.68	9.743	46.7	893.2	16.48
S1447_116	2444.43941	20.9	0.1	0.05523	0.00079	0.29401	0.0045	0.03872	0.00049	244.9	3.02	261.7	3.53	421.6	31.58	-6.420	-41.9	244.9	3.02
S1447_117	2512.10555	11.4	0.7	0.05507	0.00098	0.14481	0.00264	0.01912	0.00025	122.1	1.59	137.3	2.34	415.1	39.12	-11.071	-70.6	122.1	1.59
S1447_118	1053.05435	3.2	1.1	0.04499	0.00212	0.08662	0.00392	0.014	0.00027	89.6	1.71	84.3	3.66	0.1	54.55	6.287	89500.0	89.6	1.71
S1447_119	4066.31226	6.4	0.5	0.04911	0.00115	0.03852	0.00089	0.0057	8.00E-05	36.7	0.51	38.4	0.87	152.9	53.91	-4.427	-76.0	36.7	0.51
S1447_120	2114.56696	16.6	1.0	0.05159	0.00133	0.11588	0.00291	0.01634	0.00024	104.5	1.53	111.3	2.65	267.3	57.9	-6.110	-60.9	104.5	1.53
S1447_121	148.019687	0.4	0.4	0.04521	0.00633	0.06734	0.00912	0.01084	0.00042	69.5	2.67	66.2	8.68	0.1	264.68	4.985	69400.0	69.5	2.67
S1447_122	2224.52444	54.2	0.4	0.06983	0.00084	0.99001	0.01327	0.10312	0.00127	632.7	7.39	698.7	6.77	923.3	24.44	-9.446	-31.5	632.7	7.39
S1447_123	1124.94962	18.6	0.6	0.05753	0.00117	0.35912	0.00729	0.0454	0.00063	286.2	3.87	311.6	5.44	511.5	44.29	-8.151	-44.0	286.2	3.87
S1447_124	395.424022	34.2	0.6	0.1114	0.00153	3.88274	0.05751	0.25351	0.00334	1456.5	17.16	1610.1	11.96	1822.3	24.67	-9.540	-20.1	1822.3	24.67
S1447_125	289.695674	1.6	0.7	0.04916	0.00241	0.17873	0.00847	0.02644	0.00051	168.2	3.22	167	7.29	155.4	111.08	0.719	8.2	168.2	3.22
S1447_126	304.497642	1.7	0.5	0.04587	0.00279	0.15866	0.00926	0.02516	0.00056	160.2	3.53	149.5	8.12	0.1	131.17	7.157	160100.0	160.2	3.53
S1447_127	556.131111	48.0	0.5	0.11184	0.00131	5.4097	0.07165	0.3518	0.00438	1943.2	20.89	1886.4	11.35	1829.5	21.04	3.011	6.2	1829.5	21.04
S1447_128	737.983869	3.0	0.6	0.05442	0.00195	0.10561	0.00362	0.01412	0.00024	90.4	1.54	101.9	3.33	388.2	77.62	-11.286	-76.7	90.4	1.54
S1447_129	3076.69493	67.6	1.2	0.05846	0.00074	0.66451	0.00928	0.08266	0.00102	512	6.07	517.4	5.66	547.2	27.44	-1.044	-6.4	512	6.07
S1447_130	243.1752	0.8	0.8	0.04982	0.00374	0.09347	0.00679	0.01365	0.00033	87.4	2.08	90.7	6.31	186.5	166.06	-3.638	-53.1	87.4	2.08
S1447_131	1772.00711	4.1	0.7	0.07835	0.00236	0.08186	0.00232	0.0076	0.00013	48.8	0.83	79.9	2.17	1155.7	58.53	-38.924	-95.8		
S1447_132	987.50277	38.4	0.5	0.07837	0.00097	2.29264	0.0315	0.21276	0.00265	1243.5	14.08	1210	9.71	1156.2	24.33	2.769	7.6	1156.2	24.33
S1447_133	2698.18744	7.0	0.5	0.05539	0.00119	0.08568	0.00183	0.01125	0.00016	72.1	1	83.5	1.71	427.8	46.69	-13.653	-83.1		
S1447_135	4643.58904	0.8	0.5	0.04906	0.00079	0.1253	0.00212	0.01857	0.00024	118.6	1.5	119.9	1.91	150.7	37.53	-1.084	-21.3	118.6	1.5
S1447_136	630.140954	37.3	0.5	0.11306	0.00136	4.82921	0.06516	0.31065	0.0039	1743.9	19.18	1790	11.35	1849.1	21.59	-2.575	-5.7	1849.1	21.59
S1447_137	799.306311	51.7	0.3	0.11909	0.00138	5.65921	0.07426	0.34561	0.00429	1913.6	20.53	1925.2	11.32	1942.6	20.51	-0.603	-1.5	1942.6	20.51
S1447_138	1685.30987	25.2	0.5	0.05559	0.00078	0.63102	0.00956	0.08255	0.00104	511.3	6.18	496.7	5.95	435.9	30.65	2.939	17.3	511.3	6.18
S1447_139	429.257093	1.0	1.0	0.04428	0.00368	0.04479	0.00358	0.00736	0.00019	47.2	1.24	44.5	3.48	0.1	95.92	6.067	47100.0	47.2	1.24
S1447_140	2277.38862	199.0	0.2	0.1632	0.00175	10.96723	0.13684	0.48872	0.00592	2565.1	25.61	2520.4	11.61	2489.1	17.98	1.774	3.1	2489.1	17.98
S1447_141	1526.71735	52.6	0.8	0.07641	0.00092	1.95995	0.02643	0.18654	0.0023	1102.6	12.51	1101.9	9.07	1105.8	23.91	0.064	-0.3	1105.8	23.91
S1447_142	4802.18157	23.5	1.3	0.04928	0.00081	0.10727	0.00184	0.01583	2.00E-04	101.2	1.29	103.5	1.68	161.1	38.17	-2.222	-37.2	101.2	1.29
S1447_143	236.8315	6.0	0.4	0.07229	0.00155	1.5832	0.034	0.15928	0.00237	952.8	13.2	963.6	13.36	994	43.01	-1.121	-4.1	952.8	13.2
S1447_144	16586.6632	46.1	3.1	0.08173	0.00154	0.06259	0.00117	0.00557	8.00E-05	35.8	0.49	61.6	1.12	1239.1	36.28	-41.883	-97.1		
S1447_145	458.86103	6.3	0.2	0.05992	0.00127	0.63899	0.01354	0.07755	0.0011	481.5	6.55	501.7	8.39	600.8	45.23	-4.026	-19.9	481.5	6.55
S1447_146	2241.44098	209.9	0.3	0.11943	0.00132	5.89939	0.07496	0.35923	0.00438	1978.5	20.75	1961.1	11.03	1947.7	19.59	0.887	1.6	1947.7	19.59
S1447_147	1494.99884	6.2	0.4	0.04687	0.00107	0.10296	0.00234	0.01598	0.00022	102.2	1.41	99.5	2.15	42.2	52.88	2.714	142.2	102.2	1.41
S1447_148	270.664571	1.1	0.8	0.05714	0.00339	0.11098	0.00621	0.01412	0.00034	90.4	2.18	106.9	5.68	496.4	126.13	-15.435	-81.8		
S1447_149	1042.48151	151.0	0.5	0.14787	0.00167	9.59469	0.12414	0.47186	0.00584	2491.7	25.57	2396.7	11.9	2321.4	19.2	3.964	7.3	2321.4	19.2
S1447_150	1440.0201	5.8	0.4	0.04899	0.00129	0.11693	0.00301	0.01736	0.00025	110.9	1.61	112.3	2.74	147.4	60.4	-1.247	-24.8	110.9	1.61
S1447_151	589.964182	1.4	1.0	0.05014	0.00345	0.05507	0.0036	0.00799	2.00E-04	51.3	1.31	54.4	3.47	201.5	152.3	-5.699	-74.5	51.3	1.31
S1447_152	693.577963	49.3	0.4	0.11234	0.00134	4.96288	0.06656	0.32127	0.00402	1795.9	19.59	1813	11.33	1837.5	21.43	-0.943	-2.3	1837.5	21.43
S1447_153	81.645	0.7	0.9	0.04195	0.00403	0.00788	0.00737	0.04547	0.04182	50.6	1.35	45.1	4.12	0.1	0	12.195	50500.0	50.6	1.35
S1447_154	1065.74175	37.9	0.5	0.07113	0.00095	1.65475	0.02413	0.16918	0.00214	1007.6	11.78	991.4	9.23	961.1	26.9	1.634	4.8	1007.6	11.78
S1447_155	974.815369	2.6	0.7	0.04588	0.00181	0.07864	0.003	0.01246	0.00021	79.9	1.35	76.9	2.82	0.1	82.9	3.901	79800.0	79.9	1.35
S1447_156	6703.17726	19.0	0.8	0.04718	0.00088	0.06949	0.00132	0.01071	0.00014	68.7	0.9	68.2	1.25	58.1	44.38	0.733	18.2	68.7	0.9
S1447_157	549.78741	1.8	0.9	0.04766	0.00226	0.11378	0.00522	0.01736	0.00032	111	2.03	109.4	4.76	81.7	109.79	1.463	35.9	111	2.03
S1447_159	712.609066	32.6	0.2	0.07535	0.001	2.04273	0.02956	0.19713	0.00249	1159.9	13.42	1129.9	9.87	1077.9	26.41	2.655	7.6	1077.9	26.41
S1447_160	638.599222	2.4	0.6	0.05011	0.00239	0.09288	0.00422	0.01348	0.00027	86.3	1.73	90.2	3.92	200	107	-4.324	-56.9	86.3	1.73
S1447_161	245.289767	0.6	1.2	0.05135	0.00445	0.10027	0.0083	0.0142	0.00042	90.9	2.64	97	7.66	256.7	187.34	-6.289	-64.6	90.9	2.64
S1447_162	537.100008	15.0	1.0	0.06201	0.00117	0.91799	0.01757	0.10765	0.00148	659.1	8.61	661.3	9.3	674.4	39.78	-0.333	-2.3	659.1	8.61
S1447_163	979.044503	44.8	0.5	0.074	0.00117	1.29368	0.02139	0.12713	0.00168	771.5	9.62	842.9	9.47	1041.4	31.68	-8.471	-25.9	771.5	9.62
S1447_164	1668.39333	73.7	0.4	0.15404	0.00173	6.96679	0.08943	0.32888	0.00404	1832.9	19.58	2107.2	11.4	2391.3	18.97	-13.017	-23.4	2391.3	18.97
S1447_165	3598.99297	118.3	0.2	0.066	0.00081	1.29305	0.01772	0.14246	0.00176	858.6	9.91	842.6	7.85	806.4	25.61	1.899	6.5	858.6	9.91
S1447_166	803.535445	3.9	1.2	0.04679	0.00153	0.11087	0.00353	0.01723	0.00027	110.1	1.73	106.8	3.23	38.3	76.88	3.090	187.5	110.1	1.73
S1447_167	1213.76144	9.1	0.6	0.05273	0.00103	0.33142	0.00654	0.04571	0.00062	288.1	3.8	290.7	4.99	317	43.7	-0.894	-9.1	288.1	3.8
S1447_168	782.389775	3.0	0.5	0.0525	0.00317	0.08121	0.00462	0.01125	0.00028	72.1	1.78	79.3	4.34	307.4	131.81	-9.079	-76.5	72.1	1.78
S1447_169	735.869302	12.0	0.6	0.05733	0.00103	0.75474	0.01393	0.09573	0.00128	589.4	7.54	571	8.06	503.7	39.62	3.222	17.0	589.4	7.54
S1447_170	1287.77128	5.2	0.8	0.04871	0.00166	0.12185	0.00402	0.01819	3.00E-04	116.2	1.9	116.8	3.64	134	78.37	-0.514	-13.3	116.2	1.9
S1447_171	998.075605	14.7	0.3	0.05766	0.00127	0.52782	0.01155	0.06657	0.00095	415.4	5.76	430.4	7.67	516.4	47.93	-3.485	-19.6	415.4	5.76
S1447_172	2577.65712	5.5	1.3	0.05065	0.00156	0.08715	0.0026	0.01251	2.00E-04	80.2	1.26	84.8	2.42	224.9	69.65	-5.425	-64.3	80.2	1.26
S1447_173	795.077177	65.0	0.3	0.11624	0.00151	5.13456	0.07338	0.32118	0.00416	1795.5	20.28	1841.8	12.15	1899.3	23.18	-2.514	-5.5	1899.3	23.18
S1447_174	1072.08545	36.8	0.0	0.08078	0.001	1.86414	0.02552	0.1678	0.00208	1000	11.48	1068.5	9.05	1216.1	24.08	-6.411	-17.8	1000	11.48
S1447_175	913.492927	2.6	0.8	0.05183	0.00238	0.08832	0.00386	0.01239	0.00024	79.4	1.56	85.9	3.6	278	101.55	-7.567	-71.4	79.4	1.56
S1447_176	2554.39689	6.9	0.6	0.04756	0.00113	0.11464	0.00271	0.01753	0.00025	112	1.56	110.2	2.46	76.8	56.39	1.633	45.8	112	1.56
S1447_177	1346.97915	2.5	1.1	0.13365	0.00627	0.11956	0.00488	0.00651	0.00018	41.8	1.13	114.7	4.42	2146.4	79.74	-63.557	-98.1		
S1447_178	814.10828	71.6	0.2	0.15861	0.00201	11.29413	0.16074	0.51775	0.00686	2689.6	29.13	2547.7	13.28	2440.9	21.34	5.570	10.2	2440.9	21.34
S1447_179	357.361816	18.0	0.8	0.16335	0.00292	11.14476	0.21244	0.49609	0.00832	2597	35.87	2535.3	17.76	2490.6	29.85	2.434	4.3	2490.6	29.85
S1447_180	856.399619	0.8	0.5	0.05154	0.00448	0.07848	0.00646	0.01107	0.00035	71	2.25	76.7	6.08	265.2	187.94	-7.432	-73.2	71	2.25
S1447_181	2691.84374	6.6	0.6	0.04643	0.00187	0.07514	0.0029	0.01177	0.00021	75.4	1.35	73.6	2.74	19.8	94.01	2.446	280.8	75.4	1.35
S1447_182	4298.91463	11.0	0.9	0.05174	0.00132	0.08728	0.00218	0.01227	0.00018	78.6	1.15	85	2.04	273.9	57.48	-7.529	-71.3	78.6	1.15
S1447_183	5656.46662	13.6	1.5	0.04872	0.00149	0.14106	0.00419	0.02105	0.00033	134.3	2.11	134	3.73	134.4	70.57	0.224	-0.1	134.3	2.11
S1447_184	154.363388	0.208	0.7	0.05837	0.01254	0.12037	0.02489	0.01499	0.00092	95.9	5.85	115.4	22.55	543.7	411.09	-16.898	-82.4		
S1447_185	653.401191	17.58	0.4	0.06812	0.00138	1.45934	0.0298	0.15576	0.00225	933.2	12.56	913.7	12.3	872.3	41.41	2.134	7.0	933.2	12.56
S1447_186	651.286624	60.932	0.5	0.15968	0.00222	10.55063	0.16121	0.48042	0.00671	2529.1	29.2	2484.4	14.17	2452.3	23.32	1.799	3.1	2452.3	23.32
S1447_187	2287.96145	9.261	0.2	0.04583	0.00093	0.11621	0.00238	0.01844	0.00025	117.8	1.56	111.6	2.16	0.1	36.75	5.556	117700.0	117.8	1.56
S1447_188	1566.89412	40.985	0.5	0.06381	0.00081	1.05596	0.01479	0.12033	0.00149	732.5	8.56	731.8	7.3	735.2	26.71	0.096	-0.4	732.5	8.56
S1447_189	6259.1182	24.378	0.5	0.05164	0.00075	0.13764	0.00212	0.01938	0.00024	123.7	1.53	130.9	1.9	269.3	32.93	-5.500	-54.1	123.7	1.53
S1447_190	2600.91736	80.253	0.6	0.10851	0.00124	2.49433	0.03229	0.16713	0.00204	996.3	11.26	1270.4	9.38	1774.6	20.72	-21.576	-43.9		
S1447_191	141.24	1.186	0.9	0.04127	0.00286	0.00021	0.00016	0.00424	0.00281	47.3	1	41.6	2.74	0.1	0	13.702	47200.0	47.3	1
S1447_192	1163.01183	66.2268	0.6	0.11497	0.00133	4.22262	0.05531	0.26704	0.00328	1525.8	16.71	1678.4	10.75	1879.4	20.71	-9.092	-18.8	1879.4	20.71
S1447_193	1871.39176	50.11	0.3	0.06611	0.0008	1.32646	0.01812	0.14588	0.00179	877.8	10.09	857.3	7.91	809.9	25.49	2.391	8.4	877.8	10.09
S1447_194	192.425933	15.542	1.1	0.11471	0.00166	5.67575	0.08843	0.35976	0.00489	1981.1	23.2	1927.7	13.45	1875.3	25.82	2.770	5.6	1875.3	25.82
S1447_195	2979.42485	291.316	0.5	0.13398	0.00146	7.24179	0.09102	0.393	0.00474	2136.7	21.93	2141.7	11.21	2150.7	18.87	-0.233	-0.7	2150.7	18.87
S1447_196	15903.6581	323.844	12.4	0.11354	0.00139	0.2821	0.0038	0.01807	0.00022	115.4	1.41	252.3	3.01	1856.8	22.01	-54.261	-93.8		
S1447_197	735.869302	1.471	1.5	0.04972	0.00262	0.04961	0.0025	0.00725	0.00015	46.6	0.95	49.2	2.42	181.7	118.26	-5.285	-74.4	46.6	0.95
S1447_198	602.651584	17.075	0.6	0.06241	0.00096	0.81406	0.01317	0.09483	0.00122	584.1	7.19	604.7	7.37	688.2	32.49	-3.407	-15.1	584.1	7.19
S1447_199	1452.7075	4.534	0.5	0.04859	0.00131	0.1109	0.00293	0.0166	0.00024	106.1	1.54	106.8	2.68	127.9	62.12	-0.655	-17.0	106.1	1.54
S1447_200	1664.1642	121.901	0.9	0.13549	0.00151	7.09852	0.09095	0.3809	0.00464	2080.5	21.68	2123.9	11.4	2170.4	19.35	-2.043	-4.1	2170.4	19.35
S1447_201	490.579535	15.131	1.1	0.06502	0.00106	1.16628	0.01984	0.13041	0.00172	790.2	9.81	784.9	9.3	775	34.01	0.675	2.0	790.2	9.81
S1447_202	1023.45041	51.073	0.4	0.07641	0.001	2.0307	0.02898	0.19323	0.00243	1138.8	13.11	1125.9	9.71	1105.8	25.83	1.146	3.0	1105.8	25.83
S1447_203	296.039374	2.219	0.8	0.16854	0.00551	0.46319	0.01321	0.01998	0.00043	127.5	2.72	386.5	9.17	2543.2	53.79	-67.012	-95.0		
S1447_204	78.2389775	0.349	0.7	0.12458	0.00969	0.25264	0.01774	0.01474	0.00055	94.4	3.47	228.7	14.38	2022.8	131.75	-58.723	-95.3		
S1447_205	3415.02564	3.094	0.7	0.04423	0.00221	0.01701	0.00081	0.0028	6.00E-05	18	0.36	17.1	0.81	0.1	20.47	5.263	17900.0	18	0.36
S1447_206	2084.96302	20.212	0.1	0.05861	0.00085	0.34983	0.0054	0.04339	0.00055	273.8	3.38	304.6	4.06	552.7	31.38	-10.112	-50.5	273.8	3.38
S1447_207	1786.80908	26.651	0.1	0.05799	0.00084	0.41903	0.0068	0.05253	0.00067	330	4.11	355.4	4.86	529.2	33.93	-7.147	-37.6	330	4.11
S1447_208	1038.25238	17.332	0.4	0.05184	0.00106	0.35298	0.00725	0.0495	0.00068	311.5	4.16	307	5.44	278.5	46.12	1.466	11.8	311.5	4.16
S1447_209	2958.27918	292.306	0.2	0.15015	0.00165	6.35087	0.08046	0.30751	0.00372	1728.4	18.34	2025.5	11.11	2347.6	18.72	-14.668	-26.4		
S1447_210	515.954338	3.206	0.4	0.08018	0.00265	0.17774	0.00551	0.01612	0.00029	103.1	1.85	166.1	4.75	1201.3	63.85	-37.929	-91.4		

Sample S1455 Indus River @ Kalabagh		359 grains analysed		282 concordant ages

	concentrations			isotopic ratios						ages						discordance		preferred age	
grain	U [ppm]	Pb [ppm]	Th/U	Pb207/Pb206	2σ 76	Pb207/U235	2σ 75	Pb206/U238	2σ 68	age 206/238	2σ age 68	age 207/235	2σ age 75	age 207/206	2σ age 76	Δ 68-75 [%]	Δ 68-76 [%]	age	2σ age
S1455_001	412.1	2.3	0.8	0.05345	0.00274	0.11368	0.00551	0.01547	0.00032	99.0	2.1	109.3	5.0	348.0	111.3	-9.4	-71.6	99.0	2.1
S1455_003	534.0	3.8	0.7	0.10848	0.00304	0.25392	0.00651	0.01703	0.00028	108.9	1.8	229.8	5.3	1773.9	50.4	-52.6	-93.9		
S1455_004	421.7	2.3	0.8	0.05091	0.00257	0.11694	0.00562	0.01671	0.00033	106.8	2.1	112.3	5.1	236.7	112.2	-4.9	-54.9	106.8	2.1
S1455_005	1361.4	6.8	0.8	0.05130	0.00119	0.10865	0.00244	0.01541	0.00020	98.6	1.3	104.7	2.2	254.1	52.5	-5.8	-61.2	98.6	1.3
S1455_006	8046.6	32.2	0.2	0.04967	0.00074	0.10785	0.00160	0.01580	0.00018	101.0	1.2	104.0	1.5	179.6	34.2	-2.9	-43.8	101.0	1.2
S1455_007	647.8	98.1	0.6	0.16059	0.00181	9.69805	0.11516	0.43933	0.00493	2347.6	22.1	2406.5	10.9	2461.9	19.0	-2.4	-4.6	2461.9	19.0
S1455_008	1327.7	6.9	0.3	0.05471	0.00134	0.12086	0.00284	0.01607	0.00022	102.8	1.4	115.9	2.6	400.1	53.9	-11.3	-74.3	102.8	1.4
S1455_009	679.9	4.5	1.4	0.06139	0.00186	0.14830	0.00427	0.01758	0.00027	112.3	1.7	140.4	3.8	652.8	63.8	-20.0	-82.8		
S1455_010	585.3	56.7	0.5	0.10158	0.00120	4.02212	0.04958	0.28805	0.00326	1631.8	16.3	1638.7	10.0	1653.2	21.8	-0.4	-1.3	1653.2	21.8
S1455_011	2448.6	145.4	0.3	0.10671	0.00119	2.62726	0.03068	0.17912	0.00197	1062.2	10.8	1308.3	8.6	1743.9	20.3	-18.8	-39.1		
S1455_012	1640.4	8.8	0.8	0.05262	0.00107	0.12164	0.00241	0.01682	0.00021	107.5	1.3	116.6	2.2	312.3	45.6	-7.8	-65.6	107.5	1.3
S1455_013	259.8	0.8	0.8	0.04403	0.00437	0.04824	0.00467	0.00797	0.00020	51.2	1.3	47.8	4.5	0.1	119.1	7.1	51100.0	51.2	1.3
S1455_014	129.9	5.3	0.4	0.06681	0.00183	0.97498	0.02559	0.10617	0.00164	650.5	9.6	691.0	13.2	831.8	56.0	-5.9	-21.8	650.5	9.6
S1455_015	2333.2	13.0	0.6	0.04751	0.00089	0.10899	0.00201	0.01669	0.00020	106.7	1.3	105.0	1.8	74.1	44.9	1.6	44.0	106.7	1.3
S1455_016	1528.2	3.9	0.6	0.04619	0.00147	0.04642	0.00142	0.00731	0.00011	47.0	0.7	46.1	1.4	7.5	73.8	2.0	526.7	47.0	0.7
S1455_017	2868.7	17.6	0.8	0.04722	0.00081	0.10745	0.00181	0.01655	0.00020	105.8	1.2	103.6	1.7	60.0	40.7	2.1	76.3	105.8	1.2
S1455_018	1106.4	44.8	0.4	0.06620	0.00084	1.15057	0.01498	0.12643	0.00143	767.5	8.2	777.5	7.1	812.8	26.3	-1.3	-5.6	767.5	8.2
S1455_019	2780.5	8.4	0.6	0.05018	0.00189	0.06355	0.00226	0.00921	0.00016	59.1	1.0	62.6	2.2	203.3	84.9	-5.6	-70.9	59.1	1.0
S1455_020	445.8	1.3	0.8	0.04675	0.00310	0.04841	0.00311	0.00753	0.00015	48.4	1.0	48.0	3.0	36.5	151.9	0.8	32.6	48.4	1.0
S1455_021	572.5	23.3	0.7	0.08582	0.00124	1.19528	0.01660	0.10132	0.00126	622.2	7.4	798.4	7.7	1334.0	27.7	-22.1	-53.4		
S1455_022	155.3	2.2	0.9	0.04353	0.00243	0.06902	0.00022	0.01154	0.00371	73.9	1.4	67.8	3.5	0.1	0.0	9.0	73800.0	73.9	1.4
S1455_023	149.1	0.7	0.6	0.14899	0.01200	0.28575	0.02085	0.01395	0.00051	89.3	3.3	255.2	16.5	2334.4	131.7	-65.0	-96.2		
S1455_024	2233.7	29.7	0.1	0.05230	0.00079	0.27695	0.00418	0.03852	0.00045	243.7	2.8	248.2	3.3	298.5	34.0	-1.8	-18.4	243.7	2.8
S1455_025	1084.0	3.6	0.7	0.04674	0.00219	0.08044	0.00360	0.01252	0.00023	80.2	1.5	78.6	3.4	35.9	108.8	2.0	123.4	80.2	1.5
S1455_026	841.9	4.7	0.6	0.05129	0.00155	0.11685	0.00338	0.01657	0.00024	106.0	1.6	112.2	3.1	253.8	68.0	-5.5	-58.2	106.0	1.6
S1455_027	1922.7	166.8	0.1	0.11811	0.00153	4.72427	0.06297	0.29098	0.00346	1646.4	17.3	1771.6	11.2	1927.8	23.1	-7.1	-14.6	1927.8	23.1
S1455_028	1444.8	4.8	0.1	0.10484	0.00258	0.15729	0.00356	0.01091	0.00017	70.0	1.1	148.3	3.1	1711.6	44.5	-52.8	-95.9		
S1455_029	867.5	121.7	0.4	0.14947	0.00172	8.37581	0.10120	0.40765	0.00461	2204.2	21.1	2272.6	11.0	2339.8	19.6	-3.0	-5.8	2339.8	19.6
S1455_030	1217.1	92.2	0.2	0.11271	0.00142	3.19282	0.04122	0.20607	0.00239	1207.8	12.8	1455.4	10.0	1843.6	22.6	-17.0	-34.5		
S1455_031	1037.5	1.0	0.4	0.04391	0.00579	0.05486	0.00694	0.00909	0.00036	58.3	2.3	54.2	6.7	0.1	180.7	7.6	58200.0	58.3	2.3
S1455_032	2070.2	4.9	0.3	0.04690	0.00164	0.05531	0.00184	0.00858	0.00013	55.1	0.9	54.7	1.8	43.6	81.7	0.7	26.4	55.1	0.9
S1455_033	1584.3	204.4	0.4	0.14905	0.00167	8.90666	0.10493	0.43469	0.00483	2326.8	21.7	2328.5	10.8	2335.1	19.0	-0.1	-0.4	2335.1	19.0
S1455_034	805.5	7.3	0.1	0.04197	0.00216	0.05356	0.00266	0.00928	0.00017	59.6	1.1	53.0	2.6	0.1	0.0	12.5	59500.0	59.6	1.1
S1455_035	255.0	0.8	1.0	0.12514	0.00992	0.15344	0.01069	0.00892	0.00036	57.2	2.3	144.9	9.4	2030.7	134.0	-60.5	-97.2		
S1455_036	283.8	8.4	0.3	0.06567	0.00235	1.19591	0.04093	0.13248	0.00251	802.0	14.3	798.7	18.9	795.7	73.4	0.4	0.8	802.0	14.3
S1455_037	11449.3	40.9	0.6	0.04856	0.00076	0.06570	0.00102	0.00984	0.00011	63.1	0.7	64.6	1.0	126.8	36.3	-2.3	-50.2	63.1	0.7
S1455_038	1143.3	3.6	0.7	0.05121	0.00350	0.06229	0.00401	0.00885	0.00023	56.8	1.5	61.4	3.8	250.3	149.8	-7.5	-77.3	56.8	1.5
S1455_039	3139.7	105.6	0.1	0.06220	0.00080	0.90721	0.01195	0.10610	0.00120	650.1	7.0	655.6	6.4	681.0	27.2	-0.8	-4.5	650.1	7.0
S1455_040	683.1	4.4	0.0	0.04746	0.00211	0.11447	0.00483	0.01754	0.00032	112.1	2.1	110.0	4.4	71.8	103.0	1.9	56.1	112.1	2.1
S1455_041	8027.4	22.1	0.8	0.04811	0.00081	0.06193	0.00103	0.00936	0.00011	60.1	0.7	61.0	1.0	104.7	39.4	-1.5	-42.6	60.1	0.7
S1455_042	5270.9	9.0	0.8	0.05179	0.00116	0.03765	0.00081	0.00529	0.00007	34.0	0.4	37.5	0.8	275.9	50.4	-9.3	-87.7	34.0	0.4
S1455_043	646.2	10.7	0.3	0.05784	0.00113	0.63745	0.01215	0.08017	0.00102	497.2	6.1	500.7	7.5	523.4	42.4	-0.7	-5.0	497.2	6.1
S1455_044	808.2	18.5	0.6	0.05788	0.00091	0.68867	0.01083	0.08656	0.00103	535.1	6.1	532.0	6.5	524.9	34.5	0.6	1.9	535.1	6.1
S1455_045	428.1	13.0	0.2	0.06807	0.00142	1.18350	0.02396	0.12648	0.00173	767.7	9.9	792.9	11.1	870.7	42.5	-3.2	-11.8	767.7	9.9
S1455_046	1011.8	3.1	0.9	0.09616	0.00268	0.09883	0.00254	0.00748	0.00012	48.0	0.8	95.7	2.4	1550.9	51.4	-49.8	-96.9		
S1455_047	1959.5	1.3	0.8	0.04967	0.00398	0.01776	0.00135	0.00260	0.00007	16.7	0.5	17.9	1.4	179.7	176.8	-6.7	-90.7	16.7	0.5
S1455_048	338.3	1.2	0.2	0.04596	0.00305	0.08877	0.00570	0.01405	0.00030	89.9	1.9	86.4	5.3	0.1	148.5	4.1	89800.0	89.9	1.9
S1455_049	434.6	1.4	0.7	0.06856	0.00363	0.10570	0.00528	0.01122	0.00024	71.9	1.5	102.0	4.9	885.4	105.9	-29.5	-91.9		
S1455_050	1558.6	5.6	0.1	0.04633	0.00121	0.09391	0.00237	0.01474	0.00020	94.4	1.3	91.1	2.2	14.8	60.8	3.6	537.8	94.4	1.3
S1455_051	671.9	23.7	0.5	0.06738	0.00097	1.27232	0.01855	0.13735	0.00162	829.7	9.2	833.4	8.3	849.6	29.7	-0.4	-2.3	829.7	9.2
S1455_052	2658.7	32.9	0.2	0.06250	0.00084	0.35641	0.00487	0.04148	0.00047	262.0	2.9	309.5	3.7	691.2	28.5	-15.3	-62.1		
S1455_053	1095.2	5.7	0.7	0.05322	0.00134	0.12043	0.00292	0.01646	0.00022	105.2	1.4	115.5	2.6	338.2	56.0	-8.9	-68.9	105.2	1.4
S1455_054	788.9	2.3	0.5	0.04723	0.00233	0.05954	0.00280	0.00917	0.00017	58.8	1.1	58.7	2.7	60.3	113.9	0.2	-2.5	58.8	1.1
S1455_055	248.5	22.2	0.4	0.10958	0.00198	4.61653	0.08335	0.30645	0.00439	1723.2	21.7	1752.3	15.1	1792.4	32.6	-1.7	-3.9	1792.4	32.6
S1455_057	126.7	5.4	1.0	0.06272	0.00154	1.03841	0.02469	0.12043	0.00173	733.1	10.0	723.1	12.3	698.7	51.4	1.4	4.9	733.1	10.0
S1455_058	5498.6	14.9	0.2	0.05691	0.00095	0.07588	0.00125	0.00970	0.00012	62.2	0.7	74.3	1.2	487.4	36.7	-16.3	-87.2		
S1455_059	8341.6	159.4	0.1	0.05870	0.00070	0.68896	0.00857	0.08538	0.00095	528.1	5.6	532.2	5.2	555.9	25.9	-0.8	-5.0	528.1	5.6
S1455_060	1728.6	89.9	0.4	0.07304	0.00099	1.55880	0.02149	0.15524	0.00180	930.3	10.1	954.0	8.5	1015.0	27.2	-2.5	-8.3	930.3	10.1
S1455_061	1244.4	6.8	1.3	0.05041	0.00127	0.09612	0.00235	0.01387	0.00019	88.8	1.2	93.2	2.2	213.9	57.5	-4.7	-58.5	88.8	1.2
S1455_062	38.5	0.1	0.8	0.06602	0.04384	0.07070	0.04629	0.00779	0.00088	50.0	5.7	69.4	43.9	806.9	990.2	-28.0	-93.8		
S1455_063	8004.9	59.9	0.5	0.05295	0.00091	0.13965	0.00237	0.01919	0.00023	122.5	1.5	132.7	2.1	326.4	38.5	-7.7	-62.5	122.5	1.5
S1455_064	590.1	3.7	0.9	0.04820	0.00158	0.10623	0.00335	0.01603	0.00024	102.5	1.5	102.5	3.1	108.9	75.6	0.0	-5.9	102.5	1.5
S1455_065	1250.8	4.4	0.2	0.13285	0.00313	0.22862	0.00487	0.01252	0.00020	80.2	1.2	209.1	4.0	2136.0	40.7	-61.6	-96.2		
S1455_066	4177.2	5.1	0.1	0.05205	0.00209	0.03930	0.00149	0.00549	0.00010	35.3	0.6	39.1	1.5	287.7	89.0	-9.7	-87.7	35.3	0.6
S1455_067	1751.1	5.7	0.1	0.04610	0.00175	0.09096	0.00331	0.01435	0.00024	91.9	1.5	88.4	3.1	2.9	88.1	4.0	3069.0	91.9	1.5
S1455_068	2464.7	7.4	0.4	0.04772	0.00119	0.06704	0.00161	0.01022	0.00014	65.5	0.9	65.9	1.5	84.4	59.1	-0.6	-22.4	65.5	0.9
S1455_069	118.7	2.5	0.3	0.05686	0.00381	0.64161	0.04082	0.08207	0.00228	508.5	13.6	503.3	25.3	485.6	142.0	1.0	4.7	508.5	13.6
S1455_070	484.3	19.4	0.3	0.07058	0.00108	1.40308	0.02161	0.14460	0.00175	870.6	9.8	890.2	9.1	945.1	31.2	-2.2	-7.9	870.6	9.8
S1455_071	910.8	26.5	0.8	0.06047	0.00100	0.79866	0.01310	0.09607	0.00117	591.3	6.9	596.1	7.4	620.4	35.2	-0.8	-4.7	591.3	6.9
S1455_072	213.5	2.9	0.7	0.04400	0.00172	0.06946	0.00261	0.01148	0.00018	73.6	1.2	68.2	2.5	0.1	0.0	7.9	73500.0	73.6	1.2
S1455_073	6149.6	19.1	0.4	0.05430	0.00089	0.07976	0.00130	0.01068	0.00013	68.5	0.8	77.9	1.2	383.3	36.5	-12.1	-82.1	68.5	0.8
S1455_074	795.4	20.1	0.6	0.05866	0.00095	0.67671	0.01090	0.08391	0.00101	519.4	6.0	524.8	6.6	554.5	34.9	-1.0	-6.3	519.4	6.0
S1455_075	1425.6	12.9	0.2	0.05671	0.00130	0.27939	0.00619	0.03584	0.00048	227.0	3.0	250.2	4.9	479.4	50.3	-9.3	-52.6	227.0	3.0
S1455_076	59477.1	72.0	0.1	0.09234	0.00125	0.05391	0.00073	0.00425	0.00005	27.3	0.3	53.3	0.7	1474.3	25.5	-48.8	-98.1		
S1455_077	1011.8	38.6	0.9	0.06750	0.00113	1.11323	0.01844	0.11995	0.00148	730.3	8.5	759.7	8.9	853.4	34.3	-3.9	-14.4	730.3	8.5
S1455_078	2697.2	10.9	0.7	0.04922	0.00103	0.09173	0.00187	0.01356	0.00017	86.8	1.1	89.1	1.7	158.3	48.2	-2.6	-45.2		
S1455_079	923.6	143.4	0.6	0.16149	0.00188	10.01170	0.12282	0.45092	0.00511	2399.3	22.7	2435.9	11.3	2471.4	19.6	-1.5	-2.9	2471.4	19.6
S1455_080	1796.0	30.0	0.3	0.05769	0.00080	0.60494	0.00852	0.07626	0.00088	473.8	5.3	480.4	5.4	517.9	30.4	-1.4	-8.5	473.8	5.3
S1455_081	768.1	23.7	1.9	0.05812	0.00094	0.64096	0.01033	0.08022	0.00096	497.4	5.7	502.9	6.4	533.7	35.5	-1.1	-6.8	497.4	5.7
S1455_082	718.4	3.7	0.9	0.05489	0.00175	0.12292	0.00374	0.01629	0.00025	104.2	1.6	117.7	3.4	407.8	69.2	-11.5	-74.4	104.2	1.6
S1455_083	1072.8	2.3	0.8	0.04878	0.00235	0.04892	0.00226	0.00729	0.00014	46.9	0.9	48.5	2.2	137.2	109.6	-3.3	-65.8	46.9	0.9
S1455_084	3558.3	5.1	0.3	0.04810	0.00163	0.03789	0.00122	0.00573	0.00009	36.8	0.6	37.8	1.2	104.3	78.1	-2.6	-64.7	36.8	0.6
S1455_085	1627.6	61.0	0.2	0.07394	0.00104	1.62261	0.02310	0.15962	0.00188	954.7	10.4	979.0	8.9	1039.8	28.0	-2.5	-8.2	954.7	10.4
S1455_086	1167.4	50.7	0.3	0.06895	0.00089	1.46749	0.01945	0.15480	0.00176	927.8	9.9	917.1	8.0	897.3	26.4	1.2	3.4	927.8	9.9
S1455_087	1329.3	9.6	0.4	0.05145	0.00114	0.18093	0.00390	0.02558	0.00033	162.8	2.1	168.9	3.4	261.0	50.3	-3.6	-37.6	162.8	2.1
S1455_088	384.9	1.9	0.9	0.04724	0.00268	0.12380	0.00673	0.01906	0.00039	121.7	2.5	118.5	6.1	61.0	130.3	2.7	99.5	121.7	2.5
S1455_089	421.7	12.8	0.5	0.06029	0.00115	0.84002	0.01579	0.10133	0.00130	622.2	7.6	619.2	8.7	614.1	40.8	0.5	1.3	622.2	7.6
S1455_090	1217.1	0.8	0.6	0.05604	0.00729	0.01909	0.00235	0.00248	0.00011	16.0	0.7	19.2	2.3	453.5	265.8	-16.7	-96.5		
S1455_091	367.2	50.7	1.0	0.15777	0.00203	10.69038	0.14377	0.49281	0.00598	2582.8	25.8	2496.6	12.5	2431.9	21.6	3.5	6.2	2431.9	21.6
S1455_092	383.2	12.5	0.4	0.06590	0.00137	1.08882	0.02207	0.12018	0.00162	731.6	9.3	747.9	10.7	803.1	42.9	-2.2	-8.9	731.6	9.3
S1455_093	322.3	1.1	0.9	0.06432	0.00495	0.10758	0.00776	0.01217	0.00036	77.9	2.3	103.8	7.1	752.2	154.7	-25.0	-89.6		
S1455_094	365.6	35.5	0.7	0.11604	0.00162	5.19205	0.07446	0.32544	0.00401	1816.2	19.5	1851.3	12.2	1896.0	25.0	-1.9	-4.2	1896.0	25.0
S1455_095	380.0	1.1	0.6	0.04955	0.00426	0.07028	0.00578	0.01032	0.00029	66.2	1.9	69.0	5.5	173.8	189.1	-4.1	-61.9	66.2	1.9
S1455_096	1621.2	9.0	0.5	0.08021	0.00237	0.16759	0.00459	0.01520	0.00025	97.2	1.6	157.3	4.0	1202.2	57.1	-38.2	-91.9		
S1455_097	336.7	0.6	0.8	0.04558	0.00631	0.04685	0.00634	0.00748	0.00024	48.0	1.5	46.5	6.2	0.1	280.4	3.2	47900.0	48.0	1.5
S1455_098	524.4	2.4	0.6	0.05192	0.00209	0.09877	0.00381	0.01384	0.00023	88.6	1.4	95.6	3.5	281.9	89.3	-7.3	-68.6	88.6	1.4
S1455_099	821.0	97.8	0.4	0.16320	0.00196	10.73856	0.13525	0.47856	0.00550	2521.0	24.0	2500.8	11.7	2489.1	20.1	0.8	1.3	2489.1	20.1
S1455_100	829.0	21.3	0.6	0.06083	0.00097	0.84975	0.01354	0.10159	0.00122	623.7	7.2	624.5	7.4	633.3	34.0	-0.1	-1.5	623.7	7.2
S1455_101	575.7	17.1	0.3	0.06676	0.00104	1.11736	0.01739	0.12173	0.00146	740.5	8.4	761.7	8.3	830.2	32.0	-2.8	-10.8	740.5	8.4
S1455_102	737.6	33.7	0.4	0.08062	0.00116	2.15310	0.03134	0.19423	0.00232	1144.2	12.5	1166.1	10.1	1212.3	28.0	-1.9	-5.6	1212.3	28.0
S1455_103	285.4	0.6	0.8	0.04425	0.00548	0.04190	0.00503	0.00689	0.00023	44.2	1.5	41.7	4.9	0.1	182.4	6.0	44100.0	44.2	1.5
S1455_104	3657.7	35.5	0.4	0.05923	0.00081	0.34180	0.00476	0.04197	0.00048	265.0	3.0	298.5	3.6	575.6	29.4	-11.2	-54.0	265.0	3.0
S1455_105	277.4	10.0	0.6	0.06679	0.00137	1.27881	0.02571	0.13925	0.00189	840.4	10.7	836.3	11.5	831.3	42.2	0.5	1.1	840.4	10.7
S1455_106	771.3	24.2	0.4	0.07107	0.00115	1.59902	0.02582	0.16362	0.00202	976.9	11.2	969.8	10.1	959.5	32.6	0.7	1.8	976.9	11.2
S1455_107	340.0	1.2	0.4	0.08846	0.00727	0.15414	0.01152	0.01267	0.00047	81.2	3.0	145.6	10.1	1392.6	149.9	-44.2	-94.2	81.2	3.0
S1455_108	1545.8	6.3	0.9	0.04957	0.00153	0.08421	0.00249	0.01236	0.00018	79.2	1.2	82.1	2.3	174.7	70.5	-3.5	-54.7	79.2	1.2
S1455_109	3595.2	16.8	0.5	0.04941	0.00096	0.12683	0.00241	0.01867	0.00023	119.2	1.5	121.2	2.2	167.3	44.6	-1.7	-28.8	119.2	1.5
S1455_110	883.6	3.9	0.7	0.05320	0.00250	0.11707	0.00520	0.01601	0.00032	102.4	2.0	112.4	4.7	337.1	102.8	-8.9	-69.6	102.4	2.0
S1455_111	806.6	3.7	0.8	0.04763	0.00181	0.10914	0.00398	0.01666	0.00027	106.5	1.7	105.2	3.6	80.2	88.9	1.2	32.8	106.5	1.7
S1455_112	681.5	3.2	0.7	0.04936	0.00181	0.10979	0.00386	0.01618	0.00026	103.4	1.6	105.8	3.5	164.9	83.5	-2.3	-37.3	103.4	1.6
S1455_113	3024.3	6.4	1.1	0.04941	0.00136	0.04937	0.00131	0.00727	0.00010	46.7	0.7	48.9	1.3	167.1	63.0	-4.5	-72.1	46.7	0.7
S1455_114	421.7	2.6	0.7	0.06183	0.00262	0.36387	0.01463	0.04280	0.00081	270.2	5.0	315.1	10.9	668.2	88.3	-14.2	-59.6		
S1455_115	1329.3	39.4	0.2	0.06911	0.00098	1.42035	0.02053	0.14948	0.00176	898.0	9.9	897.5	8.6	901.9	29.1	0.1	-0.4	898.0	9.9
S1455_116	1246.0	4.3	1.2	0.04694	0.00172	0.06005	0.00212	0.00930	0.00015	59.7	0.9	59.2	2.0	45.7	85.8	0.8	30.6	59.7	0.9
S1455_117	449.0	4.7	0.2	0.08053	0.00184	0.43117	0.00937	0.03894	0.00055	246.2	3.4	364.0	6.7	1210.0	44.4	-32.4	-79.7		
S1455_118	420.1	14.4	0.8	0.07685	0.00145	1.69821	0.03143	0.16070	0.00214	960.6	11.9	1007.9	11.8	1117.4	37.1	-4.7	-14.0	960.6	11.9
S1455_119	825.8	19.1	0.5	0.06836	0.00170	0.97840	0.02341	0.10409	0.00155	638.3	9.1	692.8	12.0	879.4	50.7	-7.9	-27.4	638.3	9.1
S1455_120	952.5	2.1	1.1	0.05137	0.00275	0.04883	0.00249	0.00691	0.00014	44.4	0.9	48.4	2.4	257.4	118.6	-8.3	-82.8	44.4	0.9
S1455_121	269.4	8.4	0.7	0.06488	0.00144	1.06408	0.02294	0.11927	0.00166	726.4	9.6	735.8	11.3	770.5	46.0	-1.3	-5.7	726.4	9.6
S1455_122	458.6	1.8	0.8	0.05139	0.00276	0.11606	0.00594	0.01642	0.00034	105.0	2.2	111.5	5.4	258.5	118.9	-5.8	-59.4	105.0	2.2
S1455_123	1146.5	6.9	0.4	0.06347	0.00148	0.22206	0.00498	0.02544	0.00035	162.0	2.2	203.6	4.1	723.9	48.7	-20.4	-77.6		
S1455_124	2751.7	17.4	1.1	0.08583	0.00136	0.25673	0.00400	0.02175	0.00026	138.7	1.7	232.0	3.2	1334.4	30.3	-40.2	-89.6		
S1455_125	157.1	0.4	0.6	0.05192	0.00859	0.06418	0.01022	0.00899	0.00042	57.7	2.7	63.2	9.8	281.9	339.9	-8.7	-79.5	57.7	2.7
S1455_126	501.9	10.9	0.0	0.06780	0.00159	1.10643	0.02517	0.11867	0.00172	722.9	9.9	756.5	12.1	862.6	48.0	-4.4	-16.2	722.9	9.9
S1455_127	1207.5	4.9	0.7	0.04903	0.00163	0.10611	0.00338	0.01574	0.00024	100.7	1.5	102.4	3.1	149.0	76.0	-1.7	-32.4	100.7	1.5
S1455_128	224.5	0.7	0.7	0.04527	0.00688	0.07276	0.01067	0.01169	0.00050	74.9	3.2	71.3	10.1	0.1	291.7	5.0	74800.0	74.9	3.2
S1455_129	139.5	0.4	0.4	0.06933	0.00706	0.12027	0.01175	0.01261	0.00040	80.8	2.5	115.3	10.7	908.6	196.7	-29.9	-91.1		
S1455_130	2660.3	219.2	0.1	0.12421	0.00151	5.33891	0.06786	0.31257	0.00354	1753.4	17.4	1875.1	10.9	2017.5	21.5	-6.5	-13.1	2017.5	21.5
S1455_131	365.6	1.1	0.6	0.04649	0.00580	0.06443	0.00769	0.01008	0.00040	64.6	2.5	63.4	7.3	23.2	275.2	1.9	178.4	64.6	2.5
S1455_132	383.2	0.8	1.0	0.05371	0.00469	0.07670	0.00643	0.01038	0.00028	66.6	1.8	75.0	6.1	358.9	185.9	-11.2	-81.4	66.6	1.8
S1455_133	1175.4	14.2	0.5	0.05411	0.00122	0.35648	0.00778	0.04791	0.00064	301.7	3.9	309.6	5.8	375.6	49.8	-2.6	-19.7	301.7	3.9
S1455_134	248.5	0.6	0.7	0.04152	0.00554	0.06108	0.00799	0.01070	0.00031	68.6	2.0	60.2	7.6	0.1	51.9	14.0	68500.0	68.6	2.0
S1455_135	1497.7	6.1	0.4	0.04916	0.00151	0.11947	0.00352	0.01767	0.00026	112.9	1.7	114.6	3.2	155.6	70.4	-1.5	-27.4	112.9	1.7
S1455_136	984.6	57.5	0.4	0.12029	0.00158	4.13880	0.05609	0.25020	0.00294	1439.5	15.2	1662.0	11.1	1960.6	23.3	-13.4	-26.6		
S1455_137	1284.4	26.2	0.2	0.06058	0.00107	0.86797	0.01514	0.10419	0.00130	638.9	7.6	634.5	8.2	624.2	37.5	0.7	2.4	638.9	7.6
S1455_138	1202.7	54.3	0.2	0.09237	0.00121	2.94448	0.03985	0.23182	0.00269	1344.0	14.1	1393.4	10.3	1474.8	24.8	-3.5	-8.9	1474.8	24.8
S1455_139	1023.1	35.0	0.6	0.07101	0.00106	1.61116	0.02434	0.16499	0.00198	984.5	10.9	974.6	9.5	957.7	30.1	1.0	2.8	984.5	10.9
S1455_140	1577.9	41.0	0.3	0.06786	0.00108	1.37695	0.02195	0.14756	0.00180	887.3	10.1	879.1	9.4	864.2	32.6	0.9	2.7	887.3	10.1
S1455_141	667.1	61.4	0.5	0.13717	0.00179	7.36987	0.09995	0.39071	0.00463	2126.1	21.5	2157.3	12.1	2191.7	22.5	-1.4	-3.0	2191.7	22.5
S1455_142	476.3	13.5	0.5	0.06797	0.00122	1.22748	0.02183	0.13132	0.00167	795.4	9.5	813.2	10.0	867.7	36.8	-2.2	-8.3	795.4	9.5
S1455_143	970.1	2.9	0.3	0.04850	0.00180	0.11456	0.00408	0.01718	0.00028	109.8	1.8	110.1	3.7	123.6	85.2	-0.3	-11.2	109.8	1.8
S1455_144	222.9	0.6	0.5	0.04485	0.00505	0.07625	0.00833	0.01236	0.00037	79.2	2.4	74.6	7.9	0.1	190.2	6.2	79100.0	79.2	2.4
S1455_145	9913.1	11.5	0.4	0.05867	0.00152	0.04689	0.00116	0.00581	0.00008	37.4	0.5	46.5	1.1	554.8	55.6	-19.6	-93.3		
S1455_146	7222.4	805.6	0.2	0.20514	0.00245	15.29469	0.19165	0.54216	0.00606	2792.5	25.3	2833.8	11.9	2867.5	19.3	-1.5	-2.6	2867.5	19.3
S1455_147	788.9	7.3	0.5	0.05180	0.00162	0.31854	0.00956	0.04471	0.00069	282.0	4.3	280.8	7.4	276.7	70.1	0.4	1.9	282.0	4.3
S1455_148	1541.0	2.9	0.8	0.05267	0.00190	0.05131	0.00177	0.00711	0.00011	45.5	0.7	50.8	1.7	314.5	80.0	-10.4	-85.5	45.5	0.7
S1455_149	3226.3	155.5	0.3	0.15367	0.00188	5.57274	0.07114	0.26369	0.00298	1508.7	15.2	1911.9	11.0	2387.2	20.7	-21.1	-36.8		
S1455_150	639.8	2.4	0.6	0.06709	0.00293	0.14975	0.00613	0.01623	0.00032	103.8	2.0	141.7	5.4	840.7	88.5	-26.7	-87.7		
S1455_151	3529.4	14.0	1.5	0.05195	0.00104	0.13414	0.00263	0.01878	0.00024	119.9	1.5	127.8	2.4	283.0	45.2	-6.2	-57.6	119.9	1.5
S1455_152	633.4	42.7	1.7	0.11768	0.00163	5.77538	0.08259	0.35684	0.00433	1967.2	20.6	1942.7	12.4	1921.4	24.7	1.3	2.4	1921.4	24.7
S1455_153	322.3	20.8	0.7	0.11393	0.00182	5.38764	0.08739	0.34386	0.00454	1905.2	21.8	1882.9	13.9	1863.0	28.5	1.2	2.3	1863.0	28.5
S1455_154	1454.4	55.6	0.6	0.09236	0.00126	2.78800	0.03895	0.21949	0.00257	1279.2	13.6	1352.3	10.4	1474.7	25.7	-5.4	-13.3	1474.7	25.7
S1455_155	413.7	15.5	0.7	0.09819	0.00178	3.46177	0.06239	0.25636	0.00352	1471.2	18.1	1518.6	14.2	1590.0	33.4	-3.1	-7.5	1590.0	33.4
S1455_156	24766.8	40.0	1.7	0.11672	0.00173	0.14770	0.00217	0.00920	0.00011	59.0	0.7	139.9	1.9	1906.5	26.4	-57.8	-96.9		
S1455_157	75.4	0.3	1.0	0.05648	0.00900	0.15906	0.02469	0.02048	0.00080	130.7	5.1	149.9	21.6	470.4	319.3	-12.8	-72.2	130.7	5.1
S1455_158	1026.3	2.8	0.8	0.05902	0.00329	0.10315	0.00539	0.01271	0.00030	81.4	1.9	99.7	5.0	567.9	117.0	-18.4	-85.7		
S1455_159	1662.9	15.1	0.3	0.05127	0.00093	0.36433	0.00652	0.05167	0.00063	324.7	3.9	315.4	4.9	253.1	41.0	2.9	28.3	324.7	3.9
S1455_160	1199.5	11.1	0.3	0.05284	0.00100	0.44170	0.00829	0.06078	0.00076	380.4	4.6	371.5	5.8	321.8	42.5	2.4	18.2	380.4	4.6
S1455_161	1808.8	6.3	0.5	0.04995	0.00123	0.11738	0.00281	0.01709	0.00023	109.2	1.5	112.7	2.6	192.8	56.4	-3.1	-43.4	109.2	1.5
S1455_162	3883.8	5.3	0.7	0.05577	0.00147	0.05988	0.00152	0.00781	0.00011	50.1	0.7	59.0	1.5	443.1	57.5	-15.1	-88.7		
S1455_163	5798.4	15.4	0.6	0.05134	0.00094	0.11037	0.00199	0.01563	0.00019	100.0	1.2	106.3	1.8	256.3	41.5	-5.9	-61.0	100.0	1.2
S1455_164	391.3	1.0	0.6	0.05386	0.00358	0.09379	0.00596	0.01266	0.00029	81.1	1.9	91.0	5.5	364.9	142.9	-10.9	-77.8	81.1	1.9
S1455_165	1637.2	23.5	0.3	0.05838	0.00092	0.69552	0.01099	0.08662	0.00103	535.5	6.1	536.1	6.6	544.2	34.0	-0.1	-1.6	535.5	6.1
S1455_166	1813.6	23.4	0.9	0.05761	0.00097	0.58216	0.00973	0.07347	0.00089	457.0	5.4	465.9	6.3	514.8	36.7	-1.9	-11.2	457.0	5.4
S1455_167	787.3	1.0	0.5	0.04793	0.00347	0.05089	0.00354	0.00772	0.00018	49.6	1.2	50.4	3.4	94.8	164.0	-1.6	-47.7	49.6	1.2
S1455_168	1752.7	6.1	1.1	0.05257	0.00232	0.09327	0.00390	0.01290	0.00024	82.6	1.6	90.5	3.6	310.2	97.6	-8.7	-73.4	82.6	1.6
S1455_169	1109.7	43.5	0.3	0.11537	0.00156	3.78950	0.05280	0.23882	0.00281	1380.6	14.7	1590.5	11.2	1885.6	24.2	-13.2	-26.8		
S1455_170	1197.8	139.7	0.5	0.18122	0.00227	13.58088	0.17824	0.54487	0.00624	2803.8	26.0	2720.9	12.4	2664.1	20.7	3.0	5.2	2664.1	20.7
S1455_171	503.5	1.4	0.6	0.04582	0.00380	0.10258	0.00816	0.01628	0.00044	104.1	2.8	99.2	7.5	0.1	177.2	4.9	104000.0	104.1	2.8
S1455_172	1234.7	19.4	0.4	0.06034	0.00105	0.83551	0.01441	0.10067	0.00124	618.3	7.3	616.7	8.0	615.9	37.0	0.3	0.4	618.3	7.3
S1455_173	641.4	1.9	1.5	0.06328	0.00449	0.10627	0.00706	0.01221	0.00034	78.2	2.2	102.6	6.5	717.6	143.9	-23.8	-89.1		
S1455_174	1634.0	4.1	0.1	0.05172	0.00146	0.11462	0.00311	0.01611	0.00023	103.0	1.5	110.2	2.8	273.2	63.4	-6.5	-62.3	103.0	1.5
S1455_175	1587.5	39.0	0.8	0.06565	0.00095	1.28334	0.01899	0.14212	0.00167	856.7	9.4	838.3	8.4	795.3	30.2	2.2	7.7	856.7	9.4
S1455_176	413.7	1.6	0.7	0.10961	0.00418	0.20739	0.00719	0.01376	0.00028	88.1	1.8	191.4	6.1	1793.0	67.9	-54.0	-95.1		
S1455_177	2261.0	308.5	0.4	0.30738	0.00384	31.15716	0.40705	0.73696	0.00838	3559.3	31.1	3524.0	12.9	3507.8	19.2	1.0	1.5	3507.8	19.2
S1455_178	1666.1	2.4	1.1	0.07211	0.00265	0.06507	0.00224	0.00656	0.00012	42.1	0.7	64.0	2.1	989.2	72.9	-34.2	-95.7		
S1455_179	1395.1	53.1	0.4	0.11434	0.00198	3.44354	0.05932	0.21895	0.00295	1276.4	15.6	1514.4	13.6	1869.6	31.0	-15.7	-31.7		
S1455_180	41225.6	60.2	4.9	0.07357	0.00111	0.04233	0.00064	0.00418	0.00005	26.9	0.3	42.1	0.6	1029.7	30.2	-36.1	-97.4		
S1455_181	2285.1	5.0	0.8	0.04833	0.00157	0.06894	0.00215	0.01037	0.00016	66.5	1.0	67.7	2.0	115.7	74.9	-1.8	-42.5	66.5	1.0
S1455_182	934.9	73.8	0.6	0.15156	0.00200	9.49269	0.13003	0.45536	0.00535	2419.0	23.7	2386.8	12.6	2363.6	22.3	1.3	2.3	2363.6	22.3

Sample S1455 Indus River @ Kalabagh 359 grains analysed 282 concordant ages

grain	concentrations U [ppm]	Pb [ppm]	Th/U	isotopic ratios Pb207/Pb206	2σ 76	Pb207/U235	2σ 75	Pb206/U238	2σ 68	ages age 206/238	2σ age 68	age 207/235	2σ age 75	age 207/206	2σ age 76	discordance Δ 68-75 [%]	Δ 68-76 [%]	preferred age age	2σ age
S1455_183	1853.7	8.9	0.3	0.04991	0.00120	0.22506	0.00524	0.03278	0.00044	207.9	2.8	206.1	4.3	190.9	54.9	0.9	8.9	207.9	2.8
S1455_184	3866.2	5.1	0.8	0.05155	0.00250	0.04633	0.00212	0.00653	0.00013	42.0	0.8	46.0	2.1	265.6	107.6	-8.7	-84.2	42.0	0.8
S1455_185	495.5	0.6	1.1	0.05921	0.00779	0.06789	0.00856	0.00834	0.00034	53.5	2.2	66.7	8.1	574.8	262.9	-19.8	-90.7		
S1455_186	1265.2	2.8	1.8	0.11887	0.00649	0.14399	0.00694	0.00881	0.00025	56.5	1.6	136.6	6.2	1939.3	94.6	-58.6	-97.1		
S1455_187	418.5	1.0	0.9	0.04520	0.00396	0.09390	0.00797	0.01510	0.00038	96.6	2.4	91.1	7.4	0.1	155.2	6.0	96500.0	96.6	2.4
S1455_188	7597.6	107.7	0.2	0.06116	0.00082	0.89598	0.01243	0.10651	0.00122	652.5	7.1	649.6	6.7	644.7	28.7	0.4	1.2	652.5	7.1
S1455_189	1092.0	1.8	0.4	0.04480	0.00237	0.05184	0.00264	0.00841	0.00016	54.0	1.0	51.3	2.6	0.1	57.0	5.3	53900.0	54.0	1.0
S1455_190	3919.1	19.3	0.2	0.04694	0.00086	0.10518	0.00192	0.01629	0.00020	104.2	1.3	101.5	1.8	45.9	42.7	2.7	127.0	104.2	1.3
S1455_191	2228.9	3.4	1.6	0.05319	0.00223	0.05815	0.00232	0.00795	0.00014	51.0	0.9	57.4	2.2	337.0	92.1	-11.1	-84.9	51.0	0.9
S1455_192	147.5	0.3	0.3	0.05359	0.00729	0.11224	0.01475	0.01523	0.00058	97.4	3.7	108.0	13.5	353.7	281.2	-9.8	-72.5	97.4	3.7
S1455_193	2836.7	2.6	0.7	0.05359	0.00203	0.04072	0.00147	0.00552	0.00009	35.5	0.6	40.5	1.4	353.9	83.0	-12.3	-90.0	35.5	0.6
S1455_194	3510.2	7.3	0.6	0.04828	0.00171	0.10007	0.00338	0.01507	0.00024	96.4	1.5	96.8	3.1	113.1	81.5	-0.4	-14.8	96.4	1.5
S1455_195	3125.3	4.0	0.4	0.04788	0.00141	0.05595	0.00159	0.00850	0.00012	54.5	0.8	55.3	1.5	92.1	69.5	-1.4	-40.8	54.5	0.8
S1455_196	1840.9	3.1	0.2	0.05772	0.00201	0.07532	0.00249	0.00949	0.00016	60.9	1.0	73.7	2.4	518.9	75.1	-17.4	-88.3		
S1455_197	824.2	23.8	1.0	0.06279	0.00121	0.94867	0.01803	0.10983	0.00142	671.8	8.3	677.4	9.4	701.2	40.5	-0.8	-4.2	671.8	8.3
S1455_198	771.3	2.6	0.7	0.04696	0.00236	0.11871	0.00572	0.01838	0.00035	117.4	2.2	113.9	5.2	47.1	116.2	3.1	149.3	117.4	2.2
S1455_199	1095.2	34.3	0.8	0.06775	0.00101	1.10117	0.01670	0.11817	0.00140	720.0	8.1	753.9	8.1	860.8	30.7	-4.5	-16.4	720.0	8.1
S1455_200	434.6	21.9	1.2	0.07185	0.00120	1.56411	0.02615	0.15824	0.00197	947.0	11.0	956.1	10.4	981.8	33.6	-1.0	-3.5	947.0	11.0
S1455_201	2806.2	13.4	0.8	0.05355	0.00105	0.11259	0.00216	0.01529	0.00019	97.8	1.2	108.3	2.0	351.9	43.7	-9.7	-72.2	97.8	1.2
S1455_202	10320.4	82.1	1.7	0.05256	0.00075	0.13629	0.00199	0.01885	0.00022	120.4	1.4	129.7	1.8	310.0	32.3	-7.2	-61.2	120.4	1.4
S1455_203	2586.5	69.8	0.4	0.05763	0.00081	0.68976	0.00997	0.08700	0.00101	537.8	6.0	532.7	6.0	515.5	31.0	1.0	4.3	537.8	6.0
S1455_204	3558.3	72.0	1.0	0.05933	0.00084	0.67332	0.00980	0.08249	0.00096	511.0	5.7	522.7	5.9	579.4	30.6	-2.2	-11.8	511.0	5.7
S1455_205	6430.2	662.3	0.1	0.16117	0.00210	5.62573	0.07618	0.25374	0.00290	1457.7	14.9	1920.0	11.7	2468.0	21.9	-24.1	-40.9		
S1455_207	2195.3	113.8	0.6	0.06807	0.00099	1.14377	0.01692	0.12215	0.00144	742.9	8.3	774.3	8.0	870.6	29.8	-4.1	-14.7	742.9	8.3
S1455_209	2012.5	44.8	0.6	0.06005	0.00088	0.54615	0.00818	0.06611	0.00078	412.7	4.7	442.5	5.4	605.4	31.5	-6.7	-31.8	412.7	4.7
S1455_210	6932.1	42.8	0.0	0.05019	0.00074	0.15048	0.00226	0.02179	0.00025	139.0	1.6	142.3	2.0	204.0	33.9	-2.3	-31.9	139.0	1.6
S1455_211	3312.9	100.4	0.4	0.05999	0.00083	0.69543	0.00985	0.08427	0.00097	521.6	5.8	536.1	5.9	603.0	29.5	-2.7	-13.5	521.6	5.8
S1455_213	2628.2	10.7	0.9	0.04931	0.00103	0.07582	0.00155	0.01118	0.00014	71.7	0.9	74.2	1.5	162.4	48.1	-3.4	-55.8	71.7	0.9
S1455_214	346.4	25.6	0.9	0.07808	0.00122	1.82303	0.02883	0.16971	0.00207	1010.5	11.4	1053.8	10.4	1149.0	30.8	-4.1	-12.1	1010.5	11.4
S1455_215	1779.9	177.1	0.3	0.11671	0.00158	4.11999	0.05776	0.25660	0.00298	1472.4	15.3	1658.3	11.5	1906.5	24.2	-11.2	-22.8	1906.5	24.2
S1455_216	17746.5	129.1	0.0	0.05091	0.00071	0.18244	0.00260	0.02605	0.00030	165.8	1.9	170.2	2.2	236.9	31.6	-2.6	-30.0	165.8	1.9
S1455_217	9555.5	210.9	0.2	0.06218	0.00084	0.62631	0.00874	0.07322	0.00084	455.5	5.1	493.8	5.5	680.3	28.6	-7.8	-33.0	455.5	5.1
S1455_218	383.2	20.9	0.6	0.06969	0.00113	1.45608	0.02386	0.15187	0.00186	911.4	10.4	912.4	9.9	919.3	33.1	-0.1	-0.9	911.4	10.4
S1455_219	784.1	138.8	0.6	0.17213	0.00231	10.42727	0.14534	0.44034	0.00512	2352.2	22.9	2473.5	12.9	2578.4	22.3	-4.9	-8.8	2578.4	22.3
S1455_220	2168.0	13.4	0.7	0.05475	0.00103	0.12918	0.00240	0.01715	0.00021	109.6	1.4	123.4	2.2	402.0	41.4	-11.2	-72.7	109.6	1.4
S1455_221	1205.9	112.3	0.5	0.11551	0.00157	4.58391	0.06456	0.28845	0.00335	1633.8	16.8	1746.3	11.7	1887.9	24.3	-6.4	-13.5	1887.9	24.3
S1455_222	2034.9	92.4	1.1	0.06761	0.00114	0.63149	0.01059	0.06789	0.00083	423.4	5.0	497.0	6.6	856.8	34.6	-14.8	-50.6		
S1455_223	15932.8	47.9	0.5	0.05689	0.00085	0.06973	0.00106	0.00891	0.00010	57.2	0.7	68.4	1.0	486.7	33.0	-16.4	-88.2		
S1455_224	2323.5	141.9	0.5	0.08739	0.00119	2.22132	0.03133	0.18476	0.00214	1092.9	11.6	1187.8	9.9	1369.1	26.1	-8.0	-20.2	1092.9	11.6
S1455_225	1646.8	80.2	0.5	0.07123	0.00100	1.38594	0.02007	0.14143	0.00165	852.7	9.3	883.0	8.5	964.0	28.5	-3.4	-11.5	852.7	9.3
S1455_226	3122.1	17.1	0.5	0.04993	0.00114	0.09568	0.00212	0.01393	0.00018	89.2	1.2	92.8	2.0	191.8	52.2	-3.9	-53.5	89.2	1.2
S1455_227	12589.4	9.5	0.2	0.04870	0.00101	0.01767	0.00036	0.00264	0.00003	17.0	0.2	17.8	0.4	133.6	47.9	-4.5	-87.3	17.0	0.2
S1455_228	6196.1	12.0	1.8	0.05117	0.00111	0.03244	0.00068	0.00461	0.00006	29.6	0.4	32.4	0.7	248.5	49.0	-8.6	-88.1	29.6	0.4
S1455_229	2107.1	151.3	0.5	0.11083	0.00156	3.09978	0.04482	0.20329	0.00239	1193.0	12.8	1432.6	11.1	1813.1	25.4	-16.7	-34.2		
S1455_230	4398.5	9.5	1.7	0.09972	0.00223	0.10134	0.00213	0.00739	0.00011	47.4	0.7	98.0	2.0	1618.8	41.0	-51.6	-97.1		
S1455_231	2225.7	6.4	0.6	0.09636	0.00335	0.09695	0.00307	0.00731	0.00014	47.0	0.9	94.0	2.8	1554.9	63.9	-50.0	-97.0		
S1455_232	1385.5	71.6	0.4	0.07176	0.00112	1.50152	0.02366	0.15208	0.00184	912.6	10.3	931.0	9.6	979.2	31.4	-2.0	-6.8	912.6	10.3
S1455_233	2668.3	49.2	0.5	0.06109	0.00095	0.71208	0.01122	0.08473	0.00101	524.3	6.0	546.0	6.7	642.2	33.1	-4.0	-18.4	524.3	6.0
S1455_234	9491.4	736.0	0.1	0.11673	0.00159	4.37684	0.06157	0.27252	0.00314	1553.6	15.9	1708.0	11.6	1906.8	24.2	-9.0	-18.5	1906.8	24.2
S1455_235	2254.6	37.4	0.3	0.06652	0.00101	0.71923	0.01109	0.07859	0.00093	487.7	5.6	550.2	6.6	822.7	31.4	-11.4	-40.7	487.7	5.6
S1455_236	782.5	92.7	1.2	0.12851	0.00180	6.15574	0.08912	0.34815	0.00411	1925.8	19.6	1998.2	12.7	2077.7	24.5	-3.6	-7.3	2077.7	24.5
S1455_237	894.8	2.8	1.2	0.05107	0.00195	0.08473	0.00309	0.01206	0.00020	77.3	1.3	82.6	2.9	243.8	85.4	-6.4	-68.3	77.3	1.3
S1455_238	1205.1	10.3	0.6	0.05596	0.00101	0.13739	0.00259	0.01785	0.00025	114.1	1.6	130.7	2.3	450.5	39.4	-12.7	-74.7	114.1	1.6
S1455_239	1466.0	5.1	0.7	0.05210	0.00134	0.05826	0.00149	0.00813	0.00012	52.2	0.8	57.5	1.4	289.8	57.8	-9.2	-82.0	52.2	0.8
S1455_240	164.7	1.5	0.6	0.06046	0.00279	0.13068	0.00573	0.01571	0.00033	100.5	2.1	124.7	5.1	620.2	96.7	-19.4	-83.8		
S1455_241	702.8	3.5	0.8	0.06452	0.00187	0.08404	0.00237	0.00947	0.00016	60.8	1.0	81.9	2.2	758.6	60.1	-25.8	-92.0		
S1455_242	407.7	3.8	1.6	0.05505	0.00321	0.10137	0.00557	0.01339	0.00033	85.7	2.1	98.0	5.1	414.1	124.6	-12.6	-79.3	85.7	2.1
S1455_243	1909.6	16.6	0.2	0.05290	0.00087	0.14432	0.00253	0.01983	0.00027	126.6	1.7	136.9	2.2	324.6	36.7	-7.5	-61.0	126.6	1.7
S1455_244	715.9	6.6	0.3	0.04827	0.00138	0.11034	0.00311	0.01662	0.00026	106.3	1.7	106.3	2.8	112.4	66.1	0.0	-5.4	106.3	1.7
S1455_245	1813.4	113.2	0.1	0.06733	0.00076	1.19238	0.01619	0.12876	0.00166	780.8	9.5	797.1	7.5	847.9	23.3	-2.0	-7.9	780.8	9.5
S1455_246	658.8	39.9	0.5	0.06594	0.00082	1.27988	0.01850	0.14111	0.00185	850.9	10.4	836.8	8.2	804.5	25.9	1.7	5.8	850.9	10.4
S1455_247	300.1	12.0	0.6	0.05955	0.00108	0.87415	0.01659	0.10672	0.00151	653.7	8.8	637.8	9.0	587.2	38.7	2.5	11.3	653.7	8.8
S1455_248	1275.2	53.1	0.3	0.06055	0.00073	0.84619	0.01192	0.10160	0.00132	623.8	7.7	622.6	6.6	623.2	25.6	0.2	0.1	623.8	7.7
S1455_249	109.3	8.7	0.9	0.06875	0.00195	1.24707	0.03479	0.13188	0.00232	798.6	13.2	822.1	15.7	891.1	57.6	-2.9	-10.4	798.6	13.2
S1455_250	140.2	1.0	0.9	0.04753	0.00322	0.08472	0.00555	0.01296	0.00030	83.0	1.9	82.6	5.2	75.2	154.1	0.5	10.4	83.0	1.9
S1455_251	1632.4	20.1	0.2	0.05337	0.00078	0.19058	0.00308	0.02596	0.00035	165.2	2.2	177.1	2.6	344.5	32.8	-6.7	-52.0	165.2	2.2
S1455_252	3135.9	162.3	0.1	0.06028	0.00066	0.89708	0.01193	0.10819	0.00138	662.2	8.1	650.2	6.4	613.7	23.4	1.8	7.9	662.2	8.1
S1455_253	318.0	30.0	2.3	0.06136	0.00089	0.78960	0.01267	0.09356	0.00126	576.5	7.4	590.9	7.2	651.8	30.9	-2.4	-11.6	576.5	7.4
S1455_254	1743.2	174.5	0.4	0.10404	0.00120	1.62746	0.02232	0.11373	0.00148	694.3	8.6	980.9	8.6	1697.4	21.1	-29.2	-59.1		
S1455_255	5131.9	42.1	0.9	0.05822	0.00076	0.08889	0.00132	0.01110	0.00015	71.2	0.9	86.5	1.2	537.4	28.8	-17.7	-86.8		
S1455_256	6674.6	21.7	0.4	0.05164	0.00075	0.04378	0.00070	0.00616	0.00008	39.6	0.5	43.5	0.7	269.3	33.1	-9.0	-85.3	39.6	0.5
S1455_257	1084.4	7.1	0.6	0.04808	0.00106	0.07288	0.00163	0.01102	0.00016	70.6	1.0	71.4	1.5	103.3	51.3	-1.1	-31.7	70.6	1.0
S1455_258	1335.6	540.5	0.3	0.26043	0.00272	21.89447	0.28420	0.61121	0.00781	3074.9	31.2	3179.1	12.6	3249.3	16.3	-3.3	-5.4	3249.3	16.3
S1455_259	140.2	1.8	0.3	0.04754	0.00204	0.13613	0.00569	0.02082	0.00038	132.8	2.4	129.6	5.1	75.7	99.9	2.5	75.4	132.8	2.4
S1455_260	1722.0	13.0	0.1	0.05233	0.00086	0.12928	0.00228	0.01796	0.00024	114.7	1.5	123.4	2.1	299.9	37.1	-7.1	-61.8	114.7	1.5
S1455_261	678.4	138.4	0.5	0.16493	0.00181	7.19014	0.09609	0.31694	0.00412	1774.8	20.2	2135.3	11.9	2506.9	18.4	-16.9	-29.2		
S1455_262	213.6	2.3	0.9	0.04511	0.00218	0.08723	0.00405	0.01406	0.00029	90.0	1.8	84.9	3.8	0.1	63.5	6.0	89900.0	90.0	1.8
S1455_263	2713.5	249.2	0.4	0.07061	0.00076	1.48200	0.01951	0.15258	0.00195	915.4	10.9	923.1	8.0	946.3	21.8	-0.8	-3.3	915.4	10.9
S1455_264	1205.1	5.3	1.0	0.06736	0.00183	0.05951	0.00157	0.00642	0.00010	41.3	0.7	58.7	1.5	848.9	55.4	-29.6	-95.1		
S1455_265	407.7	26.7	0.2	0.06889	0.00095	1.09959	0.01700	0.11604	0.00155	707.7	9.0	753.2	8.2	895.5	28.2	-6.0	-21.0	707.7	9.0
S1455_266	1774.2	121.8	0.8	0.05920	0.00073	0.70198	0.01010	0.08620	0.00112	533.0	6.7	540.0	6.0	574.6	26.7	-1.3	-7.2	533.0	6.7
S1455_267	2356.4	5.8	0.8	0.10009	0.00264	0.03838	0.00096	0.00279	0.00005	17.9	0.3	38.2	0.9	1625.8	48.2	-53.1	-98.9		
S1455_268	309.8	2.1	0.7	0.05443	0.00243	0.06796	0.00289	0.00908	0.00018	58.3	1.2	66.8	2.8	388.8	96.5	-12.7	-85.0	58.3	1.2
S1455_269	373.4	2.8	0.9	0.04674	0.00167	0.07278	0.00254	0.01132	0.00019	72.6	1.2	71.3	2.4	36.0	83.5	1.8	101.7	72.6	1.2
S1455_270	831.7	257.4	0.6	0.15612	0.00165	10.47726	0.13716	0.48790	0.00626	2561.6	27.1	2477.9	12.1	2414.1	17.8	3.4	6.1	2414.1	17.8
S1455_271	427.3	16.6	0.2	0.07113	0.00138	0.81753	0.01625	0.08356	0.00123	517.4	7.3	606.7	9.1	961.0	39.0	-14.7	-46.2		
S1455_272	1143.1	10.9	0.8	0.04728	0.00090	0.09555	0.00189	0.01469	0.00020	94.0	1.3	92.7	1.8	62.7	45.3	1.4	49.9	94.0	1.3
S1455_273	2273.2	25.3	1.4	0.05097	0.00077	0.09900	0.00163	0.01412	0.00019	90.4	1.2	95.9	1.5	239.4	34.3	-5.7	-62.2	90.4	1.2
S1455_274	810.5	8.0	1.0	0.04863	0.00106	0.09420	0.00208	0.01408	0.00020	90.1	1.3	91.4	1.9	130.0	50.3	-1.4	-30.7	90.1	1.3
S1455_275	3587.6	27.4	0.3	0.04669	0.00065	0.08213	0.00128	0.01279	0.00017	81.9	1.1	80.1	1.2	33.2	32.7	2.2	146.7	81.9	1.1
S1455_276	1935.7	23.9	0.9	0.04998	0.00074	0.12027	0.00197	0.01749	0.00023	111.8	1.5	115.3	1.8	194.1	34.2	-3.0	-42.4	111.8	1.5
S1455_277	1511.7	282.2	0.7	0.11446	0.00121	4.63308	0.06067	0.29427	0.00377	1662.8	18.8	1755.2	10.9	1871.4	19.0	-5.3	-11.1	1871.4	19.0
S1455_278	696.3	39.5	0.3	0.06134	0.00077	0.97344	0.01416	0.11538	0.00151	703.9	8.7	690.2	7.3	651.2	26.7	2.0	8.1	703.9	8.7
S1455_279	22189.3	144.3	0.5	0.04758	0.00053	0.08069	0.00109	0.01233	0.00016	79.0	1.0	78.8	1.0	77.7	27.1	0.3	1.7	79.0	1.0
S1455_280	4460.0	45.2	0.3	0.05365	0.00104	0.11254	0.00225	0.01525	0.00022	97.6	1.4	108.3	2.1	356.3	43.8	-9.9	-72.6	97.6	1.4
S1455_281	1391.0	13.7	0.6	0.05109	0.00087	0.11941	0.00215	0.01699	0.00023	108.6	1.5	114.5	2.0	245.0	38.6	-5.2	-55.7	108.6	1.5
S1455_282	4813.9	31.4	0.5	0.04812	0.00066	0.08042	0.00124	0.01215	0.00016	77.9	1.0	78.5	1.2	105.1	32.1	-0.8	-25.9	77.9	1.0
S1455_283	424.0	79.4	0.8	0.15270	0.00169	8.99516	0.12112	0.42825	0.00559	2297.8	25.2	2337.5	12.3	2376.4	18.7	-1.7	-3.3	2376.4	18.7
S1455_284	2697.2	15.3	0.7	0.04945	0.00082	0.12242	0.00217	0.01800	0.00024	115.0	1.6	117.3	2.0	169.2	38.3	-2.0	-32.0	115.0	1.6
S1455_285	1133.4	44.1	0.1	0.06065	0.00074	0.83115	0.01189	0.09964	0.00130	612.3	7.6	614.2	6.6	626.7	26.2	-0.3	-2.3	612.3	7.6
S1455_286	476.2	38.3	0.6	0.06905	0.00087	1.28767	0.01879	0.13558	0.00179	819.6	10.1	840.3	8.3	900.2	25.8	-2.5	-9.0	819.6	10.1
S1455_288	512.0	2.4	0.6	0.04959	0.00180	0.12304	0.00435	0.01804	0.00031	115.3	2.0	117.8	3.9	175.6	82.7	-2.1	-34.3	115.3	2.0
S1455_289	1042.0	52.1	0.1	0.06091	0.00097	0.58673	0.01006	0.07003	0.00096	436.4	5.8	468.8	6.4	636.0	33.9	-6.9	-31.4	436.4	5.8
S1455_290	740.3	70.3	2.0	0.07015	0.00084	1.31829	0.01862	0.13661	0.00178	825.5	10.1	853.8	8.2	932.9	24.4	-3.3	-11.5	825.5	10.1
S1455_291	2734.7	124.5	0.3	0.06160	0.00068	0.86349	0.01164	0.10191	0.00131	625.6	7.7	632.0	6.3	660.3	23.6	-1.0	-5.3	625.6	7.7
S1455_292	2509.7	272.0	0.1	0.11918	0.00129	3.71531	0.04919	0.22664	0.00292	1316.8	15.3	1574.7	10.6	1944.0	19.2	-16.4	-32.3		
S1455_293	1190.4	58.3	0.2	0.06147	0.00073	0.91926	0.01289	0.10873	0.00141	665.4	8.2	662.0	6.8	655.6	25.2	0.5	1.5	665.4	8.2
S1455_294	130.5	0.9	0.8	0.06034	0.00469	0.10854	0.00788	0.01308	0.00042	83.8	2.7	104.6	7.2	615.7	159.6	-19.9	-86.4		
S1455_295	479.4	34.1	0.4	0.06953	0.00088	1.57442	0.02311	0.16463	0.00218	982.4	12.0	960.2	9.1	914.4	25.9	2.3	7.4	982.4	12.0
S1455_296	327.8	28.2	1.2	0.06672	0.00092	1.25731	0.01948	0.13701	0.00184	827.7	10.4	826.7	8.8	829.0	28.5	0.1	-0.2	827.7	10.4
S1455_297	616.4	259.4	1.1	0.27368	0.00289	22.08159	0.28955	0.58658	0.00756	2975.5	30.7	3187.3	12.7	3327.2	16.4	-6.6	-10.6	3327.2	16.4
S1455_298	1268.7	155.4	0.5	0.11318	0.00126	2.84014	0.03827	0.18244	0.00236	1080.3	12.9	1366.2	10.1	1851.1	20.0	-20.9	-41.6		
S1455_299	288.6	2.3	0.8	0.04904	0.00189	0.09262	0.00348	0.01373	0.00024	87.9	1.6	89.9	3.2	149.7	88.1	-2.2	-41.3	87.9	1.6
S1455_300	1045.3	12.5	0.8	0.05230	0.00093	0.12387	0.00232	0.01722	0.00024	110.1	1.5	118.6	2.1	298.7	40.0	-7.2	-63.1	110.1	1.5
S1455_301	2137.9	120.3	0.4	0.06314	0.00070	0.76808	0.01039	0.08844	0.00114	546.3	6.7	578.7	6.0	712.9	23.6	-5.6	-23.4	546.3	6.7
S1455_302	357.1	3.2	0.9	0.04878	0.00157	0.08452	0.00266	0.01260	0.00021	80.7	1.3	82.4	2.5	137.4	73.9	-2.1	-41.3	80.7	1.3
S1455_303	2349.9	23.3	0.4	0.04928	0.00072	0.11353	0.00183	0.01675	0.00022	107.1	1.4	109.2	1.7	161.3	33.7	-1.9	-33.6	107.1	1.4
S1455_304	5047.1	29.5	0.7	0.04852	0.00068	0.06376	0.00100	0.00955	0.00013	61.3	0.8	62.8	1.0	124.9	32.6	-2.4	-50.9	61.3	0.8
S1455_305	2009.1	10.1	0.6	0.04959	0.00095	0.05638	0.00112	0.00827	0.00012	53.1	0.7	55.7	1.1	175.8	44.0	-4.7	-69.8	53.1	0.7
S1455_306	1580.2	195.3	0.2	0.11228	0.00123	3.40081	0.04538	0.22020	0.00284	1282.9	15.0	1504.6	10.5	1836.7	19.6	-14.7	-30.2		
S1455_307	327.8	2.9	0.8	0.16420	0.00637	0.21905	0.00733	0.00970	0.00024	62.2	1.6	201.1	6.1	2499.4	63.9	-69.1	-97.5		
S1455_308	419.1	84.4	0.5	0.10243	0.00114	4.27139	0.05786	0.30318	0.00394	1707.0	19.5	1687.9	11.2	1668.5	20.5	1.1	2.3	1668.5	20.5
S1455_309	546.3	13.5	0.3	0.05380	0.00121	0.29555	0.00669	0.03994	0.00059	252.4	3.7	262.9	5.3	362.6	49.9	-4.0	-30.4	252.4	3.7
S1455_310	1366.5	119.6	0.6	0.06577	0.00073	1.29752	0.01757	0.14342	0.00185	864.0	10.4	844.6	7.8	799.1	23.2	2.3	8.1	864.0	10.4
S1455_311	4458.4	50.4	0.9	0.06268	0.00077	0.15102	0.00217	0.01752	0.00023	111.9	1.5	142.8	1.9	697.5	26.1	-21.6	-84.0		
S1455_312	1761.2	549.1	0.3	0.15128	0.00160	9.62297	0.12632	0.46244	0.00594	2450.3	26.2	2399.4	12.1	2360.5	17.9	2.1	3.8	2360.5	17.9
S1455_313	2031.9	10.5	0.9	0.04792	0.00108	0.04903	0.00112	0.00744	0.00011	47.8	0.7	48.6	1.1	94.2	53.5	-1.6	-49.3	47.8	0.7
S1455_314	2389.0	512.5	0.2	0.17083	0.00179	9.62888	0.12578	0.40978	0.00525	2213.9	24.0	2399.9	12.0	2565.8	17.4	-7.8	-13.7	2565.8	17.4
S1455_315	1498.6	236.8	0.2	0.11358	0.00122	4.86999	0.06449	0.31172	0.00401	1749.2	19.7	1797.1	11.2	1857.5	19.3	-2.7	-5.8	1857.5	19.3
S1455_316	1371.4	4.1	0.3	0.04962	0.00134	0.03763	0.00101	0.00551	0.00008	35.4	0.5	37.5	1.0	177.3	61.7	-5.6	-80.0	35.4	0.5
S1455_317	228.3	40.4	0.7	0.08972	0.00109	3.14315	0.04494	0.25469	0.00337	1462.6	17.3	1443.3	11.0	1419.5	23.0	1.3	3.0	1419.5	23.0
S1455_318	295.2	26.1	0.4	0.06739	0.00090	1.45776	0.02219	0.15725	0.00210	941.5	11.7	913.1	9.2	850.0	27.6	3.1	10.8	941.5	11.7
S1455_319	1479.1	8.1	2.6	0.04966	0.00122	0.04544	0.00112	0.00665	0.00010	42.7	0.6	45.1	1.1	178.9	56.2	-5.3	-76.1	42.7	0.6
S1455_320	234.8	60.5	0.6	0.13452	0.00152	7.28155	0.09980	0.39354	0.00518	2139.2	24.0	2146.6	12.2	2157.8	19.6	-0.3	-0.9	2157.8	19.6
S1455_321	552.8	3.2	0.9	0.05022	0.00162	0.06074	0.00192	0.00879	0.00015	56.4	0.9	59.9	1.8	205.3	73.2	-5.8	-72.5	56.4	0.9
S1455_322	329.4	68.3	0.4	0.21833	0.00247	12.79852	0.17541	0.42618	0.00568	2288.5	25.7	2664.9	12.9	2968.4	18.1	-14.1	-22.9		
S1455_323	557.7	4.5	0.9	1.05514	0.02257	1.74825	0.02817	0.01205	0.00025	77.2	1.6	1026.5	10.4	5312.7	29.6	-92.5	-98.5		
S1455_324	756.7	93.6	0.3	0.11331	0.00127	5.21255	0.07075	0.33444	0.00436	1859.9	21.1	1854.7	11.6	1853.2	20.1	0.3	0.4	1853.2	20.1
S1455_325	2720.0	505.7	0.0	0.25358	0.00266	12.30127	0.16070	0.35268	0.00452	1947.4	21.5	2627.7	12.3	3207.2	16.5	-25.9	-39.3		
S1455_326	409.3	20.3	0.9	0.05914	0.00090	0.76721	0.01280	0.09431	0.00128	581.0	7.6	578.2	7.4	572.4	32.8	0.5	1.5	581.0	7.6
S1455_327	24542.4	103.1	0.4	0.06684	0.00083	0.06931	0.00100	0.00754	0.00010	48.4	0.6	68.0	1.0	832.9	25.7	-28.8	-94.2		
S1455_328	618.0	5.0	1.3	0.05462	0.00148	0.09245	0.00247	0.01231	0.00019	78.8	1.2	89.8	2.3	396.7	59.3	-12.2	-80.1	78.8	1.2
S1455_329	133.7	2.1	0.6	0.55204	0.02910	1.14221	0.03997	0.01504	0.00065	96.2	4.1	773.6	18.9	4386.6	75.0	-87.6	-97.8		
S1455_330	249.5	49.4	0.6	0.11349	0.00150	4.81422	0.07234	0.30838	0.00422	1732.7	20.8	1787.4	12.6	1856.1	23.6	-3.1	-6.6	1856.1	23.6
S1455_331	4342.6	9.9	1.0	0.04852	0.00097	0.04051	0.00083	0.00607	0.00009	39.0	0.6	40.3	0.8	124.6	46.4	-3.2	-68.7	39.0	0.6
S1455_332	500.6	54.2	0.6	0.11544	0.00133	5.40632	0.07488	0.34047	0.00449	1888.9	21.6	1885.9	11.9	1886.7	20.6	0.2	0.1	1886.7	20.6
S1455_333	466.4	29.2	0.7	0.07130	0.00094	1.65962	0.02504	0.16921	0.00226	1007.8	12.5	993.2	9.6	966.2	26.7	1.5	4.3	1007.8	12.5
S1455_334	4791.1	333.2	0.8	0.12911	0.00147	2.70616	0.03690	0.15238	0.00199	914.3	11.1	1330.1	10.1	2085.9	19.8	-31.3	-56.2		
S1455_335	728.9	18.5	0.5	0.05753	0.00086	0.72949	0.01205	0.09218	0.00125	568.4	7.4	556.3	7.1	511.6	33.0	2.2	11.1	568.4	7.4
S1455_336	1143.1	58.8	0.6	0.06322	0.00078	0.92621	0.01330	0.10650	0.00139	652.4	8.1	665.6	7.0	715.8	25.8	-2.0	-8.9	652.4	8.1
S1455_337	3135.9	739.5	0.1	0.18293	0.00192	12.10097	0.15827	0.48093	0.00616	2531.3	26.8	2612.3	12.3	2679.6	17.2	-3.1	-5.5	2679.6	17.2
S1455_338	1686.2	155.1	0.6	0.08341	0.00091	2.42751	0.03248	0.21157	0.00273	1237.2	14.5	1250.8	9.6	1278.7	21.2	-1.1	-3.2	1278.7	21.2
S1455_339	2067.8	18.0	0.6	0.04833	0.00077	0.11394	0.00196	0.01714	0.00023	109.5	1.5	109.6	1.8	115.5	37.1	-0.1	-5.2	109.5	1.5
S1455_340	1376.3	12.0	0.6	0.04917	0.00088	0.11836	0.00223	0.01750	0.00024	111.8	1.5	113.6	2.0	156.1	41.3	-1.6	-28.4	111.8	1.5
S1455_341	3315.3	10.1	0.5	0.04869	0.00093	0.04018	0.00080	0.00600	0.00008	38.6	0.5	40.0	0.8	133.1	44.3	-3.5	-71.0	38.6	0.5
S1455_342	146.8	39.1	1.4	0.13833	0.00182	5.50248	0.08269	0.28918	0.00402	1637.4	20.1	1901.0	12.9	2206.4	22.6	-13.9	-25.8		
S1455_343	1280.1	204.1	0.9	0.08869	0.00096	2.96904	0.03956	0.24339	0.00314	1404.3	16.3	1399.7	10.1	1397.4	20.6	0.3	0.5	1397.4	20.6
S1455_344	864.3	61.4	0.8	0.06594	0.00079	1.07465	0.01517	0.11847	0.00155	721.8	8.9	741.0	7.4	804.6	24.8	-2.6	-10.3	721.8	8.9
S1455_345	1094.2	64.7	0.4	0.06047	0.00072	0.88942	0.01250	0.10693	0.00139	654.9	8.1	646.1	6.7	620.4	25.3	1.4	5.6	654.9	8.1
S1455_346	8525.4	60.8	0.3	0.04880	0.00059	0.08911	0.00127	0.01328	0.00017	85.0	1.1	86.7	1.2	138.4	28.3	-2.0	-38.6	85.0	1.1
S1455_347	10748.1	576.2	0.1	0.06171	0.00066	0.93044	0.01226	0.10961	0.00141	670.5	8.2	667.9	6.5	664.2	22.6	0.4	0.9	670.5	8.2
S1455_348	1945.5	125.4	1.0	0.05885	0.00067	0.72976	0.00999	0.09016	0.00117	556.5	6.9	556.4	5.9	561.4	24.5	0.0	-0.9	556.5	6.9
S1455_349	3116.3	196.8	0.2	0.07087	0.00078	1.36429	0.01837	0.13994	0.00181	844.3	10.2	873.7	7.9	953.8	22.4	-3.4	-11.5	844.3	10.2
S1455_350	12910.5	279.9	0.8	0.12086	0.00131	0.74150	0.00986	0.04460	0.00058	281.3	3.6	563.3	5.8	1969.0	19.2	-50.1	-85.7		
S1455_351	1612.8	295.9	0.2	0.15034	0.00160	9.33938	0.12346	0.45162	0.00583	2402.5	25.9	2371.9	12.1	2349.8	18.1	1.3	2.2	2349.8	18.1
S1455_352	2605.9	328.0	0.3	0.14806	0.00161	6.43825	0.08607	0.31612	0.00410	1770.7	20.1	2037.5	11.8	2323.7	18.5	-13.1	-23.8		
S1455_353	1656.8	209.6	0.6	0.08734	0.00094	2.92533	0.03898	0.24349	0.00314	1404.8	16.3	1388.5	10.1	1368.1	20.7	1.2	2.7	1368.1	20.7
S1455_354	952.3	11.8	0.7	0.06493	0.00114	0.17188	0.00316	0.01925	0.00027	122.9	1.7	161.0	2.7	772.0	36.5	-23.7	-84.1		
S1455_355	1961.8	126.0	0.4	0.07209	0.00080	1.38950	0.01879	0.14012	0.00181	845.3	10.2	884.5	8.0	988.6	22.4	-4.4	-14.5	845.3	10.2
S1455_357	233.2	14.6	0.5	0.06472	0.00115	1.32393	0.02490	0.14872	0.00214	893.8	12.0	856.2	10.9	765.2	37.0	4.4	16.8	893.8	12.0
S1455_358	1444.8	36.2	1.0	0.05569	0.00083	0.35223	0.00575	0.04598	0.00062	289.8	3.8	306.4	4.3	439.7	32.2	-5.4	-34.1	289.8	3.8
S1455_359	1161.1	5.2	0.5	0.04879	0.00177	0.07267	0.00255	0.01083	0.00019	69.4	1.2	71.2	2.4	137.5	83.1	-2.5	-49.5	69.4	1.2

Thal Desert dune @ Mangera 13 grains analysed 11 concordant ages

	concentrations			isotopic ratios						ages						discordance		preferred age	
grain	U [ppm]	Pb [ppm]	Th/U	Pb207/Pb206	2σ 76	Pb207/U235	2σ 75	Pb206/U238	2σ 68	age 206/238	2σ age 68	age 207/235	2σ age 75	age 207/206	2σ age 76	Δ 68-75 [%]	Δ 68-76 [%]	age	2σ age
S1462_001	1273.284245	349.9	0.5	0.18498	0.002	12.95422	0.17172	0.50905	0.00654	2652.6	27.93	2676.3	12.5	2698	17.71	-0.9	-1.7	2698	17.71
S1462_002	2386.89619	22.5	0.9	0.04719	0.00086	0.10785	0.00206	0.01661	0.00023	106.2	1.44	104	1.89	58.5	43.18	2.1	81.5	106.2	1.44
S1462_003	8194.464365	77.2	0.0	0.04859	0.00063	0.10966	0.00164	0.01641	0.00021	104.9	1.35	105.7	1.5	128	30.43	-0.8	-18.0	104.9	1.35
S1462_004	2108.493204	87.6	0.1	0.10402	0.00148	2.55223	0.04027	0.17835	0.00245	1057.9	13.41	1287.1	11.51	1697.1	26	-17.8	-37.7		
S1462_005	1265.095922	10.9	0.4	0.04747	0.001	0.11196	0.00241	0.01714	0.00024	109.6	1.55	107.8	2.2	72.3	50.03	1.7	51.6	109.6	1.55
S1462_006	350.0508135	1.9	1.1	0.04662	0.00214	0.06081	0.0027	0.00948	0.00018	60.8	1.15	59.9	2.58	29.8	106.43	1.5	104.0	60.8	1.15
S1462_007	820.879393	39.6	1.5	0.05764	0.00081	0.70463	0.01102	0.08886	0.00118	548.8	6.98	541.6	6.56	515.9	30.68	1.3	6.4	548.8	6.98
S1462_008	798.3615044	130.2	0.3	0.11433	0.00126	5.08757	0.06822	0.32345	0.00416	1806.5	20.27	1834	11.38	1869.4	19.75	-1.5	-3.4	1869.4	19.75
S1462_009	3893.547645	9.9	0.0	0.04831	0.00106	0.04249	0.00095	0.00639	9.00E-05	41.1	0.59	42.3	0.92	114.2	51.06	-2.8	-64.0	41.1	0.59
S1462_010	2268.165505	17.0	0.7	0.04563	0.00097	0.06575	0.00144	0.01047	0.00015	67.2	0.93	64.7	1.38	0.1	28.51	3.9	67100.0	67.2	0.93
S1462_011	2962.125889	44.0	0.1	0.05147	0.00073	0.249	0.00394	0.03517	0.00046	222.8	2.88	225.8	3.2	261.8	32.25	-1.3	-14.9	222.8	2.88
S1462_012	585.4651032	111.2	0.4	0.11276	0.00125	5.3137	0.07167	0.34255	0.00442	1898.9	21.23	1871.1	11.53	1844.3	19.98	1.5	3.0	1844.3	19.98

Thal Desert dune @ Muzaffarghar 56 grains analysed 48 concordant ages

	concentrations			isotopic ratios						ages						discordance		preferred age	
grain	U [ppm]	Pb [ppm]	Th/U	Pb207/Pb206	2σ 76	Pb207/U235	2σ 75	Pb206/U238	2σ 68	age 206/238	2σ age 68	age 207/235	2σ age 75	age 207/206	2σ age 76	Δ 68-75 [%]	Δ 68-76 [%]	age	2σ age
S1470_#1	4573.314936		0.7	0.06529	0.00096	0.00988	0.00013	0.04804	0.00063	63.4	0.81	64.2	0.91	101.5	30.62	-1.2	-37.5	63.4	0.81
S1470_53_#2	482.66753		0.9	0.04022	0.00143	0.0059	1.00E-04	0.04952	0.00182	38	0.65	40	1.4	172.3	83.47	-5.0	-77.9	38	0.65
S1470_259_#3	288.6383901		0.9	7.98736	0.10426	0.38693	0.00492	0.15007	0.00163	2108.6	22.85	2229.6	11.78	2346.7	18.45	-5.4	-10.1	2346.7	18.45
S1470_90_#4	1330.943687		0.7	0.07239	0.00137	0.01125	0.00015	0.04677	0.00085	72.1	0.97	71	1.3	37.3	42.27	1.5	93.3	72.1	0.97
S1470_238_#5	118.6624492		0.8	1.13169	0.01993	0.12626	0.00174	0.06516	0.00108	766.5	9.95	768.6	9.49	779.5	34.6	-0.3	-1.7	766.5	9.95
S1470_234_#6	551.6200343		0.6	4.74556	0.06274	0.30404	0.00387	0.11347	0.00126	1711.3	19.14	1775.3	11.09	1855.6	19.91	-3.6	-7.8	1855.6	19.91
S1470_245_#7	1715.794874		0.3	0.76715	0.01059	0.09145	0.00116	0.06098	0.00073	564.1	6.87	578.1	6.08	638.7	25.37	-2.4	-11.7	564.1	6.87
S1470_227_#8	258.1710044		1.6	0.09344	0.00299	0.00726	0.00014	0.09361	0.00323	46.6	0.91	90.7	2.78	1500.3	63.94	-48.6	-96.9		
S1470_180_#9	2838.277502		0.0	0.20427	0.00285	0.02944	0.00037	0.05045	0.00061	187	2.34	188.7	2.4	215.6	27.75	-0.9	-13.3	187	2.34
S1470_500_#10	397.6795596		0.3	0.07513	0.00227	0.01152	0.00018	0.04741	0.00146	73.8	1.16	73.6	2.15	69.5	72.34	0.3	6.2	73.8	1.16
S1470_470_#11	253.3603646		0.8	0.09791	0.003	0.01313	0.00022	0.05422	0.00171	84.1	1.38	94.8	2.77	379.9	69.3	-11.3	-77.9	84.1	1.38
S1470_457_#12	1090.411696		0.4	4.21442	0.05428	0.26988	0.00339	0.11352	0.00121	1540.2	17.23	1676.8	10.57	1856.5	19.07	-8.1	-17.0	1856.5	19.07
S1470_404_#13	432.9575851		0.3	4.74463	0.06227	0.30445	0.00386	0.11329	0.00124	1713.3	19.09	1775.2	11.01	1852.8	19.65	-3.5	-7.5	1852.8	19.65
S1470_383_#14	7791.632985		0.2	0.11107	0.0015	0.01692	0.00021	0.04772	0.00055	108.2	1.35	106.9	1.37	84.5	27.96	1.2	28.0	108.2	1.35
S1470_381_#15	1371.032353		0.2	4.37875	0.05626	0.28088	0.00353	0.11333	0.0012	1595.8	17.75	1708.3	10.62	1853.4	18.97	-6.6	-13.9	1853.4	18.97
S1470_388_#16	450.5965978		0.9	0.08718	0.00228	0.01218	0.00018	0.05205	0.00138	78	1.18	84.9	2.13	287.6	59.28	-8.1	-72.9	78	1.18
S1470_703_#17	2615.384523		0.8	0.04869	0.0013	0.00686	0.00011	0.0516	0.0014	44.1	0.68	48.3	1.26	267.9	61.21	-8.7	-83.5	44.1	0.68
S1470_705_#18	12028.20313		2.9	0.04666	0.00066	0.0073	9.00E-05	0.04646	0.00057	46.9	0.59	46.3	0.64	21.3	28.99	1.3	120.2	46.9	0.59
S1470_704_#19	574.0696869		0.5	0.10763	0.00238	0.01596	0.00023	0.04903	0.00107	102.1	1.44	103.8	2.18	149	50.43	-1.6	-31.5	102.1	1.44
S1470_359_#20	1481.677069		0.2	0.08093	0.00145	0.01201	0.00016	0.04898	0.00083	77	1.02	79	1.36	146.9	39.38	-2.5	-47.6	77	1.02
S1470_351_#21	6192.897013		0.1	6.24097	0.07977	0.29766	0.00373	0.15242	0.00159	1679.7	18.53	2010.2	11.19	2373.2	17.71	-16.4	-29.2		
S1470_333_#22	4239.777241		0.1	0.38616	0.0051	0.04957	0.00062	0.05663	0.00062	311.9	3.84	331.6	3.73	476.5	24.4	-5.9	-34.5		
S1470_757_#23	234.1178053		0.9	0.05938	0.00257	0.00949	0.00018	0.04549	0.00204	60.9	1.14	58.6	2.46	0.1	75.02	3.9	60800.0	60.9	1.14
S1470_630_#25	2546.432019		0.5	0.10661	0.00163	0.01595	0.00021	0.04859	0.00067	102	1.31	102.9	1.49	127.9	32.02	-0.9	-20.3	102	1.31
S1470_810_#26	830.6371447		0.3	0.46293	0.00804	0.05879	0.00079	0.05724	0.00094	368.3	4.84	386.3	5.58	500.4	35.55	-4.7	-26.4	368.3	4.84
S1470_820_#27	1191.435132		0.2	2.63107	0.03441	0.17006	0.00215	0.11247	0.00122	1012.4	11.85	1309.4	9.62	1839.7	19.53	-22.7	-45.0		
S1470_829_#28	2538.414286		0.7	0.05509	0.00096	0.00674	9.00E-05	0.05946	0.00099	43.3	0.58	54.5	0.93	584.1	35.64	-20.6	-92.6	43.3	0.58
S1470_599_#29	784.134293		0.8	0.03768	0.0011	0.00593	9.00E-05	0.0462	0.00137	38.1	0.59	37.6	1.08	8.2	69.32	1.3	364.6	38.1	0.59
S1470_852_#30	559.6377674		0.7	0.05869	0.00315	0.00686	0.00017	0.06221	0.00357	44.1	1.12	57.9	3.02	681.3	118.12	-23.8	-93.5	44.1	1.12
S1470_846_#31	1390.274912		0.2	1.3601	0.01807	0.14205	0.0018	0.0696	0.00077	856.3	10.16	871.9	7.78	916.6	22.68	-1.8	-6.6	856.3	10.16
S1470_919_#32	1114.464895		0.3	4.17214	0.05451	0.26761	0.00339	0.11333	0.00122	1528.6	17.22	1668.6	10.7	1853.5	19.39	-8.4	-17.5	1853.5	19.39
S1470_923_#33	721.5959751		0.3	4.72829	0.06217	0.30137	0.00383	0.11405	0.00124	1698.1	18.95	1772.3	11.02	1864.9	19.55	-4.2	-8.9	1864.9	19.55
S1470_1207_#34	3959.156584		1.6	0.05168	0.00084	0.00721	1.00E-04	0.05208	0.00079	46.3	0.61	51.2	0.82	289	34.07	-9.6	-84.0	46.3	0.61
S1470_1186_#35	8737.725486		0.1	0.07263	0.00102	0.01101	0.00014	0.04794	0.00058	70.6	0.89	71.2	0.96	95.4	29.39	-0.8	-26.0	70.6	0.89
S1470_1079_#36	636.6080047		0.6	8.54603	0.11202	0.38142	0.00485	0.16288	0.00176	2082.9	22.61	2290.8	11.92	2485.7	18.14	-9.1	-16.2	2485.7	18.14
S1470_1066_#37	487.4781699		1.0	0.08367	0.00217	0.01255	0.00019	0.04847	0.00127	80.4	1.21	81.6	2.03	122.2	60.43	-1.5	-34.2	80.4	1.21
S1470_1021_#38	4313.540385		0.8	0.09947	0.00144	0.01534	2.00E-04	0.04713	6.00E-04	98.2	1.25	96.3	1.33	55.3	29.41	2.0	77.6	98.2	1.25
S1470_1051_#39	745.6491743		0.3	4.5961	0.06062	0.294	0.00373	0.11364	0.00124	1661.5	18.61	1748.6	11	1858.4	19.62	-5.0	-10.6	1858.4	19.62
S1470_1065_#40	323.9164155		0.4	1.25451	0.0187	0.12243	0.00161	0.07449	0.00099	744.5	9.24	825.4	8.42	1054.4	26.76	-9.8	-29.4		
S1470_1418_#41	1326.133048		0.5	4.25002	0.05579	0.27118	0.00344	0.11393	0.00124	1546.8	17.43	1683.7	10.79	1863	19.46	-8.1	-17.0	1863	19.46
S1470_1359_#42	934.8676745		0.3	0.10818	0.00211	0.01557	0.00021	0.05051	0.00095	99.6	1.36	104.3	1.93	218.7	43.06	-4.5	-54.5	99.6	1.36
S1470_1106_#43	915.6251151		0.5	0.04591	0.00121	0.00693	0.00011	0.04815	0.00129	44.5	0.67	45.6	1.18	106.6	61.89	-2.4	-58.3	44.5	0.67
S1470_1336_#44	2761.307265		0.1	0.88548	0.01236	0.09803	0.00126	0.06566	0.00079	602.8	7.39	643.9	6.66	795.6	24.9	-6.4	-24.2		
S1470_1127_#45	5142.573983		0.1	6.30037	0.08211	0.33107	0.00418	0.13834	0.00148	1843.6	20.24	2018.5	11.42	2206.5	18.45	-8.7	-16.4	2206.5	18.45
S1470_1475_#46	477.8568902		0.8	1.21976	0.01763	0.13306	0.00173	0.06664	0.00084	805.3	9.83	809.7	8.07	826.4	26.09	-0.5	-2.6	805.3	9.83
S1470_1280_#47	3232.749969		0.2	0.02458	0.00056	0.00347	5.00E-05	0.05149	0.00116	22.3	0.32	24.7	0.55	262.8	50.78	-9.7	-91.5	22.3	0.32
S1470_1514_#48	397.6795596		0.9	0.05481	0.002	0.00825	0.00014	0.04828	0.00182	53	0.92	54.2	1.93	113	86.45	-2.2	-53.1	53	0.92
S1470_1535_#49	1013.441458		0.6	6.80654	0.08983	0.31305	0.00398	0.15805	0.00172	1755.7	19.53	2086.6	11.68	2434.9	18.36	-15.9	-27.9		
S1470_1490_#50	2584.917138		0.3	0.59007	0.00806	0.07495	0.00096	0.05723	0.00066	465.9	5.73	470.9	5.14	499.9	25.42	-1.1	-6.8	465.9	5.73
S1470_1489_#51	218.0823392		0.8	0.09213	0.00338	0.01299	0.00023	0.05157	0.00196	83.2	1.47	89.5	3.14	266.4	84.72	-7.0	-68.8	83.2	1.47
S1470_1480_#52	1016.648552		0.7	0.62546	0.00891	0.07965	0.00103	0.05708	7.00E-04	494	6.12	493.3	5.56	494.1	27.25	0.1	0.0	494	6.12
S1470_1553_#53	429.7504919		0.4	0.07786	0.00209	0.01161	0.00018	0.04874	0.00132	74.4	1.14	76.1	1.97	135.5	62.64	-2.2	-45.1	74.4	1.14
S1470_1465_#54	78.57378396		0.3	0.08486	0.00701	0.01407	0.00034	0.04384	0.00371	90.1	2.19	82.7	6.56	0.1	76.27	8.9	90000.0	90.1	2.19
S1470_1572_#55	160.3546611		0.7	0.06787	0.00334	0.00973	0.00021	0.05071	0.0026	62.4	1.31	66.7	3.17	227.8	114.45	-6.4	-72.6	62.4	1.31
S1470_1449_#56	1919.445294		1.2	0.0458	0.00093	0.00691	1.00E-04	0.04816	0.00094	44.4	0.62	45.5	0.9	107	45.68	-2.4	-58.5	44.4	0.62

Sample S1474 Thal Desert dune @ Munda 54 grains analysed 32 concordant ages

	concentrations			isotopic ratios						ages						discordance		preferred age	
grain	U [ppm]	Pb [ppm]	Th/U	Pb207/Pb206	2σ 76	Pb207/U235	2σ 75	Pb206/U238	2σ 68	age 206/238	2σ age 68	age 207/235	2σ age 75	age 207/206	2σ age 76	Δ 68-75 [%]	Δ 68-76 [%]	age	2σ age
S1474_49_#1	543.2014146		0.3	0.05053	0.00205	0.06888	0.00271	0.00991	0.00017	63.6	1.1	67.6	2.57	219.3	91.22	-5.9	-71.0	63.6	1.1
S1474_57_#2	1749.87024		0.8	-0.03063	0.00159	-0.06703	0.00347	0.01591	0.00023	101.8	1.43	-70.4	3.78	0.1	0	-244.6	101700.0		
S1474_58_#3	1000.212199		0.2	0.03766	0.0014	0.07934	0.00294	0.01531	0.00023	98	1.44	77.5	2.76	0.1	0	26.5	97900.0		
S1474_42_#4	362.8024208		1.0	0.07365	0.00103	1.81974	0.02784	0.17963	0.00233	1065	12.75	1052.6	10.02	1031.8	27.92	1.2	3.2	1065	12.75
S1474_40_#5	815.8043386		0.6	0.15097	0.00175	6.26975	0.08419	0.3019	0.00384	1700.7	19.02	2014.2	11.76	2357	19.71	-15.6	-27.8		
S1474_11_#6	8418.61971		0.3	0.04669	0.00071	0.07206	0.00118	0.01122	0.00014	71.9	0.91	70.7	1.12	33	35.32	1.7	117.9	71.9	0.91
S1474_12_#7	1110.456028		0.5	0.0263	0.00128	0.06448	0.00314	0.01783	0.00026	113.9	1.64	63.4	3	0.1	0	79.7	113800.0		
S1474_15_#8	2204.876591		0.1	0.11139	0.00121	3.97559	0.05127	0.25945	0.00323	1487	16.53	1629.2	10.46	1822.2	19.62	-8.7	-18.4		
S1474_75_#9	2098.641628		1.2	0.04189	0.00144	0.0381	0.00129	0.00661	1.00E-04	42.5	0.64	38	1.27	0.1	0	11.8	42400.0	42.5	0.64
S1474_80_#10	597.3211128		0.4	0.04857	0.00177	0.0741	0.00262	0.01109	0.00018	71.1	1.16	72.6	2.48	126.9	83.37	-2.1	-44.0	71.1	1.16
S1474_145_#11	2401.311051		0.2	0.1062	0.00123	2.25555	0.03022	0.15439	0.00194	925.5	10.84	1198.5	9.43	1735.1	21.12	-22.8	-46.7		
S1474_166_#12	1697.754975		0.3	0.11435	0.00137	5.30431	0.07287	0.33717	0.0043	1873	20.73	1869.6	11.74	1869.7	21.49	0.2	0.2	1869.7	21.49
S1474_170_#13	863.9107369		0.1	0.03638	0.0014	0.11056	0.00424	0.02209	0.00032	140.9	2.04	106.5	3.87	0.1	0	32.3	140800.0		
S1474_92_#14	1136.513661		1.3	0.0703	0.00093	1.68035	0.02463	0.17373	0.00222	1032.6	12.2	1001.1	9.33	937.2	26.75	3.1	10.2	1032.6	12.2
S1474_126_#15	579.2812134		0.2	0.06289	0.00105	0.97819	0.01729	0.11305	0.0015	690.4	8.66	692.7	8.87	704.6	35.24	-0.3	-2.0	690.4	8.66
S1474_107_#16	6045.370725		0.1	0.03675	0.00102	0.02644	0.00074	0.00523	7.00E-05	33.6	0.46	26.5	0.73	0.1	0	26.8	33500.0		
S1474_109_#17	1433.169784		0.2	0.11229	0.00131	4.55948	0.06125	0.29511	0.00372	1667	18.51	1741.9	11.19	1836.8	20.9	-4.3	-9.2		
S1474_205_#18	2471.466215		0.6	0.0642	0.00078	1.16323	0.01607	0.13169	0.00165	797.5	9.41	783.5	7.54	748.2	25.36	1.8	6.6	797.5	9.41
S1474_121_#19	434.9620183		0.6	0.10896	0.00148	3.39476	0.05073	0.22643	0.00295	1315.7	15.53	1503.2	11.72	1782.1	24.64	-12.5	-26.2	1782.1	24.64
S1474_112_#20	1192.637792		0.3	0.11953	0.00139	3.2689	0.04383	0.19875	0.0025	1168.6	13.45	1473.7	10.43	1949.2	20.64	-20.7	-40.0		
S1474_272_#21	1441.187517		0.3	0.15402	0.00171	8.61848	0.11219	0.40666	0.00507	2199.6	23.24	2298.5	11.84	2391.1	18.73	-4.3	-8.0		
S1474_278_#22	132.2925954		0.6	0.06396	0.00148	1.17378	0.02727	0.13336	0.00197	807	11.18	788.4	12.74	740.4	48.28	2.4	9.0	807	11.18
S1474_325_#23	1653.657443		0.8	0.02947	0.00181	0.06971	0.00422	0.01719	0.00029	109.9	1.85	68.4	4.01	0.1	0	60.7	109800.0		
S1474_387_#24	883.9550695		0.5	0.14826	0.00166	9.04538	0.1185	0.44336	0.00554	2365.7	24.73	2342.6	11.98	2325.9	19.07	1.0	1.7	2325.9	19.07
S1474_396_#25	222.4920923		0.5	0.16859	0.00231	10.85623	0.16358	0.46794	0.00637	2474.5	27.96	2510.9	14.01	2543.7	22.75	-1.4	-2.7	2543.7	22.75
S1474_488_#26	3112.884859		0.2	0.04796	0.00073	0.15814	0.00258	0.02396	0.00031	152.7	1.94	149.1	2.26	96	36.72	2.4	59.1	152.7	1.94
S1474_482_#27	370.8201539		0.6	-0.01121	0.00423	-0.01762	0.00664	0.01142	0.00026	73.2	1.63	-18.1	6.86	0.1	0	-504.4	73100.0		
S1474_434_#28	3078.809494		0.3	0.04777	0.00159	0.0221	0.00072	0.00336	5.00E-05	21.6	0.34	22.2	0.71	86.7	77.83	-2.7	-75.1	21.6	0.34
S1474_468_#29	3068.787328		0.1	0.05509	0.00072	0.53948	0.00782	0.07116	9.00E-04	443.1	5.39	438.1	5.16	415.6	28.55	1.1	6.6	443.1	5.39
S1474_341_#30	1555.440213		0.6	0.07015	0.00255	0.07763	0.00273	0.00804	0.00014	51.6	0.86	75.9	2.57	932.8	72.78	-32.0	-94.5		
S1474_517_#31	924.0437348		0.6	0.04555	0.00128	0.11779	0.00329	0.01879	0.00028	120	1.75	113.1	2.99	0.1	40.54	6.1	119900.0	120	1.75
S1474_523_#32	258.5718911		1.0	0.0487	0.00336	0.07928	0.00528	0.01183	0.00027	75.8	1.73	77.5	4.97	133.5	154.56	-2.2	-43.2	75.8	1.73
S1474_543_#33	7077.653856		0.2	0.046	7.00E-04	0.09862	0.00161	0.01558	2.00E-04	99.6	1.26	95.5	1.49	0.1	33.43	4.3	99500.0	99.6	1.26
S1474_558_#34	1322.925954		0.5	0.06881	0.00089	1.54411	0.02222	0.16303	0.00206	973.6	11.43	948.1	8.87	893.1	26.37	2.7	9.0	973.6	11.43
S1474_560_#35	1306.890488		0.8	0.04943	0.00171	0.05178	0.00174	0.00761	0.00012	48.9	0.78	51.3	1.68	168.3	78.65	-4.7	-70.9	48.9	0.78
S1474_601_#36	1234.730891		0.6	0.03635	0.00139	0.08601	0.00327	0.01719	0.00026	109.9	1.63	83.8	3.06	0.1	0	31.1	109800.0		
S1474_569_#37	503.1127493		0.2	0.61059	0.05378	1.23373	0.0726	0.01468	0.001	93.9	6.37	816	33	4533.4	122.11	-88.5	-97.9		
S1474_567_#38	1461.23185		0.7	0.04801	0.00147	0.05039	0.00152	0.00763	0.00012	49	0.74	49.9	1.47	98.3	72.13	-1.8	-50.2	49	0.74
S1474_499_#39	348.771388		0.4	-0.02982	0.00557	-0.03092	0.00572	0.00753	0.00022	48.4	1.41	-31.9	5.99	0.1	0	-251.7	48300.0		
S1474_578_#40	1034.287564		1.2	0.06931	9.00E-04	1.55234	0.02241	0.16272	0.00206	971.9	11.4	951.4	8.92	907.9	26.47	2.2	7.0	971.9	11.4
S1474_576_#41	202.4477597		2.3	0.06868	0.00122	1.75447	0.03244	0.18557	0.00254	1097.3	13.79	1028.8	11.96	889.2	36.25	6.7	23.4		
S1474_491_#42	4672.333939		0.2	0.12153	0.00141	4.63729	0.06187	0.2772	0.00344	1577.2	17.38	1756	11.14	1978.7	20.53	-10.2	-20.3		
S1474_696_#43	382.8467535		0.2	0.06071	0.00139	0.87644	0.02014	0.10486	0.00152	642.8	8.87	639.1	10.9	629.1	48.69	0.6	2.2	642.8	8.87
S1474_663_#44	707.5649423		0.7	0.11226	0.00148	5.48908	0.08026	0.35519	0.00458	1959.3	21.8	1898.9	12.56	1836.3	23.72	3.2	6.7	1836.3	23.72
S1474_651_#45	86.19063036		0.8	0.113	0.00195	5.34967	0.09621	0.3439	0.00492	1905.4	23.6	1876.8	15.38	1848.1	30.9	1.5	3.1	1848.1	30.9
S1474_666_#46	366.8112874		0.9	-0.04242	0.00558	-0.07104	0.00927	0.01216	0.00026	77.9	1.66	-74.8	10.13	0.1	0	-204.1	77800.0		
S1474_705_#47	1044.309731		0.2	0.10944	0.00134	4.85895	0.06722	0.32248	0.00405	1801.8	19.75	1795.2	11.65	1790.1	22.13	0.4	0.7	1790.1	22.13
S1474_640_#48	1924.255934		0.9	0.05155	0.00117	0.10359	0.00236	0.0146	2.00E-04	93.4	1.29	100.1	2.17	265.5	51.24	-6.7	-64.8	93.4	1.29
S1474_639_#49	8061.830589		0.3	0.04726	0.00115	0.02188	0.00053	0.00336	5.00E-05	21.6	0.3	22	0.53	61.8	57.23	-1.8	-65.0	21.6	0.3
S1474_714_#50	1234.730891		0.2	0.05584	0.00083	0.63432	0.01018	0.08251	0.00106	511.1	6.3	498.8	6.32	445.6	32.5	2.5	14.7	511.1	6.3
S1474_901_#51	296.6561231		0.7	0.26577	0.00797	0.55387	0.01419	0.01514	0.00032	96.8	2.04	447.5	9.27	3281.2	46.36	-78.4	-97.0		
S1474_774_#52	531.174815		0.6	0.04865	0.00255	0.07418	0.00376	0.01107	0.00022	71	1.4	72.7	3.55	131.2	119.03	-2.3	-45.9	71	1.4
S1474_766_#53	3385.487783		0.3	0.02779	0.00194	0.01105	0.00077	0.00289	5.00E-05	18.6	0.31	11.2	0.77	0.1	0	66.1	18500.0		
S1474_840_#54	1088.407263		0.5	0.04307	0.00155	0.09785	0.00345	0.0165	0.00026	105.5	1.64	94.8	3.19	0.1	0	11.3	105400.0	105.5	1.64

Acknowledgment

Firstly, my adorable tutor Prof. Eduardo Garzanti is heartily acknowledged for his great support, constructive guidance and advices through the years. His rich knowledge and innovative ideas could always be the inexhaustible "provenance" in solving the problems encountered during my Ph.D study.

Besides, I would like to express my sincere gratitude to Sergio Andò, Giovanni Vezzoli, Alberto Resentini and Mara Limonta, who patiently "transport" the necessary skills in the experiment and show me the way to trace the "provenance" step by step.

Prof. Xiumian Hu is greatly acknowledged for providing Himalayan river samples and sponsoring an excellent Alps fieldwork.

My sincere thanks also goes to Paolo, Marta, Laura, Giovanni, Guido, Ronghua, Hanpu, Chiara, Giuditta and all other fellows and students in the Laboratory of Provenance Studies for the enjoyable experience in the lab work, and to Pierfrancesco, Xishan, Yiping, Renzhi, Zhao, Min, Jie, Shunli and all other Chinese and Italian friends who make the life colourful and wonderful in the foreign country.

Last but not the least, I would like to thank my family for their understanding and supporting of my abroad studying. In particular, my wife Huiwen, who accompany and support me all the time. Hi, girl, living and studying in the same time zone means a lot to me.